frontiers | Research Topics

Molecular mechanisms of glutamatergic synapse function and dysfunction

Edited by
Dhrubajyoti Chowdhury, James P. Clement and Argel Aguilar-Valles

Published in
Frontiers in Molecular Neuroscience

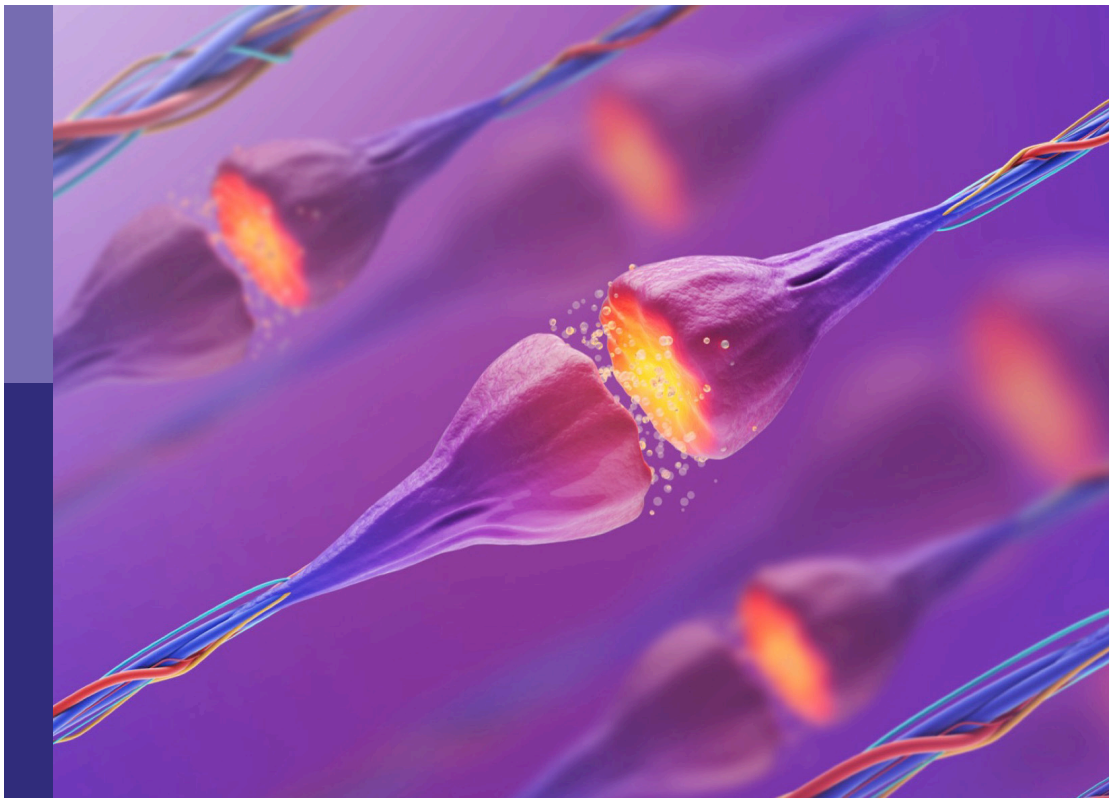

ISSN 1664-8714
ISBN 978-2-83250-944-9
DOI 10.3389/978-2-83250-944-9

About Frontiers

Frontiers is more than just an open access publisher of scholarly articles: it is a pioneering approach to the world of academia, radically improving the way scholarly research is managed. The grand vision of Frontiers is a world where all people have an equal opportunity to seek, share and generate knowledge. Frontiers provides immediate and permanent online open access to all its publications, but this alone is not enough to realize our grand goals.

Frontiers journal series

The Frontiers journal series is a multi-tier and interdisciplinary set of open-access, online journals, promising a paradigm shift from the current review, selection and dissemination processes in academic publishing. All Frontiers journals are driven by researchers for researchers; therefore, they constitute a service to the scholarly community. At the same time, the *Frontiers journal series* operates on a revolutionary invention, the tiered publishing system, initially addressing specific communities of scholars, and gradually climbing up to broader public understanding, thus serving the interests of the lay society, too.

Dedication to quality

Each Frontiers article is a landmark of the highest quality, thanks to genuinely collaborative interactions between authors and review editors, who include some of the world's best academicians. Research must be certified by peers before entering a stream of knowledge that may eventually reach the public - and shape society; therefore, Frontiers only applies the most rigorous and unbiased reviews. Frontiers revolutionizes research publishing by freely delivering the most outstanding research, evaluated with no bias from both the academic and social point of view. By applying the most advanced information technologies, Frontiers is catapulting scholarly publishing into a new generation.

What are Frontiers Research Topics?

Frontiers Research Topics are very popular trademarks of the *Frontiers journals series*: they are collections of at least ten articles, all centered on a particular subject. With their unique mix of varied contributions from Original Research to Review Articles, Frontiers Research Topics unify the most influential researchers, the latest key findings and historical advances in a hot research area.

Find out more on how to host your own Frontiers Research Topic or contribute to one as an author by contacting the Frontiers editorial office: frontiersin.org/about/contact

Molecular mechanisms of glutamatergic synapse function and dysfunction

Topic editors

Dhrubajyoti Chowdhury — Yale University, United States

James P. Clement — Jawaharlal Nehru Centre for Advanced Scientific Research, India

Argel Aguilar-Valles — Carleton University, Canada

Citation

Chowdhury, D., Clement, J. P., Aguilar-Valles, A., eds. (2022). *Molecular mechanisms of glutamatergic synapse function and dysfunction*. Lausanne: Frontiers Media SA. doi: 10.3389/978-2-83250-944-9

Table of contents

frontiers in Molecular Neuroscience

ORIGINAL RESEARCH
published: 14 September 2021
doi: 10.3389/fnmol.2021.712609

NMDARs Drive the Expression of Neuropsychiatric Disorder Risk Genes Within GABAergic Interneuron Subtypes in the Juvenile Brain

*Vivek Mahadevan[1], Apratim Mitra[2], Yajun Zhang[3], Xiaoqing Yuan[1], Areg Peltekian[1], Ramesh Chittajallu[1], Caroline Esnault[2], Dragan Maric[4], Christopher Rhodes[3], Kenneth A. Pelkey[1], Ryan Dale[2], Timothy J. Petros[3] and Chris J. McBain[1]**

[1] Section on Cellular and Synaptic Physiology, Eunice Kennedy Shriver National Institute of Child Health and Human Development (NICHD), Bethesda, MD, United States, [2] Bioinformatics and Scientific Programming Core, NICHD, Bethesda, MD, United States, [3] Unit on Cellular and Molecular Neurodevelopment, NICHD, Bethesda, MD, United States, [4] Flow and Imaging Cytometry Core Facility, National Institute of Neurological Disorders and Stroke (NINDS), Bethesda, MD, United States

OPEN ACCESS

Edited by:
Argel Aguilar-Valles, Carleton University, Canada

Reviewed by:
Stewart Alan Anderson, University of Pennsylvania, United States
Christopher Rudyk, Carleton University, Canada
Isabel Perez-Otaño, Consejo Superior de Investigaciones Científicas (CSIC), Spain

***Correspondence:**
Chris J. McBain
mcbainc@mail.nih.gov

Specialty section:
This article was submitted to Molecular Signalling and Pathways, a section of the journal Frontiers in Molecular Neuroscience

Received: 20 May 2021
Accepted: 19 July 2021
Published: 14 September 2021

Citation:
Mahadevan V, Mitra A, Zhang Y, Yuan X, Peltekian A, Chittajallu R, Esnault C, Maric D, Rhodes C, Pelkey KA, Dale R, Petros TJ and McBain CJ (2021) NMDARs Drive the Expression of Neuropsychiatric Disorder Risk Genes Within GABAergic Interneuron Subtypes in the Juvenile Brain. Front. Mol. Neurosci. 14:712609. doi: 10.3389/fnmol.2021.712609

Medial ganglionic eminence (MGE)-derived parvalbumin (PV)+, somatostatin (SST)+and Neurogliaform (NGFC)-type cortical and hippocampal interneurons, have distinct molecular, anatomical, and physiological properties. However, the molecular mechanisms regulating their maturation remain poorly understood. Here, via single-cell transcriptomics, we show that the obligate NMDA-type glutamate receptor (NMDAR) subunit gene *Grin1* mediates transcriptional regulation of gene expression in specific subtypes of MGE-derived interneurons, leading to altered subtype abundances. Notably, MGE-specific early developmental Grin1 loss results in a broad downregulation of diverse transcriptional, synaptogenic and membrane excitability regulatory programs in the juvenile brain. These widespread gene expression abnormalities mirror aberrations that are typically associated with neurodevelopmental disorders. Our study hence provides a road map for the systematic examination of NMDAR signaling in interneuron subtypes, revealing potential MGE-specific genetic targets that could instruct future therapies of psychiatric disorders.

Keywords: GABAergic interneurons, medial ganglionic eminence, transcriptional regulation, neurodevelopmental disorders, schizophrenia, NMDAR-hypofunction, scRNAseq, Ribotag-seq

INTRODUCTION

Medial ganglionic eminence (MGE)-derived forebrain GABAergic interneurons comprise the parvalbumin- containing (PV) and somatostatin-containing (SST) subpopulations throughout the entire forebrain accounting for approximately 60% of all cortical interneurons (Pelkey et al., 2017; Wamsley and Fishell, 2017). In addition, approximately half of all hippocampal neurogliaform-type cells (NGFCs), including the Ivy cells, originate from the MGE (Tricoire et al., 2010, 2011). Interestingly, though only rarely found in rodent neocortex, such MGE-derived

NGFCs are significantly more populous in primate and human neocortex (Krienen et al., 2020). While PV neurons exert robust somatic inhibition, the SST and NGFCs mediate domain-specific dendritic inhibition on their downstream pyramidal neuron targets (Pelkey et al., 2017; Wamsley and Fishell, 2017). Collectively, the interneurons shape diverse aspects of cortical and hippocampal circuit maturation and regulate information processing in mature circuits by maintaining appropriate excitation-inhibition (E-I) balance. Interneuron-specific impairments are increasingly considered central to the etiology of a number of neural circuit disorders because, numerous human CNS-disorder risk-genes are expressed in a manner specific to the development of GABAergic interneurons (Marín, 2012). Hence, there is a critical need to examine the molecular mechanisms that regulate the development and maturation of GABAergic interneurons.

Immature interneurons express different glutamate receptor subunits including the NMDA-type iGluR (NMDAR) and AMPA/Kainate-type iGluR (AMPAR/KAR) (Monyer et al., 1994; Soria, 2002; Manent, 2006), prior to the expression of any functional synapses. Multiple evidence indicates a critical role for neuronal activity, particularly through ionotropic glutamate receptors (iGluRs), in driving the development of MGE-derived interneurons (Matta et al., 2013; De Marco García et al., 2015; Pelkey et al., 2017; Priya et al., 2018; Zoodsma et al., 2020). But unlike the mature interneurons, where iGluRs are established to mediate synaptic transmission and plasticity, the precise roles for the iGluR subunits within developing interneurons are only emerging. Since the developing brain contains higher ambient glutamate than the adult brain (Hanson et al., 2019), the interneuron-expressed-iGluRs are thought to mediate trophic signaling while regulating the migration, survival, morphological and physiological maturation of interneuron development (Manent, 2006; Yozu et al., 2007; Bortone and Polleux, 2009; Desfeux et al., 2010; De Marco García et al., 2011, 2015; Kelsch et al., 2012; Le Magueresse and Monyer, 2013; Chittajallu et al., 2017; Hanson et al., 2019; Akgül and McBain, 2020).

An impairment in NMDAR signaling within GABAergic interneurons is emerging to be a key driver of juvenile-onset neural circuit disorders (Belforte et al., 2010; Rico and Marín, 2011; Nakazawa et al., 2017; Nakazawa and Sapkota, 2020). Particularly, early postnatal ablation of the obligate NMDAR subunit gene *Grin1* in GABAergic interneurons (Belforte et al., 2010; Nakao et al., 2018; Bygrave et al., 2019; Alvarez et al., 2020) resembles global *Grin1*-loss in their constellation of schizophrenia-like behavioral and neural circuit aberrations (Mohn et al., 1999). But an adult-onset (Belforte et al., 2010), or PV-exclusive (Korotkova et al., 2010; Bygrave et al., 2016), or glutamatergic neuron-exclusive *Grin1* ablation (Tatard-Leitman et al., 2015), fails to recapitulate similar behavioral abnormalities in mice. This demonstrates that NMDAR signaling plays a crucial role in determining GABAergic interneuron development that later impacts on a variety of neural circuit properties in the juvenile brain. Despite the importance of developmental NMDAR function in interneurons and its relevance to human neural circuit disorders, a comprehensive interrogation of the impact of developmental NMDAR ablation in MGE-derived interneurons, particularly across the juvenile brain is currently lacking.

NMDARs are multi-functional molecular machines that uniquely couple glutamate-induced Ca^{2+} influx pathways with gene expression regulatory programs, referred to as excitation-transcription (E-T) coupling in mature circuits (Yap and Greenberg, 2018). However, it is not clear whether the NMDAR-mediated Ca^{2+} cascades engage the transcriptional programs necessary for development and maturation in developing MGE-derived interneurons (Komuro and Rakic, 1992; Soria, 2002; Bortone and Polleux, 2009). In the present study, we examine the impact of, (i) an early developmental loss of NMDAR function in GABAergic interneurons and, (ii) the juvenile-onset NMDAR-mediated E-T coupling within MGE-derived interneurons. In particular, we conditionally deleted *Grin1* in MGE progenitors that give rise to cortical and hippocampal PV, SST, and NGFC subsets, using the *Nkx2-1*-Cre mouse line (Xu et al., 2008; Tricoire et al., 2010, 2011). In this model, the *Nkx2-1*-driven Cre expression reported in proliferating interneuron progenitors, allows for examining of the impact of embryonic loss of *Grin1* activity across all subsets of MGE-derived interneurons. Applying unbiased single-cell RNA sequencing (scRNAseq), MGE-interneuron-specific Ribotag-seq, quantitative immunostaining and *in situ* RNAscope analyses in the juvenile-brain, we establish that NMDAR-mediated transcriptional cascades regulate MGE subtype abundances, and the expression of diverse transcriptional, synaptogenic and membrane excitability genetic programs. Notably, we identify several disease-relevant genes that are misexpressed in MGE-derived interneurons upon *Grin1*-ablation, providing a broad road map for examination of MGE-derived interneuron-subtype-specific regulation via NMDAR signaling.

RESULTS

scRNAseq Recapitulates Cardinal MGE Subtypes and a Continuum of Molecular Profiles

To examine the molecular heterogeneity of MGE-derived GABAergic interneurons by scRNAseq, we microdissected frontal cortex/neocortex (nCX) and hippocampus (HPC) from fresh brain slices obtained from PD18-20 *Nkx2.1-Cre:Ai14* mouse (**Figure 1A** and **Figure 1-Supplement 1A**). Ai14-TdTomato (TdT^+) single-cell suspensions were harvested by fluorescence-activated cell sorting (FACS) using stringent gating constraints including viability and doublet discrimination (**Figure 1-Supplement 1B**) as previously described (Tanaka et al., 2008; Harris et al., 2018; Muñoz-Manchado et al., 2018), and subsequently processed through the 10X Genomics Chromium controller. 9064 and 9964 TdT^+ cells were recovered from cortex and hippocampus, respectively across 3 biological replicates. To minimize the effect of excitotoxicity and stress-related transcriptional noise, the tissue processing, FACS, and sample collection steps were performed in buffers supplemented with

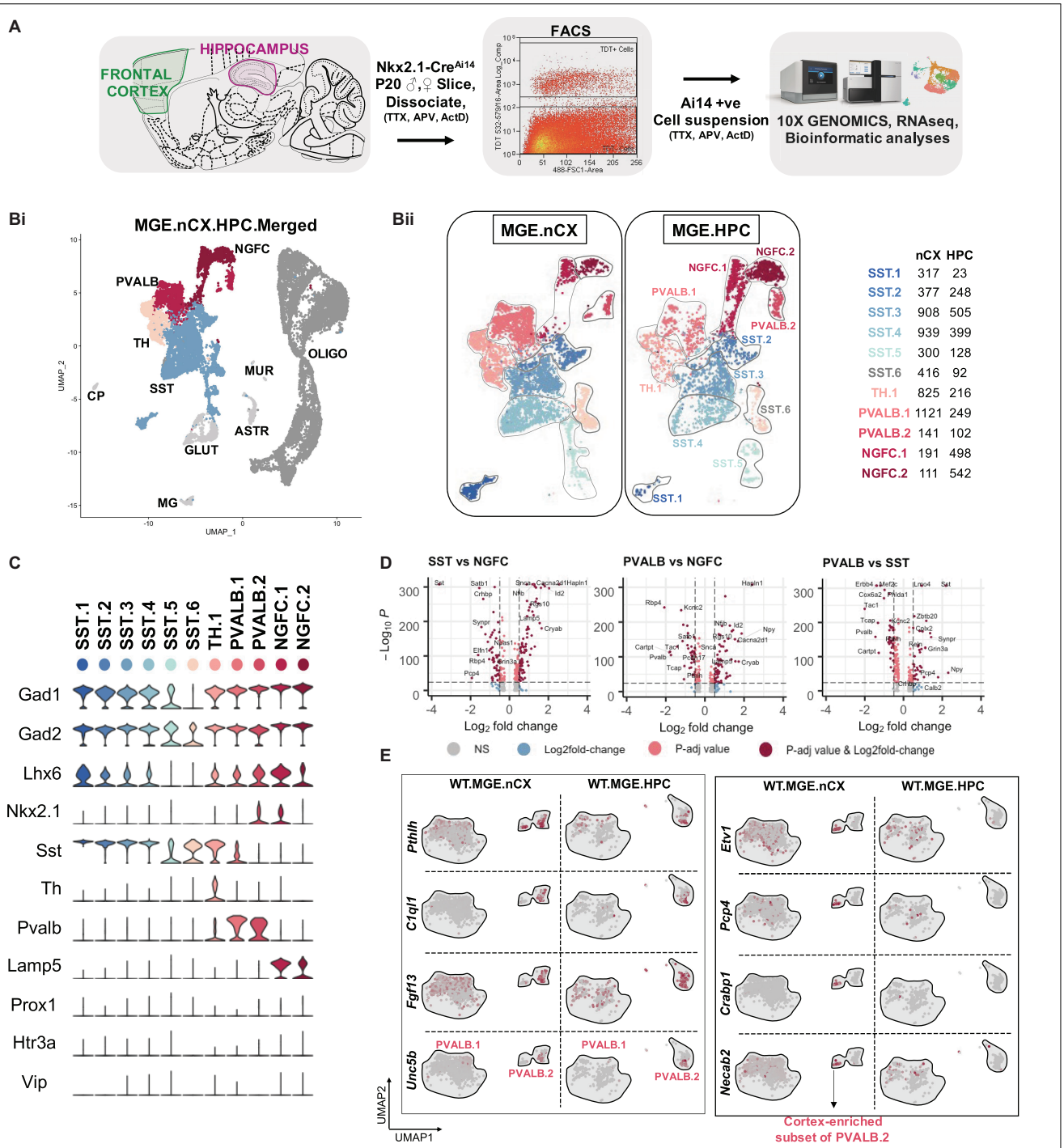

FIGURE 1 | Identification of MGE-derived interneuron subtypes in the cortex and hippocampus. **(A)** Overview of the experimental workflow. **(Bi)** Uniform Manifold Approximation and Projection (UMAP) dimensional reduction of 19,028 single-cell transcriptomes (9,064 from frontal cortex and 9,964 from hippocampus of 6 mouse brains, 3 biological replicates), showing the cardinal MGE populations. Cell clusters were color coded and annotated *post hoc* based on their transcriptional profile identities (Cell type abbreviations: PVALB, Parvalbumin; NGFC, Neurogliaform; TH, Tyrosine Hydroxylase; SST, Somatostatin; GLUT, Glutamatergic; CP, Choroid Plexus; MG, Microglia; ASTR, Astrocyte; MUR, Mural; OLIGO, Oligodendrocyte). **(Bii)** UMAP visualization of 11 MGE-derived interneuron subtypes from neocortex (MGE.nCX) and hippocampus (MGE.HPC), and the recovery of cell numbers from the subtypes. **(Biii)** Table indicating the number of *Gad1/Gad2* + cells recovered in each MGE subtype from the neocortex and hippocampus, and the defining genes enriched in each subtype. **(C)** Violin plot showing the distribution of expression levels of well-known representative cell-type-enriched marker genes across the11 MGE subtypes. **(D)** –log10 False Discovery Rate (FDR) vs. log2 fold change (FC) between each of the MGE cardinal class, representing the top enriched markers at a fold change $\geq$ 0.5 and FDR $<$ 10e-25. **(E)** UMAP representation of PVALB clusters highlighting the cortex-specific enrichment of *Pthlh*-expressing PVALB.2 subtype that is not observed in the hippocampus.

Tetrodotoxin (TTX), DL -2-Amino-5-phosphonopentanoic acid (APV) and Actinomycin-D (Act-D) (Wu Y. E. et al., 2017). Because we observed concordant cell clustering across the replicates during preliminary analysis by Seurat v3 (Butler et al., 2018; Stuart et al., 2019; **Figure 1-Supplement 2A**), the replicates were pooled for in-depth analysis. Subsequent clustering and marker gene analyses revealed that ∼62 and 33% of the TdT^+ MGE-sorts from cortex and hippocampus, respectively, express classical GABA markers including *Gad1*, *Gad2*, *Lhx6*; and the MGE-subclass markers *Pvalb*, *Sst*, and *Lamp5*, marking PV and SST, NGFC subsets, respectively (**Figure 1B** and **Figure 1-Supplement 3A**). While we did not recover cells expressing the CGE-markers *Prox1*, *Htr3a* or *Vip*, we recovered a minor fraction of cells corresponding to glutamatergic neurons, astrocytes and microglia. In addition, ∼25 and 71% TdT^+ MGE-sorts from cortex and hippocampus, respectively were enriched in oligodendrocytes marked by *Olig1* expression across all replicates (**Figure 1-Supplements 2B,C**). However, we focused our subsequent analyses on the 5656 and 3002 *Gad1*/*Gad2* positive cortical and hippocampal MGE-derived interneurons.

Unbiased cell clustering by Seurat v3 identified six subtypes of SST, two subtypes of PV, two subtypes of NGFCs, and one subtype of Tyrosine hydroxylase (TH) expressing interneurons, expressing the markers *Sst*, *Pvalb*, *Lamp5,* and *Th,* respectively, across the two brain regions examined (**Figure 1C**). Notably, all but two subtypes (SST.5 and SST.6) expressed high levels of *Lhx6*, and 2 clusters corresponding to PV.2 and NGFC.1 expressed *Nkx2.1* at this developmental time. While the PV- SST- and NGFC- clusters clearly exhibited robust gene expression differences among each other (**Figure 1D**), the TH cluster appeared to express genes that correspond to both PV: SST clusters, including *Sst* and *Pvalb* expression (**Figure 1C** and **Figure 1-Supplement 3B**). Particularly, at this developmental window we could not observe robustly different gene expression variances between the cortical and hippocampal counterparts, barring a few marginal, but significant differences (**Figure 1-Supplement 4B**). This gave us sufficient rationale to perform subsequent analyses using the MGE-derived interneurons pooled from cortex and hippocampus.

Among the SST sub clusters, SST.1–5 uniquely expresses *Chodl*, *Igf2bp3*, *Cdh7*, *Pld5,* and *Nfix,* respectively, while SST.6 expresses only markers that are common with other SST clusters (**Figure 1-Supplement 3B**). With the exception of SST.6 the remaining SST-expressing subclusters are described in previous scRNAseq assays (Tasic et al., 2016; Paul et al., 2017; **Figure 1-Supplement 5A**). For example, the *Chodl*-expressing SST.1 cluster co-expresses high *Nos1*, *Tacr1*, *Penk*, and *Npy*, and it has been previously described as putative GABAergic long-range projection neurons. Clusters SST.2/3/4 express *Elfn1*, *Reln,* and *Grm1* characteristic of putative cortical martinotti and their hippocampal counterpart, oriens-lacunosum/moleculare (O-LM) cells (Tasic et al., 2016; Harris et al., 2018; Winterer et al., 2019; **Figure 1-Supplement 5B**). Lastly, *Zbtb20*-expressing SST.5 is predicted to be septal-projecting interneurons (Harris et al., 2018). Among the PV sub clusters, while both PVALB.1&2 coexpresses several common markers including *Pvalb*, *Kcnip2*, *Tcap,* and *Kcnc1* there are several notable differences between the two clusters. PVALB.1 appears to contain continuous, but non-overlapping populations expressing *Syt2* representing putative fast-spiking basket cells or *Rbp4*/*Sst* containing putative bistratified cells (Pelkey et al., 2017; Harris et al., 2018; Tasic et al., 2018; **Figure 1-Supplement 5D**). PVALB.2 contains cells that uniquely expresses *Pthlh*, *C1ql1*, *Fgf13,* and *Unc5b* representing putative axo-axonic chandelier cells (Paul et al., 2017; Harris et al., 2018; Favuzzi et al., 2019). We also observed a TH cluster, which, in addition to expressing several genes common to the SST: PV clusters, expresses several unique genes including *Rasgrp1*, *Bcl6*, *Myo1b* that segregated into mutually exclusive cluster space expressing *Crh* or *Nr4a2* (**Figure 1-Supplements 3B, 5B**). This cluster is also described previously as putative bistratified-like cells (Harris et al., 2018; Tasic et al., 2018). Among the NGFC sub clusters, while both NGFC.1&2 coexpress several common markers including *Lamp5*, *Hapln1*, *Cacna2d1*, *Sema3c,* and *Id2*, the NGFC.1 cluster uniquely expresses several genes like *Reln*, *Ngf*, *Egfr*, *Gabra5* that are not expressed by NGFC.2 (**Figure 1-Supplement 3B**). While the *Reln*-positive population represents MGE-derived neurogliaforms, the *Reln*-negative population may represent putative ivy cells (Harris et al., 2018; **Figure 1-Supplement 5C**). While the majority of the UMAP space aligns well between the cortical and hippocampal MGE-derived interneurons, we observed some regional differences as well (**Figure 1-Supplements 3Ai,iii**).

(i) First, we observed an increase in the HPC-expressed NGFC.1&2 in comparison to their cortical counterparts, consistent with preferential localization of MGE-derived NGFCs to HPC over nCX in rodents (Tricoire et al., 2011; Pelkey et al., 2017; Krienen et al., 2020). (ii) Next, the *Pthlh*-expressing PVALB.2 subcluster splits into two islands, only in the cortex and distinctly lacking from the hippocampus. Only one of the PVALB.2 islands expresses *C1ql1*, while the other cortex-enriched island expresses unique markers *Etv1*, *Cnr1*, *Pcp4*, *Crabp1*, *Necab2*, *Epha4,* and *Hapln1* (**Figure 1E** and **Figure 1-Supplement 5D**). Whether this represents a novel subclass of chandelier cells remains to be determined. (iii) Lastly, we also observed a distinction in the hippocampal SST.3 corresponding to a subset of O-LM interneurons (**Figure 1-Supplement 3Aii**). The overall MGE cell numbers indicate that the SST cells account for the majority of MGE cell population recovered in the scRNAseq assay from both brain regions (**Figure 1-Supplements 3Aii,iii**). The PV and TH clusters accounted for a greater share of MGE-derived interneurons in the nCX than in the HPC. While it is plausible these relative cell proportions may be skewed by differential survivability of these subtypes during tissue dissociation, sorting and single-cell barcoding, these relative percentages were similar across biological replicates.

NMDAR Signaling Maintains MGE-Derived Interneuron Subtype Abundance

Because neuronal activity and glutamatergic signaling are known to regulate multiple facets of interneuronal development (De Marco García et al., 2011, 2015; Wamsley and Fishell, 2017;

Denaxa et al., 2018; Priya et al., 2018; Wong et al., 2018), we hypothesized that the key obligate subunit *Grin1* and the NMDAR signaling complex may play an instructive role in determining MGE subtype identities. To test whether NMDAR signaling impacts the development and function of MGE-derived interneurons, we ablated them in MGE progenitors by crossing floxed-*Grin1* mice with the *Nkx2.1*^{Cre} mouse line (Xu et al., 2008; **Figure 1-Supplement 1A**). The earliest expressions of *Nkx2.1* and *Grin1* in the developing rodent brains is reported around ∼embryonic day (ED) 10.5 and ∼ED14, respectively (Laurie and Seeburg, 1994; Monyer et al., 1994; Butt et al., 2008). Moreover, NMDAR-mediated Ca^{2+} signaling in migrating interneurons is reported by ∼ED16 (Soria, 2002). Because the expression and activity of *Nkx2.1* precedes *Grin1* expression, we rationalized that utilizing *Nkx2.1*^{Cre} mouse will ablate *Grin1* and NMDAR signaling in MGE progenitors from the earliest developmental point. We sorted TdT^{+} cells from the cortex and hippocampus of *Nkx2.1*^{Cre}:*Grin1*$^{fl/fl:Ai14}$ mice and performed scRNAseq using the 10X platform. The scRNAseq experiments were performed using juvenile mice (PD18–20) of both sexes and from the same litters as the wildtypes (WT) to enable subsequent direct comparison. Similar to the WT-datasets, the MGE-*Grin1*$^{fl/fl}$ mutants also revealed an enrichment of TdT + oligodendrocytes (**Figure 2-Supplement 4B**), however, we again focused our attention on the *Gad1/Gad2* positive interneurons.

We next performed integrated analyses of the MGE-*Grin1*^{wt} and MGE-*Grin1*$^{fl/fl}$ cortical and hippocampal scRNAseq datasets. Applying similar unbiased clustering parameters used for the MGE-*Grin1*^{wt} analyses, we observed a total of twelve *Gad1/Gad2* positive clusters in the integrated dataset (**Figures 2A,B**). As a robust control, *Grin1* appeared to be absent or vastly reduced in all MGE subsets in both brain regions from MGE-*Grin1*$^{fl/fl}$ (**Figure 2C**), but not in the *Slc17a7* expressing glutamatergic neurons (**Figure 2-Supplement 4A**). Overlaying the WT and NULL datasets from the brain regions revealed differential enrichments among the recovered cells between the genotypes (**Figure 2D**). Intriguingly, *Grin1*-ablation did not seem to alter the SST or PV recovery percentages, with the exception of a modest increase in the cortical NGFCs (χ^2 = 11.6, p = 0.003), but not hippocampal NGFCs (χ^2 = 4.07, p = 0.13) (**Figure 2Ei** and **Figure 2-Supplements 2Ai,B**). To independently examine whether *Grin1* ablation impacts interneuron abundances, we conducted immunostaining experiments to probe the PV and SST subtypes from postnatal days (PD) 30 brains from both genotypes. First, we observed no change in the total TdT^{+} cell counts from both cortex and hippocampus (**Figure 2-Supplements 1Ai,Bi**). Next, while we observed no change in hippocampal expressed total PV/SST cell type counts at PD30 (**Figure 2-Supplement 1Bii**), we observed a modest reduction in cortical PV cell type counts along with an increase in cortical SST cell type counts at the same age (**Figure 2-Supplement 1Aii**). This indicated differential impact of *Grin1*-ablation on cortical and hippocampal interneurons.

Despite observing no major changes in the recoveries of cardinal MGE-interneuron subtypes by scRNAseq, we observed marked changes in the recovery percentages of the subsets of SST, PV and NGFCs from both cortex and hippocampus (**Figures 2Eii-iv** and **Figure 2-Supplements 2Aii,C**). Particularly, we observed a robust increase in cortical *Chodl*-expressing cortical SST.1 population, hippocampal *Reln*-expressing SST2-4 populations, and a decrease in hippocampal SST.6 population in MGE-*Grin1*$^{fl/fl}$ (nCX, HPC: χ^2 = 286, 209; p = 2.2e-16 for both regions). In addition, we found a reduction in the cortical PVALB.1 population, and a compensatory increase in PVALB.2/3 populations in MGE-*Grin1*$^{fl/fl}$ (nCX, HPC: χ^2 = 236, 8.4; p = 2.2e-16, 0.14). Finally, we observed an increase in the NGFC.1 along with a compensatory decrease in NGFC.2 in both cortex and hippocampus (nCX, HPC: χ^2 = 13, 232; p = 0.0003, 0.14). Among the differentially enriched subclusters, *Pthlh*-expressing PVALB.3 is quite notable (**Figure 2B** and **Figure 2-Supplements 3A,B**). This cortex-enriched cluster lacking in the hippocampus was identified within the PVALB.2 putative-chandelier cells in the MGE-*Grin1*$^{wt/wt}$ (**Figure 1E** and **Figure 1-Supplement 5D**), However, subsequent to integration of the MGE-*Grin1*$^{fl/fl}$ scRNAseq dataset, it segregated as a unique cluster, far from other PVALB clusters in the UMAP space. We observed robust expressions of genes associated with NGFCs such as *Hapln1* and *Reln* expression in PVALB.3 (**Figure 2-Supplements 3A,B**). Also, we observed an increase in recovery of the cortical PVALB.3 cell numbers, including the emergence of these cells in the hippocampus subsequent to *Grin1*-ablation (**Figure 2-Supplements 2A,B**).

Increased SST and NGFC Subtypes in the Juvenile Brain Due to Loss of *Grin1*

To independently establish whether the predicted differences in cell recovery percentages among the cardinal MGE subtypes are true, we conducted RNAscope *in situ* hybridization assays from PD20-25 cortex and hippocampus from both genotypes. We particularly focused on the subtypes of SST interneurons, namely the high-*Nos1*-expressing *Chodl*-SST.1 and the *Reln*-expressing SST.2-4 subtypes. First, similar to our scRNAseq prediction, we observed a significant increase in cortical Sst^{+} cells that co-express *Nos1* and a concomitant reduction in the Sst^{+} cells that lack *Nos1* after *Grin1*-ablation in MGE-derived interneurons (**Figures 3Ai,ii**). Next, similar to our scRNAseq prediction, we observed an increase in hippocampal Sst^{+} cells that co-express *Reln* (**Figures 3Bi,ii**), without changes in total Sst^{+} cell numbers in both brain regions.

Next, we set out to examine whether the subtypes of PV and NGFC interneurons also exhibit such differences amongst their subtypes following *Grin1* ablation. We were particularly intrigued by the expression of *Nkx2.1* marker gene in subtypes of PV.3 and NGFC.1 from our scRNAseq data at ∼P20. Nkx2.1 protein is established to be expressed in cycling-MGE progenitors around ∼ED10.5 and it is thought to be turned-off in the postnatal cortex. However, it was recently indicated that subsets of late-born axo-axonic interneurons (He et al., 2016), and subsets of NGFC interneurons (Valero et al., 2021) may continue to express Nkx2.1 protein in the postnatal mouse cortex. Because both PV and NGFC

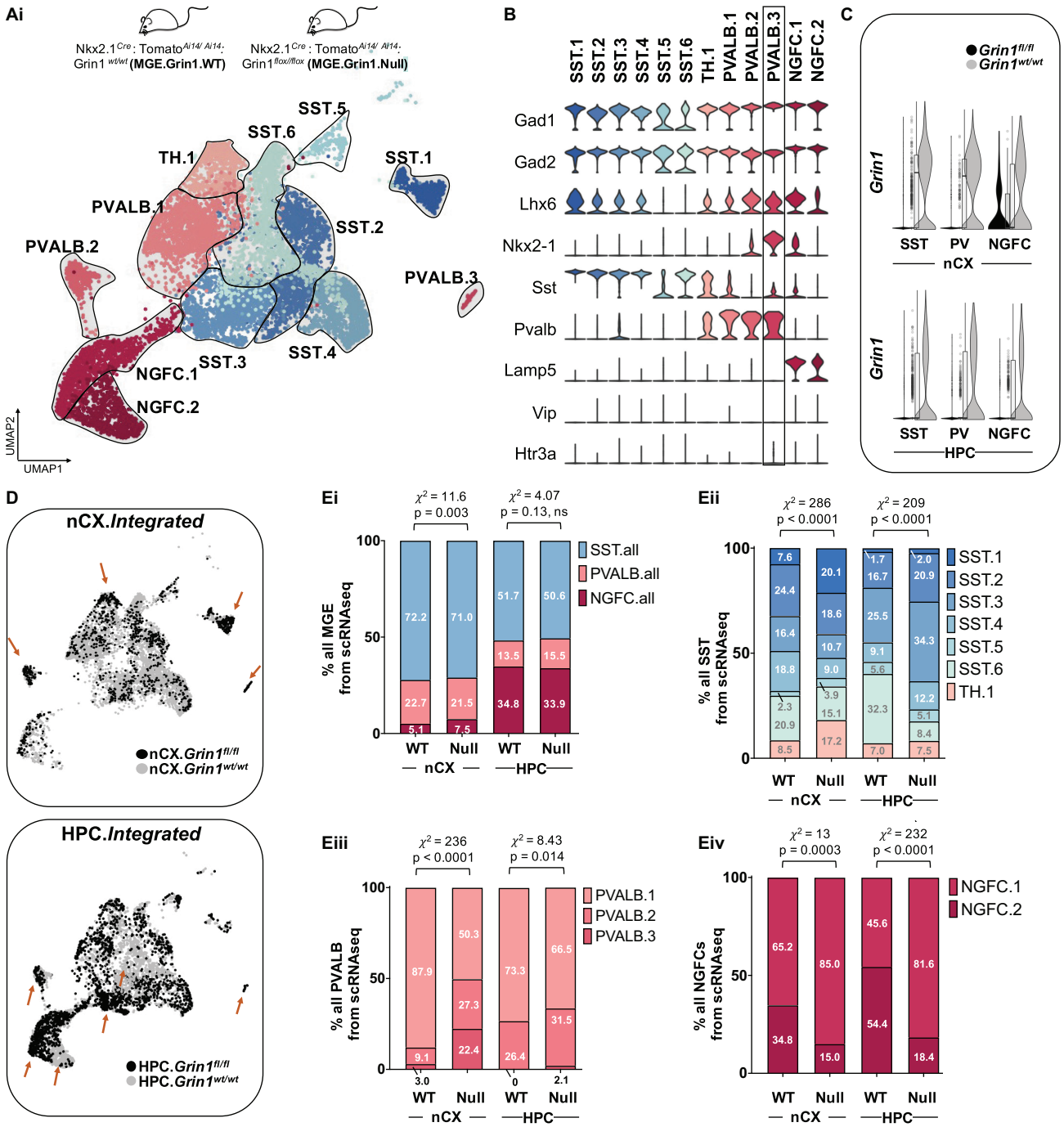

FIGURE 2 | Altered interneuron subtype proportions upon *Grin1*-ablation. **(A)** Integrated UMAP visualization of 12 subtypes of MGE-derived interneurons obtained from neocortex (nCX) and hippocampus (HPC) of $Grin1^{wt/wt}$ and $Grin1^{fl/fl}$ mice. UMAP represents the following numbers of MGE-derived interneurons from $Grin1^{wt/wt}$ and $Grin1^{fl/fl}$, respectively: 5624 (nCX.WT) and 1387 (nCX.NULL); 2998 (HPC.WT) and 2309 (HPC.NULL). 3 and 2 independent biological replicates of the scRNAseq assay from $Grin1^{wt/wt}$ and $Grin1^{fl/fl}$, respectively. **(B)** Violin plot showing the distribution of expression levels of well-known representative cell-type-enriched marker genes across the 12 interneuron subtypes. **(C)** Violin plot from both genotypes indicating the expression of *Grin1* in the cardinal of MGE-derived interneuron subtypes. **(D)** UMAP representation colored by brain-region, highlighting the differential enrichments of cells (brown arrows) within interneuron subsets in $Grin1^{wt/wt}$ and $Grin1^{fl/fl}$ from nCX and HPC. **(E)** Stacked-barplots representing the proportions of recovered cell numbers within **(Ei)**, pooled cardinal MGE subtypes, **(Eii)**, SST subtypes; **(Eiii)**, PVALB subtypes, and **(Eiv)**, NGFC subtypes in *Grin1*-WT and *Grin1*-null from neocortex or hippocampus.x^2, Chi-square test of proportions; ns, not significant.

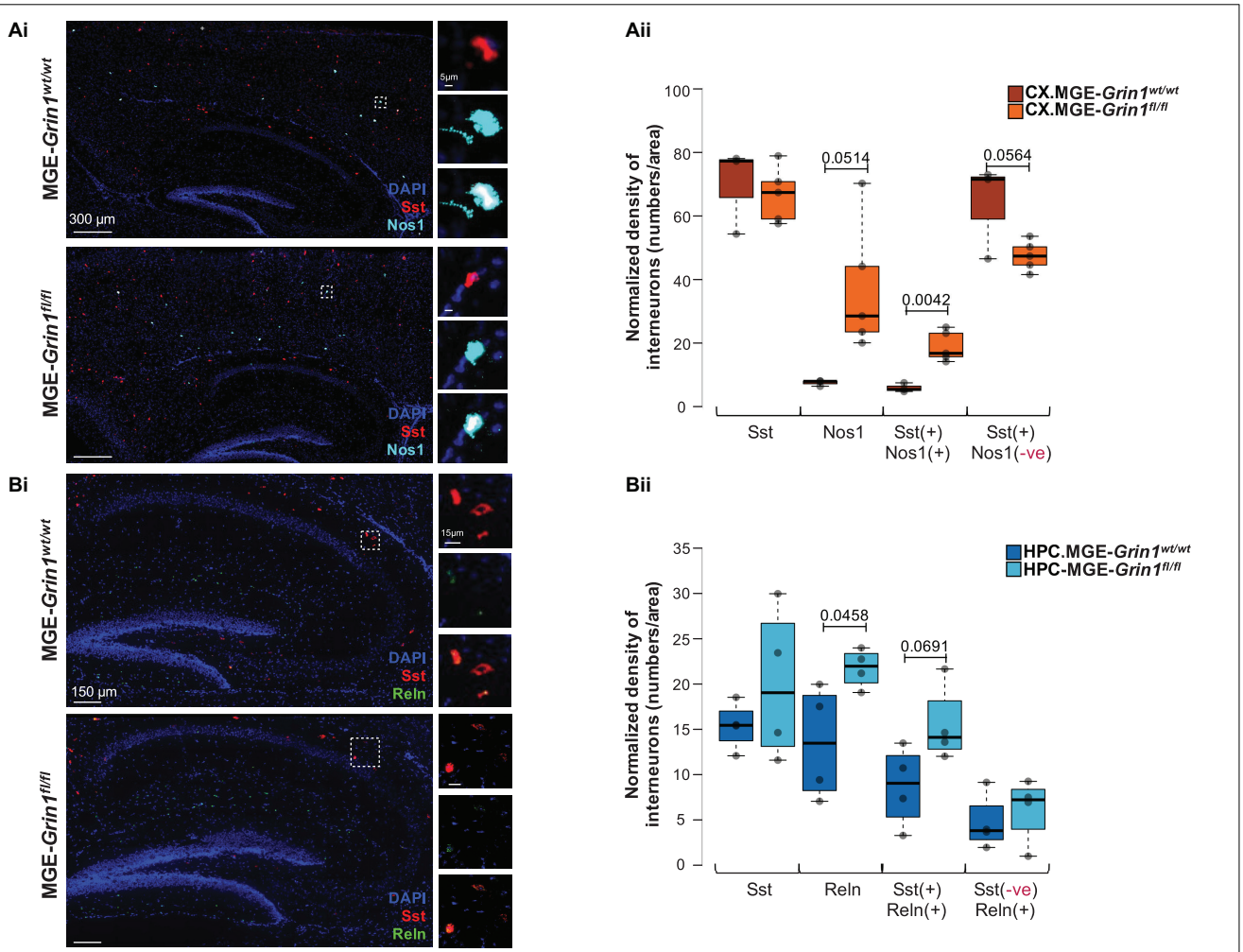

FIGURE 3 | Validation of SST interneuron subtype abundances subsequent to *Grin1*-ablation by RNA *in situ* hybridization. **(A)** Examination of cortical *Nos1*-expressing *Chodl*-SST.1 subtype abundances by **(Ai)** *in situ* hybridization using *Sst* and *Nos1* RNAscope probes from P20-25 somatosensory cortex, counterstained with DAPI. **(Aii)** Boxplots indicate *Sst*(+), *Nos1*(+), *Sst*(+):*Nos1*(+) or *Sst*(+):*Nos1*(–) cell counts. **(B)** Examination of hippocampal *Reln*-expressing SST.2-4 subtype abundances by **(Bi)** *in situ* hybridization using *Sst* and *Reln* RNAscope probes from P20-25 hippocampus, counterstained with DAPI. **(Bii)** Boxplots indicate *Sst*(+), *Reln*(+), *Sst*(+):*Reln*(+) or *Sst*(–):*Reln*(+) cell counts. *n* = 4–6 brains from each genotype for immunostaining; *n* = 2 brains (4–6 sections/brain) from each genotype for RNAscope. Error bars reflect SEM; two-tailed unpaired *t*-test, for statistical analysis.

interneuron subsets that express *Nkx2-1* gene appeared to be having increased cell recoveries in our scRNAseq assay, we examined the expression of Nkx2-1 protein in the postnatal brain with a verified antibody. First, anti-Nkx2-1 immunostaining revealed a clear expression of putative-nuclear staining in the cortex and the hippocampus, albeit at a lesser density than in the adjacent striatum on saggital sections. In the cortex, Nkx2-1-signal was observed frequently in the deep layers5/6 and less in the superficial layers, and hippocampal Nkx2-1-signal were observed frequently in the *stratum laconosum-moleculare* and *stratum oriens* and less in other layers (**Figure 4-Supplement 1Ai,ii**). While the Nkx2-1 expressing cells were all Ai14^{+}, the proportion of Ai14-cells expressing Nkx2-1 was significantly higher in the hippocampus in comparison with the cortical regions. Next, co-immunostaining of anti-Nkx2-1 with anti-PV or anti-SST antibodies revealed that these Nkx2-1 cells were not double-positive with either PV or SST in both brain regions in MGE-*Grin1*$^{wt/wt}$ sections (**Figure 4-Supplements 1B,Ci**). However, we were able to observe as few as 4 cells that were double-positive for both PV and Nkx2-1 from the hippocampus of MGE-*Grin1*$^{fl/fl}$ across all sections counted (4 sections/animal and 3 animals/genotype) (**Figure 4-Supplement Cii**). While we cannot discount the possibility that some striatal *Nkx2-1*$^{+}$ cells could have polluted the scRNAseq datasets, independent immunostaining validation indicates that PV-labeled Nkx2-1 cells are indeed rare, and they could be erroneously increased upon loss of *Grin1* in the hippocampus. Since the axo-axonic cells are very weak PV or PV-negative when assayed by immunostaining (Gallo et al., 2020), one cannot discount that some proportion of these cells that indeed expresses Nkx2-1, and were missed during our counting. However, since the Nkx2-1^{+}

cells in MGE-*Grin1*$^{wt/wt}$ sections lack PV/SST, it indicates that the majority of these cells are likely MGE-derived NGFCs, which are well established to be abundant in the hippocampus than in the cortex (Tricoire et al., 2011; Pelkey et al., 2017; Krienen et al., 2020).

Because we predicted an expansion of cortical NGFC.1 following loss of *Grin1*, we anticipated an increased proportion of Nkx2-1^{+} cells in the null tissue. Unsurprisingly, we observed a significant increase in the total numbers of Ai14^{+}:Nkx2-1^{+} and also an increased in the percentage Nkx2-1^{+} cells as a proportion of total Ai14^{+} cells in the MGE-*Grin1*$^{fl/fl}$ cortex compared with MGE- *Grin1*$^{wt/wt}$ sections (**Figure 4A**). But, despite observing increased cell recoveries of hippocampal NGFC.1 in the scRNAseq following loss of *Grin1*, we could not observe significant changes to the hippocampal Ai14^{+}:Nkx2-1^{+} double positives from the saggital sections from the *Grin1*-null tissue (**Figure 4B**). Since the hippocampal expressed-MGE-NGFCs are more densely expressed in the ventral hippocampus (unpublished observations, McBain lab), it is also possible that our quantitative cell counts from mid-dorsal hippocampal sections might have missed such an expansion in the hippocampus. It is unclear whether the changes in subtype numbers reflect a change in cell identity or whether this is altered subtype proportions due to differential survival. Nevertheless, our independent examination strongly supports the role for *Grin1*-mediated alterations in MGE-derived interneuron subtype abundances in the juvenile cortex.

NMDAR Signaling Shapes the Transcriptional Landscape in MGE-Derived Interneurons

It is now well-established that transcriptional signatures define the subtype identities of GABAergic interneurons (Fishell and Kepecs, 2020). To examine the full range of transcriptional impairments triggered by *Grin1* ablation in MGE-derived interneurons, we next performed differential gene expression testing by pooling the SST/PVALB/NGFC subtypes into their

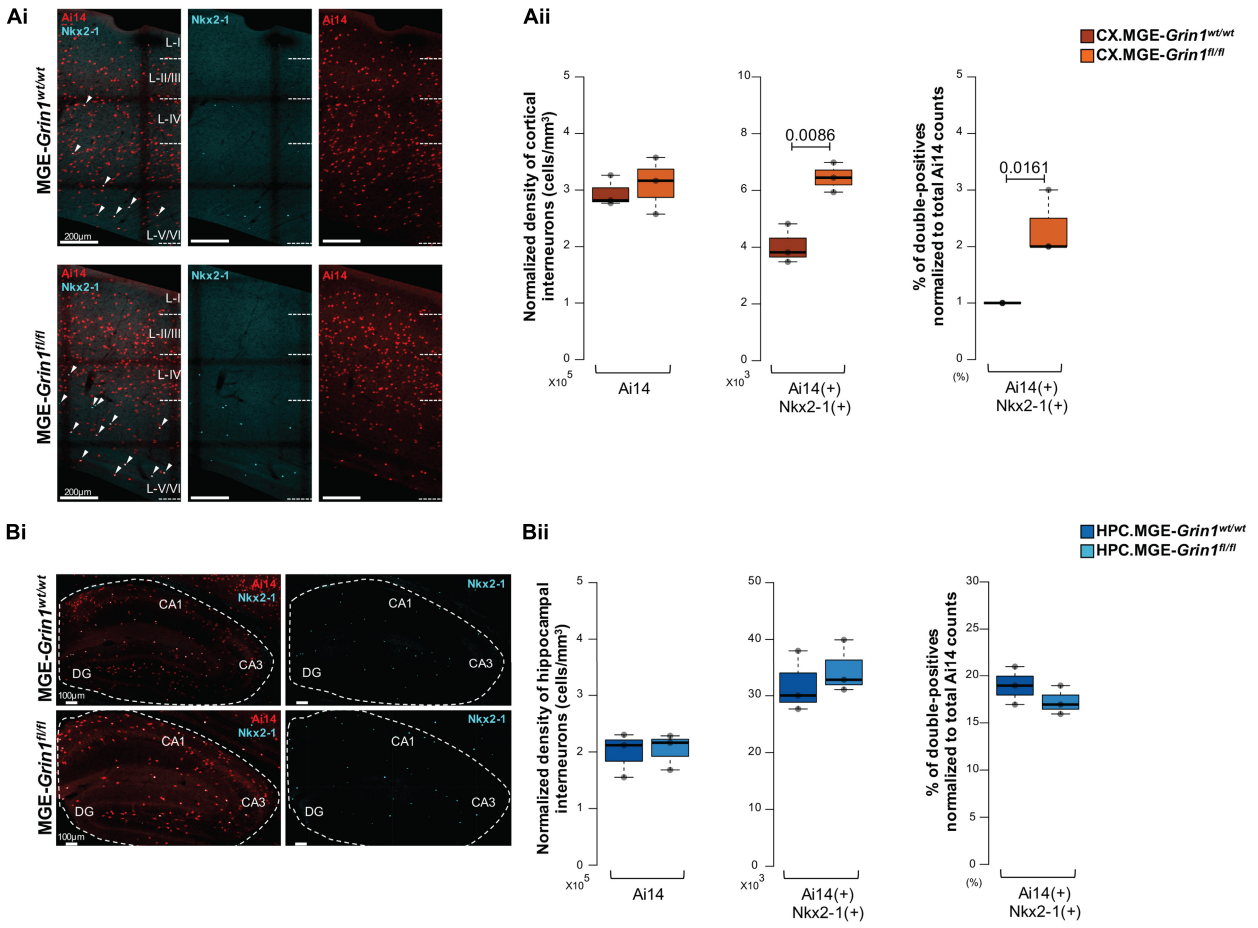

FIGURE 4 | Validation of Nkx2.1-expressing interneuron abundances subsequent to *Grin1*-ablation by immunostaining. **(Ai)**, Representative immunostaining of P25-30 somatosensory cortex using anti-Nkx2-1 (cyan), and endogenous Ai14 reporter expression. **(Aii)** Boxplots indicate the normalized density of cortical Ai14(+) and Ai14(+): Nkx2-1(+) double-positive cell counts. **(Bi)** Representative immunostaining of P25-30 hippocampus using anti-Nkx2-1 (cyan), and endogenous Ai14 reporter expression (red). **(Bii)** Boxplots indicate the normalized density of hippocampal Ai14(+) and Ai14(+): Nkx2-1(+) double-positive cell counts. *n* = 3 brains (4 sections/brain) from each genotype for immunostaining; Error bars reflect SEM from individual sections; two-tailed unpaired *t*-test, for statistical analysis.

cardinal MGE classes to identify the genes that are differentially expressed between the genotypes. For instance, SST1-6 and TH.1 are pooled together as SST; PVALB1-3 are pooled together as PVALB, and NGFC1-2 are pooled together as NGFC cardinal classes for this assay. At a stringent false-discovery rate (FDR) < 0.01, 802 genes passed the 10%-fold-change (FC) threshold across the MGE subtypes from both brain regions (**Figure 5A** and **Supplementary Table 1**). Several interesting features were observed in the differentially expressed gene (DEG) pattern upon MGE-specific *Grin1*-ablation. *(i)* Among all DEGs only ∼10 and 1% are upregulated in the cortex and hippocampus, respectively, while the remaining genes were all downregulated (**Figure 5-Supplements 1Aii,B,C**). *(ii)* While *Grin1* ablation resulted in several unique DEGs between the MGE classes, ∼10 and 27% of the DEGs are common within cortex and hippocampus, respectively (**Figures 5A,B**). For instance, while *S100a10*, *Hapln1*, *Hcrt2* are uniquely upregulated in cortical SST, PV, and NGFC, respectively (**Figure 5A**), *Apoe*, *Kcns3*, *Wnt5a* were uniquely altered in hippocampal SST, PV, and NGFC, respectively. In contrast, *Grin1* ablation induced common changes in *Penk1* and *Erbb4* expression patterns across all MGE-derived interneuron classes in the cortex and hippocampus, respectively. *(iii)* ∼27–43% of all DEGs were shared by MGE classes across brain regions (**Figure 5B**). For example, *Npas3*, *Cdh9*, *Grm1* are commonly downregulated in all SST subclasses; *Bcl6*, *Epha7*, *Gabra4* common to PV class; and *Rgs12*, *Gabrad*, *Sema5a* common to NGFCs from both brain regions. *(iv)* Lastly, 28 genes are commonly differentially expressed across both brain regions, across all MGE subtypes. For example, *Grin1*, *Neto1*, *Cdh2*, *Scn2b* are commonly downregulated across the board, while *Epha5*, *Olfm1* are commonly downregulated across all, but cortical PV cells (**Figure 5A**).

To examine the broad biological impact of the DEGs, we performed Gene Ontology (GO) analyses. Broad GO analyses on all DEGs indicates that these genes serve to regulate multiple molecular functions in interneurons, including regulation of GABAergic and glutamatergic synapses, additional to biological pathways related to addiction and circadian entrainment (**Figure 5-Supplement 2A**). Further classification of DEGs based on their cellular functions within the MGE

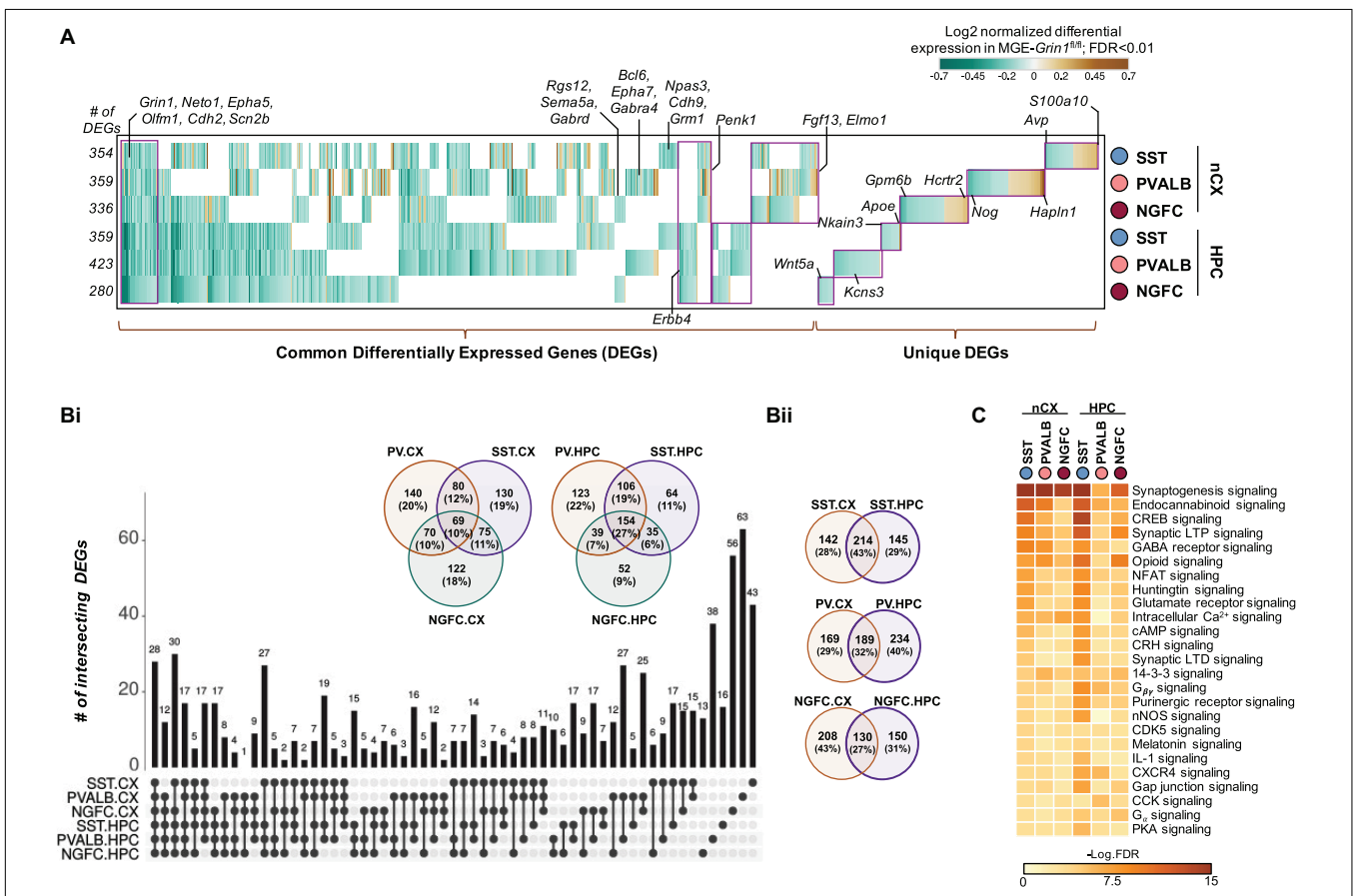

FIGURE 5 | Cell-autonomous transcriptional changes subsequent to MGE-specific developmental *Grin1*-ablation. **(A)** Combined heatmap representing the 802 differentially expressed (DEGs) in the neocortical and hippocampal MGE-derived interneurons upon *Grin1*-ablation, at a FDR < 0.01 and FC > 10%, as determined by MAST analysis (see details in section "Materials and Methods"). **(Bi)** UpSet plot and Venn-diagrams, respectively indicating the intersection and percentages of DEGs common across MGE subtypes from neocortex or hippocampus. **(Bii)** Venn-diagrams indicating the percentages of DEGs common within individual MGE subtypes from neocortex and hippocampus. **(C)** Ingenuity Pathway Analysis of significantly overrepresented molecular pathways in each MGE-subtype. FDR determined by Fisher's Exact Test.

subtypes revealed genes critical for regulation of membrane excitability, gene expression, synaptic partnering and assembly, as well as major intracellular Ca^{2+} signaling cascades, second messengers and regulators of cellular energetics (**Figure 5C**, **Figure 5-Supplement 2B**, and **Supplementary Table 2**).

Transcription Factor Expression Is a Key Component of NMDAR-Mediated Regulation of MGE-Derived Interneurons

Because transcriptional regulation underlies numerous fundamental processes including the expression of other classes of genes, we next examined the DE-transcriptional regulators in detail. We first examined the 67 genes that are differentially expressed upon *Grin1*-ablation and are known to mediate transcriptional regulation of gene expression. Of these, 35 genes are previously established to be expressed in different GABAergic interneuron classes including some notable MGE-expressed transcription factors (TFs) (**Figure 6Ai**). The remaining 32 are broadly expressed TFs (**Figure 6Aii**), that include a small subset of 15 genes that are regulated by neuronal activity. Barring a few genes, we observed the majority of TFs to be down regulated in both brain regions. Intracellular Ca^{2+} signaling cascades and second messenger systems are key mediators of NMDAR signaling to the nucleus for transcriptional regulation. Theoretically, an early first wave impairment of Ca^{2+} signaling in *Grin1*-lacking MGE progenitors could result in transcriptional silencing of the mediators of Ca^{2+} signaling cascades and second messenger systems, which would sustain the transcriptional impairments. Indeed, we also observed a downregulation of various Ca^{2+} homeostasis-regulators, kinases, phosphatases and second messengers that are activated downstream of NMDAR signaling, including regulators of cellular energetics and mitochondrial function (**Figure 6-Supplements 1A–D**). Furthermore, we noted that hippocampal MGE neurons had a greater proportion of DE-TFs and kinase signaling cascade effectors that were downregulated across all 3 subtypes compared to their cortical counterparts. Together, this suggests that hippocampal MGE-derived interneurons may be more vulnerable than cortical MGE-derived interneurons toward *Grin1*-mediated Ca^{2+} transcriptional silencing at this age.

Interestingly, among the early TF cascades in the progenitors that sequentially determine and maintain MGE fate, several members appear to be expressed at ∼P20, and starkly downregulated upon *Grin1*-ablation. For instance, *Lhx6*, *Maf*, *Arx*, *Myt1l*, *Dlx1* are among the genes broadly downregulated across all hippocampal MGE subtypes and within specific class(es) in their cortical parallels (**Figure 6A**). Other MGE fate-determining TFs, *Nkx2-1*, *Mafb*, *Satb1*, *Nr2f1* (*CoupTf1*), *Sp9*, also appear to be downregulated in discrete populations. This also includes a downregulation of *Bcl11b* (*Ctip2*) in both hippocampal and cortical NGFCs, a gene recently linked to regulation of NGFC morphology and function (Nikouei et al., 2016). Among the few transcriptional regulators upregulated are *Sirt2*, *Elmo1*, *Zcchc12*, none of which have been extensively characterized by overexpression or knockout studies to examine their specific roles within MGE-derived interneurons (**Figure 6B**). *Sirt2* is an established transcriptional repressor (Erburu et al., 2017) that may regulate the repression of several target genes in an MGE-specific manner. *Elmo1* has been previously characterized during the activity-dependent migration of CGE subtypes (De Marco García et al., 2011), and more recently predicted to be a candidate marker of immature *Pvalb* + interneurons in the hippocampus (Ling-Lin Pai et al., 2020). Finally, a recent study has predicted that the expression of *Zcchc12* correlates with slower intrinsic firing among hippocampal CA1 interneurons (Harris et al., 2018). This suggests that increased *Zcchc12* expression might regulate the expression of synaptic genes enabling reduced intrinsic excitability in the MGE subsets. Related to such putative decreased excitability in the MGE-derived interneurons, among the activity-regulated TFs, we observe broad downregulation of *Jun*, *Egr1*, *Fos*, *Fosb*, *Arc*, *Satb1*, *Arnt2* across all classes of MGE in both brain regions (**Figures 6A,B**, indicated by *), and a subtype-specific down regulation in *Npas4*.

MGE-Ribotag-Seq Cross-Validates Impaired Transcription Factor Expressions Due to MGE-*Grin1*-Ablation

To independently validate the changes in gene expressions observed by scRNAseq, we employed a Ribotag-based strategy where we generated a triple-transgenic mice by breeding the $Nkx2.1^{cre}$:$Grin1^{fl/fl}$ with the $Rpl22^{HA/HA}$-containing Ribotag mice (Sanz et al., 2009), hereafter called MGE-Ribotag (**Figure 6Bi** and **Figure 6-Supplement 1E**). We recently established that this is a robust tool to examine the mRNAs associated with the translational machinery, in a manner exclusive to MGE-derived GABAergic interneurons (Mahadevan et al., 2020). mRNAs copurified with anti-HA immunoprecipitation were utilized to prepare cDNA libraries that were subsequently sequenced in order to investigate changes in gene expression changes resulting from MGE-specific *Grin1*-ablation. By utilizing cortical and hippocampal tissues from age-matched MGE-Ribotag from both genotypes, we first established a robust reduction in *Grin1* expression in both brain regions (**Figure 6Bii**). Similar to the observed changes in the scRNAseq assay we observed robust changes in several key TFs by MGE-Ribotag-seq, particularly in genes that have established functions in maintaining MGE-identities. Notably, we observed a significant downregulation of hippocampus expressed *Lhx6* and *Id2*, an upregulation in cortical *Mafb* and hippocampal *Npas1*, and an increased expression of *Npas3* in both brain regions, after *Grin1* ablation (**Figure 6C**, top).

Key differences exist between the two strategies scRNAseq and MGE-Ribotag-seq. The scRNAseq assays only the mRNAs present in the neuronal soma while providing a single-cell resolution across the subtypes of MGE-derived interneurons. The MGE-Ribotag-seq, however, lacks the single-cell resolution across MGE-interneuron subtypes but includes the mRNAs that are bound to the translational machinery and much closer to the cellular proteome. Moreover, MGE-Ribotag-seq includes the translating-mRNAs present in the neuronal processes. Despite

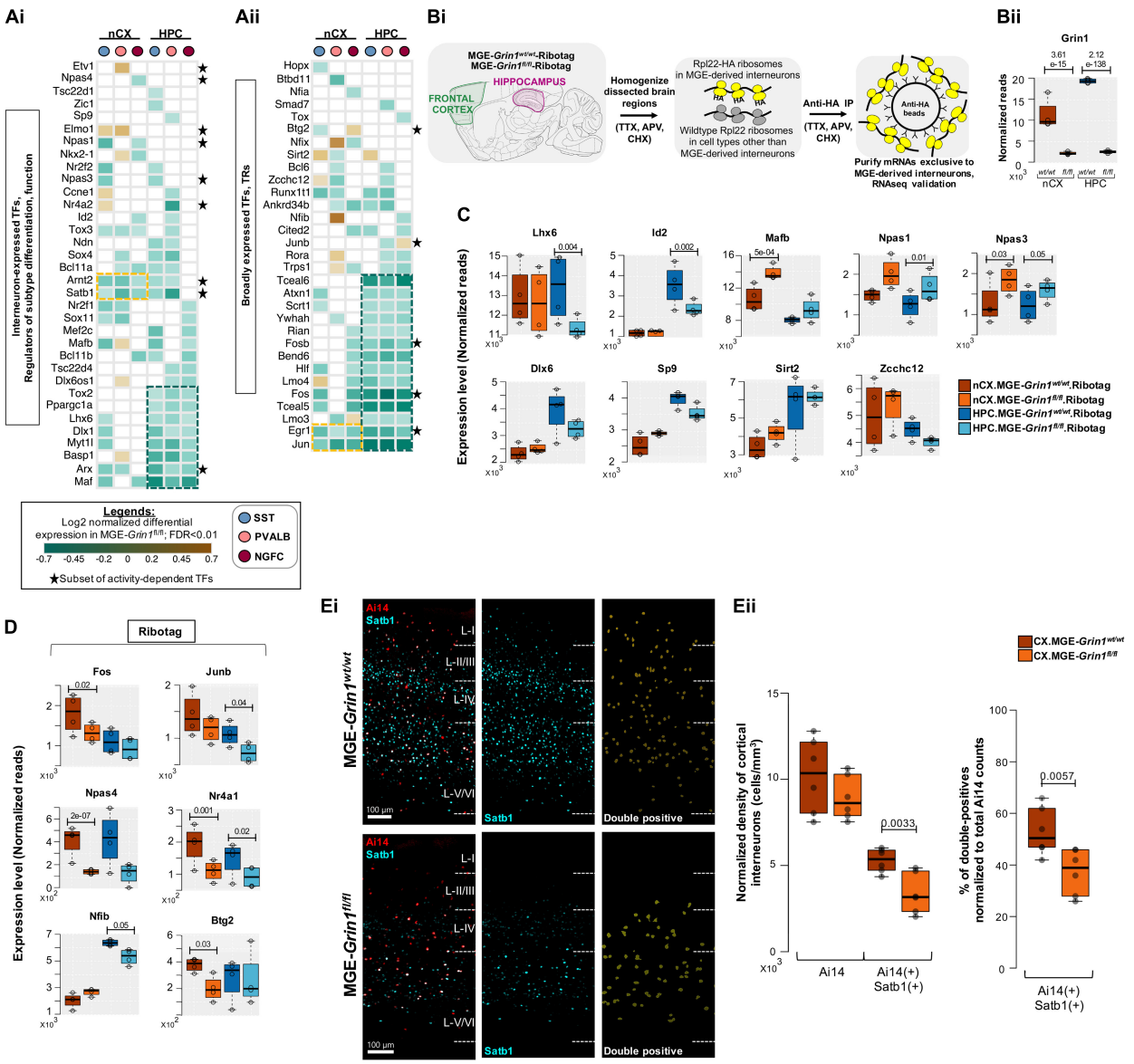

FIGURE 6 | NMDAR signaling in MGE-derived interneurons are highly dedicated to the transcriptional control of interneuron identity. **(A)** Heatmap of log2 FC of significant DEGs in neocortical and hippocampal MGE cardinal subtypes, showing a subset of **(Ai)**, Transcription factors (TFs) that are previously established to regulate MGE subtype identity and function; **(Aii)**, broadly expressed TFs and transcriptional regulators (TRs) that are not currently known to regulate MGE function. Clusters of commonly differentially expressed genes in neocortex and hippocampus are indicated in yellow or green boxes. * indicates a subset of neuronal activity-regulated TFs. **(Bi)** Overview of the experimental workflow for RNAseq validation, by ribosomal tagging/Ribotag strategy specific to MGE-derived interneurons. *n* = 4 biological replicates from each genotype for MGE-Ribotag-seq; Error bars reflect SEM; DeSeq2 for statistical analysis. **(Bii)** MGE-Ribotag-seq normalized reads for *Grin1* expression in neocortex and hippocampus. MGE-Ribotag-seq normalized reads cross-validating the differential expressions of **(C)**, MGE-enriched TFs, and **(D)**, neuronal activity-regulated TFs. **(Ei)** Representative immunostaining of P25-30 somatosensory cortex using anti-Satb1 (cyan), and endogenous Ai14 reporter expression. Ai14:Satb1 double-positive cells are represented as yellow surfaces using Imaris9.6. **(Eii)** Boxplots indicate the normalized density of cortical Ai14(+) and Ai14(+): Satb1(+) double-positive cell counts. *n* = 3 brains from each genotype for immunostaining; Error bars reflect SEM from individual sections; two-tailed unpaired *t*-test, for statistical analysis.

these technical differences, the congruity in the DEGs after *Grin1*-ablation strongly favors our claims related to NMDAR-signaling dependent regulation of key transcription factors. Having a gene not validated by MGE-Ribotag-seq does not imply a false-positive scRNAseq result, and the above-described technical differences could contribute to it. Also, the genes that are commonly differentially expressed across the PV-SST-NGFC subtypes by scRNAseq will have a greater possibility of being identified as a DEG via MGE-Ribotag-seq. Accordingly, genes such as *Dlx6*, *Sp9*, *Sirt2,* and *Zcchc12* that showed alternating differences among subtypes in the scRNAseq, did not reveal significant differences via MGE-Ribotag-seq (**Figure 6C**, bottom).

We also observed a significant decrease in the expressions of several activity-regulated TFs by MGE-Ribotag-seq in both brain regions (**Figure 6D**). While *Fos*, *Junb*, *Btg2*, *Nfib* expressions were significantly downregulated in either cortex or hippocampal MGE-derived interneurons, the expressions of *Nr4a1* and *Npas4* appear to be commonly downregulated in both brain regions after *Grin1*-ablation. *Satb1* is a key activity-regulated TF that is expressed in MGE-derived interneurons, critically regulating the identity and survival of different subtypes (Close et al., 2012; Pachnis et al., 2012). Independent immunostaining experiments revealed that *Grin1*-ablation resulted in a robust reduction in MGE-derived interneurons co-expressing Satb1 in PD30 somatosensory cortex (**Figures 6Ei,ii**), further substantiating our findings from scRNAseq. Taken together, this establishes a framework for simultaneous regulation of neuronal activity and expression of distinct sets of TFs (including the activity-regulated TFs) by NMDAR-signaling in MGE-derived interneurons.

Impaired NMDAR Signaling Alters Region-Specific MGE Subtype Marker Expression

Several GABAergic MGE markers were misregulated upon *Grin1*-ablation (**Figure 7A**). For example, genes *S100a0, Pthlh, Hcrtr2* that are normally expressed in SST, PV and NGFCs, respectively, are upregulated in the same clusters of MGE-*Grin1*$^{fl/fl}$ (**Figure 7Bi**), indicating a misexpression in a subtype-specific manner. Next, while certain genes such as *Reln*, *Tenm1* are broadly downregulated across MGE classes, some genes like *Thsd7a* show an upregulation in certain classes but a downregulation in the other classes (**Figure 7Bii**). Interestingly, a few genes that are normally abundant in one MGE class, appear to be misexpressed in another MGE class where they are not abundant. For instance, *Tcap (telethonin)*, that is expressed in PV cells, in addition to being decreased in PV cells, is upregulated in NGFCs in both cortex and hippocampus. Similarly, *Hapln1* expression, which appears to be abundant in NGFCs (Harris et al., 2018; Krienen et al., 2020), is upregulated in PV subsets (**Figure 7Biii**). Indeed, MGE-Ribotag-seq cross-validates a robust downregulation in *Tcap*, *Tenm1,* and *Hapln1*, and a robust upregulation in *S100a0*, *Tacr1,* and *Nos1* (**Figure 7C**). Lastly, we observed an upregulation in the *Gad1* and *Slc32a1* (vesicular GABA transporter, vGAT) and a downregulation in *Gad2* and *Slc6a1* (Na^+-Cl^- dependent GABA transporter, GAT1), corresponding with GABA synthesis and reuptake machineries, respectively (**Figure 7-Supplement 1A**). These findings closely match the trending differences observed via MGE-Ribotag-seq.

NMDAR Signaling Regulates MGE Subtype-Specific Expression of Neurodevelopmental Disorder Risk Genes

Interneuron-centric disease etiology is an emerging centrality in multiple psychiatric disorders (Marín, 2012). Thus, we questioned whether the *Grin1* ablation induced DEGs presently identified correlate with disease etiology. Disease-ontology based Fisher's Exact Test conducted on the DEGs showed significant over-representation of genes implicated in "Schizophrenia,"

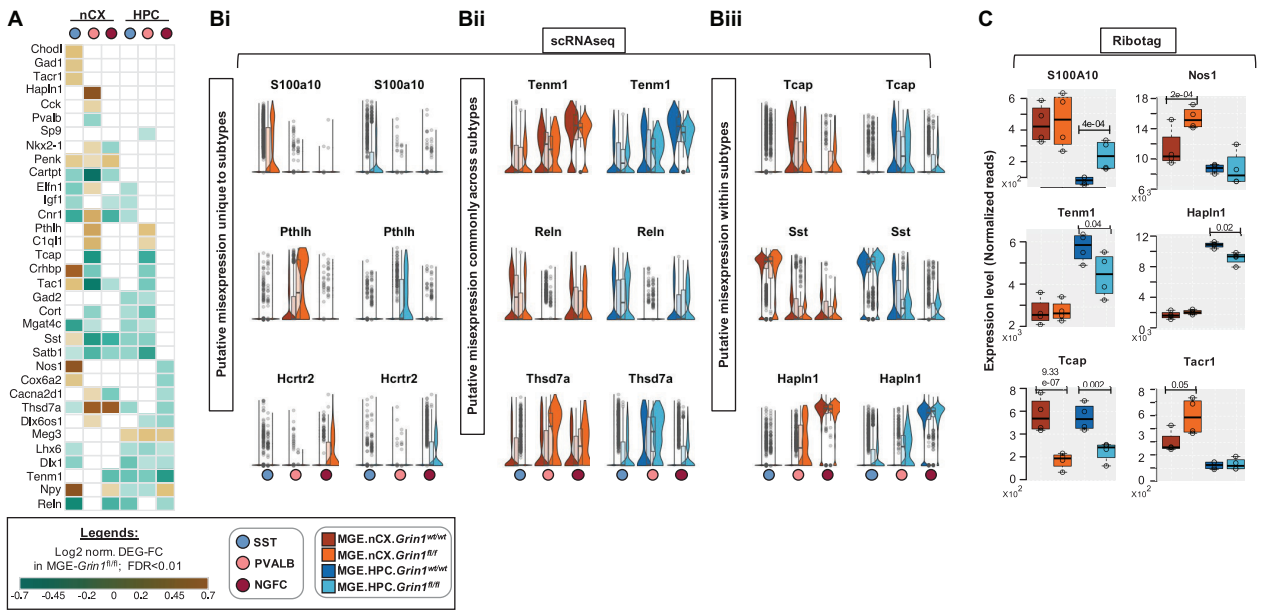

FIGURE 7 | Differential expression of interneuron marker genes across subtypes upon *Grin1*-ablation. **(A)** Heatmap of log2 FC of significant DEGs in neocortical and hippocampal MGE cardinal subtypes, showing notable MGE marker genes. Representative box-violin plots of top differentially expressed genes from the above that represent **(Bi)**, a misexpression unique to a single MGE-interneuron subtype in the *Grin1*$^{fl/fl}$ **(Bii)**, a misexpression across all MGE-derived interneuron subtypes in the *Grin1*$^{fl/fl}$; **(Biii)**, a misexpression between MGE-derived interneuron subtypes in the *Grin1*$^{fl/fl}$. **(C)** MGE-Ribotag-seq normalized reads, cross-validating the misexpressed interneuron marker genes in neocortex and hippocampus.

"Psychiatric disorders" and "Movement disorders," among other cellular impairments involving aberrant morphology of neurons (**Figure 8A** and **Supplementary Table 3**). To independently examine the DEGs for potential enrichment for neurodevelopmental disorders, we obtained the risk genes for schizophrenia (Sz) and autism spectrum (As) from the SZDB (Wu Y. et al., 2017) and SFARI (Simons Foundation, 2018) databases, respectively. These databases curate and rank disease-relevant gene sets, based on multiple evidence sources including genome-wide association studies, copy-number variations, known human mutations and other integrative analyses. In particular, we mapped the DEGs with the top-ranked genes from these disease datasets (see methods for details). While 592 DEGs could not be mapped with either disease genes, 25 genes mapped exclusively with the SFARI-AS gene list, 164 genes mapped exclusively with the SZDB-Sz gene list and 21 genes mapped with both datasets (**Figure 8Bi** and **Supplementary Table 4**). It is now well-established that several neurodevelopmental disorders exhibit a high degree of converging molecular pathways employing proteins that exist in physical complexes (Cristino et al., 2014). Therefore, we examined whether these disease-associated DEGs are known to form protein complexes between each other, by mapping curated protein-protein interaction (PPI) datasets for all 802 DEG products. Indeed, we observed that > 95% of disease annotated DEG products are known to exist with PPIs, while only ∼75% of DEG products not annotated with Sz/As are known to exist with PPIs (**Supplementary Table 4C**). Interestingly, despite not mapping directly with the high-ranked disease gene sets, the remaining 592 genes are observed to exist in tightly knit PPIs with the disease annotated genes. However, the PPIs mapped with SZDB form the most interconnected clusters in comparison to the SFARI-mapped PPI network (**Figure 8Bii**), as indicated by relatively higher clustering coefficient. Put together, both unbiased disease ontology prediction, targeted analysis of high-confidence neuropsychiatric disorder genes, indicate that members of the DEGs share physical, and functional pathways in MGE-derived interneurons, contributing toward disease etiology.

Among the 210 DEGs mapped with to Sz and As, 45 genes are established regulators of axon pathfinding, synapse formation and assembly, while 38 members are established regulators of membrane excitability and neuronal firing. Because both gene classes are intimately associated with interneuron function, we examined these classes in detail. We observed multiple classes of secreted ligands and cognate receptor families corresponding to semaphorin, netrin, slit, chemokine and growth factors, and their intracellular effectors that are downregulated upon MGE-*Grin1*-ablation (**Figures 8Ci,iv**). These include *Ntng1*, *Sema3e*, *Slit2*, *Cx3cl1*, and some of their receptors, *Unc5c*, *Nrp1*, *Neto1/2*, *Robo2* that are decreased in MGE-class-specific manner. We observed *Fgf13* that was recently demonstrated to mediate MGE-subtype specific synapse assembly, to be upregulated in cortical PV cells, but downregulated in cortical SST, while *Apoe* to be upregulated in hippocampal SST cells. In addition to synaptic assembly molecules, we observed DE in a variety of synaptic adhesion molecules, corresponding to protocadherin, cadherin, ephrin, and contactin families (**Figure 8Cii**). Notably, we also observed a downregulation of *Erbb4* across all hippocampal MGE-subtypes. Lastly, we observed increased expression of extracellular matrix components *Mgp*, *Ndst4*, *Hapln1*, *Adamts5*, *Mxra7*, *Thsd7a*, and the matrix modifying enzymes *Hs3st2/4* in cortical SST/PV subtypes (**Figure 8Ciii**). In parallel, MGE-Ribotag-seq cross-validates a robust down regulation in hippocampal *Erbb4*, and a robust differential expression of several synaptic partnering and adhesion molecules including *Cdh9*, *Ntng1*, *Ephb6*, *Pcdh1*, *Cdh12*, *Sema5a*, and key members of CAM modifiers *St3gal1* and *St8sia2* (**Figure 8D**).

Among the regulators of neuronal excitability, we observed a downregulation of multiple members of postsynaptic glutamate receptor subunits, GABA receptors and their associated partners (**Figure 8-Supplement 1Bii**). Interestingly, while we noted a broad downregulation of several members of potassium and sodium channel subunits, a few discrete members of the Kcn-families were upregulated in cortical PV and NGFC subtypes. Finally, we also observed multiple members of presynaptic GABA synthesis, release and uptake machineries including *Gad1*, *Syt2/10*, and *Slc6a1* differentially expressed in discrete MGE subtypes (**Figure 8** and **Figure 8-Supplement 1Bi**). Collectively, these findings highlight the centrality of MGE-expressed *Grin1*-signaling during synapse formation and connectivity, which when aberrantly expressed, can lead to neurodevelopmental disorders.

DISCUSSION

Centrality of MGE-Derived Interneuron-Expressed NMDARs From Juvenile Brain

NMDARs serve as critical activity dependent signaling hubs for myriad neuronal functions due to their innate ability to directly link network dynamics to cellular calcium events and associated transcriptional coupling. Such NMDAR-dependent E-T coupling is widely established in glutamatergic neurons and in specific interneurons (Wamsley and Fishell, 2017; Yap and Greenberg, 2018) using candidate approaches within mature circuits. However, the detailed unbiased evaluation of the transcriptional landscape of NMDAR signaling within interneurons in developing circuits undergoing refinement is lacking. Our study provides the first systematic "fingerprinting" of the transcriptional coupling associated with NMDAR signaling, exclusive to MGE-derived interneurons, providing a road map for examining NMDAR regulation of MGE-derived interneurons in a subtype specific manner. Our unbiased transcriptional profiling approach indicates that developmental NMDAR signaling participates in driving MGE-derived interneuron development and maturation by regulating the expression of transcription factors (67 genes), synaptogenic (53 genes) and connectivity factors/adhesion molecules (61 genes), and regulators of membrane excitability (78 genes), among the 802 DEGs in interneurons (**Figure 9**). While the present study reflects a longer-term impact of the developmental loss of

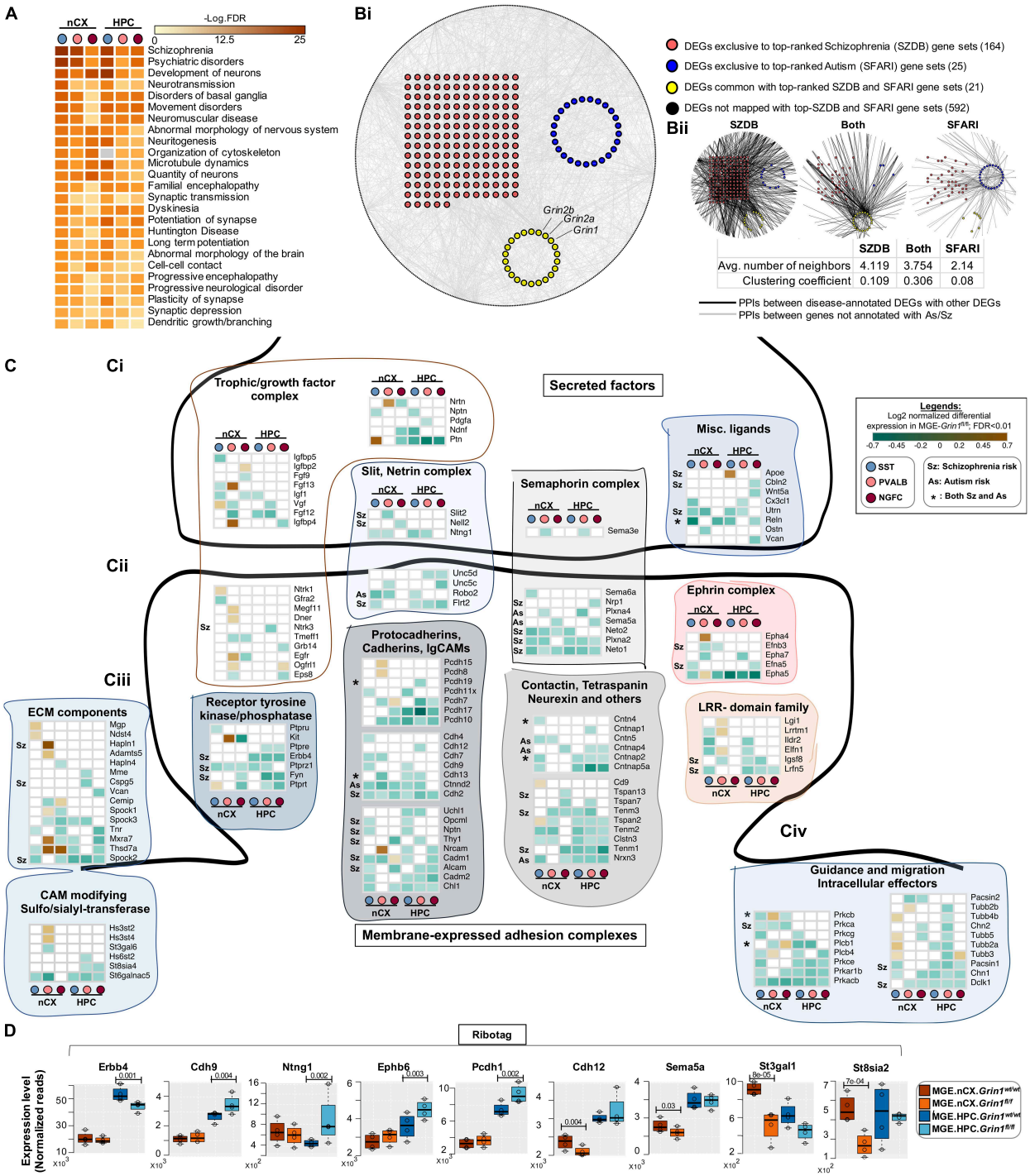

FIGURE 8 | Aberrant NMDAR signaling results in misexpression of high-risk Sz genes. **(A)** Ingenuity Pathway Analysis of significantly overrepresented disease pathways in each MGE-subtype. FDR determined by Fisher's Exact Test. **(Bi)** Global protein-protein interaction (PPI) map among all differentially expressed genes (DEGs). Red circles indicate the DEGs annotated to be top-ranked Sz-risk genes; Blue circles indicate the DEGs annotated to be top-ranked As-risk genes; Yellow circles indicate the DEGs annotated with both Sz and As-risk genes. Black circles in the periphery indicate the DEGs not annotated with high-risk Sz/As genes. The PPIs between DEGs indicated in gray lines. **(Bii)** PPIs between Sz/As/dually enriched clusters, and other genes. The PPIs between disease-annotated DEGs and other disease-annotated DEGs or with other non-annotated DEGs are indicated in black lines. The PPI between non-annotated DEGs indicated in gray lines. **(C)** Heatmap of log2 FC of significant DEGs in cortical and hippocampal MGE cardinal subtypes, showing a subset of **(Ci)**, secreted trophic factors and secreted ligands and guidance cues. **(Cii)** Membrane-bound synaptogenic receptors and cell adhesion molecules (CAMs) **(Ciii)**, extracellular Matrix (ECM) components and matrix modifying enzymes. **(Civ)** Intracellular effectors of guidance and synaptogenic cues. **(D)** MGE-Ribotag-seq normalized reads, cross-validating the differentially expressed synaptic partnering molecules.

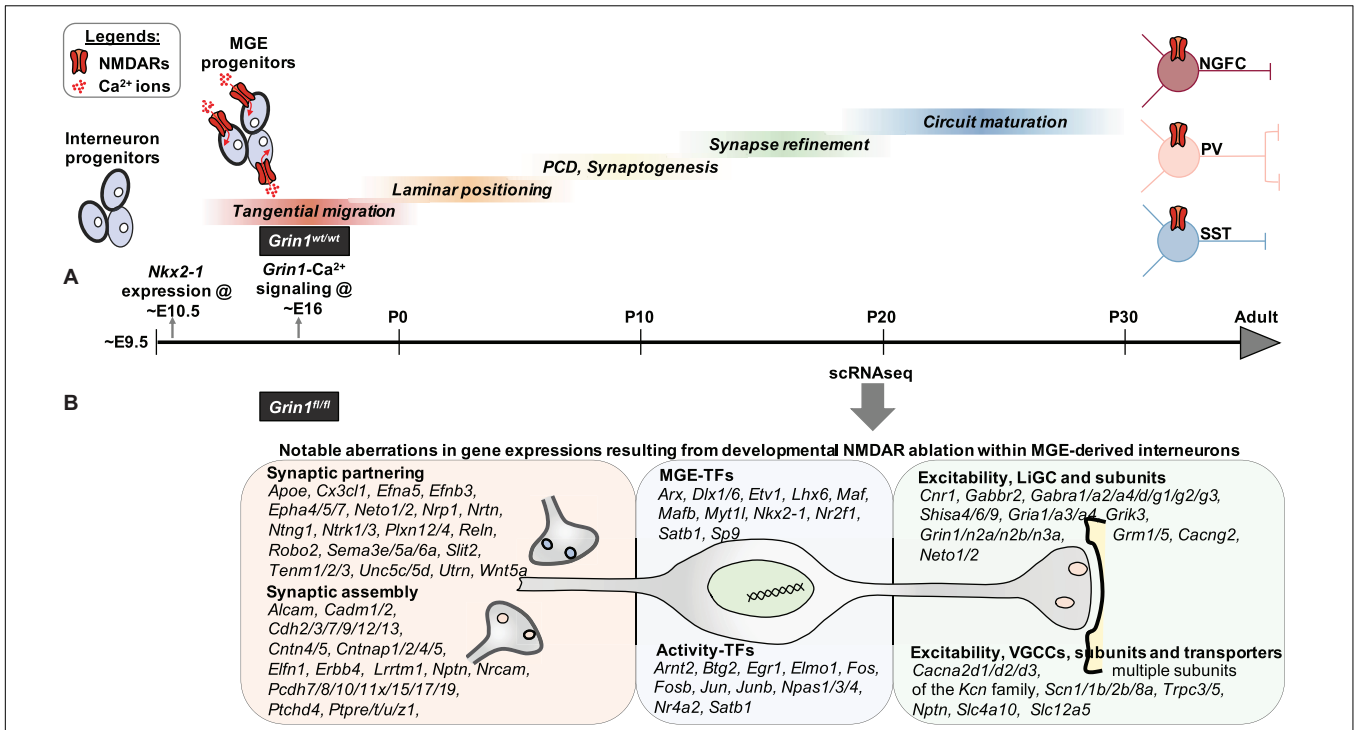

FIGURE 9 | Transcriptional control of MGE-derived interneuron development, synaptic partnering, and excitability are mediated by NMDAR signaling. **(A)** *Nkx2.1* expression appears at ∼ED10.5, driving subtype fate in MGE-expressed interneuronal progenitors. Subsequently, their sequential developmental milestones toward circuit refinement appears to be under a combination of innate genetic mechanisms and neuronal activity. While the earliest *Grin1* expression is reported at ∼ED14 in developing brain, MGE-specific NMDAR mediated Ca^{2+} is recorded at ∼ED16. However, the broad role played by interneuron-expressed NMDAR signaling during interneuron development and maturation until now is not well delineated. **(B)** By driving *Grin1*-ablation using *Nkx2.1*-driven Cre-recombinase expression, we report the earliest developmental loss of NMDAR signaling, across MGE-derived interneuron subtypes. In particular, by performing scRNAseq assay in MGE-derived interneurons from the neocortex and hippocampus of juvenile mouse brain, we report a broad transcriptional aberration subsequent to loss of NMDAR-signaling. Notably, this expression abnormality involves numerous TFs, synaptogenic and regulators of interneuron excitability, that collectively establish MGE subtype identities and drive their maturation. (TF, transcription factors; LiGC, Ligand-gated ion channel; VGCC, Voltage-gated ion channel).

NMDAR-signaling in MGE-derived interneurons, based on broad transcriptional downregulation of target genes, we can make several predictions that should guide future investigations.

Role for NMDAR-Signaling Regulated TFs in Shaping Interneuron Identity and Granularity Amongst Subtypes

Three key possibilities that enable NMDAR-dependent interneuron development exists, and our dataset provides potential examples for all three scenarios. *(i)* First, it is possible that NMDAR-dependent Ca^{2+} signaling in the developing interneuron progenitors provides a combinatorial cue that will couple with innate genetic programs to generate the diversity in interneuron subtypes. We observe key MGE-specification genes *Lhx6* and *Id2* downregulated and other genes such as *Mafb*, *Npas1,* and *Npas3* upregulated in *Grin1*-lacking interneurons in both scRNAseq and MGE-Ribotag-seq assays. *(ii)* It is also possible that NMDAR signaling critically regulates neuronal activity that further shapes the expressions of MGE-subtype determining and distinct activity-dependent TFs. In line with this possibility, we establish a robust downregulation in the activity-regulated TF, *Satb1*, and a robust reduction in Satb1 + cortical interneurons that lack *Grin1*. It is notable that *Satb1* is a key activity-regulated TF that critically regulates the identity and survival of different subtypes of SST-interneurons (Close et al., 2012; Pachnis et al., 2012). Additionally, we observe an increase in *Etv1* expression in cortical PV cells, and *Etv1* was previously demonstrated to be an activity-dependent TF that inversely correlates Ca^{2+} influx (Dehorter et al., 2015), regulating the properties of a subset of PV-interneurons. *(iii)* Lastly, it is possible that altered neuronal activity due to aberrant NMDAR -signaling result in differential survival and/or cell-death in developing interneurons (De Marco García et al., 2011, 2015; Wamsley and Fishell, 2017; Denaxa et al., 2018; Priya et al., 2018). Indicating that the *Grin1*-lacking MGE-derived interneurons have altered interneuron survival and/or cell-death, we observe differential recoveries of the subtypes within SST and NGFC in the scRNAseq assay. Particularly, we observe an abundance of cortical *Chodl*-SST.1 in the *Grin1*-ablated MGE-derived interneurons, and a concomitant decrease in cortical SST.2-4 subtypes. We also observe an increase in Nkx2-1 expressing putative neocortical NGFCs in the *Grin1*-ablated MGE-derived interneurons. Moreover, we report an increase in hippocampal *Reln*-SST2-4 subtypes upon *Grin1*-ablation by RNA *in situ* hybridization. Additionally, by

independent immunostaining experiments, we observe a robust decrease in cortical MGE-derived interneurons that coexpress the TF *Satb1*, which is established to promote interneuron survival. However, detailed future studies are necessary to uncover which of the above indicated NMDAR-dependent mechanisms regulate the abundances and diversity within PV/SST/NGFC subclasses.

Shaping Interneuron Subtype-Specific Synaptic Assembly and Connectivity

What is the biological context of differential expression of the TFs, in the juvenile forebrain when MGE-derived interneuron fate is assumed to be already sealed, and subtype identities established? It is emerging that some of these TFs are continually required for the maintenance of MGE fate, post development (Fishell and Kepecs, 2020). One of the ways the TFs maintain MGE subtype fate into adulthood, is by controlling the expression of genes that are essential for ongoing interneuron function. Accordingly, we predict that NMDAR-dependent expression of synaptogenic and synaptic partnering molecules regulate the assembly of synapses with appropriate targets. Secreted semaphorin, ephrin, slit, netrin and neurotrophin-based signaling systems have been investigated in GABAergic neurons, during axonal pathfinding, and cell migration (Marín et al., 2001; Polleux et al., 2002; Andrews et al., 2008; Nóbrega-Pereira et al., 2008; Zimmer et al., 2008). However, only recently have inroads been made into delineating their expression, and interaction with appropriate receptor systems in target synapses during accurate synaptogenesis. In addition, the NMDAR-dependent expression of synaptic adhesion molecules will further promote stability of newly formed synapses. Here, the mis-expression of diverse secreted cues, their receptors and adhesion molecules by MGE subtypes during *Grin1*-ablation, provides unique insight into the molecular diversity employed during synapse establishment. Our findings also reveal numerous candidates for examining subtype specific synapse assembly, which are centrally regulated by NMDAR signaling.

After synapse formation, nascent connections remain susceptible to strength modifications according to neuronal activity. Again, NMDAR-signaling in MGE-derived interneurons seems to regulate this process by the transcriptional regulation of the expressions of both presynaptic and postsynaptic members, including excitatory and inhibitory synaptic molecules and their auxiliary subunits, as well as presynaptic GABA release machinery molecules such as *Cplx1/2, Stx1b, Rab3c*. Cell-specific ablation of *Grin1* is previously reported to regulate neuronal intrinsic excitability (Hou and Zhang, 2017). Here, we observe a broad down regulation of several members of the potassium channel subunits and their auxiliary subunits across MGE subtypes, except for an upregulation of a few *Kcn*-genes in cortical PVs and NGFCs. While the precise impact of the diverse changes in these genes on MGE firing are currently unclear, the pattern of expression of the activity-dependent transcription factors provides us an indication.

Notable activity-dependent TFs such as *Jun, Egr1* are downregulated across all MGE sub-types, while *Fosb, Fos, Arx* are down regulated across all hippocampal MGEs, and *Satb1*, *Arnt2* are downregulated across all cortical MGEs. In addition, *Npas4*, an established early response TF activated upon neuronal activity and Ca^{2+} influx in MGE-derived interneurons (Spiegel et al., 2014), was downregulated in cortical NGFCs upon *Grin1*-ablation. Lastly, *Ostn* was recently established as an activity-regulated secreted factor (Ataman et al., 2016), and we observed *Ostn* to be downregulated specifically in cortical PV subtypes. Together, these changes are consistent with reduced neuronal activity in MGE subtypes upon *Grin1*-ablation, recapitulating previous reports indicating that NMDAR-antagonists can directly reduce the activity of GABAergic interneurons in adult mice (Homayoun and Moghaddam, 2007). The differential expressions of these activity-TFs also serve as ripe candidates to examine activity-dependent survival of specific interneuron subtypes in the juvenile brain. Interpreting the differential expressions of activity-dependent genes during scRNAseq has been challenging, particularly, when these genes could get activated by the very process involved in cell dissociation and sorting (Wu Y. E. et al., 2017). However, our use of activity-blockers and actinomycin-D throughout our MGE-*Grin1*^{wt} and MGE-*Grin1*$^{fl/fl}$ scRNAseq pipelines and independent validations via MGE-Ribotag-seq gives confidence that the differential expressions of activity-dependent TFs reflect biological relevance.

NMDAR Signaling in NGFCs

Among the MGE subtypes, the PV and SST interneurons are traditionally widely studied in comparison to the dendrite-targeting NGFC subtypes (that include the Ivy cells). In the present study we provide the first detailed molecular insight into the cortical and hippocampal NGFCs, subsequent to NMDAR ablation. We anticipated that these cell types could be particularly susceptible to loss of NMDARs, since we previously reported that NGFCs exhibit the most robust synaptic NMDAR conductances among the MGE subtypes (Matta et al., 2013). While our study was being corresponded, a recent study demonstrated the existence of deep layer neocortical NGFCs that continue to express Nkx2-1 in the postnatal mouse brain (Valero et al., 2021). In the present study we establish the existence of Nkx2-1-expressing MGE-derived interneurons in the juvenile mouse cortex and hippocampus through immunostaining. Moreover, we report that neocortical but not hippocampal Nkx2-1-expressing putative NGFC abundance is regulated by NMDAR-signaling. While we conducted the cell counting across the entire saggital section, we are confident of the robustness of our neocortical Nkx2-1 cell counts. However, since we missed the ventral hippocampus in our saggital brain sections, our quantitative cell counts from mid-dorsal hippocampal sections might have missed such an expansion in the hippocampus. We also identified many TFs (*Bcl11b, Id2*) and activity-TFs (*Npas4*) differentially expressed in these NGFCs after the loss of *Grin1*, and thus our dataset provides novel targets for examining activity-dependent survival of NGFCs. Finally, NGFCs exhibited dendritic arborization impairments subsequent to impaired NMDA signaling (De Marco García et al., 2015; Chittajallu et al., 2017). Indeed, we observe 49 genes among the DEGs

(**Supplementary Table 1**) that have established roles in regulating neuronal cytoskeleton and associated signaling. Therefore, our dataset is a robust repository for detailed examination of NGFC function by providing several candidates.

Developmental NMDAR Ablation in Interneurons and Schizophrenia

Impaired NMDAR function observed during human NMDAR gene mutations, and anti-NMDAR-encephalitis results in a wide range of neuropsychiatric disorders including autism spectrum disorders, intellectual disability, psychosis, epilepsy and associated comorbidities (Lakhan et al., 2013). While broadly aberrant NMDAR signaling in neurons is thought to underlie a wide range of these neurological disorders, an interneuron-centric developmental NMDAR aberration is emerging central to schizophrenia-related syndromes (Nakazawa and Sapkota, 2020). Indeed, in the present study, disease mapping of the DEGs using high-ranked SZDB-Sz and SFARI-As datasets indicate that many more DEGs map with the Sz than the As database. Moreover, proteins encoded by these disease relevant DEGs exist in physical and functional complexes with the ones encoded by DEGs that are not directly mapped to the Sz database. We used only stringent, high-ranked disease genes from the database that pass several disease-relevant criteria. However, there are other DEGs that still map to lower-ranked Sz and As datasets that are "non-annotated" in present study. While our study can be argued as an "extreme" case of NMDAR hypofunction in MGE-derived interneurons, it provides a starting point highlighting the centrality and broad range of interneuronal NMDAR-transcriptional pathways during development. Several studies implicate NMDAR-hypofunction specific to PV cell types as a central underlying feature of schizophrenia etiology (Lewis et al., 2005). However, the measurable NMDAR conductances within PV interneurons are relatively small in comparison to other MGE subtypes (Matta et al., 2013). In addition, $Pvalb^{Cre}$-driven recombination and *Grin1*-ablation were demonstrated only by 8 weeks (Carlén et al., 2011), indicating that a developmental requirement of NMDAR functions was not examined in these studies. Hence it is unsurprising that while NMDAR-ablation in $Pvalb^{Cre}$ lines produces other behavioral deficits unrelated to the Sz-like phenotypes (Korotkova et al., 2010; Bygrave et al., 2016), a developmental, but not adult-onset *Grin1*-ablation in $Ppp1r2^{Cre}$ line that targets a subset of PV interneurons among other subtypes, recapitulates core Sz-like behavioral phenotypes (Belforte et al., 2010). Emerging new mouse lines that provide genetic access into PV cells earlier than $Pvalb^{Cre}$ (Harris et al., 2014; Wamsley et al., 2018) could address the specific requirement of developmental *Grin1* function in PV interneurons. Lastly, NMDA signaling in non-PV interneuron subtypes are also known to drive robust dendritic inhibition in pyramidal neurons (Chittajallu et al., 2017; Ali et al., 2020).

Integrating these ideas and based on findings from the present study, we propose the following: *(i)* Despite a smaller NMDAR conductance in PV interneurons, we observe a robust transcriptional coupling via NMDARs, as observed by several distinct gene expression abnormalities in this cell type relevant to human Sz. Therefore, PV-expressed NMDARs primarily serve to regulate transcriptional coupling, mediating PV-subtype abundances. *(ii)* The developmental window for NMDAR loss of function is particularly important because, its transcriptional regulation maintains the correct synaptogenic and assembly cues, which when lost, lead to disease-causing impaired connectivity. Perhaps, in the $Grin1^{fl/fl}$: $Pvalb^{Cre}$ mouse line, the *Grin1*-ablation occurs only at a developmental window when synaptic connectivity is sufficiently complete, explaining why the animal model does not lead to profound Sz-like behavioral impairments (Bygrave et al., 2016). ***(iii)*** The dendrite targeting SST and NGFC interneurons also exhibit robust NMDAR signaling and transcriptional coupling. During aberrant NMDAR-transcriptional coupling, it is therefore likely that impaired dendritic connectivity and inhibition onto pyramidal neurons also contributes toward disease etiology. Therefore, our dataset provides credence to interneuronal subtype-specific granularity, connectivity and excitability, all playing combinatorial and mutually supporting roles during disease etiology. Taken together, our study presents a rich resource, laying the road map for systematic examination of NMDAR signaling in interneuron subtypes, by providing multiple molecular targets for examination in both normal and impaired circuits.

MATERIALS AND METHODS

Contact for Reagent and Resource Sharing

Further information and requests for resources and reagents should be directed to and reasonable requests will be fulfilled by the Lead Contact, Chris J. McBain.[1]

Animals

All experiments were conducted in accordance with animal protocols approved by the National Institutes of Health. MGE-derived interneuron-specific $Grin1^{fl/fl}$ line, and Ribotag crosses were conducted as indicated in **Figure 1-Supplement 1A** and **Figure 6-Supplement 1E**. Littermate MGE-$Grin1^{wt/wt}$ controls, and MGE-$Grin1^{fl/fl}$ male and female mice were used during this study. Mice were housed and bred in conventional vivarium with standard laboratory chow and water in standard animal cages under a 12hr circadian cycle. Genotyping of the mice were performed as indicated in the appropriate Jackson Laboratory mice catalog.

Single-Cell Dissociation and FACS

P18-20 juvenile $Nkx2\text{-}1^{Cre}$:$Grin1^{wt/wt}$:TdT^{+} and $Nkx2\text{-}1^{Cre}$:$Grin1^{fl/fl}$:TdT^{+} mice were used for single-cell sequencing experiments. All mice were deeply anesthetized with isoflurane and then rapidly decapitated. Brain dissection, slicing and FACS sorting were carried out as described (Tanaka et al., 2008; Harris et al., 2018; Muñoz-Manchado et al., 2018), with slight modifications. NMDG-HEPES–based solution

[1] mcbainc@mail.nih.gov

(Tanaka et al., 2008) was used in all steps to enable better recovery of the cells during FACS sorting and single-cell bar coding. Briefly, the brain sectioning solution contained NMDG-HEPES–based high-Mg^{2+} cutting solution contained 93 mM NMDG, 2.5 mM KCl, 1.2 mM NaH_2PO_4, 30 mM $NaHCO_3$, 20 mM HEPES, 25 mM glucose, 5 mM sodium ascorbate, 3 mM sodium pyruvate, 2 mM Thiourea, 10 mM $MgSO_4$*$7H_2O$, and 0.5 mM $CaCl_2$*$2H_2O$; it was adjusted to pH 7.4 with 12.1N HCl, an osmolarity of 300–310 mOsm, and carbogenated (mix of 95% O_2 and 5% CO_2) before use. This solution was chilled, and the process of sectioning were conducted on an ice-chamber in the vibratome.

3-4, *Nkx2-1*^{Cre}:*Grin1*$^{wt/wt}$:TdT^{+} or *Nkx2-1*^{Cre}:*Grin1*$^{fl/fl}$:TdT^{+} mice were processed on consecutive days for single-cell sequencing experiments. TdT negative animals were processed in parallel for initially setting FACS gate for the Tomato-channel. Across the replicates, 10X MGE-*Grin1*$^{wt/wt}$ and 6X MGE-*Grin1*$^{fl/fl}$ animals were used for the scRNAseq. Coronal slices containing frontal cortex and hippocampus (350 mM) were cut using VT-1000S vibratome (Leica Microsystems) in cold NMDG-HEPES–based high-Mg^{2+} cutting solution. Slices were recovered in the same solution at 20°C for 30 min during when, they were visually inspected under fluorescence microscope and micro dissected, all under constant carbogenation. The recovery and microdissection were conducted in the NMDG-HEPES high-Mg^{2+} solution supplemented with 0.5 μM tetrodotoxin (TTX), 50 μM DL -2-Amino-5-phosphonopentanoic acid (APV) and 10 μM Actinomycin-D (Act-D).

Cell dissociation was performed using the Worthington Papain Dissociation System according to manufacturer instructions with minor modifications. Briefly, single-cell suspensions of the micro dissected frontal cortices or hippocampus were prepared using sufficiently carbogenated dissociation solution (containing Papain, DNAse in Earle's Balanced Salt Solution, EBSS), supplemented with 1 μM TTX, 100 μM APV, and 20 μM Act-D. After a 60 min enzymatic digestion at 37°C, followed by gentle manual trituration with fire-polished Pasteur pipettes, the cell dissociates were centrifuged at 300 g for 5 min at 20°C, and the supernatants were discarded. The enzymatic digestion was quenched in the next step by the addition of ovomucoid protease inhibitor. Albumin density gradient was performed on the pellets, using a sufficiently carbogenated debris removal solution (containing albumin-ovomucoid inhibitor, DNAse in EBSS). The resulting cell pellets were resuspended in 1 ml FACS buffer containing 10% FBS, 10 U/μl of DNAse, 1 μM TTX, 100 μM APV, and 20 μM Act-D in a 50:50 mix of carbogenated EBSS: NMDG-HEPES–based cutting saline (with 1 mM $MgSO_4$*$7H_2O$, it is important to not use High-Mg^{2+} in the FACS buffer, as it interferes with the subsequent 10X scRNAseq reaction). Cells were placed in polystyrene tubes (Falcon 352235) on ice during the FACS.

For single cell sorting of TdT^{+} expressing cells by FACS, resuspended cell dissociates were filtered through 35 mm cell strainer (Falcon 352235) to remove cell clumps. The single cell suspensions were then incubated with 1 μg/ml DAPI and 1 μM DRAQ5 at 4°C for 5 min to label dead cells and live cells, respectively. Samples were analyzed for TdTomato expression and sorted using a MoFlo Astrios EQ high speed cell sorter (Beckman Coulter). TdT-negative cells were used as a control to set the thresholding FACS gate for the detection and sorting of the Ai14-TdTomato-expressing cells, and the same gate was then applied for all subsequent experiments. Flow data analysis and setting of sorting gates on live (DAPI-negative, DRAQ5-positive) and Ai14-TdTomato-expressing cells were carried out using Summit software V6.3.016900 (Beckman Coulter). Per sample/session, 20,000–40,000 individual cells were sorted into a FBS-precoated, Eppendorf LoBind Microcentrifuge tubes containing carbogenated 10 ml FACS buffer, that served as the starting material for 10X Genomics barcoding.

10X Genomics Chromium

The cells were inspected for viability, counted, and loaded on the 10X Genomics Chromium system, aiming to recover ∼5,000 cells per condition. 12 PCR cycles were conducted for cDNA amplification, and the subsequent library preparation and sequencing were carried out in accordance with the manufacturer recommendation (Chromium^{TM} Single Cell 3′ Library and Gel Bead Kit v2 and v3, 16 reactions). Sequencing of the libraries were performed on the Illumina HiSeq 2500 at the NICHD, Molecular Genomics Core facility. **Replicate 1** of the scRNAseq were performed using 10X v2 reaction from which, the cell estimates, mean reads per cell (raw), median genes per cell, respectively, are as follows Cortical WT: 1277, 149K, 4615; Cortical NULL: 181, 159K, 4826; Hippocampal WT: 2221, 92K, 2578; Hippocampal NULL: 404, 154K, 4903. **Replicate 2** of the scRNAseq were performed using 10X v3 reaction from which, the cell estimates, mean reads per cell (raw), median genes per cell, respectively, are as follows Cortical WT: 3851, 22.8K, 1536; Cortical NULL: 2898, 23.5K, 2759; Hippocampal WT: 4600, 23.6K, 850; Hippocampal NULL: 4436, 25.8K, 3143. Replicate 3 of the scRNAseq were performed using 10X v3 reaction from which, cell estimates, mean reads per cell (raw), median genes per cell respectively, are as follows Cortical WT: 3960, 24.8K, 2870; Hippocampal WT: 3159, 26.9K, 2956. Representative quality metrics from Replicate 2 are indicated in **Figure 1-Supplements 1B–E**. Demultiplexed samples were aligned to the mouse reference genome (mm10). The end definitions of genes were extended 4 k bp downstream (or halfway to the next feature if closer) and converted to mRNA counts using the Cell Ranger Version 2.1.1, provided by the manufacturer.

MGE-Ribotag-Seq

This assay was performed as recently described (Sanz et al., 2009; Mahadevan et al., 2020). Notably, *Nkx2.1*^{cre}: *Grin1*$^{fl/wt}$ were bred with Ribotag mice for > 10 generations to obtain homozygosity in *Rpl22*$^{HA/HA}$. Age-matched *Nkx2-1*^{Cre}: *Grin1*$^{wt/wt}$: *Rpl22*$^{HA/HA}$ or *Nkx2-1*^{Cre}: *Grin1*$^{fl/fl}$: *Rpl22*$^{HA/HA}$ littermates (2 males and 2 females per genotype) were utilized for the MGE-Ribotag-seq. RNAs bound with anti-HA immunoprecipitates and RNA from bulk tissue (input) were purified using RNeasy Plus Micro Kit and the quality of RNA were measured using RNA 6000 Pico kit and 2100 Bioanalyzer system. cDNA libraries were constructed from 250 pg RNA using the SMARTer Stranded Total RNA-Seq. Kit v2 only from samples

with RNA Integrity Numbers > 6. Sequencing of the libraries were performed on the Illumina HiSeq2500, at 50 million 2 × 100 bp paired-end reads per sample. ∼75% of reads were uniquely mapped to genomic features in the reference genome. Bioconductor package DESeq2 (Love et al., 2014) was used to identify differentially expressed genes (DEG). This package allows for statistical determination of DEGs using a negative binomial distribution model. The resulting values were then adjusted using the Benjamini and Hochberg's method for controlling the false discovery rate (FDR).

Data Processing, Analyses, Visualization, and Differential Expression Testing

Processing (load, align, merge, cluster, differential expression testing) and visualization of the scRNAseq datasets were performed with the R statistical programming environment (R Core Team, 2013) (v3.5.1) and Seurat package (Butler et al., 2018; Stuart et al., 2019) (v3.1.5, a development version of Seurat v3.1.5.9000 was used to generate violin plots in **Figures 2C**, **7B**, **Figure 7-Supplement 1**, and **Figure 2-Supplement 4A**). Data set preprocessing, comparison of WT- and NULL-Ai14 cells, canonical correlation analyses, and differential expression of genes (padj < 0.01) within the same cluster between WT- and NULL-Ai14 cells were performed according to default Seurat parameters, unless otherwise mentioned. Quality control filtering was performed by only including cells that had between 200 and 6,000 unique genes, and that had < 30% of reads from mitochondrial genes. While the WT replicates had no cells above 30% mitochondrial genes, only NULL replicates from both brain regions exhibited 7–12% of cells above this threshold. Suggestive of inherent biological impact of *Grin1*-ablation, we repeated the clustering and subsequent analyses without excluding any cells. These analyses did not alter the clustering or skew the gene list. Clustering was performed on the top 25 PCs using the function FindClusters() by applying the shared nearest neighbor modularity optimization with varying clustering resolution. A cluster resolution of 1.0 was determined to be biologically meaningful, that yielded all known MGE cardinal classes. Initial analyses were performed on the WT datasets separately (WT.alone), and similar set of analysis parameters were applied when the WT and NULL samples were merged (WT.NULL.integrated) for subsequent differential expression testing. Phylogenetic tree relating the "average" cell from each identity class based on a distance matrix constructed in gene expression space using the BuildClusterTree() function. Overall, we identified 27, and 33 clusters using this approach in the WT.alone, and WT.NULL.integrated assays, respectively. The WT.alone correspond to 11 MGE.*Gad1/Gad2* clusters (**Figure 1C**), while the WT.NULL.integrated assay correspond to 12 clusters (**Figure 2B**). We first searched for the top differential markers for each MGE subcluster using the FindAllMarkers() function. The genes thus identified for the integrated data is presented in **Supplementary Table 1B**. Determination of MGE and non-MGE identities are performed based on existing interneuron literature and other scRNAseq datasets (Tasic et al., 2016, 2018; Paul et al., 2017; Pelkey et al., 2017; Harris et al., 2018; Fishell and Kepecs, 2020). The labels from **Figures 1**, **2** are matched with the top gene markers identified by the FindAllMarkers() function and the similarly named clusters in **Figures 1**, **2** have the same identities. Lastly, for the integrated analyses and differential expression testing, we first merged the identities of the subclusters SST.1-SST.6 and TH.1 and relabeled as SST subset; PVALB.1-3 relabeled as PVALB subset; and NGFC.1-2 relabeled as the NGFC subset during subsequent analysis (**Figures 5–8**).

Differential gene expression testing was performed using the MAST package (Finak et al., 2015) within the FindMarkers function to identify the differentially expressed genes between two subclusters. MAST utilizes a hurdle model with normalized UMI as covariate to generate the differential fold changes and is known to result in underestimation of the magnitude of fold change (FC) (Ximerakis et al., 2019). Therefore, while applying a stringent false-discovery rate < 0.01, we determined the minimum FC based on the control gene *Grin1*, which is the target gene knocked out in MGE-derived interneuron cell types. Notably for *Grin1*, we had previously demonstrated that the NGFCs which carry maximum NMDAR component among MGEs, are devoid of NMDAR current at this comparable age (Chittajallu et al., 2017). In the present scRNAseq assay, we observe a logFC for *Grin1* ranging between −0.1 and −0.35 across both brain regions and all MGE subtypes. Therefore, we determined a minimum logFC in our DEGs as ± 0.1 to be meaningful. Previous studies have demonstrated the MAST approach for DEG testing to be powerful in determining subtle changes in highly transcribed genes, and among abundant populations, additional to underrepresenting changes among weakly transcribed genes (Finak et al., 2015; Ximerakis et al., 2019). Volcano plots and Heat maps for the DEG were generated using EnhancedVolcano package (Blighe et al., 2021) and Morpheus package (Broad Institute) within the R framework. UpSet plots were generated using the Intervene package s within the R framework. Associated scRNAseq source data, including sequencing reads and single cell expression matrices, is available from the Gene Expression Omnibus (GEO) under accession number GSE156201.

Pathway Analyses PPI Network Mapping and Disease Mapping

Ingenuity Pathway Analyses were conducted on the differentially expressed genes to generate the molecular functional annotation and to identify the biological pathways and disease pathways overrepresented. This tool was also used to annotate genes with their known cellular functional classes. Additional Gene Ontology mapping and KEGG analyses were conducted using ShinyGO (Ge et al., 2020). Protein-protein interaction (PPI) mapping datasets from a variety of curated databases were conducted as previously described (Mahadevan et al., 2017) using the Cytoscape platform (v3.8.0) (Smoot et al., 2011). Schizophrenia risk genes integrated from various sources including genome-wide association studies (GWAS), copy number variation (CNV), association and linkage studies, post-mortem human brain gene expression, expression

quantitative trait loci (eQTL) and encyclopedia of DNA elements (ENCODE), were downloaded from http://www.szdb.org/ (Wu Y. et al., 2017). Autism Spectrum Disorder risk genes integrated from various sources were downloaded from Simons Foundation https://gene.sfari.org/ (Simons Foundation, 2018). SZDB genes that had an integrated total score of 3-6 (1419 genes, 22% out of 6387) were considered "high-risk" for DEG mapping (**Supplementary Table 4A**). SFARI genes scored 1-2 with accounting for a high strength of evidence (392 genes, 42% out of 943), were considered "high-risk" for DEG mapping (**Supplementary Table 4B**).

Immunostaining

All solutions were freshly prepared and filtered using 0.22μm syringe filters for parallel treatments of wildtype and MGE-*Grin1*-null groups. Adult mice of postnatal day (PD) 25–30 were mice were deeply anesthetized with isoflurane and perfused transcardially with 1X phosphate buffer saline (PBS) and followed by the fixative 4% paraformaldehyde. The brains were post-fixed in the same fixative for overnight at 4°C for the immunostaining assays. Postfixed brains were serially dehydrated using 10%/20%/30% sucrose solutions at 4°C. Coronal or saggital sections (50 μm) were cut on a freezing microtome. Immunostaining was performed on free-floating sections. Tissue sections were permeabilized and blocked in 1 × PBS + 1% bovine serum albumin + 10% normal goat serum + 0.5% Triton X-100 (Carrier PB) at room temperature for 2 h, followed by incubation in primary antibodies, listed below, diluted with 1 × PBS + 1% bovine serum albumin + 1% normal goat serum + 0.1% Triton X-100 overnight at 4°C. Tissue sections were then incubated with secondary antibodies, listed below, diluted in Carrier Solution (1:1,000), and DAPI (1:2,000) at room temperature for 1–2 h and mounted on Superfrost glass slides, and coverslipped using Mowiol mounting medium and 1.5 mm cover glasses.

Antibodies

The following primary antibodies were used: mouse anti-PV (1:1,000; Sigma-Aldrich Cat# P3088, RRID: AB_477329), rat anti-SST (1:1,000; Millipore Cat# MAB354, RRID: AB_2255365), rabbit anti-Satb1 (1:1,000; Abcam Cat# ab109122, RRID: AB_10862207), rabbit anti-HA (Abcam, Cat#ab9110, RRID AB_307019), rabbit anti Nkx2-1 (1:500, Abcam:Cat#ab76013/Epitomics:Cat#2044-1, RRID: AB_1310784). Secondary antibodies were conjugated with Alexa Fluor dyes 488 or 633 (1:1,000; Thermo Fisher Scientific).

RNAscope HiPlex *in situ* Hybridization

All apparatus, dissection instruments for this assay were treated to maintain RNAse-free conditions. Brains from two sets of P20-25 littermates from both genotypes were rapidly dissected and rinsed in fresh ice-cold RNAse-free 1XPBS. Individual brains were placed into cryomolds and snap-frozen by dipping into isopentene:dry ice mix. Frozen brains were stored in −80°C. 15μm fresh frozen saggital sections were obtained using a RNAse-free cryostat, and sections serially mounted on RNAse-free Superfrost glass slides. After a series of pretreatments with 4% fresh PFA and dehydration using 50, 70, and 100% EtOH, the slides were processed for HiPlex assay according to ACDBio manufacturer's instructions within a week. A panel of HiPlex probes were utilized counterstained with DAPI (1:2,000), but only data from *Reln, Sst, Nos1* are presented in this study.

Image Acquisition and Analysis

Immunostaining

Mouse brains from 3 to 6 animals (2–4 sections per animal) were used for each condition, and section depth were matched between the genotypes for parallel immunostaining. Fluorescent images were captured using the 20X objective of a Nikon Widefield Fluorescence, Spinning Disk Confocal microscope. For all slices with immunostained or genetically reported signal, 50 μm thin sections were imaged using 20x/0.45 CFI Plan Apo objective (imaging settings: Numerical Aperture 0.75, bit depth 16-bit, Exposure 100 ms). 10–20 Confocal z-stacks were acquired at a depth of 2 μM, and were stitched using NIS Elements (Nikon) before importing them into Imaris software (Bitplane, version 9.6). Cell bodies were marked in Imaris software using the "Spots" function. *Nkx2.1*^{Cre} TdT^{+}, PV^{+}, SST^{+}, SATB1^{+}, NKX2-1^{+} cell bodies were detected using the automatic function, with a signal detection radius of 15 μm. The Imaris "Quality" filter was set above an empirically determined threshold to maximize the number of detected cells while minimizing observed false positives. SST + cell bodies were marked manually using the Imaris "Spots" function. ROI 3D borders around hippocampus or somatosensory cortex, drawn manually using the Imaris function "Surfaces." Spots were then split within each ROI using the Imaris function "Split Spots." Overlap of TdT^{+} cells with other markers (PV, SST, SATB1, NKX2-1) was addressed by filtering the TdT^{+} Spots above an empirically determined threshold intensity in the channel relative to the marker of interest. Each image with an automatic analysis by Imaris was checked by an expert and incorrectly identified cell bodies where refined if required. Total numbers of cell counts are normalized to the volume of the section imaged and normalized to the TdT cell numbers where applicable. In **Figure 2-Supplement 1**, **Figure 4**, **Figure 4-Supplement 1**, and **Figure 6E**, error bars reflect standard error of mean (SEM); Two-tailed unpaired *t*-test was performed using Prism8.

RNAscope-HiPlex

Mouse brains from 2 animals (3–5 sections per animal) were used for each condition, and section depth were matched between the genotypes for parallel HiPlex assay. Fluorescent images were captured using the 40X-oil objective of a Nikon Widefield Fluorescence, Spinning Disk Confocal microscope. All sections were imaged using 10x/0.45 CFI Plan Apo objective (imaging settings: Numerical Aperture 0.75, bit depth 16-bit, Exposure 100 ms). Confocal stacks were stitched using NIS Elements (Nikon) before importing them into Imaris software (Bit-plane, version 9.6). *Sst* + *Reln* + *Nos1* + RNA signals that contain DAPI were identified using "Spot" function as described above, and the overlap of *Sst* + spots with *Reln* + or *Nos1* + spots were identified by thresholding the signals of *Reln* or *Nos1,* respectively. Total numbers of cell counts are normalized

to the area of the thin section imaged. In **Figure 3**, error bars reflect standard error of mean (SEM); Two-tailed unpaired *t*-test was performed using Prism8.

DATA AVAILABILITY STATEMENT

scRNAseq source data are available from the Gene Expression Omnibus (GEO) under accession number GSE156201 (https://www.ncbi.nlm.nih.gov/geo/query/acc.cgi?acc=GSE156201).

ETHICS STATEMENT

All experiments were conducted in accordance with animal protocols approved by the National Institutes of Health.

AUTHOR CONTRIBUTIONS

VM and CJM conceived the project and wrote the manuscript. VM, TJP, RC, KAP, and CJM designed the experiments. DM performed FACS sorting and analysis. VM, YZ, and TJP performed 10X scRNAseq. VM performed Ribotag assays. VM, AM, CR, CE, and RD performed 10X scRNAseq bioinformatic analyses. VM, XY, and KAP conducted RNAscope, immunofluorescent staining, imaging, and analysis. CJM supervised the study. All authors edited the manuscript.

FUNDING

This work was supported by the *Eunice Kennedy Shriver* NICHD Intramural Award to CJM.

ACKNOWLEDGMENTS

We thank Steven L. Coon, Tianwei Li, and James R. Iben at the Molecular Genomics Core, NICHD, for RNA sequencing support. We thank Vincent Schram and Lynne Holtzclaw of the NICHD Microscopy and Imaging Core for imaging support, and we thank Carolina Bengtsson Gonzales for assistance with improving cell viability during dissociation and FACS. We also thank Steven Hunt and Daniel Abebe for assistance with animal colony maintenance.

SUPPLEMENTARY MATERIAL

The Supplementary Material for this article can be found online at: https://www.frontiersin.org/articles/10.3389/fnmol.2021.712609/full#supplementary-material

REFERENCES

Akgül, G., and McBain, C. J. (2020). AMPA receptor deletion in developing MGE-derived hippocampal interneurons causes a redistribution of excitatory synapses and attenuates postnatal network oscillatory activity. *Sci. Rep.* 10:1333.

Ali, F., Gerhard, D. M., Sweasy, K., Pothula, S., Pittenger, C., Duman, R. S., et al. (2020). Ketamine disinhibits dendrites and enhances calcium signals in prefrontal dendritic spines. *Nat. Commun.* 11:72.

Alvarez, R. J., Pafundo, D. E., Zold, C. L., and Belforte, J. E. (2020). Interneuron NMDA receptor ablation induces hippocampus-prefrontal cortex functional hypoconnectivity after adolescence in a mouse model of schizophrenia. *J. Neurosci.* 40, 3304–3317. doi: 10.1523/jneurosci.1897-19.2020

Andrews, W., Barber, M., Hernadez-Miranda, L. R., Xian, J., Rakic, S., Sundaresan, V., et al. (2008). The role of Slit-Robo signaling in the generation, migration and morphological differentiation of cortical interneurons. *Dev. Biol.* 313, 648–658. doi: 10.1016/j.ydbio.2007.10.052

Ataman, B., Boulting, G. L., Harmin, D. A., Yang, M. G., Baker-Salisbury, M., Yap, E.-L., et al. (2016). Evolution of Osteocrin as an activity-regulated factor in the primate brain. *Nature* 539:242. doi: 10.1038/nature20111

Belforte, J. E., Zsiros, V., Sklar, E. R., Jiang, Z., Yu, G., Li, Y., et al. (2010). Postnatal NMDA receptor ablation in corticolimbic interneurons confers schizophrenia-like phenotypes. *Nat. Neurosci.* 13, 76–83. doi: 10.1038/nn.2447

Blighe, K., Rana, S., and Lewis, M. (2021). *EnhancedVolcano: Publication-Ready Volcano Plots With Enhanced Colouring and Labeling*. R package version 1.10.0. Available online at: https://bioconductor.org/packages/release/bioc/html/EnhancedVolcano.html

Bortone, D., and Polleux, F. (2009). KCC2 expression promotes the termination of cortical interneuron migration in a voltage-sensitive calcium-dependent manner. *Neuron* 62, 53–71. doi: 10.1016/j.neuron.2009.01.034

Broad Institute. *Morpheus*. Available online at: https://software.broadinstitute.org/morpheus

Butler, A., Hoffman, P., Smibert, P., Papalexi, E., and Satija, R. (2018). Integrating single-cell transcriptomic data across different conditions, technologies, and species. *Nat. Biotechnol.* 36, 411–420. doi: 10.1038/nbt.4096

Butt, S. J. B., Sousa, V. H., Fuccillo, M. V., Hjerling-Leffler, J., Miyoshi, G., Kimura, S., et al. (2008). The requirement of Nkx2-1 in the temporal specification of cortical interneuron subtypes. *Neuron* 59, 722–732. doi: 10.1016/j.neuron.2008.07.031

Bygrave, A. M., Masiulis, S., Kullmann, D. M., Bannerman, D. M., and Kätzel, D. (2019). Gene-environment interaction in a conditional NMDAR-knockout model of schizophrenia. *Front. Behav. Neurosci.* 12:332. doi: 10.3389/fnbeh.2018.00332

Bygrave, A. M., Masiulis, S., Nicholson, E., Berkemann, M., Barkus, C., Sprengel, R., et al. (2016). Knockout of NMDA-receptors from parvalbumin interneurons sensitizes to schizophrenia-related deficits induced by MK-801. *Transl. Psychiatry* 6:e778. doi: 10.1038/tp.2016.44

Carlén, M., Meletis, K., Siegle, J., Cardin, J., Futai, K., Vierling-Claassen, D., et al. (2011). A critical role for NMDA receptors in parvalbumin interneurons for gamma rhythm induction and behavior. *Mol. Psychiatry.* 17, 537–548. doi: 10.1038/mp.2011.31

Chittajallu, R., Wester, J. C., Craig, M. T., Barksdale, E., Yuan, X. Q., Akgül, G., et al. (2017). Afferent specific role of NMDA receptors for the circuit integration of hippocampal neurogliaform cells. *Nat. Commun.* 8:152.

Close, J., Xu, H., De Marco Garcia, N., Batista-Brito, R., Rossignol, E., Rudy, B., et al. (2012). Satb1 is an activity-modulated transcription factor required for the terminal differentiation and connectivity of medial ganglionic eminence-derived cortical interneurons. *J. Neurosci.* 32, 17690–17705. doi: 10.1523/jneurosci.3583-12.2012

Cristino, A. S., Williams, S. M., Hawi, Z., An, J.-Y., Bellgrove, M. A., Schwartz, C. E., et al. (2014). Neurodevelopmental and neuropsychiatric disorders represent an interconnected molecular system. *Mol. Psychiatry.* 19, 294–301. doi: 10.1038/mp.2013.16

De Marco García, N. V., Karayannis, T., and Fishell, G. (2011). Neuronal activity is required for the development of specific cortical interneuron subtypes. *Nature* 472, 351–355. doi: 10.1038/nature09865

De Marco García, N. V., Priya, R., Tuncdemir, S. N., Fishell, G., and Karayannis, T. (2015). Sensory inputs control the integration of neurogliaform

interneurons into cortical circuits. *Nat. Neurosci.* 18, 393–401. doi: 10.1038/nn.3946

Dehorter, N., Ciceri, G., Bartolini, G., Lim, L., del Pino, I., and Marin, O. (2015). Tuning of fast-spiking interneuron properties by an activity-dependent transcriptional switch. *Science* 349, 1216–1220. doi: 10.1126/science.aab3415

Denaxa, M., Neves, G., Rabinowitz, A., Kemlo, S., Liodis, P., Burrone, J., et al. (2018). Modulation of apoptosis controls inhibitory interneuron number in the cortex. *Cell Rep.* 22, 1710–1721. doi: 10.1016/j.celrep.2018.01.064

Desfeux, A., El Ghazi, F., Jégou, S., Legros, H., Marret, S., Laudenbach, V., et al. (2010). Dual effect of glutamate on GABAergic interneuron survival during cerebral cortex development in mice neonates. *Cereb. Cortex.* 20, 1092–1108. doi: 10.1093/cercor/bhp181

Erburu, M., Muñoz-Cobo, I., Diaz-Perdigon, T., Mellini, P., Suzuki, T., Puerta, E., et al. (2017). SIRT2 inhibition modulate glutamate and serotonin systems in the prefrontal cortex and induces antidepressant-like action. *Neuropharmacology* 117, 195–208. doi: 10.1016/j.neuropharm.2017.01.033

Favuzzi, E., Deogracias, R., Marques-Smith, A., Maeso, P., Jezequel, J., Exposito-Alonso, D., et al. (2019). Distinct molecular programs regulate synapse specificity in cortical inhibitory circuits. *Science* 363, 413–417. doi: 10.1126/science.aau8977

Finak, G., McDavid, A., Yajima, M., Deng, J., Gersuk, V., Shalek, A. K., et al. (2015). MAST: a flexible statistical framework for assessing transcriptional changes and characterizing heterogeneity in single-cell RNA sequencing data. *Genome Biol.* 16:278. doi: 10.1186/s13059-015-0844-5

Fishell, G., and Kepecs, A. (2020). Interneuron types as attractors and controllers. *Annu. Rev. Neurosci.* 43, 1–30. doi: 10.1146/annurev-neuro-070918-050421

Gallo, N. B., Paul, A., and Van Aelst, L. (2020). Shedding light on chandelier cell development, connectivity, and contribution to neural disorders. *Trends Neurosci.* 43, 565–580. doi: 10.1016/j.tins.2020.05.003

Ge, S. X., Jung, D., and Yao, R. (2020). ShinyGO: a graphical gene-set enrichment tool for animals and plants. *Bioinformatics* 36, 2628–2629. doi: 10.1093/bioinformatics/btz931

Hanson, E., Armbruster, M., Lau, L. A., Sommer, M. E., Klaft, Z.-J., Swanger, S. A., et al. (2019). Tonic activation of GluN2C/GluN2D-containing NMDA receptors by ambient glutamate facilitates cortical interneuron maturation. *J. Neurosci.* 39, 3611–3626. doi: 10.1523/jneurosci.1392-18.2019

Harris, J. A., Hirokawa, K. E., Sorensen, S. A., Gu, H., Mills, M., Ng, L. L., et al. (2014). Anatomical characterization of Cre driver mice for neural circuit mapping and manipulation. *Front. Neural Circuits* 8:76. doi: 10.3389/fncir.2014.00076

Harris, K. D., Hochgerner, H., Skene, N. G., Magno, L., Katona, L., Bengtsson Gonzales, C., et al. (2018). Classes and continua of hippocampal CA1 inhibitory neurons revealed by single-cell transcriptomics. *PLoS Biol.* 16:e2006387. doi: 10.1371/journal.pbio.2006387

He, M., Tucciarone, J., Lee, S., Nigro, M. J., Kim, Y., Levine, J. M., et al. (2016). Strategies and tools for combinatorial targeting of GABAergic neurons in mouse cerebral cortex. *Neuron* 91, 1228–1243. doi: 10.1016/j.neuron.2016.08.021

Homayoun, H., and Moghaddam, B. (2007). NMDA receptor hypofunction produces opposite effects on prefrontal cortex interneurons and pyramidal neurons. *J. Neurosci.* 27, 11496–11500. doi: 10.1523/jneurosci.2213-07.2007

Hou, G., and Zhang, Z.-W. (2017). NMDA receptors regulate the development of neuronal intrinsic excitability through cell-autonomous mechanisms. *Front. Cell. Neurosci.* 11:353. doi: 10.3389/fncel.2017.00353

Kelsch, W., Li, Z., Eliava, M., Goengrich, C., and Monyer, H. (2012). GluN2B-containing NMDA receptors promote wiring of adult-born neurons into olfactory bulb circuits. *J. Neurosci.* 32, 12603–12611. doi: 10.1523/jneurosci.1459-12.2012

Komuro, H., and Rakic, P. (1992). Selective role of N-type calcium channels in neuronal migration. *Science* 257, 806–809. doi: 10.1126/science.1323145

Korotkova, T., Fuchs, E. C., Ponomarenko, A., von Engelhardt, J., and Monyer, H. (2010). NMDA receptor ablation on parvalbumin-positive interneurons impairs hippocampal synchrony, spatial representations, and working memory. *Neuron* 68, 557–569. doi: 10.1016/j.neuron.2010.09.017

Krienen, F. M., Goldman, M., Zhang, Q., del Rosario, R. C. H., Florio, M., Machold, R., et al. (2020). Innovations present in the primate interneuron repertoire. *Nature* 586, 262–269. doi: 10.1038/s41586-020-2781-z

Lakhan, S. E., Caro, M., and Hadzimichalis, N. (2013). NMDA receptor activity in neuropsychiatric disorders. *Front. Psychiatry* 4:52. doi: 10.3389/fpsyt.2013.00052

Laurie, D., and Seeburg, P. (1994). Regional and developmental heterogeneity in splicing of the rat brain NMDAR1 mRNA. *J. Neurosci.* 14, 3180–3194. doi: 10.1523/jneurosci.14-05-03180.1994

Le Magueresse, C., and Monyer, H. (2013). GABAergic interneurons shape the functional maturation of the cortex. *Neuron* 77, 388–405. doi: 10.1016/j.neuron.2013.01.011

Lewis, D. A., Hashimoto, T., and Volk, D. W. (2005). Cortical inhibitory neurons and schizophrenia. *Nat. Rev. Neurosci.* 6, 312–324. doi: 10.1038/nrn1648

Ling-Lin Pai, E., Chen, J., Fazel Darbandi, S., Cho, F. S., Chen, J., Chu, J. S., et al. (2020). Maf and Mafb control mouse pallial interneuron fate and maturation through neuropsychiatric disease gene regulation. *Elife* 9:e54903.

Love, M. I., Huber, W., and Anders, S. (2014). Moderated estimation of fold change and dispersion for RNA-seq data with DESeq2. *Genome Biol.* 15:550.

Mahadevan, V., Khademullah, C. S. S., Dargaei, Z., Chevrier, J., Uvarov, P., Kwan, J., et al. (2017). Native KCC2 interactome reveals PACSIN1 as a critical regulator of synaptic inhibition. *Elife* 6, 1–34.

Mahadevan, V., Peltekian, A., and McBain, C. J. (2020). Translatome analyses using conditional ribosomal tagging in GABAergic interneurons and other sparse cell types. *Curr. Protoc. Neurosci.* 92:e93.

Manent, J.-B. (2006). Glutamate acting on AMPA but not NMDA receptors modulates the migration of hippocampal interneurons. *J. Neurosci.* 26, 5901–5909. doi: 10.1523/jneurosci.1033-06.2006

Marín, O. (2012). Interneuron dysfunction in psychiatric disorders. *Nat. Rev. Neurosci.* 13, 107–120. doi: 10.1038/nrn3155

Marín, O., Yaron, A., Bagri, A., Tessier-Lavigne, M., and Rubenstein, J. L. R. (2001). Sorting of striatal and cortical interneurons regulated by semaphorin-neuropilin interactions. *Science* 293, 872–875. doi: 10.1126/science.1061891

Matta, J. A., Pelkey, K. A., Craig, M. T., Chittajallu, R., Jeffries, B. W., and McBain, C. J. (2013). Developmental origin dictates interneuron AMPA and NMDA receptor subunit composition and plasticity. *Nat. Neurosci.* 16, 1032–1041. doi: 10.1038/nn.3459

Mohn, A. R., Gainetdinov, R. R., Caron, M. G., and Koller, B. H. (1999). Mice with reduced NMDA receptor expression display behaviors related to schizophrenia. *Cell* 98, 427–436. doi: 10.1016/s0092-8674(00)81972-8

Monyer, H., Burnashev, N., Laurie, D. J., Sakmann, B., and Seeburg, P. H. (1994). Developmental and regional expression in the rat brain and functional properties of four NMDA receptors. *Neuron* 12, 529–540. doi: 10.1016/0896-6273(94)90210-0

Muñoz-Manchado, A. B., Gonzales, C. B., Zeisel, A., Munguba, H., Bekkouche, B., Skene, N. G., et al. (2018). Diversity of interneurons in the dorsal striatum revealed by single-cell RNA sequencing and patchseq. *Cell Rep.* 24, 2179–2190.e7.

Nakao, K., Jeevakumar, V., Jiang, S. Z., Fujita, Y., Diaz, N. B., Pretell Annan, C. A., et al. (2018). Schizophrenia-like dopamine release abnormalities in a mouse model of NMDA receptor hypofunction. *Schizophr. Bull.* 31:2018. doi: 10.1093/schbul/sby003

Nakazawa, K., Jeevakumar, V., and Nakao, K. (2017). Spatial and temporal boundaries of NMDA receptor hypofunction leading to schizophrenia. *NPJ Schizophr.* 3:7.

Nakazawa, K., and Sapkota, K. (2020). The origin of NMDA receptor hypofunction in schizophrenia. *Pharmacol. Ther.* 205:107426. doi: 10.1016/j.pharmthera.2019.107426

Nikouei, K., Muñoz-Manchado, A. B., and Hjerling-Leffler, J. (2016). BCL11B/CTIP2 is highly expressed in GABAergic interneurons of the mouse somatosensory cortex. *J. Chem. Neuroanat.* 71, 1–5. doi: 10.1016/j.jchemneu.2015.12.004

Nóbrega-Pereira, S., Kessaris, N., Du, T., Kimura, S., Anderson, S. A., and Marín, O. (2008). Postmitotic Nkx2-1 controls the migration of telencephalic interneurons by direct repression of guidance receptors. *Neuron* 59, 733–745. doi: 10.1016/j.neuron.2008.07.024

Pachnis, V., Achimastou, A., Lasrado, R., Garefalaki, A., Maes, T., Kalaitzidou, M., et al. (2012). Maturation-promoting activity of SATB1 in MGE-derived cortical interneurons. *Cell Rep.* 2, 1351–1362. doi: 10.1016/j.celrep.2012.10.003

Paul, A., Crow, M., Raudales, R., Gillis, J., and Huang, Z. J. (2017). Transcriptional architecture of synaptic communication delineates cortical GABAergic neuron identity. *Cell* 171, 522–539. doi: 10.1016/j.cell.2017.08.032

Pelkey, K. A., Chittajallu, R., Craig, M. T., Tricoire, L., Wester, J. C., and McBain, C. J. (2017). Hippocampal GABAergic inhibitory interneurons. *Physiol. Rev.* 97, 1619–1747. doi: 10.1152/physrev.00007.2017

Polleux, F., Whitford, K. L., Dijkhuizen, P. A., Vitalis, T., and Ghosh, A. (2002). Control of cortical interneuron migration by neurotrophins and PI3-kinase signaling. *Development* 129, 3147–3160. doi: 10.1242/dev.129.13.3147

Priya, R., Paredes, M. F., Karayannis, T., Yusuf, N., Liu, X., Jaglin, X., et al. (2018). activity regulates cell death within cortical interneurons through a calcineurin-dependent mechanism. *Cell Rep.* 22, 1695–1709. doi: 10.1016/j.celrep.2018.01.007

R Core Team. (2013). *R: A Language and Environment for Statistical Computing*. Vienna: R Foundation for Statistical Computing.

Rico, B., and Marín, O. (2011). Neuregulin signaling, cortical circuitry development and schizophrenia. *Curr. Opin. Genet. Dev.* 21, 262–270. doi: 10.1016/j.gde.2010.12.010

Sanz, E., Yang, L., Su, T., Morris, D. R., McKnight, G. S., and Amieux, P. S. (2009). Cell-type-specific isolation of ribosome-associated mRNA from complex tissues. *Proc. Natl. Acad. Sci. U.S.A.* 106, 13939–13944. doi: 10.1073/pnas.0907143106

Simons Foundation (2018). *SFARI Gene. Simons Found.* Available onlie at: https://gene.sfari.org/ (accessed May 11, 2020).

Smoot, M. E., Ono, K., Ruscheinski, J., Wang, P. L., and Ideker, T. (2011). Cytoscape 2.8: new features for data integration and network visualization. *Bioinformatics* 27, 431–432. doi: 10.1093/bioinformatics/btq675

Soria, J. M. (2002). Receptor-activated calcium signals in tangentially migrating cortical cells. *Cereb. Cortex* 12, 831–839. doi: 10.1093/cercor/12.8.831

Spiegel, I., Mardinly, A. R., Gabel, H. W., Bazinet, J. E., Couch, C. H., Tzeng, C. P., et al. (2014). Npas4 regulates excitatory-inhibitory balance within neural circuits through cell-type-specific gene programs. *Cell* 157, 1216–1229. doi: 10.1016/j.cell.2014.03.058

Stuart, T., Butler, A., Hoffman, P., Hafemeister, C., Papalexi, E., Mauck, W. M., et al. (2019). Comprehensive integration of single-cell data. *Cell* 177, 1888–1902.e21. doi: 10.1016/j.cell.2019.05.031

Tanaka, Y., Tanaka, Y., Furuta, T., Yanagawa, Y., and Kaneko, T. (2008). The effects of cutting solutions on the viability of GABAergic interneurons in cerebral cortical slices of adult mice. *J. Neurosci. Methods* 171, 118–125. doi: 10.1016/j.jneumeth.2008.02.021

Tasic, B., Menon, V., Nguyen, T. N. T., Kim, T. T. K., Jarsky, T., Yao, Z., et al. (2016). Adult mouse cortical cell taxonomy revealed by single cell transcriptomics. *Nat. Neurosci.* 19, 335–346. doi: 10.1038/nn.4216

Tasic, B., Yao, Z., Graybuck, L. T., Smith, K. A., Nguyen, T. N., Bertagnolli, D., et al. (2018). Shared and distinct transcriptomic cell types across neocortical areas. *Nature* 563, 72–78.

Tatard-Leitman, V. M., Jutzeler, C. R., Suh, J., Saunders, J. A., Billingslea, E. N., Morita, S., et al. (2015). Pyramidal cell selective ablation of N-methyl-D-aspartate receptor 1 causes increase in cellular and network excitability. *Biol. Psychiatry* 77, 556–568. doi: 10.1016/j.biopsych.2014.06.026

Tricoire, L., Pelkey, K. A., Daw, M. I., Sousa, V. H., Miyoshi, G., Jeffries, B., et al. (2010). Common origins of hippocampal Ivy and nitric oxide synthase expressing neurogliaform cells. *J. Neurosci.* 30, 2165–2176. doi: 10.1523/jneurosci.5123-09.2010

Tricoire, L., Pelkey, K. A., Erkkila, B. E., Jeffries, B. W., Yuan, X., and McBain, C. J. A. (2011). Blueprint for the spatiotemporal origins of mouse hippocampal interneuron diversity. *J. Neurosci.* 31, 10948–10970. doi: 10.1523/jneurosci.0323-11.2011

Valero, M., Viney, T. J., Machold, R., Mederos, S., Zutshi, I., Schuman, B., et al. (2021). Sleep down state-active ID2/Nkx2.1 interneurons in the neocortex. *Nat. Neurosci.* 24, 401–411. doi: 10.1038/s41593-021-00797-6

Wamsley, B., and Fishell, G. (2017). Genetic and activity-dependent mechanisms underlying interneuron diversity. *Nat. Rev. Neurosci.* 18, 299–309. doi: 10.1038/nrn.2017.30

Wamsley, B., Jaglin, X. H., Favuzzi, E., Quattrocolo, G., Nigro, M. J., Yusuf, N., et al. (2018). Rbfox1 mediates cell-type-specific splicing in cortical interneurons. *Neuron* 100, 846–859.e7.

Winterer, J., Lukacsovich, D., Que, L., Sartori, A. M., Luo, W., and Földy, C. (2019). Single−cell RNA−Seq characterization of anatomically identified OLM interneurons in different transgenic mouse lines. *Eur. J. Neurosci.* 50, 3750–3771. doi: 10.1111/ejn.14549

Wong, F. K., Bercsenyi, K., Sreenivasan, V., Portalés, A., Fernández-Otero, M., and Marín, O. (2018). Pyramidal cell regulation of interneuron survival sculpts cortical networks. *Nature* 557, 668–673. doi: 10.1038/s41586-018-0139-6

Wu, Y., Yao, Y. G., and Luo, X. J. (2017). A database for schizophrenia genetic research. *Schizophr. Bull.* 43, 459–471.

Wu, Y. E., Pan, L., Zuo, Y., Li, X., and Hong, W. (2017). Detecting activated cell populations using single-cell RNA-Seq. *Neuron* 96, 1–27.

Ximerakis, M., Lipnick, S. L., Innes, B. T., Simmons, S. K., Adiconis, X., Dionne, D., et al. (2019). Single-cell transcriptomic profiling of the aging mouse brain. *Nat. Neurosci.* 22, 1696–1708. doi: 10.1038/s41593-019-0491-3

Xu, Q., Tam, M., and Anderson, S. A. (2008). Fate mapping Nkx2.1-lineage cells in the mouse telencephalon. *J. Comp. Neurol.* 506, 16–29. doi: 10.1002/cne.21529

Yap, E. L., and Greenberg, M. E. (2018). Activity-regulated transcription: bridging the gap between neural activity and behavior. *Neuron* 100, 330–348. doi: 10.1016/j.neuron.2018.10.013

Yozu, M., Tabata, H., König, N., and Nakajima, K. (2007). Migratory behavior of presumptive interneurons is affected by AMPA receptor activation in slice cultures of embryonic mouse neocortex. *Dev. Neurosci.* 30, 105–116. doi: 10.1159/000109856

Zimmer, G., Garcez, P., Rudolph, J., Niehage, R., Weth, F., Lent, R., et al. (2008). Ephrin-A5 acts as a repulsive cue for migrating cortical interneurons. *Eur. J. Neurosci.* 28, 62–73. doi: 10.1111/j.1460-9568.2008.06320.x

Zoodsma, J. D., Chan, K., Bhandiwad, A. A., Golann, D. R., Liu, G., Syed, S. A., et al. (2020). A model to study NMDA receptors in early nervous system development. *J. Neurosci.* 40, 3631–3645. doi: 10.1523/jneurosci.3025-19.2020

Conflict of Interest: The authors declare that the research was conducted in the absence of any commercial or financial relationships that could be construed as a potential conflict of interest.

Publisher's Note: All claims expressed in this article are solely those of the authors and do not necessarily represent those of their affiliated organizations, or those of the publisher, the editors and the reviewers. Any product that may be evaluated in this article, or claim that may be made by its manufacturer, is not guaranteed or endorsed by the publisher.

frontiers in Molecular Neuroscience

ORIGINAL RESEARCH
published: 08 October 2021
doi: 10.3389/fnmol.2021.716675

Opposing Changes in Synaptic and Extrasynaptic N-Methyl-D-Aspartate Receptor Function in Response to Acute and Chronic Restraint Stress

*Yiu Chung Tse[1], Moushumi Nath[1,2], Amanda Larosa[1,2] and Tak Pan Wong[1,3]**

[1] Neuroscience Division, Douglas Research Centre, Montreal, QC, Canada, [2] Integrated Program in Neuroscience, McGill University, Montreal, QC, Canada, [3] Department of Psychiatry, McGill University, Montreal, QC, Canada

A pertinent mechanism by which stress impacts learning and memory is through stress-induced plastic changes in glutamatergic transmission in the hippocampus. For instance, acute stress has been shown to alter the expression, binding, and function of the ionotropic glutamate N-methyl-D-aspartate receptor (NMDAR). However, the consequences of chronic stress, which could lead to various stress-related brain disorders, on NMDAR function remain unclear. While most studies on NMDARs focused on these receptors in synapses (synaptic NMDARs or sNMDARs), emerging findings have revealed functional roles of NMDARs outside synapses (extrasynaptic NMDARs or exNMDARs) that are distinct from those of sNMDARs. Using a restraint stress paradigm in adult rats, the objective of the current study is to examine whether sNMDARs and exNMDARs in the hippocampus are differentially regulated by acute and chronic stress. We examined sNMDAR and exNMDAR function in dorsal CA1 hippocampal neurons from brain slices of adult rats that were acutely (1 episode) or chronically (21 daily episodes) stressed by restraint (30 min). We found that acute stress increases sNMDAR but suppresses exNMDAR function. Surprisingly, we only observed a reduction in exNMDAR function after chronic stress. Taken together, our findings suggest that sNMDARs and exNMDARs may be differentially regulated by acute and chronic stress. Most importantly, the observed suppression in exNMDAR function by both acute and chronic stress implies crucial but overlooked roles of hippocampal exNMDARs in stress-related disorders.

Keywords: brain slice, corticosterone, electrophysiology, hippocampus, synaptic plasticity

OPEN ACCESS

Edited by:
Argel Aguilar-Valles, Carleton University, Canada

Reviewed by:
John J. Woodward, Medical University of South Carolina, United States
Thomas J. Papouin, Washington University School of Medicine in St. Louis, United States

***Correspondence:**
Tak Pan Wong
takpan.wong@mcgill.ca

Specialty section:
This article was submitted to Molecular Signaling and Pathways, a section of the journal Frontiers in Molecular Neuroscience

Received: *29 May 2021*
Accepted: *16 September 2021*
Published: *08 October 2021*

Citation:
Tse YC, Nath M, Larosa A and Wong TP (2021) Opposing Changes in Synaptic and Extrasynaptic N-Methyl-D-Aspartate Receptor Function in Response to Acute and Chronic Restraint Stress. Front. Mol. Neurosci. 14:716675. doi: 10.3389/fnmol.2021.716675

INTRODUCTION

N-methyl-D-aspartate receptor (NMDAR) is an ionotropic glutamate receptor that mediates synaptic plasticity and neuronal fate (Hardingham and Bading, 2003; Lau and Zukin, 2007; Paoletti et al., 2013). NMDARs also play crucial roles in mediating the biological impacts of stress on the nervous system. For instance, the facilitating effect of acute stress on pain sensation (Alexander et al., 2009) and fear conditioning (Shors and Servatius, 1995; Shors and Mathew, 1998) can be

abolished by NMDAR antagonists. The atrophy and loss of spines on cortical and hippocampal neurons in stressed rodents can also be rescued by the blockade or the genetic knockdown of NMDARs (Magarinos and McEwen, 1995; Christian et al., 2011; Li N. et al., 2011; Martin and Wellman, 2011). The impact of stress on NMDAR expression and function has been extensively examined. Acute stress can increase the expression (Gore et al., 2000; Yamamoto et al., 2008; Yuen et al., 2012), binding (Krugers et al., 1993) and function of NMDARs (Yuen et al., 2009, 2011). The effect of chronic stress on NMDAR expression and function is less clear. Previous studies have revealed increased (Calabrese et al., 2012; Costa-Nunes et al., 2014; Pacheco et al., 2017), decreased (Pacheco et al., 2017) or stable (Schwendt and Jezova, 2000; Nasca et al., 2015) NMDAR expression in the hippocampus after chronic stress exposure. These somewhat conflicting findings may be due to differences in the type and duration of stressors used in these studies. Finally, only a few studies have examined the impact of chronic stress on NMDAR function (Karst and Joels, 2003; Yuen et al., 2012; Tse et al., 2019). Since chronic stress is associated with the pathogenesis of mood disorders (McEwen, 2003; Hammen, 2005), it is imperative to further examine if NMDAR function can also be regulated by chronic stress.

While our current understanding of the functional roles of NMDARs is based on studies of these receptors in synapses (sNMDARs), emerging findings have revealed functional roles for NMDARs that are located outside synapses (extrasynaptic NMDARs or exNMDARs). With high levels in the early postnatal age (Tovar and Westbrook, 1999), the proportion of exNMDAR decreases with development. However, close to 30% NMDARs in adult hippocampal slices remain extrasynaptic (Papouin et al., 2012). In addition to its substantial presence in the brain, exNMDARs can be physiologically activated through various means (for review, see Petralia et al., 2010; Papouin and Oliet, 2014). For instance, exNMDARs can be activated by glutamate from extracellular space (Le Meur et al., 2007), astrocytes (Carmignoto and Fellin, 2006; Nie et al., 2010) and repetitive stimulation of glutamate synapses (Suzuki et al., 2008). Back-propagating actional potentials also facilitate exNMDAR activation (Wu et al., 2012). Functional roles mediated by exNMDARs include neuronal synchrony (Fellin et al., 2004), synaptic computation (Oikonomou et al., 2012) and plasticity (Lu et al., 2001; Liu et al., 2013). These findings provide a more complete picture of exNMDAR physiology in addition to its contribution to neuronal death (Hardingham and Bading, 2010; Parsons and Raymond, 2014). Notably, these emerging functional roles of exNMDARs beg the question of whether these receptors are subjected to stress-related regulation.

Using a restraint stressor, the objective of this study is to examine the impact of acute and chronic stress on sNMDAR and exNMDAR functions in the hippocampal CA1 region, a region that is sensitive to stress and highly implicated in stress-related mood disorders (Brown et al., 1999; McEwen, 1999; Campbell and Macqueen, 2004; Duman and Monteggia, 2006). We found that exNMDAR function can be reduced by both acute and chronic stress.

MATERIALS AND METHODS

Animals

All care and use of animals were in accordance with the guidelines and policies of the Canadian Council on Animal Care and approved by the Facility Animal Care Committee of the Douglas Research Centre (DRC), McGill University (animal use protocol number 2010-5935). Adult (8–12-week old) male Sprague Dawley (SD) rats were obtained from *Charles River Laboratories*. They were housed in the DRC animal facility and maintained on a 12/12 light cycle with lights on at 08:00 AM. Food and water were available *ad libitum*. Rats were used for experiments after being housed in the animal facility for at least 1 week to reduce the influence of stress from transportation.

Stress Paradigm

Each episode of restraint stress was performed by putting a rat into a DecapiCone (*BrainTree Scientific*) for 30 min. For acute stress, rats were sacrificed 30 min after the end of one episode of restraint stress. For chronic stress, rats were restrained once daily for 21 days. Rats were sacrificed within a week after chronic stress (3.0 ± 0.4 days) for electrophysiological recording. Control rats for the acute stress and chronic stress experiments were handled daily for 1 and 21 days, respectively.

Brain Slice Preparation

Unless specified otherwise, all materials and chemicals were purchased from *Sigma Aldrich*. Rats were anesthetized with isoflurane (5%) and decapitated using a guillotine. Trunk blood was collected after decapitation in EDTA-containing tubes to prepare serum for CORT (corticosterone) ELISA (*Abcam*. ELISA was performed using manufacturer's procedures). Coronal brain slices were cut in a hyperosmotic, ice-cold and carbogenated (5% CO_2, 95% O_2) slice-cutting solution (in mM: 252 sucrose, 2.5 KCl, 4 $MgCl_2$, 0.1 $CaCl_2$, 1.25 KH_2PO_4, 26 $NaHCO_3$ and 10 glucose, ~360 mOsmol/L) using a vibrating blade microtome (*Leica*). Slices were then transferred to carbogenated artificial cerebrospinal fluid (aCSF; in mM: 125 NaCl, 2.5 KCl, 1 $MgCl_2$, 2 $CaCl_2$, 1.25 NaH_2PO_4, 26 $NaHCO_3$ and 25 glucose, ~310 mOsmol/L) at 32°C for 1 h, followed by room temperature incubation before recordings.

Electrophysiology

General Procedures

All recordings were performed in the dorsal hippocampal CA1 region at room temperature. Synaptic responses were evoked by stimulating the Schaffer collateral-commissural pathway through a tungsten bipolar electrode (*FHC*) using constant current pulses (0.08 ms) at 0.05 Hz. Electrophysiological data were amplified by the Multiclamp 700 B amplifier (*Molecular Devices*), digitized by the Digidata 1440 (*Molecular Devices*), and stored in a PC for offline analysis.

Field Excitatory Postsynaptic Potential

Recordings of evoked AMPA receptor (AMPAR)-mediated field excitatory postsynaptic potentials (fEPSPs) were performed with

an aCSF-containing glass pipette in the *stratum radiatum*. $GABA_A$ receptors ($GABA_ARs$) were blocked by bicuculline methobromide (10 μM) and picrotoxin (20 μM). To record NMDAR-mediated-fEPSP, we reduced the concentration of $MgCl_2$ in aCSF to 0.05 mM. AMPARs were blocked by DNQX (20 μM).

Excitatory Postsynaptic Current

Recordings of evoked excitatory postsynaptic currents (EPSCs) from CA1 pyramidal neurons were performed using a patch pipette containing (in mM) 110 Cs-gluconate, 17.5 CsCl, 2 $MgCl_2$, 0.5 EGTA, 10 HEPES (*Wisent Inc.*), 4 ATP, and 5 QX-314 (*Alomone Labs*), with the pH adjusted to 7.2 by CsOH (∼290 mOsmol/L). Only recordings with an access resistance lower than 20 MΩ were kept. We did not observe differences between the input resistance of CA1 neurons from different animal groups (control: 152.3 ± 6.4 MΩ; acute stress: 159.9 ± 7.0 MΩ; chronic stress: 162.1 ± 14.0 MΩ). The AMPAR- and NMDAR-mediated component of EPSCs were evoked while voltage clamping the membrane potential at –60 and + 40 mV, respectively. In EPSCs evoked at + 40 mV, the magnitude of EPSC at 150 ms post-stimulation was used to represent the NMDAR component, since the AMPAR component has returned to baseline at this time point (see **Figure 1A**). To examine exNMDAR currents, EPSCs mediated by sNMDARs were recorded while voltage clamping the neuron at + 40 mV in the presence of DNQX to block the AMPAR component and maintained at around 100 pA. After a > 90% blockade of sNMDAR currents by a 30-min-long application of MK801 (40 μM, EPSCs were evoked at 0.1 Hz during MK801 blockade), exNMDAR currents were induced by (i) the blockade of glutamate transporters by DL-threo-β-benzyloxyaspartic acid (TBOA, 20 μM; Milnerwood et al., 2010; Li S. et al., 2011), or (ii) a brief 10-pulse tetanus at 100 Hz as previously described (Luscher et al., 1998).

Statistical Analysis

All data are presented as mean ± SEM. Statistical analyses were performed using JMP 13. Normality of data was examined using the Shapiro-Wilk test. Student's *t*-tests were used for comparisons of normally distributed data between two groups. Two-way ANOVA was also used to compare the effect of stress on the input/output relationship of evoked fEPSPs. For data that are not normally distributed, Mann-Whitney tests were used for comparisons between two groups and Kruskal-Wallis tests and *post hoc* Wilcoxon tests were used for comparing data from three groups. Statistical significance (2-tailed) was set at $p < 0.05$.

RESULTS

Acute Stress Enhances sNMDAR and Suppresses exNMDAR Functions

We first examined the effect of acute restraint stress on sNMDAR and exNMDAR functions in the hippocampal CA1 region of control and acutely stressed adult male rats. Acute restraint stress significantly increased CORT blood levels [CORT levels in controls: 48.5 ± 16.8 ng/ml; CORT levels in stressed rats: 495.4 ± 36.8 ng/ml; $t(4) = 13.5$; $p = 1.73E-04$]. In the presence of AMPAR and $GABA_AR$ antagonists, we isolated evoked fEPSPs that were mediated by sNMDARs (**Figure 2A**). To compare fEPSP between slices, we examined the relationship between the amplitude of fiber volley (*fv*; input), which represents the depolarization of synaptic inputs, and the slope of fEPSP (output). We found that acute stress significantly increases the input/output relationship of NMDAR-mediated fEPSPs when compared to controls {two-way ANOVA, stress—[$F(1, 10) = 5.16$, $p = 0.046$]; *fv* amplitudes (as repeated measures)—[$F(4, 40) = 142.5$, $p = 4.24E-23$]; stress × *fv* amplitudes—[$F(4, 40) = 3.46$, $p = 0.016$]}. However, acute stress did not affect the input/output relationship of AMPAR-mediated fEPSPs when compared to controls {**Figure 2B**; two-way ANOVA, stress—[$F(1, 23) = 0.01$, $p = 0.918$]; *fv* amplitudes (as repeated measures)—[$F(4, 92) = 55.2$, $p = 1.21E-23$]; stress × *fv* amplitudes—[$F(4, 92) = 0.58$, $p = 0.681$]}.

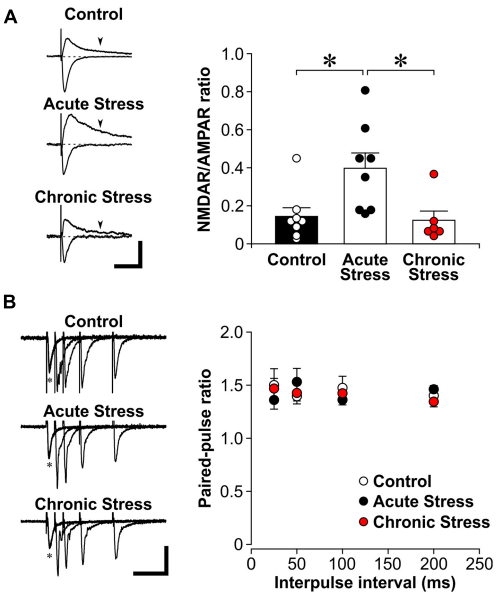

FIGURE 1 | Acute stress enhances the NMDAR/AMPAR ratio. **(A)** *Left*: Representative traces of evoked excitatory postsynaptic currents (EPSCs) while voltage clamping hippocampal CA1 neurons at either –60 mV (inward currents) or +40 mV (outward currents). The AMPAR component is represented by the EPSC amplitude recorded at –60 mV. The NMDAR component is estimated by the magnitude of +40 current at 150 ms post stimulation (arrowheads), when the AMPAR component has returned to baseline (dotted line). Scale bar = 100 pA, 100 ms. *Right:* Histograms of NMDAR/AMPAR ratio in EPSCs recorded from control (8 recordings, 4 rats), acutely stressed rats (8 recordings, 4 rats) and chronically stressed rats (6 recordings, 3 rats). Mean ± SEM. *$p < 0.05$, *post hoc* Wilcoxon test after Kruskal-Wallis test. **(B)** *Left:* Representative traces of paired-pulse stimulation of evoked field excitatory postsynaptic potential (fEPSP) at different interpulse intervals (*represent the first pulse, followed by the second pulse at 25, 50, 100, or 200 ms in overlapping traces) that were recorded from brain slices of control, acutely stressed and chronically stressed rats. Scale bar = 0.2 mV, 100 ms. *Right:* Scatter plots show the paired-pulse ratios of fEPSP slope in control (12 recordings, 5 rats), acutely stressed rats (12 recordings, 5 rats) and chronically stressed rats (15 recordings, 4 rats). Mean ± SEM.

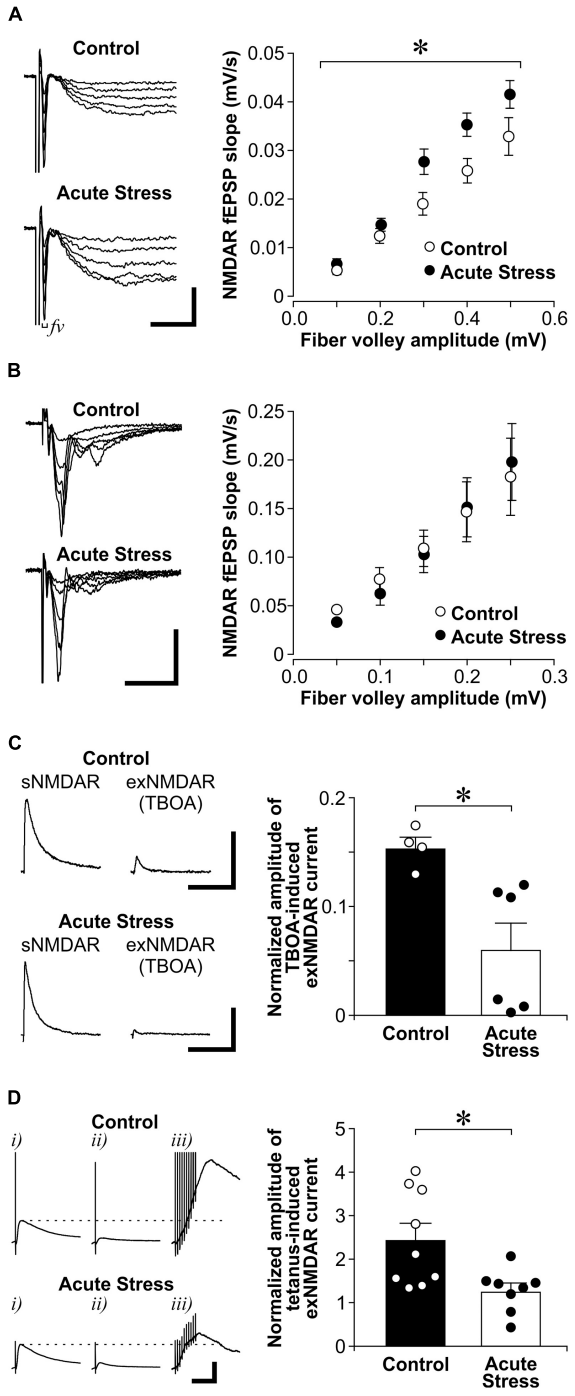

FIGURE 2 | Acute stress enhances sNMDAR and reduces exNMDAR functions. **(A)** *Left*: Representative traces of evoked NMDAR-mediated evoked field excitatory postsynaptic potential (fEPSP) that were recorded from brain slices of control and acutely stressed rats (restrained for 30 min). Scale bar = 0.2 mV, 10 ms. *Right:* Scatter plots show the relationship between fiber volley (*fv*) amplitude and the slope of NMDAR fEPSP in control (6 recordings, 3 rats) and stressed rats (6 recordings, 3 rats). Mean ± SEM. *$p < 0.05$, interaction between the effect of stress and fiber volley amplitudes [repeated measures ANOVA, $F(4, 40) = 3.46$]. **(B)** *Left:* Representative traces of evoked AMPAR-mediated fEPSP that were recorded from brain slices of control and *(Continued)*

FIGURE 2 | (Continued)
acutely stressed rats. Scale bar = 0.4 mV, 25 ms. *Right:* Scatter plots show the relationship between fiber volley amplitude and the slope of AMPAR fEPSP in control (15 recordings, 4 rats) and stressed rats (10 recordings, 3 rats). Mean ± SEM. **(C)** *Left:* Representative traces of sNMDAR and TBOA-induced exNMDAR currents that were recorded from brain slices of control and acutely stressed rats. Scale bar = 50 pA, 500 ms. *Right:* Histogram shows the normalized amplitude of exNMDAR currents recorded from slices of control (4 recordings, 4 rats) and acutely stressed rats (6 recordings, 3 rats). Mean ± SEM. *$p < 0.05$, Student's *t*-test. **(D)** *Left:* Representative traces of evoked NMDAR mediated currents that were recorded from brain slices of control and acutely stressed rats before (*i*) and after a 30 min-long MK801 blockade (*ii*). Five minutes after washing out MK801, exNMDAR currents were induced by a brief tetanus stimulation [*iii*, 10-pulse (100 Hz)]. Dotted lines represent the level of sNMDAR current before MK801 blockade. Scale bar = 100 pA, 100 ms. *Right:* Histograms of normalized amplitude of exNMDAR currents recorded from brain slices of control (9 recordings, 9 rats) or acutely stressed rats (8 recordings, 5 rats). Mean ± SEM. *$p < 0.05$, Student's *t*-test.

We next examined the impact of acute stress on exNMDAR function (**Figure 2C**). To isolate exNMDAR-mediated currents, we first blocked evoked sNMDAR currents by MK801. MK801 produced a sustained use-dependent blockade of NMDARs (Tse et al., 2019). We next induced a spillover of synaptic glutamate release by blocking glutamate transporter with TBOA to activate exNMDARs (Milnerwood et al., 2010; Li S. et al., 2011). Compared to controls, we found that acute stress reduces the normalized amplitude of exNMDAR currents [normalized by the amplitude of sNMDAR currents before MK801 blockade from the same cell; $t(8) = 3.06$, $p = 0.016$]. Apart from using TBOA, we used a brief tetanus (Luscher et al., 1998; 10-pulse at 100 Hz) to increase extracellular glutamate levels after MK801 blockade of sNMDAR to activate exNMDARs in another set of slices from stressed and control rats. Like the TBOA findings, we found that the amplitude of exNMDAR current in slices from acutely stressed rats is significantly smaller than that in slices from control rats (**Figure 2D**; U = 11, $p = 0.018$). These findings suggest that acute stress enhances sNMDAR and reduces exNMDAR function in dorsal hippocampal CA1 neurons.

Acute Stress Reduces Ambient Glutamate-Mediated exNMDAR Currents

Since exNMDAR currents induced by TBOA and a brief tetanus after MK801 blockade was normalized by sNMDAR currents, the reduced exNMDAR function may also be due to the enhanced sNMDAR function caused by stress. To address this limitation, we used another method to directly measure exNMDAR function. exNMDARs can be activated by ambient levels of glutamate in brain slices, which can be revealed by the shift in whole-cell holding currents caused by NMDAR antagonists such as MK801 or APV (Le Meur et al., 2007; Papouin et al., 2012). To show that the shift in whole-cell currents caused by a NMDAR antagonist does not affect sNMDAR function, we recorded sNMDAR-mediated EPSCs from CA1 pyramidal neurons before and after perfusing slices with MK801. Although MK801 treatment caused a shift in whole-cell currents, it did not affect the amplitude of sNMDAR EPSCs (**Figures 3A,B**). Next, we

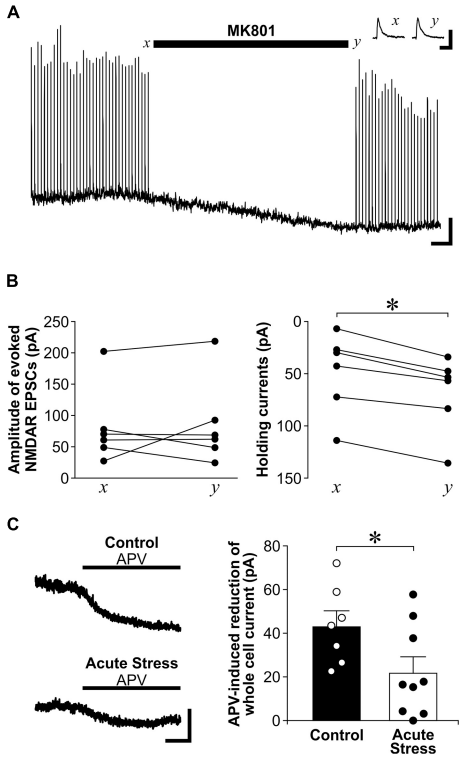

FIGURE 3 | Acute stress reduces exNMDAR currents mediated by ambient glutamate. **(A)** Representative trace shows the effect of MK801 on evoked NMDAR-mediated EPSCs and whole-cell holding currents recorded from a CA1 neuron. Stimulations for evoking EPSCs were stopped at *x* and during MK801 application. MK801 reduced whole-cell holding currents. However, the amplitudes of evoked NMDAR-mediated EPSCs were not affected when stimulation was resumed at time *y*. The reduction of EPSC amplitude near the end of the trace was likely due to residual levels of MK801 in the recording chamber. Scale bar = 40 pA, 1 min. Inset: traces of sNMDAR before (*x*) and after (*y*) MK801 application. Scale bar = 200 pA, 200 ms. **(B)** Line plots show changes in evoked NMDAR-mediated EPSCs (*left*; 6 recordings, 3 rats) and whole-cell holding currents (*right*; 6 recordings, 3 rats) before (*x*) and after MK801 application (*y*). $^*p < 0.05$, paired Student's *t*-test; current at time *x* vs. time *y*. **(C)** *Left:* Representative traces of APV (50 μM) -induced blockade of whole-cell current of CA1 neurons in brain slices from control or acutely stressed rats. Scale bar = 40 pA, 1 min. *Right:* Histograms of the APV-induced blockade of whole-cell currents recorded from hippocampal slices of control (7 recordings, 3 rats) or acutely stressed rats (9 recordings, 4 rats). Mean ± SEM. $^*p < 0.05$, Student's *t*-test.

compared the shift in whole-cell currents caused by APV between control and acutely stressed rats. Compared to slices from control rats, we found that APV-sensitive holding currents recorded from CA1 pyramidal neurons are significantly smaller in slices from acutely stressed rats [**Figure 3C**; $t(14) = 2.17$, $p = 0.048$]. These findings corroborated data from the spillover experiments to show that acute stress reduces exNMDAR function.

Chronic Stress Suppresses exNMDAR Functions

After being stressed by restraint daily for 21 days, chronically stressed rats displayed lower body weight gain over 21 days of stress than control rats [**Figure 4A**; $t(13) = 3.65$, $p = 0.003$]. In addition, we found higher plasma CORT levels in chronically stressed rats when compared to non-stressed controls rats [$t(13) = 2.74$, $p = 0.017$]. Surprisingly, we found no difference in sNMDAR function between chronically stressed and control rats {**Figure 4B**; two-way ANOVA, stress—[$F(1, 13) = 0.291$, $p = 0.599$]; *fv* amplitudes (as repeated measures)—[$F(4, 52) = 125.0$, $p = 5.24E\text{-}26$]; stress × *fv* amplitudes—[$F(4, 52) = 0.546$, $p = 0.703$]}. Chronic stress also did not affect the input/output function of AMPAR-mediated fEPSP {**Figure 4C**; two-way ANOVA, stress—[$F(1, 21) = 0.113$, $p = 0.741$]; *fv* amplitudes (as repeated measures)—[$F(4, 84) = 32.2$, $p = 2.94E\text{-}17$]; stress × *fv* amplitudes—[$F(4, 84) = 0.733$, $p = 0.572$]}. Nonetheless, chronically stressed rats displayed lower TBOA-induced exNMDAR currents than control rats {**Figure 4D**, [$t(10) = 2.69$, $p = 0.023$]}. In addition, chronically stressed rats also showed lower APV-induced shifts in holding currents of CA1 neurons than control rats {**Figure 4E**, [$t(8) = 3.31$, $p = 0.011$]}. Taken together, chronic stress reduced exNMDAR function.

To further show the specific impact of acute stress on sNMDAR function, we performed whole-cell recordings of the NMDAR/AMPAR ratio of evoked EPSC. We found that acute stress significantly increased the NMDAR/AMPAR ratio of evoked EPSC when compared to control and chronic stress (**Figure 1A**; Kruskal-Wallis test, $Z = 9.75$, $p = 0.008$; *post hoc* Wilcoxon tests: control vs. acute stress: $p = 0.010$; acute stress vs. chronic stress: $p = 0.012$; control vs. chronic stress: $p = 0.478$).

Acute and Chronic Stress Do Not Affect Presynaptic Glutamate Release

High presynaptic glutamate release might recruit exNMDARs during MK801 blockade and result in the reduced exNMDAR currents we observed in slices from stressed rats. If acute or chronic stress enhances presynaptic glutamate release, we expect MK801 would need a shorter time to block sNMDAR currents. However, comparing the time for blocking 50% of sNMDAR currents by MK801 between slices from control and acutely stressed rats (control: 10.2 ± 1.4 min; acute stress: 9.2 ± 1.0 min; [$t(10) = 0.58$; $p = 0.578$]), or between control and chronically stressed rats (control: 9.8 ± 0.7 min; chronic stress: 9.0 ± 1.1 min; [$t(10) = 0.60$; $p = 0.562$]), revealed no differences. We also compared the paired-pulse ratios of fEPSP at different interpulse intervals (25–200 ms) in slices from control and stressed rats. We found no differences in paired-pulse facilitation between the 3 groups {**Figure 1B**; two-way ANOVA, animal groups—[$F(2, 34) = 0.370$, $p = 0.694$]; interpulse interval (as repeated measures)—[$F(3, 102) = 1.6$, $p = 0.187$]; animal groups × interpulse interval—[$F(6, 102) = 0.814$, $p = 0.561$]}. Together, these findings suggest that the impact of stress on exNMDAR function is not related to changes in presynaptic glutamate release.

DISCUSSION

Stress-induced plasticity of NMDAR function depends on stress duration and the locations of these receptors. We show in this study that acute stress enhanced sNMDAR and reduced

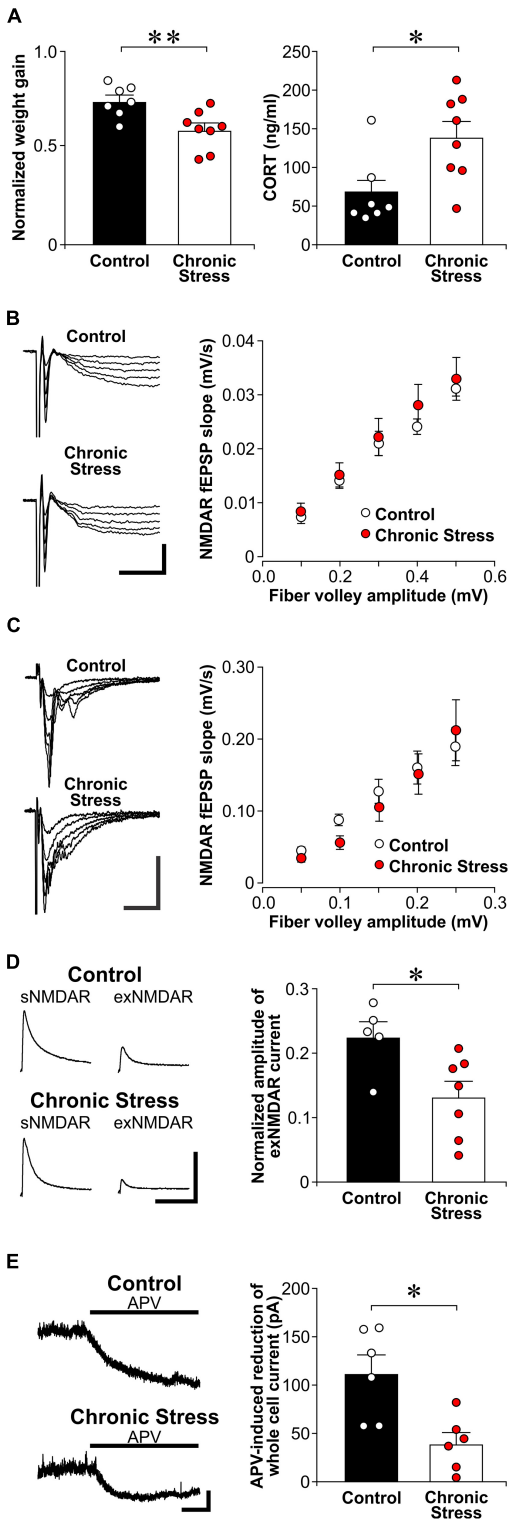

FIGURE 4 | Chronic stress reduces exNMDAR functions. **(A)** *Left:* Histograms of normalized weight gain of control (n = 7) and chronically stressed rats (n = 8) in 21 days. *Right:* Histograms of CORT levels in trunk blood in control (n = 7) and chronically stressed rats (n = 8) collected right before brain slice preparation. Stressed rats were sacrificed 7 days within the end of chronic restraint stress. Mean ± SEM. *p < 0.05, **p < 0.01, Student's t-test. **(B)** *Left:* Representative traces of evoked NMDAR-mediated field excitatory postsynaptic potential (fEPSP) that were recorded from brain slices of control and chronically stressed rats. Scale bar = 0.2 mV, 40 ms. *Right:* Scatter plots show the relationship between fiber volley amplitude and the slope of NMDAR fEPSP in control (7 recordings, 4 rats) and stressed rats (8 recordings, 4 rats). Mean ± SEM. **(C)** *Left:* Representative traces of evoked AMPAR-mediated fEPSP that were recorded from brain slices of control and chronically stressed rats. Scale bar = 0.4 mV, 25 ms. *Right:* Scatter plots show the relationship between fiber volley amplitude and the slope of AMPAR fEPSP in control (10 recordings, 4 rats) and stressed rats (13 recordings, 4 rats). Mean ± SEM. **(D)** *Left:* Representative traces of sNMDAR and TBOA-induced exNMDAR currents from brain slices of control or chronically stressed rats. Scale bar = 50 pA, 500 ms. *Right:* Histogram shows the normalized amplitude of exNMDAR currents recorded from brain slices of control (5 recordings, 4 rats) and chronically stressed rats (7 recordings, 6 rats). Mean ± SEM. *p < 0.05, Student's t-test. **(E)** *Left:* Representative traces of APV (50 μM) -induced blockade of whole-cell current of CA1 neurons in brain slices from control and chronically stressed mice. Scale bar = 40 pA, 1 min. *Right:* Histograms of the APV-induced blockade of whole-cell currents recorded from control (6 recordings, 3 rats) and chronically stressed mice (6 recordings, 3 rats). Mean ± SEM. *p < 0.05, Student's t-test.

exNMDAR functions. Interestingly, reduced exNMDAR function was also induced by chronic stress. Apart from sNMDARs (Yuen et al., 2009; Tse et al., 2011), we reveal in this study that exNMDARs are highly susceptible to stress-induced regulation.

Our findings are in parallel to previous findings that while acute stress exposure increases sNMDAR function, this increase may be transient and may not be sustained by repeated exposure to the same stressor. In the prefrontal cortex (PFC), both acute restraint and forced swim stress have been shown to increase postsynaptic AMPAR and NMDAR responses (Yuen et al., 2009, 2012). However, recording these postsynaptic responses from rats that were stressed by a similar restraint stressor daily revealed a decrease in synaptic AMPAR and NMDAR function after 7 days when compared to controls (Yuen et al., 2012). In the same study, 7-day restraint stress did not affect AMPAR function in the CA1. Finally, both synaptic AMPAR and NMDAR responses recorded from granule cells of the dentate gyrus were not affected in rats that have received 21 daily episodes of chronic unpredictable stress (Karst and Joels, 2003). Since there was a mean delay of 3 days between the end of chronic stress and electrophysiology recording, we cannot rule out the possibility that sNMDAR was enhanced immediately after chronic stress but returned to baseline when we sacrificed the animals. Even if sNMDAR function is transiently increased after chronic stress, this change is unlike the persistent decrease in exNMDAR function.

We found that exNMDAR function was reduced by both acute and chronic restraint stress. Although glutamate spillover caused by either a brief tetanus or the blockade of glutamate transporters has been used to estimate exNMDAR function, these indirect methods have limitations. To compare exNMDAR function between slices, exNMDAR function was normalized by sNMDAR currents from the same slice in the current study. The increase in sNMDAR function caused by acute stress could be a factor that may lead to a decrease in normalized exNMDAR function. The more direct method of estimating

exNMDAR function by using the blockade of exNMDAR-mediated whole-cell currents was used to address this limitation (Le Meur et al., 2007; Yao et al., 2018). The spillover method may also target a specific population of exNMDARs. In **Figure 3**, we found that the MK801 treatment we used to block sNMDARs could block exNMDARs that are activated by ambient glutamate. This finding suggests that the spillover approach recruits a different population of exNMDARs (also called perisynaptic NMDARs) (Mitani and Komiyama, 2018) that are not sensitive to ambient glutamate. Despite these limitations, we found that both acute and chronic stress reduce exNMDAR currents that are sensitive to ambient glutamate. In addition, chronic stress reduced TBOA- and tetanus-induced exNMDAR currents without affecting sNMDAR function. Together, our findings suggest that exNMDARs are reduced by both acute and chronic stress.

Mechanisms underlying the reduction of exNMDAR function after stress remains to be determined. After acute stress, the reduction of exNMDARs may be due to surface trafficking of these receptors to synapses for enhancing sNMDAR function (e.g., see Tovar and Westbrook, 2002; Groc et al., 2006). Nonetheless, how a reduction of exNMDARs was maintained when sNMDAR function is no longer enhanced after chronic stress is not clear. Since the expression of glutamate transporter can be reduced by chronic stress (Liu et al., 2016, 2017; Zhu et al., 2017), the increase in ambient glutamate after a reduction in transporter function may downregulate exNMDAR expression, which are more sensitive to ambient glutamate than sNMDARs. The loss of astrocytes, a suggested source of glutamate for activating exNMDARs (Carmignoto and Fellin, 2006), in the stressed brain (Czeh et al., 2006) could also contribute to reduced exNMDAR function.

A loss of exNMDAR function could contribute to the impact of chronic stress on hippocampal function. Since exNMDARs mediate NMDAR spikes (Suzuki et al., 2008; Oikonomou et al., 2012) that amplify synaptic signals (Harris and Pettit, 2008) and enhance neuronal excitability (Sah et al., 1989; Oikonomou et al., 2012), reduced exNMDAR function could contribute to the negative impact of chronic stress on rats' performance in spatial working and reference memory tasks (Luine et al., 1994; Henningsen et al., 2009; Veena et al., 2009). However, not all hippocampus-related cognitive functions are impaired by chronic stress. For instance, contextual fear conditioning is enhanced in chronically stressed rats (Conrad et al., 1999; Sandi et al., 2001). Given that exNMDARs are associated with forgetting mechanisms such as long-term depression (Liu et al., 2013), reduction in exNMDARs may be related to the enhanced encoding of aversive information in stressed mice. Recently, we have shown that mice that are susceptible to a chronic social defeat stressor show enhanced negative memory engrams formation in the hippocampal CA1 region (Zhang et al., 2019). In addition, we observed a reduction of exNMDAR function in this hippocampal region of mice that are susceptible, but not resilient to this stressor (Tse et al., 2019). These findings suggest that the enhanced encoding of aversive information could be related to a reduction in exNMDARs. Further studies could investigate if enhancing exNMDAR function, for example using drug-coating nanoparticles that are too big to enter synaptic cleft (Savchenko et al., 2016; Tse et al., 2019; Valente et al., 2020), will ameliorate the enhancement of aversive memory in stressed rats.

CONCLUSION

In conclusion, we show that apart from sNMDAR function, exNMDAR function can be modulated by both acute and chronic stress. Given the emerging functional roles of exNMDARs, changes in exNMDAR function could be related to the pathogenesis of stress-related brain disorders.

DATA AVAILABILITY STATEMENT

The raw data supporting the conclusions of this article will be made available by the authors, without undue reservation.

ETHICS STATEMENT

The animal study was reviewed and approved by Facility Animal Care Committee, McGill University.

AUTHOR CONTRIBUTIONS

YT, MN, and TW conducted all experiments. YT and TW designed the study. YT, AL, and TW analyzed the data and wrote the manuscript. All authors have approved the submitted version.

FUNDING

This work was supported by the Canadian Institutes of Health Research (137003).

ACKNOWLEDGMENTS

We would like to thank Alice Wong for her technical assistance.

REFERENCES

Alexander, J. K., DeVries, A. C., Kigerl, K. A., Dahlman, J. M., and Popovich, P. G. (2009). Stress exacerbates neuropathic pain via glucocorticoid and NMDA receptor activation. *Brain Behav. Immun.* 23, 851–860. doi: 10.1016/j.bbi.2009.04.001

Brown, E. S., Rush, A. J., and McEwen, B. S. (1999). Hippocampal remodeling and damage by corticosteroids: implications for mood disorders. *Neuropsychopharmacology* 21, 474–484. doi: 10.1016/s0893-133x(99)00054-8

Calabrese, F., Guidotti, G., Molteni, R., Racagni, G., Mancini, M., and Riva, M. A. (2012). Stress-induced changes of hippocampal

NMDA receptors: modulation by duloxetine treatment. *PLoS One* 7:e37916.

Campbell, S., and Macqueen, G. (2004). The role of the hippocampus in the pathophysiology of major depression. *J. Psychiatry Neurosci.* 29, 417–426.

Carmignoto, G., and Fellin, T. (2006). Glutamate release from astrocytes as a non-synaptic mechanism for neuronal synchronization in the hippocampus. *J. Physiol. Paris* 99, 98–102. doi: 10.1016/j.jphysparis.2005.12.008

Christian, K. M., Miracle, A. D., Wellman, C. L., and Nakazawa, K. (2011). Chronic stress-induced hippocampal dendritic retraction requires CA3 NMDA receptors. *Neuroscience* 174, 26–36. doi: 10.1016/j.neuroscience.2010.11.033

Conrad, C. D., LeDoux, J. E., Magarinos, A. M., and McEwen, B. S. (1999). Repeated restraint stress facilitates fear conditioning independently of causing hippocampal CA3 dendritic atrophy. *Behav. Neurosci.* 113, 902–913. doi: 10.1037/0735-7044.113.5.902

Costa-Nunes, J., Zubareva, O., Araujo-Correia, M., Valenca, A., Schroeter, C. A., Pawluski, J. L., et al. (2014). Altered emotionality, hippocampus-dependent performance and expression of NMDA receptor subunit mRNAs in chronically stressed mice. *Stress* 17, 108–116. doi: 10.3109/10253890.2013.872619

Czeh, B., Simon, M., Schmelting, B., Hiemke, C., and Fuchs, E. (2006). Astroglial plasticity in the hippocampus is affected by chronic psychosocial stress and concomitant fluoxetine treatment. *Neuropsychopharmacology* 31, 1616–1626. doi: 10.1038/sj.npp.1300982

Duman, R. S., and Monteggia, L. M. (2006). A neurotrophic model for stress-related mood disorders. *Biol. Psychiatry* 59, 1116–1127. doi: 10.1016/j.biopsych.2006.02.013

Fellin, T., Pascual, O., Gobbo, S., Pozzan, T., Haydon, P. G., and Carmignoto, G. (2004). Neuronal synchrony mediated by astrocytic glutamate through activation of extrasynaptic NMDA receptors. *Neuron* 43, 729–743. doi: 10.1016/j.neuron.2004.08.011

Gore, A. C., Yeung, G., Morrison, J. H., and Oung, T. (2000). Neuroendocrine aging in the female rat: the changing relationship of hypothalamic gonadotropin-releasing hormone neurons and N-methyl-D-aspartate receptors. *Endocrinology* 141, 4757–4767. doi: 10.1210/endo.141.12.7841

Groc, L., Heine, M., Cousins, S. L., Stephenson, F. A., Lounis, B., Cognet, L., et al. (2006). NMDA receptor surface mobility depends on NR2A-2B subunits. *Proc. Natl. Acad. Sci. USA* 103, 18769–18774. doi: 10.1073/pnas.0605238103

Hammen, C. (2005). Stress and depression. *Annu. Rev. Clin. Psychol.* 1, 293–319.

Hardingham, G. E., and Bading, H. (2003). The Yin and Yang of NMDA receptor signalling. *Trends Neurosci.* 26, 81–89. doi: 10.1016/s0166-2236(02)00040-1

Hardingham, G. E., and Bading, H. (2010). Synaptic versus extrasynaptic NMDA receptor signalling: implications for neurodegenerative disorders. *Nat. Rev. Neurosci.* 11, 682–696. doi: 10.1038/nrn2911

Harris, A. Z., and Pettit, D. L. (2008). Recruiting extrasynaptic NMDA receptors augments synaptic signaling. *J. Neurophysiol.* 99, 524–533. doi: 10.1152/jn.01169.2007

Henningsen, K., Andreasen, J. T., Bouzinova, E. V., Jayatissa, M. N., Jensen, M. S., Redrobe, J. P., et al. (2009). Cognitive deficits in the rat chronic mild stress model for depression: relation to anhedonic-like responses. *Behav. Brain Res.* 198, 136–141. doi: 10.1016/j.bbr.2008.10.039

Karst, H., and Joels, M. (2003). Effect of chronic stress on synaptic currents in rat hippocampal dentate gyrus neurons. *J. Neurophysiol.* 89, 625–633. doi: 10.1152/jn.00691.2002

Krugers, H. J., Koolhaas, J. M., Bohus, B., and Korf, J. (1993). A single social stress-experience alters glutamate receptor-binding in rat hippocampal CA3 area. *Neurosci. Lett.* 154, 73–77. doi: 10.1016/0304-3940(93)90174-j

Lau, C. G., and Zukin, R. S. (2007). NMDA receptor trafficking in synaptic plasticity and neuropsychiatric disorders. *Nat. Rev. Neurosci.* 8, 413–426. doi: 10.1038/nrn2153

Le Meur, K., Galante, M., Angulo, M. C., and Audinat, E. (2007). Tonic activation of NMDA receptors by ambient glutamate of non-synaptic origin in the rat hippocampus. *J. Physiol.* 580, 373–383. doi: 10.1113/jphysiol.2006.123570

Li, N., Liu, R. J., Dwyer, J. M., Banasr, M., Lee, B., Son, H., et al. (2011). Glutamate N-methyl-D-aspartate receptor antagonists rapidly reverse behavioral and synaptic deficits caused by chronic stress exposure. *Biol. Psychiatry* 69, 754–761. doi: 10.1016/j.biopsych.2010.12.015

Li, S., Jin, M., Koeglsperger, T., Shepardson, N. E., Shankar, G. M., and Selkoe, D. J. (2011). Soluble Abeta oligomers inhibit long-term potentiation through a mechanism involving excessive activation of extrasynaptic NR2B-containing NMDA receptors. *J. Neurosci.* 31, 6627–6638. doi: 10.1523/jneurosci.0203-11.2011

Liu, D. D., Yang, Q., and Li, S. T. (2013). Activation of extrasynaptic NMDA receptors induces LTD in rat hippocampal CA1 neurons. *Brain Res. Bull.* 93, 10–16. doi: 10.1016/j.brainresbull.2012.12.003

Liu, F., Wu, J., Gong, Y., Wang, P., Zhu, L., Tong, L., et al. (2017). Harmine produces antidepressant-like effects via restoration of astrocytic functions. *Prog. Neuropsychopharmacol. Biol. Psychiatry* 79, 258–267. doi: 10.1016/j.pnpbp.2017.06.012

Liu, W. X., Wang, J., Xie, Z. M., Xu, N., Zhang, G. F., Jia, M., et al. (2016). Regulation of glutamate transporter 1 via BDNF-TrkB signaling plays a role in the anti-apoptotic and antidepressant effects of ketamine in chronic unpredictable stress model of depression. *Psychopharmacology* 233, 405–415. doi: 10.1007/s00213-015-4128-2

Lu, W., Man, H., Ju, W., Trimble, W. S., MacDonald, J. F., and Wang, Y. T. (2001). Activation of synaptic NMDA receptors induces membrane insertion of new AMPA receptors and LTP in cultured hippocampal neurons. *Neuron* 29, 243–254. doi: 10.1016/s0896-6273(01)00194-5

Luine, V., Villegas, M., Martinez, C., and McEwen, B. S. (1994). Repeated stress causes reversible impairments of spatial memory performance. *Brain Res.* 639, 167–170. doi: 10.1016/0006-8993(94)91778-7

Luscher, C., Malenka, R. C., and Nicoll, R. A. (1998). Monitoring glutamate release during LTP with glial transporter currents. *Neuron* 21, 435–441. doi: 10.1016/s0896-6273(00)80552-8

Magarinos, A. M., and McEwen, B. S. (1995). Stress-induced atrophy of apical dendrites of hippocampal CA3c neurons: involvement of glucocorticoid secretion and excitatory amino acid receptors. *Neuroscience* 69, 89–98. doi: 10.1016/0306-4522(95)00259-l

Martin, K. P., and Wellman, C. L. (2011). NMDA receptor blockade alters stress-induced dendritic remodeling in medial prefrontal cortex. *Cereb. Cortex.* 21, 2366–2373. doi: 10.1093/cercor/bhr021

McEwen, B. S. (1999). Stress and hippocampal plasticity. *Annu. Rev. Neurosci.* 22, 105–122. doi: 10.1146/annurev.neuro.22.1.105

McEwen, B. S. (2003). Mood disorders and allostatic load. *Biol. Psychiatry* 54, 200–207. doi: 10.1016/s0006-3223(03)00177-x

Milnerwood, A. J., Gladding, C. M., Pouladi, M. A., Kaufman, A. M., Hines, R. M., Boyd, J. D., et al. (2010). Early increase in extrasynaptic NMDA receptor signaling and expression contributes to phenotype onset in Huntington's disease mice. *Neuron* 65, 178–190. doi: 10.1016/j.neuron.2010.01.008

Mitani, A., and Komiyama, T. (2018). Real-Time processing of two-photon calcium imaging data including lateral motion artifact correction. *Front. Neuroinform.* 12:98. doi: 10.3389/fninf.2018.00098

Nasca, C., Zelli, D., Bigio, B., Piccinin, S., Scaccianoce, S., Nistico, R., et al. (2015). Stress dynamically regulates behavior and glutamatergic gene expression in hippocampus by opening a window of epigenetic plasticity. *Proc. Natl. Acad. Sci. USA* 112, 14960–14965. doi: 10.1073/pnas.1516016112

Nie, H., Zhang, H., and Weng, H. R. (2010). Bidirectional neuron-glia interactions triggered by deficiency of glutamate uptake at spinal sensory synapses. *J. Neurophysiol.* 104, 713–725. doi: 10.1152/jn.00282.2010

Oikonomou, K. D., Short, S. M., Rich, M. T., and Antic, S. D. (2012). Extrasynaptic glutamate receptor activation as cellular bases for dynamic range compression in pyramidal neurons. *Front. Physiol.* 3:334. doi: 10.3389/fphys.2012.00334

Pacheco, A., Aguayo, F. I., Aliaga, E., Munoz, M., Garcia-Rojo, G., Olave, F. A., et al. (2017). Chronic stress triggers expression of immediate early genes and differentially affects the expression of AMPA and NMDA subunits in dorsal and ventral hippocampus of rats. *Front. Mol. Neurosci.* 10:244. doi: 10.3389/fnmol.2017.00244

Paoletti, P., Bellone, C., and Zhou, Q. (2013). NMDA receptor subunit diversity: impact on receptor properties, synaptic plasticity and disease. *Nat. Rev. Neurosci.* 14, 383–400. doi: 10.1038/nrn3504

Papouin, T., Ladepeche, L., Ruel, J., Sacchi, S., Labasque, M., Hanini, M., et al. (2012). Synaptic and Extrasynaptic NMDA receptors are gated by different endogenous coagonists. *Cell* 150, 633–646. doi: 10.1016/j.cell.2012.06.029

Papouin, T., and Oliet, S. H. (2014). Organization, control and function of extrasynaptic NMDA receptors. *Philos. Trans. R Soc. Lond. B Biol. Sci.* 369:20130601. doi: 10.1098/rstb.2013.0601

Parsons, M. P., and Raymond, L. A. (2014). Extrasynaptic NMDA receptor involvement in central nervous system disorders. *Neuron* 82, 279–293. doi: 10.1016/j.neuron.2014.03.030

Petralia, R. S., Wang, Y. X., Hua, F., Yi, Z., Zhou, A., Ge, L., et al. (2010). Organization of NMDA receptors at extrasynaptic locations. *Neuroscience* 167, 68–87. doi: 10.1016/j.neuroscience.2010.01.022

Sah, P., Hestrin, S., and Nicoll, R. A. (1989). Tonic activation of NMDA receptors by ambient glutamate enhances excitability of neurons. *Science* 246, 815–818. doi: 10.1126/science.2573153

Sandi, C., Merino, J. J., Cordero, M. I., Touyarot, K., and Venero, C. (2001). Effects of chronic stress on contextual fear conditioning and the hippocampal expression of the neural cell adhesion molecule, its polysialylation, and L1. *Neuroscience* 102, 329–339. doi: 10.1016/s0306-4522(00)00484-x

Savchenko, A., Braun, G. B., and Molokanova, E. (2016). Nanostructured Antagonist of Extrasynaptic NMDA Receptors. *Nano. Lett.* 16, 5495–5502. doi: 10.1021/acs.nanolett.6b01988

Schwendt, M., and Jezova, D. (2000). Gene expression of two glutamate receptor subunits in response to repeated stress exposure in rat hippocampus. *Cell Mol. Neurobiol.* 20, 319–329.

Shors, T. J., and Mathew, P. R. (1998). NMDA receptor antagonism in the lateral/basolateral but not central nucleus of the amygdala prevents the induction of facilitated learning in response to stress. *Learn Mem.* 5, 220–230.

Shors, T. J., and Servatius, R. J. (1995). Stress-induced sensitization and facilitated learning require NMDA receptor activation. *Neuroreport* 6, 677–680. doi: 10.1097/00001756-199503000-00023

Suzuki, T., Kodama, S., Hoshino, C., Izumi, T., and Miyakawa, H. (2008). A plateau potential mediated by the activation of extrasynaptic NMDA receptors in rat hippocampal CA1 pyramidal neurons. *Eur. J. Neurosci.* 28, 521–534. doi: 10.1111/j.1460-9568.2008.06324.x

Tovar, K. R., and Westbrook, G. L. (1999). The incorporation of NMDA receptors with a distinct subunit composition at nascent hippocampal synapses in vitro. *J. Neurosci.* 19, 4180–4188. doi: 10.1523/jneurosci.19-10-04180.1999

Tovar, K. R., and Westbrook, G. L. (2002). Mobile NMDA receptors at hippocampal synapses. *Neuron* 34, 255–264. doi: 10.1016/s0896-6273(02)00658-x

Tse, Y. C., Bagot, R. C., Hutter, J. A., Wong, A. S., and Wong, T. P. (2011). Modulation of synaptic plasticity by stress hormone associates with plastic alteration of synaptic NMDA receptor in the adult hippocampus. *PLoS One* 6:e27215. doi: 10.1371/journal.pone.0027215

Tse, Y. C., Lopez, J., Moquin, A., Wong, S. A., Maysinger, D., and Wong, T. P. (2019). The susceptibility to chronic social defeat stress is related to low hippocampal extrasynaptic NMDA receptor function. *Neuropsychopharmacology* 44, 1310–1318. doi: 10.1038/s41386-019-0325-8

Valente, P., Kiryushko, D., Sacchetti, S., Machado, P., Cobley, C. M., Mangini, V., et al. (2020). Conopeptide-functionalized nanoparticles selectively antagonize extrasynaptic n-methyl-d-aspartate receptors and protect hippocampal neurons from excitotoxicity in vitro. *ACS Nano.* 14, 6866–6877. doi: 10.1021/acsnano.0c00866

Veena, J., Srikumar, B. N., Mahati, K., Bhagya, V., Raju, T. R., and Shankaranarayana Rao, B. S. (2009). Enriched environment restores hippocampal cell proliferation and ameliorates cognitive deficits in chronically stressed rats. *J. Neurosci. Res.* 87, 831–843. doi: 10.1002/jnr.21907

Wu, Y. W., Grebenyuk, S., McHugh, T. J., Rusakov, D. A., and Semyanov, A. (2012). Backpropagating action potentials enable detection of extrasynaptic glutamate by NMDA receptors. *Cell Rep.* 1, 495–505. doi: 10.1016/j.celrep.2012.03.007

Yamamoto, S., Morinobu, S., Fuchikami, M., Kurata, A., Kozuru, T., and Yamawaki, S. (2008). Effects of single prolonged stress and D-cycloserine on contextual fear extinction and hippocampal NMDA receptor expression in a rat model of PTSD. *Neuropsychopharmacology* 33, 2108–2116. doi: 10.1038/sj.npp.1301605

Yao, L., Grand, T., Hanson, J. E., Paoletti, P., and Zhou, Q. (2018). Higher ambient synaptic glutamate at inhibitory versus excitatory neurons differentially impacts NMDA receptor activity. *Nat. Commun.* 9:4000.

Yuen, E. Y., Liu, W., Karatsoreos, I. N., Feng, J., McEwen, B. S., and Yan, Z. (2009). Acute stress enhances glutamatergic transmission in prefrontal cortex and facilitates working memory. *Proc. Natl. Acad. Sci. USA* 106, 14075–14079.

Yuen, E. Y., Liu, W., Karatsoreos, I. N., Ren, Y., Feng, J., McEwen, B. S., et al. (2011). Mechanisms for acute stress-induced enhancement of glutamatergic transmission and working memory. *Mol. Psychiatry* 16, 156–170. doi: 10.1038/mp.2010.50

Yuen, E. Y., Wei, J., Liu, W., Zhong, P., Li, X., and Yan, Z. (2012). Repeated stress causes cognitive impairment by suppressing glutamate receptor expression and function in prefrontal cortex. *Neuron* 73, 962–977. doi: 10.1016/j.neuron.2011.12.033

Zhang, T. R., Larosa, A., Di Raddo, M. E., Wong, V., Wong, A. S., and Wong, T. P. (2019). Negative memory engrams in the hippocampus enhance the susceptibility to chronic social defeat stress. *J. Neurosci.* 39, 7576–7590. doi: 10.1523/jneurosci.1958-18.2019

Zhu, X., Ye, G., Wang, Z., Luo, J., and Hao, X. (2017). Sub-anesthetic doses of ketamine exert antidepressant-like effects and upregulate the expression of glutamate transporters in the hippocampus of rats. *Neurosci. Lett.* 639, 132–137. doi: 10.1016/j.neulet.2016.12.070

Conflict of Interest: The authors declare that the research was conducted in the absence of any commercial or financial relationships that could be construed as a potential conflict of interest.

Publisher's Note: All claims expressed in this article are solely those of the authors and do not necessarily represent those of their affiliated organizations, or those of the publisher, the editors and the reviewers. Any product that may be evaluated in this article, or claim that may be made by its manufacturer, is not guaranteed or endorsed by the publisher.

frontiers in Molecular Neuroscience

MINI REVIEW
published: 15 November 2021
doi: 10.3389/fnmol.2021.796912

Evolutionarily Established Palmitoylation-Dependent Regulatory Mechanisms of the Vertebrate Glutamatergic Synapse and Diseases Caused by Their Disruption

*Takashi Hayashi**

Biomedical Research Institute, National Institute of Advanced Industrial Science and Technology (AIST), Tsukuba, Japan

Glutamate is the major excitatory neurotransmitter in the vertebrate brain and various modifications have been established in the glutamatergic synapses. Generally, many neuronal receptors and ion channels are regulated by *S*-palmitoylation, a reversible post-translational protein modification. Genome sequence databases show the evolutionary acquisition and conservation concerning vertebrate-specific palmitoylation of synaptic proteins including glutamate receptors. Moreover, palmitoylation of some glutamate receptor-binding proteins is subsequently acquired only in some mammalian lineages. Recent progress in genome studies has revealed that some palmitoylation-catalyzing enzymes are the causative genes of neuropsychiatric disorders. In this review, I will summarize the evolutionary development of palmitoylation-dependent regulation of glutamatergic synapses and their dysfunctions which are caused by the disruption of palmitoylation mechanism.

Keywords: palmitoylation, glutamate receptor (GluR), PDZ protein, excitatory synapse, vertebrate, eutherian, evolution

OPEN ACCESS

Edited by:
Dhrubajyoti Chowdhury, Yale University, United States

Reviewed by:
Darren Boehning, Cooper Medical School of Rowan University, United States

***Correspondence:**
Takashi Hayashi
takashi.hayashi@aist.go.jp

Specialty section:
This article was submitted to Molecular Signalling and Pathways, a section of the journal Frontiers in Molecular Neuroscience

Received: *18 October 2021*
Accepted: *26 October 2021*
Published: *15 November 2021*

Citation:
Hayashi T (2021) Evolutionarily Established Palmitoylation-Dependent Regulatory Mechanisms of the Vertebrate Glutamatergic Synapse and Diseases Caused by Their Disruption. Front. Mol. Neurosci. 14:796912. doi: 10.3389/fnmol.2021.796912

INTRODUCTION

Vertebrates comprise a lot of animal species classified within the subphylum Vertebrata, which consists of a majority of the phylum Chordata. Variety of species in mammals, birds, reptiles, amphibians, lobe-finned fishes, ray-finned fishes, cartilaginous fishes, and jawless fishes belong to vertebrates. They have diverged from the common ancestral chordate. Other subphyla Cephalochordata and Urochordata in the phylum Chordata are composed of lancelets and sea squirts (also known as ascidians), respectively. The vertebrate brain has been naturally developed from the primitive chordate nervous system. Almost as if a language is deeply rooted in the accumulated history of speakers (Cavalli-Sforza, 2000), essential structure, operating principles, and components of vertebrate brain basically hold the evolutionary accumulation in the history of life. Regarding many vertebrate synaptic protein orthologs including ion channels and neurotransmitter receptors, these component parts commonly exist in the whole chordates as well as species in other animal phyla. In this review, I will discuss recent findings supporting the evolutionarily developed modification in the vertebrate brain and will address their functional significance.

EVOLUTIONARY ACQUISITION AND CONSERVATION OF SYNAPTIC PALMITOYLATION IN THE VERTEBRATE LINEAGE

Among various neurotransmitters available in animals, glutamate was evolutionarily selected as the major excitatory neurotransmitter in the vertebrate central nervous system. Thus, glutamate receptor (GluR) family proteins play central roles in excitatory synaptic transmission and plasticity in the vertebrate brain (Shepherd and Huganir, 2007; Kessels and Malinow, 2009; Anggono and Huganir, 2012; Diering and Huganir, 2018). GluRs are composed of ionotropic and metabotropic GluRs. The ionotropic glutamate receptors (iGluRs) are pharmacologically and electrophysiologically classified into four groups, α-amino-3-hydroxy-5-methyl-4-isoxazolepropionate (AMPA)-type, kainate (KA)-type, δ-type, and *N*-methyl-D-aspartate (NMDA)-type receptors, basically named after their selective agonist drugs (Seeburg, 1993; Hollmann and Heinemann, 1994; Mori and Mishina, 2003). Ancestral animal GluR genes are supposed to be developed from prokaryotic potassium-selective ion channel GluR0 (Arinaminpathy et al., 2003).

Essential biological functions of proteins are basically determined by the amino acid sequence of proteins. Moreover, post-translational protein modifications (PTPMs) enable precise and dynamic control of protein localization, membrane trafficking, and fine-tuning of protein functions. In many types of PTPMs, protein *S*-palmitoylation is a prominent type of fatty acylation, characterized by the reversible covalent attachment of lipid palmitate on target proteins (Resh, 2016). Palmitate is a saturated fatty acid, which most abundantly exists in the vertebrate brain as well as in the whole body. The biochemical process of *S*-palmitoylation is enzymatically mediated transfer of palmitoyl group from palmitoyl-coenzyme A (palmitoyl-CoA) to intracellular cysteine residues of target proteins *via* thioester bonds. Accumulating genome information in animal species increasingly clarifies that low rates of substitution occur at structurally or functionally significant amino acid residues during molecular evolution against continuous mutation pressure.

Previous studies have shown the vertebrate-specific conservation of palmitoylated cysteine residues in GluRs orthologs (**Figure 1**). Concretely, synaptic palmitoylation sites in AMPA receptor subunits GluA1, GluA2, GluA3, and GluA4 (also known as GluR1-4, GluRA-D, or GluRα1-4) orthologs (Hayashi et al., 2005; Itoh et al., 2018, 2019; Iizumi et al., 2021), NMDA receptor regulatory subunits GluN2A and GluN2B (also known as NR2A and NR2B or GluRε1 and GluRε2) orthologs (Hayashi et al., 2009; Mattison et al., 2012) and KA receptor subunit GluK2 (also known as GluR6 or GluRβ2) orthologs (Pickering et al., 1995) are almost completely conserved only in the vertebrate lineage (Hayashi, 2014, 2021). AMPA receptors and NMDA receptors are palmitoylated at their two distinct sites (Hayashi et al., 2005, 2009; Hayashi, 2021). Another palmitoylation site causes the receptors to accumulate in the Golgi apparatus (**Figure 1**). Cysteine residues at the corresponding sites are widely conserved in both vertebrates and invertebrates besides nematodes (Thomas and Hayashi, 2013). This Golgi apparatus localizing palmitoylation thus appears to act as a "quality control" mechanism to ensure correct receptor maturation. In contrast, vertebrate-specific synaptic palmitoylation sites in AMPA receptors and NMDA receptors are implicated in "quantitative regulation" of synaptic strength, which relate to complex neuronal events such as long-lasting synaptic plasticity. Evolutionarily, the sudden appearance of many animal phyla had occurred in the Cambrian period. These data strongly indicate that synaptic palmitoylation-dependent GluRs regulation had established just after the divergence of the common vertebrate ancestor from chordates around 500 million years ago in the late Cambrian to the early Ordovician periods (**Figure 2**). The GluR palmitoylation mechanisms have been evolutionarily conserved against mutation pressure throughout whole vertebrate species, presumably because the protein palmitoylation plays essential and irreplaceable roles for vertebrate-specific excitatory synaptic functions. Extremely conserved synaptic palmitoylation sites in the vertebrate lineage from jawless fishes to humans indicate that this modification may form the basis of vertebrate-specific brain functions.

Similarly, vertebrate-specific conservations of palmitoylation sites are also observed in other ion channels and neurotransmitter receptors (Borroni et al., 2016), such as HCN2 (hyperpolarization-activated cyclic nucleotide-gated channel 2) orthologs (Itoh et al., 2017), a water channel AQP4 (aquaporin family protein 4) orthologs (Hayashi, 2017), and serotonin (chemically known as 5-hydroxytryptamine, 5-HT) receptors 5-HT_{1A}, 5-HT_4, 5-HT_7 receptor orthologs (Kaizuka and Hayashi, 2018).

STEPWISE REFINEMENT OF PALMITOYLATION-DEPENDENT REGULATION OF GluR-BINDING PROTEINS

As the major excitatory neurotransmitter receptors, GluRs ensure the minimal and essential excitatory synaptic transmission in the vertebrate brain. Furthermore, additional participation of GluR-binding proteins greatly refines temporal and spatial control of excitatory synaptic functions (Thomas and Hayashi, 2013). The most well-studied palmitoylated GluRs regulators are PDZ (PSD95/Dlg1/zo-1) domain-containing proteins, such as PSD-95 (postsynaptic density protein 95), GRIP1 (GluR-interacting protein 1), GRIP2, and PICK1 (protein interacting with C-kinase 1), which make complex with GluRs, respectively. These vertebrate PDZ domain proteins have orthologs in other phyla (**Figure 1**).

PSD-95 binds to NMDA receptor subunits GluN2A-2D and KA receptor subunit GluK2 through its PDZ domain. PSD-95 also interacts with AMPA receptors-transmembrane AMPAR regulatory proteins (TARPs) complex and regulates AMPA receptors ion channel properties as well as their membrane localization in many animal species. Orthologs of PSD-95, also known as SAP-90 (synapse-associated protein

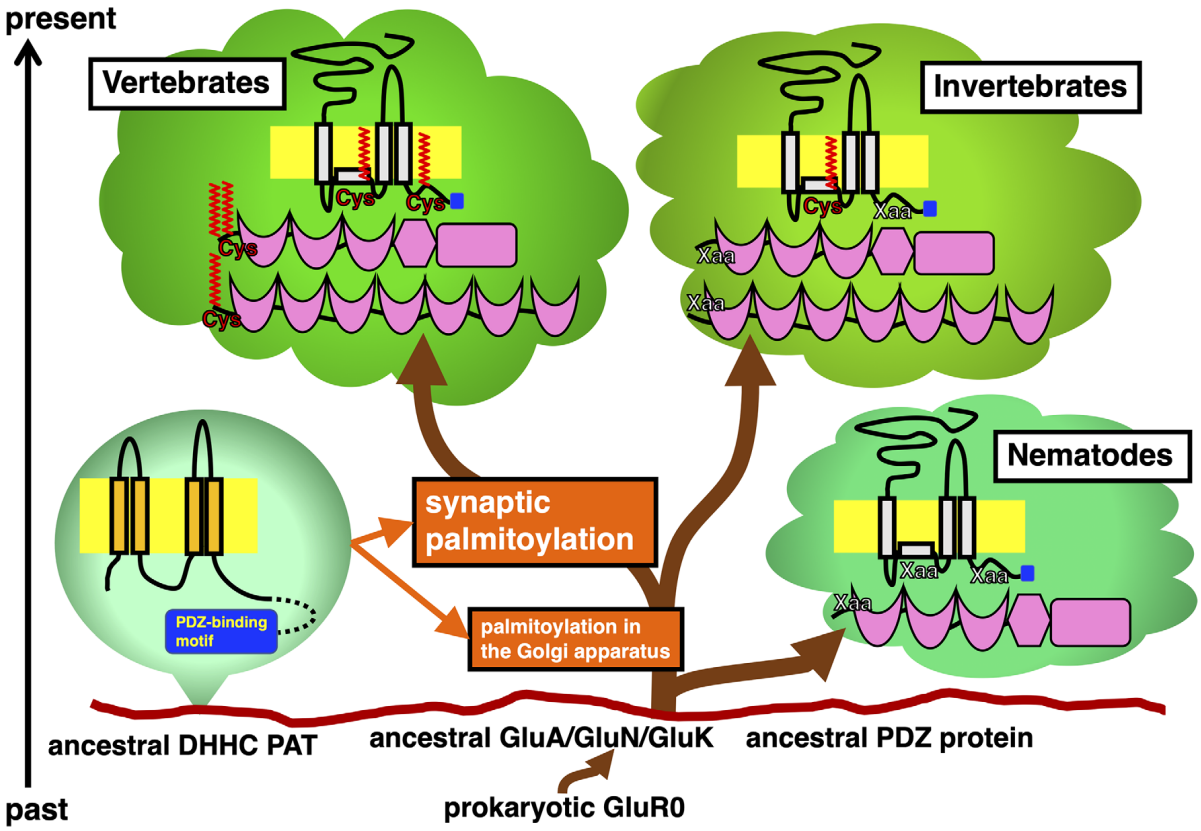

FIGURE 1 | Timeline of appearance of GluR and PDZ protein orthologs in the animal phylogenetic tree diverged from the same primitive root on the eukaryotic ground. Stepwise establishment of GluR palmitoylation in the Golgi apparatus and synaptic palmitoylation in vertebrate GluRs and PDZ proteins are shown in orange. DHHC PATs, which evolutionarily expand, catalyze these modifications. Ancestral AMPA receptor GluA, NMDA receptor GluN, and KA receptor GluK had been developed from the prokaryotic GluR0. Divergence of orthologs of these GluRs and PDZ proteins in vertebrate and invertebrate lineages are shown. Schematic of these proteins indicate the location of palmitoylation sites (colored in red) and PDZ-binding motif (colored in blue).

90), broadly exist in vertebrates and many invertebrates. The fruit fly *Drosophila melanogaster* protein Discs large (DLG) and a nematode *Caenorhabditis elegans* protein DLG-1 are orthologs of vertebrate PSD-95. While vertebrate PSD-95 possess N-terminal palmitoylated cysteine residues, invertebrate PSD-95 orthologs lack these motifs at the corresponding site. N-terminal palmitoylation sites are lost in DLG orthologs from primitive chordates (e.g., an ascidian *Ciona intestinalis*, sometimes known by the common name of vase tunicate) and hemichordates (e.g., an acorn worm *Saccoglossus kowalevskii*). Therefore, synaptic regulation through PSD-95 palmitoylation appears unique to vertebrates (**Figure 1**).

Other PDZ proteins GRIP1a and its related GRIP2a/ABP-L (AMPA receptor-binding protein-L), are alternatively spliced to generate palmitoylated isoforms, GRIP1b, GRIP2b/pABP-L. PDZ domains of these proteins interact with GluA2 C-terminus. The neuronal trafficking and localization of vertebrate AMPA receptor complexes can be regulated by these binding partners *via* palmitoylation (Thomas et al., 2012). The GRIP1b N-terminal palmitoylation sequence is widely present in vertebrate genomes. However, GRIP1 sequences in primitive chordates (*C. intestinalis*) and hemichordates (*S. kowalevskii*) lack this palmitoylation site. Generally, palmitoylation motifs are lost in invertebrate GRIP1 and GRIP2 orthologs including insects. Although the dGRIP, a *Drosophila* GRIP1 ortholog, exceptionally contains a cysteine residue at the corresponding position to vertebrate GRIP1, amino acids around the dGRIP cysteine are poorly conserved compared with vertebrate GRIP1b. Thus, it remains unclear whether dGRIP can serve similar functions to mammalian GRIP1b even if dGRIP is palmitoylated. Palmitoylation of iGluRs, PSD-95, GRIP1b, GRIP2b, HCN2, AQP4, and 5-HT receptor orthologs seem to be acquired in the ancestor of vertebrates at about the same time around 500 million years ago (**Figure 2**).

The PDZ domain of PICK1 competitively binds to the AMPA receptor subunit GluA2 C-terminus (**Figure 2**). PICK1 controls GluA2-containing AMPA receptor endocytosis from the synaptic surface (Shepherd and Huganir, 2007; Thomas et al., 2013). Sequence databases show that the PICK1 C-terminal palmitoylation is limited in some orders in mammals (Hayashi, 2015). In contrast to the evolutionary establishment of palmitoylation in other neuronal protein orthologs, widely and specifically recognized in vertebrates as mentioned above, palmitoylation of PICK1 had been

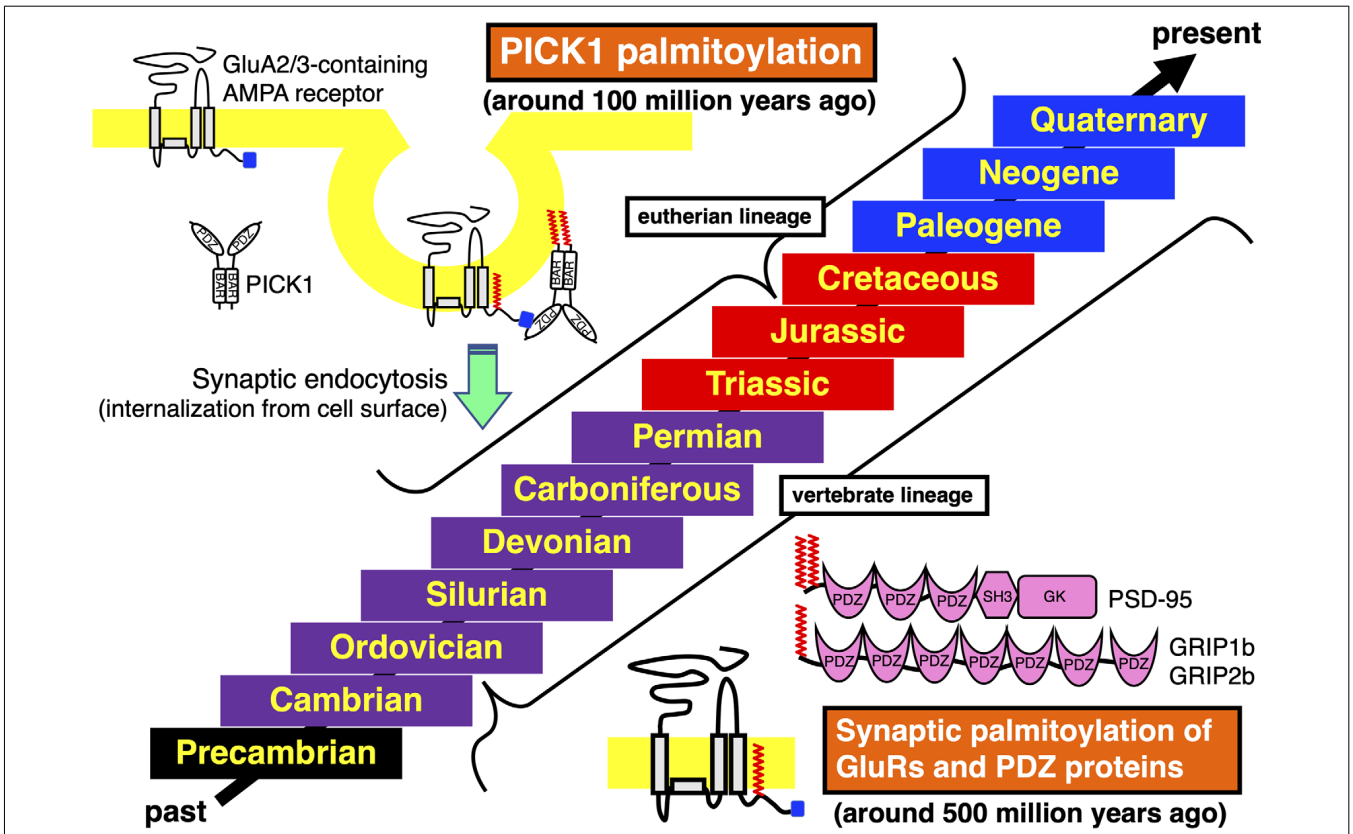

FIGURE 2 | Acquisition and conservation of vertebrate-specific palmitoylation in GluRs and PDZ proteins and eutherian-specific palmitoylation in PICK1. Geologic time scale from the past to the present is shown. The Phanerozoic Eon, during which abundant animal species have expanded and became partly extinct, is majorly classed into the Paleozoic Era (Cambrian, Ordovician, Silurian, Devonian, Carboniferous, and Permian periods, marked in purple), the Mesozoic Era (Triassic, Jurassic, and Cretaceous periods, marked in red) and the Cenozoic Era (Paleogene, Neogene, and Quaternary periods, marked in blue). The preceding Precambrian period is marked in black. Synaptic palmitoylation was established only in the common vertebrate ancestors of GluRs, PSD-95, GRIP1b, or GRIP2b around 500 million years ago in the late Cambrian to the early Ordovician periods, which has been almost completely conserved in the whole vertebrate lineage. Moreover, PICK1 palmitoylation has been conserved in most eutherian lineage, which was acquired in the common ancestor of eutherian species belonging to the superorders Xenarthra, Laurasiatheria, Euarchontoglires, and the orders Sirenia and Proboscidea around 100 million years ago in the early Cretaceous period.

acquired step by step along the divergence of mammalian species. The class Mammalia consists of three living groups, the subclasses Prototheria (e.g., platypus), Metatheria (extant marsupials, such as gray short-tailed opossum and wallaby), and Eutheria (extant placentals). PICK1 orthologs in both subclasses Prototheria and Metatheria lack palmitoylation sites. Placental mammals are further classified into the four major superorders, Afrotheria, Xenarthra, Laurasiatheria, and Euarchontoglires (Springer and Murphy, 2007). All these eutherian (placental) species diverged from the same root around 100 million years ago in the early Cretaceous period (Springer et al., 2011). In the superorder Afrotheria, aardvark PICK1 ortholog shows the primitive C-terminal sequence (-Gly-Ser in the order Tubulidentata). Some afrotherian PICK1 orthologs have additional short Cys non-containing motif to the anticipated original (-Gly-Ser-Trp-Xaa-Gly-Ser in the order Macroscelidea, e.g., Cape elephant shrew and in the order Afrosoricida e.g., Cape golden mole, lesser hedgehog tenrec). The Cys-containing PICK1 palmitoylation motif is found in species belonging to the superorders Afrotheria (-Gly-Ser-Trp-Cys-Gly-Ser in the order Sirenia, e.g., Florida manatee and in the order Proboscidea, e.g., African elephant), Xenarthra (-Gly-Ser-Trp-Cys-Gly-Ser in the order Cingulata, e.g., armadillo), Laurasiatheria (-Gly-Ser-Trp-Cys-Asp-Ser, e.g., dog) and Euarchontoglires (-Gly-Ser-Trp-Cys-Asp-Ser, e.g., mouse, human). The PICK1 palmitoylation-dependent refined control of AMPA receptors should originate in the common ancestor of these eutherian (placental) species (Hayashi, 2015). This improved PICK1 regulation mechanism has been broadly conserved during evolution in the extant eutherian (placental) lineage, whereas a cysteine residue at the corresponding site is lost in some exceptional species such as hedgehog (the order Erinaceomorpha in the superorder Laurasiatheria: -Gly-Ser-Trp-Ser-Asp-Ser) and American pika (the order Lagomorpha in the superorder Euarchontoglires: -Gly-Ser-Trp-Ser-Asp-Ser). Furthermore, PICK1 orthologs in all reported species in the family Bovidae (cattle, yak, water buffalo, sheep, goat, antelope: -Gly-Ser-Trp-Cys-Asn-Ser) possess different Cys-containing sequences from the standard eutherian motif, which may imply ongoing

molecular evolution of PICK1 palmitoylation (Hayashi, 2015).

ENZYMES CATALYZING PALMITOYLATION IN NEURODEGENERATIVE DISEASE AND MENTAL DISORDERS AND THEIR EVOLUTIONARY EXPANSION

Biochemical researches have revealed that cycles of palmitoylation by palmitoyl acyl transferases (PATs) and depalmitoylation by palmitoyl-protein thioesterases (PPTs) serve as a cellular regulatory mechanism from yeast to human (Fukata and Fukata, 2010; Matt et al., 2019). Presently, 23 human and 24 mouse genes have been identified in a PAT family containing the Asp-His-His-Cys (DHHC) catalytic motif within a cysteine-rich, zinc finger-like domain (Korycka et al., 2012; Gottlieb and Linder, 2017; De and Sadhukhan, 2018). As PPTs, acyl-protein thioesterase (also called as Lypla) 1 and 2 (APT1 and APT2), APT-like, palmitoyl-protein thioesterase 1 and 2 (PPT1 and PPT2), and 17 α/β-hydrolase domain-containing family proteins are currently known (Lin and Conibear, 2015; Yokoi et al., 2016). About 40% of PATs are known to be linked to human diseases (Chavda et al., 2014). Palmitoylation deficiency leads to neuropsychiatric disorders. Especially, mutations in DHHC PATs are related to neurogenerative diseases (DHHC7, DHHC12, and DHHC21 in Alzheimer's disease, DHHC17/HIP14 (huntingtin-interacting protein 14) and DHHC13/HIP14L (HIP14-like) in Huntington's disease) and mental disorders (DHHC5 in bipolar disorder, DHHC8 in schizophrenia, DHHC9, and DHHC15 in X-linked intellectual disability).

Comparison of animal genomes suggests that DHHC PATs homologs seem to have expanded during animal evolution. PDZ-binding motifs are present in C-termini of several DHHC PATs, which are recognized by PDZ domain-containing proteins (**Figure 1**). Predicted C-terminal PDZ-binding motifs on DHHC PATs are increasingly recognized in DHHC PAT homologs (Thomas and Hayashi, 2013): a nematode worm (*C. elegans*, 6.7%), fruit fly (*D. melanogaster*, 18.2%), Zebrafish (*Danio rerio*, 36.4%), frog (*Xenopus tropicalis*, 38.1%), mouse (*Mus musculus*, 33.3%), and humans (*Homo sapiens*, 39.1%). The proportion of PDZ-binding PATs goes up from 6.7% in worms to around 36.7% in vertebrates as DHHC PAT numbers increase. All eight PDZ-binding mouse PATs (DHHC3, DHHC5, DHHC7, DHHC8, DHHC14, DHHC16, DHHC17, and DHHC21 orthologs) are detected in 14 neuronal tissue-expressing PATs (57.1%), indicating that PDZ-dependent interaction of PATs is likely to play crucial roles in the vertebrate brain.

CONCLUSION AND PERSPECTIVE

So far, there is no direct evidence that implicates mutations at the palmitoylation sites of iGluRs and that their binding proteins cause any neuropsychiatric disorders. However, palmitoylation of these orthologs was established in the very early stage of vertebrate evolution and they have been extremely well conserved in the whole vertebrate species or in specific eutherian lineage as summarized in this review. This essential synaptic modification system may be protected by multiple layers of regulatory mechanisms to prevent disturbance of vertebrate brain functions. Further accumulation of genome sequence data will fill in the blanks of the animal order, family, and genus list concerning vertebrate divergence. Additional information will reveal the timeline of establishment and divergence of these palmitoylation sites-containing motifs in more detail. Especially, sequence information on urochordates (sea squirts or ascidians), cephalochordates (lancelets), and cyclostomes (lampreys and hagfishes) will clarify the initial acquisition of the mechanism of synaptic palmitoylation.

AUTHOR CONTRIBUTIONS

The author confirms being the sole contributor of this work and has approved it for publication.

FUNDING

This work was supported in part by Grants-in-Aid from the Ministry of Education, Culture, Sports, Science and Technology of Japan (MEXT)/Japan Society for the Promotion of Science (JSPS; Grant numbers 22680029, 23650187, 24111512, 16K07078), RRIME and FORCE from Japan Agency for Medical Research and Development (AMED; Grant number JP18gm5910009, JP20gm4010004), the Takeda Science Foundation, the Mitsubishi Foundation, the Brain Science Foundation, the Suzuken Memorial Foundation, and the Astellas Foundation for Research on Metabolic Disorders.

ACKNOWLEDGMENTS

I am grateful to Dr. A. Oota-Ishigaki and Ms. N. Suzuki for excellent assistance. Dr. P. Kumar kindly proofread the manuscript.

REFERENCES

Anggono, V., and Huganir, R. L. (2012). Regulation of AMPA receptor trafficking and synaptic plasticity. *Curr. Opin. Neurobiol.* 22, 461–469. doi: 10.1016/j.conb.2011.12.006

Arinaminpathy, Y., Biggin, P. C., Shrivastava, I. H., and Sansom, M. S. (2003). A prokaryotic glutamate receptor: homology modelling and molecular dynamics simulations of GluR0. *FEBS Lett.* 553, 321–327. doi: 10.1016/s0014-5793(03)01036-6

Borroni, M. V., Valles, A. S., and Barrantes, F. J. (2016). The lipid habitats of neurotransmitter receptors in brain. *Biochim. Biophys. Acta* 1858, 2662–2670. doi: 10.1016/j.bbamem.2016.07.005

Cavalli-Sforza, L. L. (2000). *Genes, Peoples and Languages*. New York: North Point Press.

Chavda, B., Arnott, J. A., and Planey, S. L. (2014). Targeting protein palmitoylation: selective inhibitors and implications in disease. *Expert Opin. Drug Discov.* 9, 1005–1019. doi: 10.1517/17460441.2014.933802

De, I., and Sadhukhan, S. (2018). Emerging roles of DHHC-mediated protein S-palmitoylation in physiological and pathophysiological context. *Eur. J. Cell Biol.* 97, 319–338. doi: 10.1016/j.ejcb.2018.03.005

Diering, G. H., and Huganir, R. L. (2018). The AMPA receptor code of synaptic plasticity. *Neuron* 100, 314–329. doi: 10.1016/j.neuron.2018.10.018

Fukata, Y., and Fukata, M. (2010). Protein palmitoylation in neuronal development and synaptic plasticity. *Nat. Rev. Neurosci.* 11, 161–175. doi: 10.1038/nrn2788

Gottlieb, C. D., and Linder, M. E. (2017). Structure and function of DHHC protein S-acyltransferases. *Biochem. Soc. Trans.* 45, 923–928. doi: 10.1042/BST20160304

Hayashi, T. (2014). Evolutionarily conserved palmitoylation-dependent regulation of ionotropic glutamate receptors in vertebrates. *Neurotransmitter* 1:e388. doi: 10.14800/nt.388

Hayashi, T. (2015). The origin and diversity of PICK1 palmitoylation in the eutheria. *Neurotransmitter* 2:e802. doi: 10.14800/nt.802

Hayashi, T. (2017). Conservation and phylogenetic stepwise changes of aquaporin (AQP) 4 palmitoylation in vertebrate evolution. *Neurotransmitter* 4:e1608. doi: 10.14800/nt.1608

Hayashi, T. (2021). Post-translational palmitoylation of ionotropic glutamate receptors in excitatory synaptic functions. *Br. J. Pharmacol.* 178, 784–797. doi: 10.1111/bph.15050

Hayashi, T., Rumbaugh, G., and Huganir, R. L. (2005). Differential regulation of AMPA receptor subunit trafficking by palmitoylation of two distinct sites. *Neuron* 47, 709–723. doi: 10.1016/j.neuron.2005.06.035

Hayashi, T., Thomas, G. M., and Huganir, R. L. (2009). Dual palmitoylation of NR2 subunits regulates NMDA receptor trafficking. *Neuron* 64, 213–226. doi: 10.1016/j.neuron.2009.08.017

Hollmann, M., and Heinemann, S. (1994). Cloned glutamate receptors. *Annu. Rev. Neurosci.* 17, 31–108. doi: 10.1146/annurev.ne.17.030194.000335

Iizumi, M., Oota-Ishigaki, A., Yamashita, M., and Hayashi, T. (2021). Reduced effect of anticonvulsants on AMPA receptor palmitoylation-deficient mice. *Front. Pharmacol.* 12:711737. doi: 10.3389/fphar.2021.711737

Itoh, M., Kaizuka, T., and Hayashi, T. (2017). Evolutionary acquisition and divergence of vertebrate HCN2 palmitoylation. *Neurotransmitter* 4:e1603. doi: 10.14800/nt.1603

Itoh, M., Okuno, H., Yamada, D., Yamashita, M., Abe, M., Natsume, R., et al. (2019). Perturbed expression pattern of the immediate early gene Arc in the dentate gyrus of GluA1 C-terminal palmitoylation-deficient mice. *Neuropsychopharmacol. Rep.* 39, 61–66. doi: 10.1002/npr2.12044

Itoh, M., Yamashita, M., Kaneko, M., Okuno, H., Abe, M., Yamazaki, M., et al. (2018). Deficiency of AMPAR-palmitoylation aggravates seizure susceptibility. *J. Neurosci.* 38, 10220–10235. doi: 10.1523/JNEUROSCI.1590-18.2018

Kaizuka, T., and Hayashi, T. (2018). Comparative analysis of palmitoylation sites of serotonin (5-HT) receptors in vertebrates. *Neuropsychopharmacol. Rep.* 38, 75–85. doi: 10.1002/npr2.12011

Kessels, H. W., and Malinow, R. (2009). Synaptic AMPA receptor plasticity and behavior. *Neuron* 61, 340–350. doi: 10.1016/j.neuron.2009.01.015

Korycka, J., Lach, A., Heger, E., Boguslawska, D. M., Wolny, M., Toporkiewicz, M., et al. (2012). Human DHHC proteins: a spotlight on the hidden player of palmitoylation. *Eur. J. Cell Biol.* 91, 107–117. doi: 10.1016/j.ejcb.2011.09.013

Lin, D. T., and Conibear, E. (2015). Enzymatic protein depalmitoylation by acyl protein thioesterases. *Biochem. Soc. Trans.* 43, 193–198. doi: 10.1042/BST20140235

Matt, L., Kim, K., Chowdhury, D., and Hell, J. W. (2019). Role of palmitoylation of postsynaptic proteins in promoting synaptic plasticity. *Front. Mol. Neurosci.* 12:8. doi: 10.3389/fnmol.2019.00008

Mattison, H. A., Hayashi, T., and Barria, A. (2012). Palmitoylation at two cysteine clusters on the C-terminus of GluN2A and GluN2B differentially control synaptic targeting of NMDA receptors. *PLoS One* 7:e49089. doi: 10.1371/journal.pone.0049089

Mori, H., and Mishina, M. (2003). Roles of diverse glutamate receptors in brain functions elucidated by subunit-specific and region-specific gene targeting. *Life Sci.* 74, 329–336. doi: 10.1016/j.lfs.2003.09.020

Pickering, D. S., Taverna, F. A., Salter, M. W., and Hampson, D. R. (1995). Palmitoylation of the GluR6 kainate receptor. *Proc. Natl. Acad. Sci. U S A* 92, 12090–12094. doi: 10.1073/pnas.92.26.12090

Resh, M. D. (2016). Fatty acylation of proteins: the long and the short of it. *Prog. Lipid Res.* 63, 120–131. doi: 10.1016/j.plipres.2016.05.002

Seeburg, P. H. (1993). The TINS/TiPS lecture. the molecular biology of mammalian glutamate receptor channels. *Trends Neurosci.* 16, 359–365. doi: 10.1016/0166-2236(93)90093-2

Shepherd, J. D., and Huganir, R. L. (2007). The cell biology of synaptic plasticity: AMPA receptor trafficking. *Annu. Rev. Cell Dev. Biol.* 23, 613–643. doi: 10.1146/annurev.cellbio.23.090506.123516

Springer, M. S., Meredith, R. W., Janecka, J. E., and Murphy, W. J. (2011). The historical biogeography of mammalia. *Philos. Trans. R. Soc. Lond B Biol. Sci.* 366, 2478–2502. doi: 10.1098/rstb.2011.0023

Springer, M. S., and Murphy, W. J. (2007). Mammalian evolution and biomedicine: new views from phylogeny. *Biol. Rev. Camb. Philos. Soc.* 82, 375–392. doi: 10.1111/j.1469-185X.2007.00016.x

Thomas, G. M., and Hayashi, T. (2013). Smarter neuronal signaling complexes from existing components: how regulatory modifications were acquired during animal evolution: evolution of palmitoylation-dependent regulation of AMPA-type ionotropic glutamate receptors. *Bioessays* 35, 929–939. doi: 10.1002/bies.201300076

Thomas, G. M., Hayashi, T., Chiu, S. L., Chen, C. M., and Huganir, R. L. (2012). Palmitoylation by DHHC5/8 targets GRIP1 to dendritic endosomes to regulate AMPA-R trafficking. *Neuron* 73, 482–496. doi: 10.1016/j.neuron.2011.11.021

Thomas, G. M., Hayashi, T., Huganir, R. L., and Linden, D. J. (2013). DHHC8-dependent PICK1 palmitoylation is required for induction of cerebellar long-term synaptic depression. *J. Neurosci.* 33, 15401–15407. doi: 10.1523/JNEUROSCI.1283-13.2013

Yokoi, N., Fukata, Y., Sekiya, A., Murakami, T., Kobayashi, K., and Fukata, M. (2016). Identification of PSD-95 depalmitoylating enzymes. *J. Neurosci.* 36, 6431–6444. doi: 10.1523/JNEUROSCI.0419-16.2016

Conflict of Interest: The author declares that the research was conducted in the absence of any commercial or financial relationships that could be construed as a potential conflict of interest.

Publisher's Note: All claims expressed in this article are solely those of the authors and do not necessarily represent those of their affiliated organizations, or those of the publisher, the editors and the reviewers. Any product that may be evaluated in this article, or claim that may be made by its manufacturer, is not guaranteed or endorsed by the publisher.

frontiers in Molecular Neuroscience

REVIEW
published: 03 January 2022
doi: 10.3389/fnmol.2021.801882

Tetraspanins as Potential Modulators of Glutamatergic Synaptic Function

*Amina Becic†, Jennifer Leifeld†, Javeria Shaukat† and Michael Hollmann**

Department of Biochemistry I – Receptor Biochemistry, Faculty of Chemistry and Biochemistry, Ruhr University Bochum, Bochum, Germany

Tetraspanins (Tspans) comprise a membrane protein family structurally defined by four transmembrane domains and intracellular N and C termini that is found in almost all cell types and tissues of eukaryotes. Moreover, they are involved in a bewildering multitude of diverse biological processes such as cell adhesion, motility, protein trafficking, signaling, proliferation, and regulation of the immune system. Beside their physiological roles, they are linked to many pathophysiological phenomena, including tumor progression regulation, HIV-1 replication, diabetes, and hepatitis. Tetraspanins are involved in the formation of extensive protein networks, through interactions not only with themselves but also with numerous other specific proteins, including regulatory proteins in the central nervous system (CNS). Interestingly, recent studies showed that Tspan7 impacts dendritic spine formation, glutamatergic synaptic transmission and plasticity, and that Tspan6 is correlated with epilepsy and intellectual disability (formerly known as mental retardation), highlighting the importance of particular tetraspanins and their involvement in critical processes in the CNS. In this review, we summarize the current knowledge of tetraspanin functions in the brain, with a particular focus on their impact on glutamatergic neurotransmission. In addition, we compare available resolved structures of tetraspanin family members to those of auxiliary proteins of glutamate receptors that are known for their modulatory effects.

Keywords: tetraspanins, CNS, synaptic function, glutamate receptor, modulator structures

OPEN ACCESS

Edited by:
Dhrubajyoti Chowdhury, Yale University, United States

Reviewed by:
Janosch P. Heller, Dublin City University, Ireland
Alexander I. Sobolevsky, Columbia University Irving Medical Center, United States

****Correspondence:***
Michael Hollmann
michael.hollmann@rub.de

† These authors have contributed equally to this work and share first authorship

Specialty section:
This article was submitted to Molecular Signalling and Pathways, a section of the journal Frontiers in Molecular Neuroscience

Received: *25 October 2021*
Accepted: *07 December 2021*
Published: *03 January 2022*

Citation:
Becic A, Leifeld J, Shaukat J and Hollmann M (2022) Tetraspanins as Potential Modulators of Glutamatergic Synaptic Function. Front. Mol. Neurosci. 14:801882. doi: 10.3389/fnmol.2021.801882

INTRODUCTION

A large family of abundantly expressed transmembrane proteins, found in all multicellular eukaryotes and comprising 33 members in humans, create an important protein network involved in a wide range of cellular processes such as cell proliferation, adhesion, signaling, fusion, and migration (Boucheix and Rubinstein, 2001). Back in 1988, a melanoma-associated antigen (ME491) was identified to consist of four transmembrane domains (TMs) (Hotta et al., 1988). Two years later its sequence homology to the Sm23 antigen found in the parasitic trematode *Schistosoma mansoni* was recognized (Wright et al., 1990). Further investigations revealed that the proteins CD37 (Classon et al., 1989) and TAPA-1 (target of the antiproliferative antibody 1, later denoted as CD81) (Oren et al., 1990) also share structural similarity. For classification purposes, the term "tetraspanins" was proposed for all members of the transmembrane four superfamily (TM4SF) (Maecker et al., 1997) (see **Table 1** for overview of tetraspanin nomenclature). These proteins are believed to function through their shared exceptional ability to interact with each other and numerous partner proteins to create a dynamic network of interactions known as the "tetraspanin

TABLE 1 | Summary of human tetraspanins with their alternative names, tissue specificity and the functions.

Name	Alternative names *	Tissue specificity*	Protein function
Tetraspanin1	TSPAN-1, NET-1	Intestine, testis	Regulation of cell development, activation, growth and motility (Liu et al., 2019; Wang L. et al., 2021). Prognostic role in prostate (Stinnesbeck et al., 2021), pancreatic (Ma C. et al., 2021), and cervical (Wollscheid et al., 2002) cancer
Tetraspanin2	TSPAN-2, FLJ12082, TSN2	Smooth muscle	Contribution to oligodendrocyte differentiation into myelin-forming glia (Yaseen et al., 2017). Modulation of microglial cells (Reynolds and Mahajan, 2020). Association with migraine (Esserlind et al., 2013)
Tetraspanin3	TSPAN-3, TM4-A, TM4SF8	Low tissue specificity	Regulation of the expression of ADAM10, presenilin and the amyloid precursor protein (Seipold and Saftig, 2016). Associated with progression of acute myeloid leukemia (Kwon et al., 2015; Yang et al., 2016; Sun et al., 2020; Zhang Z. Y. et al., 2020)
Tetraspanin4	TSPAN-4, NAG-2, TM4SF7	Low tissue specificity	Potential biomarker in hepatocellular carcinoma and plays a critical role in promoting cancer cell proliferation (Li et al., 2021). Interacts with histamine H4 receptor (Ma X. et al., 2021)
Tetraspanin5	TSPAN-5, NET-4, TM4SF9	Brain and ovary	Promotes metastasis of hepatocellular carcinoma through Notch signaling (Xie et al., 2021). Involved in dendritic spine maturation process (Moretto et al., 2019). Plays a role in regulation of ADAM10 compartmentalization (Jouannet et al., 2016) and trafficking (Dornier et al., 2012) to the cell surface
Tetraspanin6	TSPAN-6, T245, TM4SF6	Salivary gland	Regulator of carcinogenesis in colorectal cancer (Andrijes et al., 2021), retinoic acid-inducible gene I-like receptor-mediated immune signaling (Wang et al., 2012) and Amyloid Precursor Protein metabolism (Guix et al., 2017)
Tetraspanin7	TSPAN-7, A15, CD231, DXS1692E, MRX58, MXS1, TALLA-1, TM4SF2	Brain	Involved in HIV-1 host-virus interaction (Ménager, 2017; Perot et al., 2020) regulates AMPA receptor trafficking (Bassani et al., 2012) and is autoantibody target in type 1 diabetes (McLaughlin et al., 2020)
Tetraspanin8	TSPAN-8, CO-029, TM4SF3	Intestine	Target candidate for immunotherapy of pancreatic adenocarcinoma (Schäfer et al., 2021). Highly expressed in renal carcinoma (Tang et al., 2020) and involved in lung adenocarcinoma migration (Xu et al., 2020)
Tetraspanin9	TSPAN9, NET-5	Brain, heart muscle	Regulates gastric cancer cell migration and invasion (Li et al., 2016; Qi et al., 2019) platelet function (Protty et al., 2009) and modulates the early endosome in virus entry (Stiles and Kielian, 2016)
Tetraspanin10	TSPAN10, OCSP	Retina	Involved in trafficking regulation of the transmembrane metalloprotease ADAM10 (Dornier et al., 2012). Genetic variant within the TSPAN10 gene is associated with strabismus (Plotnikov et al., 2019)
Tetraspanin11	TSPAN11	Intestine	Participates in determining the direction of bone matrix organization (Nakanishi et al., 2019)
Tetraspanin12	TSPAN12, NET-2, TM4SF12	Low tissue specificity	Involved in retinal vascularization by regulating norrin (NDP) signal transduction (Junge et al., 2009). Promotes ADAM10 maturation, facilitating ADAM10-dependent proteolysis of APP (Xu et al., 2009). Heterozygous mutation in TSPAN12 gene is associated with familial exudative vitreoretinopathy (Carroll and Kim, 2019)
Tetraspanin13	TSPAN13, NET-6, TM4SF13	Low tissue specificity	Potential marker indicating the outcome of breast cancer (Jiang et al., 2019). Involved in pathophysiology of thyroid cancer (Li et al., 2019)
Tetraspanin14	TSPAN14, DC-TM4F2, MGC11352, TM4SF14	Low tissue specificity	Regulates maturation and trafficking of the transmembrane metalloprotease ADAM10 (Dornier et al., 2012; Haining et al., 2017; Moretto et al., 2019; Noy et al., 2019)
Tetraspanin15	TSPAN15, NET-7, TM4SF15	Low tissue specificity	Essential subunit of an ADAM10 scissor complex (Koo et al., 2020). Overexpression positively regulates development oral squamous cell carcinoma (Hiroshima et al., 2019). Stemness-related marker in hepatocellular carcinoma (Sidahmed-Adrar et al., 2019)
Tetraspanin16	TSPAN16, TM-8, TM4-B, TM4SF16	Blood, testis	Under-expressed in acute lymphoblastic leukemia (Juric et al., 2007)
Tetraspanin17	TSPAN17, FBX23, FBXO23, TM4SF17	Low tissue specificity	Involved in regulation of ADAM10 trafficking (Dornier et al., 2012; Reyat et al., 2017). Decreased levels associated with improved survival in glioblastoma multiforme (Guo et al., 2019)
Tetraspanin18	TSPAN18	Low tissue specificity	Regulator of thrombo-inflamation (Noy et al., 2019; Gavin et al., 2020). Involved in the development of psychotic symptoms and schizophrenia (Yuan et al., 2013; Zhang et al., 2015; Liu et al., 2016; Wu et al., 2016)
Tetraspanin19	TSPAN19	Lung, pituitary gland	Specific function unclear
Tetraspanin20	TSPAN20, UPK1B, UPK1, Uroplakin 1B	Placenta, urinary bladder	Plays an important role in normal bladder epithelial physiology (Wu et al., 1995; Lobban et al., 1998). Involved in renal cell carcinoma (Yuasa et al., 1998; Finch et al., 1999; Wang et al., 2018; Zhang Z. Y. et al., 2020) and urinary tract inflammation prediction (Bulut et al., 2014)

(Continued)

TABLE 1 | (Continued)

Name	Alternative names *	Tissue specificity*	Protein function
Tetraspanin21	TSPAN21, UPK1A, Uroplakin 1A	Prostate, urinary bladder	Plays an important role in normal bladder epithelial physiology (Wu et al., 1995; Lobban et al., 1998; Ogawa et al., 1999; Hall et al., 2005). Upregulation connected with lung cancer cells (Byun et al., 2020), downregulation enhances apoptosis of bladder carcinoma cells (Zhu et al., 2015) and reduced expression associated with gastric adenocarcinoma (Zheng et al., 2014)
Tetraspanin22	TSPAN22, PRPH2, CACD2, rd2, RDS, RP7, Peripherin 2	Retina	Essential for retina photoreceptor outer segment disk morphogenesis (Donato et al., 2021) and involved in retinal degeneration (Travis et al., 1991), macular dystrophy (Kumaran et al., 1993; Çavdarli et al., 2020) and retinitis pigmentosa (Kajiwara et al., 1991; Farrar et al., 1992; Jordan et al., 1992; Li et al., 2021)
Tetraspanin23	TSPAN23, ROM1, ROM, Retinal outer segment membrane protein 1	Retina	Plays a role in rod outer segment (ROS) morphogenesis (Conley et al., 2017). Involved in retinitis pigmentosa (Kajiwara et al., 1991; Bascom et al., 1992; Böhm et al., 2017). Potential tumor suppressor for lung cancer (Zhang M. et al., 2021)
Tetraspanin24	TSPAN24, CD151 molecule (Raph blood group), CD151 (PETA-3, RAPH, SFA-1	Low tissue specificity	Essential in kidney and skin morphogenesis (Karamatic Crew et al., 2004). Downregulation induces apoptosis in trophoblast cells in preeclampsia (Wang Z. et al., 2021). Marker for activated T cells (Perez et al., 2020)
Tetraspanin25	TSPAN25, CD53, MOX44	Blood, lymphoid tissue	Immune cell function regulator (Dunlock, 2020). Associated with tuberculosis (Omae et al., 2017; Jin et al., 2019). Leukocyte surface antigen (Angelisová et al., 1990; Horejsí and Vlcek, 1991)
Tetraspanin26	TSPAN26, CD37	Blood, lymphoid tissue	Potential biomarker in acute myeloid leukemia (Stilgenbauer et al., 2019; Zhang Q. et al., 2020). Leukocyte antigen (Classon et al., 1989; Horejsí and Vlcek, 1991). Associates with MHC class II glycoproteins (Angelisová et al., 1994)
Tetraspanin27	TSPAN27, CD82, IA4, KAI1, R2, ST6	Low tissue specificity	Suppresses migration in prostate cancer (Ichikawa et al., 1992; Dodla et al., 2020; Ma et al., 2020). Involved in pancreatic cancer (Liu X. et al., 2021). Regulation of oligodendrocyte progenitor cell myelination (Mela and Goldman, 2009)
Tetraspanin28	TSPAN28, CD81, TAPA-1, TAPA1	Low tissue specificity	Involved in lymphocyte cell membrane organization (Schaffer and Minguet, 2020). Knockout disrupts engraftment in acute lymphoblastic leukemia (Quagliano et al., 2020). Expressed on microglia (Reynolds and Mahajan, 2020)
Tetraspanin29	TSPAN29, CD9, BA2, MIC3, MRP-1, P24	Low tissue specificity	Regulates development of acute myeloid leukemia (Liu Y. et al., 2021). Associated with integrins (Torres-Gómez et al., 2021). Leukocyte surface protein (Horejsí and Vlcek, 1991). Expressed on microglia (Reynolds and Mahajan, 2020). Maintenance of the myelin sheet (Nakamura et al., 1996)
Tetraspanin30	TSPAN30, CD63, ME491, MLA1	Low tissue specificity	Negatively regulates hepatocellular carcinoma (Yu S. et al., 2021). Leukocyte surface glycoprotein (Horejsí and Vlcek, 1991). Involved in neural stem cell adhesion and migration (Lee et al., 2014)
Tetraspanin31	TSPAN31, SAS	Low tissue specificity	Suppresses cell proliferation of cervical cancer (Xia et al., 2020). Amplified in human sarcomas (Jankowski et al., 1995)
Tetraspanin32	TSPAN32, PHEMX, TSSC6	Blood, bone marrow, heart muscle, lymphoid tissue	Significantly reduced levels in CD4 T cells of multiple sclerosis patients (Lombardo et al., 2019)
Tetraspanin33	TSPAN33, MGC50844, Penumbra	Kidney	Regulates migration of human B lymphocytes (Navarro-Hernandez et al., 2020) and used as s marker of activated and malignant B cells (Luu et al., 2013). Regulates trafficking of the metalloprotease ADAM10 (Dornier et al., 2012). Highly expressed in erythroid progenitors (Heikens et al., 2007)

Data marked with (*) is obtained from the protein atlas database (proteinatlas.org). The "Tissue specificity" category is based on mRNA expression levels in the analyzed samples based on a combination of data from HPA, GTEX, and FANTOM5 obtained from proteinatlas.org.

web" or "tetraspanin-enriched microdomains" (TEMs) on the cell surface (Hemler, 2003; Charrin et al., 2009; Dornier et al., 2012). Consequently, tetraspanins are also regarded as molecular organizers (Boucheix and Rubinstein, 2001). For example, the interaction of tetraspanins with integrins has been well documented (Schmidt et al., 1996; Bassani and Cingolani, 2012). Integrins are cell adhesion molecules consisting of an α- and a β-subunit and can mediate both cell–cell and cell–extracellular matrix interactions (Hynes, 2002; Bassani and Cingolani, 2012). In this contect, tetraspanins, in the form of TEMs, are believed to exert a scaffolding function and organize proteins spatially and temporally in biological membranes (Perot and Ménager, 2020). For example, TEMs may be enriched in integrins and thus act as functional units involved in cell adhesion (Termini and Gillette, 2017; Perot and Ménager, 2020). With respect to the role of TEMs in the brain, interactions between Tspan28 (CD81) and Tspan29 (CD9) with integrins α3β1 and α6β1 have been shown to influence neurite growth (Schmidt et al., 1996; Stipp and Hemler, 2000; Bassani and Cingolani, 2012). Thus, these distinct units organized by tetraspanins play diverse roles in a variety of biological processes such as in viral infections, in cell–cell adhesion through interplay with the aforementioned integrins,

and in cancer development and metastasis (Perot and Ménager, 2020). Viruses have been reported to preferentially enter cells via TEMs, which presumably can happen with or without direct binding to tetraspanins as receptors for virus entry (Pileri et al., 1998; Martin et al., 2005; Charrin et al., 2009; He et al., 2013; Hantak et al., 2019).

THE STRUCTURE OF TETRASPANINS

Tetraspanins are small integral membrane proteins that range in size from 204 (Tspan13) to 355 (Tspan10) amino acids (Charrin et al., 2009) and have a molecular weight of 20–30 kDa (Bassani and Cingolani, 2012). Topologically, tetraspanins possess four TMs, where the first two (TM1 and TM2) are linked by a small extracellular loop (EC1) of 20–28 amino acids and the last two (TM3 and TM4) are connected by a large extracellular loop (EC2) of 76–131 amino acids (Berditchevski, 2001; Huang et al., 2005; Lazo, 2007). TM2 and TM3 are joined by a very short intracellular loop (IL) (**Figure 1**). In addition, tetraspanins comprise short cytosolic N- and C-termini (Huang et al., 2005; Seigneuret, 2006). Tetraspanins are distinguished from other proteins with four TMs by several distinct features. These include the unequal size of the two extracellular loops, the presence of two to four cysteine pairs, and a CCG motif (Cys-Cys-Gly sequence) in EC2 (**Figure 1**). In addition, over 50% of tetraspanins carry a PxxCC (Pro-x-x-Cys-Cys) motif, where x can be any amino acid (Berditchevski, 2001; Huang et al., 2005; Seigneuret, 2006). The cysteine pairs in EC2 play an essential role for the correct folding of the domain by forming disulfide bridges (Berditchevski, 2001). Furthermore, a highly conserved subfamily of tetraspanins known as TspanC8, comprising Tspan5, Tspan10, Tspan14, Tspan15, Tspan17, and Tspan33, is characterized by their unique property of possessing eight cysteines within their EC2 (Boucheix and Rubinstein, 2001; Huang et al., 2005). Most tetraspanins are potentially N-glycosylated in EC2 (Maecker et al., 1997). Tetraspanins known to be un-glycosylated are Tspan28 (CD81) and Tspan12 (Net-2), while Tspan29 (CD9) contains an N-glycosylation site in EC1 (Boucheix and Rubinstein, 2001). Presumably, most tetraspanins are also S-acylated. For example, palmitoylation has been demonstrated in three independent studies for each tetraspanin tested (Seehafer et al., 1988; Berditchevski et al., 2002; Charrin et al., 2002; Yang et al., 2002; Stipp et al., 2003). In addition, ubiquitination has already been demonstrated for Tspan6 (Wang et al., 2012), Tspan24 (CD151), Tspan27 (CD82) (Tsai et al., 2007), and Tspan28 (CD81) (Lineberry et al., 2008; Charrin et al., 2009; Termini and Gillette, 2017).

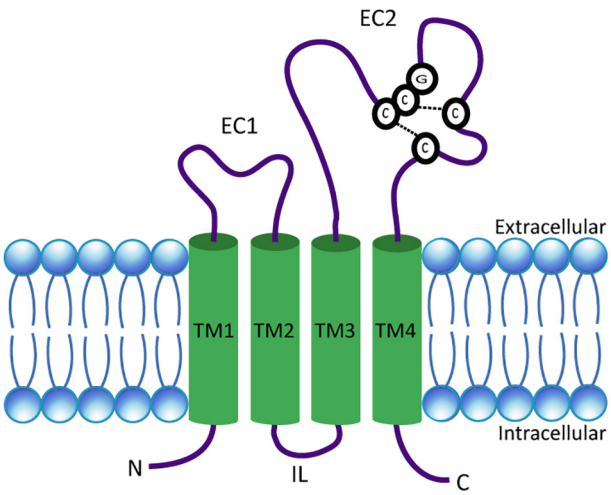

FIGURE 1 | Schematic presentation of a tetraspanin. The model depicts the conserved structural features of tetraspanins. EC1 and EC2 represent the short and large extracellular domains, respectively. Transmembrane domains TM1–TM4 and the CCG motif along with disulfide bonds between two pairs of cysteine residues in EC2 are shown. N- and C-termini as well as the intracellular loop (IL) are located in the cytosol.

PHYSIOLOGICAL FUNCTIONS OF TETRASPANINS

In addition to the research dedicated to uncovering all of the structural peculiarities of this protein family, a major effort has been made over the last 20 years to shed more light on the involvement of these proteins in various physiological functions in the body. Many tetraspanins are involved in the process of cell development, activation, growth regulation, and motility. It has been shown that Tspan1 significantly reduces cell migration, tissue invasion, and increases apoptosis of human pancreatic cancer cells (Tian et al., 2018). Furthermore, the expression of Tspan3, Tspan4, and Tspan7 in cells with high migratory potential suggests a role in the regulation of migration processes (Kashef et al., 2013). Down-regulation of Tspan8 inhibits the proliferation and migration of colorectal cancer cells, while over-expression promotes the opposite effects (Zhang et al., 2019). Overexpression of Tspan9 significantly inhibits the proliferation, migration, and invasion of human gastric cancer cells (Li et al., 2016). Direction of bone matrix organization orthogonal to osteoblast alignment is controlled by Tspan11-mediated focal adhesion assembly (Nakanishi et al., 2019).

Another context in which tetraspanins are involved, is the immune system and regulation of inflammatory pathways. Tspan18 knockout mice have reduced thrombus size in a deep vein thrombosis model, and reduced platelet deposition in the microcirculation following myocardial ischemia-reperfusion injury (Noy et al., 2019). Tspan26 is a B-cell surface antigen widely expressed on mature B cells, and it is involved in immune regulation and tumor suppression (Xu-Monette et al., 2016). Tspan28 (CD81) knockout cells show impaired viral DNA replication and produce greatly diminished viral titers in Herpes simplex virus 1 infection in a neuroblastoma cell model (Benayas et al., 2020).

Since Tspan28, Tspan29, and Tspan30 are abundantly expressed on extracellular vesicles categorized as exosomes, they are also used as exosomal markers (Lai et al., 2010; Oksvold et al., 2015). Tspan31 is a critical regulator of transduction of survival and apoptotic signals in hepatocellular carcinoma cells

(Wang et al., 2018). Two tetraspanins (Tspan20 and Tspan21), better known as uroplakins (UPKs), are involved in normal bladder epithelial physiology. Tspan20, also known as uroplakin 1B (UPK1B), promotes the invasion and metastasis of bladder cancer via regulation of the Wnt/β-catenin pathway (Wang et al., 2018; Zhang Z. Y. et al., 2020), while the reduced expression of Tspan21 (UPK1A) might play a role in the progression of gastric cancer (Zheng et al., 2014).

The standardized tetraspanin nomenclature (Charrin et al., 2009) utilizes a simple numbering system from Tspan1 to Tspan33. However, in certain research fields other names for some of the tetraspanin proteins are more frequently used. A summary of all human tetraspanins including their alternative names, tissue-specific RNA expression, and their reported involvement in different physiological or pathophysiological processes is listed in **Table 1**.

TETRASPANINS IN THE CENTRAL NERVOUS SYSTEM

One of the first evidences of tetraspanins playing an important role in the CNS came from research on the *Drosophila melanogaster* tetraspanin late bloomer (lbl) in the middle of the 1990s. It was observed that in fly mutants lacking this protein, adjacent motoneurons showed increased ectopic sprouting, and synapse formation was delayed. These results, which indicate that lbl promotes the formation of motor neuron synapses in the fruit fly, suggest that other tetraspanins may also be involved in this process and that a similar mechanism may also be found in mammals (Kopczynski et al., 1996). Furthermore, RNA *in situ* analyses of all tetraspanin family genes found in *Drosophila* revealed that most tetraspanins are either specifically expressed in the nervous system or intestines or have ubiquitously low levels of expression. In addition, other studies suggested that the tetraspanins are not critical for neurite growth but that their absence delays the formation of the final synaptic contact points of motor neuron axons. Moreover, the tetraspanins expressed by motor neurons showed partial compensation for the role of deleted lbl (Fradkin et al., 2002).

Following these studies in *Drosophila*, numerous research efforts in the following years focused on demonstrating the importance and involvement of tetraspanins in various processes in the CNS. Since the tetraspanins are referred to as "molecular organizers," it became clear that certain tetraspanins playing an important role in regulating ADAM10 (A disintegrin and metalloproteinase 10), are involved in the Notch signaling pathway, and are essential for photoreceptor function.

ADAM10 Regulation by Tetraspanins

Tetraspanins have been reported to regulate metalloproteases. Particularly important for the nervous system is ADAM10 also known as Kuzbanian in *Drosophila*, which works as "molecular scissors" and is responsible for cleaving the extracellular portion of dozens of transmembrane proteins including amyloid precursor protein (APP), notch, and cadherin (Hartmann et al., 2002; Reiss et al., 2005; Kuhn et al., 2010; Dornier et al., 2012; Groot et al., 2014; Seipold and Saftig, 2016). It has been shown that Tspan3 acts as a stabilizing factor of active ADAM10, APP, and the γ-secretase complex at the plasma membrane and Tspan12 and Tspan15 may be involved in Alzheimer's disease physiopathology (Seipold et al., 2017). It was found that all members of the TspanC8 subfamily are directly involved in the regulation of ADAM10 exit from the ER and play an important role in its enzymatic maturation by promoting its trafficking to the cell surface (Dornier et al., 2012). TspanC8s, indeed, differentially regulate ADAM10 membrane compartmentalization through atypical association. Four TspanC8 members, in particular Tspan5, Tspan14, Tspan15, and Tspan33, increase ADAM10 expression at the cell surface (Dornier et al., 2012). Mass spectrometric analysis suggested a reduced interaction of ADAM10 with other components of the tetraspanin web in Tspan15-expressing cells. By contrast, ADAM10 association with other members of the C8 tetraspanin subfamily was increased in Tspan5-transfected cells (Jouannet et al., 2016). Recently, with the help of the first monoclonal antibodies generated against Tspan15, it was shown that ADAM10 and Tspan15 exist together at the cell surface and that ADAM10 is required for Tspan15 expression in cell lines (Koo et al., 2020). This suggests that the direct interaction of Tspan15 with ADAM10 makes it crucial for the ADAM10 scissor complex (Koo et al., 2020). In an independent study, mass spectrometric analysis revealed Tspan12 as a partner for ADAM10 that is involved in its maturation and increases ADAM10-mediated cleavage of the APP (Xu et al., 2009). Tspan15 was identified as the only member of the TspanC8 family involved in the promotion of ADAM10-dependent N-cadherin cleavage when overexpressed in human embryonic kidney cells (Noy et al., 2016). Some integrin–tetraspanin interactions facilitate maturation and cell surface expression of the integrin receptors. Since many tetraspanins contain PDZ domain-binding motifs, it is possible that some of them serve as linkers between integrins and intracellular PDZ scaffolding proteins or signal transduction molecules (Bassani and Cingolani, 2012).

Role of Tetraspanins in Notch Signaling

Notch has been established as one of the major substrates of the ADAM10 protease (Groot et al., 2014). Several studies have suggested that Notch has a crucial role in the synaptic plasticity of the mammalian brain (Costa et al., 2003, 2005; Wang et al., 2004). Depending on the level of receptor activation, Notch might decrease or increase long-term potentiation (LTP) (Wang et al., 2004; Dahlhaus et al., 2008). Human Tspan5 and Tspan33, the orthologs of *Caenorhabditis elegans* TSP-12, appear to facilitate γ-secretase-mediated cleavage and thus promote Notch activity (Dunn et al., 2010). Further investigation revealed that other members of TspanC8, Tspan5, and Tspan14, also appear to be promoters of ligand-induced Notch activity in U2OS and HeLa cells, while Tspan15 has the opposite effect (Dornier et al., 2012; Jouannet et al., 2016). The latter observation explains why the knockdown of Tspan15 enhances Notch activation (Jouannet et al., 2016).

The Tspan22 (peripherin 2) Connection to Photoreceptors

Human Tspan22, also known as peripherin 2 (PRPH2) or retinal degeneration slow (RDS), is located in the retina and abundantly expressed in the outer segment (OS) of photoreceptors (Molday and Molday, 1987; Milstein et al., 2020). PRPH2 is thought to be essential for the vision and morphogenesis of the OS, which consists of hundreds of disc membranes mainly responsible for the conversion of light signals into electrical signals. Membranous discs in OS undergo constant renewal (Young, 1967). In this regard, PRPH2 in a complex with rom-1 (rod outer segment membrane protein 1, which is another related tetraspanin) is required for the regulation of morphogenesis and structural integrity of the OS (Stuck et al., 2016; Murru et al., 2018). It was found that any gene-level mutation or defect in PRPH2 leads to a broad range of progressive retinal degeneration events in humans (Kohl et al., 1998), affecting mainly either rod or cone cell photoreceptors (Stuck et al., 2016). PRPH2-deficient mice show disrupted photoreceptor morphogenesis (Sanyal et al., 1980). In addition, PRPH2 serves as a molecular bridge between rhodopsin and the rod cyclic nucleotide-gated (CNG) channel complex in rod OS (Becirovic et al., 2014).

TETRASPANINS IN THE BRAIN

To point out other tetraspanins that may play important roles in the CNS, we extracted RNA expression level data in different brain regions from "The Human Protein Atlas" database (Uhlén et al., 2015) in **Figure 2**.

The tetraspanin with the strongest expression in the brain tissue is Tspan7 (**Table 1**), which also shows the strongest localization in cerebral cortex in comparison to other regions of the brain (**Figure 2**). Tspan7 was characterized as a key player in the morphological and functional maturation of glutamatergic synapses (Bassani and Passafaro, 2012). Tspan3 stands out as having one of the highest RNA expression levels in the brain among all tetraspanins (**Figure 2**).

Interestingly, the tetraspanins Tspan28, Tspan29, and Tspan30 exhibit overall high levels of RNA expression. Tspan29 and Tspan28 are shown to be expressed on microglial cells (Reynolds and Mahajan, 2020). Tspan29, more commonly called CD9, is involved in neurite outgrowth and cell migration, and it is associated with the α6β1 integrin and the neural adhesion molecule L1 in mouse brain (Schmidt et al., 1996). Tspan29 was also detected in human adult nervous tissue, and its expression is correlated with myelination where it may interact with the extracellular matrix and participate in the maintenance of the myelin sheath (Nakamura et al., 1996). It also enhances myelin membrane adhesion to extracellular matrices at very late stages of development (Kagawa et al., 1997). Furthermore, Tspan29 plays a role in glial cells in pathological conditions such as the devastating transmissible spongiform encephalopathy (TSE) (Doh-Ura et al., 2000).

Involvement of Tspan13 in modulating the coupling between the voltage sensor activation and pore opening of voltage-gated Ca^{2+} channels (encoded by the caveolin genes, abbreviated as CAV) was confirmed where Tspan13 has been identified as an interaction partner of the α1 subunit of N-type CaV2.2 (Mallmann et al., 2013).

Tspan27 (CD82) is a critical molecule in the regulation of oligodendrocyte progenitor cell migration and myelination (Mela and Goldman, 2009). Downregulation of this molecule in oligodendrocytes inhibits differentiation, reduces myelin protein accumulation, and leads to regression to less mature stages (Mela and Goldman, 2013). In addition, there is evidence that the CD82-TRPM7-Numb pathway is associated with age-related synapse/memory impairments (Zhao et al., 2020). Further, TIMP-1 (tissue inhibitor of metalloproteinase-1) has been identified as a potent key regulator of Tspan30 (CD63) and β1-integrin-mediated signaling that regulates human neural stem cell adhesion and migration (Lee et al., 2014).

TETRASPANINS AT GLUTAMATERGIC SYNAPSES

Ionotropic glutamate receptors (iGluRs) are ligand-gated cation selective ion channels that can be activated by the brain's major excitatory neurotransmitter L-glutamate. The family of iGluRs can be further subdivided into kainate (KA), N-methyl-D-aspartate (NMDA), α-amino-3-hydroxy-5-methyl-4-isoxazole propionate (AMPA) and Delta receptors (Hollmann and Heinemann, 1994; Sobolevsky et al., 2009; Traynelis et al., 2010). AMPARs are typically located at the post-synapse and mediate the majority of rapid excitatory neurotransmission (Gasic and Hollmann, 1992). They play a critical role in mechanisms such as synaptic plasticity and are associated with various neurodegenerative and neuropsychiatric disorders (Palmer et al., 2005). The AMPA receptor (AMPAR) subfamily consists of a total of four members (GluA1–GluA4) and they are functional as homomeric and heteromeric tetramers (Sager et al., 2009). Many different auxiliary subunits have been discovered, which influence AMPAR function in the CNS with respect to trafficking and gating. The most prominent and intensively studied auxiliary proteins are the so-called transmembrane AMPAR modulatory proteins (TARPs), of which there are six members in total (γ2, γ3, γ4, γ5, γ7, and γ8) (Tomita, 2010), with γ2 being the most extensively member studied to date. For example, γ2 promotes trafficking of AMPARs to the plasma membrane and influences their biophysical functions (Tomita, 2010). Thus, γ2 is able to slow receptor deactivation and at the same time strongly reduces receptor desensitization accompanied by a faster recovery from desensitization (Priel et al., 2005; Tomita, 2010; Ben-Yaacov et al., 2017). In addition, γ2 increases agonist affinity and influences receptor gating by increasing channel conductance and opening probability (Tomita, 2010; Ben-Yaacov et al., 2017).

Research over the last 20 years has revealed many interacting proteins that play a key role in the regulation of glutamate receptor trafficking and functions, which in turn leads to stabilization and strengthening of synaptic plasticity. Major directly interacting proteins of AMPARs include GRIP1 (glutamate receptor-interacting proteins 1) (Osten et al., 2000)

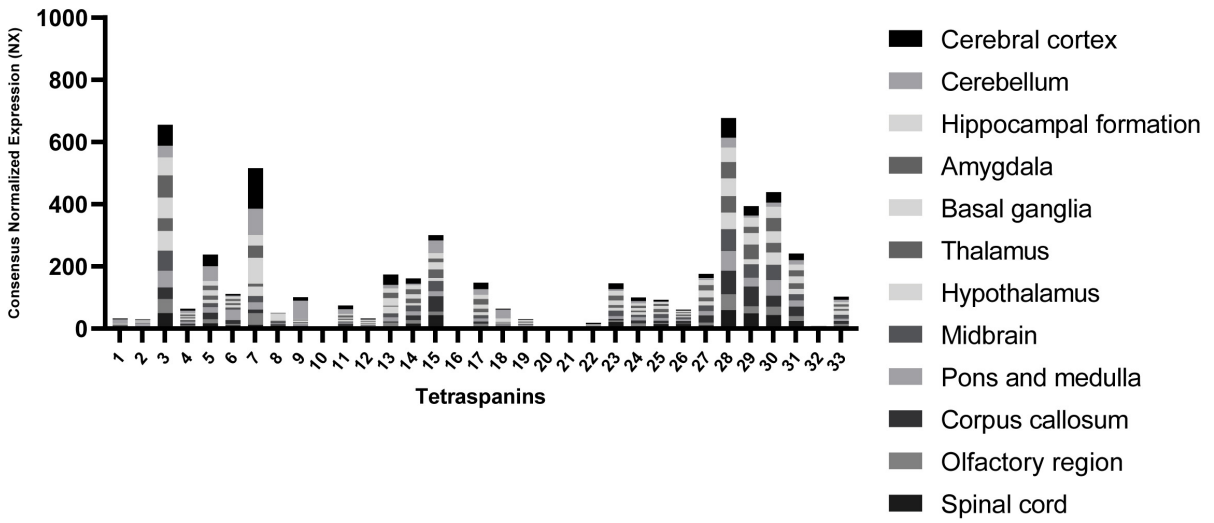

FIGURE 2 | RNA expression levels of tetraspanins in different regions of the brain. Consensus Normalized eXpression (NX) levels shown are created by combining the data from three transcriptomics datasets (HPA, GTEx, and FANTOM5) using normalization pipeline. Each bar contains combined data of all brain regions indicated. Data used to compose the graph obtained from the Human Protein Atlas database (proteinatlas.org).

and PICK1 (protein interacting with C kinase 1) (Xia et al., 1999), required for either insertion of AMPARs at the synaptic surface (Osten et al., 2000) or removal from the synaptic membrane (Braithwaite et al., 2002) as well as for the regulation of spine morphology.

Tspan6, associated with the neurological condition EFMR (epilepsy female-restricted with mental retardation, now referred to as intellectual disability), has been identified as a novel regulator of hippocampal synaptic transmission and LTP, with a key role in synapse development and AMPAR trafficking (Depienne et al., 2011; Vincent et al., 2012; Salas et al., 2017). It was speculated that the increased synaptic transmission observed by some authors was caused by an increased response to glutamate (Salas et al., 2017). However, no altered expression of synaptic proteins was detected (Salas et al., 2017). In fact, the expression of postsynaptic density protein 95 (PSD-95), AMPARs, NMDARs, and metabotropic glutamate receptors (mGluRs) was unchanged in the postsynaptic membrane (Salas et al., 2017). This observation applies equally to intracellular receptors, which are receptors that are not located in the plasma membrane but in intracellular compartments of the neuron, such as the ER or endosomes, and cell-surface receptors as well as to synaptically and non-synaptically localized GluA1-containing AMPARs (Salas et al., 2017). Moreover, no change in phosphorylation could be detected for the GluA1 subunit (Salas et al., 2017). The authors combine their seemingly contradictory results of an observed increase in basal synaptic transmission in combination with reduced LTP in the hypothesis of "occluded" LTP (Salas et al., 2017). This hypothesis posits that sustained, increased basal synaptic transmission inhibits the induction of LTP because further excitatory stimulation is not possible anymore. It has also been speculated that Tspan6 alters the biophysical properties of AMPARs, possibly in a TARP-like manner (Salas et al., 2017), so a direct interaction between Tspan6 and AMPARs may be possible.

Tspan7, which is highly homologous to Tspan6, is associated with the neurological disease X-linked intellectual disability (Zemni et al., 2000; Abidi et al., 2002; Bassani et al., 2012). Mutation of the TM4SF2 gene (=Tspan7) is a cause of a severe intellectual disability and cognitive impairment. The mutation is connected with alterations in AMPAR expression levels, which cause changes in excitatory synapse structure and function (Murru et al., 2017). The ampakine CX516 has been shown to have positive effects on Tspan7 knockout mice, rescuing the intellectual disability phenotype, suggesting pharmacological modulation of AMPARs as a potential therapeutic target (Murru et al., 2017).

Tspan7 has also been found to modulate glutamatergic synaptic transmission as well as synaptic plasticity (Bassani et al., 2012; Salas et al., 2017). In particular, it was shown to promote dendritic spine formation (Bassani et al., 2012). Effectively, Tspan7 influences neuronal morphogenesis by regulating filopodia density and dendritic spine morphology (Bassani et al., 2012). This is presumably mediated by interactions with integrin β1 and/or phosphatidylinositol 4-kinase (PI4K), and ultimately results in remodeling of the actin cytoskeleton, as speculated by the authors (Bassani et al., 2012). The authors furthermore demonstrated that Tspan7 interacts with the PDZ domain of PICK1 to regulate AMPAR trafficking and hippocampal spine development *in vitro* (Bassani et al., 2012). It was shown that the interaction of Tspan7 with PICK1 attenuates the internalization of AMPARs, which is typically mediated by the interaction of the latter with PICK1 (Perez et al., 2001). This subsequently leads to an increased availability of AMPARs at the postsynaptic membrane and thus to an enhanced excitability of the postsynaptic neuron (Bassani et al., 2012). Because co-immunoprecipitation experiments have shown

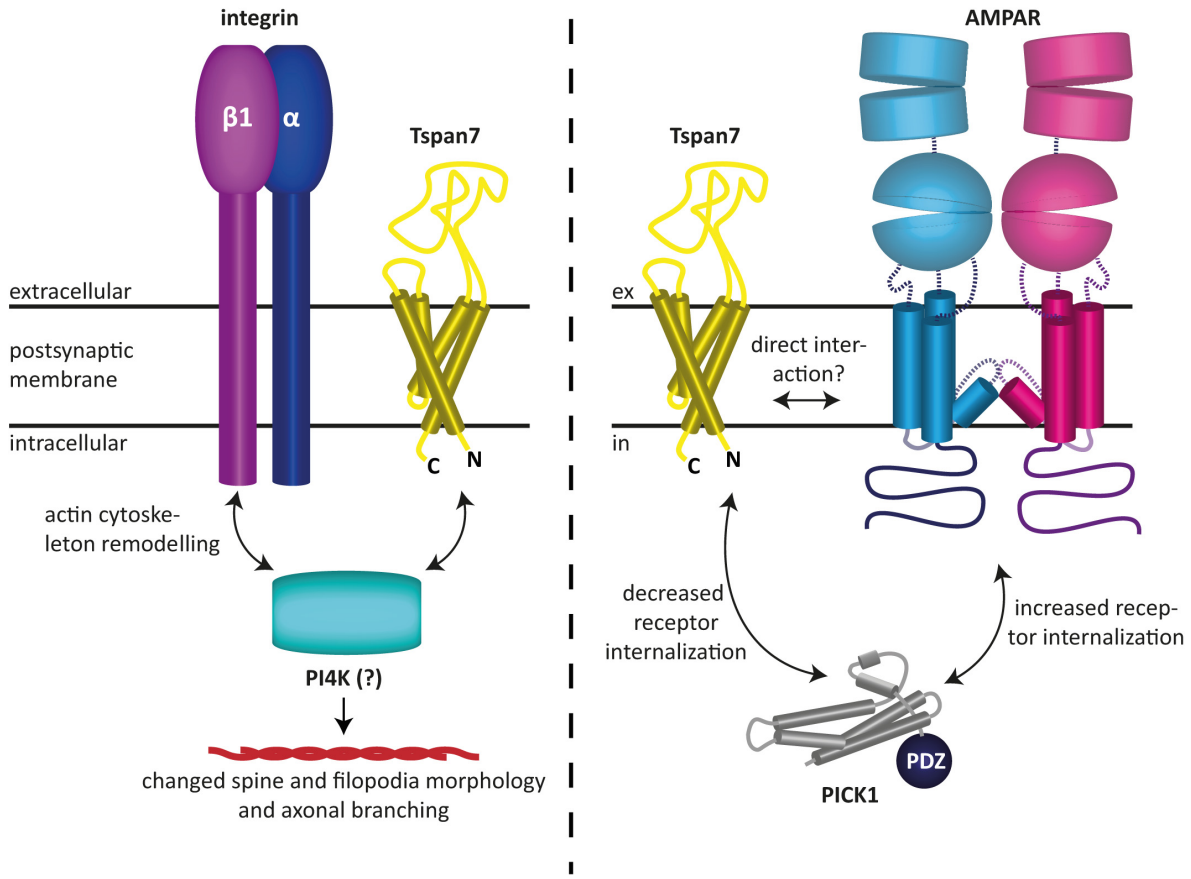

FIGURE 3 | Reported functions of Tspan7 in neurons. (Left) Tspan7 influences neuronal morphogenesis by regulating filopodia density and dendritic spine morphology. This is presumably mediated by interactions with integrin β1 and/or PI4K and ultimately results in remodeling of the actin cytoskeleton (Bassani et al., 2012). (Right) Tspan7 regulates synaptic function at glutamatergic synapses. Interaction of Tspan7 with PICK1 attenuates the internalization of AMPARs, which is typically mediated by the interaction of the latter with PICK1 (Perez et al., 2001). This subsequently leads to an increased availability of AMPARs at the postsynaptic membrane and thus to an enhanced excitability of the postsynaptic neuron. In this process, Tspan7 interacts with PICK1 via its C-terminus (Bassani et al., 2012). The figures are based on the illustrations of Bassani and Passafaro (2012) and Perot and Ménager (2020).

that the C-terminus of Tspan7 knocks down PICK1 and β1 integrin as well as the two AMPAR subunits GluA2 and GluA3, a macromolecular complex between the aforementioned proteins, in which Tspan7 serves as an organizer, has been hypothesized (Bassani et al., 2012). However, a direct modulation of AMPARs by Tspan7, similar to what has been proposed for Tspan6, appears equally plausible, as it could also explain the findings described in Bassani et al. (2012). In fact, like the prototypical TARP γ2, Tspan7 may preferentially interact with the GluA2 subunit, as it colocalizes with it most predominantly (Bassani et al., 2012), and hence could be responsible for the maintenance of normal synaptic plasticity. The fact that in the co-immunoprecipitation experiments Tspan7 pulled down two AMPAR subunits, namely GluA2 and GluA3, in addition to other proteins, may also indicate a direct interaction between the aforementioned proteins, although none of the proteomics studies published to date have found tetraspanins among the AMPAR-associated proteins discovered with these methods (Schwenk et al., 2012, 2014; Li et al., 2013; Chen et al., 2014; Bettler and Fakler, 2017). However, this does not necessarily mean that tetraspanins do not interact with AMPARs, as these studies rely on the specific properties of certain mild detergents, which may not, however, be suitable for maintaining the specific interactions of tetraspanins. An overview of the functions of Tspan7 in neurons described here and found by Bassani et al. (2012) is shown in **Figure 3**.

STRUCTURAL HOMOLOGIES BETWEEN TETRASPANINS AND KNOWN AMPA RECEPTOR MODULATORS

From the entire tetraspanin family, only the full-length structures of Tspan28 (CD81) (Zimmerman et al., 2016; Yang et al., 2020; Susa et al., 2021), Tspan29 (CD9) (Umeda et al., 2020), and Tspan25 (CD53) (Yang et al., 2020) have been resolved to date, and the structures were found to be highly similar. Thus, the four TMs of Tspan25, Tspan28, and Tspan29 each form an ice

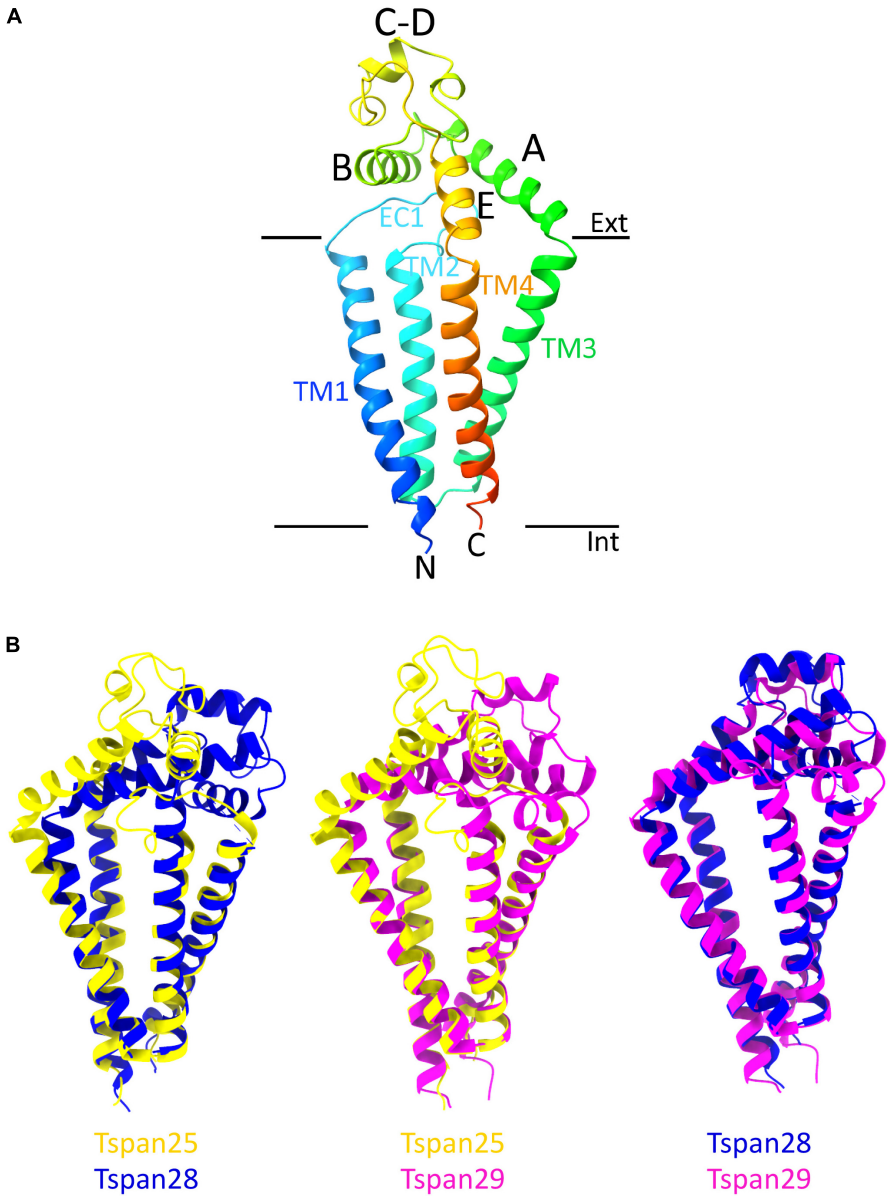

FIGURE 4 | Overall structure of a tetraspanin **(A)**. Helices A–E are indicated in the EC2 domain between TM3 and TM4. Helices A, B, and E represent conserved regions, while helices C–D are variable among tetraspanins. Superposition of all previously resolved structures of tetraspanins **(B)**. Shown is the overlay of Tspan25 (pdb model 6WVG in yellow) with Tspan28 (pdb model 5TCX in blue) and of Tspan25 (yellow) with Tspan29 (pdb model 6K4J in magenta) as well as of Tspan28 (blue) with Tspan29 (magenta).

cream cone-shaped structure with two TM pairs forming the sides of this structure (**Figure 4B**; Zimmerman et al., 2016; Umeda et al., 2020; Yang et al., 2020). The TM domains of all solved tetraspanins structures are virtually superimposable (**Figure 4B**), with Tspan25 in the open conformation, without bound lipid, adopting the same structure as Tspan28 and Tspan29 in the closed form with bound cholesterol (Yang et al., 2020). The EC2 domains of the beforementioned tetraspanins can be generally described as mushroom-like structures that have a total of five helices A to E. Here, helices A and E form the fungal stem, while helix B forms the fungal head together with the variable C–D region (**Figure 4A**) (Zimmerman et al., 2016; Umeda et al., 2020; Yang et al., 2020). The general mushroom shape is visible in all resolved structures, whereas slightly larger structural variations are apparent in the C–D region (**Figure 4B**).

The EC2 domain is thought to be responsible for the partnering of the respective tetraspanins with other proteins, a property facilitated by its sequence and structural variability (Zimmerman et al., 2016; Umeda et al., 2020; Yang et al., 2020). The shorter EC1 domain appears disordered in most structural resolutions representing the closed state of the respective

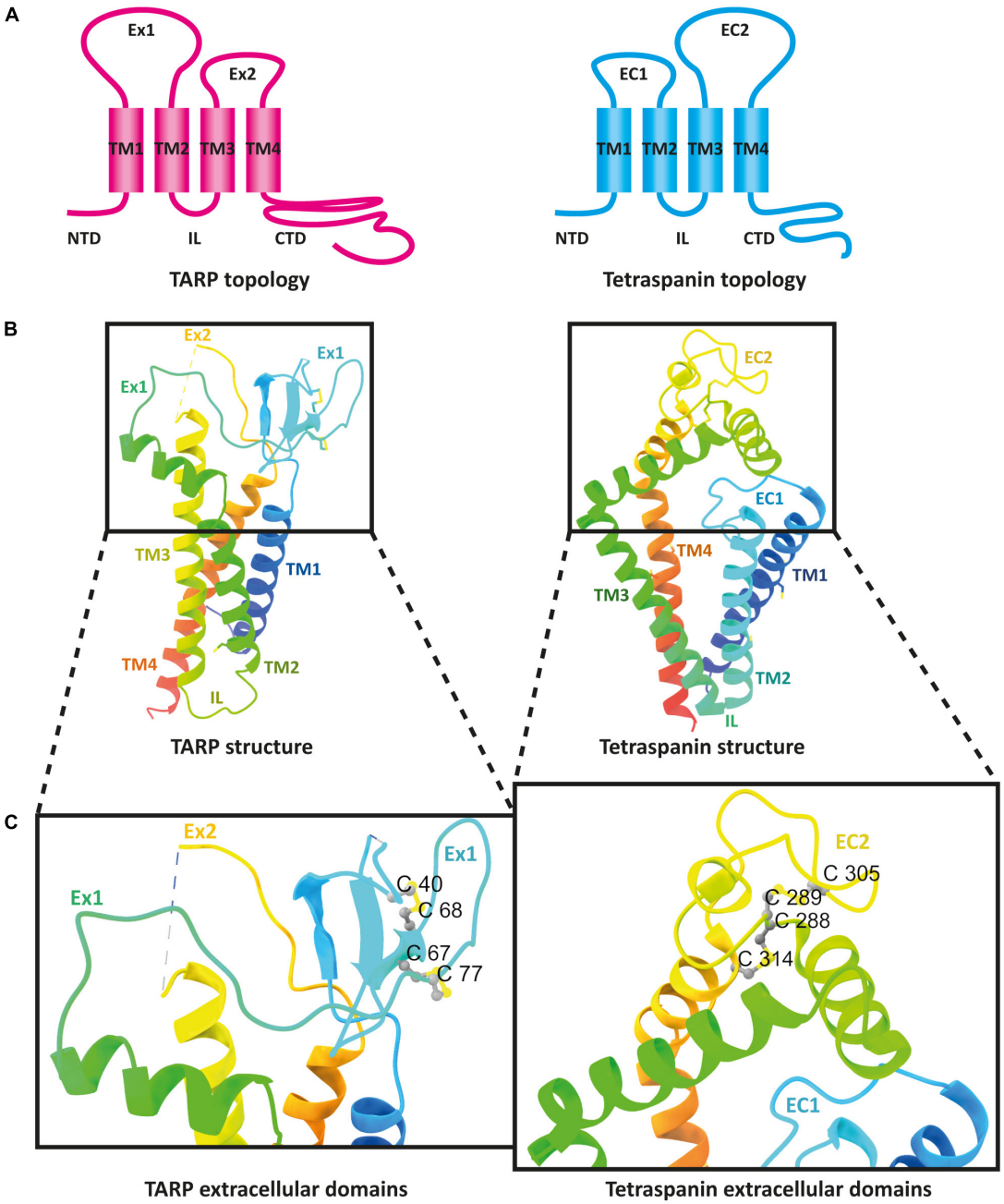

FIGURE 5 | The architecture of transmembrane AMPAR regulatory proteins (TARPs) and tetraspanins (TSPANs). **(A)** Overall topology of TARPs (left) in comparison to tetraspanins (right). **(B)** Ribbon diagrams, rainbow-colored (from N-terminus in blue to C-terminus in red), representing the structures of TARPs (left) based on the structure of human TARP γ2, originally named stargazin and resolved by cryo-EM (pdb model 6DLZ, published by Twomey et al., 2018), and human Tspan25 (right), also known as CD53, resolved by crystallization and X-ray diffraction (pdb model 6WVG, published by Yang et al., 2020). Cysteine residues and disulfide bridges are presented as yellow heteroatoms and sticks, respectively. Distinct domains are labeled. Black boxes indicate the areas of TARPs and tetraspanins enlarged in panel **(C)**. Cysteine residues forming disulfide bridges in the big loops are labeled (one-letter amino acid code with number of each residue) and presented in ball and stick style with sulfur and carbon shown in yellow and gray, respectively.

molecule, suggesting a high flexibility of this domain (Yang et al., 2020; Susa et al., 2021). Based on the recently resolved structures of the open state, in which the EC1 domain is well visible, it can be assumed that EC1 stabilizes the open conformation through interaction with EC2 (Yang et al., 2020; Susa et al., 2021).

Looking at the membrane topology, the close similarity between TARPs and tetraspanins is obvious (**Figure 5A**). Both proteins have four TM domains, although these adopt a more conical form in the previously resolved structures of tetraspanins compared with those of TARPs (**Figure 5B**). In the extracellular

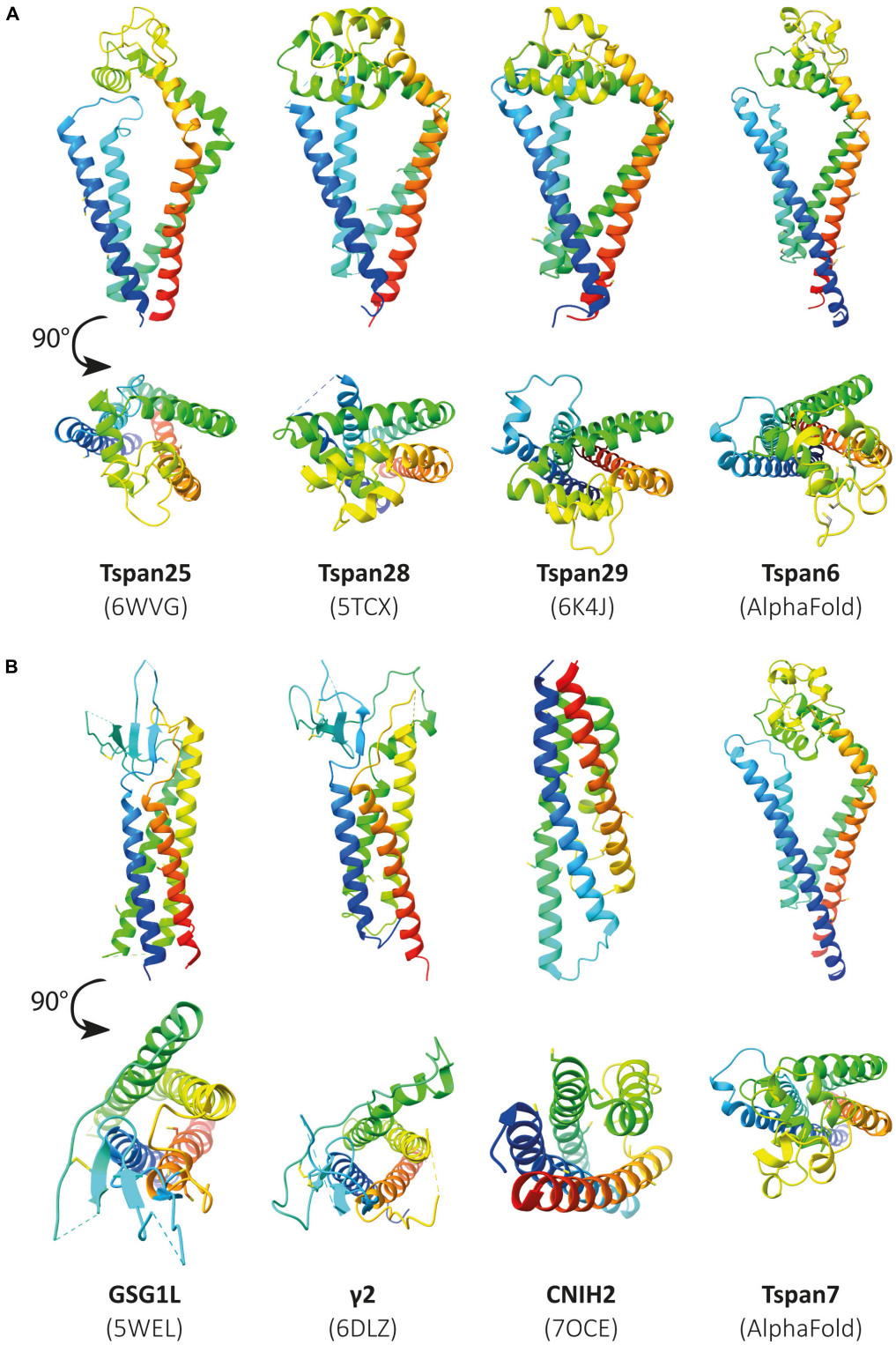

FIGURE 6 | Illustration of previously resolved and predicted tetraspanin structures in comparison to resolved structures of known AMPAR auxiliary subunits. Ribbon diagrams rainbow-colored (from N-terminus in blue to C-terminus in red) showing the structures of the chosen proteins from *Homo sapiens*, displayed with different views, one parallel to the membrane (upper) and another from the extracellular side rotated by a 90° angle (lower). In panel **(A)** the following structures are depicted (from left to right): Tspan25 (pdb model 6WVG), Tspan28 (pdb model 5TCX), Tspan29 (pdb model 6K4J), and Tspan6 (AlphaFold database). Panel **(B)** shows the structures of GSG1L (pdb model 5WEL), γ2 (pdb model 6DLZ), CNIH2 (pdb model 7OCE), and Tspan7 (AlphaFold database) from left to right.

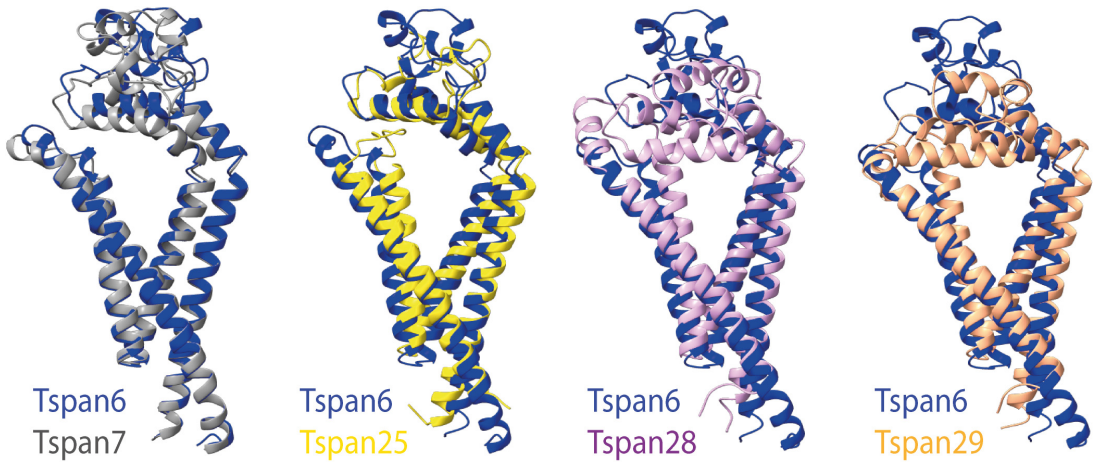

FIGURE 7 | Superposition of selected tetraspanin structures with the predicted structure of Tspan6. The left side shows the superposition of the structures of Tspan6 (blue) and Tspan7 (gray) predicted by AlphaFold; both tetraspanins are known to influence glutamatergic synapses. For comparison, the overlays of the structure of Tspan6 with already known resolved structures of tetraspanins are shown on the right (from left to right): overlay of Tspan6 with Tspan25 (yellow) (PDB model 6WVG) as well as with Tspan28 (pale pink) (PDB model 5TCX), and with Tspan29 (orange) (PDB model 6K4J).

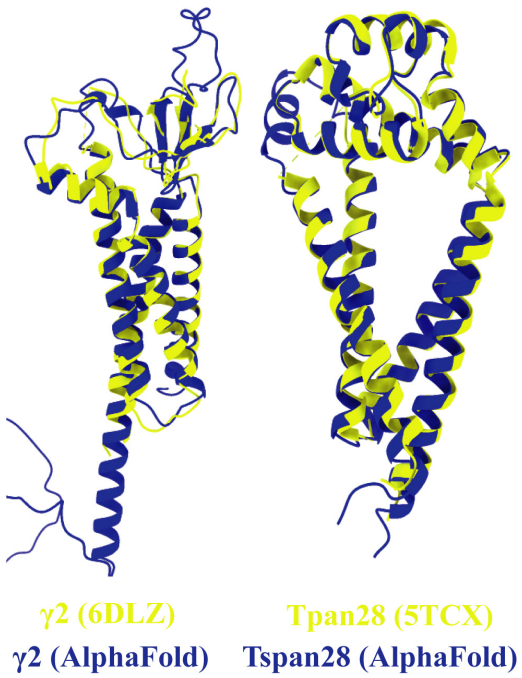

FIGURE 8 | Overlays of predicted and resolved structures. To obtain an impression of the accuracy and reliability of the structures predicted by AlphaFold, the corresponding pdb files of the solved structures of γ2 [(left) pdb model 6DLZ, colored in yellow] and Tspan28 [(right) pdb model 5TCX, colored in yellow] were superimposed on the respective AlphaFold predictions (colored in blue).

domain, both protein families are topologically very similar. Both feature a large extracellular loop (Ex1 in TARPs and EC2 in tetraspanins) and a small loop (Ex2 in TARPs and EC1 in tetraspanins). These loops are folded differently in the structures resolved so far. The small Ex2 domain in TARPs contains a β-sheet and a loop according to the available resolved structures, which unfortunately have been fully resolved so far only for TARP γ5 (pdb model 7RZ5) (Klykov et al., 2021). In tetraspanins, the small EC1 loop either does not contain a secondary structure element, i.e., comprises exclusively a loop, as in Tspan25 (pdb model 6WVG) (Yang et al., 2020), or EC1 contains an α-helix along with a loop, as in Tspan28 (pdb model 7JIC) (Susa et al., 2021) and Tspan29 (pdb model 6K4J) (Umeda et al., 2020).The small loops are overall shorter in tetraspanins than in TARPs and presumably serve to stabilize the larger EC2 loop (Yang et al., 2020). For TARPs, both loops are thought to have a receptor-modulating function, although there is no consensus so far, as different observations have been reported (Twomey et al., 2016; Riva et al., 2017; Herguedas et al., 2019). Remarkable differences exist in the formation of secondary structural elements. The Ex1 loop forms one α-helix and four β-strands in TARPs, whereas the large loop in the tetraspanins exclusively forms α-helical elements (**Figures 5B,C**). The formation of disulfide bridges in the large EC2 domain of tetraspanins is likely important for proper folding. However, TARPs also have several cysteine residues in their large Ex1 loop that form disulfide bridges (**Figure 5C**).

Unfortunately, the structures resolved to date do not include tetraspanins associated with CNS functions such as Tspan6 or Tspan7. So far, the structure of many different proteins, identified as auxiliary subunits of AMPARs, has been elucidated. These include structures of the TARPs γ2 (Twomey et al., 2016), γ5 (Klykov et al., 2021), and γ8 (Herguedas et al., 2019), GSG1L (germ cell-specific gene 1-like protein) (Chen and Gouaux, 2019), and CNIH3 (cornichon family AMPA receptor auxiliary protein 3) (Nakagawa, 2019) as well as cornichon family AMPA receptor auxiliary protein 2 (CNIH2) (Zhang D. et al., 2021). If some tetraspanins do indeed interact with or modulate the function of AMPARs, as has

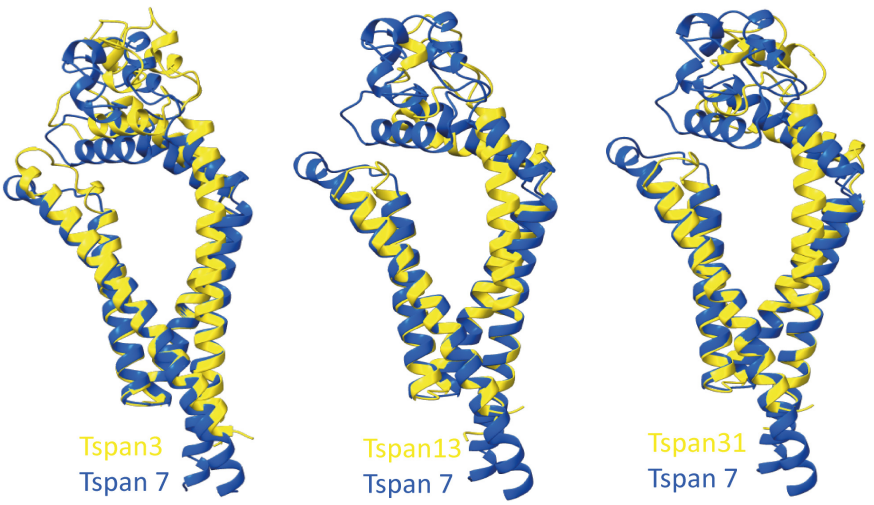

FIGURE 9 | Superimposition of AlphaFold-predicted structures of Tspan3, Tspan13, and Tspan31 with Tspan7 using ChimeraX. Aligned structures of Tspan3, Tspan13, and Tspan31 (yellow) and Tspan7 (blue). RMSD values for Tspan3/7, Tspan13/7, and Tspan31/7 are 0.9, 0.829, and 0.854 Å, respectively.

TABLE 2 | RMSD values (in Å) for human Tspan1-Tspan33 in alignment with Tspan7.

Tspan7 aligned with	RMSD between superimposed atoms (angstroms)	Tspan7 aligned with	RMSD between superimposed atoms (angstroms)
Tspan1	0.983	**Tspan18**	1.008
Tspan2	1.019	**Tspan19**	1.237
Tspan3	**0.90**	**Tspan20**	1.161
Tspan4	1.029	**Tspan21**	1.089
Tspan5	1.077	**Tspan22**	1.038
Tspan6	**0.774**	**Tspan23**	1.113
Tspan7	**0.000**	**Tspan24**	1.005
Tspan8	1.145	**Tspan25**	1.144
Tspan9	1.158	**Tspan26**	1.227
Tspan10	1.159	**Tspan27**	1.459
Tspan11	1.092	**Tspan28**	1.050
Tspan12	1.041	**Tspan29**	1.062
Tspan13	**0.829**	**Tspan30**	1.042
Tspan14	1.080	**Tspan31**	**0.854**
Tspan15	0.960	**Tspan32**	1.028
Tspan16	1.155	**Tspan33**	1.136
Tspan17	1.024		

All tetraspanin structures were obtained from AlphaFold and aligned using Chimera-X. Smaller RMSD values indicate a higher similarity between the aligned protein structures. The color scheme used to highlight the values in the table refers to ***Figure 9****, so Tspan7, which served as the template for the overlay, is shown in blue. The tetraspanins Tspan3, Tspan6, Tspan13, and Tspan31, closely related to Tspan7 according to the calculated RMSD values, are highlighted in red with bold RMSD numbers. An overlay of Tspan6 and Tspan7 is shown in* ***Figure 7****.*

been postulated, it may be assumed that they are structurally similar to already known AMPAR auxiliary subunits. In **Figure 6**, already known structures of selected AMPAR auxiliary subunits are shown in comparison to the previously resolved structures of Tspan25, Tspan28, and Tspan29. In the absence of solved structures for Tspan6 and Tspan7, which serve essential roles in the CNS (Bassani et al., 2012; Salas et al., 2017), predicted structures of Tspan6 and Tspan7 were used which have been mapped using the predictions of DeepMind's new artificial intelligence called AlphaFold (Jumper et al., 2021; Tunyasuvunakool et al., 2021).

Figure 6A (three structures on the left) shows all previously known tetraspanin structures (Tspan25 or CD53, Tspan28 or CD81, and Tspan29 or CD9) in two views: parallel to the membrane, and in a birds-eye view from above the membrane. Both views are compared to three selected AMPAR auxiliary subunits (**Figure 6B**): GSG1L, TARP γ2, and CNIH2. GSG1L and γ2 are structurally strikingly similar, whereas CNIH2 adopts a different fold. The structures predicted by AlphaFold for Tspan6 and Tspan7 (**Figures 6A,B**, two structures on the right), for each of which an essential function in the CNS has already been demonstrated (Bassani et al., 2012;

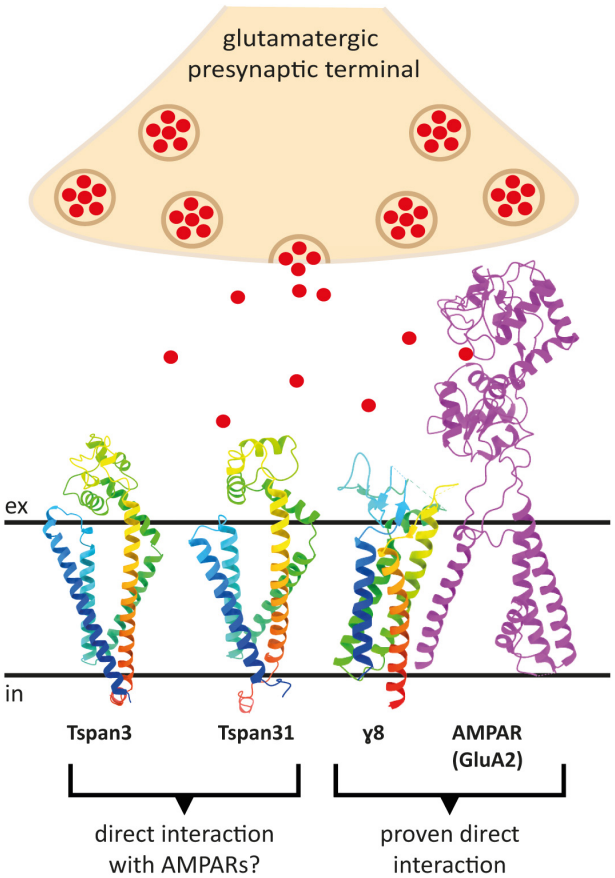

FIGURE 10 | Putative direct interactions of tetraspanins with AMPARs at the postsynaptic membrane of a glutamatergic synapse. Shown is a GluA2 subunit in the D position in magenta, which has been proven to interact with the TARP γ8 (in rainbow colors) (right). To the left are the AlphaFold prediction models of Tspan3 and Tspan31, also colored in rainbow colors, which may also affect AMPAR function in a TARP-like manner. Red dots represent glutamate molecules. The proteins are displayed in ribbon style. The AMPAR subunit GluA2 lacks the C-terminus as well as the amino terminal domain (ATD) (PDB model: 7LEP) (Yu J. et al., 2021).

Murru et al., 2017; Salas et al., 2017), are shown in comparison to γ2 (**Figure 6B**, center). Both are predicted to have a similar conformation, which differs markedly from that of the previously resolved tetraspanin structures (see **Figure 7**). Tspan6 (blue) and Tspan7 (gray) are generally less conical, their first as well as last TM domains are much longer, and the large extracellular loop, while also forming α-helices, has a significantly different spatial structure by comparison. Of all the tetraspanin structures resolved so far, Tspan25 (yellow) has the most similar structure to Tspan6, whereas Tspan28 (pink) and Tspan29 (orange) show stronger structural deviations from Tspan6.

To compare the prediction of AlphaFold with experimentally resolved protein structures, the prediction for γ2 was superimposed on a structure of γ2 elucidated by cryo-EM (**Figure 8**, left). Overall, the two structures from *Homo sapiens* match well. As expected, the motile parts of the loops diverge slightly as they represent flexible elements. Somewhat unexpectedly, the TM4 of γ2 is predicted by AlphaFold to be much longer than was determined by experimental analysis. The predicted structure for Tspan28 (AlphaFold), on the other hand, overlaps almost perfectly with the resolved structure (**Figure 8**, right), confirming AlphaFold as a trustworthy, powerful tool for *in silico* analysis of the proteins studied here.

To predict which other tetraspanins might play an important role in the glutamatergic synapse, we superimposed structures of all other tetraspanins (predicted by AlphaFold) with Tspan7 using the ChimeraX program. Out of all aligned structures, four tetraspanins (Tspan3, Tspan6, Tspan13, and Tspan31) stand out (**Figure 9**) because of their small Root mean square distance (RMSD) value in comparison to other tetraspanins when aligned with Tspan7 (**Table 2**). On the basis of the small RMSD values which indicate high structural similarity of aligned proteins (Carugo, 2007), we hypothesize that these particular tetraspanins (Tspan3, Tspan13, and Tspan31) may share functional characteristics with Tspan7, that have already been demonstrated for Tspan6 (Salas et al., 2017) and thus may play an important role in the CNS. Both direct and indirect interactions with CNS proteins are conceivable. **Figure 10** shows a hypothetical direct interaction of Tspan3 and Tspan31 with the AMPAR subunit GluA2 at a glutamatergic synapse. Next to it, TARP γ8 is shown, which functions in a similar manner as γ2 with respect to its AMPAR-modulating effects. Further investigation is required to characterize their functional properties in relevance to the CNS expression pattern of these tetraspanins.

CONCLUSION AND PERSPECTIVES

Studies in the past two decades have deepened our knowledge about the role of tetraspanins in diverse cellular processes. Although there has been considerable progress in understanding the relation between tetraspanins and its partner molecules involved in the regulation of numerous cellular functions, not much is known about structure-related functions, interaction, expression, and localization of tetraspanins in association with glutamate receptors.

Data from "The Human Protein Atlas" database indicated that Tspan3, Tspan5, Tspan6, Tspan7, Tspan15, Tspan28, Tspan29, and Tspan30 RNA is detected in functionally relevant quantities in different brain regions. According to the literature, all these tetraspanins have significant role in CNS, whereas only for Tspan6 and Tspan7 it has been proven to interact with glutamate receptors. However, since only three tetraspanin structures have been resolved so far, therefore we suggest that the structural similarity of predicted tetraspanin structures with the Tspan7 might indicate other unexplored members of tetraspanin family with the potential to contribute to the organization of the glutamatergic synapse. Moreover, beside the reported role of Tspan6 and its closest paralog Tspan7 at AMPAR-mediated synaptic transmission, three additional tetraspanins, Tspan3, Tspan13, and Tspan31 also point toward their potential involvement in important processes at the

glutamatergic synapse based on their smaller RMSD value in comparison to other tetraspanins.

In addition, Tspan7 mutation and Tspan6 mRNA upregulation has been linked to intellectual disability and Alzheimer's disease, respectively, therefore, understanding the regulation of glutamatergic synapses by tetraspanins may help to develop new targets for therapeutic interventions of several CNS diseases. Considering the abundant expression and broad spectrum of functions of tetraspanins in CNS, further investigation is required into the synaptic role of structurally related members of the tetraspanin family as well as understanding the mechanism of their actions as potential auxiliary subunits of AMPARs.

AUTHOR CONTRIBUTIONS

All authors contributed to the article and approved the submitted version.

FUNDING

This work was supported by in-house funding of the Faculty of Chemistry and Biochemistry, Ruhr University Bochum (AB, JL, and JS). We acknowledge support by the Open Access Publication Funds of the Ruhr University Bochum.

REFERENCES

Abidi, F. E., Holinski-Feder, E., Rittinger, O., Kooy, F., Lubs, H. A., Stevenson, R. E., et al. (2002). A novel 2 bp deletion in the TM4SF2 gene is associated with MRX58. *J. Med. Genet.* 39, 430–433. doi: 10.1136/jmg.39.6.430

Andrijes, R., Hejmadi, R. K., Pugh, M., Rajesh, S., Novitskaya, V., Ibrahim, M., et al. (2021). Tetraspanin 6 is a regulator of carcinogenesis in colorectal cancer. *Proc. Natl. Acad. Sci. U.S.A.* 118:e2011411118. doi: 10.1073/pnas.2011411118

Angelisová, P., Hilgert, I., and Horejsí, V. (1994). Association of four antigens of the tetraspans family (CD37, CD53, TAPA-1, and R2/C33) with MHC class II glycoproteins. *Immunogenetics* 39, 249–256. doi: 10.1007/bf00188787

Angelisová, P., Vlcek, C., Stefanová, I., Lipoldová, M., and Horejsí, V. (1990). The human leucocyte surface antigen CD53 is a protein structurally similar to the CD37 and MRC OX-44 antigens. *Immunogenetics* 32, 281–285. doi: 10.1007/bf00187099

Bascom, R. A., Manara, S., Collins, L., Molday, R. S., Kalnins, V. I., and Mcinnes, R. R. (1992). Cloning of the cDNA for a novel photoreceptor membrane protein (rom-1) identifies a disk rim protein family implicated in human retinopathies. *Neuron* 8, 1171–1184. doi: 10.1016/0896-6273(92)90137-3

Bassani, S., and Cingolani, L. A. (2012). Tetraspanins: interactions and interplay with integrins. *Int. J. Biochem. Cell Biol.* 44, 703–708. doi: 10.1016/j.biocel.2012.01.020

Bassani, S., Cingolani, L. A., Valnegri, P., Folci, A., Zapata, J., Gianfelice, A., et al. (2012). The X-linked intellectual disability protein TSPAN7 regulates excitatory synapse development and AMPAR trafficking. *Neuron* 73, 1143–1158. doi: 10.1016/j.neuron.2012.01.021

Bassani, S., and Passafaro, M. (2012). TSPAN7: a new player in excitatory synapse maturation and function. *Bioarchitecture* 2, 95–97. doi: 10.4161/bioa.20829

Becirovic, E., Nguyen, O. N., Paparizos, C., Butz, E. S., Stern-Schneider, G., Wolfrum, U., et al. (2014). Peripherin-2 couples rhodopsin to the CNG channel in outer segments of rod photoreceptors. *Hum. Mol. Genet.* 23, 5989–5997. doi: 10.1093/hmg/ddu323

Benayas, B., Sastre, I., López-Martín, S., Oo, A., Kim, B., Bullido, M. J., et al. (2020). Tetraspanin CD81 regulates HSV-1 infection. *Med. Microbiol. Immunol.* 209, 489–498. doi: 10.1007/s00430-020-00684-0

Ben-Yaacov, A., Gillor, M., Haham, T., Parsai, A., Qneibi, M., and Stern-Bach, Y. (2017). Molecular mechanism of AMPA receptor modulation by TARP/Stargazin. *Neuron* 93, 1126–1137.e4. doi: 10.1016/j.neuron.2017.01.032

Berditchevski, F. (2001). Complexes of tetraspanins with integrins: more than meets the eye. *J. Cell Sci.* 114, 4143–4151.

Berditchevski, F., Odintsova, E., Sawada, S., and Gilbert, E. (2002). Expression of the palmitoylation-deficient CD151 weakens the association of alpha 3 beta 1 integrin with the tetraspanin-enriched microdomains and affects integrin-dependent signaling. *J. Biol. Chem.* 277, 36991–37000. doi: 10.1074/jbc.M205265200

Bettler, B., and Fakler, B. (2017). Ionotropic AMPA-type glutamate and metabotropic GABA(B) receptors: determining cellular physiology by proteomes. *Curr. Opin. Neurobiol.* 45, 16–23. doi: 10.1016/j.conb.2017.02.011

Böhm, S., Riedmayr, L. M., Nguyen, O. N. P., Gießl, A., Liebscher, T., Butz, E. S., et al. (2017). Peripherin-2 and Rom-1 have opposing effects on rod outer segment targeting of retinitis pigmentosa-linked peripherin-2 mutants. *Sci. Rep.* 7:2321. doi: 10.1038/s41598-017-02514-5

Boucheix, C., and Rubinstein, E. (2001). Tetraspanins. *Cell. Mol. Life Sci.* 58, 1189–1205. doi: 10.1007/pl00000933

Braithwaite, S. P., Xia, H., and Malenka, R. C. (2002). Differential roles for NSF and GRIP/ABP in AMPA receptor cycling. *Proc. Natl. Acad. Sci. U.S.A.* 99, 7096–7101. doi: 10.1073/pnas.102156099

Bulut, I. K., Mir, S., Berdeli, A., and Sozeri, B. (2014). The predictive value of urinary UPIb mRNA levels in VUR and recurrent urinary tract infections. *Clin. Nephrol.* 81, 152–158. doi: 10.5414/cn107778

Byun, Y., Choi, Y. C., Jeong, Y., Yoon, J., and Baek, K. (2020). Long Noncoding RNA Expression Profiling Reveals Upregulation of Uroplakin 1A and Uroplakin 1A Antisense RNA 1 under Hypoxic Conditions in Lung Cancer Cells. *Mol. Cells* 43, 975–988. doi: 10.14348/molcells.2020.0126

Carroll, R. M., and Kim, B. J. (2019). Asymptomatic adults in a single family with familial exudative vitreoretinopathy and TSPAN12 variant. *Ophthalmic Genet.* 40, 474–479. doi: 10.1080/13816810.2019.1686157

Carugo, O. (2007). Statistical validation of the root-mean-square-distance, a measure of protein structural proximity. *Protein Eng. Des. Sel.* 20, 33–37. doi: 10.1093/protein/gzl051

Çavdarli, C., Çavdarlı, B., and Alp, M. N. (2020). Investigating the role of BEST1 and PRPH2 variants in the molecular aetiology of adult-onset vitelliform macular dystrophies. *Ophthalmic Genet.* 41, 585–590. doi: 10.1080/13816810.2020.1821385

Charrin, S., Le Naour, F., Silvie, O., Milhiet, P. E., Boucheix, C., and Rubinstein, E. (2009). Lateral organization of membrane proteins: tetraspanins spin their web. *Biochem. J.* 420, 133–154. doi: 10.1042/bj20082422

Charrin, S., Manié, S., Oualid, M., Billard, M., Boucheix, C., and Rubinstein, E. (2002). Differential stability of tetraspanin/tetraspanin interactions: role of palmitoylation. *FEBS Lett.* 516, 139–144. doi: 10.1016/s0014-5793(02)02522-x

Chen, N., Pandya, N. J., Koopmans, F., Castelo-Székelv, V., Van Der Schors, R. C., Smit, A. B., et al. (2014). Interaction proteomics reveals brain region-specific AMPA receptor complexes. *J. Proteome Res.* 13, 5695–5706. doi: 10.1021/pr500697b

Chen, S., and Gouaux, E. (2019). Structure and mechanism of AMPA receptor - auxiliary protein complexes. *Curr. Opin. Struct. Biol.* 54, 104–111. doi: 10.1016/j.sbi.2019.01.011

Classon, B. J., Williams, A. F., Willis, A. C., Seed, B., and Stamenkovic, I. (1989). The primary structure of the human leukocyte antigen CD37, a species homologue of the rat MRC OX-44 antigen. *J. Exp. Med.* 169, 1497–1502. doi: 10.1084/jem.169.4.1497

Conley, S. M., Stuck, M. W., Watson, J. N., and Naash, M. I. (2017). Rom1 converts Y141C-Prph2-associated pattern dystrophy to retinitis pigmentosa. *Hum. Mol. Genet.* 26, 509–518. doi: 10.1093/hmg/ddw408

Costa, R. M., Drew, C., and Silva, A. J. (2005). Notch to remember. *Trends Neurosci.* 28, 429–435. doi: 10.1016/j.tins.2005.05.003

Costa, R. M., Honjo, T., and Silva, A. J. (2003). Learning and memory deficits in Notch mutant mice. *Curr. Biol.* 13, 1348–1354. doi: 10.1016/s0960-9822(03)00492-5

Dahlhaus, M., Hermans, J. M., Van Woerden, L. H., Saiepour, M. H., Nakazawa, K., Mansvelder, H. D., et al. (2008). Notch1 signaling in pyramidal neurons

regulates synaptic connectivity and experience-dependent modifications of acuity in the visual cortex. *J. Neurosci.* 28, 10794–10802. doi: 10.1523/jneurosci.1348-08.2008

Depienne, C., Trouillard, O., Bouteiller, D., Gourfinkel-An, I., Poirier, K., Rivier, F., et al. (2011). Mutations and deletions in PCDH19 account for various familial or isolated epilepsies in females. *Hum. Mutat.* 32, E1959–E1975. doi: 10.1002/humu.21373

Dodla, P., Bhoopalan, V., Khoo, S. K., Miranti, C., and Sridhar, S. (2020). Gene expression analysis of human prostate cell lines with and without tumor metastasis suppressor CD82. *BMC Cancer* 20:1211. doi: 10.1186/s12885-020-07675-7

Doh-Ura, K., Mekada, E., Ogomori, K., and Iwaki, T. (2000). Enhanced CD9 expression in the mouse and human brains infected with transmissible spongiform encephalopathies. *J. Neuropathol. Exp. Neurol.* 59, 774–785. doi: 10.1093/jnen/59.9.774

Donato, L., Abdalla, E. M., Scimone, C., Alibrandi, S., Rinaldi, C., Nabil, K. M., et al. (2021). Impairments of photoreceptor outer segments renewal and phototransduction due to a peripherin rare haplotype variant: insights from molecular modeling. *Int. J. Mol. Sci.* 22:3484. doi: 10.3390/ijms22073484

Dornier, E., Coumailleau, F., Ottavi, J. F., Moretti, J., Boucheix, C., Mauduit, P., et al. (2012). TspanC8 tetraspanins regulate ADAM10/Kuzbanian trafficking and promote Notch activation in flies and mammals. *J. Cell Biol.* 199, 481–496. doi: 10.1083/jcb.201201133

Dunlock, V. E. (2020). Tetraspanin CD53: an overlooked regulator of immune cell function. *Med. Microbiol. Immunol.* 209, 545–552. doi: 10.1007/s00430-020-00677-z

Dunn, C. D., Sulis, M. L., Ferrando, A. A., and Greenwald, I. (2010). A conserved tetraspanin subfamily promotes Notch signaling in *Caenorhabditis elegans* and in human cells. *Proc. Natl. Acad. Sci. U.S.A.* 107, 5907–5912. doi: 10.1073/pnas.1001647107

Esserlind, A. L., Christensen, A. F., Le, H., Kirchmann, M., Hauge, A. W., Toyserkani, N. M., et al. (2013). Replication and meta-analysis of common variants identifies a genome-wide significant locus in migraine. *Eur. J. Neurol.* 20, 765–772. doi: 10.1111/ene.12055

Farrar, G. J., Kenna, P., Jordan, S. A., Kumar-Singh, R., Humphries, M. M., Sharp, E. M., et al. (1992). Autosomal dominant retinitis pigmentosa: a novel mutation at the peripherin/RDS locus in the original 6p-linked pedigree. *Genomics* 14, 805–807. doi: 10.1016/s0888-7543(05)80193-4

Finch, J. L., Miller, J., Aspinall, J. O., and Cowled, P. A. (1999). Cloning of the human uroplakin 1B cDNA and analysis of its expression in urothelial-tumor cell lines and bladder-carcinoma tissue. *Int. J. Cancer* 80, 533–538. doi: 10.1002/(sici)1097-0215(19990209)80:4<533::aid-ijc9>3.0.co;2-5

Fradkin, L. G., Kamphorst, J. T., Diantonio, A., Goodman, C. S., and Noordermeer, J. N. (2002). Genomewide analysis of the Drosophila tetraspanins reveals a subset with similar function in the formation of the embryonic synapse. *Proc. Natl. Acad. Sci. U.S.A.* 99, 13663–13668. doi: 10.1073/pnas.212511099

Gasic, G. P., and Hollmann, M. (1992). Molecular neurobiology of glutamate receptors. *Annu. Rev. Physiol.* 54, 507–536. doi: 10.1146/annurev.ph.54.030192.002451

Gavin, R. L., Koo, C. Z., and Tomlinson, M. G. (2020). Tspan18 is a novel regulator of thrombo-inflammation. *Med. Microbiol. Immunol.* 209, 553–564. doi: 10.1007/s00430-020-00678-y

Groot, A. J., Habets, R., Yahyanejad, S., Hodin, C. M., Reiss, K., Saftig, P., et al. (2014). Regulated proteolysis of NOTCH2 and NOTCH3 receptors by ADAM10 and presenilins. *Mol. Cell. Biol.* 34, 2822–2832. doi: 10.1128/mcb.00206-14

Guix, F. X., Sannerud, R., Berditchevski, F., Arranz, A. M., Horré, K., Snellinx, A., et al. (2017). Tetraspanin 6: a pivotal protein of the multiple vesicular body determining exosome release and lysosomal degradation of amyloid precursor protein fragments. *Mol. Neurodegener.* 12:25. doi: 10.1186/s13024-017-0165-0

Guo, X. B., Zhang, X. C., Chen, P., Ma, L. M., and Shen, Z. Q. (2019). miR-378a-3p inhibits cellular proliferation and migration in glioblastoma multiforme by targeting tetraspanin 17. *Oncol. Rep.* 42, 1957–1971. doi: 10.3892/or.2019.7283

Haining, E. J., Matthews, A. L., Noy, P. J., Romanska, H. M., Harris, H. J., Pike, J., et al. (2017). Tetraspanin Tspan9 regulates platelet collagen receptor GPVI lateral diffusion and activation. *Platelets* 28, 629–642. doi: 10.1080/09537104.2016.1254175

Hall, G. D., Weeks, R. J., Olsburgh, J., Southgate, J., Knowles, M. A., Selby, P. J., et al. (2005). Transcriptional control of the human urothelial-specific gene, uroplakin Ia. *Biochim. Biophys. Acta* 1729, 126–134. doi: 10.1016/j.bbaexp.2005.04.004

Hantak, M. P., Qing, E., Earnest, J. T., and Gallagher, T. (2019). Tetraspanins: architects of viral entry and exit platforms. *J. Virol.* 93:e01429-17. doi: 10.1128/jvi.01429-17

Hartmann, D., De Strooper, B., Serneels, L., Craessaerts, K., Herreman, A., Annaert, W., et al. (2002). The disintegrin/metalloprotease ADAM 10 is essential for Notch signalling but not for alpha-secretase activity in fibroblasts. *Hum. Mol. Genet.* 11, 2615–2624. doi: 10.1093/hmg/11.21.2615

He, J., Sun, E., Bujny, M. V., Kim, D., Davidson, M. W., and Zhuang, X. (2013). Dual function of CD81 in influenza virus uncoating and budding. *PLoS Pathog.* 9:e1003701. doi: 10.1371/journal.ppat.1003701

Heikens, M. J., Cao, T. M., Morita, C., Dehart, S. L., and Tsai, S. (2007). Penumbra encodes a novel tetraspanin that is highly expressed in erythroid progenitors and promotes effective erythropoiesis. *Blood* 109, 3244–3252. doi: 10.1182/blood-2006-09-046672

Hemler, M. E. (2003). Tetraspanin proteins mediate cellular penetration, invasion, and fusion events and define a novel type of membrane microdomain. *Annu. Rev. Cell Dev. Biol.* 19, 397–422. doi: 10.1146/annurev.cellbio.19.111301.153609

Herguedas, B., Watson, J. F., Ho, H., Cais, O., García-Nafría, J., and Greger, I. H. (2019). Architecture of the heteromeric GluA1/2 AMPA receptor in complex with the auxiliary subunit TARP γ8. *Science* 364:eaav9011. doi: 10.1126/science.aav9011

Hiroshima, K., Shiiba, M., Oka, N., Hayashi, F., Ishida, S., Fukushima, R., et al. (2019). Tspan15 plays a crucial role in metastasis in oral squamous cell carcinoma. *Exp. Cell Res.* 384:111622. doi: 10.1016/j.yexcr.2019.111622

Hollmann, M., and Heinemann, S. (1994). Cloned glutamate receptors. *Annu. Rev. Neurosci.* 17, 31–108. doi: 10.1146/annurev.ne.17.030194.000335

Horejsí, V., and Vlcek, C. (1991). Novel structurally distinct family of leucocyte surface glycoproteins including CD9, CD37, CD53 and CD63. *FEBS Lett.* 288, 1–4. doi: 10.1016/0014-5793(91)80988-f

Hotta, H., Ross, A. H., Huebner, K., Isobe, M., Wendeborn, S., Chao, M. V., et al. (1988). Molecular cloning and characterization of an antigen associated with early stages of melanoma tumor progression. *Cancer Res.* 48, 2955–2962.

Huang, S., Yuan, S., Dong, M., Su, J., Yu, C., Shen, Y., et al. (2005). The phylogenetic analysis of tetraspanins projects the evolution of cell-cell interactions from unicellular to multicellular organisms. *Genomics* 86, 674–684. doi: 10.1016/j.ygeno.2005.08.004

Hynes, R. O. (2002). Integrins: bidirectional, allosteric signaling machines. *Cell* 110, 673–687. doi: 10.1016/s0092-8674(02)00971-6

Ichikawa, T., Ichikawa, Y., Dong, J., Hawkins, A. L., Griffin, C. A., Isaacs, W. B., et al. (1992). Localization of metastasis suppressor gene(s) for prostatic cancer to the short arm of human chromosome 11. *Cancer Res.* 52, 3486–3490.

Jankowski, S. A., De Jong, P., and Meltzer, P. S. (1995). Genomic structure of SAS, a member of the transmembrane 4 superfamily amplified in human sarcomas. *Genomics* 25, 501–506. doi: 10.1016/0888-7543(95)80051-m

Jiang, L., Zhang, X., Geradts, J., Wei, Q., Hochwald, S., Xu, H., et al. (2019). Expression of tetraspanins NET-6 and CD151 in breast cancer as a potential tumor biomarker. *Clin. Exp. Med.* 19, 377–384. doi: 10.1007/s10238-019-00554-x

Jin, H. S., Cho, J. E., and Park, S. (2019). Association between CD53 genetic polymorphisms and tuberculosis cases. *Genes Genomics* 41, 389–395. doi: 10.1007/s13258-018-0764-3

Jordan, S. A., Farrar, G. J., Kumar-Singh, R., Kenna, P., Humphries, M. M., Allamand, V., et al. (1992). Autosomal dominant retinitis pigmentosa (adRP; RP6): cosegregation of RP6 and the peripherin-RDS locus in a late-onset family of Irish origin. *Am. J. Hum. Genet.* 50, 634–639.

Jouannet, S., Saint-Pol, J., Fernandez, L., Nguyen, V., Charrin, S., Boucheix, C., et al. (2016). TspanC8 tetraspanins differentially regulate the cleavage of ADAM10 substrates, Notch activation and ADAM10 membrane compartmentalization. *Cell. Mol. Life Sci.* 73, 1895–1915. doi: 10.1007/s00018-015-2111-z

Jumper, J., Evans, R., Pritzel, A., Green, T., Figurnov, M., Ronneberger, O., et al. (2021). Highly accurate protein structure prediction with AlphaFold. *Nature* 596, 583–589. doi: 10.1038/s41586-021-03819-2

Junge, H. J., Yang, S., Burton, J. B., Paes, K., Shu, X., French, D. M., et al. (2009). TSPAN12 regulates retinal vascular development by promoting Norrin- but not

Wnt-induced FZD4/beta-catenin signaling. *Cell* 139, 299–311. doi: 10.1016/j.cell.2009.07.048

Juric, D., Lacayo, N. J., Ramsey, M. C., Racevskis, J., Wiernik, P. H., Rowe, J. M., et al. (2007). Differential gene expression patterns and interaction networks in BCR-ABL-positive and -negative adult acute lymphoblastic leukemias. *J. Clin. Oncol.* 25, 1341–1349. doi: 10.1200/jco.2006.09.3534

Kagawa, T., Mekada, E., Shishido, Y., and Ikenaka, K. (1997). Immune system-related CD9 is expressed in mouse central nervous system myelin at a very late stage of myelination. *J. Neurosci. Res.* 50, 312–320. doi: 10.1002/(SICI)1097-4547(19971015)50:2<312::AID-JNR19>3.0.CO;2-9

Kajiwara, K., Hahn, L. B., Mukai, S., Travis, G. H., Berson, E. L., and Dryja, T. P. (1991). Mutations in the human retinal degeneration slow gene in autosomal dominant retinitis pigmentosa. *Nature* 354, 480–483. doi: 10.1038/354480a0

Karamatic Crew, V., Burton, N., Kagan, A., Green, C. A., Levene, C., Flinter, F., et al. (2004). CD151, the first member of the tetraspanin (TM4) superfamily detected on erythrocytes, is essential for the correct assembly of human basement membranes in kidney and skin. *Blood* 104, 2217–2223. doi: 10.1182/blood-2004-04-1512

Kashef, J., Diana, T., Oelgeschläger, M., and Nazarenko, I. (2013). Expression of the tetraspanin family members Tspan3, Tspan4, Tspan5 and Tspan7 during *Xenopus laevis* embryonic development. *Gene Expr. Patterns* 13, 1–11. doi: 10.1016/j.gep.2012.08.001

Klykov, O., Gangwar, S. P., Yelshanskaya, M. V., Yen, L., and Sobolevsky, A. I. (2021). Structure and desensitization of AMPA receptor complexes with type II TARP γ5 and GSG1L. *Mol. Cell*. [Epub ahead of print]. doi: 10.1016/j.molcel.2021.09.030

Kohl, S., Giddings, I., Besch, D., Apfelstedt-Sylla, E., Zrenner, E., and Wissinger, B. (1998). The role of the peripherin/RDS gene in retinal dystrophies. *Acta Anat.* 162, 75–84. doi: 10.1159/000046471

Koo, C. Z., Harrison, N., Noy, P. J., Szyroka, J., Matthews, A. L., Hsia, H. E., et al. (2020). The tetraspanin Tspan15 is an essential subunit of an ADAM10 scissor complex. *J. Biol. Chem.* 295, 12822–12839. doi: 10.1074/jbc.RA120.012601

Kopczynski, C. C., Davis, G. W., and Goodman, C. S. (1996). A neural tetraspanin, encoded by late bloomer, that facilitates synapse formation. *Science* 271, 1867–1870. doi: 10.1126/science.271.5257.1867

Kuhn, P. H., Wang, H., Dislich, B., Colombo, A., Zeitschel, U., Ellwart, J. W., et al. (2010). ADAM10 is the physiologically relevant, constitutive alpha-secretase of the amyloid precursor protein in primary neurons. *EMBO J.* 29, 3020–3032. doi: 10.1038/emboj.2010.167

Kumaran, N., Pennesi, M. E., Yang, P., Trzupek, K. M., Schlechter, C., Moore, A. T., et al. (1993). "Leber congenital amaurosis/early-onset severe retinal dystrophy overview," in *GeneReviews(®)*, eds M. P. Adam, H. H. Ardinger, R. A. Pagon, S. E. Wallace, L. J. H. Bean, G. Mirzaa, et al. (Seattle, WA: University of Washington).

Kwon, H. Y., Bajaj, J., Ito, T., Blevins, A., Konuma, T., Weeks, J., et al. (2015). Tetraspanin 3 is required for the development and propagation of acute myelogenous leukemia. *Cell Stem Cell* 17, 152–164. doi: 10.1016/j.stem.2015.06.006

Lai, R. C., Arslan, F., Lee, M. M., Sze, N. S., Choo, A., Chen, T. S., et al. (2010). Exosome secreted by MSC reduces myocardial ischemia/reperfusion injury. *Stem Cell Res.* 4, 214–222. doi: 10.1016/j.scr.2009.12.003

Lazo, P. A. (2007). Functional implications of tetraspanin proteins in cancer biology. *Cancer Sci.* 98, 1666–1677. doi: 10.1111/j.1349-7006.2007.00584.x

Lee, S. Y., Kim, J. M., Cho, S. Y., Kim, H. S., Shin, H. S., Jeon, J. Y., et al. (2014). TIMP-1 modulates chemotaxis of human neural stem cells through CD63 and integrin signalling. *Biochem. J.* 459, 565–576. doi: 10.1042/bj20131119

Li, K. W., Chen, N., and Smit, A. B. (2013). Interaction proteomics of the AMPA receptor: towards identification of receptor sub-complexes. *Amino Acids* 44, 1247–1251. doi: 10.1007/s00726-013-1461-9

Li, P., Dong, M., and Wang, Z. (2019). Downregulation of TSPAN13 by miR-369-3p inhibits cell proliferation in papillary thyroid cancer (PTC). *Bosn. J. Basic Med. Sci.* 19, 146–154. doi: 10.17305/bjbms.2018.2865

Li, P. Y., Lv, J., Qi, W. W., Zhao, S. F., Sun, L. B., Liu, N., et al. (2016). Tspan9 inhibits the proliferation, migration and invasion of human gastric cancer SGC7901 cells via the ERK1/2 pathway. *Oncol. Rep.* 36, 448–454. doi: 10.3892/or.2016.4805

Li, W. N., Du, X. J., Zhang, Y. T., Wang, L. Y., and Zhu, J. (2021). A novel mutation in the PRPH2 gene in a Chinese pedigree with retinitis pigmentosa and angle-closure glaucoma. *BMC Ophthalmol.* 21:302. doi: 10.1186/s12886-021-02064-5

Lineberry, N., Su, L., Soares, L., and Fathman, C. G. (2008). The single subunit transmembrane E3 ligase gene related to anergy in lymphocytes (GRAIL) captures and then ubiquitinates transmembrane proteins across the cell membrane. *J. Biol. Chem.* 283, 28497–28505. doi: 10.1074/jbc.M805092200

Liu, G., Wang, Y., Yang, L., Zou, B., Gao, S., Song, Z., et al. (2019). Tetraspanin 1 as a mediator of fibrosis inhibits EMT process and Smad2/3 and beta-catenin pathway in human pulmonary fibrosis. *J. Cell Mol. Med.* 23, 3583–3596. doi: 10.1111/jcmm.14258

Liu, J., Li, M., and Su, B. (2016). GWAS-identified schizophrenia risk SNPs at TSPAN18 are highly diverged between Europeans and East Asians. *Am. J. Med. Genet. B Neuropsychiatr. Genet.* 171, 1032–1040. doi: 10.1002/ajmg.b.32471

Liu, X., Guo, X., Li, H., Chen, J., and Han, H. (2021). Effects of KAI gene expression on ferroptosis in pancreatic cancer cells. *Mol. Med. Rep.* 23:163. doi: 10.3892/mmr.2020.11802

Liu, Y., Wang, G., Zhang, J., Chen, X., Xu, H., Heng, G., et al. (2021). CD9, a potential leukemia stem cell marker, regulates drug resistance and leukemia development in acute myeloid leukemia. *Stem Cell Res. Ther.* 12:86. doi: 10.1186/s13287-021-02155-6

Lobban, E. D., Smith, B. A., Hall, G. D., Harnden, P., Roberts, P., Selby, P. J., et al. (1998). Uroplakin gene expression by normal and neoplastic human urothelium. *Am. J. Pathol.* 153, 1957–1967. doi: 10.1016/s0002-9440(10)65709-4

Lombardo, S. D., Mazzon, E., Basile, M. S., Campo, G., Corsico, F., Presti, M., et al. (2019). Modulation of Tetraspanin 32 (TSPAN32) expression in T cell-mediated immune responses and in multiple sclerosis. *Int. J. Mol. Sci.* 20:4323. doi: 10.3390/ijms20184323

Luu, V. P., Hevezi, P., Vences-Catalan, F., Maravillas-Montero, J. L., White, C. A., Casali, P., et al. (2013). TSPAN33 is a novel marker of activated and malignant B cells. *Clin. Immunol.* 149, 388–399. doi: 10.1016/j.clim.2013.08.005

Ma, C., Cui, Z., Wang, Y., Zhang, L., Wen, J., Guo, H., et al. (2021). Bioinformatics analysis reveals TSPAN1 as a candidate biomarker of progression and prognosis in pancreatic cancer. *Bosn. J. Basic Med. Sci.* 21, 47–60. doi: 10.17305/bjbms.2020.5096

Ma, X., Verweij, E. W. E., Siderius, M., Leurs, R., and Vischer, H. F. (2021). Identification of TSPAN4 as Novel Histamine H(4) Receptor Interactor. *Biomolecules* 11:1127. doi: 10.3390/biom11081127

Ma, Z., Gao, Y., Liu, W., Zheng, L., Jin, B., Duan, B., et al. (2020). CD82 Suppresses ADAM17-Dependent E-cadherin cleavage and cell migration in prostate cancer. *Dis. Markers* 2020:8899924. doi: 10.1155/2020/8899924

Maecker, H. T., Todd, S. C., and Levy, S. (1997). The tetraspanin superfamily: molecular facilitators. *FASEB J.* 11, 428–442. doi: 10.1096/fasebj.11.6.9194523

Mallmann, R. T., Wilmes, T., Lichvarova, L., Bührer, A., Lohmüller, B., Castonguay, J., et al. (2013). Tetraspanin-13 modulates voltage-gated CaV2.2 Ca2+ channels. *Sci. Rep.* 3:1777. doi: 10.1038/srep01777

Martin, F., Roth, D. M., Jans, D. A., Pouton, C. W., Partridge, L. J., Monk, P. N., et al. (2005). Tetraspanins in viral infections: a fundamental role in viral biology? *J. Virol.* 79, 10839–10851. doi: 10.1128/jvi.79.17.10839-10851.2005

McLaughlin, K. A., Tombs, M. A., and Christie, M. R. (2020). Autoimmunity to tetraspanin-7 in type 1 diabetes. *Med. Microbiol. Immunol.* 209, 437–445. doi: 10.1007/s00430-020-00674-2

Mela, A., and Goldman, J. E. (2009). The tetraspanin KAI1/CD82 is expressed by late-lineage oligodendrocyte precursors and may function to restrict precursor migration and promote oligodendrocyte differentiation and myelination. *J. Neurosci.* 29, 11172–11181. doi: 10.1523/jneurosci.3075-09.2009

Mela, A., and Goldman, J. E. (2013). CD82 blocks cMet activation and overcomes hepatocyte growth factor effects on oligodendrocyte precursor differentiation. *J. Neurosci.* 33, 7952–7960. doi: 10.1523/jneurosci.5836-12.2013

Ménager, M. M. (2017). TSPAN7, effector of actin nucleation required for dendritic cell-mediated transfer of HIV-1 to T cells. *Biochem. Soc. Trans.* 45, 703–708. doi: 10.1042/bst20160439

Milstein, M. L., Cavanaugh, B. L., Roussey, N. M., Volland, S., Williams, D. S., and Goldberg, A. F. X. (2020). Multistep peripherin-2/rds self-assembly drives membrane curvature for outer segment disk architecture and photoreceptor viability. *Proc. Natl. Acad. Sci. U.S.A.* 117, 4400–4410. doi: 10.1073/pnas.1912513117

Molday, L. L., and Molday, R. S. (1987). Glycoproteins specific for the retinal rod outer segment plasma membrane. *Biochim. Biophys. Acta* 897, 335–340. doi: 10.1016/0005-2736(87)90430-5

Moretto, E., Longatti, A., Murru, L., Chamma, I., Sessa, A., Zapata, J., et al. (2019). TSPAN5 enriched microdomains provide a platform for dendritic spine maturation through neuroligin-1 clustering. *Cell Rep.* 29, 1130–1146.e8. doi: 10.1016/j.celrep.2019.09.051

Murru, L., Moretto, E., Martano, G., and Passafaro, M. (2018). Tetraspanins shape the synapse. *Mol. Cell. Neurosci.* 91, 76–81. doi: 10.1016/j.mcn.2018.04.001

Murru, L., Vezzoli, E., Longatti, A., Ponzoni, L., Falqui, A., Folci, A., et al. (2017). Pharmacological Modulation of AMPAR rescues intellectual disability-like phenotype in Tm4sf2-/y Mice. *Cereb. Cortex* 27, 5369–5384. doi: 10.1093/cercor/bhx221

Nakagawa, T. (2019). Structures of the AMPA receptor in complex with its auxiliary subunit cornichon. *Science* 366, 1259–1263. doi: 10.1126/science.aay2783

Nakamura, Y., Iwamoto, R., and Mekada, E. (1996). Expression and distribution of CD9 in myelin of the central and peripheral nervous systems. *Am. J. Pathol.* 149, 575–583.

Nakanishi, Y., Matsugaki, A., Kawahara, K., Ninomiya, T., Sawada, H., and Nakano, T. (2019). Unique arrangement of bone matrix orthogonal to osteoblast alignment controlled by Tspan11-mediated focal adhesion assembly. *Biomaterials* 209, 103–110. doi: 10.1016/j.biomaterials.2019.04.016

Navarro-Hernandez, I. C., López-Ortega, O., Acevedo-Ochoa, E., Cervantes-Díaz, R., Romero-Ramírez, S., Sosa-Hernández, V. A., et al. (2020). Tetraspanin 33 (TSPAN33) regulates endocytosis and migration of human B lymphocytes by affecting the tension of the plasma membrane. *FEBS J.* 287, 3449–3471. doi: 10.1111/febs.15216

Noy, P. J., Gavin, R. L., Colombo, D., Haining, E. J., Reyat, J. S., Payne, H., et al. (2019). Tspan18 is a novel regulator of the Ca(2+) channel Orai1 and von Willebrand factor release in endothelial cells. *Haematologica* 104, 1892–1905. doi: 10.3324/haematol.2018.194241

Noy, P. J., Yang, J., Reyat, J. S., Matthews, A. L., Charlton, A. E., Furmston, J., et al. (2016). TspanC8 Tetraspanins and A Disintegrin and Metalloprotease 10 (ADAM10) Interact via Their Extracellular Regions: EVIDENCE FOR DISTINCT BINDING MECHANISMS FOR DIFFERENT TspanC8 PROTEINS. *J. Biol. Chem.* 291, 3145–3157. doi: 10.1074/jbc.M115.703058

Ogawa, K., Johansson, S. L., and Cohen, S. M. (1999). Immunohistochemical analysis of uroplakins, urothelial specific proteins, in ovarian Brenner tumors, normal tissues, and benign and neoplastic lesions of the female genital tract. *Am. J. Pathol.* 155, 1047–1050. doi: 10.1016/s0002-9440(10)65206-6

Oksvold, M. P., Neurauter, A., and Pedersen, K. W. (2015). Magnetic bead-based isolation of exosomes. *Methods Mol. Biol.* 1218, 465–481. doi: 10.1007/978-1-4939-1538-5_27

Omae, Y., Toyo-Oka, L., Yanai, H., Nedsuwan, S., Wattanapokayakit, S., Satproedprai, N., et al. (2017). Pathogen lineage-based genome-wide association study identified CD53 as susceptible locus in tuberculosis. *J. Hum. Genet.* 62, 1015–1022. doi: 10.1038/jhg.2017.82

Oren, R., Takahashi, S., Doss, C., Levy, R., and Levy, S. (1990). TAPA-1, the target of an antiproliferative antibody, defines a new family of transmembrane proteins. *Mol. Cell. Biol.* 10, 4007–4015. doi: 10.1128/mcb.10.8.4007-4015.1990

Osten, P., Khatri, L., Perez, J. L., Köhr, G., Giese, G., Daly, C., et al. (2000). Mutagenesis reveals a role for ABP/GRIP binding to GluR2 in synaptic surface accumulation of the AMPA receptor. *Neuron* 27, 313–325. doi: 10.1016/s0896-6273(00)00039-8

Palmer, C. L., Cotton, L., and Henley, J. M. (2005). The molecular pharmacology and cell biology of alpha-amino-3-hydroxy-5-methyl-4-isoxazolepropionic acid receptors. *Pharmacol. Rev.* 57, 253–277. doi: 10.1124/pr.57.2.7

Perez, J. L., Khatri, L., Chang, C., Srivastava, S., Osten, P., and Ziff, E. B. (2001). PICK1 targets activated protein kinase Calpha to AMPA receptor clusters in spines of hippocampal neurons and reduces surface levels of the AMPA-type glutamate receptor subunit 2. *J. Neurosci.* 21, 5417–5428. doi: 10.1523/jneurosci.21-15-05417.2001

Perez, M. D., Seu, L., Lowman, K. E., Moylan, D. C., Tidwell, C., Samuel, S., et al. (2020). The tetraspanin CD151 marks a unique population of activated human T cells. *Sci. Rep.* 10:15748. doi: 10.1038/s41598-020-72719-8

Perot, B. P., García-Paredes, V., Luka, M., and Ménager, M. M. (2020). Dendritic cell maturation regulates TSPAN7 function in HIV-1 transfer to CD4(+) T lymphocytes. *Front. Cell. Infect. Microbiol.* 10:70. doi: 10.3389/fcimb.2020.00070

Perot, B. P., and Ménager, M. M. (2020). Tetraspanin 7 and its closest paralog tetraspanin 6: membrane organizers with key functions in brain development, viral infection, innate immunity, diabetes and cancer. *Med. Microbiol. Immunol.* 209, 427–436. doi: 10.1007/s00430-020-00681-3

Pileri, P., Uematsu, Y., Campagnoli, S., Galli, G., Falugi, F., Petracca, R., et al. (1998). Binding of hepatitis C virus to CD81. *Science* 282, 938–941. doi: 10.1126/science.282.5390.938

Plotnikov, D., Shah, R. L., Rodrigues, J. N., Cumberland, P. M., Rahi, J. S., Hysi, P. G., et al. (2019). A commonly occurring genetic variant within the NPLOC4-TSPAN10-PDE6G gene cluster is associated with the risk of strabismus. *Hum. Genet.* 138, 723–737. doi: 10.1007/s00439-019-02022-8

Priel, A., Kolleker, A., Ayalon, G., Gillor, M., Osten, P., and Stern-Bach, Y. (2005). Stargazin reduces desensitization and slows deactivation of the AMPA-type glutamate receptors. *J. Neurosci.* 25, 2682–2686. doi: 10.1523/jneurosci.4834-04.2005

Protty, M. B., Watkins, N. A., Colombo, D., Thomas, S. G., Heath, V. L., Herbert, J. M., et al. (2009). Identification of Tspan9 as a novel platelet tetraspanin and the collagen receptor GPVI as a component of tetraspanin microdomains. *Biochem. J.* 417, 391–400. doi: 10.1042/bj20081126

Qi, Y., Lv, J., Liu, S., Sun, L., Wang, Y., Li, H., et al. (2019). TSPAN9 and EMILIN1 synergistically inhibit the migration and invasion of gastric cancer cells by increasing TSPAN9 expression. *BMC Cancer* 19:630. doi: 10.1186/s12885-019-5810-2

Quagliano, A., Gopalakrishnapillai, A., Kolb, E. A., and Barwe, S. P. (2020). CD81 knockout promotes chemosensitivity and disrupts in vivo homing and engraftment in acute lymphoblastic leukemia. *Blood Adv.* 4, 4393–4405. doi: 10.1182/bloodadvances.2020001592

Reiss, K., Maretzky, T., Ludwig, A., Tousseyn, T., De Strooper, B., Hartmann, D., et al. (2005). ADAM10 cleavage of N-cadherin and regulation of cell-cell adhesion and beta-catenin nuclear signalling. *EMBO J.* 24, 742–752. doi: 10.1038/sj.emboj.7600548

Reyat, J. S., Chimen, M., Noy, P. J., Szyroka, J., Rainger, G. E., and Tomlinson, M. G. (2017). ADAM10-Interacting Tetraspanins Tspan5 and Tspan17 Regulate VE-Cadherin Expression and Promote T Lymphocyte Transmigration. *J. Immunol.* 199, 666–676. doi: 10.4049/jimmunol.1600713

Reynolds, J. L., and Mahajan, S. D. (2020). Transmigration of Tetraspanin 2 (Tspan2) siRNA Via Microglia Derived Exosomes across the Blood Brain Barrier Modifies the Production of Immune Mediators by Microglia Cells. *J. Neuroimmune Pharmacol.* 15, 554–563. doi: 10.1007/s11481-019-09895-6

Riva, I., Eibl, C., Volkmer, R., Carbone, A. L., and Plested, A. J. (2017). Control of AMPA receptor activity by the extracellular loops of auxiliary proteins. *eLife* 6:e28680. doi: 10.7554/eLife.28680

Sager, C., Tapken, D., Kott, S., and Hollmann, M. (2009). Functional modulation of AMPA receptors by transmembrane AMPA receptor regulatory proteins. *Neuroscience* 158, 45–54. doi: 10.1016/j.neuroscience.2007.12.046

Salas, I. H., Callaerts-Vegh, Z., Arranz, A. M., Guix, F. X., D'hooge, R., Esteban, J. A., et al. (2017). Tetraspanin 6: a novel regulator of hippocampal synaptic transmission and long term plasticity. *PLoS One* 12:e0171968. doi: 10.1371/journal.pone.0171968

Sanyal, S., De Ruiter, A., and Hawkins, R. K. (1980). Development and degeneration of retina in rds mutant mice: light microscopy. *J. Comp. Neurol.* 194, 193–207. doi: 10.1002/cne.901940110

Schäfer, D., Tomiuk, S., Küster, L. N., Rawashdeh, W. A., Henze, J., Tischler-Höhle, G., et al. (2021). Identification of CD318, TSPAN8 and CD66c as target candidates for CAR T cell based immunotherapy of pancreatic adenocarcinoma. *Nat. Commun.* 12:1453. doi: 10.1038/s41467-021-21774-4

Schaffer, A. M., and Minguet, S. (2020). Caveolin-1, tetraspanin CD81 and flotillins in lymphocyte cell membrane organization, signaling and immunopathology. *Biochem. Soc. Trans.* 48, 2387–2397. doi: 10.1042/bst20190387

Schmidt, C., Künemund, V., Wintergerst, E. S., Schmitz, B., and Schachner, M. (1996). CD9 of mouse brain is implicated in neurite outgrowth and cell migration in vitro and is associated with the alpha 6/beta 1 integrin and the neural adhesion molecule L1. *J. Neurosci. Res.* 43, 12–31. doi: 10.1002/jnr.490430103

Schwenk, J., Baehrens, D., Haupt, A., Bildl, W., Boudkkazi, S., Roeper, J., et al. (2014). Regional diversity and developmental dynamics of the AMPA-receptor

proteome in the mammalian brain. *Neuron* 84, 41–54. doi: 10.1016/j.neuron.2014.08.044

Schwenk, J., Harmel, N., Brechet, A., Zolles, G., Berkefeld, H., Müller, C. S., et al. (2012). High-resolution proteomics unravel architecture and molecular diversity of native AMPA receptor complexes. *Neuron* 74, 621–633. doi: 10.1016/j.neuron.2012.03.034

Seehafer, J. G., Tang, S. C., Slupsky, J. R., and Shaw, A. R. (1988). The functional glycoprotein CD9 is variably acylated: localization of the variably acylated region to a membrane-associated peptide containing the binding site for the agonistic monoclonal antibody 50H.*19. Biochim. Biophys. Acta* 957, 399–410. doi: 10.1016/0167-4838(88)90231-2

Seigneuret, M. (2006). Complete predicted three-dimensional structure of the facilitator transmembrane protein and hepatitis C virus receptor CD81: conserved and variable structural domains in the tetraspanin superfamily. *Biophys. J.* 90, 212–227. doi: 10.1529/biophysj.105.069666

Seipold, L., Damme, M., Prox, J., Rabe, B., Kasparek, P., Sedlacek, R., et al. (2017). Tetraspanin 3: a central endocytic membrane component regulating the expression of ADAM10, presenilin and the amyloid precursor protein. *Biochim. Biophys. Acta* 1864, 217–230. doi: 10.1016/j.bbamcr.2016.11.003

Seipold, L., and Saftig, P. (2016). The emerging role of tetraspanins in the proteolytic processing of the amyloid precursor protein. *Front. Mol. Neurosci.* 9:149. doi: 10.3389/fnmol.2016.00149

Sidahmed-Adrar, N., Ottavi, J. F., Benzoubir, N., Ait Saadi, T., Bou Saleh, M., Mauduit, P., et al. (2019). Tspan15 is a new stemness-related marker in hepatocellular carcinoma. *Proteomics* 19:e1900025. doi: 10.1002/pmic.201900025

Sobolevsky, A. I., Rosconi, M. P., and Gouaux, E. (2009). X-ray structure, symmetry and mechanism of an AMPA-subtype glutamate receptor. *Nature* 462, 745–756. doi: 10.1038/nature08624

Stiles, K. M., and Kielian, M. (2016). Role of TSPAN9 in Alphavirus Entry and Early Endosomes. *J. Virol.* 90, 4289–4297. doi: 10.1128/jvi.00018-16

Stilgenbauer, S., Aurran Schleinitz, T., Eichhorst, B., Lang, F., Offner, F., Rossi, J. F., et al. (2019). Phase 1 first-in-human trial of the anti-CD37 antibody BI 836826 in relapsed/refractory chronic lymphocytic leukemia. *Leukemia* 33, 2531–2535. doi: 10.1038/s41375-019-0475-z

Stinnesbeck, M., Kristiansen, A., Ellinger, J., Hauser, S., Egevad, L., Tolkach, Y., et al. (2021). Prognostic role of TSPAN1, KIAA1324 and ESRP1 in prostate cancer. *APMIS* 129, 204–212. doi: 10.1111/apm.13117

Stipp, C. S., and Hemler, M. E. (2000). Transmembrane-4-superfamily proteins CD151 and CD81 associate with alpha 3 beta 1 integrin, and selectively contribute to alpha 3 beta 1-dependent neurite outgrowth. *J. Cell Sci.* 113(Pt 11), 1871–1882.

Stipp, C. S., Kolesnikova, T. V., and Hemler, M. E. (2003). Functional domains in tetraspanin proteins. *Trends Biochem. Sci.* 28, 106–112. doi: 10.1016/s0968-0004(02)00014-2

Stuck, M. W., Conley, S. M., and Naash, M. I. (2016). PRPH2/RDS and ROM-1: historical context, current views and future considerations. *Prog. Retin. Eye Res.* 52, 47–63. doi: 10.1016/j.preteyeres.2015.12.002

Sun, H., Sun, Y., Chen, Q., and Xu, Z. (2020). LncRNA KCNQ1OT1 contributes to the progression and chemoresistance in acute myeloid leukemia by modulating Tspan3 through suppressing miR-193a-3p. *Life Sci.* 241:117161. doi: 10.1016/j.lfs.2019.117161

Susa, K. J., Rawson, S., Kruse, A. C., and Blacklow, S. C. (2021). Cryo-EM structure of the B cell co-receptor CD19 bound to the tetraspanin CD81. *Science* 371, 300–305. doi: 10.1126/science.abd9836

Tang, Y., Xie, J., Chen, Y., Zhang, T., Zhuo, H., Chen, J., et al. (2020). Tspan8 is highly expressed in clear cell renal cell carcinoma and indicates poor prognosis. *Ann. Clin. Lab. Sci.* 50, 638–644.

Termini, C. M., and Gillette, J. M. (2017). Tetraspanins function as regulators of cellular signaling. *Front. Cell. Dev. Biol.* 5:34. doi: 10.3389/fcell.2017.00034

Tian, J., Zhang, R., Piao, H., Li, X., Sheng, W., Zhou, J., et al. (2018). Silencing Tspan1 inhibits migration and invasion, and induces the apoptosis of human pancreatic cancer cells. *Mol. Med. Rep.* 18, 3280–3288. doi: 10.3892/mmr.2018.9331

Tomita, S. (2010). Regulation of ionotropic glutamate receptors by their auxiliary subunits. *Physiology* 25, 41–49. doi: 10.1152/physiol.00033.2009

Torres-Gómez, Á, Cardeñes, B., Díez-Sainz, E., Lafuente, E. M., and Cabañas, C. (2021). Functional integrin regulation through interactions with tetraspanin CD9. *Methods Mol. Biol.* 2217, 47–56. doi: 10.1007/978-1-0716-0962-0_5

Travis, G. H., Christerson, L., Danielson, P. E., Klisak, I., Sparkes, R. S., Hahn, L. B., et al. (1991). The human retinal degeneration slow (RDS) gene: chromosome assignment and structure of the mRNA. *Genomics* 10, 733–739. doi: 10.1016/0888-7543(91)90457-p

Traynelis, S. F., Wollmuth, L. P., Mcbain, C. J., Menniti, F. S., Vance, K. M., Ogden, K. K., et al. (2010). Glutamate receptor ion channels: structure, regulation, and function. *Pharmacol. Rev.* 62, 405–496. doi: 10.1124/pr.109.002451

Tsai, Y. C., Mendoza, A., Mariano, J. M., Zhou, M., Kostova, Z., Chen, B., et al. (2007). The ubiquitin ligase gp78 promotes sarcoma metastasis by targeting KAI1 for degradation. *Nat. Med.* 13, 1504–1509. doi: 10.1038/nm1686

Tunyasuvunakool, K., Adler, J., Wu, Z., Green, T., Zielinski, M., Žídek, A., et al. (2021). Highly accurate protein structure prediction for the human proteome. *Nature* 596, 590–596. doi: 10.1038/s41586-021-03828-1

Twomey, E. C., Yelshanskaya, M. V., Grassucci, R. A., Frank, J., and Sobolevsky, A. I. (2016). Elucidation of AMPA receptor-stargazin complexes by cryo-electron microscopy. *Science* 353, 83–86. doi: 10.1126/science.aaf8411

Twomey, E. C., Yelshanskaya, M. V., Vassilevski, A. A., and Sobolevsky, A. I. (2018). Mechanisms of channel block in calcium-permeable AMPA receptors. *Neuron* 99, 956–968.e4. doi: 10.1016/j.neuron.2018.07.027

Uhlén, M., Fagerberg, L., Hallström, B. M., Lindskog, C., Oksvold, P., Mardinoglu, A., et al. (2015). Proteomics. Tissue-based map of the human proteome. *Science* 347:1260419. doi: 10.1126/science.1260419

Umeda, R., Satouh, Y., Takemoto, M., Nakada-Nakura, Y., Liu, K., Yokoyama, T., et al. (2020). Structural insights into tetraspanin CD9 function. *Nat. Commun.* 11:1606. doi: 10.1038/s41467-020-15459-7

Vincent, A. K., Noor, A., Janson, A., Minassian, B. A., Ayub, M., Vincent, J. B., et al. (2012). Identification of genomic deletions spanning the PCDH19 gene in two unrelated girls with intellectual disability and seizures. *Clin. Genet.* 82, 540–545. doi: 10.1111/j.1399-0004.2011.01812.x

Wang, F. H., Ma, X. J., Xu, D., and Luo, J. (2018). UPK1B promotes the invasion and metastasis of bladder cancer via regulating the Wnt/β-catenin pathway. *Eur. Rev. Med. Pharmacol. Sci.* 22, 5471–5480. doi: 10.26355/eurrev_201809_15807

Wang, L., Gao, P., Yuan, P., Zhou, P., Fan, H., Lin, X., et al. (2021). miR-573 suppresses pancreatic cancer cell proliferation, migration, and invasion through targeting TSPAN1. *Strahlenther. Onkol.* 197, 438–448. doi: 10.1007/s00066-020-01728-3

Wang, Z., Cai, B., Cao, C., Lv, H., Dai, Y., Zheng, M., et al. (2021). Downregulation of CD151 induces oxidative stress and apoptosis in trophoblast cells via inhibiting ERK/Nrf2 signaling pathway in preeclampsia. *Free Radic. Biol. Med.* 164, 249–257. doi: 10.1016/j.freeradbiomed.2020.12.441

Wang, Y., Chan, S. L., Miele, L., Yao, P. J., Mackes, J., Ingram, D. K., et al. (2004). Involvement of Notch signaling in hippocampal synaptic plasticity. *Proc. Natl. Acad. Sci. U.S.A.* 101, 9458–9462. doi: 10.1073/pnas.0308126101

Wang, Y., Tong, X., Omoregie, E. S., Liu, W., Meng, S., and Ye, X. (2012). Tetraspanin 6 (TSPAN6) negatively regulates retinoic acid-inducible gene I-like receptor-mediated immune signaling in a ubiquitination-dependent manner. *J. Biol. Chem.* 287, 34626–34634. doi: 10.1074/jbc.M112.390401

Wollscheid, V., Kühne-Heid, R., Stein, I., Jansen, L., Köllner, S., Schneider, A., et al. (2002). Identification of a new proliferation-associated protein NET-1/C4.8 characteristic for a subset of high-grade cervical intraepithelial neoplasia and cervical carcinomas. *Int. J. Cancer* 99, 771–775. doi: 10.1002/ijc.10442

Wright, M. D., Henkle, K. J., and Mitchell, G. F. (1990). An immunogenic Mr 23,000 integral membrane protein of Schistosoma mansoni worms that closely resembles a human tumor-associated antigen. *J. Immunol.* 144, 3195–3200.

Wu, L., Chen, F., Wei, J., Shen, Y., and Xu, Q. (2016). Study of the tetraspanin 18 association with schizophrenia in a Han Chinese population. *Psychiatry Res.* 241, 263–266. doi: 10.1016/j.psychres.2016.03.057

Wu, X. R., Medina, J. J., and Sun, T. T. (1995). Selective interactions of UPIa and UPIb, two members of the transmembrane 4 superfamily, with distinct single transmembrane-domained proteins in differentiated urothelial cells. *J. Biol. Chem.* 270, 29752–29759. doi: 10.1074/jbc.270.50.29752

Xia, J., Zhang, X., Staudinger, J., and Huganir, R. L. (1999). Clustering of AMPA receptors by the synaptic PDZ domain-containing protein PICK1. *Neuron* 22, 179–187. doi: 10.1016/s0896-6273(00)80689-3

Xia, Y., Deng, Y., Zhou, Y., Li, D., Sun, X., Gu, L., et al. (2020). TSPAN31 suppresses cell proliferation in human cervical cancer through down-regulation of its antisense pairing with CDK4. *Cell Biochem. Funct.* 38, 660–668. doi: 10.1002/cbf.3526

Xie, Q., Guo, H., He, P., Deng, H., Gao, Y., Dong, N., et al. (2021). Tspan5 promotes epithelial-mesenchymal transition and tumour metastasis of hepatocellular carcinoma by activating Notch signalling. *Mol. Oncol.* 15, 3184–3202. doi: 10.1002/1878-0261.12980

Xu, D., Sharma, C., and Hemler, M. E. (2009). Tetraspanin12 regulates ADAM10-dependent cleavage of amyloid precursor protein. *FASEB J.* 23, 3674–3681. doi: 10.1096/fj.09-133462

Xu, Y., Wu, H., Wu, L., Xu, L., Li, J., Wang, Q., et al. (2020). Silencing of long non-coding RNA SOX21-AS1 inhibits lung adenocarcinoma invasion and migration by impairing TSPAN8 via transcription factor GATA6. *Int. J. Biol. Macromol.* 164, 1294–1303. doi: 10.1016/j.ijbiomac.2020.07.172

Xu-Monette, Z. Y., Li, L., Byrd, J. C., Jabbar, K. J., Manyam, G. C., Maria De Winde, C., et al. (2016). Assessment of CD37 B-cell antigen and cell of origin significantly improves risk prediction in diffuse large B-cell lymphoma. *Blood* 128, 3083–3100. doi: 10.1182/blood-2016-05-715094

Yang, X., Claas, C., Kraeft, S. K., Chen, L. B., Wang, Z., Kreidberg, J. A., et al. (2002). Palmitoylation of tetraspanin proteins: modulation of CD151 lateral interactions, subcellular distribution, and integrin-dependent cell morphology. *Mol. Biol. Cell* 13, 767–781. doi: 10.1091/mbc.01-05-0275

Yang, Y., Liu, X. R., Greenberg, Z. J., Zhou, F., He, P., Fan, L., et al. (2020). Open conformation of tetraspanins shapes interaction partner networks on cell membranes. *EMBO J.* 39:e105246. doi: 10.15252/embj.2020105246

Yang, Y. G., Sari, I. N., Zia, M. F., Lee, S. R., Song, S. J., and Kwon, H. Y. (2016). Tetraspanins: spanning from solid tumors to hematologic malignancies. *Exp. Hematol.* 44, 322–328. doi: 10.1016/j.exphem.2016.02.006

Yaseen, I. H., Monk, P. N., and Partridge, L. J. (2017). Tspan2: a tetraspanin protein involved in oligodendrogenesis and cancer metastasis. *Biochem. Soc. Trans.* 45, 465–475. doi: 10.1042/bst20160022

Young, R. W. (1967). The renewal of photoreceptor cell outer segments. *J. Cell Biol.* 33, 61–72. doi: 10.1083/jcb.33.1.61

Yu, J., Rao, P., Clark, S., Mitra, J., Ha, T., and Gouaux, E. (2021). Hippocampal AMPA receptor assemblies and mechanism of allosteric inhibition. *Nature* 594, 448–453. doi: 10.1038/s41586-021-03540-0

Yu, S., Chen, J., Quan, M., Li, L., Li, Y., and Gao, Y. (2021). CD63 negatively regulates hepatocellular carcinoma development through suppression of inflammatory cytokine-induced STAT3 activation. *J. Cell. Mol. Med.* 25, 1024–1034. doi: 10.1111/jcmm.16167

Yuan, J., Jin, C., Qin, H. D., Wang, J., Sha, W., Wang, M., et al. (2013). Replication study confirms link between TSPAN18 mutation and schizophrenia in Han Chinese. *PLoS One* 8:e58785. doi: 10.1371/journal.pone.0058785

Yuasa, T., Yoshiki, T., Tanaka, T., Kim, C. J., Isono, T., and Okada, Y. (1998). Expression of uroplakin Ib and uroplakin III genes in tissues and peripheral blood of patients with transitional cell carcinoma. *Jpn. J. Cancer Res.* 89, 879–882. doi: 10.1111/j.1349-7006.1998.tb00643.x

Zemni, R., Bienvenu, T., Vinet, M. C., Sefiani, A., Carrié, A., Billuart, P., et al. (2000). A new gene involved in X-linked mental retardation identified by analysis of an X;2 balanced translocation. *Nat. Genet.* 24, 167–170. doi: 10.1038/72829

Zhang, B., Li, D. X., Lu, N., Fan, Q. R., Li, W. H., and Feng, Z. F. (2015). Lack of Association between the TSPAN18 Gene and Schizophrenia Based on New Data from Han Chinese and a Meta-Analysis. *Int. J. Mol. Sci.* 16, 11864–11872. doi: 10.3390/ijms160611864

Zhang, D., Watson, J. F., Matthews, P. M., Cais, O., and Greger, I. H. (2021). Gating and modulation of a hetero-octameric AMPA glutamate receptor. *Nature* 594, 454–458. doi: 10.1038/s41586-021-03613-0

Zhang, M., Jiang, J., and Ma, C. (2021). The Outer Retinal Membrane Protein 1 Could Inhibit Lung Cancer Progression as a Tumor Suppressor. *Comput. Math. Methods Med.* 2021:6651764. doi: 10.1155/2021/6651764

Zhang, Q., Han, Q., Zi, J., Song, C., and Ge, Z. (2020). CD37 high expression as a potential biomarker and association with poor outcome in acute myeloid leukemia. *Biosci. Rep.* 40:BSR20200008. doi: 10.1042/bsr20200008

Zhang, Z. Y., Zhang, J. L., Zhao, L. X., Yang, Y., Guo, R., Zhou, N., et al. (2020). NAA10 promotes proliferation of renal cell carcinoma by upregulating UPK1B. *Eur. Rev. Med. Pharmacol. Sci.* 24, 11553–11560. doi: 10.26355/eurrev_202011_23796

Zhang, T., Sun, X., Han, J., and Han, M. (2019). Genetic variants of TSPAN12 gene in patients with retinopathy of prematurity. *J. Cell. Biochem.* 120, 14544–14551. doi: 10.1002/jcb.28715

Zhao, Y., Kiss, T., Delfavero, J., Li, L., Li, X., Zheng, L., et al. (2020). CD82-TRPM7-Numb signaling mediates age-related cognitive impairment. *Geroscience* 42, 595–611. doi: 10.1007/s11357-020-00166-4

Zheng, Y., Wang, D. D., Wang, W., Pan, K., Huang, C. Y., Li, Y. F., et al. (2014). Reduced expression of uroplakin 1A is associated with the poor prognosis of gastric adenocarcinoma patients. *PLoS One* 9:e93073. doi: 10.1371/journal.pone.0093073

Zhu, H., Tang, Y., Zhang, X., Jiang, X., Wang, Y., Gan, Y., et al. (2015). Downregulation of UPK1A suppresses proliferation and enhances apoptosis of bladder transitional cell carcinoma cells. *Med. Oncol.* 32:84. doi: 10.1007/s12032-015-0541-y

Zimmerman, B., Kelly, B., Mcmillan, B. J., Seegar, T. C. M., Dror, R. O., Kruse, A. C., et al. (2016). Crystal Structure of a Full-Length Human Tetraspanin Reveals a Cholesterol-Binding Pocket. *Cell* 167, 1041–1051.e11. doi: 10.1016/j.cell.2016.09.056

Conflict of Interest: The authors declare that the research was conducted in the absence of any commercial or financial relationships that could be construed as a potential conflict of interest.

Publisher's Note: All claims expressed in this article are solely those of the authors and do not necessarily represent those of their affiliated organizations, or those of the publisher, the editors and the reviewers. Any product that may be evaluated in this article, or claim that may be made by its manufacturer, is not guaranteed or endorsed by the publisher.

frontiers in Molecular Neuroscience

ORIGINAL RESEARCH
published: 02 February 2022
doi: 10.3389/fnmol.2022.801757

Metabotropic Glutamate Receptor 5 Antagonism Reduces Pathology and Differentially Improves Symptoms in Male and Female Heterozygous zQ175 Huntington's Mice

Si Han Li[1,2], Tash-Lynn L. Colson[1,2], Khaled S. Abd-Elrahman[1,2,3†] and Stephen S. G. Ferguson[1,2†]*

[1] Brain and Mind Research Institute, University of Ottawa, Ottawa, ON, Canada, [2] Department of Cellular and Molecular Medicine, Faculty of Medicine, University of Ottawa, Ottawa, ON, Canada, [3] Department of Pharmacology and Toxicology, Faculty of Pharmacy, Alexandria University, Alexandria, Egypt

OPEN ACCESS

Edited by:
Argel Aguilar-Valles,
Carleton University, Canada

Reviewed by:
Gerald W. Zamponi,
University of Calgary, Canada
Jean-Martin Beaulieu,
University of Toronto, Canada

***Correspondence:**
Stephen S. G. Ferguson
sferguso@uottawa.ca

[†] These authors share senior authorship

Specialty section:
This article was submitted to Molecular Signalling and Pathways, a section of the journal Frontiers in Molecular Neuroscience

Received: 25 October 2021
Accepted: 07 January 2022
Published: 02 February 2022

Citation:
Li SH, Colson T-LL, Abd-Elrahman KS and Ferguson SSG (2022) Metabotropic Glutamate Receptor 5 Antagonism Reduces Pathology and Differentially Improves Symptoms in Male and Female Heterozygous zQ175 Huntington's Mice.
Front. Mol. Neurosci. 15:801757.
doi: 10.3389/fnmol.2022.801757

Huntington's disease (HD) is an inherited autosomal dominant neurodegenerative disorder that leads to progressive motor and cognitive impairment. There are currently no available disease modifying treatments for HD patients. We have previously shown that pharmacological blockade of metabotropic glutamate receptor 5 (mGluR5) signaling rescues motor deficits, improves cognitive impairments and mitigates HD neuropathology in male zQ175 HD mice. Mounting evidence indicates that sex may influence HD progression and we have recently reported a sex-specific pathological mGluR5 signaling in Alzheimer's disease (AD) mice. Here, we compared the outcomes of treatment with the mGluR5 negative allosteric modulator CTEP (2-chloro-4-[2-[2,5-dimethyl-1-[4-(trifluoromethoxy)phenyl]imidazol-4-yl]ethynyl]pyridine) in both male and female symptomatic zQ175 mice. We found that female zQ175 mice required a longer treatment duration with CTEP than male mice to show improvement in their rotarod performance. Unlike males, chronic CTEP treatment did not improve the grip strength nor reverse the cognitive decline of female zQ175 mice. However, CTEP reduced the number of huntingtin aggregates, improved neuronal survival and decreased microglia activation in the striatum of both male and female zQ175 mice. Together, our results indicate that mGluR5 antagonism can reduce HD neuropathology in both male and female zQ175 HD mice, but sex has a clear impact on the efficacy of the treatment and must be taken into consideration for future HD drug development.

Keywords: neurodegenerative disease, huntingtin (Htt), G protein-coupled receptor (GPCR), sex differences, striatum, neuroglia, neuronal nuclei (NeuN)

Abbreviations: AD, Alzheimer's disease; HD, Huntington's disease; Iba1, ionized calcium binding adapter molecule 1; mGluR, metabotropic glutamate receptor; mHtt, mutant huntingtin; NeuN, neuronal nuclei; NMDAR, N-methyl-D-aspartate receptor; PKC, protein kinase C; PLC, phospholipase C.

INTRODUCTION

Huntington's disease (HD) is an inherited autosomal dominant neurodegenerative disease characterized by the early loss of medium spiny neurons in the striatum (Martin and Gusella, 1986). HD symptoms typically manifests between the age of 30–50 and includes choreatic movements, dementia and behavioral difficulties (Roos, 2010). HD is caused by the expansion of a polyglutamine repeat in the N-terminal region of the huntingtin protein (MacDonald et al., 1993). Mutant huntingtin proteins (mHtt) with this expanded polyglutamine repeats have been shown to be targeted for proteolysis and their cleavage at the N-terminus results in the formation of cytoplasmic and intranuclear aggregates that strongly correlate with HD symptoms and severity (DiFiglia et al., 1997). Indeed, longer polyglutamine repeats are associated with earlier disease onset and more severe symptoms (Andrew et al., 1993; Furtado et al., 1996). Despite this well-characterized etiology, disease modifying approaches to treat HD are lacking.

Glutamate is the major mediator of excitatory transmission in the brain and considerable evidence suggests glutamate-induced toxicity and reduction in glutamate uptake contribute to the selective loss of striatal neurons in HD (Hassel et al., 2008; Ribeiro et al., 2011, 2017). Metabotropic glutamate receptor 5 (mGluR5) is a member of the G protein-coupled receptor (GPCR) superfamily that is highly expressed in the striatum and cortex, the two brain regions most affected in HD (Shigemoto et al., 1993; Ribeiro et al., 2017). We have previously reported that mutant but not wildtype huntingtin can disrupt mGluR5 signaling by interacting with it as a part of a protein complex that includes the huntingtin-binding protein optineurin (Anborgh et al., 2005). We have also demonstrated that genetic deletion of mGluR5 in a Q111 mutant huntingtin knock in mouse model reduces mutant huntingtin aggregate size and improves disease pathology (Ribeiro et al., 2014). The prolonged pharmacological blockade of mGluR5 signaling with the negative allosteric modulator CTEP (2-chloro-4-[2-[2,5-dimethyl-1-[4-(trifluoromethoxy)phenyl]imidazol-4-yl]ethynyl]pyridine) also improves HD symptoms and promotes autophagic removal of mutant huntingtin aggregates in the brains of zQ175 HD mouse model (Abd-Elrahman et al., 2017; Abd-Elrahman and Ferguson, 2019). These findings indicate that targeted antagonism of mGluR5 may be effective for the treatment of HD. However, these studies were conducted exclusively in male HD mice and the effects of mGluR5 antagonism on HD pathology in female mice have not yet been investigated.

There is growing evidence that sex may influence HD phenotype and neuropathology in HD rodent models and patients (Dorner et al., 2007; Bode et al., 2008; Zielonka et al., 2013). We recently showed that activation of mGluR2/3 in male and female HD mice led to differential regulation of cell signaling pathways and there are sex-specific differences in cell signaling mechanisms contributing to the pathogenesis of HD (Li et al., 2021). More importantly, we have also reported sex-specific signaling of mGluR5 in AD mice (Abd-Elrahman et al., 2020a; Abd-Elrahman and Ferguson, 2022). Therefore, it is particularly important to study the disease modifying properties of CTEP and assess the contribution of pathological mGluR5 signaling to HD progression in female mice.

Here, we investigated whether targeted antagonism of mGluR5 using CTEP differentially improves HD symptoms and neuropathology in male versus female zQ175 HD mice. We find indeed that chronic treatment with CTEP differentially improves motor and cognitive deficits in male and female zQ175 mice. We also find that CTEP reduces mHtt aggregate pathology, neuronal loss and microgliosis in both male and female zQ175 mice. Our findings point to potential sex-specific differences in the contribution of mGluR5 to HD pathology.

MATERIALS AND METHODS

Reagents

CTEP (1972) was purchased from Axon Medchem (Reston, United States). Rabbit anti-Iba1 (Abcam Cat# ab178847, RRID:AB_2832244) was from Abcam (Cambridge, United States). Mouse anti-NeuN (Millipore Cat# ABN78, RRID:AB_10807945) and anti-Huntingtin clone mEM48 (Millipore Cat# MAB5374, RRID:AB_177645) were from Sigma-Aldrich (St. Louis, MO, United States).

Animals

All animal experimental protocols were approved by the University of Ottawa Institutional Animal Care Committee and were in accordance with the Canadian Council of Animal Care guidelines. Animals were group caged and housed under a constant 12-h light/dark cycle and food and water were given *ad libitum*. Wildtype and Heterozygous zQ175 HD mice carrying ∼188 CAG repeats were obtained from the Jackson Laboratory and bred to establish littermate-controlled male and female wildtype (Wt) and heterozygous zQ175 (zQ175) mice. Groups of 22 male and female Wt and zQ175 mice were aged to 12 months of age and 11 mice from each group were treated with either DMSO or CTEP (2 mg/kg; dissolved in 10% DMSO and then mixed with chocolate pudding; final DMSO concentration was 0.1%) for 12 weeks. This drug dose was calculated weekly according to weight and was based on our previous studies in male HD mice and AD mice (Hamilton et al., 2016; Abd-Elrahman et al., 2017, 2018, 2020a,b; de Souza et al., 2020). All groups were assessed in a battery of behavioral experiments after 4 and 12 weeks of drug treatment. At the end of the 12-week treatment, mice were sacrificed by exsanguination, and the brains were collected and randomized for immunostaining.

Behavioral Analysis

All animals were habituated in the testing room for a minimum of 30 min before testing. All behavioral tests were performed blindly and during the animal's dark cycle.

Forelimb Grip Strength

The grip strength of each mouse was measured using the Chatillon DEF II Grip Strength Meter (Columbus Instruments). Mice were held over the grid of the instrument by their tails and allowed to firmly grip the bar. The mice were then

pulled horizontally away from the bar using constant force and at a speed of ∼2.5 cm/s until they released the bar. Each mouse was tested 8 times with a break of 5 s in between each trial and the values of maximal peak force were recorded (Abd-Elrahman et al., 2017).

Rotarod Test

Mice were introduced to the rotarod apparatus (IITC Life Science, Woodlands Hills, CA, United States) by placing them on the rotarod at rest for 3 min on the first day. Four 5-min-long trails were then performed daily for two consecutive days using an accelerating protocol (from 5 to 45 RPM in 300 s) with 10 min of rest between each trial. Any mice remaining on the rotarod after 300 s were removed and the time scored as 300 s. Average of the latency to fall obtained from the four trials of the second day was used for analysis (Abd-Elrahman et al., 2017).

Novel Object Recognition

Mice were placed in a square arena measuring 45 cm × 45 cm × 45 cm and tracked using an overhead camera fed to a computer in a separate room. Mice were allowed to explore the empty arena for 5 min, and 5 min later, two identical objects were placed in the arena 5 cm from the edge and 5 cm apart. Mice were returned to the arena for 5 min and allowed to explore. The time spent exploring each object was recorded, and mice were considered exploring the object if their snout was within 1 cm of the object. Twenty-four hours after first exposure, the experiment was repeated with one object replaced with a novel object. The time spent exploring each object was recorded and analyzed using the Noldus EthoVision 10 software. Data were interpreted using the recognition index (time spent exploring the familiar object or the novel object over the total time spent exploring both objects multiplied by 100) and was used to measure the recognition memory [TA or $TB/(TA + TB)$] × 100, where T represents the time, A represents a familiar object, and B represents a novel object (Abd-Elrahman et al., 2017).

Immunohistochemistry

One hemisphere of each brain sample was fixed in 4%-paraformaldehyde and then transferred to 70% ethanol for storage at 4°C. The samples were embedded in paraffin and then coronally sectioned through the striatum at a thickness of 5 μm. Sections were then incubated with the mouse monoclonal EM48 antibody at 1:100, Neuronal Nuclei (NeuN) antibody at 1:1500, or Iba1 antibody at 1:8000 dilution for 30 min at room temperature and staining was done using Leica Bond III automatic stainer using BOND polymer Refine Detection Kit (Leica Biosystems Cat# DS9800, RRID:AB_2891238) from Leica Biosystems. Slide were scanned using a Leica Aperio Slide scanner at 20× and the number of EM positive aggregates, NeuN or Iba1 positive cells were counted in representative 300 × 300 μm^2 areas of the striatum. Experimenters were blinded to analysis and six sections per mouse were analyzed and for each section two ROIs in the striatum were quantified using the cell counter tool in ImageJ (Abd-Elrahman et al., 2017, 2020b, 2021a; Li et al., 2021).

Statistical Analysis

Means ± SEM are shown for each independent experiment and $P < 0.05$ was used as the threshold for statistical significance. Statistical significance was assessed using GraphPad Prism 9 software and was determined by Two-way or Three-way Analysis of Variance (ANOVAs) as appropriate, followed by Tukey's *post hoc* test to determine the source of significant interactions. Statistical details of individual experiments are indicated in figure legends.

RESULTS

CTEP Treatment Differentially Rescues Motor Deficits in Male and Female Heterozygous zQ175 Huntington's Disease Mice

To investigate potential sex-specific differences in the contribution of pathological mGluR5 signaling to HD progression and pathology, we first assessed whether targeted mGluR5 antagonism would improve motor deficits in symptomatic heterozygous male and female zQ175 mice. Twelve-month-old male and female wildtype and heterozygous zQ175 mice were treated with either vehicle or CTEP (2 mg/kg) every 48 h and their motor performance was assessed 4 weeks (13-month-old) and 12 weeks (15-month-old) after the initiation of treatment. The ANOVA indicated that vehicle-treated 13- and 15-month-old male and female heterozygous zQ175 mice showed significant impairment in forelimb grip strength compared to age- and sex-matched, vehicle-treated wildtype mice, F's(1,80) = 343.8 and 323.4; $p < 0.0001$, for 13- and 15-month-old vehicle-treated mice, respectively (**Figures 1A,B**). After both 4 and 12 weeks of treatment, the forelimb grip strength varied as a function of the Treatment × Genotype × Sex interaction, F's(1,80) = 5.298 and 16.39, $p = 0.0239$ and 0.0001, for 4 and 12 weeks, respectively. The follow-up tests of the simple effects of this interaction confirmed that CTEP treatment for either 4 or 12 weeks led to a statistically significant improvement in grip strength in male but not in female heterozygous zQ175 mice when compared to their sex-matched, vehicle-treated heterozygous zQ175 mice (**Figures 1A,B**). However, the forelimb grip force of CTEP-treated male heterozygous zQ175 mice remained lower than that of sex- and age-matched, vehicle-treated wildtypes (**Figures 1A,B**).

Vehicle-treated (4 and 12 weeks) male and female heterozygous zQ175 mice remained on the rotarod for a shorter time compared to age- and sex-matched, vehicle-treated wildtypes, F's(1,80) = 36.88 and 72.85, $p < 0.0001$, for 13- and 15-month-old vehicle-treated mice, respectively (**Figures 2A,B**). After 4 weeks of CTEP treatment, the rotarod performance varied as a function of the Treatment × Genotype × Sex interaction, $F(1,80) = 4.705$, $p = 0.0330$. Comparisons of the simple effects of this interaction indicated that 4 weeks of CTEP treatment improved the rotarod performance of male heterozygous zQ175 mice so that their performance was significantly better than that of age- and sex-matched, vehicle-treated zQ175 counterparts

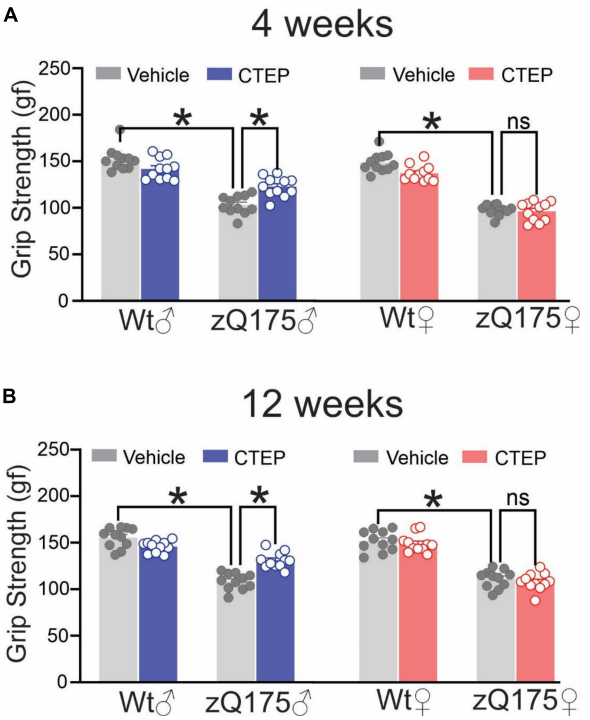

FIGURE 1 | Effect of chronic administration of CTEP on grip strength in male and female zQ175 mice. Mean ± SEM of grip strength [gram-force (gf)] after 4 weeks **(A)** and 12 weeks **(B)** of treatment with either vehicle or CTEP (2 mg/kg/48 h) of 12-month-old heterozygous zQ175 (zQ175) and wildtype (Wt) male and female mice (n = 11 for each group). *P < 0.05 by three-way analysis of variance (ANOVA) and Tukey's multiple comparisons test.

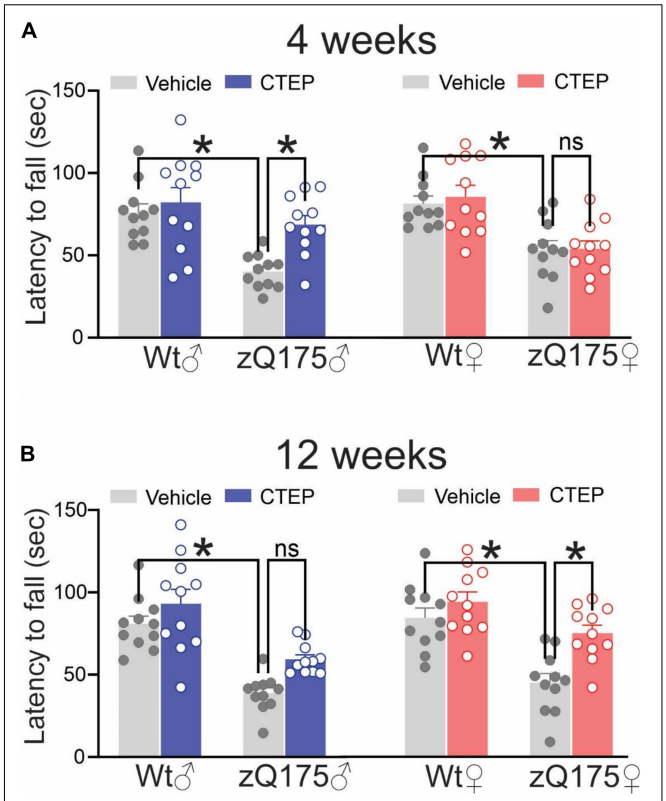

FIGURE 2 | Effect of chronic administration of CTEP on rotarod performance in male and female zQ175. Mean ± SEM of latency to fall (sec) from accelerating rotarod after 4 weeks **(A)** and 12 weeks **(B)** of treatment with either vehicle or CTEP (2 mg/kg/48 h) of 12-month-old heterozygous zQ175 (zQ175) and wild-type (Wt) male and female mice (n = 11 for each group). *P < 0.05 by three-way analysis of variance (ANOVA) and Tukey's multiple comparisons test.

(**Figure 2A**). However, CTEP failed to elicit any significant improvement in female heterozygous zQ175 mice (**Figure 2A**). A comparable interaction was not apparent after 12 weeks of CTEP treatment, $F(1,80) = 0.5789$, $p = 0.4490$. Specifically, after 12 weeks of CTEP treatment, both male and female heterozygous zQ175 mice showed significantly better rotarod performance relative to vehicle treated heterozygous mice of the same sex, $F(1,80) = 21.49$, $p < 0.0001$ (**Figure 2B**). In effect, CTEP improved the rotarod performance of both male and female heterozygous zQ175 mice after 12 weeks of treatment, however, the magnitude of this effect was larger in the females than in the males, although the interaction involving this variable was not significant (**Figure 2B**). Collectively, these data indicated that CTEP treatment differentially rescues motor deficits in female and male heterozygous zQ175 mice and highlight how sex can influence the efficacy of potential drug candidates in reversing specific HD symptoms.

CTEP Treatment Improves Cognitive Impairment in Male but Not Female Heterozygous zQ175 Huntington's Disease Mice

Huntington's disease was associated with cognitive impairment in addition to motor deficits (Lemiere et al., 2004). We previously reported that CTEP treatment for 12 weeks improved cognitive impairments in 15-month-old male heterozygous zQ175 mice (Abd-Elrahman et al., 2017). Thus, we assessed whether female heterozygous zQ175 mice exhibited memory impairment in the novel object recognition test at the same age and whether CTEP treatment could alleviate the impairment in female mice. Analysis of the recognition scores revealed a significant interaction between Genotype × Treatment, F's(1,72) = 90.37 and 22.07, $p < 0.0001$ for male and female, respectively. The follow up tests confirmed that unlike wildtypes, where comparable performance was observed irrespective of treatment at 15 months of age, both vehicle-treated male and female heterozygous zQ175 mice failed to distinguish between novel and familiar objects (**Figures 3A,B**). At the end of the 12 weeks of CTEP treatment, male heterozygous zQ175 mice regained their ability to discriminate between familiar and novel objects but female heterozygous zQ175 mice remained cognitively impaired (**Figures 3A,B**). Collectively, these data indicated that while both male and female heterozygous zQ175 mice present with cognitive deficits, mGluR5 antagonism does not rescue these deficits in HD mice on a female background.

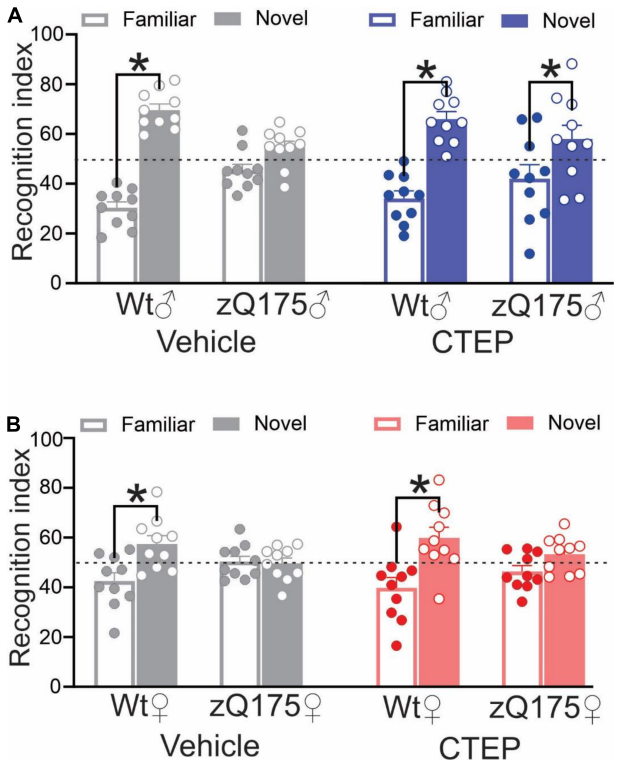

FIGURE 3 | Effect of chronic administration of CTEP on novel object recognition in male and female zQ175 mice. Mean ± SEM of the recognition index, for exploring a novel object versus a familiar object on the second day of novel object recognition test, after 12 weeks of treatment with either vehicle or CTEP (2 mg/kg/48 h) of 12-month-old heterozygous zQ175 (zQ175) and wild-type (Wt) male **(A)** and female **(B)** mice (n = 10 for all groups). *$P < 0.05$ by two-way analysis of variance (ANOVA) and Tukey's multiple comparisons test.

CTEP Treatment Reduced Huntingtin Aggregate Number and Neuronal Loss in Both Male and Female Heterozygous zQ175 Huntington's Disease Mice

The formation of intranuclear and cytoplasmic mHtt aggregates are the pathological hallmark of HD (DiFiglia et al., 1997). We have reported that genetic silencing and pharmacological blockade of mGluR5 reduced the number of mHtt aggregates in male Q111 and zQ175 HD mice, respectively (Ribeiro et al., 2014; Abd-Elrahman et al., 2017). Therefore, we examined whether chronic CTEP treatment can also reduce the number of mHtt aggregates in female zQ175 HD mice. After 12 weeks of CTEP treatment, the number of mHtt aggregates in the striatum of both male and female heterozygous zQ175 mice were significantly reduced compared to age- and sex-matched, vehicle-treated heterozygous zQ175 mice, $F(1,16) = 23.19$, $p = 0.0002$ (**Figures 4A,B**). Next, we examined whether the improvement in motor function and the decrease in aggregates accumulation were associated with the rescue of neuronal survival. The number of neuronal nuclei (NeuN)-positive cells in the striatum of vehicle-treated 15-month-old male and female heterozygous zQ175 mice was significantly lower than that of age- and sex-matched, vehicle-treated wildtype mice, $F(1,32) = 48.82$, $p < 0.0001$ (**Figures 5A–C**). Twelve week-treatment with CTEP significantly increased the number of NeuN-positive striatal neurons of both male and female heterozygous zQ175 mice compared to age-and sex-matched, vehicle-treated heterozygous zQ175 mice, $F(1,32) = 9.361$, $p = 0.0045$, and to values that are not different from age- and sex-matched, vehicle-treated wildtype mice (**Figures 5A–C**). Collectively, these findings indicate that chronic CTEP treatment can reduce HD pathology and rescue neuronal loss in both male and female heterozygous zQ175 mice.

CTEP Treatment Reduces Microglial Activation in Heterozygous zQ175 Huntington's Disease Mice

Microglia activation has been suggested to contribute to the pathogenesis of several neurodegenerative diseases, including AD, Parkinson's disease, Amyotrophic Lateral Sclerosis and HD (Perry et al., 2010; Abd-Elrahman et al., 2021b). Activation of microglia has been observed in both pre-symptomatic HD gene carriers and symptomatic patients (Pavese et al., 2006; Tai et al., 2007; Björkqvist et al., 2008). Therefore, we assessed the number of activated microglia in the striatum of our mice by staining for ionized calcium-binding adapter molecule 1 (Iba1), a protein that is specifically expressed during microgliosis (Ito et al., 1998). The number of Iba1-positive cells was significantly higher in the striatum of 15-month-old vehicle-treated male and female heterozygous zQ175 mice compared to age- and sex-matched, vehicle-treated wildtypes, $F(1,32) = 41.48$, $p < 0.0001$ (**Figures 6A–C**). Twelve weeks of CTEP treatment reduced the number of Iba1-positive cells in the striatum of both male and female zQ175 mice, $F(1,32) = 6.573$, $p = 0.0153$, to values that are not significantly different than age- and sex-matched, vehicle-treated wildtypes (**Figures 6A–C**).

DISCUSSION

Despite the discovery of its underlying genetic cause decades ago, the exact mechanism(s) underlying HD progression remain poorly understood and treatment options for HD patients are largely symptomatic. Glutamate signaling plays a significant role in the pathophysiology of HD, and the pharmacological blockade of mGluR5 using NAMs delays disease progression in male zQ175 HD mice (Abd-Elrahman et al., 2017). However, several reports have emerged suggesting that sex can influence age of onset and disease progression in HD (Roos et al., 1991; Bode et al., 2008; Zajac et al., 2010; Cao et al., 2018). Furthermore, sex-specific differences in mGluR5 signaling and response to mGluR5 NAMs have been reported in AD mice (Abd-Elrahman et al., 2020a; Abd-Elrahman and Ferguson, 2022). Here, we show that CTEP can indeed improve the performance of male HD mice in all motor and cognitive tasks but fails to elicit similar outcomes in female HD mice. We also demonstrate that CTEP reduces mHtt pathology, microgliosis and neuronal death in both sexes. Our findings point to distinct sex-specific differences in the outcomes of chronic mGluR5 blockade between male

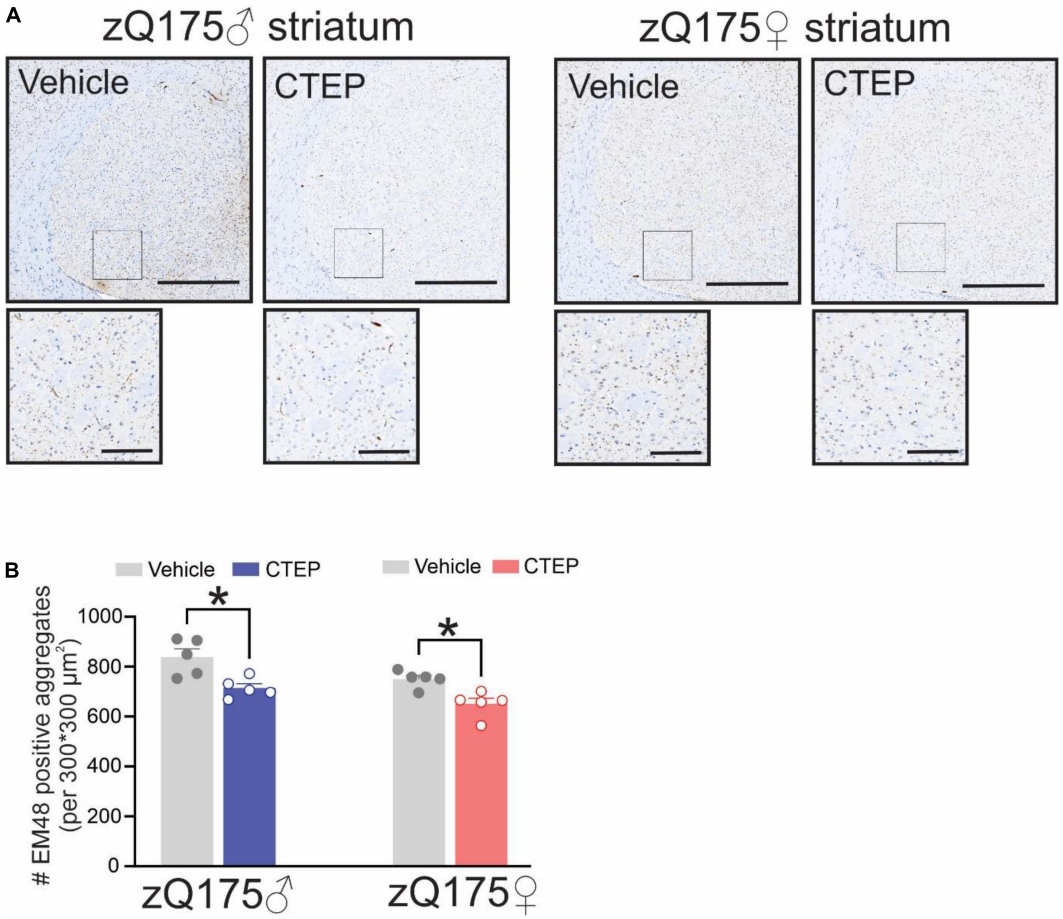

FIGURE 4 | Effect of chronic administration CTEP on mutant huntingtin aggregates in male and female zQ175 mouse striatum. Representative images of staining for mHtt aggregates using the antibody EM48 **(A)** and quantification of the number of huntingtin aggregates **(B)** in striatal brain slices from 15-month-old male and female heterozygous zQ175 mice after 12 weeks of treatment with either vehicle or CTEP (2 mg/kg/48 h). Scale bar = 500 μm for whole striatum and 100 μm for magnified areas. Data are quantified from two different 300 × 300 μm^2 striatal regions of 6 sections per mouse and five independent mouse brains from each group were used for analysis. Data are mean ± SEM. *$P < 0.05$ by two-way analysis of variance (ANOVA) and Tukey's multiple comparisons test.

and female HD mice that warrants investigating the plausible underlying mechanism(s).

We have previously shown that male heterozygous zQ175 mice at 12 months of age have significant deficits in both motor and cognitive functions that can be reversed by 12-week treatment with CTEP (Abd-Elrahman et al., 2017; Li et al., 2021). Here, we find that both male and female heterozygous zQ175 mice present with significant and comparable impairments in their grip strength and motor coordination that are consistent with previous findings by our group and others using the same mouse model (Menalled et al., 2012; Smith et al., 2014; Abd-Elrahman et al., 2017; Li et al., 2021). We also show that the short (4 weeks) and the long (12 weeks) treatment paradigms are to a great extent equally effective in reversing impairments in grip force and motor coordination of male zQ175 mice during rotarod test. Despite both age-matched male and female HD mice showing deficits in grip strength and motor function, CTEP was not able to improve the performance of female zQ175 mice in most of the motor tasks. Specifically, CTEP did not improve grip strength and only longer treatment with CTEP was able to significantly improve the rotarod performance of female zQ175 mice. Sex-dependent differences in the onset of some motor symptoms were previously reported in another knock-in model of HD, HdhQ350/+ mice (Cao et al., 2018). Moreover, the expression of brain-derived neurotrophic factor (BDNF) was found to be severely affected in female R6/1 mice compared to age-matched males (Zajac et al., 2010). Therefore, it is possible that motor deficits present earlier in female compared to male zQ175 mice and extended treatment is required to reverse these impairments in females. Interestingly, impairment in precision grip control is an early predictor of disease onset and manifest in the pre-HD stage in patients (Rao et al., 2011). Thus, it is also possible that deficits in grip force manifests even earlier than limb coordination and an extended treatment paradigm (beyond 12 weeks) is required to detect a significant improvement in grip strength in female zQ175 mice.

Progressive cognitive decline is another debilitating symptom of HD and MRI study show that HD pathology spreads to the

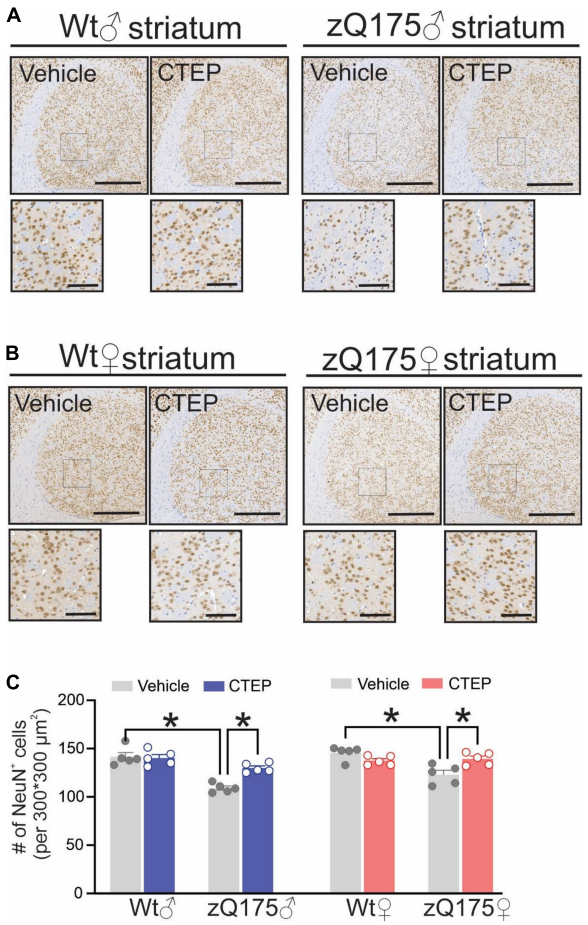

FIGURE 5 | Effect of chronic administration of CTEP on neuronal survival in male and female zQ175 mouse striatum. Representative images of staining for neuronal nuclei (NeuN)-positive cells in striatal brain slices from 15-month-old male **(A)** and female **(B)** heterozygous zQ175 (zQ175) and wild-type (Wt) mice after 12 weeks of treatment with either vehicle or CTEP (2 mg/kg/48 h). Scale bar = 500 μm for whole striatum and 100 μm for magnified areas. **(C)** Quantification of the number of NeuN-positive cells in striatal brain slices from 15-month-old male and female zQ175 and Wt mice after 12 weeks of treatment with either vehicle or CTEP. Data are quantified from two different 300 × 300 μm^2 striatal regions of 6 sections per mouse and five independent mouse brains from each group were used for analysis. Data are mean ± SEM. *$P < 0.05$ by three-way analysis of variance (ANOVA) and Tukey's multiple comparisons test.

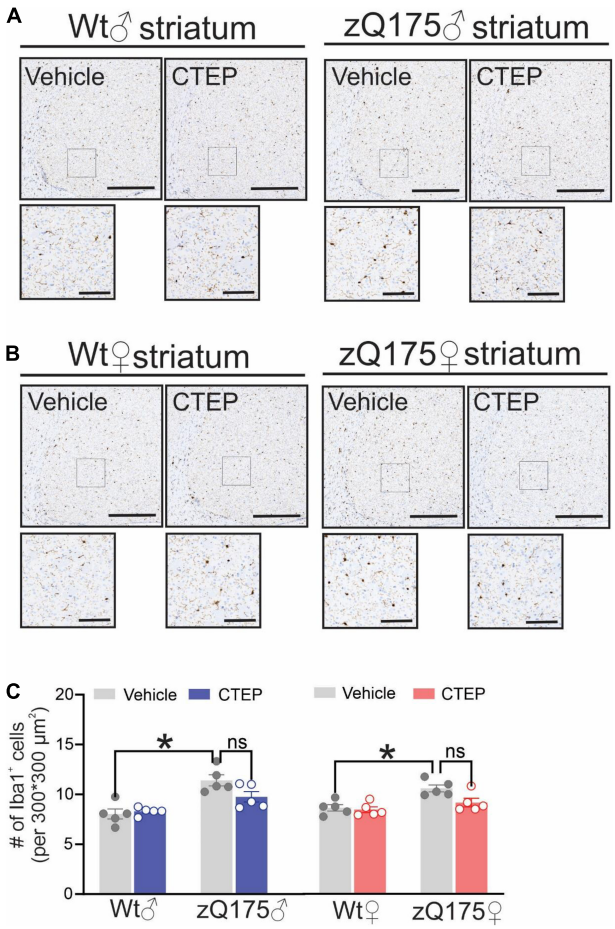

FIGURE 6 | Effect of chronic administration of CTEP on microglia activation in male and female zQ175 mouse striatum. Representative images of staining for ionized calcium binding adaptor molecule 1 (Iba1)-positive cells in striatal brain slices from 15-month-old male **(A)** and female **(B)** heterozygous zQ175 (zQ175) and wild-type (Wt) mice after 12 weeks of treatment with either vehicle or CTEP (2 mg/kg/48 h). Scale bar = 500 μm for whole striatum and 100 μm for magnified areas. **(C)** quantification of the number of Iba1-positive cells in striatal brain slices from 15-month-old male and female zQ175 and Wt mice after 12 weeks of treatment with either vehicle or CTEP. Data are quantified from two different 300 × 300 μm^2 striatal regions of 6 sections per mouse and five independent mouse brains from each group were used for analysis. Data are mean ± SEM. *$P < 0.05$ by three-way analysis of variance (ANOVA) and Tukey's multiple comparisons test.

hippocampus, a brain region well-known to be important for learning and memory (Rosas et al., 2003; Lemiere et al., 2004; Bird and Burgess, 2008; van den Bogaard et al., 2011). Additionally, impaired neurogenesis and appearance of mHtt aggregates in the hippocampus have also been reported in animal models of HD (Morton et al., 2000; Simpson et al., 2011; Abd-Elrahman et al., 2017). Here, we show that CTEP reverses cognitive impairment in the novel object recognition test in male but not female zQ175 mice. Interestingly, such an observation is consistent with our most recent work showing that CTEP can reverse deficits in spatial and working memory in male but not female AD mice (Abd-Elrahman et al., 2020a). mGluR5 signaling is differentially regulated between male and female AD mice due to sex-specific differences in the composition of the pathological scaffold formed between amyloid β (Aβ) and mGluR5 (Abd-Elrahman et al., 2020a; Abd-Elrahman and Ferguson, 2022). Thus, it is possible that similar to Aβ, mHtt triggers a sex-specific pathological signaling of mGluR5 that alters the efficacy of mGluR5 NAMs in reversing memory and motor deficits in female HD mice.

Deposition of insoluble mHtt aggregates in the striatum is one of the distinguishing features of HD pathology and mGluR5 is highly expressed in striatum (Shigemoto et al., 1993; DiFiglia et al., 1997). We show that mGluR5 antagonism results in a significant reduction in the number of mHtt aggregates

and rescues neuronal loss in the striatum of both male and female zQ175 mice. Since mHtt is known to alter transcriptional regulation and apoptosis (Kim et al., 1999; Rigamonti et al., 2000; Cui et al., 2006), it is likely that the reduction in mHtt following chronic mGluR5 inhibition reduces the loss of striatal neurons and nurture the neurotrophic capacity in HD brains. We have previously reported a similar reduction in apoptotic neuronal loss and mHtt aggregates in male zQ175 mice that was attributed to reactivation of a ZBTB16-dependent autophagy pathway that facilitates the clearance of mHtt aggregates from the striatum (Abd-Elrahman et al., 2017). However, ZBTB16 autophagic pathway is regulated in a sex-specific manner in zQ175 and AD mice and therefore it is likely that the mechanisms underling such reduction in mHtt load and neuronal loss after mGluR5 antagonism are different between both sexes (Abd-Elrahman et al., 2020a; Li et al., 2021). Further investigation in the mechanism(s) underlying such reduction in mHtt pathology in CTEP-treated female zQ175 mice is required in the future.

Activated microglia and elevated levels of pro-inflammatory cytokines have been found in the brains of HD patients and are thought to contribute to HD pathology (Tai et al., 2007; Björkqvist et al., 2008; Silvestroni et al., 2009). mGluR5 is heavily expressed in microglia and the genetic deletion of mGluR5 in BACHD mouse model of HD triggers cortical microgliosis (Biber et al., 1999; Carvalho et al., 2019). We detected microgliosis in the striatum of both male and female zQ175 mice that was abrogated by CTEP, suggesting that mGluR5 antagonism can be effective in reducing neuroinflammation in HD brains of both sexes. It is worth noting that pharmacological silencing of mGluR5 using CTEP in amyotrophic lateral sclerosis (ALS) and AD mice, two neurodegenerative diseases in which glutamate-mediated excitotoxicity plays a crucial role, reduced the number of activated microglia (Abd-Elrahman et al., 2020b; Milanese et al., 2021). Therefore, it is possible that in HD, glutamate excitotoxicity triggers microglial mGluR5 overactivation leading to microgliosis and exacerbation of neuroinflammation that can be abolished by mGluR5 NAMs.

Metabotropic glutamate receptor 5 NAMs remain a promising disease modifying treatment in HD since they are capable of reversing disease pathology in both sexes, but it is possible that extended treatment in females is required to accomplish a significant recovery in motor and cognitive symptoms. The mechanism(s) underlying the sex-specific differences in the efficacy of mGluR5 NAMs in zQ175 HD mice remains unclear. So far, no differences in the subcellular localization, expression, and function of mGluR5 between males and females have been reported in HD. However, mGluR5 can directly interact with mHtt in male Q111 HD mice leading to altered receptor signaling but such interaction has not been investigated in female HD mice (Anborgh et al., 2005; Ribeiro et al., 2010). Furthermore, membrane estrogen receptors are coupled to mGluR5 in female rat striatum and can activate mGluR5 signaling in the presence of estradiol (Grove-Strawser et al., 2010). Therefore, it is possible that mGluR5 interaction with mHtt in HD brain is either intrinsically different between males and females or is influenced by the crosstalk between mGluR5 and sex hormone receptors. Additionally, membrane mGluR5 forms heterodimers and it is possible that the composition of these dimers is regulated in a sex-specific manner leading to differential binding and/or efficacy of mGluR5 allosteric ligands (Prinster et al., 2005; Lee et al., 2020).

CONCLUSION

We demonstrate that mGluR5 contributes to HD pathophysiology in male and female zQ175 HD mice and that while mGluR5 NAMs can reverse neuropathology in both sexes, they are less efficacious in reversing symptoms in female compared with male mice. Thus, there are important sex-specific differences in the signaling pathways downstream of mGluR5 that contributes to the pathophysiology zQ175 HD mice that should be investigated in the future. We also emphasize the importance of designing individualized HD treatments that takes both the sex and disease stage of the patient into account.

DATA AVAILABILITY STATEMENT

The original contributions presented in the study are included in the article/supplementary material, further inquiries can be directed to the corresponding author.

ETHICS STATEMENT

All animal experimental protocols were approved by the University of Ottawa Institutional Animal Care Committee and were in accordance with the Canadian Council of Animal Care guidelines.

AUTHOR CONTRIBUTIONS

SL, KA-E, and SF were responsible for the conception and design of all experiments. SL, KA-E, and T-LC performed the experiments and data analysis. SL and KA-E wrote the manuscript. SF edited the manuscript and supervised the study. All authors contributed to the article and approved the submitted version.

FUNDING

This study was supported by the Huntington's Society of Canada, Krembil Foundation and Canadian Institutes of Health Research (CIHR) grants PJT-148656, PJT-153317, and PJT-165967 to SF, Ontario Graduate Scholarship to SL, and clinician postdoctoral fellowship from the Alberta Innovates Health Solutions and CIHR to KA-E.

ACKNOWLEDGMENTS

The authors thank Shaunessy Hutchinson for her breeding the animals, Behavior and Physiology Core at the University of Ottawa for their assistance, and Hymie Anisman (Carleton University) for assistance in the statistical analysis.

REFERENCES

Abd-Elrahman, K. S., Albaker, A., de Souza, J. M., Ribeiro, F. M., Schlossmacher, M. G., Tiberi, M., et al. (2020a). Aβ oligomers induce pathophysiological mGluR5 signaling in Alzheimer's disease model mice in a sex-selective manner. *Sci. Signal.* 13:eabd2494. doi: 10.1126/scisignal.abd2494

Abd-Elrahman, K. S., Hamilton, A., Albaker, A., and Ferguson, S. S. (2020b). mGluR5 contribution to neuropathology in Alzheimer mice is disease stage-dependent. *ACS Pharmacol. Transl. Sci.* 3, 334–344. doi: 10.1021/acsptsci.0c00013

Abd-Elrahman, K. S., and Ferguson, S. S. (2019). Modulation of mTOR and CREB pathways following mGluR5 blockade contribute to improved Huntington's pathology in zQ 175 mice. *Mol. Brain* 12, 1–9. doi: 10.1186/s13041-019-0456-1

Abd-Elrahman, K. S., and Ferguson, S. S. (2022). Noncanonical metabotropic glutamate receptor 5 signaling in Alzheimer's disease. *Annu. Rev. Pharmacol. Toxicol.* 62, 235–254. doi: 10.1146/annurev-pharmtox-021821-091747

Abd-Elrahman, K. S., Hamilton, A., Hutchinson, S. R., Liu, F., Russell, R. C., and Ferguson, S. S. (2017). mGluR5 antagonism increases autophagy and prevents disease progression in the zQ175 mouse model of Huntington's disease. *Sci. Signal.* 10:eaan6387. doi: 10.1126/scisignal.aan6387

Abd-Elrahman, K. S., Hamilton, A., Vasefi, M., and Ferguson, S. S. (2018). Autophagy is increased following either pharmacological or genetic silencing of mGluR5 signaling in Alzheimer's disease mouse models. *Mol. Brain* 11, 1–8. doi: 10.1186/s13041-018-0364-9

Abd-Elrahman, K. S., Sarasija, S., Colson, T. L. L., and Ferguson, S. S. (2021a). A M1 muscarinic acetylcholine receptor positive allosteric modulator improves pathology and cognitive deficits in female APPswe/PSEN1ΔE9 mice. *Br. J. Pharmacol. [Online ahead of print]* doi: 10.1111/bph.15750

Abd-Elrahman, K. S., Sarasija, S., and Ferguson, S. S. (2021b). The role of neuroglial metabotropic glutamate receptors in Alzheimer's disease. *Curr. Neuropharmacol. [Online ahead of print]* doi: 10.2174/1570159X19666210916102638

Anborgh, P. H., Godin, C., Pampillo, M., Dhami, G. K., Dale, L. B., Cregan, S. P., et al. (2005). Inhibition of metabotropic glutamate receptor signaling by the huntingtin-binding protein optineurin. *J. Biol. Chem.* 280, 34840–34848. doi: 10.1074/jbc.M504508200

Andrew, S. E., Goldberg, Y. P., Kremer, B., Telenius, H., Theilmann, J., Adam, S., et al. (1993). The relationship between trinucleotide (CAG) repeat length and clinical features of Huntington's disease. *Nat. Genet.* 4, 398–403. doi: 10.1038/ng0893-398

Biber, K., Laurie, D. J., Berthele, A., Sommer, B., Tolle, T. R., Gebicke-Härter, P. J., et al. (1999). Expression and signaling of group I metabotropic glutamate receptors in astrocytes and microglia. *J. Neurochem.* 72, 1671–1680. doi: 10.1046/j.1471-4159.1999.721671.x

Bird, C. M., and Burgess, N. (2008). The hippocampus and memory: insights from spatial processing. *Nat. Rev. Neurosci.* 9, 182–194. doi: 10.1038/nrn2335

Björkqvist, M., Wild, E. J., Thiele, J., Silvestroni, A., Andre, R., Lahiri, N., et al. (2008). A novel pathogenic pathway of immune activation detectable before clinical onset in Huntington's disease. *J. Exp. Med.* 205, 1869–1877. doi: 10.1084/jem.20080178

Bode, F. J., Stephan, M., Suhling, H., Pabst, R., Straub, R. H., Raber, K. A., et al. (2008). Sex differences in a transgenic rat model of Huntington's disease: decreased 17β-estradiol levels correlate with reduced numbers of DARPP32+ neurons in males. *Hum. Mol. Genet.* 17, 2595–2609. doi: 10.1093/hmg/ddn159

Cao, J. K., Detloff, P. J., Gardner, R. G., and Stella, N. (2018). Sex-dependent behavioral impairments in the HdhQ350/+ mouse line. *Behav. Brain Res.* 337, 34–45. doi: 10.1016/j.bbr.2017.09.026

Carvalho, T. G., Alves-Silva, J., de Souza, J. M., Real, A. L., Doria, J. G., Vieira, E. L., et al. (2019). Metabotropic glutamate receptor 5 ablation accelerates age-related neurodegeneration and neuroinflammation. *Neurochem. Int.* 126, 218–228. doi: 10.1016/j.neuint.2019.03.020

Cui, L., Jeong, H., Borovecki, F., Parkhurst, C. N., Tanese, N., and Krainc, D. (2006). Transcriptional repression of PGC-1α by mutant huntingtin leads to mitochondrial dysfunction and neurodegeneration. *Cell* 127, 59–69. doi: 10.1016/j.cell.2006.09.015

de Souza, J. M., Abd-Elrahman, K. S., Ribeiro, F. M., and Ferguson, S. S. (2020). mGluR5 regulates REST/NRSF signaling through N-cadherin/β-catenin complex in Huntington's disease. *Mol. Brain* 13, 1–15.

DiFiglia, M., Sapp, E., Chase, K. O., Davies, S. W., Bates, G. P., Vonsattel, J., et al. (1997). Aggregation of huntingtin in neuronal intranuclear inclusions and dystrophic neurites in brain. *Science* 277, 1990–1993. doi: 10.1126/science.277.5334.1990

Dorner, J. L., Miller, B. R., Barton, S. J., Brock, T. J., and Rebec, G. V. (2007). Sex differences in behavior and striatal ascorbate release in the 140 CAG knock-in mouse model of Huntington's disease. *Behav. Brain Res.* 178, 90–97. doi: 10.1016/j.bbr.2006.12.004

Furtado, S., Suchowersky, O., Rewcastle, N. B., Graham, L., Klimek, M. L., and Garber, A. (1996). Relationship between trinucliotide repeats and neuropathological changes in Huntington's diease. *Ann. Neurol.* 39, 132–136.

Grove-Strawser, D., Boulware, M. I., and Mermelstein, P. G. (2010). Membrane estrogen receptors activate the metabotropic glutamate receptors mGluR5 and mGluR3 to bidirectionally regulate CREB phosphorylation in female rat striatal neurons. *Neuroscience* 170, 1045–1055. doi: 10.1016/j.neuroscience.2010.08.012

Hamilton, A., Vasefi, M., Vander Tuin, C., McQuaid, R. J., Anisman, H., and Ferguson, S. S. (2016). Chronic pharmacological mGluR5 inhibition prevents cognitive impairment and reduces pathogenesis in an Alzheimer disease mouse model. *Cell Rep.* 15, 1859–1865. doi: 10.1016/j.celrep.2016.04.077

Hassel, B., Tessler, S., Faull, R. L., and Emson, P. C. (2008). Glutamate uptake is reduced in prefrontal cortex in Huntington's disease. *Neurochem. Res.* 33, 232–237. doi: 10.1007/s11064-007-9463-1

Ito, D., Imai, Y., Ohsawa, K., Nakajima, K., Fukuuchi, Y., and Kohsaka, S. (1998). Microglia-specific localisation of a novel calcium binding protein, Iba1. *Mol. Brain Res.* 57, 1–9. doi: 10.1016/s0169-328x(98)00040-0

Kim, M., Lee, H., LaForet, G., McIntyre, C., Martin, E. J., Chang, P., et al. (1999). Mutant huntingtin expression in clonal striatal cells: dissociation of inclusion formation and neuronal survival by caspase inhibition. *J. Neurosci.* 19, 964–973. doi: 10.1523/JNEUROSCI.19-03-00964.1999

Lee, J., Munguba, H., Gutzeit, V. A., Singh, D. R., Kristt, M., Dittman, J. S., et al. (2020). Defining the homo-and heterodimerization propensities of metabotropic glutamate receptors. *Cell Rep.* 31:107605.

Lemiere, J., Decruyenaere, M., Evers-Kiebooms, G., Vandenbussche, E., and Dom, R. (2004). Cognitive changes in patients with Huntington's disease (HD) and asymptomatic carriers of the HD mutation. *J. Neurol.* 251, 935–942.

Li, S. H., Colson, T.-L. L., Abd-Elrahman, K. S., and Ferguson, S. S. (2021). mGluR2/3 activation improves motor performance and reduces pathology in heterozygous zQ175 Huntington's disease mice. *J. Pharmacol. Exp. Therapeutics* 2021:JET–AR–2021–000735. doi: 10.1124/jpet.121.000735

MacDonald, M. E., Ambrose, C. M., Duyao, M. P., Myers, R. H., Lin, C., Srinidhi, L., et al. (1993). A novel gene containing a trinucleotide repeat that is expanded and unstable on Huntington's disease chromosomes. *Cell* 72, 971–983. doi: 10.1016/0092-8674(93)90585-e

Martin, J. B., and Gusella, J. F. (1986). Huntingtons disease. *N. Engl. J. Med.* 315, 1267–1276.

Menalled, L. B., Kudwa, A. E., Miller, S., Fitzpatrick, J., Watson-Johnson, J., Keating, N., et al. (2012). Comprehensive behavioral and molecular characterization of a new knock-in mouse model of Huntington's disease: zQ175. *PLoS One* 7:e49838. doi: 10.1371/journal.pone.0049838

Milanese, M., Bonifacino, T., Torazza, C., Provenzano, F., Kumar, M., Ravera, S., et al. (2021). Blocking metabotrobic glutamate receptor 5 by the negative allosteric modulator CTEP improves disease course of ALS in SOD1G93A mice. *Br. J. Pharmacol.* 178, 3747–3764. doi: 10.1111/bph.15515

Morton, A., Lagan, M., Skepper, J., and Dunnett, S. (2000). Progressive formation of inclusions in the striatum and hippocampus of mice transgenic for the human Huntington's disease mutation. *J. Neurocytol.* 29, 679–702. doi: 10.1023/a:1010887421592

Pavese, N., Gerhard, A., Tai, Y., Ho, A., Turkheimer, F., Barker, R., et al. (2006). Microglial activation correlates with severity in Huntington disease: a clinical and PET study. *Neurology* 66, 1638–1643. doi: 10.1212/01.wnl.0000222734.56412.17

Perry, V. H., Nicoll, J. A., and Holmes, C. (2010). Microglia in neurodegenerative disease. *Nat. Rev. Neurol.* 6:193.

Prinster, S. C., Hague, C., and Hall, R. A. (2005). Heterodimerization of g protein-coupled receptors: specificity and functional significance. *Pharmacol. Rev.* 57, 289–298. doi: 10.1124/pr.57.3.1

Rao, A. K., Gordon, A. M., and Marder, K. S. (2011). Coordination of fingertip forces during precision grip in premanifest Huntington's disease. *Mov. Disord.* 26, 862–869. doi: 10.1002/mds.23606

Ribeiro, F. M., DeVries, R. A., Hamilton, A., Guimaraes, I. M., Cregan, S. P., Pires, R. G., et al. (2014). Metabotropic glutamate receptor 5 knockout promotes motor and biochemical alterations in a mouse model of Huntington's disease. *Hum. Mol. Genet.* 23, 2030–2042. doi: 10.1093/hmg/ddt598

Ribeiro, F. M., Paquet, M., Ferreira, L. T., Cregan, T., Swan, P., Cregan, S. P., et al. (2010). Metabotropic glutamate receptor-mediated cell signaling pathways are altered in a mouse model of Huntington's disease. *J. Neurosci.* 30, 316–324. doi: 10.1523/JNEUROSCI.4974-09.2010

Ribeiro, F. M., Pires, R. G., and Ferguson, S. S. (2011). Huntington's disease and Group I metabotropic glutamate receptors. *Mol. Neurobiol.* 43, 1–11. doi: 10.1007/s12035-010-8153-1

Ribeiro, F. M., Vieira, L. B., Pires, R. G., Olmo, R. P., and Ferguson, S. S. (2017). Metabotropic glutamate receptors and neurodegenerative diseases. *Pharmacol. Res.* 115, 179–191. doi: 10.1016/j.phrs.2016.11.013

Rigamonti, D., Bauer, J. H., De-Fraja, C., Conti, L., Sipione, S., Sciorati, C., et al. (2000). Wild-type huntingtin protects from apoptosis upstream of caspase-3. *J. Neurosci.* 20, 3705–3713. doi: 10.1523/JNEUROSCI.20-10-03705.2000

Roos, R., Vegter-Van Der Vlis, M., Hermans, J., Elshove, H., Moll, A., Van de Kamp, J., et al. (1991). Age at onset in Huntington's disease: effect of line of inheritance and patient's sex. *J. Med. Genet.* 28, 515–519. doi: 10.1136/jmg.28.8.515

Roos, R. A. (2010). Huntington's disease: a clinical review. *Orphanet J. Rare Dis.* 5, 1–8.

Rosas, H., Koroshetz, W., Chen, Y., Skeuse, C., Vangel, M., Cudkowicz, M., et al. (2003). Evidence for more widespread cerebral pathology in early HD: an MRI-based morphometric analysis. *Neurology* 60, 1615–1620. doi: 10.1212/01.wnl.0000065888.88988.6e

Shigemoto, R., Nomura, S., Ohishi, H., Sugihara, H., Nakanishi, S., and Mizuno, N. (1993). Immunohistochemical localization of a metabotropic glutamate receptor, mGluR5, in the rat brain. *Neurosci. Lett.* 163, 53–57. doi: 10.1016/0304-3940(93)90227-c

Silvestroni, A., Faull, R. L., Strand, A. D., and Möller, T. (2009). Distinct neuroinflammatory profile in post-mortem human Huntington's disease. *Neuroreport* 20, 1098–1103. doi: 10.1097/WNR.0b013e32832e34ee

Simpson, J. M., Gil-Mohapel, J., Pouladi, M. A., Ghilan, M., Xie, Y., Hayden, M. R., et al. (2011). Altered adult hippocampal neurogenesis in the YAC128 transgenic mouse model of Huntington disease. *Neurobiol. Dis.* 41, 249–260. doi: 10.1016/j.nbd.2010.09.012

Smith, G. A., Rocha, E. M., McLean, J. R., Hayes, M. A., Izen, S. C., Isacson, O., et al. (2014). Progressive axonal transport and synaptic protein changes correlate with behavioral and neuropathological abnormalities in the heterozygous Q175 KI mouse model of Huntington's disease. *Hum. Mol. Genet.* 23, 4510–4527. doi: 10.1093/hmg/ddu166

Tai, Y. F., Pavese, N., Gerhard, A., Tabrizi, S. J., Barker, R. A., Brooks, D. J., et al. (2007). Microglial activation in presymptomatic Huntington's disease gene carriers. *Brain* 130, 1759–1766. doi: 10.1093/brain/awm044

van den Bogaard, S. J., Dumas, E. M., Acharya, T. P., Johnson, H., Langbehn, D. R., Scahill, R. I., et al. (2011). Early atrophy of pallidum and accumbens nucleus in Huntington's disease. *J. Neurol.* 258, 412–420. doi: 10.1007/s00415-010-5768-0

Zajac, M., Pang, T., Wong, N., Weinrich, B., Leang, L., Craig, J. M., et al. (2010). Wheel running and environmental enrichment differentially modify exon-specific BDNF expression in the hippocampus of wild-type and pre-motor symptomatic male and female Huntington's disease mice. *Hippocampus* 20, 621–636. doi: 10.1002/hipo.20658

Zielonka, D., Marinus, J., Roos, R. A., De Michele, G., Di Donato, S., Putter, H., et al. (2013). The influence of gender on phenotype and disease progression in patients with Huntington's disease. *Parkinsonism Related Disord.* 19, 192–197. doi: 10.1016/j.parkreldis.2012.09.012

Conflict of Interest: SF holds a Tier I Canada Research Chair in Brain and Mind. KA-E is a Lecturer at the Department of Pharmacology and Toxicology, Faculty of Pharmacy, University of Alexandria, Egypt.

The remaining authors declare that the research was conducted in the absence of any commercial or financial relationships that could be construed as a potential conflict of interest.

Publisher's Note: All claims expressed in this article are solely those of the authors and do not necessarily represent those of their affiliated organizations, or those of the publisher, the editors and the reviewers. Any product that may be evaluated in this article, or claim that may be made by its manufacturer, is not guaranteed or endorsed by the publisher.

frontiers in Molecular Neuroscience

MINI REVIEW
published: 14 February 2022
doi: 10.3389/fnmol.2022.836255

The Impact of Glutamatergic Synapse Dysfunction in the Corticothalamocortical Network on Absence Seizure Generation

*Beulah Leitch**

Department of Anatomy, School of Biomedical Sciences, Brain Health Research Centre, University of Otago, Dunedin, New Zealand

Childhood absence epilepsy (CAE) is the most common pediatric epilepsy affecting 10–18% of all children with epilepsy. It is genetic in origin and the result of dysfunction within the corticothalamocortical (CTC) circuitry. Network dysfunction may arise from multifactorial mechanisms in patients from different genetic backgrounds and thus account for the variability in patient response to currently available anti-epileptic drugs; 30% of children with absence seizures are pharmaco-resistant. This review considers the impact of deficits in AMPA receptor-mediated excitation of feed-forward inhibition (FFI) in the CTC, on absence seizure generation. AMPA receptors are glutamate activated ion channels and are responsible for most of the fast excitatory synaptic transmission throughout the CNS. In the stargazer mouse model of absence epilepsy, the genetic mutation is in stargazin, a transmembrane AMPA receptor trafficking protein (TARP). This leads to a defect in AMPA receptor insertion into synapses in parvalbumin-containing (PV+) inhibitory interneurons in the somatosensory cortex and thalamus. Mutation in the *Gria4* gene, which encodes for the AMPA receptor subunit GluA4, the predominant AMPA receptor subunit in cortical and thalamic PV + interneurons, also leads to absence seizures. This review explores the impact of glutamatergic synapse dysfunction in the CTC network on absence seizure generation. It also discusses the cellular and molecular mechanisms involved in the pathogenesis of childhood absence epilepsy.

Keywords: AMPA receptors, excitatory synapses, feed-forward inhibition, absence epilepsy, corticothalamocortical network, DREADD technology

OPEN ACCESS

Edited by:
James P. Clement, Jawaharlal Nehru Centre for Advanced Scientific Research, India

Reviewed by:
Olga Shevtsova, Italian Institute of Technology (IIT), Italy
Narendrakumar Ramanan, Indian Institute of Science (IISc), India

***Correspondence:**
Beulah Leitch
beulah.leitch@otago.ac.nz

Specialty section:
This article was submitted to Molecular Signalling and Pathways, a section of the journal Frontiers in Molecular Neuroscience

Received: *15 December 2021*
Accepted: *18 January 2022*
Published: *14 February 2022*

Citation:
Leitch B (2022) The Impact of Glutamatergic Synapse Dysfunction in the Corticothalamocortical Network on Absence Seizure Generation. Front. Mol. Neurosci. 15:836255. doi: 10.3389/fnmol.2022.836255

INTRODUCTION

Childhood absence epilepsy (CAE) is classified as a genetic, generalized type of pediatric epilepsy, which is non-convulsive (Scheffer et al., 2017). It occurs in early childhood (peak onset is between 4–10 years) and accounts for approximately 18% of epilepsy in school-aged children. Absence seizures are characterized by sudden, brief impairment of consciousness, accompanied by behavioral arrest. Loss of awareness and unresponsiveness is manifested as vacant episodes (termed absences) during which the child appears to be staring into space. Typical absence seizures are brief lasting 3–20 s but can occur multiple times a day and thus severely impact learning. They appear on electroencephalogram (EEG) as bilaterally synchronous spike and wave discharges

(SWDs) at approximately 2.5–4 Hz. Absence seizures, formerly known as "*petit mal*" seizures, were until recently thought to be relatively benign due to their non-convulsive nature and high incidence of remission during childhood and early adulthood (Fisher et al., 2017). However, it is now known that absence seizures in children are also accompanied by comorbid conditions (Tellez-Zenteno et al., 2007). Anxiety and depression are the most frequent comorbidities (Sarkisova et al., 2017). Cognitive, behavioral, and psychiatric comorbidities, including attention deficit hyperactivity disorder, intellectual disability, autism spectrum disorder, depression, unstable mood, and suicidal tendencies are reported in 11–40% of children affected by epilepsy (Austin et al., 2011; Reilly et al., 2014; Terra et al., 2014; Quvile and Wilmshurst, 2016). Furthermore, there is also evidence of morphological changes during development in the cortex of some CAE patients compared to healthy controls, which could affect cognitive abilities (Tosun et al., 2011).

Seizures and Treatment

Seizures are caused by disruption of the normal excitatory/inhibitory (E/I) balance within brain networks resulting in hyperexcitation. However, the precise cellular and molecular events that transform normal brain circuits into epileptic circuits and the mechanisms that generate seizures in different types of epilepsy are still unclear. Although seizures can be controlled in many patients using anti-epileptic drugs (AEDs), there are often severe side-effects and one-third of patients will continue to have uncontrolled seizures because current AEDs don't work for them. AEDs even aggravate seizures in some cases (Glauser et al., 2013). As epilepsy is a spectrum disorder, it presents uniquely in each patient, so a "one size fits all" approach to treatment does not work. The variability in response to drug treatment and disease outcome in children with CAE suggests that complex and multifactorial mechanisms may underlie absence seizure generation in patients from different genetic backgrounds. Deciphering the potential mechanisms involved in generation of absence seizures is important for future identification of novel therapeutic targets with higher efficacy for patient-specific treatment.

The Stargazer Model of Absence Epilepsy

Several rodent models have proved invaluable in studying the cellular and molecular mechanisms underlying absence epilepsy. There appear to be multiple mechanisms through which absence seizures can be generated; with altered glutamatergic excitation implicated in epileptogenesis in many experimental models. Alterations in the expression and function of alpha-amino-3-hydroxy-5-methyl-4-isoxazolepropionic acid (AMPA) receptors, which mediate most of the fast excitatory glutamatergic synaptic transmission in the brain, have been implicated in some models. The stargazer mouse, in particular, has been the focus of studies to understand how a genetic defect resulting in AMPAR deficits at synapses, contributes to the generation of absence seizures. The mutation underlying the epileptic phenotype in stargazers was first identified as a defect in the voltage-dependent calcium channel (VDCC) γ2 subunit gene, *Cacng2* (Noebels et al., 1990; Letts et al., 1998). This severely reduces the normal expression of the γ2 subunit protein called stargazin. Stargazin is involved in trafficking, synaptic targeting and modulation of AMPA receptors at excitatory synapses (Hashimoto et al., 1999; Chen et al., 2000; Tomita et al., 2003, 2005; Nicoll et al., 2006). It belongs to a family of transmembrane AMPA receptor regulatory proteins (TARPs) which are differentially expressed in different brain regions and neurons (Tomita et al., 2003). It was the first TARP to be identified; and was named TARP-γ2, due to its homology to the γ1 subunit of skeletal muscle VDCCs. Absence of stargazin (TARP-γ2) in the stargazer mutant mouse leads to absence epilepsy and cerebellar ataxia (Noebels et al., 1990). Absence seizures are known to originate from disturbance within the corticothalamocortical (CTC) network. Stargazin expression in the cortex and thalamus is limited to inhibitory gamma-aminobutyric acid (GABA) interneurons (Tao et al., 2013), and specifically to parvalbumin containing (PV +) GABAergic interneurons (Maheshwari et al., 2013).

The Corticothalamocortical Network

The CTC network comprises reciprocal connections between the thalamus and the cortex (**Figure 1**). In normal functioning of the CTC network, the thalamus receives sensory information from the periphery. Glutamatergic relay neurons within the ventral posterior (VP) thalamic nucleus send excitatory thalamocortical (TC) projections to glutamatergic pyramidal cells in layer IV of the cortex. The pyramidal cells in turn send corticothalamic (CT) projections back to the relay neurons in the thalamus from cortical layers V/VI, which are the output layers of the cortex (Jones, 1998; Constantinople and Bruno, 2013). Both the TC and CT projections also send collateral branches into the reticular thalamic nucleus (RTN), which forms a thin sheath of inhibitory GABAergic PV + interneurons that surrounds the thalamic relay nuclei. These CT and TC projections to the RTN are reciprocally connected, allowing the RTN to evaluate the sensory information transmitted to-and-from the cortex. The RTN inhibitory interneurons do not project out of the thalamus; they send feed-forward inhibition (FFI) to the thalamic relay neurons. In this way, the RTN plays an important role in regulating the excitability of thalamic relay cells (Bal et al., 1995; Sohal and Huguenard, 1998). CT collateral activation of RTN feed-forward inhibitory neurons is much stronger than direct CT activation of relay neurons in the VP, therefore cortical activation is mainly inhibitory *via* the collateral RTN pathway (Destexhe et al., 1998; Golshani et al., 2001; Beenhakker and Huguenard, 2009).

The SWDs, which are the hallmark of absence seizures on EEG, arise from aberrant hypersynchronous activity within this network (Snead, 1995; McCormick and Contreras, 2001). However, the precise cellular and molecular mechanisms underlying the genesis of absence seizures are still largely unknown and appear multifactorial. There are potentially different microcircuits within the CTC network that could be dysfunctional in different patients, hence accounting for the variability in response to drug treatment. It is critical to understand the microcircuit and neuron-specific mechanisms

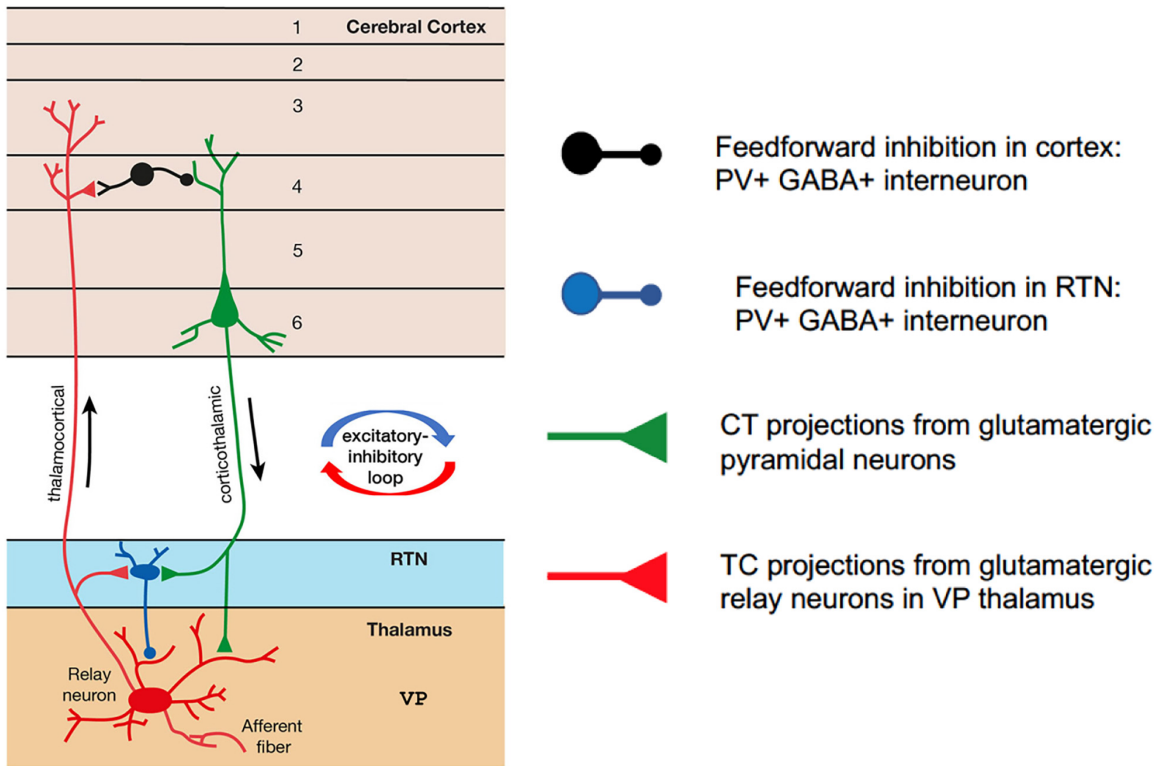

FIGURE 1 | Simplified schematic of the corticothalamocortical (CTC) network in the rodent brain. Relay neurons in the ventral posterior (VP) thalamus are reciprocally connected with the pyramidal neurons in the cortex. Feedforward PV + inhibitory interneurons in the reticular thalamic nucleus (RTN) project onto the relay neurons and are excited at AMPA synapses by corticothalamic projections from pyramidal cells. Feedforward PV + inhibitory interneurons in the cortex are excited at AMPA synapses by thalamocortical projections from relay neurons in VP thalamus.

that underlie generation of absence seizures, which arise from different genetic backgrounds, in order to identify novel therapeutic targets for treatment of this type of seizure.

Feed-Forward Inhibition in the Corticothalamocortical Network

Research using the stargazer mouse model of absence epilepsy (Barad et al., 2012, 2017; Seo and Leitch, 2014, 2015, 2017; Adotevi and Leitch, 2016, 2017, 2019) has demonstrated that region-specific alterations in AMPA receptor expression in inhibitory microcircuits within the CTC network may be a key factor contributing to pathological hypersynchronous oscillatory activity in some forms of absence epilepsy. Specifically, a selective decrease in AMPA receptor expression at excitatory input synapses on RTN inhibitory interneurons from CT afferent projections (CT-RTN) but not at excitatory input synapses onto VP relay neurons (CT-VP) has been identified by Barad et al. (2012). As the inhibitory interneurons in RTN provide FFI to relay neurons in the VP, loss of AMPA receptors at CT-RTN synapses could lead to a loss of FFI within this microcircuit. A similar loss of AMPARs within inhibitory feed-forward microcircuits in the somatosensory cortex has also been reported (Adotevi and Leitch, 2016, 2017, 2019). FFI is essential to prevent runaway excitation within the CTC network. Epilepsy is caused by disruption of the normal excitatory-inhibitory (E/I) balance within brain networks, resulting in hyperexcitation and seizures. GABAergic feed-forward interneurons play a crucial role in the prevention of seizures by regulating this delicate E/I balance. A specific loss in CT-RTN excitation, leading to impaired FFI of thalamic relay nuclei, has also been demonstrated in the absence epileptic Gria4 knockout mouse, which lacks the AMPAR GluA4 subunit (Paz et al., 2011). GluA4-AMPARs are more abundant in RTN neurons than on TC relay cells (Golshani et al., 2001). Loss of GluA4 expression in the Gria4$^{-/-}$ mouse (Beyer et al., 2008) resulted in a selective impairment in CT-RTN firing, but not in CT-relay neuron or feedback relay neuron-RTN synaptic function (Paz et al., 2011). Collectively, these findings suggest that impairment of thalamic FFI due to weakened AMPAR-mediated excitatory input to inhibitory RTN neurons may contribute to seizures in these two absence epilepsy mouse models.

Impact of Silencing Feed-Forward Inhibition Using Designer Receptors Exclusively Activated by Designer Drug Technology

To test whether loss of FFI is directly related to the generation and maintenance of absence seizures, Panthi and Leitch (2019) used Designer Receptors Exclusively Activated by Designer Drug (DREADD) technology to selectively silence PV + interneurons

in the CTC network. DREADD technology involves insertion of engineered receptors (designer receptors) that are only activated by synthetic ligands (designer drugs) into specific neurons (Roth, 2016). DREADD receptors are mutated muscarinic G-protein receptors, which are either excitatory (hM3Dq) or inhibitory (hM4Di). They can be inserted into transgenic mice *in vivo* using viral vector methods (Zhu et al., 2014; Urban and Roth, 2015). Alternatively, strains of DREADD mice can be used that express either the activating Gq-DREADD or inhibiting Gi-DREADD, under the control of a strong ubiquitous promoter, which is separated from the DREADD by a loxP site-flanked Stop signal. Mating of these strains with any Cre-driver mouse line removes the Stop signal only in the cell type specified by the Cre-driver used. This cell-specific DREADD can then be activated by injection or oral application of the designer drug i.e., clozapine-N-oxide (CNO) (Zhu et al., 2016). This later method was used by Panthi and Leitch (2019) to express inhibiting Gi-DREADDs in PV + interneurons. They found that inactivating FFI (either in the somatosensory cortex or the RTN thalamus by focal injections of CNO) generates absence-like SWDs in normal non-epileptic mice. Furthermore, selectively activating PV + inhibitory interneurons within the CTC network during chemically-induced absence seizures, was sufficient to prevent or reduce seizure activity (Panthi and Leitch, 2021). In contrast, focal injection of CNO into either the somatosensory cortex or RTN thalamus of non-DREADD wildtype control animals, had no effect on chemical-induced absence seizures. These data demonstrate a potential for targeting FFI interneurons within the CTC network in future therapeutic strategies to control seizures in some cases of human absence epilepsy.

CONCLUSION

This review highlights the impact of glutamatergic synapse dysfunction in the CTC network on absence seizure generation. Loss of FFI in CTC microcircuits, as a result of a mutation in the AMPA receptor trafficking protein stargazin, results in SWDs. Hence intervention strategies to regulate the activation of specific inhibitory interneurons within this network could be a potential seizure suppressing mechanism in some absence epilepsy patients. Suppression of epileptiform activity by modifying the synaptic output from specific inhibitory interneurons through the use of DREADD and optogenetic technologies is now possible (Krook-Magnuson and Soltesz, 2015). Furthermore, these approaches can be used to investigate any comorbidity between seizures and behavioral changes related to neurological and neuropsychiatric disorders.

AUTHOR CONTRIBUTIONS

The author confirms being the sole contributor of this work and has approved it for publication.

ACKNOWLEDGMENTS

The author would like to thank N. Dunstone for kindly proofreading this manuscript.

REFERENCES

Adotevi, N. K., and Leitch, B. (2016). Alterations in AMPA receptor subunit expression in cortical inhibitory interneurons in the epileptic stargazer mutant mouse. *Neuroscience* 339, 124–138. doi: 10.1016/j.neuroscience.2016.09.052

Adotevi, N. K., and Leitch, B. (2017). Synaptic changes in AMPA receptor subunit expression in cortical parvalbumin interneurons in the stargazer model of absence epilepsy. *Front. Mol. Neurosci.* 10:434. doi: 10.3389/fnmol.2017.00434

Adotevi, N. K., and Leitch, B. (2019). Cortical expression of AMPA receptors during postnatal development in a genetic model of absence epilepsy. *Int. J. Dev. Neurosci.* 73, 19–25. doi: 10.1016/j.ijdevneu.2018.12.006

Austin, J. K., Perkins, S. M., Johnson, C. S., Fastenau, P. S., Byars, A. W., deGrauw, T. J., et al. (2011). Behavior problems in children at time of first recognized seizure and changes over the following 3 years. *Epilepsy Behav.* 21, 373–381. doi: 10.1016/j.yebeh.2011.05.028

Bal, T., von Krosigk, M., and McCormick, D. A. (1995). Synaptic and membrane mechanisms underlying synchronized oscillations in the ferret LGNd *in vitro*. *J. Physiol.* 483, 641–663. doi: 10.1113/jphysiol.1995.sp020612

Barad, Z., Grattan, D., and Leitch, B. (2017). NMDA receptor expression in the thalamus of the stargazer model of absence epilepsy. *Sci. Rep.* 7:42926. doi: 10.1038/srep42926

Barad, Z., Shevtsova, O., Arbuthnott, G., and Leitch, B. (2012). Selective loss of AMPA receptors at corticothalamic synapses in the epileptic stargazer mouse. *Neuroscience* 217, 19–31. doi: 10.1016/j.neuroscience.2012.05.011

Beenhakker, M. P., and Huguenard, J. R. (2009). Neurons that fire together also conspire together: is normal sleep circuitry hijacked to generate epilepsy? *Neuron* 62, 612–632. doi: 10.1016/j.neuron.2009.05.015

Beyer, B., Deleuze, C., Letts, V. A., Mahaffey, C. L., Boumil, R. M., Lew, T. A., et al. (2008). Absence seizures in C3H/HeJ and knockout mice caused by mutation of the AMPA receptor subunit Gria4. *Hum. Mol. Genet.* 17, 1738–1749. doi: 10.1093/hmg/ddn064

Chen, L., Chetkovich, D. M., Petralia, R. S., Sweeney, N. T., Kawasaki, Y., Wenthold, R. J., et al. (2000). Stargazin regulates synaptic targeting of AMPA receptors by two distinct mechanisms. *Nature* 408, 936–943. doi: 10.1038/35050030

Constantinople, C. M., and Bruno, R. M. (2013). Deep cortical layers are activated directly by thalamus. *Science* 340, 1591–1594. doi: 10.1126/science.1236425

Destexhe, A., Contreras, D., and Steriade, M. (1998). Mechanisms underlying the synchronizing action of corticothalamic feedback through inhibition of thalamic relay cells. *J. Neurophysiol.* 79, 999–1016. doi: 10.1152/jn.1998.79.2.999

Fisher, R. S., Cross, J. H., D'Souza, C., French, J. A., Haut, S. R., Higurashi, N., et al. (2017). Instruction manual for the ILAE 2017 operational classification of seizure types. *Epilepsia* 58, 531–542. doi: 10.1111/epi.13671

Glauser, T. A., Cnaan, A., Shinnar, S., Hirtz, D. G., Dlugos, D., Masur, D., et al. (2013). Ethosuximide, valproic acid, and lamotrigine in childhood absence epilepsy: initial monotherapy outcomes at 12 months. *Epilepsia* 54, 141–155. doi: 10.1111/epi.12028

Golshani, P., Liu, X. B., and Jones, E. G. (2001). Differences in quantal amplitude reflect GluR4- subunit number at corticothalamic synapses on two populations of thalamic neurons. *Proc. Natl. Acad. Sci. U.S.A.* 98, 4172–4177. doi: 10.1073/pnas.061013698

Hashimoto, K., Fukaya, M., Qiao, X., Sakimura, K., Watanabe, M., and Kano, M. (1999). Impairment of AMPA receptor function in cerebellar granule cells of ataxic mutant mouse stargazer. *J. Neurosci.* 19, 6027–6036. doi: 10.1523/JNEUROSCI.19-14-06027.1999

Jones, E. G. (1998). Viewpoint: the core and matrix of thalamic organisation. *Neuroscience* 85, 331–345. doi: 10.1016/s0306-4522(97)00581-2

Krook-Magnuson, E., and Soltesz, I. (2015). Beyond the hammer and the scalpel: selective circuit control for the epilepsies. *Nat. Neurosci.* 18, 331–338. doi: 10.1038/nn.3943

Letts, V. A., Felix, R., Biddlecome, G. H., Arikkath, J., Mahaffey, C. L., Valenzuela, A., et al. (1998). The mouse stargazer gene encodes a neuronal Ca^{2+}-channel γ subunit. *Nat. Genet.* 19, 340–347. doi: 10.1038/1228

Maheshwari, A., Nahm, W. K., and Noebels, J. L. (2013). Paradoxical proepileptic response to NMDA receptor blockade linked to cortical interneuron defect in stargazer mice. *Front. Cell Neurosci.* 7:156. doi: 10.3389/fncel.2013.00156

McCormick, D. A., and Contreras, D. (2001). On the cellular and network bases of epileptic seizures. *Annu. Rev. Physiol.* 63, 815–846. doi: 10.1146/annurev.physiol.63.1.815

Nicoll, R. A., Tomita, S., and Bredt, D. S. (2006). Auxiliary subunits assist AMPA-type glutamate receptors. *Science* 311, 1253–1256. doi: 10.1126/science.1123339

Noebels, J. L., Qiao, X., Bronson, R. T., Spencer, C., and Davisson, M. T. (1990). Stargazer: a new neurological mutant on chromosome 15 in the mouse with prolonged cortical seizures. *Epilepsy Res.* 7, 129–135. doi: 10.1016/0920-1211(90)90098-g

Panthi, S., and Leitch, B. (2019). The impact of silencing feed-forward parvalbumin-expressing inhibitory interneurons in the corticothalamocortical network on seizure generation and behaviour. *Neurobiol. Dis.* 132:104610. doi: 10.1016/j.nbd.2019.104610

Panthi, S., and Leitch, B. (2021). Chemogenetic activation of feed-forward inhibitory parvalbumin-expressing interneurons in the cortico-thalamocortical network during absence seizures. *Front. Cell. Neurosci.* 15:688905. doi: 10.3389/fncel.2021.688905

Paz, J. T., Bryant, A. S., Peng, K., Fenno, L., Yizhar, O., Frankel, W. N., et al. (2011). A new mode of corticothalamic transmission revealed in the gria4(-/-). model of absence epilepsy. *Nat. Neurosci.* 14, 1167–1173. doi: 10.1038/nn.2896

Quvile, T., and Wilmshurst, J. M. (2016). Comorbidities affecting children with epilepsy – not a novel entity but new insights could improve holistic care. *Eur. Neurol. Rev.* 11, 16–17. doi: 10.17925/ENR.2016.11.01.16

Reilly, C., Atkinson, P., Das, K. B., Chin, R. F., Aylett, S. E., Burch, V., et al. (2014). Neurobehavioral comorbidities in children with active epilepsy: a population-based study. *Pediatrics* 133, e1586–e1593. doi: 10.1542/peds.2013-3787

Roth, B. L. (2016). DREADDs for neuroscientists. *Neuron* 89, 683–694. doi: 10.1016/j.neuron.2016.01.040

Sarkisova, K. Y., Fedotova, I. B., Surina, N. M., Nikolaev, G. M., Perepelkina, O. V., Kostina, Z. A., et al. (2017). Genetic background contributes to the comorbidity of anxiety and depression with audiogenic seizure propensity and responses to fluoxetine treatment. *Epilepsy Behav.* 68, 95–102. doi: 10.1016/j.yebeh.2016.12.025

Scheffer, I. E., Berkovic, S., Capovilla, G., Connolly, M. B., French, J., Guilhoto, L., et al. (2017). ILAE classification of the epilepsies: position paper of the ILAE commission for classification and terminology. *Epilepsia* 58, 512–521. doi: 10.1111/epi.13709

Seo, S., and Leitch, B. (2014). Altered thalamic GABAA-receptor subunit expression in the stargazer mouse model of absence epilepsy. *Epilepsia* 55, 224–232. doi: 10.1111/epi.12500

Seo, S., and Leitch, B. (2015). Synaptic changes in GABAA receptor expression in the thalamus of the Stargazer mouse model of absence epilepsy. *Neuroscience* 306, 28–38. doi: 10.1016/j.neuroscience.2015.08.021

Seo, S., and Leitch, B. (2017). Postnatal expression of thalamic GABAAR subunits in the stargazer mouse model of absence epilepsy. *Neuroreport* 28, 1255–1260. doi: 10.1097/WNR.0000000000000909

Snead, O. C. III (1995). Basic mechanisms of generalized absence seizures. *Ann. Neurol.* 37, 146–157. doi: 10.1002/ana.410370204

Sohal, V. S., and Huguenard, J. R. (1998). Long-range connections synchronize rather than spread intrathalamic oscillations: computational modeling and *in vitro* electrophysiology. *J. Neurophysiol.* 80, 1736–1751. doi: 10.1152/jn.1998.80.4.1736

Tao, Y., Chen, Y., Shen, C., Luo, Z., Bates, C. R., Lee, D., et al. (2013). Erbin interacts with TARP γ-2 for surface expression of AMPA receptors in cortical interneurons. *Nat. Neurosci.* 16, 290–299. doi: 10.1038/nn.3320

Tellez-Zenteno, J. F., Patten, S. B., Jette, N., Williams, J., and Wiebe, S. (2007). Psychiatric comorbidity in epilepsy: a population-based analysis. *Epilepsia* 48, 2336–2344. doi: 10.1111/j.1528-1167.2007.01222.x

Terra, V. C., de Paola, L., and Silvado, C. E. (2014). Are children affected by epileptic neuropsychiatric comorbidities? *Epilepsy Behav.* 38, 8–12. doi: 10.1016/j.yebeh.2013.10.003

Tomita, S., Adesnik, H., Sekiguchi, M., Zhang, W., Wada, K., Howe, J. R., et al. (2005). Stargazin modulated AMPA receptor gating and trafficking by distinct domains. *Nature* 435, 1052–1058. doi: 10.1038/nature03624

Tomita, S., Chen, L., Kawasaki, Y., Petralia, R. S., Wenthold, R. J., Nicoll, R. A., et al. (2003). Functional studies and distribution define a family of transmembrane AMPA receptor regulatory proteins. *J. Cell Biol.* 161, 805–816. doi: 10.1083/jcb.200212116

Tosun, D., Siddarth, P., Toga, A. W., Hermann, B., and Capaln, R. (2011). Effects of childhood absence epilepsy on associations between regional cortical morphometry and aging and cognitive abilities. *Hum. Brain Mapp.* 32, 580–591. doi: 10.1002/hbm.21045

Urban, D. J., and Roth, B. L. (2015). DREADDs (designer receptors exclusively activated by designer drugs): chemogenetic tools with therapeutic utility. *Ann. Rev. Pharmacol. Toxicol.* 55, 399–417. doi: 10.1146/annurev-pharmtox-010814-124803

Zhu, H., Aryal, D. K., Olsen, R. H. J., Urban, D. J., Swearingen, A., Forbes, S., et al. (2016). Cre dependent DREADD (designer receptors exclusively activated by designer drugs) mice. *Genesis* 54, 439–446. doi: 10.1002/dvg.22949

Zhu, H., Pleil, K. E., Urban, D. J., Moy, S. S., Kash, T. L., and Roth, B. L. (2014). Chemogenetic inactivation of ventral hippocampal glutamatergic neurons disrupts consolidation of contextual fear memory. *Neuropsychopharmacology* 39, 1880–1892. doi: 10.1038/npp.2014.35

Conflict of Interest: The author declares that the research was conducted in the absence of any commercial or financial relationships that could be construed as a potential conflict of interest.

Publisher's Note: All claims expressed in this article are solely those of the authors and do not necessarily represent those of their affiliated organizations, or those of the publisher, the editors and the reviewers. Any product that may be evaluated in this article, or claim that may be made by its manufacturer, is not guaranteed or endorsed by the publisher.

frontiers in Molecular Neuroscience

REVIEW
published: 23 February 2022
doi: 10.3389/fnmol.2022.823135

A Ribosomal Perspective on Neuronal Local Protein Synthesis

Sudhriti Ghosh Dastidar and Deepak Nair**

Centre for Neuroscience, Indian Institute of Science, Bengaluru, India

Continued mRNA translation and protein production are critical for various neuronal functions. In addition to the precise sorting of proteins from cell soma to distant locations, protein synthesis allows a dynamic remodeling of the local proteome in a spatially variable manner. This spatial heterogeneity of protein synthesis is shaped by several factors such as injury, guidance cues, developmental cues, neuromodulators, and synaptic activity. In matured neurons, thousands of synapses are non-uniformly distributed throughout the dendritic arbor. At any given moment, the activity of individual synapses varies over a wide range, giving rise to the variability in protein synthesis. While past studies have primarily focused on the translation factors or the identity of translated mRNAs to explain the source of this variation, the role of ribosomes in this regard continues to remain unclear. Here, we discuss how several stochastic mechanisms modulate ribosomal functions, contributing to the variability in neuronal protein expression. Also, we point out several underexplored factors such as local ion concentration, availability of tRNA or ATP during translation, and molecular composition and organization of a compartment that can influence protein synthesis and its variability in neurons.

Keywords: neurons, synapse, local translation, ribosome remodeling, *in vivo* dynamics

OPEN ACCESS

Edited by:
James P. Clement, Jawaharlal Nehru Center for Advanced Scientific Research, India

Reviewed by:
Rosalina Fonseca, New University of Lisbon, Portugal
Zach T. Campbell, The University of Texas at Dallas, United States
Dan Ohtan Wang, Kyoto University, Japan

****Correspondence:***
Sudhriti Ghosh Dastidar
sudhritig@iisc.ac.in
Deepak Nair
deepak@iisc.ac.in

Specialty section:
This article was submitted to Molecular Signalling and Pathways, a section of the journal Frontiers in Molecular Neuroscience

Received: *26 November 2021*
Accepted: *17 January 2022*
Published: *23 February 2022*

Citation:
Dastidar SG and Nair D (2022) A Ribosomal Perspective on Neuronal Local Protein Synthesis. Front. Mol. Neurosci. 15:823135. doi: 10.3389/fnmol.2022.823135

INTRODUCTION

Careful decoding of mRNA messages is a fundamental yet complex challenge for any cell. Highly arborized morphology of neurons demands precise spatial and temporal control of mRNA translation in response to synaptic or network activation (Kapur et al., 2017; Rangaraju et al., 2017; Holt et al., 2019). The last few decades of research have pointed out that mRNA translation is regulated locally in neuronal dendrites, axons, dendritic spines, presynaptic boutons, or axonal growth cones (Biever et al., 2019; Fernandopulle et al., 2021). In matured neurons, the cumulative extent of dendritic translation exceeds that of cell soma, allowing spatial variability required for network integrity and homeostasis in the brain (Job and Eberwine, 2001; Hanus and Schuman, 2013; Spillane et al., 2013). Other contemporary studies have confirmed that variability in local protein synthesis is critical for neuronal development, maintenance, synaptic signaling, and plasticity (Holt et al., 2019; Fernandopulle et al., 2021). Studies also suggest that disruptions of activity-induced local translation have drastic consequences leading to cognitive deficits observed in several neurodevelopmental disorders and neurodegenerative diseases (Bear et al., 2004; Oddo, 2012; Deshpande et al., 2020; Ma, 2020).

Ribosomes are the central components of the translation machinery (Baßler and Hurt, 2019). For a long time, all cytosolic ribosomes were believed to act similarly, following a sequence of

well-defined steps (Ramakrishnan, 2002; Wilson and Cate, 2012). However, in the past 5 years, an emerging body of evidence indicates the presence of significant heterogeneity in cellular ribosomes (Genuth and Barna, 2018; Gay et al., 2022). In addition, translation factors often shape ribosomal performance by controlling numerous aspects such as subunit loading on mRNAs, translational fidelity, ribosomal processivity, speed of translocation, probability of reloading, and more (Jackson et al., 2010; Kapur et al., 2017; Neelagandan et al., 2020). Within neurons, ribosomes are produced in the nucleolus and transported to the cytosol (Stoykova et al., 1985; Baßler and Hurt, 2019). A fraction of this population is then sorted to distant locations from the cell soma to participate in local translation (Tiedge and Brosius, 1996; Scarnati et al., 2018; Hafner et al., 2019; Koltun et al., 2020). Further, remodeling of existing ribosomes can occur in remote locations in a biogenesis-independent fashion (Sotelo-Silveira et al., 2006; Shigeoka et al., 2019; Mofatteh, 2020; Fernandopulle et al., 2021). Such remodeling events together with other parameters such as local ion concentrations, mRNA and tRNA availability, steady-state ATP content, and signaling pathways govern ribosomal activity and translation in neuronal compartments (Holt and Schuman, 2013; Rangaraju et al., 2017; Biever et al., 2019, 2020; Holt et al., 2019).

Here, we review the current understanding of ribosome biogenesis and heterogeneity within a neuron. We highlight the mechanisms and local parameters that influence stochasticity in ribosomal performance. Also, we discuss the importance of studying ribosomal dynamics to explain this translational variability required for neuronal functions.

REGULATION OF RIBOSOME BIOGENESIS WITHIN NEURONS

"Ribosome Biogenesis" results in the production of functionally matured ribosomes that determines the protein synthetic ability of a living cell (Stoykova et al., 1985; Chau et al., 2018; Hetman and Slomnicki, 2019; **Figure 1**). The biogenesis process happens primarily in the nucleolus and is guided at least by 200 associating factors (AFs) and 80 different types of small nucleolar RNAs (snoRNA) (Baßler and Hurt, 2019).

Within the brain, three of the four rRNA species are synthesized together as a single polycistronic ∼45s rRNA precursor (pre rRNA) (Thomson et al., 2013; Baßler and Hurt, 2019). In general, the ribosomal DNA (rDNA) genes are present in multiple copies within the genome grouped into 7 different clusters, known as variants. Of these variants, 5 are expressed in the brain (Tseng et al., 2008; Allen et al., 2018). However, the rRNA content in individual brain cells can vary in a cell-type-specific manner. For example, studies have revealed that rat neurons possess fourfold higher pre rRNA content than oligodendrocytes due to a reduced turnover rate (Stoykova et al., 1985). In addition, ribosome biogenesis dynamically alters with stages of brain development. For example, the nucleolar number in rat and chicken cerebellar Purkinje neurons increases from the embryonic stage to the post-natal/hatching period (Lafarga et al., 1995). In mice, the synthesis of a few ribosomal proteins (RP), ribosome biogenesis factors, and translation factors are repressed in the neuronal progenitor cells following neural tube closure. The resulting dip in protein synthesis capacity is required for a timed reduction in the rate of proliferation of these cells which, otherwise causes macrocephaly (Chau et al., 2018). However, later during forebrain development, a surge in ribosome biosynthesis promotes dendritic development and arborisation (Slomnicki et al., 2016; Chau et al., 2018). Studies in mouse hippocampal neurons have shown that a moderate depletion of ribosomal proteins S6, S14, or L4, required for subunit export, perturbs dendritic growth and development. This is due to the reduced ribosomal recruitment and translation of BDNF target mRNAs despite having signaling pathways from the TrkB receptors intact (Slomnicki et al., 2016). In addition, the ribosome content is depleted within axons during synaptogenesis (Costa et al., 2019). Together these results highlight that ribosome biogenesis and assembly are regulated in a dynamic and site-specific manner during brain and neuronal development.

Also, neuronal stimulation affects rDNA transcription. For example, 1-h stimulation of auditory nerves results in a significant rise in the rRNA content of chicken cochlear neurons (Hyson and Rubel, 1995). In Aplysia neurons, 5-HT or LTF-inducing stimulus leads to an elevation in pol I-mediated rRNA synthesis. Translocation of the chromatin remodeling protein PARP1, following the activation of the PKA-ERK pathway, mediates this rapid synapse to nucleus signaling (Hernandez et al., 2009; **Figure 1**). Another study has observed that on NMDA stimulation, AIDA1, a synaptic PSD-interacting protein, translocates from the synapse to the nucleus to regulate nucleolar numbers (Jordan et al., 2007). These observations explain the mechanistic basis of the dynamic communication between the nucleolus and synapse that shape ribosome biogenesis in response to synaptic signaling.

Following the synthesis of 45s pre-rRNA transcript, several molecules take part in rRNA maturation (Thomson et al., 2013; Sen Gupta et al., 2018). While a key enzyme Nucleolin is involved in transcriptional regulation and cleavage of the 45s rRNA, other critical proteins like Fibrillarin catalyze the modifications of hundreds of bases and backbone residues of the processed rRNA (Boisvert et al., 2007; Sen Gupta et al., 2018). These modifications, such as 2′ *O*-methylations, can influence rRNA secondary structures, the subunit RP compositions, ribosomal association with various RNA-binding proteins (RBPs), and thus allowing ribosomes with specific rRNA modifications to translate a distinct set of mRNA targets (Kondrashov et al., 2011; Polikanov et al., 2015; Simsek et al., 2017; Sloan et al., 2017; D'Souza et al., 2018; Merkurjev et al., 2018; **Figure 1**). In addition, activity-dependent changes in rRNA modifications can alter global mRNA translation. For example, the induction of experience-dependent plasticity leads to an increased rRNA production and translation in neurons. Neurons express a long nucleolus-specific lncRNA (LONA) that precludes both Nucleolin and Fibrillarin activity, reducing the pro-translational 2′ *O*-methyl marks on rRNA. However,

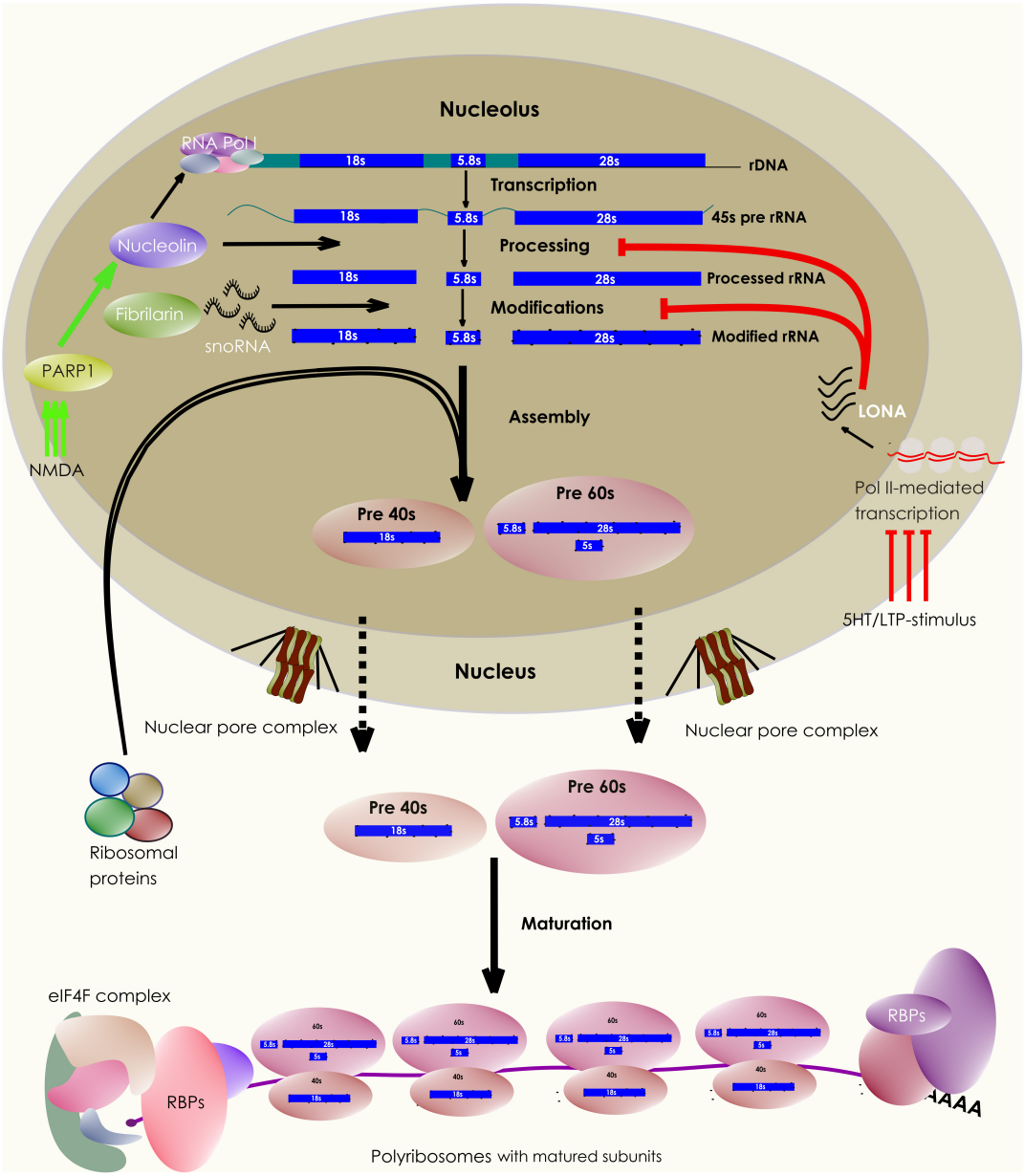

FIGURE 1 | Neuronal control of ribosome biogenesis. The schematic depicts various stages of ribosome biogenesis within the nucleolar compartment. The rRNA synthesis, modification, and maturation takes place in the nucleolus following which, they associate with ribosomal proteins produced in the cytosol. The assembled subunits are then exported out of the nucleus to undergo the final steps of cytoplasmic maturation. A pool of these matured subunits engages in translating mRNAs, a process facilitated by multiple other protein factors. Interestingly, the nucleolar biogenesis process can be influenced by synaptic stimulation through a variety of synapse to nucleus (retrograde) signaling pathways.

synaptic activation causes degradation of LONA, relieving the inhibition of global translation and upscaling the rRNA production (Li et al., 2018; **Figure 1**). However, the evidence for other types of rRNA modifications impacting local ribosomal performance in neurons is yet to come. Further experiments can reveal whether individual ribosomes carrying unique combinations of rRNA modifications (an epitranscriptomic code) can influence their functions distinctly (Li and Wang, 2020). Nevertheless, rRNA modifications represent an additional layer of ribosomal regulation in neurons (**Figure 2**).

RIBOSOMAL SORTING AND DISTRIBUTION

Localization of ribosomes to subcellular compartments allows neurons to mount a rapid translation response upon stimulation

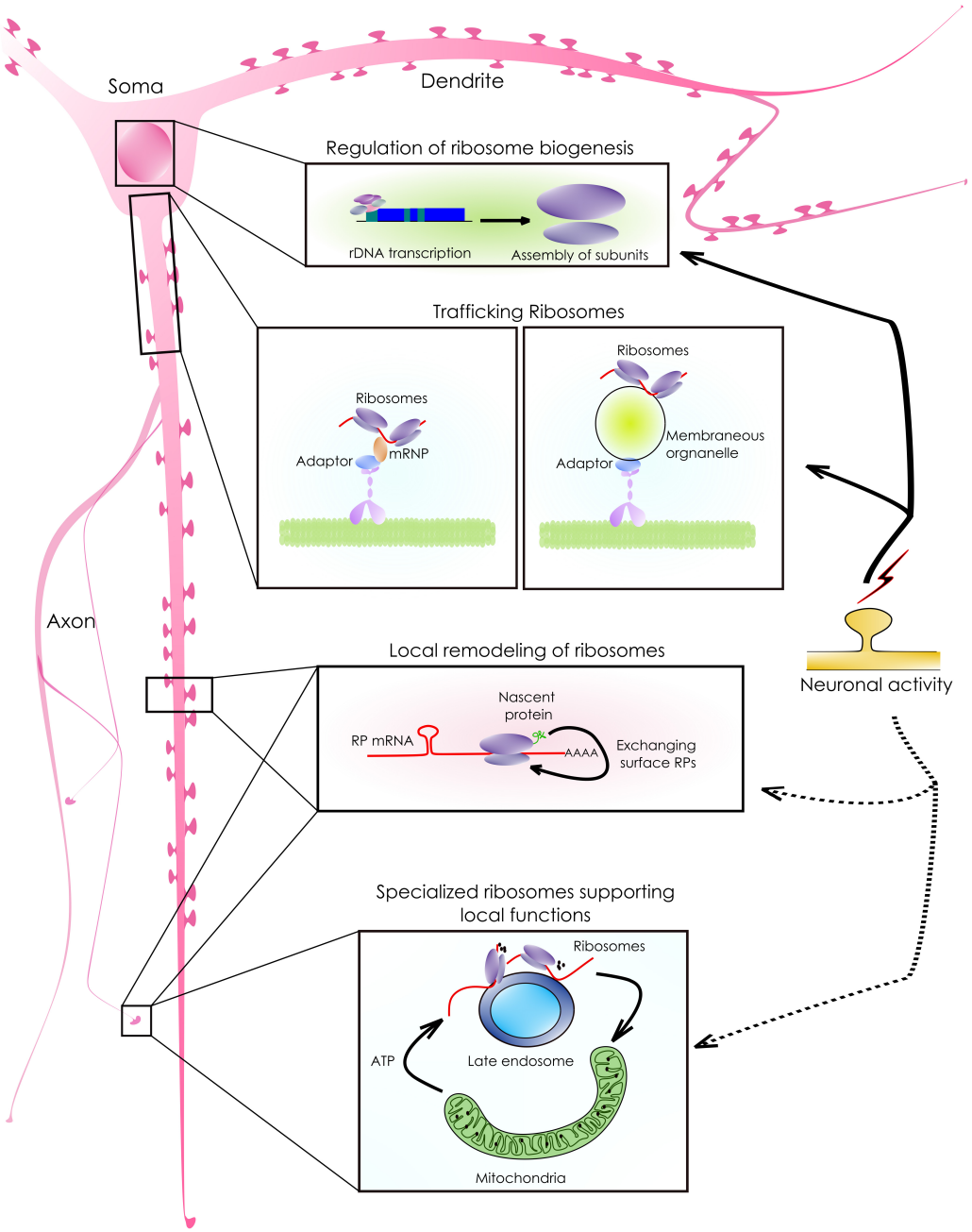

FIGURE 2 | Ribosomal synthesis, sorting, and remodeling to support local functions. As shown in the schematic, neurons have an arborized morphology. mRNA abundant. As a result, the availability of ribosomes and translation machinery in these remote locations is crucial for the abundant local mRNA translation that supports neuronal functions. Following biosynthesis, ribosomal sorting in neurons happens either *via* diffusion or by active transport. The active sorting, is achieved either by associating with mRNPs or by tethering to membrane-bound organelles targeted to distant locations. In addition, existing ribosomes can exchange locally synthesized surface proteins (RPs) giving rise to ribosomes with specialized functions. For example, RP mRNAs with a specific sequence motif are translated into the axons which, can then associate with the surface components of existing ribosomes. Such modifications allow ribosomes to translate a distinct set of transcripts that support local functions.

(**Figure 2**). It is currently believed that while the subunits diffuse freely anywhere in the cell, most assembled ribosomes reach their target location by associating with various RBPs, membraneless granules, or membrane-bound organelles (Rolls et al., 2002; Fernandopulle et al., 2021). Such association can also lead to the functional compartmentalization of ribosomes. For example, a recent study has reported that the presynaptic ribosomes, tethered to *Rab7a*-containing endosomal vesicles, drive the

translation of mRNAs relevant to mitochondrial functions (Cioni et al., 2019; **Figure 2**). In axonal growth cones, the DCC receptor and its ligand netrin regulate the translation of their target mRNAs by immobilizing the ribosomes locally (Martin, 2010; Tcherkezian et al., 2010; Kim and Martin, 2015; Koppers et al., 2019). These results highlight the importance of spatial confinement of ribosomes for compartmentalizing translation (Reid and Nicchitta, 2015; Cioni et al., 2019).

A large fraction of the cytosolic ribosome functions as polyribosomes. They often reach their target locations by piggybacking partner mRNPs or transporting granules (Fernandopulle et al., 2021). For example, TDP43 and FMRP/FUS containing transport granules are shown to carry polyribosomes to neuronal axons and dendrites, respectively (Miyashiro et al., 2003; Simsek et al., 2017; Thelen and Kye, 2020; Nagano et al., 2020). Both motor proteins such as Kinesin I, II, Myosin II, and V and adaptor proteins like RACK1 help in the precise targeting of polysomes (Hirokawa et al., 2010; Ceci et al., 2012; Spillane et al., 2013). However, given the heterogeneous properties of ribosome-associated mRNPs and the contradictory nature of evidence, it is not clear whether moving polysomes can translate actively (Wu et al., 2015; Katz et al., 2016; Mateju et al., 2020). This necessitates the study of the translatability of moving polysomes in greater depth.

While ample evidence supports the polyribosomal translation of mRNAs at somatic and dendritic compartments, evidence for axonal ribosomes has been hard to come by for a long period (Ostroff et al., 2002, 2018, 2017; Biever et al., 2019). Eventually, improved paradigms have allowed the detection of mRNAs, rRNAs, actively translating polysomes, ER-Golgi-mediated protein synthesis, and their membrane targeting in axons (Giuditta et al., 1968, 1980, 1986; Tennyson, 1970; Bassell et al., 1998; Willis, 2005; Merianda et al., 2009). Recent investigations have discovered additional mechanisms that aid in axonal ribosomal homeostasis. For example, studies on injured sciatic nerves have shown that polyribosomes are transferred to the axons from the neighboring Schwann cells through tunneling nanotubes or exosomes (Court et al., 2008). In addition, a few other current studies suggest that in the axons, monosome-mediated translation is abundant compared to polysomes (Biever et al., 2019, 2020; Koltun et al., 2020). These findings imply that neurons utilize a range of mechanisms to supply ribosomes to axons, where the translation program is modified uniquely to meet the local protein demands. The fact that several stimulations uniquely impact axonal translation corroborates this idea further (Hafner et al., 2019; Koltun et al., 2020).

LOCAL REMODELING OF RIBOSOMES

Ribosomal subunits are composed of ∼80 ribosomal proteins and 4 different rRNA species. Conventionally it is believed that the protein or rRNA composition of the ribosomal population within a cell is consistent over time (Ferretti and Karbstein, 2019). However, multiple recent reports suggest otherwise. Studies in various non-neuronal systems have detected differential transcription and splicing of RP mRNAs and change in the stoichiometry of ribosomal core proteins across a range of physiological states (Bortoluzzi et al., 2001; Sharov et al., 2003; Richards, 2004; Adjaye et al., 2005; Kondrashov et al., 2011; Slavov et al., 2015). Some of these studies also show that ribosomes with distinct RP compositions can preferentially translate a subpool of mRNAs. For example, ribosomes containing RPL10A/uL1 protein selectively translate the internal ribosome entry site (IRES)-containing mRNAs (Shi et al., 2017). Interestingly, neurons also contain a large proportion of RPL10A containing ribosomes at the dendrites (Koltun et al., 2020; Sun et al., 2021). However, it is not known whether they translate a selected set of mRNAs in these compartments. Other than the RP composition, their posttranslational modifications are necessary for ribosomal function and can be a source of significant functional variability (Belin et al., 2010; Loenarz et al., 2014; Simsek and Barna, 2017). For example, in RPL12/uS23, hydroxylation of a proline residue is required for polysome formation, without which, human patients develop microcephaly and hearing loss (Loenarz et al., 2014). In addition, phosphorylated forms of various ribosomal proteins are studied widely in the context of synaptic signaling and are implicated in Parkinson's disease (Simsek and Barna, 2017; Martin et al., 2011). Besides, a combination of methylated, acetylated, and ubiquitylated ribosomal proteins can define some form of post-translational modifications code (PTM code) that can direct a ribosome to function uniquely (Nesterchuk et al., 2011; Simsek and Barna, 2017). Such functional specifications corroborate the "ribosome filter hypothesis" that considers ribosomes as active components of the gene regulatory framework (Mauro and Edelman, 2002).

In neurons, a consistent yet intriguing finding has been an abundance of RP mRNAs in the neuronal branches away from the cell body (Poon et al., 2006; Cajigas et al., 2012; Rangaraju et al., 2017). The targeting of these mRNAs to the distal processes cannot be explained by the Brownian diffusion and requires a reassessment of their physiological roles in these compartments. Also, there is evidence to support the ubiquitous synthesis of ribosomal proteins at distant locations, where they can physically associate with the pre-existing ribosomes. For example, RP mRNAs with CUIC-sequence motifs are translated locally and are incorporated into the axonal ribosomes required to translate critical mRNAs for axonal maintenance and branching (Shigeoka et al., 2019). The translation of RP mRNAs in axons requires the survival of the motor neuron (SMN) protein in the absence of which, axonal ribosomal content dips by 27% (Fallini et al., 2012, 2016). In dendrites, 17 ribosomal proteins are synthesized locally while 12 of them are incorporated into the existing ribosomes rapidly (Fusco et al., 2021). These proteins are short-lived and are associated with the solvent-accessible surfaces of ribosomes (Shigeoka et al., 2019; Fusco et al., 2021). Such dynamic exchanges of subunit proteins are necessary for the maintenance, repair, or modification of their functions in the local compartments (**Figure 2**). Interestingly, ribosomes are often located at both dendritic and axonal branch points. Here, they colocalize with mitochondria and other RBPs to translate mRNAs critical for stabilizing branches (Cui-Wang et al., 2012; Spillane et al., 2013).

Despite our knowledge of dendritic and axonal translation, we know relatively little about the synthesis of ribosomal proteins at the synapse. Ribosome profiling from cortical synaptoneurosomes has revealed that a few RP mRNAs are synthesized locally at the synapse upon NMDAR stimulation (Kuzniewska et al., 2020). Whether they can modulate existing ribosomal function requires verification. Moreover, since solitary monosomes translate the bulk of the synaptic mRNAs, especially with shorter ORFs (Biever et al., 2020; Koltun et al., 2020), conceptually it is feasible to selectively alter the translation of such mRNAs by modifying single ribosomes. Whether such mechanisms operate at the synapse requires validation through experimentation.

Also, these studies have opened up a flurry of other questions that remain unanswered. For instance, given the distinct translation states of various neuronal compartments, whether ribosomes with unique RP compositions or rRNA modifications populate these compartments differentially remains to be seen. In addition, it is not clear whether the type of synaptic activity (i.e., excitatory vs. inhibitory) has distinct impacts on the ribosomal properties. Besides, within a synapse, there can be multiple functional zones with heterogeneous molecular compositions (Nanguneri et al., 2019; Venkatesan et al., 2020). Whether ribosomes proximal to these zones function uniquely is not understood. Also, specific biochemical mechanisms that control ribosome-RBP association needs to be identified. Intriguingly, a large part of the variability in protein expression is contributed by the stochasticity of translation elongation (Datta and Seed, 2018; Koltun et al., 2020; Sun et al., 2021). Whether rRNA modifications and subunit protein compositions contribute to the stochastic aspects of protein synthesis are not well characterized. Also, it needs to be investigated whether specialized ribosomes necessarily need to function as monosomes. In the case of a polysome, do all ribosomes harbor similar subunit compositions? Whether sequence and structural features of mRNAs dictate their affinity toward ribosomes? How does the presence or absence of an RBP affect ribosome-mRNA recognition? Some of these questions need to be addressed thoroughly for a better understanding of translation regulation in neurons. Besides, mRNA nucleotides often undergo chemical modifications posttranscriptionally, known as the epitranscriptomic changes, which represent an additional layer of translation regulation. A large number of synaptic mRNAs harbor critical modifications such as N^6-methyladenosine, m^5-cytosine, etc., because of the actions of a group of depositing (writer), binding (reader), and removing (eraser) enzymes (Flamand and Meyer, 2019). For example, almost 3,000 synaptic mRNAs are m^6A methylated (Merkurjev et al., 2018). These modifications either facilitate or occlude the binding of modified mRNAs to RBPs and translation machinery, thus, tuning translation kinetics (Merkurjev et al., 2018; Li et al., 2019). A study has shown in the past that mRNA modification such as N^6-methyladenosine (m^6A) alters the recognition time and binding probability of a cognate tRNA to an mRNA codon and consequently alters elongation dynamics (Choi et al., 2016). Also, it is established that the absence of these RNA modifying enzymes affects synaptic translation and plasticity (Li et al., 2019). Further insight would clarify whether the deficiency of such enzymes impacts the ribosome-mRNA recognition, binding, and translatability of these mRNAs. Finally, how these processes are altered in pathological conditions or with aging should be monitored. Nonetheless, on-site remodeling of ribosomes through various mechanisms represents an exciting ramification of our understanding of spatiotemporal gene expression regulation in neurons.

LOCAL FACTORS THAT AFFECT TRANSLATION KINETICS

For the holistic understanding of neuronal translation, numerous other factors need considerations. Since distant branches with smaller diameters present significant diffusion barriers, local factors are bound to influence ribosomal function. However, such studies are limited in the neuronal context. We discuss a few components from the local microenvironment that could be critical in our opinion to shape ribosomal function.

Concentration of Cations

K^+

K^+ is a major intracellular monovalent cation in neurons. Recent studies have revealed the role of K^+ ions as integral components of the ribosomal structure (Khatter et al., 2015; Rozov et al., 2019). In eukaryotic ribosomes, K^+ ions strengthen the intersubunit interactions and mediate the interactions between tRNAs and ribosomal components (Wilson and Cate, 2012; Khatter et al., 2015). This is unlike the prokaryotic ribosomes, where the role of Mg^{2+} ions is more prominent (Ramakrishnan, 2002; Nierhaus, 2014). Intriguingly, recent studies from prokaryotic ribosomes also have suggested diverse roles for K^+ ions (Rozov et al., 2019). However, our current understanding of the influence of K^+ ions upon ribosomal performance in the cellular context is limited. In the case of hippocampal neurons, while the steady-state concentration of K^+ $[(K^+)_i]$ is ∼140 mM, it can reduce rapidly up to almost ∼43 percent following glutamate-mediated depolarization (Ballanyi et al., 1984; Müller and Somjen, 2000; Somjen and Müller, 2000; Nierhaus, 2014; Shen et al., 2019). Similar observations were made for carbachol or GABA treatment [∼20% and 8.5% $(K^+)_i$ respectively (Ballanyi et al., 1984)]. Such changes would be pronounced in the small volume compartments like dendritic spines or axonal growth cones and are likely to impact ribosomal subunit interactions and subsequent functions. Considering a large body of evidence pointing to the fact that neuronal depolarization can affect protein synthesis (Sutton et al., 2004; Hsu et al., 2015; Kos et al., 2016; Brigidi et al., 2019; Dastidar et al., 2020), it is worth investigating whether such effects are mediated by the changes in $[K^+]_i$. In addition, multiple reports suggest altered neuronal firing and membrane properties upon treatment with global protein synthesis inhibitors (Kleim et al., 2003; Sharma et al., 2012; Scavuzzo et al., 2019). Whether this effect is due to the release of a large amount of ribosome-bound K^+ ions following the inhibitor actions needs verification.

Mg^{2+}

Magnesium is an abundant divalent cation within mammalian cells. In neurons, the intracellular Mg^{2+} concentration ranges between 17–20 mM (Romani, 2011). Interestingly, the concentration difference of Mg^{2+} ions across the plasma membrane is only twofold (compared to 20,000-fold of calcium). There are various mechanisms by which Mg^{2+} ions are stored in a cell, of which ribosome-bound Mg^{2+} pool represents a considerable fraction. In humans, each ribosome is bound to 239 Mg^{2+} ions (Khatter et al., 2015). Studies of diverse backgrounds have revealed that Mg^{2+} is a small electron-dense ion that helps in stabilizing the negative charges of the rRNA backbone residues (counterions) (Nierhaus, 2014). Given a neuron can have as many as 10^6–10^7 ribosomes, the amount of ribosome-bound Mg^{2+} is substantial. However, due to the shallow concentration gradient of Mg^{2+} across the membrane and the continuous exchange between their bound and the free form in the cytosol, changes in extracellular Mg^{2+} availability can severely impact the intracellular Mg^{2+} concentration and ribosomal functions. Also, the Mg^{2+} deficiency within neurons can be sensed by mTOR signaling that can alter translation in several ways (Shindo et al., 2020).

Ca^{2+} and Mn^{2+}

Apart from being a cation, Ca^{2+} acts as an important intracellular second messenger in neurons. However, its role in the context of neuronal ribosomes is less studied. Earlier observations on purified E. coli ribosomes have established that the presence of Ca^{2+} in the reaction buffer improves ribosomal performance (Gordon and Lipmann, 1967). However, later studies have found that another divalent cation Mn^{2+} can substitute Mg^{2+} in both subunits while Ca^{2+} could do so only in the small subunit (Weiss et al., 1973). In sync with these observations, Mg^{2+} depletion in pituitary GH3 cells leads to a complete abolishment of polysomes. However, replenishing Ca^{2+} quickly recovers the polysomal functions, highlighting a positive influence of calcium over eukaryotic polysomes (Chin et al., 1987). In addition, Ca^{2+} promotes the association between purified human ribosomes and the Ca^{2+}-sensitive protein Calmodulin (Behnen et al., 2012). Interestingly, at the neuronal synapse, Ca^{2+} activates several EF-hand-containing proteins such as Calmodulin, Caldendrin, Calbindin, Calreticulin, Calneuron, and others (Chard et al., 1995; Seidenbecher et al., 1998; Pangršič et al., 2015; Mundhenk et al., 2019). Some of them, such as Calneuron 1 and 2, have the highest affinity toward Ca^{2+}. Functionally, they are implicated in Golgi to plasma membrane protein trafficking (Mundhenk et al., 2019). However, not much is known whether they can influence protein synthesis. Since neuronal activation alters intracellular Ca^{2+} levels, an exciting direction would be to investigate how these various Ca^{2+}-binding proteins act together to regulate ribosomal functions following neuronal stimulation.

ATP Level

Intracellular ATP concentration is a major rate-limiting factor for almost all anabolic pathways. ATP level is particularly important for protein synthesis due to multiple ATP-consuming steps in mRNA translation (Schwanhäusser et al., 2011). Our previous study has demonstrated that neuronal activity-induced protein synthesis is responsible for a significant ATP expenditure (Dastidar et al., 2020). Others have observed that a deficiency in energy biosynthesis can attenuate activity-induced synaptic translation (Rangaraju et al., 2019). Moreover, perturbing mitochondrial function that colocalizes with the translational hotspots at the neurite branch points impairs brach-point protein synthesis and branch stabilization (Hill et al., 2012; Spillane et al., 2013; Li et al., 2004). Conversely, new proteins can support mitochondrial function locally. For example, local translation of lamin B2 at the retinal ganglionic axons of *Xenopus* maintains mitochondrial morphology and function (Yoon et al., 2012). In this context, an intriguing observation has been that an excess of intracellular ATP can negatively impact translation by binding additional Mg^{2+} ions, thus limiting Mg^{2+}-dependent ribosomal assembly (Pontes et al., 2015). Therefore, a coordinated regulation between protein synthesis and energy biosynthesis is necessary for neuronal functions and can be achieved by the actions of intracellular metabolic sensors like phosphofructokinase 1 (PFK1) or AMP-activated protein kinase (AMPK) (Jang et al., 2016; Marinangeli et al., 2018; Dastidar et al., 2020). In general, the interplay between metabolic and translation regulatory pathways remains incompletely understood and would be an active area of future research.

tRNA Availability

Transfer RNAs (tRNA) canonically function as adapter molecules during mRNA translation. The availability of tRNAs, therefore, is one of the rate-limiting parameters of the ribosomal function. The redundancy in the genetic code allows most amino acids to be encoded by multiple codons. Also, these codons are distributed non-randomly along the length of an mRNA message (Komar, 2016) and are related to the decoding times for each codon (Gardin et al., 2014; Quax et al., 2015). Indeed eukaryotic ribosomes can accommodate frequent codons more rapidly at the A site than the rare codons (Gardin et al., 2014). The codon usage bias has been estimated to account for 30% of the variation in mRNA-protein correlation in human cells (Schwanhäusser et al., 2011). Also, the difference in decoding time determines the speed of polypeptide emergence and co-translational protein folding (Waudby et al., 2019). In other words, any change in the mRNA codons influences their average decoding time, the rate of ribosomal translocation, the rate of polypeptide emergence, and hence the folding probability of a protein toward its native state. Since tRNA availability influences the average decoding time, the rapid activity-induced translation response would require various tRNA species to be readily available within local compartments. Toward this end, the presence of tRNAs was detected within neuronal dendrites back in 1996 (Tiedge and Brosius, 1996). In addition, a more recent study has determined their kinetics inside neurons (Koltun et al., 2020). In this study, the exogenously labeled tRNAs introduced in the cortical neurons showed punctate structures. In general, the tRNA puncta were bidirectionally transported in the dendrites and a fraction of them (generally larger in size) could be destabilized with puromycin, a translation inhibitor that disengages elongating ribosomes,

indicating they were part of actively translating complexes. However, chemical LTP induction led to a further increase in these large tRNA aggregation and potentially mRNA translation (Koltun et al., 2020).

Despite the advances, appreciating various dimensions of tRNA function in neuronal mRNA translation would require more information. In particular, how the concentration of individual tRNA species affects ribosomal processivity is not established clearly. Also, considering the differences in decoding time for various codons (Gardin et al., 2014), it would be compelling to probe whether mRNAs in a compartment show distinct codon usage patterns and whether the tRNAs for those codons are enriched in those locations. Finally, given the rising evidence of on-site ribosomal remodeling, one would be intrigued to know if the remodeled ribosomes prefer to bind specific tRNA species and translate mRNAs with distinct codon-usage patterns.

In cellulo Dynamics of Neuronal Ribosomes

Decades of work in biochemistry and insight from high-resolution structures have elucidated the founding principles of mRNA translation and ribosomal function. But, these approaches provide very little dynamic information in the cellular realm. More recent studies based on single-molecule tracking have been instrumental in describing the dynamic properties of ribosomes and mRNAs within cells (Volkov and Johansson, 2019). Both prokaryotic and eukaryotic ribosomes have been visualized by tagging RPs with fluorescent proteins (Katz et al., 2016; Bayas et al., 2018). These experiments have been critical in understanding the population behavior of ribosomes arising from thousands of single-molecule detection events. Especially, live tracking of ribosomal subunits allows correlating their dynamics to mRNA translation within a cell (Prabhakar et al., 2019; Volkov and Johansson, 2019). For example, single-molecule diffusion studies on E. coli ribosomes have found that while the subunits themselves can diffuse freely across the entire cell, elongating ribosomes are excluded from the nucleoid (Sanamrad et al., 2014). Besides, simultaneous tracking of mRNPs and ribosomal particles on mouse fibroblast lines has revealed that polysome-associated mRNPs move slower than the mRNPs alone. Ribosomes in these cells show two prominent diffusional states (Katz et al., 2016). While the majority display relatively less mobility, a smaller freely diffusing fraction moves more rapidly (Katz et al., 2016; Donlin-Asp et al., 2021). Interestingly, treatment with puromycin increases the mobility of both ribosomes and mRNPs in these cells. Another study noted a similar effect of puromycin treatment on the mRNP dynamics in neurons (Donlin-Asp et al., 2021). These results suggest that polyribosomes impede the movement of mRNP complexes by making them heavier while destabilizing them with puromycin increases their mobility (Katz et al., 2016). However, one problem with single-molecule experiments is that the fluorescent proteins coexpressed with the proteins of interest often show moderate brightness and photostability (Chudakov et al., 2010; Volkov and Johansson, 2019). In addition, the presence of a large number of subdiffraction ribosomal particles can complicate the detection and analysis of single-molecule trajectories (Volkov and Johansson, 2019). To this end, a combination of photoactivable or photoswitchable fluorescent proteins/fluorophores and imaging techniques that can overcome the diffraction barrier such as STED, RESOLFT, and PALM/STORM have enabled molecular tracking with relatively lesser complications (Manley et al., 2008; Nair et al., 2013; Shcherbakova et al., 2014; Kedia et al., 2021). For example, observations made through sptPALM trajectories in migrating mouse fibroblast cells describe that ribosomes near focal adhesions of the leading edge show much-confined movement compared to elsewhere in the cytosol. Since ribosomes tend to dwell more at the site of translation, such interchanges between diffusion states are envisioned to drive compartmentalization of protein synthesis (Katz et al., 2016).

Despite considerable progress, much of our understanding of the dynamics of individual ribosomes in neurons remain elusive. Considering the large variability in the mRNP composition, kinetics, and biochemical properties (Formicola et al., 2019; Tauber et al., 2020), it is necessary to probe how mRNP properties affect ribosomal movement and function. In the same context, it would be useful to generate a neuron-wide ribosomal mobility map with nanometer precision. In addition, compartments like dendritic spines or growth cones show non-homogeneous molecular distribution and organization (Frost et al., 2010; Igarashi, 2019). While functional zones like post-synaptic density (PSD) are protein-dense regions, other areas of a spine are more dynamic with varied molecular compositions (Kaizuka and Takumi, 2018; Venkatesan et al., 2020; Helm et al., 2021). Interestingly, similar to focal adhesions, PSD is also reported to associate with polyribosomes, RBPs and act as a platform of translation (Ostroff et al., 2017; Yoon et al., 2016; Zhang et al., 2012). However, ribosomal diffusion kinetics in and around PSD has not been examined yet. Using single-molecule localization microscopy (SMLM), it is now possible to track the mean square displacement of ribosomes and calculate their diffusion parameters from HMM-bayesian modeling. Given the strong correlation between ribosomal confinement and active translation, the analysis can reveal the spatial distribution of translation "hotspots" within spines in live neurons (Monnier et al., 2015; Katz et al., 2016; Volkov and Johansson, 2019; **Figure 3**). In addition, we are yet to know how neuronal stimulation may impact ribosomal localization and their dynamics within spines (Ostroff et al., 2017). As discussed before, synaptic molecules often organize into functional zones by forming nanoclusters. Signaling through these nanodomains is crucial for synaptic plasticity and protein synthesis (Nair et al., 2013; Goncalves et al., 2020; Sun et al., 2021). For example, GluA1 or GluA2 and PSD 95 nanodomains at the dendritic spines are the hubs of intracellular signaling. The efficacy of signaling depends on nanodomain sizes and the localization of receptors in these clusters (Nair et al., 2013; Tang et al., 2016; Nanguneri et al., 2019; Venkatesan et al., 2020). In addition, it is observed that within translationally active spines, PSD microdomains often associate with newly synthesized proteins which, in turn, are closely apposed to ribosomes (Sun et al., 2021). However, little

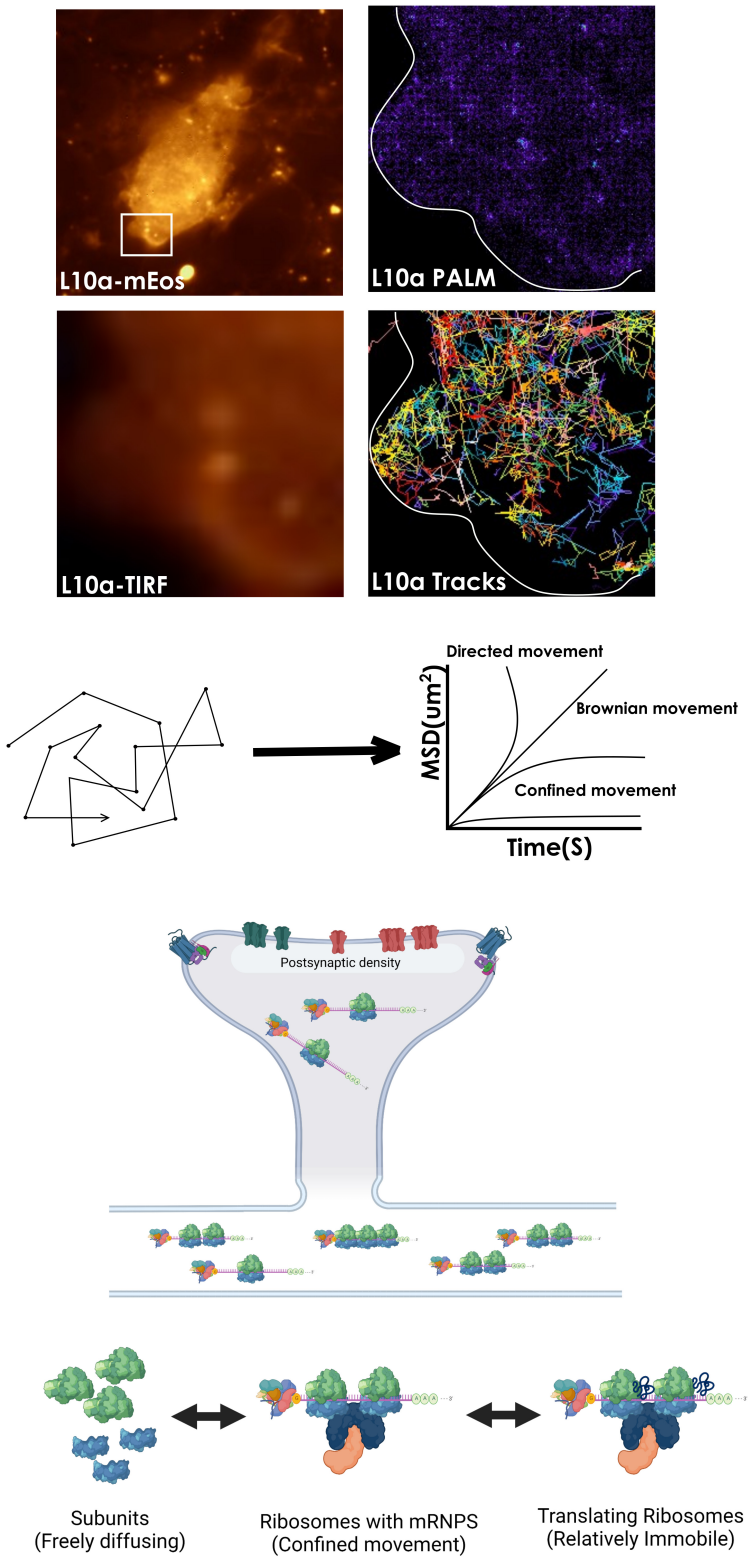

FIGURE 3 | Tracking ribosomal mobility for locating "hotspots" of active translation. Visualizing and tracking ribosomal subunits at the single-particle level is possible by tagging a subunit protein such as L10a with photoactivable fluorescent proteins such as mEos within a cell. Analysis of their mean square displacement (MSD) trajectories of single protein molecules can then be used to calculate the diffusion coefficients of various ribosomal populations, that switch between diffusional states while functioning within cells. In addition, perturbations with pharmacological agents that destabilize ribosomes can confirm their engagement in active translation. Also, an HMM-based analysis of the trajectories can be used to reveal the mechanisms underpinning the conversion between diffusional states of ribosomes (not shown).

is known whether the molecular organization of the PSD can sequester or trap ribosomes to initiate localized translation. Also, the precise nanometer level localization maps of receptors, PSD, ribosome distribution, and protein synthesis hotspots together are not available yet. These finer insights into spatio-temporal correlation and regulation of ribosomal functions would be valuable to understand the stochastic constraints that control local rates of translation. In parallel, direct visualization of single ribosomes and their kinetics can verify whether their sequestration at the PSD is necessary for localized translation. Perturbing nanodomain properties using pharmacochemical or optogenetic approaches followed by ribo-tracking can indeed delineate the relationship between the molecular organization, and protein synthesis at the individual spine level. Altogether, these approaches provide us with the opportunity to answer the previously underexplored questions of mRNA translation. They also allow us to appreciate the tremendous variability in ribosomal functions within neurons with unprecedented details.

CONCLUDING REMARKS

Proteome remodeling is a critical component of the neuronal response to several incoming stimuli. The complex morphology of neurons requires the remodeling to be done locally in a compartmentalized manner. Together with various other mechanisms, ribosomal modulation (through biogenesis, sorting, local remodeling, and dynamic properties) provides a way to create variability in protein expression. However, the spatiotemporal kinetics of such changes and their relation with synaptic signaling remains to be determined. During memory formation, information is stored from shorter to longer time scales at the synapse. Yet the mechanistic connections between the various phases of memory formation remain to be uncovered. Considering signaling events and instantaneous molecular organizations encode information for a short period while protein synthesis dictates its long-term storage, a rigorous connection between the events of these two timescales can explain how memories are stored permanently from their shorter labile versions. With the emergence of suitable technologies with high spatial and temporal precisions, we are finally in a position to address some of these pressing questions.

AUTHOR CONTRIBUTIONS

SD conceptualized and designed the manuscript. Both authors wrote and edited the manuscript and approved the submitted version.

FUNDING

This work was supported by Department of Biotechnology, Govt. of India grant (Department of Biotechnology Genomics Engineering Taskforce to DN), DBT-IISc Partnership program to DN, IISC-STAR program grant to DN, and Institute of Eminence grant from IISc to DN. Department of Biotechnology research associateship grant to SD.

REFERENCES

Adjaye, J., John, H., Ralf, H., BenKahla, A., Brink, T. C., Wierling, C., et al. (2005). "Primary Differentiation in the Human Blastocyst: Comparative Molecular Portraits of Inner Cell Mass and Trophectoderm Cells.". *Stem Cells* 23, 1514–1525. doi: 10.1634/stemcells.2005-0113

Allen, K. D., Regier, M. J., Hsieh, C., Tsokas, P., Barnard, M., Phatarpekar, S., et al. (2018). "Learning-Induced Ribosomal RNA Is Required for Memory Consolidation in Mice—Evidence of Differentially Expressed rRNA Variants in Learning and Memory." Edited by Michal Hetman. *PLoS One* 13:e0203374. doi: 10.1371/journal.pone.0203374

Ballanyi, K., Bruggencate, T., Grafe, P., and Reddy, M. M. (1984). "Different types of potassium transport linked to carbachol and y-aminobutyric acid actions in rat sympathetic neurons.". *Neuroscience* 12, 917–927. doi: 10.1016/0306-4522(84)90179-9

Bassell, G. J., Zhang, H., Byrd, A. L., Femino, A. M., Singer, R. H., Taneja, K. L., et al. (1998). "Sorting of beta-actin mRNA and protein to neurites and growth cones in culture,". *J. Neurosci.* 18, 251–265. doi: 10.1523/JNEUROSCI.18-01-00251.1998

Baßler, J., and Hurt, E. (2019). "Eukaryotic Ribosome Assembly.". *Annu. Rev. Biochem.* 88, 281–306. doi: 10.1146/annurev-biochem-013118-110817

Bayas, C. A., Wang, J., Lee, M. K., Schrader, J. M., Shapiro, L., and Moerner, W. E. (2018). "Spatial Organization and Dynamics of RNase E and Ribosomes in *Caulobacter Crescentus*.". *Proc. Natl. Acad. Sci.* 115, E3712–E3721. doi: 10.1073/pnas.1721648115

Bear, M. F., Huber, K. M., and Warren, S. T. (2004). "The mGluR Theory of Fragile X Mental Retardation.". *Trends Neurosci.* 27, 370–377. doi: 10.1016/j.tins.2004.04.009

Behnen, P., Davis, E., Delaney, E., Frohm, B., Bauer, M., Cedervall, T., et al. (2012). "Calcium-Dependent Interaction of Calmodulin with Human 80S Ribosomes and Polyribosomes.". *Biochemistry* 51, 6718–6727. doi: 10.1021/bi3005939

Belin, S., Hacot, S., Daudignon, L., Therizols, G., Pourpe, S., Mertani, H. C., et al. (2010). "Purification of Ribosomes from Human Cell Lines.". *Curr. Protoc. Cell Biol.* 49:cb0340s49. doi: 10.1002/0471143030.cb0340s49

Biever, A., Donlin-Asp, P. G., and Schuman, E. M. (2019). "Local Translation in Neuronal Processes.". *Curr. Opin. Neurobiol.* 57, 141–148. doi: 10.1016/j.conb.2019.02.008

Biever, A., Glock, C., Tushev, G., Ciirdaeva, E., Dalmay, T., Langer, J. D., et al. (2020). "Monosomes Actively Translate Synaptic mRNAs in Neuronal Processes.". *Science* 367:eaay4991. doi: 10.1126/science.aay4991

Boisvert, F., Koningsbruggen, S. V., Navascués, J., and Lamond, A. I. (2007). "The Multifunctional Nucleolus.". *Nat. Rev. Mol. Cell Biol.* 8, 574–585. doi: 10.1038/nrm2184

Bortoluzzi, S., D'Alessi, F., Romualdi, C., and Danieli, G. A. (2001). "Differential Expression of Genes Coding for Ribosomal Proteins in Different Human Tissues.". *Bioinformatics* 17, 1152–1157. doi: 10.1093/bioinformatics/17.12.1152

Brigidi, G. S., Hayes, M. G. B., Santos, N. P. D., Hartzell, A. L., Texari, L., Lin, P., et al. (2019). "Genomic Decoding of Neuronal Depolarization by Stimulus-Specific NPAS4 Heterodimers.". *Cell* 179, 373.e–391.e. doi: 10.1016/j.cell.2019.09.004

Cajigas, I. J., Tushev, G., Will, T. J., Dieck, S. T., Fuerst, N., and Schuman, E. M. (2012). "The Local Transcriptome in the Synaptic Neuropil Revealed by Deep Sequencing and High-Resolution Imaging.". *Neuron* 74, 453–466. doi: 10.1016/j.neuron.2012.02.036

Ceci, M., Welshhans, K., Ciotti, M. T., Brandi, R., Parisi, C., Paoletti, F., et al. (2012). "RACK1 Is a Ribosome Scaffold Protein for β-Actin mRNA/ZBP1 Complex.". *PLoS One* 7:e35034. doi: 10.1371/journal.pone.0035034

Chard, P. S., Jordan, J., Marcuccilli, C. J., Miller, R. J., Leiden, J. M., Roos, R. P., et al. (1995). "Regulation of Excitatory Transmission at Hippocampal Synapses by Calbindin D28k.". *Proc. Natl. Acad. Sci.* 92, 5144–5148. doi: 10.1073/pnas.92.11.5144

Chau, K. F., Shannon, M. L., Fame, R. M., Fonseca, E., Mullan, H., Johnson, M. B., et al. (2018). "Downregulation of Ribosome Biogenesis during Early Forebrain Development.". *ELife* 7:e36998. doi: 10.7554/eLife.36998

Chin, K. V., Cade, C., Brostrom, C. O., Galuska, E. M., and Brostrom, M. A. (1987). "Calcium-Dependent Regulation of Protein Synthesis at Translational Initiation in Eukaryotic Cells.". *J. Biol. Chem.* 262, 16509–16514. doi: 10.1016/S0021-9258(18)49285-X

Choi, J., Ieong, K., Demirci, H., Chen, J., Petrov, A., Prabhakar, A., et al. (2016). "N6-Methyladenosine in mRNA Disrupts tRNA Selection and Translation-Elongation Dynamics.". *Nat. Struct. Mol. Biol.* 23, 110–115. doi: 10.1038/nsmb.3148

Chudakov, D. M., Matz, M. V., Lukyanov, S., and Lukyanov, K. A. (2010). "Fluorescent Proteins and Their Applications in Imaging Living Cells and Tissues.". *Physiol. Rev.* 90, 1103–1163. doi: 10.1152/physrev.00038.2009

Cioni, J., Lin, J. Q., Holtermann, A. V., Koppers, M., Jakobs, M. A. H., Azizi, A., et al. (2019). Late Endosomes Act as mRNA Translation Platforms and Sustain Mitochondria in Axons. *Cell* 176, 56.e–72.e. doi: 10.1016/j.cell.2018.11.030

Costa, R. O., Martins, H., Martins, L. F., Cwetsch, A. W., Mele, M., Pedro, J. R., et al. (2019). Synaptogenesis Stimulates a Proteasome-Mediated Ribosome Reduction in Axons. *Cell Rep.* 28, 864.e–876.e. doi: 10.1016/j.celrep.2019.06.080

Court, F. A., Hendriks, W. T. J., MacGillavry, H. D., Alvarez, J., and Minnen, J. V. (2008). "Schwann Cell to Axon Transfer of Ribosomes: Toward a Novel Understanding of the Role of Glia in the Nervous System.". *J. Neurosci.* 28, 11024–11029. doi: 10.1523/Jneurosci.2429-08.2008

Cui-Wang, T., Hanus, C., Cui, T., Helton, T., Bourne, J., Watson, D., et al. (2012). "Local Zones of Endoplasmic Reticulum Complexity Confine Cargo in Neuronal Dendrites.". *Cell* 148, 309–321. doi: 10.1016/j.cell.2011.11.056

D'Souza, M. N., Gowda, N. K. C., Tiwari, V., Babu, R. O., Anand, P., Dastidar, S. G., et al. (2018). "FMRP Interacts with C/D Box snoRNA in the Nucleus and Regulates Ribosomal RNA Methylation.". *IScience* 9, 399–411. doi: 10.1016/j.isci.2018.11.007

Dastidar, S. G., Sharma, S. D., Chakraborty, S., Chattarji, S., Bhattacharya, A., and Muddashetty, R. S. (2020). Distinct Regulation of Bioenergetics and Translation by Group I mGluR and NMDAR. *EMBO Rep.* 2020:201948037. doi: 10.15252/embr.201948037

Datta, S., and Seed, B. (2018). "Influence of Multiplicative Stochastic Variation on Translational Elongation Rates.". *PLoS One* 13:e0191152. doi: 10.1371/journal.pone.0191152

Deshpande, P., Flinkman, D., Hong, Y., Goltseva, E., Siino, V., Sun, L., et al. (2020). "Protein Synthesis Is Suppressed in Sporadic and Familial Parkinson's Disease by LRRK2.". *FASEB J.* 34, 14217–14233. doi: 10.1096/fj.202001046R

Donlin-Asp, P. G., Polisseni, C., Klimek, R., Heckel, A., and Schuman, E. M. (2021). "Differential Regulation of Local mRNA Dynamics and Translation Following Long-Term Potentiation and Depression.". *Proc. Natl. Acad. Sci.* 118:e2017578118. doi: 10.1073/pnas.2017578118

Fallini, C., Bassell, G. J., and Rossoll, W. (2012). "Spinal Muscular Atrophy: The Role of SMN in Axonal mRNA Regulation.". *Brain Res.* 1462, 81–92. doi: 10.1016/j.brainres.2012.01.044

Fallini, C., Donlin-Asp, P. G., Rouanet, J. P., Bassell, G. J., and Rossoll, W. (2016). Deficiency of the Survival of Motor Neuron Protein Impairs mRNA Localization and Local Translation in the Growth Cone of Motor Neurons. *J. Neurosci.* 36, 3811–3820. doi: 10.1523/JNEUROSCI.2396-15.2016

Fernandopulle, M. S., Lippincott-Schwartz, J., and Ward, M. E. (2021). "RNA Transport and Local Translation in Neurodevelopmental and Neurodegenerative Disease.". *Nat. Neurosci.* 24, 622–632. doi: 10.1038/s41593-020-00785-2

Ferretti, M. B., and Karbstein, K. (2019). "Does Functional Specialization of Ribosomes Really Exist?". *RNA* 25, 521–538. doi: 10.1261/rna.069823.118

Flamand, M. N., and Meyer, K. D. (2019). "The Epitranscriptome and Synaptic Plasticity.". *Curr. Opin. Neurobiol.* 59, 41–48. doi: 10.1016/j.conb.2019.04.007

Formicola, N., Vijayakumar, J., and Besse, F. (2019). Neuronal Ribonucleoprotein Granules: Dynamic Sensors of Localized Signals. *Traffic* 2019:12672. doi: 10.1111/tra.12672

Frost, N. A., Shroff, H., Kong, H., Betzig, E., and Blanpied, T. A. (2010). "Single-Molecule Discrimination of Discrete Perisynaptic and Distributed Sites of Actin Filament Assembly within Dendritic Spines.". *Neuron* 67, 86–99. doi: 10.1016/j.neuron.2010.05.026

Fusco, C. M., Desch, K., Dörrbaum, A. R., Wang, M., Staab, A., Chan, I. C. W., et al. (2021). "Neuronal Ribosomes Exhibit Dynamic and Context-Dependent Exchange of Ribosomal Proteins.". *Nat. Commun.* 12:6127. doi: 10.1038/s41467-021-26365-x

Gardin, J., Yeasmin, R., Yurovsky, A., Cai, Y., Skiena, S., Futcher, et al. (2014). "Measurement of Average Decoding Rates of the 61 Sense Codons *in Vivo*.". *ELife* 3:e03735. doi: 10.7554/eLife.03735

Gay, D. M., Lund, A. H., and Jansson, M. D. (2022). "Translational Control through Ribosome Heterogeneity and Functional Specialization.". *Trends Biochem. Sci.* 47, 66–81. doi: 10.1016/j.tibs.2021.07.001

Genuth, N. R., and Barna, M. (2018). "The Discovery of Ribosome Heterogeneity and Its Implications for Gene Regulation and Organismal Life.". *Mol. Cell* 71, 364–374. doi: 10.1016/j.molcel.2018.07.018

Giuditta, A., Cupellot, A., and Lazzarini, G. (1980). "Ribosomal RNA in the Axoplasm of the Squid Giant Axon.". *J. Neurochem.* 34, 1757–1760. doi: 10.1111/j.1471-4159.1980.tb11271.x

Giuditta, A., Dettbarn, W. D., and Brzin, M. (1968). "Protein Synthesis in the Isolated Giant Axon of the Squid.". *Proc. Natl. Acad. Sci.* 59, 1284–1287. doi: 10.1073/pnas.59.4.1284

Giuditta, A., Tim, H., and Luigia, S. (1986). "Rapid Important Paper.". *Neurochem. Int.* 8, 435–442. doi: 10.1016/0197-0186(86)90019-7

Goncalves, J., Bartol, T. M., Camus, C., Levet, F., Menegolla, A. P., Sejnowski, T. J., et al. (2020). "Nanoscale Co-Organization and Coactivation of AMPAR, NMDAR, and mGluR at Excitatory Synapses.". *Proc. Natl. Acad. Sci.* 117, 14503–14511. doi: 10.1073/pnas.1922563117

Gordon, J., and Lipmann, F. (1967). "Role of Divalent Ions in Poly U-Directed Phenylalanine Polymerization.". *J. Mol. Biol.* 23, 23–33. doi: 10.1016/S0022-2836(67)80064-0

Hafner, A., Donlin-Asp, P. G., Leitch, B., Herzog, E., and Schuman, E. M. (2019). Local Protein Synthesis Is a Ubiquitous Feature of Neuronal Pre- and Postsynaptic Compartments. *Science* 364:eaau3644. doi: 10.1126/science.aau3644

Hanus, C., and Schuman, E. M. (2013). "Proteostasis in Complex Dendrites.". *Nat. Rev. Neurosci.* 14, 638–648. doi: 10.1038/nrn3546

Helm, M. S., Dankovich, T. M., Mandad, S., Rammner, B., Jähne, S., Salimi, V., et al. (2021). "A Large-Scale Nanoscopy and Biochemistry Analysis of Postsynaptic Dendritic Spines.". *Nat. Neurosci.* 24, 1151–1162. doi: 10.1038/s41593-021-00874-w

Hernandez, A. I., Wolk, J., Hu, J.-Y., Liu, J., Kurosu, T., Schwartz, J. H., et al. (2009). Poly-(ADP-Ribose) Polymerase-1 Is Necessary for Long-Term Facilitation in Aplysia. *J. Neurosci.* 29, 9553–9562.

Hetman, M., and Slomnicki, L. P. (2019). "Ribosomal Biogenesis as an Emerging Target of Neurodevelopmental Pathologies.". *J. Neurochem.* 148, 325–347. doi: 10.1111/jnc.14576

Hill, S. E., Parmar, M., Gheres, K. W., Guignet, M. A., Huang, Y., Jackson, F., et al. (2012). "Development of Dendrite Polarity in Drosophila Neurons.". *Neural Dev.* 7:34. doi: 10.1186/1749-8104-7-34

Hirokawa, N., Niwa, S., and Tanaka, Y. (2010). "Molecular Motors in Neurons: Transport Mechanisms and Roles in Brain Function, Development, and Disease.". *Neuron* 68, 610–638. doi: 10.1016/j.neuron.2010.09.039

Holt, C. E., and Schuman, E. M. (2013). "The Central Dogma Decentralized: New Perspectives on RNA Function and Local Translation in Neurons.". *Neuron* 80, 648–657. doi: 10.1016/j.neuron.2013.10.036

Holt, C. E., Martin, K. C., and Schuman, E. M. (2019). "Local Translation in Neurons: Visualization and Function.". *Nat. Struct. Mol. Biol.* 26, 557–566. doi: 10.1038/s41594-019-0263-5

Hsu, W., Chung, H., Wu, C., Wu, H., Lee, Y., Chen, E., et al. (2015). "Glutamate Stimulates Local Protein Synthesis in the Axons of Rat Cortical Neurons by Activating α-Amino-3-Hydroxy-5-Methyl-4-Isoxazolepropionic Acid (AMPA) Receptors and Metabotropic Glutamate Receptors.". *J. Biol. Chem.* 290, 20748–20760. doi: 10.1074/jbc.M115.638023

Hyson, R. L., and Rubel, E. W. (1995). "Activity-Dependent Regulation of a Ribosomal RNA Epitope in the Chick Cochlear Nucleus.". *Brain Res.* 672, 196–204. doi: 10.1016/0006-8993(94)01390-4

Igarashi, M. (2019). "Molecular Basis of the Functions of the Mammalian Neuronal Growth Cone Revealed Using New Methods.". *Proc. Jap. Acad. Ser. B* 95, 358–377. doi: 10.2183/pjab.95.026

Jackson, R. J., Hellen, C. U. T., and Pestova, T. V. (2010). "The Mechanism of Eukaryotic Translation Initiation and Principles of Its Regulation.". *Nat. Rev. Mol. Cell Biol.* 11, 113–127. doi: 10.1038/nrm2838

Jang, S., Nelson, J. C., Bend, E. G., Rodríguez-Laureano, L., Tueros, F. G., Cartagenova, L., et al. (2016). "Glycolytic Enzymes Localize to Synapses under Energy Stress to Support Synaptic Function.". *Neuron* 90, 278–291. doi: 10.1016/j.neuron.2016.03.011

Job, C., and Eberwine, J. (2001). "Identification of Sites for Exponential Translation in Living Dendrites.". *Proc. Natl. Acad. Sci.* 98, 13037–13042. doi: 10.1073/pnas.231485698

Jordan, B. A., Fernholz, B. D., Khatri, L., and Ziff, E. B. (2007). "Activity-Dependent AIDA-1 Nuclear Signaling Regulates Nucleolar Numbers and Protein Synthesis in Neurons.". *Nat. Neurosci.* 10, 427–435. doi: 10.1038/nn1867

Kaizuka, T., and Takumi, T. (2018). "Postsynaptic Density Proteins and Their Involvement in Neurodevelopmental Disorders.". *J. Biochem.* 163, 447–455. doi: 10.1093/jb/mvy022

Kapur, M., Monaghan, C. E., and Ackerman, S. L. (2017). "Regulation of mRNA Translation in Neurons—A Matter of Life and Death.". *Neuron* 96, 616–637. doi: 10.1016/j.neuron.2017.09.057

Katz, Z. B., English, B. P., Lionnet, T., Yoon, Y. J., Monnier, N., Ovryn, B., et al. (2016). "Mapping Translation 'hot-Spots' in Live Cells by Tracking Single Molecules of mRNA and Ribosomes.". *ELife* 5:e10415. doi: 10.7554/eLife.10415

Kedia, S., Ramakrishna, P., Netrakanti, P. R., Singh, N., Sisodia, S. S., Jose, M., et al. (2021). "Alteration in Synaptic Nanoscale Organization Dictates Amyloidogenic Processing in Alzheimer's Disease.". *IScience* 24:101924. doi: 10.1016/j.isci.2020.101924

Khatter, H., Myasnikov, A. G., Natchiar, S. K., and Klaholz, B. P. (2015). "Structure of the Human 80S Ribosome.". *Nature* 520, 640–645. doi: 10.1038/nature14427

Kim, S., and Martin, K. C. (2015). "Neuron-Wide RNA Transport Combines with Netrin-Mediated Local Translation to Spatially Regulate the Synaptic Proteome.". *ELife* 4:e04158. doi: 10.7554/eLife.04158

Kleim, J. A., Bruneau, R., Calder, K., Pocock, D., Vandenberg, P. M., MacDonald, E., et al. (2003). "Functional Organization of Adult Motor Cortex Is Dependent upon Continued Protein Synthesis.". *Neuron* 40, 167–176. doi: 10.1016/S0896-6273(03)00592-0

Koltun, B., Ironi, S., Gershoni-Emek, N., Barrera, I., Hleihil, M., Nanguneri, S., et al. (2020). "Measuring mRNA Translation in Neuronal Processes and Somata by tRNA-FRET.". *Nucleic Acids Res.* 48, e32–e32. doi: 10.1093/nar/gkaa042

Komar, A. A. (2016). The Yin and Yang of Codon Usage. *Huma. Mol. Genet.* 25, R77–R85. doi: 10.1093/hmg/ddw207

Kondrashov, N., Pusic, A., Stumpf, C. R., Shimizu, K., Hsieh, A. C., Xue, S., et al. (2011). "Ribosome-Mediated Specificity in Hox mRNA Translation and Vertebrate Tissue Patterning.". *Cell* 145, 383–397. doi: 10.1016/j.cell.2011.03.028

Koppers, M., Cagnetta, S., Shigeoka, T., Wunderlich, L. C. S., Vallejo-Ramirez, P., Lin, J. Q., et al. (2019). "Receptor-Specific Interactome as a Hub for Rapid Cue-Induced Selective Translation in Axons.". *ELife* 8:e48718. doi: 10.7554/eLife.48718

Kos, A., Wanke, K. A., Gioio, A., Martens, G. J., Kaplan, B. B., and Aschrafi, A. (2016). "Monitoring mRNA Translation in Neuronal Processes Using Fluorescent Non-Canonical Amino Acid Tagging.". *J. Histochem. Cytochem.* 64, 323–333. doi: 10.1369/0022155416641604

Kuzniewska, B., Cysewski, D., Wasilewski, M., Sakowska, P., Milek, J., Kulinski, T. M., et al. (2020). Mitochondrial Protein Biogenesis in the Synapse Is Supported by Local Translation. *EMBO Rep.* 2020:201948882. doi: 10.15252/embr.201948882

Lafarga, M., Andres, M. A., Fernandez-Viadero, C., Villegas, J., and Berciano, M. T. (1995). "Number of Nucleoli and Coiled Bodies and Distribution of Fibrillar Centres in Differentiating Purkinje Neurons of Chick and Rat Cerebellum.". *Anat. Embryol.* 191, 359–367. doi: 10.1007/BF00534689

Li, D., and Wang, J. (2020). Ribosome heterogeneity in stem cells and development. *J. Cell Biol.* 219:e202001108. doi: 10.1083/jcb.202001108

Li, D., Zhang, J., Wang, M., Li, X., Gong, H., Tang, H., et al. (2018). "Activity-Dependent LoNA Regulates Translation by Coordinating rRNA Transcription and Methylation.". *Nat. Commun.* 9:1726. doi: 10.1038/s41467-018-04072-4

Li, J., Yang, X., Qi, Z., Sang, Y., Liu, Y., Xu, B., et al. (2019). "The Role of mRNA M6A Methylation in the Nervous System.". *Cell Biosci.* 9:66. doi: 10.1186/s13578-019-0330-y

Li, Z., Okamoto, K., Hayashi, Y., and Sheng, M. (2004). "The Importance of Dendritic Mitochondria in the Morphogenesis and Plasticity of Spines and Synapses.". *Cell* 119, 873–887. doi: 10.1016/j.cell.2004.11.003

Loenarz, C., Sekirnik, R., Thalhammer, A., Ge, W., Spivakovsky, E., Mackeen, M. M., et al. (2014). "Hydroxylation of the Eukaryotic Ribosomal Decoding Center Affects Translational Accuracy.". *Proc. Natl. Acad. Sci.* 111, 4019–4024. doi: 10.1073/pnas.1311750111

Ma, T. (2020). "Dysregulation of Neuronal Protein Synthesis in Alzheimer's Disease," in *The Oxford Handbook of Neuronal Protein Synthesis*, by Tao Ma, ed. W. Sossin (Oxford: Oxford University Press), doi: 10.1093/oxfordhb/9780190686307.013.18

Manley, S., Gillette, J. M., Patterson, G. H., Shroff, H., Hess, H. F., Betzig, E., et al. (2008). High-Density Mapping of Single-Molecule Trajectories with Photoactivated Localization Microscopy. *Nat. Methods* 5, 155–157. doi: 10.1038/nmeth.1176

Marinangeli, C., Didier, S., Ahmed, T., Caillerez, R., Domise, M., Laloux, C., et al. (2018). "AMP-Activated Protein Kinase Is Essential for the Maintenance of Energy Levels during Synaptic Activation.". *IScience* 9, 1–13. doi: 10.1016/j.isci.2018.10.006

Martin, I., Dawson, V. L., and Dawson, T. M. (2011). "Recent Advances in the Genetics of Parkinson's Disease.". *Annu. Rev. Genomics Hum. Genet.* 12, 301–325. doi: 10.1146/annurev-genom-082410-101440

Martin, K. C. (2010). "Anchoring Local Translation in Neurons.". *Cell* 141, 566–568. doi: 10.1016/j.cell.2010.04.031

Mateju, D., Eichenberger, B., Voigt, F., Eglinger, J., Roth, G., and Chao, J. A. (2020). Single-Molecule Imaging Reveals Translation of mRNAs Localized to Stress Granules. *Cell* 183, 1801.e–1812.e. doi: 10.1016/j.cell.2020.11.010

Mauro, V. P., and Edelman, G. M. (2002). "The Ribosome Filter Hypothesis.". *Proc. Natl. Acad. Sci.* 99, 12031–12036. doi: 10.1073/pnas.192442499

Merianda, T. T., Lin, A. C., Lam, J. S. Y., Vuppalanchi, D., Willis, D. E., Karin, N., et al. (2009). "A Functional Equivalent of Endoplasmic Reticulum and Golgi in Axons for Secretion of Locally Synthesized Proteins.". *Mol. Cell. Neurosci.* 40, 128–142. doi: 10.1016/j.mcn.2008.09.008

Merkurjev, D., Hong, W., Iida, K., Oomoto, I., Goldie, B. J., Yamaguti, H., et al. (2018). "Synaptic N6-Methyladenosine (M6A) Epitranscriptome Reveals Functional Partitioning of Localized Transcripts.". *Nat. Neurosci.* 21, 1004–1014. doi: 10.1038/s41593-018-0173-6

Miyashiro, K. Y., Beckel-Mitchener, A., Park, T. P., Becker, K. G., Barret, T., Liu, L., et al. (2003). "RNA Cargoes Associating with FMRP Reveal Deficits in Cellular Functioning in Fmr1 Null Mice.". *Neuron* 37, 417–431. doi: 10.1016/S0896-6273(03)00034-5

Mofatteh, M. (2020). "mRNA Localization and Local Translation in Neurons.". *AIMS Neurosci.* 7, 299–310. doi: 10.3934/Neuroscience.2020016

Monnier, N., Barry, Z., Park, H. Y., Su, K., Katz, Z., English, B. P., et al. (2015). "Inferring Transient Particle Transport Dynamics in Live Cells.". *Nat. Methods* 12, 838–840. doi: 10.1038/nmeth.3483

Müller, M., and Somjen, G. G. (2000). "Na^+ and K^+ Concentrations, Extra- and Intracellular Voltages, and the Effect of TTX in Hypoxic Rat Hippocampal Slices.". *J. Neurophysiol.* 83, 735–745. doi: 10.1152/jn.2000.83.2.735

Mundhenk, J., Fusi, C., and Kreutz, M. R. (2019). "Caldendrin and Calneurons—EF-Hand CaM-Like Calcium Sensors With Unique Features and Specialized Neuronal Functions.". *Front. Mol. Neurosci.* 12:16. doi: 10.3389/fnmol.2019.00016

Nagano, S., Jinno, J., Abdelhamid, R. F., Jin, Y., Shibata, M., Watanabe, S., et al. (2020). "TDP-43 Transports Ribosomal Protein mRNA to Regulate Axonal Local Translation in Neuronal Axons.". *Acta Neuropathol.* 140, 695–713. doi: 10.1007/s00401-020-02205-y

Nair, D., Hosy, E., Petersen, J. D., Constals, A., Giannone, G., Choquet, D., et al. (2013). Super-Resolution Imaging Reveals That AMPA Receptors Inside Synapses Are Dynamically Organized in Nanodomains Regulated by PSD95. *J. Neurosci.* 33, 13204–13224. doi: 10.1523/JNEUROSCI.2381-12.2013

Nanguneri, S., Pramod, R. T., Efimova, N., Das, D., Jose, M., Svitkina, T., et al. (2019). Characterization of Nanoscale Organization of F-Actin in Morphologically Distinct Dendritic Spines *In Vitro* Using Supervised Learning. *Eneuro* 6, ENEURO.425–ENEURO.418. doi: 10.1523/ENEURO.0425-18.2019

Neelagandan, N., Lamberti, I., Carvalho, H. J. F., Gobet, C., and Naef, F. (2020). "What Determines Eukaryotic Translation Elongation: Recent Molecular and Quantitative Analyses of Protein Synthesis.". *Open Biol.* 10:200292. doi: 10.1098/rsob.200292

Nesterchuk, M. V., Sergiev, P. V., and Dontsova, O. A. (2011). "Posttranslational Modifications of Ribosomal Proteins in *Escherichia Coli*.". *Acta Naturae* 3, 22–33. doi: 10.32607/20758251-2011-3-2-22-33

Nierhaus, K. H. (2014). "Mg2+, K+, and the Ribosome.". *J. Bacteriol.* 196, 3817–3819. doi: 10.1128/JB.02297-14

Oddo, S. (2012). "The Role of mTOR Signaling in Alzheimer Disease.". *Front. Biosci.* 4:941–952. doi: 10.2741/s310

Ostroff, L. E., Botsford, B., Gindina, S., Cowansage, K. K., LeDoux, J. E., Klann, E., et al. (2017). Accumulation of Polyribosomes in Dendritic Spine Heads, But Not Bases and Necks, during Memory Consolidation Depends on Cap-Dependent Translation Initiation. *J. Neurosci.* 37, 1862–1872. doi: 10.1523/JNEUROSCI.3301-16.2017

Ostroff, L. E., Fiala, J. C., Allwardt, B., and Harris, K. M. (2002). "Polyribosomes Redistribute from Dendritic Shafts into Spines with Enlarged Synapses during LTP in Developing Rat Hippocampal Slices.". *Neuron* 35, 535–545. doi: 10.1016/S0896-6273(02)00785-7

Ostroff, L. E., Watson, D. J., Cao, G., Parker, P. H., Smith, H., and Harris, K. M. (2018). "Shifting Patterns of Polyribosome Accumulation at Synapses over the Course of Hippocampal Long-Term Potentiation.". *Hippocampus* 28, 416–430. doi: 10.1002/hipo.22841

Pangršič, T., Gabrielaitis, M., Michanski, S., Schwaller, B., Wolf, F., Strenzke, N., et al. (2015). "EF-Hand Protein Ca $^{2+}$ Buffers Regulate Ca $^{2+}$ Influx and Exocytosis in Sensory Hair Cells.". *Proc. Natl. Acad. Sci.* 112, E1028–E1037. doi: 10.1073/pnas.1416424112

Polikanov, Y. S., Melnikov, S. V., Söll, D., and Steitz, T. A. (2015). "Structural Insights into the Role of RNA Modifications in Protein Synthesis and Ribosome Assembly.". *Nat. Struct. Mol. Biol.* 22, 342–344. doi: 10.1038/nsmb.2992

Pontes, M. H., Sevostyanova, A., and Groisman, E. A. (2015). "When Too Much ATP Is Bad for Protein Synthesis.". *J. Mol. Biol.* 427, 2586–2594. doi: 10.1016/j.jmb.2015.06.021

Poon, M. M., Choi, S., Jamieson, C. A. M., Geschwind, D. H., and Martin, K. C. (2006). Identification of Process-Localized mRNAs from Cultured Rodent Hippocampal Neurons. *J. Neurosci.* 26, 13390–13399. doi: 10.1523/JNEUROSCI.3432-06.2006

Prabhakar, A., Puglisi, E. V., and Puglisi, J. D. (2019). "Single-Molecule Fluorescence Applied to Translation.". *Cold Spring Harb. Perspect. Biol.* 11:a032714. doi: 10.1101/cshperspect.a032714

Quax, T. E. F., Claassens, N. J., Söll, D., and Oost, J. V. D. (2015). "Codon Bias as a Means to Fine-Tune Gene Expression.". *Mol. Cell* 59, 149–161. doi: 10.1016/j.molcel.2015.05.035

Ramakrishnan, V. (2002). "Ribosome Structure and the Mechanism of Translation.". *Cell* 108, 557–572. doi: 10.1016/S0092-8674(02)00619-0

Rangaraju, V., Dieck, S. T., and Schuman, E. M. (2017). "Local Translation in Neuronal Compartments: How Local Is Local?". *EMBO Rep.* 18, 693–711. doi: 10.15252/embr.201744045

Rangaraju, V., Lauterbach, M., and Schuman, E. M. (2019). Spatially Stable Mitochondrial Compartments Fuel Local Translation during Plasticity. *Cell* 176, 73.e–84.e. doi: 10.1016/j.cell.2018.12.013

Reid, D. W., and Nicchitta, C. V. (2015). "Diversity and Selectivity in mRNA Translation on the Endoplasmic Reticulum.". *Nat. Rev. Mol. Cell Biol.* 16, 221–231. doi: 10.1038/nrm3958

Richards, M. (2004). "The Transcriptome Profile of Human Embryonic Stem Cells as Defined by SAGE.". *Stem Cells* 22, 51–64. doi: 10.1634/stemcells.22-1-51

Rolls, M. M., Hall, D. H., Victor, M., Stelzer, E. H. K., Tom, A., and Rapoport. (2002). "Targeting of Rough Endoplasmic Reticulum Membrane Proteins and Ribosomes in Invertebrate Neurons.". *Mol. Biol. Cell* 13, 1778–1791. doi: 10.1091/mbc.01-10-0514

Romani, A. M. P. (2011). "Cellular Magnesium Homeostasis.". *Arch. Biochem. Biophys.* 512, 1–23. doi: 10.1016/j.abb.2011.05.010

Rozov, A., Khusainov, I., Omari, K. E., Duman, R., Mykhaylyk, V., Yusupov, M., et al. (2019). "Importance of Potassium Ions for Ribosome Structure and Function Revealed by Long-Wavelength X-Ray Diffraction.". *Nat. Commun.* 10:2519. doi: 10.1038/s41467-019-10409-4

Sanamrad, A., Persson, F., Lundius, E. G., Fange, D., Gynna, A. H., and Elf, J. (2014). "Single-Particle Tracking Reveals That Free Ribosomal Subunits Are Not Excluded from the *Escherichia Coli* Nucleoid.". *Proc. Natl. Acad. Sci.* 111, 11413–11418. doi: 10.1073/pnas.1411558111

Scarnati, M. S., Kataria, R., Biswas, M., and Paradiso, K. G. (2018). "Active Presynaptic Ribosomes in the Mammalian Brain, and Altered Transmitter Release after Protein Synthesis Inhibition.". *ELife* 7:e36697. doi: 10.7554/eLife.36697

Scavuzzo, C. J., LeBlancq, M. J., Nargang, F., Lemieux, H., Hamilton, T. J., and Dickson, C. T. (2019). "The Amnestic Agent Anisomycin Disrupts Intrinsic Membrane Properties of Hippocampal Neurons *via* a Loss of Cellular Energetics.". *J. Neurophysiol.* 122, 1123–1135. doi: 10.1152/jn.00370.2019

Schwanhäusser, B., Busse, D., Li, N., Dittmar, G., Schuchhardt, J., Wolf, J., et al. (2011). "Global Quantification of Mammalian Gene Expression Control.". *Nature* 473, 337–342. doi: 10.1038/nature10098

Seidenbecher, C. I., Langnaese, K., Sanmartı̀-Vila, L., Boeckers, T. M., Smalla, K., Sabel, B. A., et al. (1998). Caldendrin, a Novel Neuronal Calcium-Binding Protein Confined to the Somato-Dendritic Compartment. *J. Biol. Chem.* 273, 21324–21331. doi: 10.1074/jbc.273.33.21324

Sen Gupta, A., Joshi, G., Pawar, S., and Sengupta, K. (2018). "Nucleolin Modulates Compartmentalization and Dynamics of Histone 2B-ECFP in the Nucleolus.". *Nucleus* 9, 350–367. doi: 10.1080/19491034.2018.1471936

Sharma, A. V., Nargang, F. E., and Dickson, C. T. (2012). Neurosilence: Profound Suppression of Neural Activity Following Intracerebral Administration of the Protein Synthesis Inhibitor Anisomycin. *J. Neurosci.* 32, 2377–2387. doi: 10.1523/JNEUROSCI.3543-11.2012

Sharov, A. A., Piao, Y., Matoba, R., Dudekula, D. D., Qian, Y., VanBuren, C., et al. (2003). "Transcriptome Analysis of Mouse Stem Cells and Early Embryos.". *PLoS Biol.* 1:e74. doi: 10.1371/journal.pbio.0000074

Shcherbakova, D. M., Sengupta, P., Lippincott-Schwartz, J., and Verkhusha, V. V. (2014). "Photocontrollable Fluorescent Proteins for Superresolution Imaging.". *Annu. Rev. Biophys.* 43, 303–329. doi: 10.1146/annurev-biophys-051013-022836

Shen, Y., Wu, S., Rancic, C., Aggarwal, A., Qian, Y., Miyashita, S., et al. (2019). "Genetically Encoded Fluorescent Indicators for Imaging Intracellular Potassium Ion Concentration.". *Commun. Biol.* 2:18. doi: 10.1038/s42003-018-0269-2

Shi, Z., Fujii, K., Kovary, K. M., Genuth, N. R., Röst, H. L., Teruel, M. N., et al. (2017). Heterogeneous Ribosomes Preferentially Translate Distinct Subpools of mRNAs Genome-Wide. *Mol. Cell* 67, 71.e–83.e. doi: 10.1016/j.molcel.2017.05.021

Shigeoka, T., Koppers, M., Wong, H. H., Lin, J. Q., Cagnetta, R., Dwivedy, A., et al. (2019). On-Site Ribosome Remodeling by Locally Synthesized Ribosomal Proteins in Axons. *Cell Rep.* 29, 3605.e–3619.e. doi: 10.1016/j.celrep.2019.11.025

Shindo, Y., Yamanaka, R., Hotta, K., and Oka, K. (2020). "Inhibition of Mg^{2+} Extrusion Attenuates Glutamate Excitotoxicity in Cultured Rat Hippocampal Neurons.". *Nutrients* 12:2768. doi: 10.3390/nu12092768

Simsek, D., and Barna, M. (2017). "An Emerging Role for the Ribosome as a Nexus for Post-Translational Modifications.". *Curr. Opin. Cell Biol.* 45, 92–101. doi: 10.1016/j.ceb.2017.02.010

Simsek, D., Tiu, G. C., Flynn, R. A., Byeon, G. W., Leppek, K., Xu, A. F., et al. (2017). The Mammalian Ribo-Interactome Reveals Ribosome Functional Diversity and Heterogeneity. *Cell* 169, 1051.e–1065.e. doi: 10.1016/j.cell.2017.05.022

Slavov, N., Semrau, S., Airoldi, E., Budnik, B., and Oudenaarden, A. V. (2015). "Differential Stoichiometry among Core Ribosomal Proteins.". *Cell Rep.* 13, 865–873. doi: 10.1016/j.celrep.2015.09.056

Sloan, K. E., Warda, A. S., Sharma, S., Entian, K., Lafontaine, D., and Bohnsack, M. T. (2017). Tuning the Ribosome: The Influence of rRNA Modification on Eukaryotic Ribosome Biogenesis and Function. *RNA Biol.* 14, 1138–1152. doi: 10.1080/15476286.2016.1259781

Slomnicki, L. P., Pietrzak, M., Vashishta, A., Jones, J., Lynch, N., Elliot, S., et al. (2016). "Requirement of Neuronal Ribosome Synthesis for Growth and Maintenance of the Dendritic Tree.". *J. Biol. Chem.* 291, 5721–5739. doi: 10.1074/jbc.M115.682161

Somjen, G. G., and Müller, M. (2000). "Potassium-Induced Enhancement of Persistent Inward Current in Hippocampal Neurons in Isolation and in Tissue Slices.". *Brain Res.* 885, 102–110. doi: 10.1016/S0006-8993(00)02948-6

Sotelo-Silveira, J. R., Calliari, A., Kun, A., Koenig, E., and Sotelo, J. R. (2006). "RNA Trafficking in Axons: RNA in Axons.". *Traffic* 7, 508–515. doi: 10.1111/j.1600-0854.2006.00405.x

Spillane, M., Ketschek, A., Merianda, T. T., Twiss, J. L., and Gallo, G. (2013). "Mitochondria Coordinate Sites of Axon Branching through Localized Intra-Axonal Protein Synthesis.". *Cell Rep.* 5, 1564–1575. doi: 10.1016/j.celrep.2013.11.022

Stoykova, A. S., Dabeva, M. D., Dimova, R. N., and Hadjiolov, A. A. (1985). "Ribosome Biogenesis and Nucleolar Ultrastructure in Neuronal and Oligodendroglial Rat Brain Cells.". *J. Neurochem.* 45, 1667–1676. doi: 10.1111/j.1471-4159.1985.tb10521.x

Sun, C., Nold, A., Fusco, C. M., Rangaraju, V., Tchumatchenko, T., Heilemann, M., et al. (2021). "The Prevalence and Specificity of Local Protein Synthesis during Neuronal Synaptic Plasticity.". *Sci. Adv.* 7:eabj0790. doi: 10.1126/sciadv.abj0790

Sutton, M. A., Wall, N. R., Akalu, G. L., and Schuman, E. M. (2004). "Regulation of Dendritic Protein Synthesis by Miniature Synaptic Events.". *Science* 304, 1979–1983. doi: 10.1126/science.1096202

Tang, A., Chen, H., Li, T. P., Metzbower, S. R., MacGillavry, H. D., and Blanpied, T. A. (2016). "A trans-synaptic Nanocolumn Aligns Neurotransmitter Release to Receptors.". *Nature* 536, 210–214. doi: 10.1038/nature19058

Tauber, D., Tauber, G., and Parker, R. (2020). "Mechanisms and Regulation of RNA Condensation in RNP Granule Formation.". *Trends Biochem. Sci.* 45, 764–778. doi: 10.1016/j.tibs.2020.05.002

Tcherkezian, J., Brittis, P. A., Thomas, F., Roux, P. P., and Flanagan, J. G. (2010). "Transmembrane Receptor DCC Associates with Protein Synthesis Machinery and Regulates Translation.". *Cell* 141, 632–644. doi: 10.1016/j.cell.2010.04.008

Tennyson, V. M. (1970). "The Fine Structure of The Axon and Growth Cone of the Dorsal Root Neuroblast of the Rabbit Embryo.". *J. Cell Biol.* 44, 62–79. doi: 10.1083/jcb.44.1.62

Thelen, M. P., and Kye, M. J. (2020). "The Role of RNA Binding Proteins for Local mRNA Translation: Implications in Neurological Disorders.". *Front. Mol. Biosci.* 6:161. doi: 10.3389/fmolb.2019.00161

Thomson, E., Ferreira-Cerca, S., and Hurt, E. (2013). "Eukaryotic Ribosome Biogenesis at a Glance.". *J. Cell Sci.* 126, 4815–4821. doi: 10.1242/jcs.111948

Tiedge, H., and Brosius, J. (1996). Translational Machinery in Dendrites of Hippocampal Neurons in Culture. *J. Neurosci.* 16, 7171–7181. doi: 10.1523/JNEUROSCI.16-22-07171.1996

Tseng, H., Chou, W., Wang, J., Zhang, X., Zhang, S., and Schultz, R. M. (2008). "Mouse Ribosomal RNA Genes Contain Multiple Differentially Regulated Variants.". *PLoS One* 3:e1843. doi: 10.1371/journal.pone.0001843

Venkatesan, S., Subramaniam, S., Rajeev, P., Chopra, Y., Jose, M., and Nair, D. (2020). Differential Scaling of Synaptic Molecules within Functional Zones of an Excitatory Synapse during Homeostatic Plasticity. *Eneuro* 7, ENEURO.407–ENEURO.419. doi: 10.1523/ENEURO.0407-19.2020

Volkov, I. L., and Johansson, M. (2019). "Single-Molecule Tracking Approaches to Protein Synthesis Kinetics in Living Cells.". *Biochemistry* 58, 7–14. doi: 10.1021/acs.biochem.8b00917

Waudby, C. A., Dobson, C. M., and Christodoulou, J. (2019). "Nature and Regulation of Protein Folding on the Ribosome.". *Trends Biochem. Sci.* 44, 914–926. doi: 10.1016/j.tibs.2019.06.008

Weiss, R. L., Kimes, B. W., and Morris, D. R. (1973). Cations and Ribosome Structure. 111. Effects on the 30s and 50s Subunits of Replacing Bound Mg^{2+}; by Inorganic Cations. *Biochemistry* 12, 450–456. doi: 10.1021/bi00727a014

Willis, D. (2005). Differential Transport and Local Translation of Cytoskeletal, Injury-Response, and Neurodegeneration Protein mRNAs in Axons. *J. Neurosci.* 25, 778–791. doi: 10.1523/JNEUROSCI.4235-04.2005

Wilson, D. N., and Cate, J. H. D. (2012). "The Structure and Function of the Eukaryotic Ribosome.". *Cold Spring Harb. Perspect. Biol.* 4, a011536–a011536. doi: 10.1101/cshperspect.a011536

Wu, B., Buxbaum, A. R., Katz, Z. B., Yoon, Y. J., and Singer, R. H. (2015). "Quantifying Protein-mRNA Interactions in Single Live Cells.". *Cell* 162, 211–220. doi: 10.1016/j.cell.2015.05.054

Yoon, B. C., Jung, H., Dwivedy, A., O'Hare, C. M., Zivraj, K. H., and Holt, C. E. (2012). "Local Translation of Extranuclear Lamin B Promotes Axon Maintenance.". *Cell* 148, 752–764. doi: 10.1016/j.cell.2011.11.064

Yoon, Y. J., Wu, B., Buxbaum, A. R., Das, S., Tsai, A., English, B. P., et al. (2016). "Glutamate-Induced RNA Localization and Translation in Neurons.". *Proc. Natl. Acad. Sci.* 113, E6877–E6886. doi: 10.1073/pnas.1614267113

Zhang, G., Neubert, T. A., and Jordan, B. A. (2012). RNA Binding Proteins Accumulate at the Postsynaptic Density with Synaptic Activity. *J. Neurosci.* 32, 599–609. doi: 10.1523/JNEUROSCI.2463-11.2012

Conflict of Interest: The authors declare that the research was conducted in the absence of any commercial or financial relationships that could be construed as a potential conflict of interest.

frontiers in Molecular Neuroscience

REVIEW
published: 24 February 2022
doi: 10.3389/fnmol.2022.831825

Hyperacute Excitotoxic Mechanisms and Synaptic Dysfunction Involved in Traumatic Brain Injury

Brendan Hoffe and Matthew R. Holahan**

Department of Neuroscience, Carleton University, Ottawa, ON, Canada

The biological response of brain tissue to biomechanical strain are of fundamental importance in understanding sequela of a brain injury. The time after impact can be broken into four main phases: hyperacute, acute, subacute and chronic. It is crucial to understand the hyperacute neural outcomes from the biomechanical responses that produce traumatic brain injury (TBI) as these often result in the brain becoming sensitized and vulnerable to subsequent TBIs. While the precise physical mechanisms responsible for TBI are still a matter of debate, strain-induced shearing and stretching of neural elements are considered a primary factor in pathology; however, the injury-strain thresholds as well as the earliest onset of identifiable pathologies remain unclear. Dendritic spines are sites along the dendrite where the communication between neurons occurs. These spines are dynamic in their morphology, constantly changing between stubby, thin, filopodia and mushroom depending on the environment and signaling that takes place. Dendritic spines have been shown to react to the excitotoxic conditions that take place after an impact has occurred, with a shift to the excitatory, mushroom phenotype. Glutamate released into the synaptic cleft binds to NMDA and AMPA receptors leading to increased Ca^{2+} entry resulting in an excitotoxic cascade. If not properly cleared, elevated levels of glutamate within the synaptic cleft will have detrimental consequences on cellular signaling and survival of the pre- and post-synaptic elements. This review will focus on the synaptic changes during the hyperacute phase that occur after a TBI. With repetitive head trauma being linked to devastating medium – and long-term maladaptive neurobehavioral outcomes, including chronic traumatic encephalopathy (CTE), understanding the hyperacute cellular mechanisms can help understand the course of the pathology and the development of effective therapeutics.

Keywords: traumatic brain injury, synaptic dysfunction, excitotoxicity, dendritic spine, neurodegeneration

OPEN ACCESS

Edited by:
James P. Clement, Jawaharlal Nehru Centre for Advanced Scientific Research, India

Reviewed by:
Vijayalakshmi Santhakumar, University of California, Riverside, United States
Poonam Thakur, Indian Institute of Science Education and Research, Thiruvananthapuram, India

****Correspondence:***
Brendan Hoffe
brendanhoffe@carleton.ca
Matthew R. Holahan
MatthewHolahan@Cunet.Carleton.ca

Specialty section:
This article was submitted to Molecular Signaling and Pathways, a section of the journal Frontiers in Molecular Neuroscience

Received: *08 December 2021*
Accepted: *07 February 2022*
Published: *24 February 2022*

Citation:
Hoffe B and Holahan MR (2022) Hyperacute Excitotoxic Mechanisms and Synaptic Dysfunction Involved in Traumatic Brain Injury. Front. Mol. Neurosci. 15:831825. doi: 10.3389/fnmol.2022.831825

INTRODUCTION

The synapse is regarded as the fundamental site of communication between cells of the nervous system and synaptic dysfunction may represent a choke point for the multitude of upstream factors and downstream responses that lead to neuron atrophy or death. Synaptic malleability is a key component to behavior and cognition, with the formation, reshaping and strengthening of synapses being a key feature underlying learning and memory (Bourne and Harris, 2007;

González-Tapia et al., 2016; Noye Tuplin and Holahan, 2019). Prolonged pathological changes at the synaptic level have been shown to play a role in several psychiatric and neurodegenerative diseases, such as Alzheimer's disease, Huntington's disease, Fragile X syndrome and schizophrenia (Calabrese et al., 2006; Herms and Dorostkar, 2016).

Over the past 15 years there has been an increase in attention to the relationship between traumatic brain injury (TBI), Alzheimer's disease and chronic traumatic encephalopathy (Omalu et al., 2005; McKee et al., 2013; Goldstein et al., 2014; Albayram et al., 2020). Given that TBI can be regarded as a singular event (Wojnarowicz et al., 2017), the cellular processes that take place at the synapse dictate how the cell responds to the change in environment. These cellular processes can be categorized into four main time phases: hyperacute, acute, subacute, and chronic (Guerriero et al., 2015; MacFarlane and Glenn, 2015). While much research exists on the changes occurring days to months after TBI, there is comparatively little research investigating the hyperacute synaptic changes occurring within minutes to hours. These short-term changes could reveal the pathological mechanisms that are responsible for the later stages of neurodegeneration which may help shed light on potential therapeutic routes for neurodegenerative diseases associated with head trauma. This review will focus on and highlight the synaptic dysfunction during the hyperacute phase post-TBI, combining crucial findings from both *in vitro* and *in vivo* data to better understand what occurs at the synapse within minutes to hours after an impact has occurred.

TIME PHASE FOLLOWING IMPACT

The timeline of cellular responses that occur after brain impact spans four phases: hyperacute (minutes to hours), acute (hours to several days), subacute (several days to weeks) and chronic (months and beyond; Guerriero et al., 2015; MacFarlane and Glenn, 2015). During the hyperacute phase, affected neurons undergo substantial and abnormal electrical and cellular activity leading to maladaptive remodeling, potentially as an attempt to regain homeostasis following impact. While the affected cells work to re-establish internal homeostasis during each phase, if damage were to remain unresolved (ex. further damage, or severity of initial damage) the pathology continues and moves into the next phase. As each phase progresses to the next, the damage severity increases. This can ultimately lead to the major neurodegeneration observed in pathologies associated with head trauma (**Figure 1**).

Hyperacute Changes to the Pre-synaptic Terminal

The promotion of excitotoxic conditions requires prolonged release and presence of glutamate within the synaptic cleft, leading to overactivation of *N*-Methyl-d-aspartate receptors (NMDAr) and of α-amino-3-hydroxy-5-methyl-4-isoxazolepropionic acid receptors (AMPAr) on the post-synaptic membrane. *In vitro* neuronal stretch models have demonstrated an increase in membrane permeability within minutes after stretch through dysregulated ionic channels or the membrane physically rupturing (Smith et al., 1999; Weber, 2012; Siedler et al., 2014). Wolf et al. (2001) found that within minutes following stretch strain, an increase in intracellular Ca^{2+} was observed with levels that continued to rise during the time course of the experiment (1-20 min). This increase was dependent on the influx of Na^{+} as blockade of the voltage gated Na^{+} channels with tetrodotoxin inhibited this rise in intracellular Ca^{2+} (Wolf et al., 2001).

Increased intracellular Ca^{2+} in the pre-synaptic neuron prime the readily releasable pool of synaptic vesicles and the SNARE complex that mediates the fusion of vesicles to the membrane wall via various docking proteins (Hackett and Ueda, 2015; Kaeser and Regehr, 2017; Chen et al., 2021). Carlson et al. (2016) found that 6 h after cortical impact to rodents, there was a noticeable increase in SNAP-25 complex, as well as syntaxin, that steadily decreased over a 2-week period. This is of importance as SNAP-25 and syntaxin are two of the three main SNARE proteins responsible for vesicle-membrane fusion at the pre-synaptic terminal (Kaeser and Regehr, 2017; Chen et al., 2021). Ahmed et al. (2012) found that within 30 min following stretch damage to *Drosophila* motor neurons, there were elevated levels of Synaptotagmin, a Ca^{2+} sensitive vesicle trafficking protein that interacts with SNAP-25, within the pre-synaptic terminal. These synaptic changes, along with changes to the post-synaptic neuron, are summarized in **Figure 2**.

Hyperacute Inflammatory Response

Neuroinflammation plays a significant role in modulating the damage after brain injuries, with the activation of numerous proinflammatory cytokines such as interleukin-1, 6, tumor necrosis factor-α (TNF- α), and interferon-γ reported within the hyperacute phase following injury (Patterson and Holahan, 2012; Smith et al., 2012; Xiong et al., 2018). Recently, attention toward molecular recognition of damage has been gaining interest as possible mechanisms for signaling the immune response after injury. Toll-like receptors (TLR) are a class of pattern recognition receptors that activate and mediate the production of cytokines involved in proinflammatory response (Vaure and Liu, 2014). TLR-4, specifically, has been shown to influence neuronal excitability through cytokine-enhanced NMDAr currents in hippocampal cultures (Balosso et al., 2014). In the context of TBI, however, TLR-4 enhances neuronal excitability through upregulation of Ca^{2+}-permeable GluR1, and not NMDAr, hours after impact (Li et al., 2015; Korgaonkar et al., 2020). Using the fluid percussion injury (FPI) model in juvenile rats, Li et al. (2015) demonstrated elevated neuronal expression of TLR-4 within the hippocampus 4 h after impact, with a peak at 24 h, then returning to similar levels as 4 h at 3 days post-impact. This early increase in TLR-4 expression was accompanied with enhanced non-NMDA excitatory postsynaptic currents in granule cell and mossy cells at 3 days. The contribution of TLR-4 to increased neuronal excitability is through the downstream effector of nuclear factor kappa B (NF-κB; Vaure and Liu, 2014). In neurons, increased synaptic expression of NF-κB has been shown to promote excitatory synapses and spinogenesis through NMDAr regulated Ca^{2+} influx (Boersma et al., 2011). In glial

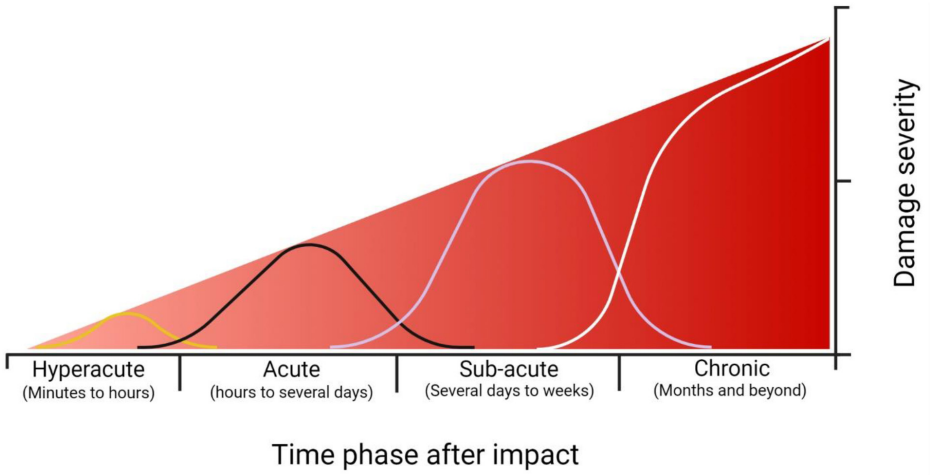

FIGURE 1 | Timescale representation of the severity of damage following impact. Each time phase has the capacity to re-establish homeostasis through cellular repair or some form of treatment. If the cellular homeostasis is unresolved, however, the damage severity increases as time progresses. At the hyperacute time phase (minutes to hours) the damage severity is low, consisting of focal changes at the synaptic level such as hyperexcitability, increased membrane permeability (either through membrane disruption or receptor activity), and onset of excitotoxic conditions. During the acute phase (hours to several days), damage consists of further receptor alterations, activation of proteases and apoptotic pathways, mitochondrial dysfunction, and prolonged excitotoxic conditions. During the subacute phase (several days to weeks), regional deficits within the brain are observed due to cellular dysfunction, prolonged neuroinflammation, and onset of phosphorylated tau accumulation. During the chronic phase (months and beyond), major *behavioral* deficits and neuropsychiatric conditions are observed, including, but not limited to, impaired learning and memory, depression, and prolonged headaches. The neuropathology of chronic traumatic encephalopathy is also observed during this time (Guerriero et al., 2015; MacFarlane and Glenn, 2015). Created with BioRender.com.

cells, TLR-4-activated NF-κB has downstream effects on the upregulation on proinflammatory factors such as interferon-beta (IFN-β) and TNF-α (Vaure and Liu, 2014). Overproduction of these factors in microglia have been shown to promote excitotoxic conditions by downregulating excitatory amino acid transporter-2, thus reducing glutamate reuptake from astrocytes (Sitcheran et al., 2005). Another mechanism includes the TNF-α induced increase in AMPAr lacking GluR2, increasing the Ca^{2+} permeability (Stellwagen et al., 2005; for review see Olmos and Lladó, 2014).

Maladaptive Role of Inhibition During Hyperacute Phase

While not directly in the scope of this review paper, the role of γ-aminobutyric acid (GABA) in the promotion of excitotoxic conditions is important. Immediately following FPI (i.e., within minutes of impact to tissue fixation), Toth et al. (1997) demonstrated that large basket-like cells within the granular layer of the rat hippocampus were damaged, as evident from positive Gallyas silver staining. The neighboring granule cells, however, showed no signs of damage indicating that, due to their size, these GABAergic interneurons were at more risk of damage compared to the tightly packed granule cells. Further, the authors note that the damage to GABAergic interneurons immediately after impact can further promote the state of hyperexcitability as there is limited inhibitory signals within this region of the hippocampus (Toth et al., 1997). More recently, studies have shown further downregulation of GABAergic subunits within the rat hippocampus, particularly α1, α2, γ2, and δ, 6 h following FPI (Raible et al., 2012; Drexel et al., 2015). Interestingly, both groups found upregulation of α4 subunits, with Raible et al. (2012) showing increase in the ipsilateral side, but not contralateral, and Drexel et al. (2015) showing increase in both ipsilateral and contralateral to region of impact. Considering how the α1, α2 and γ2 GABA subunits regulated phasic inhibition, and the α4 subunit regulates tonic inhibition, the increase in α4 subunit expression could be an indication of a compensatory mechanism to counteract the hyperexcited state occurring after impact (Drexel et al., 2015).

Electrophysiological Changes Following Impact

Excitotoxic conditions arise from the prolonged release of glutamate into the synaptic cleft with subsequent binding to and activation of post-synaptic receptors. Having established an increase in membrane permeability, which leads to influx of Na^{+} and $Ca^{2+,}$ as well as the efflux of K^{+} (MacFarlane and Glenn, 2015), one would assume that the dysregulation of ions across the membrane could be enough to trigger aberrant depolarizations and produce a hyperactive state shortly after trauma. However, much like the dynamics of the pre-synaptic terminal, there remains limited research into the hyperacute phase of TBI (Cohen et al., 2007). This could be in part due to the complexity of techniques from one study to another, or experimental limitations associated with electrophysiological recordings from slice preparations in such a protracted timeframe. Nonetheless, there have been a handful of studies looking at the electrophysiological properties that occur within the hyperacute phase following TBI.

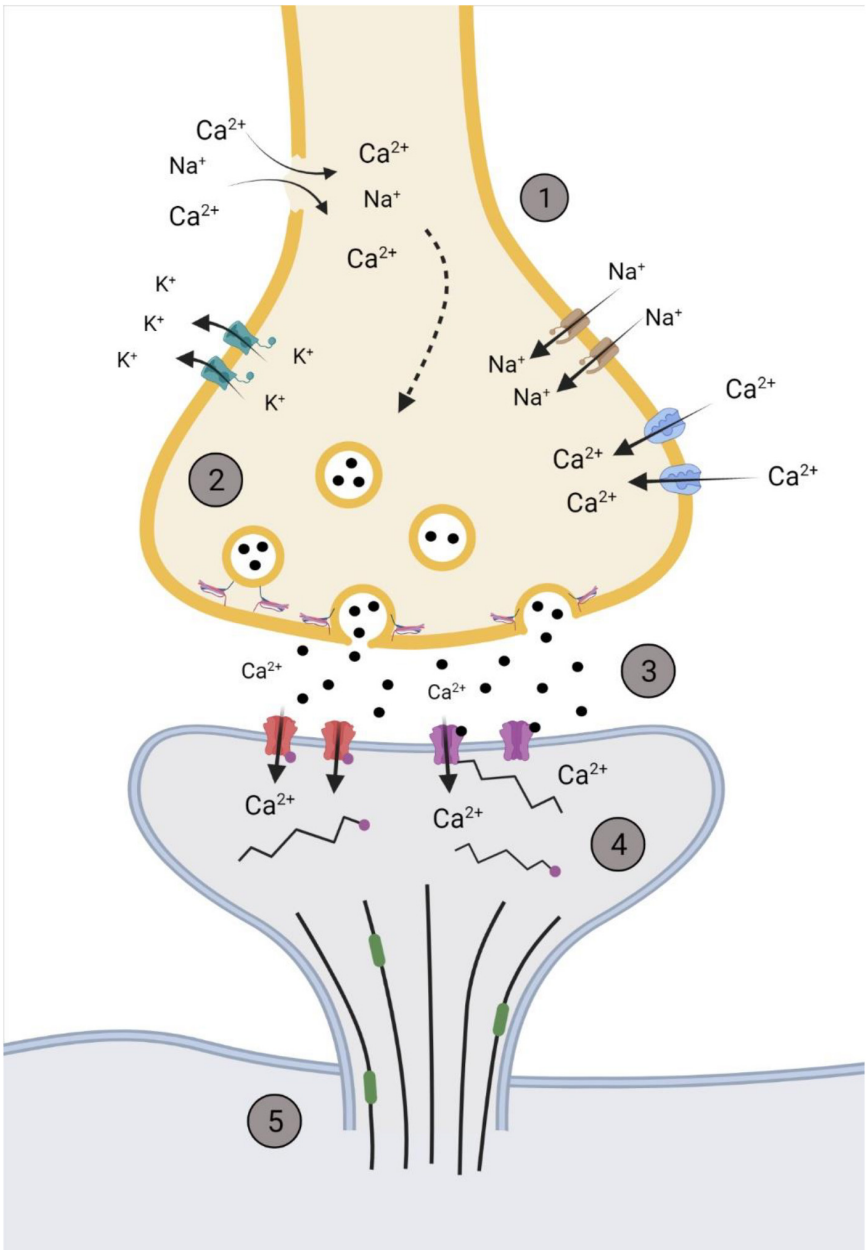

FIGURE 2 | Representation of the synapse within the hyperacute phase after impact. (1) Membrane permeability increases soon after impact through the influx/efflux of ions via voltage gated channels or rupturing of the pre-synaptic membrane. (2) The increase in Ca^{2+} primes glutamate filled vesicles and increases the rate of fusion and release of glutamate. (3) Increased and sustained release of glutamate (black dots) into the synaptic cleft activates NMDAr NR2B subunits (purple) and increases post-synaptic concentrations of Ca^{2+}. This activates various kinases that phosphorylates AMPA GluR1 subunits (red), further promoting the influx of Ca^{2+}. (4) Post-synaptic cytoskeleton alterations occur through phosphorylation (pink dots), with disinhibition of *remodeling* proteins, such as end-binding protein 3 (green), occurring to allow for the restructuring of the dendritic spine cytoskeleton. (5) Downstream cascades from the influx of Ca^{2+}alter microtubule dynamics within the cytoskeleton of the neuron. Created with BioRender.com.

Using microelectrode arrays to measure neural population activity following cortical compression, Ding et al. (2011) found a time-dependent shift in electrical activity after compression. Within minutes of injury, there was a depression in cortical activity, with a gradual rise in excitability within an hour post injury, eventually resulting in cortical hyperexcitability by the 2-h mark. Similarly, using an *in vitro* stretch model, it was shown that within 30 min there was a reduced occurrence of spontaneous action potentials in neurons that were damaged (Magou et al., 2015). Interestingly, the authors found that in the adjacent neurons that did not experience stretch damage, there was an increase in action potentials generated within that

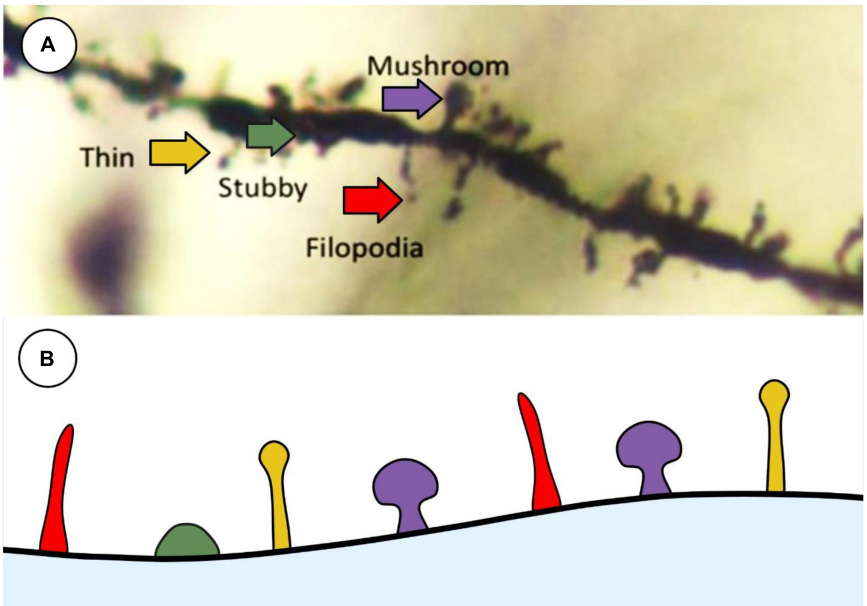

FIGURE 3 | Representative image of main spine types that are commonly used in histological analysis described by Peters and Kaiserman-Abramof (1970). **(A)** Golgi-stained neuron showcasing the 4 main types of spines: thin (yellow), stubby (green), filopodia (red), and mushroom (purple). **(B)** Schematic representation of the types of spines to illustrate differences between shapes. Created with BioRender.com.

timeframe. This could potentially indicate that due to imbalance of ionic homeostasis immediately after trauma, the depression of electrical activity could act as a primer for the hyperexcitability experienced shortly after (Berger et al., 2008; Ding et al., 2011). This enhanced activity in adjacent neurons could propagate hyperexcitatory conditions, potentially initiating the secondary, maladaptive intracellular pathways associated with TBI.

The release of ions following injury has also been shown to be enhanced within 24 h after injury and alter electrophysiological properties. In a rather paradoxical way, D'Ambrosio et al. (1998) demonstrated a loss of long term potentiation (LTP), but not long term depression (LTD), in hippocampal slice recordings, 24 h after FPI in rats. They found that rats who received FPI had higher thresholds required to evoke population spikes within the CA1. However, previous work from Katayama et al. (1990) demonstrated, *in vivo*, a massive increase in extracellular K^+ following FPI resulting in neuronal hyperexcitability. D'Ambrosio et al. (1998) attribute their opposite finding to differences in the microenvironments between *in vivo* and *in vitro* settings. They note that the elevated efflux of K^+ abolishes LTP as the sudden overactivation of NMDAr and firing of the post-synaptic neuron leaves the neuron unable to undergo further potentiation after injury; something not reproducible in an *in vitro* setting (D'Ambrosio et al., 1998). Interestingly, a year later D'Ambrosio et al. (1999) demonstrated altered neuronal activity due to excessive accumulation of extracellular K^+ 24 h after FPI in hippocampal slices. This accumulation led to a hyperexcited state in CA3 neurons, as evident by the higher percentage of burst discharges in the post-FPI slices. The authors also note a significant loss of inward rectifying K^+ currents from recruited glia cells. These findings indicate a disruption to mechanisms responsible for maintaining extracellular homeostasis, such as the decreased K^+ clearance from glia cells plus the prolonged release of K^+ from hyperactive neurons (D'Ambrosio et al., 1999).

A report by Ross and Soltesz (2000) examined the electrophysiological properties of interneurons in the dentate gyrus after lateral FPI. Within the dentate gyrus, there was an observed increase of spontaneous interneuron firing rates due to Na^+/K^+-ATPase-related depolarizations. This increase in interneuron firing rates after impact led to increased frequency and amplitude of spontaneous inhibitory postsynaptic potentials in dentate gyrus granule cells. It is important to note that this increase in spontaneous inhibitory postsynaptic potentials occurs simultaneously to a decrease in miniature inhibitory postsynaptic current frequency. The authors describe this post-FPI increase in interneuron depolarization and increased GABAergic transmission could increase the efficacy of incoming excitatory signals to further promote interneuron firing after impact. This rather paradoxical mechanism has been reported in previous models of hyperexcitability, such as kindling seizures, chronic stress-induced seizures, and febrile seizures (Nusser et al., 1998; Chen et al., 1999; MacKenzie and Maguire, 2015).

Hyperacute Changes to the Post-synaptic Terminal

Using animal models of TBI, it has been shown that extracellular glutamate levels rise drastically within minutes after impact and remained elevated for hours (Faden et al., 1989; Folkersma et al., 2011; Xiong et al., 2019). Along the post-synaptic membrane, AMPAr and NMDAr become over-activated from the increased

presence of glutamate within the synaptic cleft. The GluR1 subunit of AMPAr plays a crucial role in LTP and membrane conductance under normal conditions; however, they have been implicated in progressing neurodegenerative diseases under pathological conditions (Spaethling et al., 2012). Unlike the GluR2 subunit, which limits membrane permeability of Ca^{2+}, phosphorylated GluR1, via Ca^{2+}/calmodulin-dependent protein kinase II (CaMKII) and PKC, increases membrane permeability to Ca^{2+} and promotes the upregulation of GluR1 insertion into the membrane and the influx of Ca^{2+} (Isaac et al., 2007). In the context of TBI, *in vitro* stretch models reveal an increase in GluR1 phosphorylation within hours of injury and increased levels of intracellular Ca^{2+} (Spaethling et al., 2008, 2012). Phosphorylation of GluR1 is mediated through NMDAr activity, specifically the NR2B subunit activity, as blocking the NR2B subunit blocked the rise in Ca^{2+} levels and reduced levels of phosphorylated GluR1 in stretched neurons (Spaethling et al., 2012). This has been observed in animal models of TBI, with increased CaMKII autophosphorylation and GluR1 observed within the hippocampus as early as 15 min after using weighted drop controlled cortical impact (CCI; Schumann et al., 2008) and 1 h post FPI (Atkins et al., 2006).

Calcium influx via the activation of NMDAr is crucial for synaptic plasticity and activating various biochemical pathways responsible for neuronal physiology. However, sustained activation of NMDAr promotes pathological secondary cascades which underlie the onset of neurodegenerative diseases (Kalia et al., 2008; Shohami and Biegon, 2014). Within the hyperacute phase of TBI, phosphorylated NR2B levels begin to rise and promote the upregulation of other NMDAr subunits, such as NR1 and NR2A (Schumann et al., 2008). The NR2B subunit is responsible for high influxes on Ca^{2+} into the neuron, with dysregulation of this subunit leading to excitotoxic conditions (Arnsten et al., 2021). In cultured neurons, the loss of functional connectivity is primarily mediated through activation of NR2B subunit (Patel et al., 2014). The NR2B subunit appears to be the focal subunit of potential neurotoxic effects, as administration of inhibiting kinases involved in regulating the receptor reduced the elevated levels of phosphorylated NR2B and improved long term neurological function after trauma (Schumann et al., 2008; Zhou and Sheng, 2013; Patel et al., 2014).

DENDRITIC SPINE CLASSIFICATION

Dendritic spines are the primary site for excitatory synaptic communication between two neurons and their morphology can greatly dictate neural function. Dendritic spines are dynamic in their morphology, constantly shifting between phenotypes depending on the surrounding environment or internal cellular conditions (Hering and Sheng, 2001). The constant remodeling and development of spines is termed spinogenesis with these changes taking place in the time frame of seconds to minutes to days to weeks (Calabrese et al., 2006). The remodeling and retracting of spines is a highly conserved trait across species, with evidence to show spinogenesis rates changing during learning and memory (Tønnesen and Nägerl, 2016; Luengo-Sanchez et al., 2018), disease progression (Calabrese et al., 2006; Aguayo et al., 2018; Jamjoom et al., 2021) and naturally with age (Benavides-Piccione et al., 2013).

In their 1970 paper, Peters and Kaiserman-Abramof (1970) described the three main categories of spine type: thin, stubby and mushroom. Thin spines represent a transitory phenotype that are primed to develop into mushroom-type spines through repeated synaptic activity (Pchitskaya and Bezprozvanny, 2020). Stubby spines represent immature spines and are less likely to be a place of synaptic communication between neurons (Helm et al., 2021). Mushroom spines are considered to represent an excitatory synapse and are associated with synaptic plasticity achieved through LTP (Jaworski et al., 2009; Helm et al., 2021). Using modern neuronal reconstruction, Luengo-Sanchez et al. (2018) characterized the spine morphology in human cortical pyramidal neurons using three dimensional meshes on individual spines and quantitative features such as, but not limited to, height, growth direction of the spine, and volume. This group was able to categorize dendritic spines into six distinct clusters based on the Bayesian information criterion, which contained sub-sets of spine shapes based on the authors described criterion. Bokota et al. (2016) produced 10 distinct spine clusters using automatic three-dimensional dendritic spine reconstruction, with each cluster containing a range of spine morphology subsets. While modern imaging techniques show that spine classification exists on a continuum at any one time (Rodriguez et al., 2008; Bokota et al., 2016; Luengo-Sanchez et al., 2018), the categories set forth by Peters and Kaiserman-Abramof (1970) are still widely used to classify spines when performing histological analyses (**Figure 3**).

Dendritic Spine Physiology

The cytoskeletal filaments within the spine head are made up of an intricate network of actin filaments that form the basis for morphological spine remodeling. These filaments, along with the molecular machinery involved in the dynamics of the spine cytoskeleton, act independently from the machinery in neighboring spines (Newpher and Ehlers, 2009). The ultrastructural changes within a single dendritic spine involve the recruitment of several protein kinase families that regulate actin filament dynamics within the spine head (Meng et al., 2003; Jaworski et al., 2009; Aguayo et al., 2018; Reza-Zaldivar et al., 2020). Lim-kinase (LIMK), for example, is a major family of protein kinases that regulate the shape of dendritic spines and their function and plays a major role in LTP (Meng et al., 2003). Through the influx of $Ca2^{2+}$ via NMDAr, CaMKI, and CaMKII stimulate the activity of Rac1. The stimulation of Rac1 has downstream effects of promoting LIMK-1 activity which ultimately leads to actin polymerization and the maintenance of spine morphology [for full review see Saneyoshi et al. (2010)]. The rate in which LIMK-1 is activated and suppressed is achieved by brain derived neurotrophic factor (BDNF) and microRNA-134 (miRNA-134), respectfully, however the exact mechanisms in which this operates is not well understood (Schratt et al., 2006; Saneyoshi et al., 2010; Reza-Zaldivar et al., 2020).

In addition to the regulation of dendritic spine actin, the activity along the synaptic membrane and the scaffolding

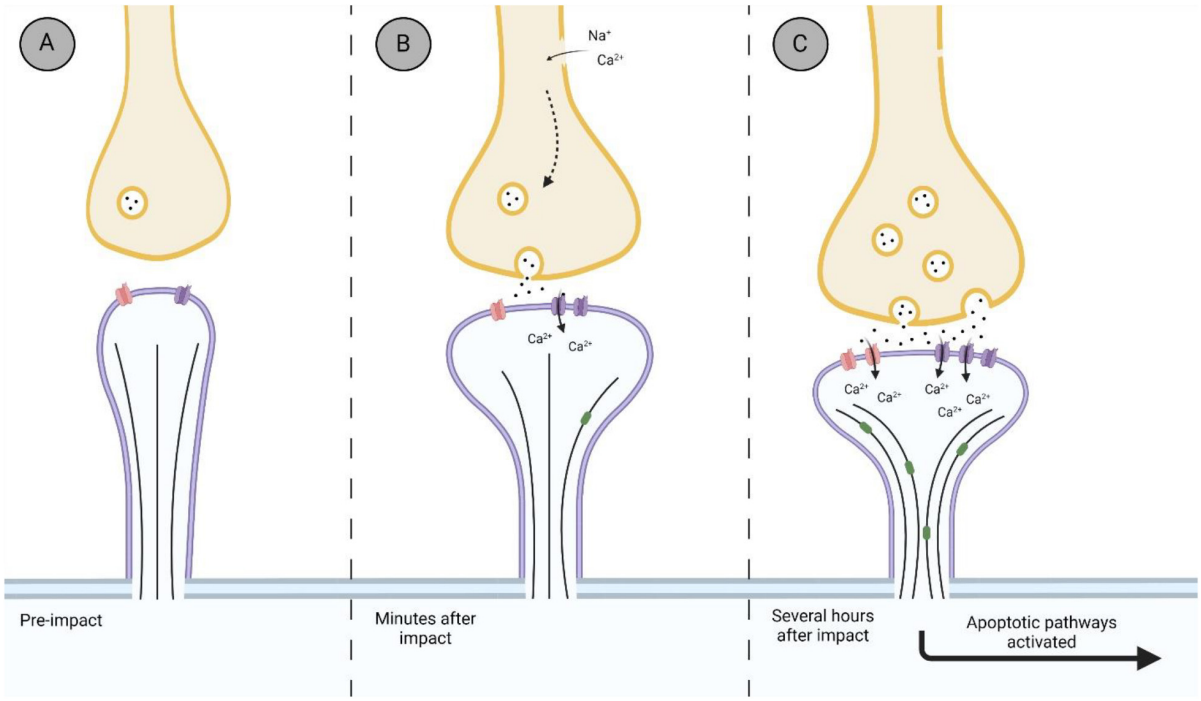

FIGURE 4 | Representation of the biological timeline of the synapse after impact. **(A)** Thin synapse before an impact. Thin spines are considered a transitory spine phenotype, with the potential to transition in an excitatory synapse. **(B)** Within minutes after impact, synaptic changes within the hyperacute phase after impact. Membrane ruptures and ionic imbalances promote the hyperexcitability of the synapse, with an influx of Ca^{2+} into the post-synaptic terminal via NMDAr (purple). **(C)** Further damage to the synapse due to hyperexcitability and sustained release of glutamate from the pre-synaptic terminal is observed several hours after impact. Increased influx of Ca^{2+} into the post-synaptic terminal promotes the further upregulation of NMDAr, as well as upregulating GluR1 subunit of AMPAr (red). Disinhibition of synaptic reconstruction proteins, such as EB3 (green), occurs as restricting proteins become inactivated, promoting excitatory mushroom spine phenotype. Hyperexcitability promotes neurodegenerative pathways via overworked mitochondria and damage to the microtubule cytoskeleton of the neuron. Created with BioRender.com.

proteins that make up the post-synaptic density (PSD) regulate cytoskeletal dynamics of the spine. The PSD is roughly 50 nm wide and is enriched in a wide variety of proteins responsible for synaptic integrity and regulating what enters the neuron (Harris and Kater, 1994). One of the most important synaptic proteins responsible for synaptic stability is PSD-95. PSD-95 is a scaffolding protein responsible for the regulation of AMPAr and NMDAr, as well as neuroligins and neurexins responsible for anchoring the pre-synaptic and post-synaptic terminals together (Keith and El-Husseini, 2008; Jeong et al., 2019). Knockdown models of PSD-95 have shown decreased spine numbers, altered formation of functional synapses and decreased rates of spinogenesis (Jeong et al., 2019). The overexpression of PSD-95 promotes development of excitatory synapses along the dendrite (Levinsoni et al., 2005).

Dendritic Spine Receptors

The basis for synaptic plasticity and LTP involves the movement of ions across the membrane through AMPAr channels and NMDAr channels. NMDAr have been largely implicated in the consequences of excitotoxicity, however there is mounting evidence to suggest the upregulation of the AMPA GluR1 subunit contributes to excitotoxic conditions (for review see Guerriero et al., 2015). AMPAr are the primary fast excitatory receptor within the nervous system, consisting of 4 subunits, GluR1 to GluR4, which form tetrameric complexes that have distinct receptor binding subtypes. Most AMPAr contain the Ca^{2+}-impermeable GluR2 subunit, however a subset of AMPAr contain the Ca^{2+}-permeable GluR1 subunit (Song and Huganir, 2002). Once glutamate is bound, the pore of the receptor opens allowing for cations (Na^{+} and Ca^{2+}) to move across the membrane resulting in depolarization (Chater and Goda, 2014). NMDAr consist of three main subfamilies, GluN1, N2, N3, with multiple subunits within each family. A combination of subfamilies makes up the NMDAr channel, with GluN1 and N2 subunits pairing together, or GluN2 and N3 together. Acting as a coincidence detector, the opening of NMDAr channels requires the depolarization of the neuron as well as the binding of glutamate followed by the removal of the Mg^{2+} ion within the membrane-spanning domain of the channel (Paoletti et al., 2013). Once Mg^{2+} is removed, the NMDAr becomes permeable to Na^{+} and Ca^{2+}. NMDAr activation and Ca^{2+} play a crucial role in the LIMK pathway through activating CaMKII and remodeling the actin cytoskeleton of the dendritic spine (Newpher and Ehlers, 2009; Saneyoshi et al., 2010). The influx of Ca^{2+} into the neuron is required for normal cellular functioning through the activation of various enzymes, protein complexes, and immediate early genes (Paoletti et al., 2013). Too large of an influx of Ca^{2+},

however, has been established as a main factor in the onset of excitotoxic conditions that put the neuron at risk of cell death, and ultimately the onset of various neurodegenerative diseases.

Cytoskeleton Changes Within the Dendritic Spine After Impact

Within the post-synaptic membrane, the synaptic architecture is stabilized primarily through PSD-95 which is regulated through the activity of NR2B subunits (Szydlowska and Tymianski, 2010; Frank et al., 2016; Jeong et al., 2019). PSD-95 has also been shown to restrict the remodeling of dendrites by mediating the activity of end-binding protein 3 (EB3); a protein responsible for growth and microtubule dynamics (Patel et al., 2019). EB3 is a well conserved member of the EB family responsible for restructuring dendritic spine cytoskeleton, maintenance of excitatory synapses, shuttling organelles into dendritic spines, and has shown to be involved in LTP (Jaworski et al., 2009; Penzes et al., 2009). The activity of PSD-95 is regulated by phosphorylation on cyclin-dependent kinase 5 (cdk5; Keith and El-Husseini, 2008). Park et al. (2013) demonstrated an increase in phosphorylated PSD-93, a similar scaffolding protein to PSD-95, several hours following FPI in the rodent cortex. These proteins are considered deactivated once phosphorylated (Nowacka et al., 2020). This could suggest that following TBI, the disruption of PSD-95/93 allows for the remodeling of the dendrite and spine through proteins such as EB3 (**Figure 4**), as their activity is no longer inhibited (Patel et al., 2019). Very few studies have investigated the remodeling of dendritic spine morphology post-TBI within the hyperacute phase. Pijet et al. (2019) found that 24 h after CCI, dendritic spines in the ipsilateral cortex became shorter and wider, a characteristic of excitatory mushroom-type spines (Jontes and Smith, 2000). The expression of shorter-wider spines was accompanied by an increase in the matrix metalloproteinase-9 (MMP-9). This extracellular protease has a role in synaptic plasticity as it is present in excitatory synapses within the hippocampus, cerebellum and cerebral cortex (for review see Michaluk and Kaczmarek, 2007). Moreover, inhibition of MMP-9 activity has been shown to make spines resistant to excitotoxic damage from TBI as well as post-impact-induced seizures (Michaluk and Kaczmarek, 2007; Hayashi et al., 2009; Pijet et al., 2019). Expression of MMP-9 has been seen to increase 30 min after TBI, and remaining elevated for hours and days (Wang et al., 2000; Truettner et al., 2005; Hayashi et al., 2009; Pijet et al., 2018). While not reported in Pijet et al. (2018), it would be interesting to see if the increase in MMP-9 expression 30 min after CCI would be accompanied by a change in dendritic spine phenotype, similar to what they found a year later at 24 h after impact.

DAMAGE TO THE DENDRITE OUTSIDE OF THE SPINE HEAD FOLLOWING IMPACT

The large influx of Ca^{2+} that follows TBI activates various downstream pathophysiological cascades that put the neuron at risk of degeneration. One of these pathways includes alterations to the neuronal microtubule network. Microtubules provide both cytoskeletal structuring to the neuron, as well as act as a "molecular highway" for proteins and organelles to travel throughout the neuron. Calpain is a family of calcium-activated proteases involved in numerous physiological functions ranging from modifications to receptors and channels, activation of apoptotic proteins and regulation of structural proteins (Saatman et al., 2010). The activation of calpain can occur within minutes of injury and be sustained for several days (Saatman et al., 2010). In particular, calpain-2 has been shown to have neurodegenerative consequences several hours post-TBI, as evidence by increased calpain-2 levels correlating with the activation of apoptotic pathways in mice (Wang et al., 2018). Calpain-2 also disrupts microtubule dynamics by phosphorylating tau, the accumulation and aggregation of which has been well documented in the onset of tauopathy's such as chronic traumatic encephalopathy and Alzheimer's disease (Goldstein et al., 2012; Baudry and Bi, 2016; for review see McKee et al., 2013).

Along with activation of neurodegenerative pathways such as calpain-2, the influx of Ca^{2+} that follows a TBI places stress upon the mitochondria of the neuron (Watts et al., 2015). In data not shown, Griesemer and Mautes (2007) noted an increase in adenosine triphosphate levels 1 h post closed head impact, with a decrease occurring by hour 4. Overworked mitochondria fail to buffer the rise in intracellular Ca^{2+} levels and as a result damaging reactive oxygen species, such as H_2O_2, are created (Vercesi et al., 2018). While these secondary pathophysiological pathways take time to develop, the initial onset of the sequelae begins with a moment of disruption shortly after impact. Further investigations into the hyperacute neuronal responses to TBI will be beneficial in the development of possible therapeutic targets and better understanding of how these chronic diseases initiate.

CONCLUSION

The hyperacute phase that follows TBI has been relatively understudied when it comes to understanding the dynamics of head trauma. The changes at the level of the synapse showcase the disrupted communication between neurons and how it reacts to the change in the environment. These subtle changes at the synapse amplify as further damage occurs, progressing the pathological pathway that is seen in the sub-acute and chronic phases of diseases associated with TBI. Understanding where the biochemical changes begin following head trauma could direct the field of research to the development of effective treatments and therapeutics soon after an impact has occurred.

AUTHOR CONTRIBUTIONS

BH contributed to the research and drafting of manuscript. MRH contributed to the revisions and final approval of manuscript. Both authors contributed to the article and approved the submitted version.

REFERENCES

Aguayo, F. I., Tejos-Bravo, M., Díaz-Véliz, G., Pacheco, A., García-Rojo, G., Corrales, W., et al. (2018). Hippocampal Memory Recovery After Acute Stress: A Behavioral, Morphological and Molecular Study. *Front. Mol. Neurosci.* 11:283. doi: 10.3389/fnmol.2018.00283

Ahmed, W. W., Li, T. C., Rubakhin, S. S., Chiba, A., Sweedler, J. V., and Saif, T. A. (2012). Mechanical tension modulates local and global vesicle dynamics in neurons. *Cell. Mol. Bioengine.* 2012, 155–164. doi: 10.1007/s12195-012-0223-1

Albayram, O., Albayram, S., and Mannix, R. (2020). Chronic traumatic encephalopathy—a blueprint for the bridge between neurological and psychiatric disorders. *Transl. Psychiatry* 10:424. doi: 10.1038/s41398-020-01111-x

Arnsten, A. F. T., Datta, D., and Preuss, T. M. (2021). Studies of aging nonhuman primates illuminate the etiology of early-stage Alzheimer's-like neuropathology: An evolutionary perspective. *Am. J. Primatol.* 83:23254. doi: 10.1002/ajp.23254

Atkins, C. M., Chen, S., Alonso, O. F., Dietrich, D., and Hu, B.-R. (2006). Activation of calcium/calmodulin-dependent protein kinases after traumatic brain injury. *J. Cereb. Blood Flow Metab.* 26, 1507–1518. doi: 10.1038/sj.jcbfm.9600301

Balosso, S., Liu, J., Bianchi, M. E., and Vezzani, A. (2014). Disulfide-containing high mobility group box-1 promotes N-methyl-d-aspartate receptor function and excitotoxicity by activating toll-like receptor 4-dependent signaling in hippocampal neurons. *Antioxid. Redox Signal.* 21, 1726–1740. doi: 10.1089/ars.2013.5349

Baudry, M., and Bi, X. (2016). Calpain-1 and Calpain-2: The Yin and Yang of Synaptic Plasticity and Neurodegeneration. *Trends Neurosci.* 39, 235–245. doi: 10.1016/j.tins.2016.01.007

Benavides-Piccione, R., Fernaud-Espinosa, I., Robles, V., Yuste, R., and DeFelipe, J. (2013). Age-Based Comparison of Human Dendritic Spine Structure Using Complete Three-Dimensional Reconstructions. *Cereb. Cortex* 23:1798. doi: 10.1093/CERCOR/BHS154

Berger, M., Speckmann, E. J., Pape, H. C., and Gorji, A. (2008). Spreading depression enhances human neocortical excitability in vitro. *Cephalalgia* 28, 558–562. doi: 10.1111/j.1468-2982.2008.01556.x

Boersma, M. C. H., Dresselhaus, E. C., de Biase, L. M., Mihalas, A. B., Bergles, D. E., and Meffert, M. K. (2011). A requirement for nuclear factor-κB in developmental and plasticity-associated synaptogenesis. *J. Neurosci.* 31, 5414–5425. doi: 10.1523/JNEUROSCI.2456-10.2011

Bokota, G., Magnowska, M., Kuśmierczyk, T., Łukasik, M., Roszkowska, M., and Piewczynski, D. (2016). Computational approach to dendritic spine taxonomy and shape transition analysis. *Front. Comput. Neurosci.* 10:140. doi: 10.3389/fncom.2016.00140

Bourne, J., and Harris, K. M. (2007). Do thin spines learn to be mushroom spines that remember? *Curr. Opin. Neurobiol.* 17, 381–386. doi: 10.1016/j.conb.2007.04.009

Calabrese, B., Wilson, M. S., and Halpain, S. (2006). Development and regulation of dendritic spine synapses. *Physiology* 21, 38–47. doi: 10.1152/physiol.00042.2005

Carlson, S. W., Yan, H., Ma, M., Li, Y., Henchir, J., and Dixon, C. E. (2016). Traumatic brain injury impairs soluble N-ethylmaleimide-sensitive factor attachment protein receptor complex formation and alters synaptic vesicle distribution in the hippocampus. *J. Neurotrauma* 33, 113–121. doi: 10.1089/neu.2014.3839

Chater, T. E., and Goda, Y. (2014). The role of AMPA receptors in postsynaptic mechanisms of synaptic plasticity. *Front. Cell. Neurosci.* 8:401. doi: 10.3389/fncel.2014.00401

Chen, F., Chen, H., Chen, Y., Wei, W., Sun, Y., Zhang, L., et al. (2021). Dysfunction of the SNARE complex in neurological and psychiatric disorders. *Pharmacol. Res.* 165, 1043–6618. doi: 10.1016/J.PHRS.2021.105469

Chen, K., Baram, T. Z., and Soltesz, I. (1999). Febrile seizures in the developing brain result in persistent modification of neuronal excitability in limbic circuits. *Nat. Med.* 5, 888–894. doi: 10.1038/11330

Cohen, A. S., Pfister, B. J., Schwarzbach, E., Sean Grady, M., Goforth, P. B., and Satin, L. S. (2007). Injury-induced alterations in CNS electrophysiology. *Prog. Brain Res.* 161, 143–169. doi: 10.1016/S0079-6123(06)61010-8

D'Ambrosio, R., Maris, D. O., Grady, M. S., Winn, H. R., and Janigro, D. (1998). Selective loss of hippocampal long-term potentiation, but not depression, following fluid percussion injury. *Brain Res.* 786, 64–79. doi: 10.1016/S0006-8993(97)01412-1

D'Ambrosio, R., Maris, D. O., Grady, M. S., Winn, H. R., and Janigro, D. (1999). Impaired K+ homeostasis and altered electrophysiological properties of post-traumatic hippocampal gila. *J. Neurosci.* 19, 8152–8162. doi: 10.1523/jneurosci.19-18-08152.1999

Ding, M. C., Wang, Q., Lo, E. H., and Stanley, G. B. (2011). Cortical excitation and inhibition following focal traumatic brain injury. *J. Neurosci.* 31, 14085–14094. doi: 10.1523/JNEUROSCI.3572-11.2011

Drexel, M., Puhakka, N., Kirchmair, E., Hörtnagl, H., Pitkänen, A., and Sperk, G. (2015). Expression of GABA receptor subunits in the hippocampus and thalamus after experimental traumatic brain injury. *Neuropharmacology* 88, 122–133. doi: 10.1016/j.neuropharm.2014.08.023

Faden, A. I., Demediuk, P., Panter, S. S., and Vink, R. (1989). The role of excitatory amino acids and NMDA receptors in traumatic brain injury. *Science* 244, 798–800. doi: 10.1126/science.2567056

Folkersma, H., Foster Dingley, J. C., van Berckel, B. N. M., Rozemuller, A., Boellaard, R., Huisman, M. C., et al. (2011). Increased cerebral (R)-[11C]PK11195 uptake and glutamate release in a rat model of traumatic brain injury: A longitudinal pilot study. *J. Neuroinflamm.* 8:67. doi: 10.1186/1742-2094-8-67

Frank, R. A. W., Komiyama, N. H., Ryan, T. J., Zhu, F., O'Dell, T. J., and Grant, S. G. N. (2016). NMDA receptors are selectively partitioned into complexes and supercomplexes during synapse maturation. *Nat. Commun.* 7:ncomms11264. doi: 10.1038/ncomms11264

Goldstein, L. E., Fisher, A. M., Tagge, C. A., Zhang, X. L., Velisek, L., Sullivan, J. A., et al. (2012). Chronic traumatic encephalopathy in blast-exposed military veterans and a blast neurotrauma mouse model. *Sci. Transl. Med.* 4:134ra60. doi: 10.1126/scitranslmed.3003716

Goldstein, L. E., McKee, A. C., and Stanton, P. K. (2014). Considerations for animal models of blast-related traumatic brain injury and chronic traumatic encephalopathy. *Alzheimers. Res. Ther.* 6:64. doi: 10.1186/s13195-014-0064-3

González-Tapia, D., Martínez-Torres, N. I., Hernández-González, M., Guevara, M. A., and González-Burgos, I. (2016). Plastic changes to dendritic spines on layer V pyramidal neurons are involved in the rectifying role of the prefrontal cortex during the fast period of motor learning. *Behav. Brain Res.* 298, 261–267. doi: 10.1016/j.bbr.2015.11.013

Griesemer, D., and Mautes, A. M. (2007). Closed head injury causes hyperexcitability in rat hippocampal CA1 but not in CA3 pyramidal cells. *J. Neurotrauma* 24, 1823–1832. doi: 10.1089/neu.2006.0237

Guerriero, R. M., Giza, C. C., and Rotenberg, A. (2015). Glutamate and GABA Imbalance Following Traumatic Brain Injury. *Curr. Neurol. Neurosci. Rep.* 15:1. doi: 10.1007/s11910-015-0545-1

Hackett, J. T., and Ueda, T. (2015). Glutamate Release. *Neurochem. Res.* 40, 2443–2460. doi: 10.1007/s11064-015-1622-1

Harris, K. M., and Kater, S. B. (1994). Dendritic spines: Cellular specializations imparting both stability and flexibility to synaptic function. *Annu. Rev. Neurosci.* 17, 341–371. doi: 10.1146/annurev.ne.17.030194.002013

Hayashi, T., Kaneko, Y., Yu, S. J., Bae, E. K., Stahl, C. E., Kawase, T., et al. (2009). Quantitative analyses of matrix metalloproteinase activity after traumatic brain injury in adult rats. *Brain Res.* 1280, 172–177. doi: 10.1016/j.brainres.2009.05.040

Helm, M. S., Dankovich, T. M., Mandad, S., Rammner, B., Jähne, S., Salimi, V., et al. (2021). A large-scale nanoscopy and biochemistry analysis of postsynaptic dendritic spines. *Nat. Neurosci.* 24, 1151–1162. doi: 10.1038/s41593-021-00874-w

Hering, H., and Sheng, M. (2001). Dentritic spines: structure, dynamics and regulation. *Nat. Rev. Neurosci.* 2, 880–888. doi: 10.1038/35104061

Herms, J., and Dorostkar, M. M. (2016). Dendritic Spine Pathology in Neurodegenerative Diseases. *Annu. Rev. Pathol. Mech. Dis.* 11, 221–250. doi: 10.1146/annurev-pathol-012615-044216

Isaac, J. T. R., Ashby, M., and McBain, C. J. (2007). The Role of the GluR2 Subunit in AMPA Receptor Function and Synaptic Plasticity. *Neuron* 54, 859–871. doi: 10.1016/j.neuron.2007.06.001

Jamjoom, A. A. B., Rhodes, J., Andrews, P. J. D., and Grant, S. G. N. (2021). The synapse in traumatic brain injury. *Brain* 144, 18–31. doi: 10.1093/brain/awaa321

Jaworski, J., Kapitein, L. C., Gouveia, S. M., Dortland, B. R., Wulf, P. S., Grigoriev, I., et al. (2009). Dynamic Microtubules Regulate Dendritic Spine Morphology and Synaptic Plasticity. *Neuron* 61, 85–100. doi: 10.1016/j.neuron.2008.11.013

Jeong, J., Pandey, S., Li, Y., Badger, J. D., Lu, W., and Roche, K. W. (2019). PSD-95 binding dynamically regulates NLGN1 trafficking and function. *Proc. Natl. Acad. Sci. U S A.* 116, 12035–12044. doi: 10.1073/pnas.1821775116

Jontes, J. D., and Smith, S. J. (2000). Filopodia, Spines, and the Generation of Synaptic Diversity. *Neuron* 27, 11–14. doi: 10.1016/s0896-6273(00)00003-9

Kaeser, P. S., and Regehr, W. G. (2017). The readily releasable pool of synaptic vesicles. *Curr. Opin. Neurobiol.* 43, 63–70. doi: 10.1016/J.CONB.2016.12.012

Kalia, L. V., Kalia, S. K., and Salter, M. W. (2008). NMDA receptors in clinical neurology: excitatory times ahead. *Lancet Neurol.* 7, 742–755. doi: 10.1016/S1474-4422(08)70165-0

Katayama, Y., Becker, D. P., Tamura, T., and Hovda, D. A. (1990). Massive increases in extracellular potassium and the indiscriminate release of glutamate following concussive brain injury. *J. Neurosurg.* 73, 889–900. doi: 10.3171/jns.1990.73.6.0889

Keith, D., and El-Husseini, A. (2008). Excitation control: Balancing PSD-95 function at the synapse. *Front. Mol. Neurosci.* 1:4. doi: 10.3389/neuro.02.004.2008

Korgaonkar, A. A., Li, Y., Sekhar, D., Subramanian, D., Guevarra, J., Swietek, B., et al. (2020). Toll-like Receptor 4 Signaling in Neurons Enhances Calcium-Permeable α-Amino-3-Hydroxy-5-Methyl-4-Isoxazolepropionic Acid Receptor Currents and Drives Post-Traumatic Epileptogenesis. *Ann. Neurol.* 87, 497–515. doi: 10.1002/ana.25698

Levinsoni, J. N., Chéry, N., Huang, K., Wong, T. P., Gerrow, K., Kang, R., et al. (2005). Neuroligins mediate excitatory and inhibitory synapse formation: Involvement of PSD-95 and neueexin-1β in neuroligin-induced synaptic specificity. *J. Biol. Chem.* 280, 17312–17319. doi: 10.1074/jbc.M413812200

Li, Y., Korgaonkar, A. A., Swietek, B., Wang, J., Elgammal, F. S., Elkabes, S., et al. (2015). Toll-like receptor 4 enhancement of non-NMDA synaptic currents increases dentate excitability after brain injury. *Neurobiol. Dis.* 74, 240–253. doi: 10.1016/j.nbd.2014.11.021

Luengo-Sanchez, S., Fernaud-Espinosa, I., Bielza, C., Benavides-Piccione, R., Larrañaga, P., and DeFelipe, J. (2018). 3D morphology-based clustering and simulation of human pyramidal cell dendritic spines. *PLoS Comput. Biol.* 14:1006221. doi: 10.1371/journal.pcbi.1006221

MacFarlane, M. P., and Glenn, T. C. (2015). Neurochemical cascade of concussion. *Brain Inj.* 29, 139–153. doi: 10.3109/02699052.2014.965208

MacKenzie, G., and Maguire, J. (2015). Chronic stress shifts the GABA reversal potential in the hippocampus and increases seizure susceptibility. *Epilepsy Res.* 109, 13–27. doi: 10.1016/j.eplepsyres.2014.10.003

Magou, G. C., Pfister, B. J., and Berlin, J. R. (2015). Effect of acute stretch injury on action potential and network activity of rat neocortical neurons in culture. *Brain Res.* 1624, 525–535. doi: 10.1016/j.brainres.2015.07.056

McKee, A. C., Stein, T. D., Nowinski, C. J., Stern, R. A., Daneshvar, D. H., Alvarez, V. E., et al. (2013). The spectrum of disease in chronic traumatic encephalopathy. *Brain* 136, 43–64. doi: 10.1093/brain/aws307

Meng, Y., Zhang, Y., Tregoubov, V., Falls, D. L., and Jia, Z. (2003). Regulation of spine morphology and synaptic function by LIMK and the actin cytoskeleton. *Rev. Neurosci.* 14, 233–240. doi: 10.1515/REVNEURO.2003.14.3.233

Michaluk, P., and Kaczmarek, L. (2007). Matrix metalloproteinase-9 in glutamate-dependent adult brain function and dysfunction. *Cell Death Differ.* 14, 1255–1258. doi: 10.1038/sj.cdd.4402141

Newpher, T. M., and Ehlers, M. D. (2009). Spine microdomains for postsynaptic signaling and plasticity. *Trends Cell Biol.* 19, 218–227. doi: 10.1016/j.tcb.2009.02.004

Nowacka, A., Borczyk, M., Salamian, A., Wójtowicz, T., Włodarczyk, J., and Radwanska, K. (2020). PSD-95 Serine 73 phosphorylation is not required for induction of NMDA-LTD. *Sci. Rep.* 10, 1–11. doi: 10.1038/s41598-020-58989-2

Noye Tuplin, E. W., and Holahan, M. R. (2019). Exploring time-dependent changes in conditioned place preference for food reward and associated changes in the nucleus accumbens. *Behav. Brain Res.* 361, 14–25. doi: 10.1016/j.bbr.2018.12.031

Nusser, Z., Hájos, N., Somogyi, P., and Mody, I. (1998). Increased number of synaptic GABA(A) receptors underlies potentiation at hippocampal inhibitory synapses. *Nature* 395, 172–177. doi: 10.1038/25999

Olmos, G., and Lladó, J. (2014). Tumor necrosis factor alpha: A link between neuroinflammation and excitotoxicity. *Mediators Inflamm.* 2014:861231. doi: 10.1155/2014/861231

Omalu, B. I., DeKosky, S. T., Minster, R. L., Kamboh, M. I., Hamilton, R. L., and Wecht, C. H. (2005). Chronic traumatic encephalopathy in a National Football League player. *Neurosurgery* 57, 128–133. doi: 10.1227/01.NEU.0000163407.92769.ED

Paoletti, P., Bellone, C., and Zhou, Q. (2013). NMDA receptor subunit diversity: Impact on receptor properties, synaptic plasticity and disease. *Nat. Rev. Neurosci.* 14, 383–400. doi: 10.1038/nrn3504

Park, Y., Luo, T., Zhang, F., Liu, C., Bramlett, H. M., Dalton Dietrich, W., et al. (2013). Downregulation of Src-kinase and glutamate-receptor phosphorylation after traumatic brain injury. *J. Cereb. Blood Flow Metab.* 33, 1642–1649. doi: 10.1038/jcbfm.2013.121

Patel, M. V., Sewell, E., Dickson, S., Kim, H., Meaney, D. F., and Firestein, B. L. (2019). A Role for Postsynaptic Density 95 and Its Binding Partners in Models of Traumatic Brain Injury. *J. Neurotrauma* 36, 2129–2138. doi: 10.1089/neu.2018.6291

Patel, T. P., Ventre, S. C., Geddes-Klein, D., Singh, P. K., and Meaney, D. F. (2014). Single-neuron NMDA receptor phenotype influences neuronal rewiring and reintegration following traumatic injury. *J. Neurosci.* 34, 4200–4213. doi: 10.1523/JNEUROSCI.4172-13.2014

Patterson, Z. R., and Holahan, M. R. (2012). Understanding the neuroinflammatory response following concussion to develop treatment strategies. *Front. Cell. Neurosci.* 0:58. doi: 10.3389/fncel.2012.00058

Pchitskaya, E., and Bezprozvanny, I. (2020). Dendritic Spines Shape Analysis—Classification or Clusterization? Perspective. *Front. Synaptic Neurosci.* 12:31. doi: 10.3389/fnsyn.2020.00031

Penzes, P., Srivastava, D. P., and Woolfrey, K. M. (2009). Not Just Actin? A Role for Dynamic Microtubules in Dendritic Spines. *Neuron* 61, 3–5. doi: 10.1016/j.neuron.2008.12.018

Peters, A., and Kaiserman-Abramof, I. R. (1970). The small pyramidal neuron of the rat cerebral cortex. The perikaryon, dendrites and spines. *Am. J. Anat.* 127, 321–355. doi: 10.1002/aja.1001270402

Pijet, B., Stefaniuk, M., and Kaczmarek, L. (2019). MMP-9 contributes to dendritic spine remodeling following traumatic brain injury. *Neural Plast.* 2019, 42–45. doi: 10.1155/2019/3259295

Pijet, B., Stefaniuk, M., Kostrzewska-Ksiezyk, A., Tsilibary, P. E., Tzinia, A., and Kaczmarek, L. (2018). Elevation of MMP-9 Levels Promotes Epileptogenesis After Traumatic Brain Injury. *Mol. Neurobiol.* 55, 9294–9306. doi: 10.1007/s12035-018-1061-5

Raible, D. J., Frey, L. C., Cruz Del Angel, Y., Russek, S. J., and Brooks-Kayal, A. R. (2012). GABAA receptor regulation after experimental traumatic brain injury. *J. Neurotrauma* 29, 2548–2554. doi: 10.1089/neu.2012.2483

Reza-Zaldivar, E. E., Hernández-Sápiens, M. A., Minjarez, B., Gómez-Pinedo, U., Sánchez-González, V. J., Márquez-Aguirre, A. L., et al. (2020). Dendritic Spine and Synaptic Plasticity in Alzheimer's Disease: A Focus on MicroRNA. *Front. Cell Dev. Biol.* 8:255. doi: 10.3389/fcell.2020.00255

Rodriguez, A., Ehlenberger, D. B., Dickstein, D. L., Hof, P. R., and Wearne, S. L. (2008). Automated three-dimensional detection and shape classification of dendritic spines from fluorescence microscopy images. *PLoS One* 3:1997. doi: 10.1371/journal.pone.0001997

Ross, S. T., and Soltesz, I. (2000). Selective depolarization of interneurons in the early posttraumatic dentate gyrus: Involvement of the Na+/K+-ATPase. *J. Neurophysiol.* 83, 2916–2930. doi: 10.1152/jn.2000.83.5.2916

Saatman, K. E., Creed, J., and Raghupathi, R. (2010). Calpain as a Therapeutic Target in Traumatic Brain Injury. *Neurotherapeutics* 7, 31–42. doi: 10.1016/j.nurt.2009.11.002

Saneyoshi, T., Fortin, D. A., and Soderling, T. R. (2010). Regulation of spine and synapse formation by activity-dependent intracellular signaling pathways. *Curr. Opin. Neurobiol.* 20, 108–115. doi: 10.1016/j.conb.2009.09.013

Schratt, G. M., Tuebing, F., Nigh, E. A., Kane, C. G., Sabatini, M. E., Kiebler, M., et al. (2006). A brain-specific microRNA regulates dendritic spine development. *Nature* 439, 283–289. doi: 10.1038/nature04367

Schumann, J., Alexandrovich, G. A., Biegon, A., and Yaka, R. (2008). Inhibition of NR2B phosphorylation restores alterations in NMDA receptor expression and improves functional recovery following traumatic brain injury in mice. *J. Neurotrauma* 25, 945–957. doi: 10.1089/neu.2008.0521

Shohami, E., and Biegon, A. (2014). Novel Approach to the Role of NMDA Receptors in Traumatic Brain Injury. *CNS Neurol. Disord. Drug Targets* 13, 567–573. doi: 10.2174/1871527313126660196

Siedler, D. G., Chuah, M. I., Kirkcaldie, M. T. K., Vickers, J. C., and King, A. E. (2014). Diffuse axonal injury in brain trauma: Insights from alterations in neurofilaments. *Front. Cell. Neurosci.* 8:429. doi: 10.3389/fncel.2014.00429

Sitcheran, R., Gupta, P., Fisher, P. B., and Baldwin, A. S. (2005). Positive and negative regulation of EAAT2 by NF-κB: A role for N-myc in TNFα-controlled repression. *EMBO J.* 24, 510–520. doi: 10.1038/sj.emboj.7600555

Smith, D. H., Wolf, J. A., Lusardi, T. A., Lee, V. M. Y., and Meaney, D. F. (1999). High tolerance and delayed elastic response of cultured axons to dynamic stretch injury. *J. Neurosci.* 19, 4263–4269. doi: 10.1523/jneurosci.19-11-04263.1999

Smith, J. A., Das, A., Ray, S. K., and Banik, N. L. (2012). Role of pro-inflammatory cytokines released from microglia in neurodegenerative diseases. *Brain Res. Bull.* 87, 10–20. doi: 10.1016/j.brainresbull.2011.10.004

Song, I., and Huganir, R. L. (2002). Regulation of AMPA receptors during synaptic plasticity. *Trends Neurosci.* 25, 578–588. doi: 10.1016/S0166-2236(02)02270-1

Spaethling, J. M., Klein, D. M., Singh, P., and Meaney, D. F. (2008). Calcium-permeable AMPA receptors appear in cortical neurons after traumatic mechanical injury and contribute to neuronal fate. *J. Neurotrauma* 2008, 1207–1216. doi: 10.1089/neu.2008.0532

Spaethling, J., Le, L., and Meaney, D. F. (2012). NMDA receptor mediated phosphorylation of GluR1 subunits contributes to the appearance of calcium-permeable AMPA receptors after mechanical stretch injury. *Neurobiol. Dis.* 46, 646–654. doi: 10.1016/j.nbd.2012.03.003

Stellwagen, D., Beattie, E. C., Seo, J. Y., and Malenka, R. C. (2005). Differential regulation of AMPA receptor and GABA receptor trafficking by tumor necrosis factor-α. *J. Neurosci.* 25, 3219–3228. doi: 10.1523/JNEUROSCI.4486-04.2005

Szydlowska, K., and Tymianski, M. (2010). Calcium, ischemia and excitotoxicity. *Cell Calcium* 47, 122–129. doi: 10.1016/j.ceca.2010.01.003

Tønnesen, J., and Nägerl, U. V. (2016). Dendritic spines as tunable regulators of synaptic signals. *Front. Psychiatry* 7:101. doi: 10.3389/fpsyt.2016.00101

Toth, Z., Hollrigel, G. S., Gorcs, T., and Soltesz, I. (1997). Instantaneous perturbation of dentate interneuronal networks by a pressure wave-transient delivered to the neocortex. *J. Neurosci.* 17, 8106–8117. doi: 10.1523/jneurosci.17-21-08106.1997

Truettner, J. S., Alonso, O. F., and Dietrich, W. D. (2005). Influence of therapeutic hypothermia on matrix metalloproteinase activity after traumatic brain injury in rats. *J. Cereb. Blood Flow Metab.* 25, 1505–1516. doi: 10.1038/sj.jcbfm.9600150

Vaure, C., and Liu, Y. (2014). A comparative review of toll-like receptor 4 expression and functionality in different animal species. *Front. Immunol.* 5:316. doi: 10.3389/fimmu.2014.00316

Vercesi, A. E., Castilho, R. F., Kowaltowski, A. J., de Oliveira, H. C. F., de Souza-Pinto, N. C., Figueira, T. R., et al. (2018). Mitochondrial calcium transport and the redox nature of the calcium-induced membrane permeability transition. *Free Radic. Biol. Med.* 129, 1–24. doi: 10.1016/j.freeradbiomed.2018.08.034

Wang, X., Jung, J., Asahi, M., Chwang, W., Russo, L., Moskowitz, M. A., et al. (2000). Effects of matrix metalloproteinase-9 gene knock-out on morphological and motor outcomes after traumatic brain injury. *J. Neurosci.* 20, 7037–7042. doi: 10.1523/jneurosci.20-18-07037.2000

Wang, Y., Liu, Y., Lopez, D., Lee, M., Dayal, S., Hurtado, A., et al. (2018). Protection against TBI-Induced Neuronal Death with Post-Treatment with a Selective Calpain-2 Inhibitor in Mice. *J. Neurotrauma* 35, 105–117. doi: 10.1089/neu.2017.5024

Watts, L. T., Shen, Q., Deng, S., Chemello, J., and Duong, T. Q. (2015). Manganese-Enhanced Magnetic Resonance Imaging of Traumatic Brain Injury. *J. Neurotrauma* 32, 1001–1010. doi: 10.1089/neu.2014.3737

Weber, J. T. (2012). Altered calcium signaling following traumatic brain injury. *Front. Pharmacol.* 3:60. doi: 10.3389/fphar.2012.00060

Wojnarowicz, M. W., Fisher, A. M., Minaeva, O., and Goldstein, L. E. (2017). Considerations for experimental animal models of concussion, traumatic brain injury, and chronic traumatic encephalopathy-these matters matter. *Front. Neurol.* 8:240. doi: 10.3389/fneur.2017.00240

Wolf, J. A., Stys, P. K., Lusardi, T., Meaney, D., and Smith, D. H. (2001). Traumatic axonal injury induces calcium influx modulated by tetrodotoxin-sensitive sodium channels. *J. Neurosci.* 21, 1923–1930. doi: 10.1523/jneurosci.21-06-01923.2001

Xiong, Y., Mahmood, A., and Chopp, M. (2018). Current understanding of neuroinflammation after traumatic brain injury and cell-based therapeutic opportunities. *Chinese J. Traumatol. English Ed.* 21, 137–151. doi: 10.1016/j.cjtee.2018.02.003

Xiong, Y., Mahmood, A., and Chopp, M. (2019). Remodeling dendritic spines for treatment of traumatic brain injury. *Neural Regen. Res.* 14, 1477–1480. doi: 10.4103/1673-5374.255957

Zhou, Q., and Sheng, M. (2013). NMDA receptors in nervous system diseases. *Neuropharmacology* 74, 69–75. doi: 10.1016/j.neuropharm.2013.03.030

Conflict of Interest: The authors declare that the research was conducted in the absence of any commercial or financial relationships that could be construed as a potential conflict of interest.

Publisher's Note: All claims expressed in this article are solely those of the authors and do not necessarily represent those of their affiliated organizations, or those of the publisher, the editors and the reviewers. Any product that may be evaluated in this article, or claim that may be made by its manufacturer, is not guaranteed or endorsed by the publisher.

frontiers in Molecular Neuroscience

MINI REVIEW
published: 31 March 2022
doi: 10.3389/fnmol.2022.864502

Advances and Barriers in Understanding Presynaptic *N*-Methyl-*D*-Aspartate Receptors in Spinal Pain Processing

Annemarie Dedek[1,2] *and Michael E. Hildebrand*[1,2]*

[1] *Department of Neuroscience, Carleton University, Ottawa, ON, Canada,* [2] *Neuroscience Department, Ottawa Hospital Research Institute, Ottawa, ON, Canada*

For decades, *N*-methyl-*D*-aspartate (NMDA) receptors have been known to play a critical role in the modulation of both acute and chronic pain. Of particular interest are NMDA receptors expressed in the superficial dorsal horn (SDH) of the spinal cord, which houses the nociceptive processing circuits of the spinal cord. In the SDH, NMDA receptors undergo potentiation and increases in the trafficking of receptors to the synapse, both of which contribute to increases in excitability and plastic increases in nociceptive output from the SDH to the brain. Research efforts have primarily focused on postsynaptic NMDA receptors, despite findings that presynaptic NMDA receptors can undergo similar plastic changes to their postsynaptic counterparts. Recent technological advances have been pivotal in the discovery of mechanisms of plastic changes in presynaptic NMDA receptors within the SDH. Here, we highlight these recent advances in the understanding of presynaptic NMDA receptor physiology and their modulation in models of chronic pain. We discuss the role of specific NMDA receptor subunits in presynaptic membranes of nociceptive afferents and local SDH interneurons, including their modulation across pain modalities. Furthermore, we discuss how barriers such as lack of sex-inclusive research and differences in neurodevelopmental timepoints have complicated investigations into the roles of NMDA receptors in pathological pain states. A more complete understanding of presynaptic NMDA receptor function and modulation across pain states is needed to shed light on potential new therapeutic treatments for chronic pain.

Keywords: dorsal horn, primary afferent, presynaptic, NMDAR, pain, spinal cord, sex differences, developmental timepoints

OPEN ACCESS

Edited by:
Dhrubajyoti Chowdhury,
Yale University, United States

Reviewed by:
Mark Baccei,
University of Cincinnati, United States
Maria Gutierrez-Mecinas,
University of Glasgow,
United Kingdom

***Correspondence:**
Michael E. Hildebrand
Mike.Hildebrand@carleton.ca

Specialty section:
This article was submitted to Molecular Signalling and Pathways, a section of the journal Frontiers in Molecular Neuroscience

Received: *28 January 2022*
Accepted: *04 March 2022*
Published: *31 March 2022*

Citation:
Dedek A and Hildebrand ME (2022) Advances and Barriers in Understanding Presynaptic N-Methyl-D-Aspartate Receptors in Spinal Pain Processing. Front. Mol. Neurosci. 15:864502. doi: 10.3389/fnmol.2022.864502

INTRODUCTION

Pain

Acute pain is a critical protective mechanism that alerts the body to tissue damage. The somatosensory nociceptive system is comprised of peripheral sensory neurons, circuits in the superficial dorsal horn (SDH) of the spinal cord and many target brain regions. The peripheral sensory neurons and the SDH are responsible for transducing and modulating nociceptive input;

once afferent signals are processed in the brain, conscious perception of nociception results in the multifaceted experience of pain. As a complex network of brain areas are involved in integrating and modulating pain [for review see Almeida et al. (2004)], a practical treatment approach is to target nociceptive input before it reaches the brain.

Nociception in the Spinal Dorsal Horn

The cellular organization of the SDH lends itself to plastic changes that can increase network excitability and nociceptive output. Lamina I and II, the outer-most laminae of the SDH, are the main sites of entry for high-threshold nociceptive primary afferents (Todd, 2010; Peirs and Seal, 2016; Peirs et al., 2021). Aδ fibers are small-diameter, myelinated primary afferent fibers that synapse onto lamina I and lamina II_{outer} neurons. C fibers also have a small diameter but are unmyelinated and synapse onto lamina I-II neurons. Most neurons in laminae I and III, and virtually all neurons in lamina II, are interneurons, meaning that they make local synaptic connections exclusively within the SDH. Interneurons can be divided into two general subtypes: excitatory (glutamatergic) and inhibitory [GABAergic (γ-aminobutyric acid-ergic) and/or glycinergic] (Todd, 2017). In addition to input from primary afferents, the SDH receives input from descending efferents from the brain (Kato et al., 2006; Todd, 2010, 2015). The final neuronal subpopulation within the SDH is a small number of projection neurons (Todd, 2015). Given this convergence of interconnected synaptic inputs from primary afferents, descending efferents, and local interneurons onto SDH projection neurons, targeting molecular determinants of excitability within this network can readily lead to altered nociceptive output.

N-Methyl-*D*-Aspartate Receptors in Spinal Nociception and Hyperexcitability

Excitatory glutamatergic *N*-methyl-*D*-aspartate receptors (NMDARs) are critical regulators of SDH plasticity and excitability. The seminal discovery of windup, which is characterized by progressively increased amplitude of SDH neuronal depolarization and firing during a course of repeated C-fiber stimulation (Mendell and Wall, 1965), paved the way for investigating the role of NMDARs in acute nociceptive processing. Both competitive and non-competitive NMDAR antagonists can block windup (Woolf and Thompson, 1991). Selective NMDAR antagonists also reverse increased excitability in SDH neurons in the subcutaneous formalin injection model of acute pain (Coderre and Melzack, 1992).

Dysregulated processing of nociceptive input results in pathological pain through hyperexcitability of the SDH (Woolf, 2011), which is dependent upon NMDAR activation (Bourinet et al., 2014). Early studies found that intrathecal injection of the NMDAR antagonist MK-801 reduced mechanical and heat hyperalgesia, while leaving acute nociception unaltered in sham-treated animals (Chapman and Dickenson, 1992; Yamamoto and Yaksh, 1992a,b). In later studies, selective knockdown of the obligatory NMDAR subunit, GluN1, in the SDH through intrathecal viral injections prevented the induction of pain hypersensitivity induced by injury but did not affect pain thresholds in uninjured animals (South et al., 2003; Garraway et al., 2007). Importantly, NMDARs can be located on both the pre- and postsynaptic membrane, and yet early research into the nociceptive roles of NMDARs has not made this critical distinction between pre- and postsynaptic receptors in the SDH.

Purpose

Historically, the role of presynaptic NMDARs has been overshadowed by their postsynaptic counterparts. For example, many of the processes mediating chronic pain have exclusively focused on postsynaptic changes. In recent years, it has become evident that presynaptic NMDARs (preNMDARs) contribute to the etiology of pathological pain. Here, we will explore how preNMDARs are modulated in the SDH and contribute to pain signaling. Further, we will highlight gaps in the literature regarding the nociceptive roles of preNMDARs.

PRESYNAPTIC *N*-METHYL-*D*-ASPARTATE RECEPTORS

Studies in the 1990s discovered that exogenous application of NMDA resulted in increased neurotransmitter release from monoaminergic terminals in the striatum (Krebs et al., 1991). This finding provided some of the first evidence for functional preNMDARs that modulate the release of neurotransmitters (Krebs et al., 1991). Electron microscopy with an antibody targeting the GluN1 NMDAR subunit in male adult Sprague Dawley rats showed extensive labeling of the presynaptic terminal in the SDH, revealing for the first time that NMDARs are present presynaptically in the dorsal horn of the spinal cord (Liu et al., 1994). In the SDH, nearly one-third of NMDARs are found to be presynaptic and are located immediately adjacent to the vesicle release site at the active zone (Liu et al., 1994). PreNMDARs in primary afferent terminals are translated in dorsal root ganglia neurons and are transported along the axon to the afferent terminal (Liu et al., 1994). The localization of NMDARs in the axon terminals of primary afferents, adjacent to the vesicle release site, allows them to influence the release of glutamate and peptide neurotransmitters from primary afferents, thus directly modulating the first nociceptive input to the central nervous system (Liu et al., 1994; Duguid and Smart, 2008; Abraira et al., 2017; Zimmerman et al., 2019).

Properties of Presynaptic *N*-Methyl-*D*-Aspartate Receptors

The type of NMDAR subunits that make up receptors in the presynaptic terminal gives insight into the function of these receptors, as well as an opportunity to selectively inhibit a subpopulation of NMDARs. Interestingly, all subunit types

(GluN2A-D and GluN3A-B) can assemble into preNMDARs in the nervous system (Bouvier et al., 2015; Oshima-Takago and Takago, 2017). Primary afferent terminals have been found to contain functional GluN2B subunits in adult rats (Boyce et al., 1999; Chen et al., 2010; Zhao et al., 2012; Yan et al., 2013). However, further studies are needed to fully characterize the expression of specific subunits in preNMDARs in the spinal cord.

Presynaptic NMDARs have different properties than their postsynaptic counterparts. Canonical postsynaptic NMDARs are blocked by Mg^{2+} at rest; they, therefore, require neuronal depolarization along with glutamate binding to become functionally active. Presynaptic NMDARs, on the other hand, can promote spontaneous neurotransmitter release in the absence of neuronal depolarization (Kavalali, 2015; Dore et al., 2017; Wong et al., 2021). This suggests that these NMDARs can be activated by endogenous glutamate without relief of the Mg^{2+} block (Mayer et al., 1984; Kunz et al., 2013; Kavalali, 2015). Studies in the cortex and hippocampus have identified GluN2C/GluN2D subunit-containing preNMDARs, which convey low Mg^{2+} sensitivity and low calcium-permeability to the NMDAR (Banerjee et al., 2009; Andrade-Talavera et al., 2016). Studies of NMDAR subunit expression patterns have identified GluN2D expression in the spinal cord (Dunah et al., 1996; Temi et al., 2021), however, further research is needed to identify if these subunits are incorporated into SDH preNMDARs. PreNMDARs in the visual cortex have been found to contain GluN1/GluN3A/GluN2B triheteromers (Larsen et al., 2011). This type of triheteromer is presumed to be less sensitive to Mg^{2+} and have lower Ca^{2+} permeability than diheteromeric GluN1/GluN2B NMDARs (Paoletti et al., 2013). GluN3A subunits have also been found in the spinal cord, however, it is unknown if they are present in SDH synaptic terminals (**Figure 1**; Kehoe et al., 2013).

Another factor that may explain preNMDAR Mg^{2+} insensitivity and associated functions in the absence of neuronal depolarization is metabotropic NMDAR signaling (Dore et al., 2017; Wong et al., 2021). In addition to ionotropic functions, NMDARs can signal via ion-flux-independent mechanisms (Dore et al., 2015, 2017). Metabotropic preNMDAR signaling has recently come to light during investigations into differences in mechanisms governing spontaneous and evoked vesicle release. Contrary to classical theories of synaptic transmission, the release of vesicles in spontaneous and evoked neurotransmission may occur by independent mechanisms that rely on different types of NMDAR function. Abrahamsson and colleagues found that, in pyramidal cells of the visual cortex, Mg^{2+}-sensitive preNMDARs upregulate the readily-releasable vesicle pool during high-frequency firing through Rab3-interacting molecules (RIMs), which provide scaffolding at presynaptic active zones. Conditional RIM1αβ deletion abolished the upregulation of vesicle replenishment, but preNMDAR-mediated spontaneous vesicle release was unaffected, even when preNMDAR ionotropic function was blocked by the channel-pore blocker MK-801 (Abrahamsson et al., 2017). Spontaneous vesicle release was found to be mediated by Mg^{2+}-insensitive preNMDARs that signal metabotropically through c-Jun *N*-terminal kinase (JNK), indicating that evoked and spontaneous vesicle release occurs through distinct processes (**Figure 1**; Abrahamsson et al., 2017; Bouvier et al., 2018).

PRESYNAPTIC MODULATION OF PLASTICITY BY PRESYNAPTIC *N*-METHYL-*D*-ASPARTATE RECEPTORS

The trafficking and function of NMDARs are regulated by protein tyrosine kinases such as Src-family kinases (SFKs). Indeed, SFK-dependent phosphorylation of NMDARs has been intricately tied to SDH plasticity (Xie et al., 2016; Suo et al., 2017) as well as the development of both inflammatory and neuropathic pain (Salter and Kalia, 2004; Liu et al., 2008; Sorge et al., 2011; Hildebrand et al., 2014, 2016). Although most studies have focused on NMDAR modulation exclusively at postsynaptic sites, SFKs have also been implicated in regulating preNMDARs in primary afferents. PreNMDAR activity at primary afferent terminals can be indirectly measured by neurokinin 1 (NK1) receptor internalization, which occurs as a result of presynaptic release of substance P (SP) (Marvizón et al., 1997). High-frequency stimulation (100 Hz) of the dorsal root induces the release of SP (a nociception-specific neuropeptide) and subsequent NK1 receptor internalization in NK1R-positive neurons in laminae I and II-outer. This NK1R internalization is also induced by administering NMDA and is abolished using AP5, a selective NMDAR antagonist, but is unaffected by the AMPAR and kainate receptor antagonist, CNQX, indicating that SP release in the SDH is regulated by NMDARs (Marvizón et al., 1997). Interestingly, NMDA-induced SP release does not require the firing of primary afferents or the opening of Ca^{2+} channels, supporting the notion that preNMDARs result in SP release via their own influx of Ca^{2+} into primary afferent terminals (Chen et al., 2010) or through metabotropic signaling (Dore et al., 2015; Bouvier et al., 2018). PreNMDAR-mediated SP release can be attenuated by blocking SFKs using PP1 or dasatinib (Chen et al., 2010). In addition, another study examining the role of SFKs in SP release found that intrathecal administration of NMDA only caused NK1 internalization when pretreated with BDNF (Chen W. et al., 2014). To investigate the role of SFKs in NK1 internalization, Chen W. et al. (2014) incubated spinal cord slices in BDNF for 60 minutes, followed by incubation in NMDA and either dasatinib, PP2 (both are SFK inhibitors), or PP3 (an inactive PP2 analog). They found that NK1R internalization resulting from preNMDAR-mediated SP release is blocked by inhibiting SFKs (using PP2 or dasatinib) and is unaffected by PP3 (Chen W. et al., 2014). Moreover, in mossy fibers of dentate granule cells, preNMDAR activation results in BDNF release from axon terminals, further promoting plastic changes (Lituma et al., 2021). These results suggest that regulating SFKs in primary afferent terminals could help modulate aberrant incoming nociceptive signals to the CNS in pathological pain states.

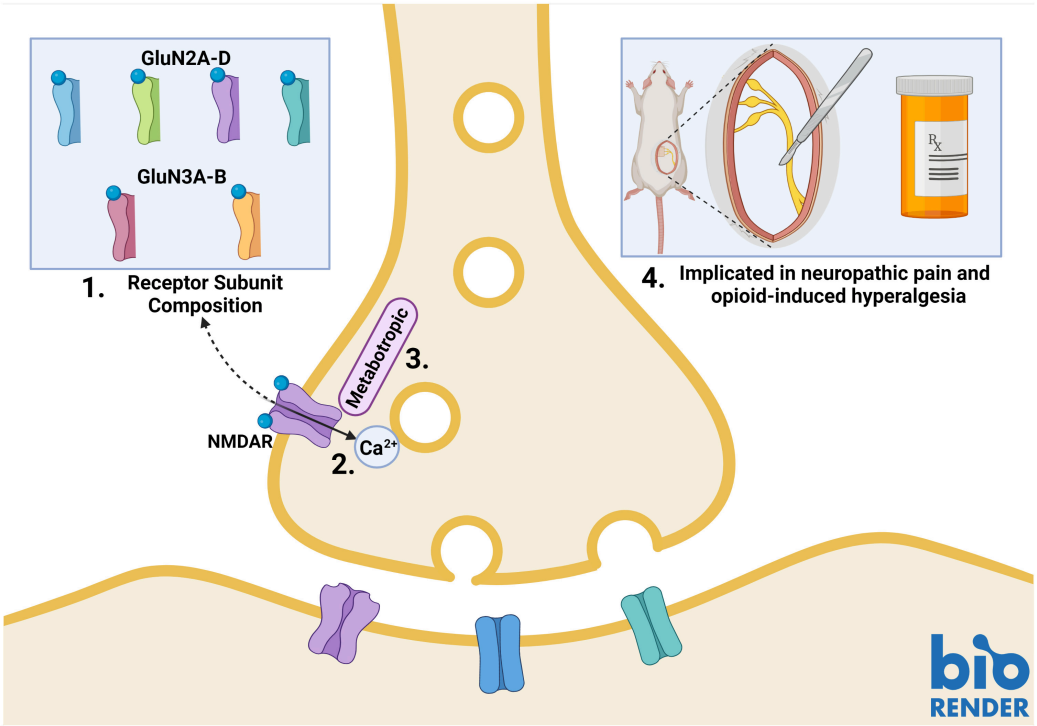

FIGURE 1 | Properties of presynaptic *N*-methyl-*D*-aspartate receptors (preNMDARs) in the superficial dorsal horn (SDH). 1. GluN2A and GluN2B-containing preNMDARs in primary afferents have been implicated in pain models. Low Mg^{2+} sensitivity suggests a potential role of GluN2D or GluN3-containing preNMDARs. 2. PreNMDARs may contribute to signaling in the SDH by either direct cation influx, or 3. By metabotropic signaling. 4. To date, preNMDARs have been found to contribute to both neuropathic pain and opioid-induced hyperalgesia, but not to non-pathological nociception. Figure was created using BioRender.com.

ROLE OF PRESYNAPTIC *N*-METHYL-*D*-ASPARTATE RECEPTORS IN PATHOLOGICAL PAIN MODELS

Presynaptic *N*-Methyl-*D*-Aspartate Receptors in Neuropathic Pain Models

Neuropathic pain is chronic pain that occurs following damage to neurons in the nociceptive pathway. To understand the role of preNMDARs in neuropathic pain, Yan et al. (2013) examined adolescent male rats subjected to the spinal nerve ligation (SNL) model of neuropathic pain. They found that evoked EPSC amplitudes in neuropathic rats were higher than sham animals. They also found a decrease in the paired-pulse ratio of neuropathic rats, indicating that SNL increased the probability of neurotransmitter release from presynaptic terminals (Yan et al., 2013). PreNMDARs that are upregulated in this model were found to be predominantly GluN2B subunit-containing (**Figure 1**; Yan et al., 2013). This has interesting implications, as studies have found that GluN2B NMDARs mediate baseline dorsal horn postsynaptic NMDAR responses in naïve rats as well as spinal hyperexcitability in a neuropathic pain model, but these studies did not examine the role of GluN2B-containing preNMDARs (Hildebrand et al., 2014, 2016; Tong and MacDermott, 2014). Increases in preNMDAR activation are dependent on activation of protein kinase C (PKC), as demonstrated by reversal with the PKC inhibitor GF109203 in spinal slices from SNL rats (Yan et al., 2013). Activation of preNMDARs was also linked to increased release of substance P, increased frequency of miniature EPSCs and associated pain hypersensitivity in multiple models of neuropathic pain, including the chronic constriction injury (CCI) and SNL models, in adolescent or young adult male rats (Chen W. et al., 2014; Chen S. R. et al., 2014; Li et al., 2016).

In addition to the CCI and SNL models of neuropathic pain, preNMDARs have been implicated in the development of paclitaxel-induced neuropathic pain in male rats. Xie and colleagues found similar preNMDAR-induced increases in mEPSC frequency and a reduction in paired-pulse ratio in paclitaxel-treated rats (Xie et al., 2016). However, unlike the peripheral nerve injury models (Yan et al., 2013), the increase in preNMDAR activity by PKC in the paclitaxel model was mediated through phosphorylation of GluN2A-containing NMDARs (Xie et al., 2016) instead of GluN2B. Interestingly, glutamate release in sham animals was not regulated by presynaptic NMDARs in any of the above-described experiments. This suggests that neuropathic injury results in recruitment of preNMDAR regulation pathways to enhance glutamate release and drive an increase in excitability in the SDH and that preNMDARs are not involved in neurotransmitter release in uninjured male adolescent animals (**Figure 1**; Yan et al., 2013; Li et al., 2016; Xie et al., 2016). In support of this, selective knockdown of

primary afferent NMDARs did not affect phase I, the acute phase, of the formalin model of pain (McRoberts et al., 2011). Importantly, presynaptic glutamate receptors may still be a target of anesthetics (Kubota et al., 2020), but further research is needed to understand the role of preNMDARs in non-pathological nociceptive SDH signaling.

Gabapentin is a common pain therapeutic; although it has been used for decades to treat pain, new mechanisms of action are still being uncovered (Kukkar et al., 2013). One of gabapentin's targets, α2δ-1, a voltage-activated calcium channel subunit, has recently been shown to interact with preNMDARs to augment glutamatergic input to the SDH. Nerve injury increases the expression of α2δ-1 in the DRG and spinal dorsal horn (Luo et al., 2001; Huang et al., 2019). Recent studies have shown that the C-terminal of α2δ-1 interacts with preNMDARs to promote synaptic/plasma membrane trafficking of α2δ-1-bound NMDARs (Chen et al., 2018; Huang et al., 2020). Blocking NMDARs reverses the SNL-mediated over-expression of α2δ-1 and the increase in frequency of mEPSCs in male rats. Gabapentin disrupts the interaction of α2δ-1 with NMDARs and thus blocks nerve injury-induced potentiation of presynaptic and postsynaptic NMDAR activity in the SDH (Chen et al., 2018; Zhang et al., 2021). Interestingly, this suggests clinical use of gabapentin may be modulating preNMDARs in human neuropathic pain.

Presynaptic *N*-Methyl-*D*-Aspartate Receptors in Opioid-Induced Hyperalgesia

Prolonged exposure to opioids results in paradoxical opioid-induced hyperalgesia. This phenomenon has long been tied to NMDAR signaling. In a study on the role of preNMDARs in opioid-induced hyperalgesia, Zeng et al. performed whole-cell patch clamp recordings on lamina I neurons while using the NMDAR antagonist MK-801 to block postsynaptic NMDARs. They perfused NMDA onto spinal slices from unsexed opioid-tolerant juvenile rats and found an increase in mEPSC frequency. Morphine-tolerant animals also had increased numbers of SDH primary afferents containing NMDARs, as determined using immunogold labeling of GluN1 subunits and electron microscopy (Zeng et al., 2006). Furthermore, the effects of preNMDARs on opioid tolerance was blocked by PKC inhibitors in male rats, suggesting that PKC may be potentiating preNMDARs to increase glutamate, resulting in opioid-induced hypersensitivity (Zhao et al., 2012). Moreover, co-administration of NMDAR antagonists with opioids also attenuates the development of opioid tolerance (**Figure 1**; Chapman and Dickenson, 1992; Zeng et al., 2006; Shen et al., 2018).

Inflammatory Pain

Presynaptic *N*-methyl-*D*-aspartate receptors are known to play a role in both neuropathic pain and opioid-induced hyperalgesia, however, they do not seem to be involved in inflammatory pain. In a study examining the effects of inflammatory pain modeled by plantar injection of complete Freud's adjuvant (CFA) in young adult male rats, increased glutamatergic input to lamina I (but not lamina II) was found to occur via presynaptic TRPA1 and TRPV1, as opposed to preNMDARs (Deng et al., 2019; Huang et al., 2019). This study looked at animals 10-16 days following injection of CFA. This is noteworthy because Weyerbacher and colleagues have previously shown, using both sexes of mice, that the maintenance of inflammatory pain occurs via an NMDAR-independent mechanism. They show, using knockout of GluN1 subunits in SDH neurons, that 96 h post-CFA injection, knockout animals are no longer protected from the effects of CFA, indicating that although NMDARs are involved in the development of inflammatory pain, they are not involved in its maintenance (Weyerbacher et al., 2010). Unfortunately, this study did not specifically evaluate the role of preNMDARs. To investigate the potential role of preNMDARs in the initiation of inflammatory pain hypersensitivity, future studies that include timepoints during the "induction phase" (1–3 days post-CFA injection) (Fehrenbacher et al., 2012); of CFA-induced inflammatory pain are needed.

UNANSWERED QUESTIONS ON PRESYNAPTIC *N*-METHYL-*D*-ASPARTATE RECEPTORS

Presynaptic *N*-Methyl-*D*-Aspartate Receptors Across Development

The expression pattern of NMDARs in the CNS varies across the lifespan, enabling distinct NMDAR subunit-specific mechanisms of plasticity at discrete developmental stages. For example, in the prenatal and early postnatal brain, there is a high expression of GluN2B and GluN2D NMDARs (Crair and Malenka, 1995; Hsia et al., 1998). The properties of GluN2B and GluN2D subunits promote temporal summation and integration at developing synapses due to their slow deactivation kinetics (Paoletti et al., 2013). In the weeks following birth, there is a developmental switch in the brain that promotes GluN2A-NMDAR expression, while expression and synaptic localization of GluN2B and GluN2D are decreased. This results in decreased synaptic strength and dampens the probability of further NMDAR-dependent functional circuit reorganization in the adult brain (Gray et al., 2011). However, the GluN2B/GluN2D to GluN2A developmental switch does not occur in the SDH of male rats (females have not been studied) (Mahmoud et al., 2020). Instead, the relative contributions of GluN2A- and GluN2B-mediated NMDAR postsynaptic responses at lamina II synapses remain constant throughout early postnatal development in male rats (Mahmoud et al., 2020). Consistent with this, the GluN2A, GluN2B, and GluN2D subunits are all found to be expressed in the SDH of male and female juvenile rats (Temi et al., 2021). However, many foundational findings from both the brain and spinal cord do not separate pre- from postsynaptic NMDARs, which is problematic given the differential functions of these populations in synaptic physiology.

Of the available evidence on preNMDARs in nociceptive processing, results from early postnatal animals appear to

contrast with findings from adolescent and adult models. For example, inhibiting NMDARs in the SDH of SNL or opioid-tolerant adult rats reduced the frequency of mEPSCs, and did not affect mEPSC frequency in naïve animals (Zhao et al., 2012; Yan et al., 2013). This suggests that in mature animals preNMDARs increase glutamatergic vesicle release in some pathological pain states, and do not affect baseline transmission. However, in naïve postnatal day 12–17 rats, Zeng and colleagues found that application of NMDA to activate preNMDARs reduced mEPSC frequency and reduced the amplitude of evoked EPSCs (Zeng et al., 2006). Additionally, Bardoni et al. (2004) showed that bath application of NMDA to spinal slices from postnatal day 6–12 rats caused an increase in synaptic latency, as well as the failure of monosynaptic AMPAR EPSCs in lamina I, with some heterogeneity in responses between individual neurons (Bardoni et al., 2004). They also found that NMDA application decreased the amplitude of the AMPAR EPSCs, which was attenuated by the NMDAR antagonist D-APV, suggesting that preNMDAR stimulation decreases glutamate release in these young animals (Bardoni et al., 2004). Since NMDAR expression and subunit composition varies greatly throughout development (Ewald and Cline, 2008), studies examining preNMDAR function across development can address the disparity between these studies. This is necessary for a complete understanding of the role preNMDARs play in the control of neurotransmitter release both in normal physiological conditions and in pathological pain (**Figure 2**). An important clinical consideration relating to these studies is that specific pain conditions affect patients of discrete ages. For example, osteoarthritis primarily affects older adults (Zhang and Jordan, 2010), and thus, adult rodent models best represent that pathology (Bapat et al., 2018). The varied function of NMDARs across development, combined with age-specific pain pathologies requires using age-appropriate rodent models to accurately study preNMDAR contribution to pathological pain.

Potential Sex Differences in Pain-Processing Presynaptic *N*-Methyl-*D*-Aspartate Receptors

Building on age-related developmental differences in NMDAR function, recent studies have highlighted the importance of considering sex and sex-hormone-related factors in pain models (Sorge et al., 2015; Mapplebeck et al., 2019; Dedek et al., 2021). Specifically, some of these differences have been tied to NMDAR function and regulation (Mogil et al., 1993; Dedek et al., 2021). For example, we found a sex-hormone-dependant sexual dimorphism in postsynaptic NMDAR potentiation in CFA-mediated inflammatory and *ex vivo* BDNF-treatment models of pathological pain, which is conserved from rodents to humans (Dedek et al., 2021). Additionally, we identified differences in baseline NMDAR localization within the SDH between male

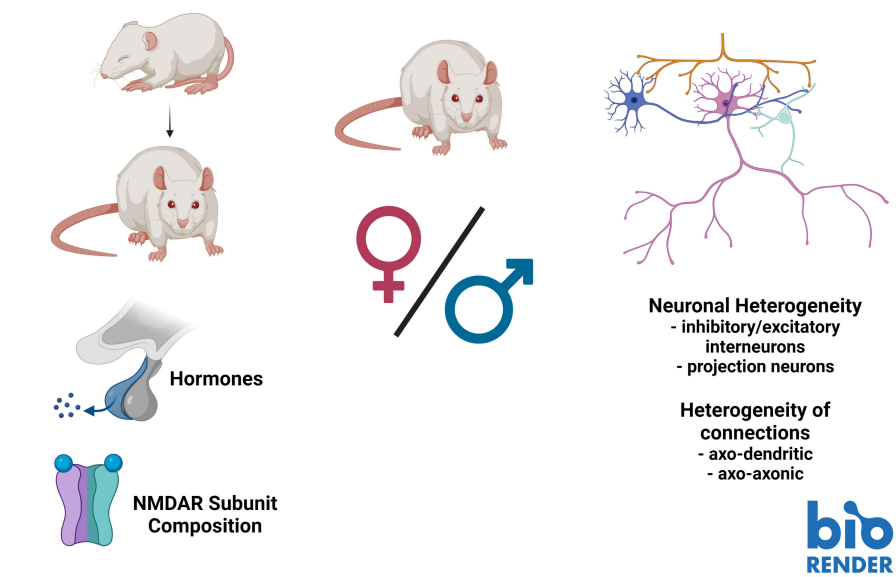

FIGURE 2 | Barriers to understanding the role of presynaptic *N*-methyl-*D*-aspartate receptors (preNMDARs) in superficial dorsal horn (SDH) nociception. **(A)**. Existing literature on preNMDARs in the SDH spans several developmental timepoints. This makes comparison between studies problematic, as NMDAR expression and composition may change throughout development. **(B)**. Almost all studies on preNMDARs in the SDH have been conducted in male or unsexed animals. Because data in recent years has demonstrated substantial sex differences in not only pain and nociception, but in the role of NMDARs in pain, it is critical for future studies to examine preNMDARs in females. **(C)**. The complex circuitry and unknown connectivity of the SDH makes interpreting overall output from the contributions of preNMDARs difficult. Increased mapping of the connectivity of distinct neuronal subpopulations, such as primary afferent terminals, inhibitory and excitatory interneurons, as well as projection neurons, in addition to understanding the distinct contributions of axo-dendritic and axo-axonic connections, will be vital to fully understand the role of preNMDARs in nociception in the SDH. Figure was created using BioRender.com.

and female juvenile rats: GluN2B and GluN2D are preferentially localized to the SDH in males, but in females only GluN2B is preferentially localized to the SDH, and in males, but not females, GluN2B expression was enhanced in the medial SDH (Temi et al., 2021; **Figure 2**). Almost the entire body of the above-discussed literature on preNMDARs in the SDH is based on studies in male or unsexed rodents, and thus a critical gap exists in addressing possible sex differences in the roles of SDH preNMDARs in physiological and pathological pain processing.

Complex Superficial Dorsal Horn Circuitry

A final barrier to fully understanding the role of preNMDARs in mediating nociceptive spinal cord signaling is the complex connectivity making up SDH circuitry. Unlike some other areas of the CNS where circuitry has been mapped out with knowledge of the exact connectivity between defined neuronal populations, like in the hippocampus, the exact connectivity within the SDH is unknown. With high collateralization of primary afferents and a complex network of modulatory interneurons that are either inhibitory or excitatory, inferring the effect on SDH output from specific molecular inputs is extremely difficult (**Figure 2**). For example, at first glance, it may seem straightforward that an increase in vesicle release from primary afferents would always have an overall excitatory effect in the SDH. However, primary afferents make axo-axonic connections that have been found to result in depression of primary afferent vesicle release. These mechanisms are not yet fully understood (Hochman et al., 2010). In addition, preNMDARs can contribute to the release of a diverse array of neurotransmitter-containing vesicles in either a spontaneous or depolarization-evoked manner (Pittaluga, 2021). Across various regions of the brain, NMDA application results in an increased spontaneous release of dopamine and glutamate, while having no effect on spontaneous GABA release (Pittaluga, 2021). In the SDH, studies performed in juvenile animals suggest a role of preNMDARs in mediating long-term depression (LTD) and presynaptic inhibition of primary afferent terminals (Bardoni et al., 1998, 2004, 2013; Zimmerman et al., 2019; Comitato and Bardoni, 2021), but further investigation is needed across the developmental spectrum. It is also important to consider that the majority of cells in the SDH are locally synapsing excitatory and inhibitory neurons (Todd, 2017), and that preNMDARs are found in the terminals of both of these classes of interneurons (Liu et al., 1994). PreNMDARs are thus likely to regulate the local release of excitatory and inhibitory neurotransmitters within SDH nociceptive networks. For this reason, it is necessary to understand the neuronal identities and connections within the SDH to paint a complete picture of the role of preNMDARs in nociceptive signaling and shed light on potential new therapeutic interventions for the treatment of pain.

CONCLUSION

Though preNMDARs have been known to exist for decades, only recently has their contribution to spinal cord physiology come into the spotlight. Thus far, it is clear that preNMDARs play a critical role in modulating the release of glutamate from primary afferents by directly permitting Ca^{2+} entry to the presynaptic terminal and/or by metabotropic signaling. Although progress has been made in understanding the role of preNMDARs in the SDH, several critical barriers remain. Further exploration of potential differences in preNMDARs by sex and across development is needed, as well as integrating this information into the rapidly evolving understanding of the complex molecular and cellular circuitry of the SDH.

AUTHOR CONTRIBUTIONS

AD wrote this manuscript, with editing and feedback from MEH. Both authors contributed to the article and approved the submitted version.

FUNDING

This study was supported by a Discovery Grant from the Natural Sciences and Engineering Research Council of Canada to MEH as well as by a MITACs Accelerate Industrial Fellowship to AD, in partnership with Eli Lilly research grant funding to MEH.

ACKNOWLEDGMENTS

We thank Natalina Salmaso and Melissa Chee for their helpful feedback in the preparation of this manuscript.

REFERENCES

Abrahamsson, T., Chou, C. Y. C., Li, S. Y., Mancino, A., Costa, R. P., Brock, J. A., et al. (2017). Differential regulation of evoked and spontaneous release by presynaptic NMDA receptors. *Neuron* 96, 839–855.e5. doi: 10.1016/j.neuron.2017.09.030

Abraira, V. E., Kuehn, E. D., Chirila, A. M., Springel, M. W., Toliver, A. A., Zimmerman, A. L., et al. (2017). The cellular and synaptic architecture of the mechanosensory dorsal horn. *Cell* 168, 295–310.e19. doi: 10.1016/j.cell.2016.12.010watswa

Almeida, T. F., Roizenblatt, S., and Tufik, S. (2004). Afferent pain pathways: a neuroanatomical review. *Brain Res.* 1000, 40–56. doi: 10.1016/j.brainres.2003.10.073

Andrade-Talavera, Y., Duque-Feria, P., Paulsen, O., and Rodríguez-Moreno, A. (2016). Presynaptic spike timing-dependent long-term depression in the mouse hippocampus. *Cereb. Cortex* 26, 3637–3654. doi: 10.1093/cercor/bhw172

Banerjee, A., Meredith, R. M., Rodríguez-Moreno, A., Mierau, S. B., Auberson, Y. P., and Paulsen, O. (2009). Double dissociation of spike timing-dependent potentiation and depression by subunit-preferring NMDA receptor antagonists in mouse barrel cortex. *Cereb. Cortex* 19, 2959–2969. doi: 10.1093/cercor/bhp067

Bapat, S., Hubbard, D., Munjal, A., Hunter, M., and Fulzele, S. (2018). Pros and cons of mouse models for studying osteoarthritis. *Clin. Transl. Med.* 7:36. doi: 10.1186/s40169-018-0215-4

Bardoni, R., Torsney, C., Tong, C. K., Prandini, M., and MacDermott, A. B. (2004). Presynaptic NMDA receptors modulate glutamate release from primary

sensory seurons in rat spinal cord dorsal horn. *J. Neurosci.* 24, 2774–2781. doi: 10.1523/JNEUROSCI.4637-03.2004

Bardoni, R., Magherini, P. C., and MacDermott, A. B. (1998). NMDA EPSCs at glutamatergic synapses in the spinal cord dorsal horn of the postnatal rat. *J. Neurosci.* 18, 6558–6567. doi: 10.1523/jneurosci.18-16-06558.1998

Bardoni, R., Takazawa, T., Tong, C. K., Choudhury, P., Scherrer, G., and Macdermott, A. B. (2013). Pre- and postsynaptic inhibitory control in the spinal cord dorsal horn. *Ann. N. Y. Acad. Sci.* 1279, 90–96. doi: 10.1111/nyas.12056

Bourinet, E., Altier, C., Hildebrand, M. E., Trang, T., Salter, M. W., and Zamponi, G. W. (2014). Calcium-permeable ion channels in pain signaling. *Physiol. Rev.* 94, 81–140. doi: 10.1152/physrev.00023.2013

Bouvier, G., Bidoret, C., Casado, M., and Paoletti, P. (2015). Presynaptic NMDA receptors: roles and rules. *Neuroscience* 311, 322–340. doi: 10.1016/j.neuroscience.2015.10.033

Bouvier, G., Larsen, R. S., Rodríguez-Moreno, A., Paulsen, O., and Sjöström, P. J. (2018). Towards resolving the presynaptic NMDA receptor debate. *Curr. Opin. Neurobiol.* 51, 1–7. doi: 10.1016/j.conb.2017.12.020

Boyce, S., Wyatt, A., Webb, J. K., O'Donnell, R., Mason, G., Rigby, M., et al. (1999). Selective NMDA NR2B antagonists induce antinociception without motor dysfunction: correlation with restricted localisation of NR2B subunit in dorsal horn. *Neuropharmacology* 38, 611–623. doi: 10.1016/S0028-3908(98)00218-4

Chapman, V., and Dickenson, A. H. (1992). The combination of NMDA antagonism and morphine produces profound antinociception in the rat dorsal horn. *Brain Res.* 573, 321–323. doi: 10.1016/0006-8993(92)90780-D

Chen, J., Li, L., Chen, S.-R., Chen, H., Xie, J.-D., Sirrieh, R. E., et al. (2018). The α2δ-1-NMDA receptor complex is critically involved in neuropathic pain development and gabapentin therapeutic actions. *Cell Rep.* 22, 2307–2321. doi: 10.1016/J.CELREP.2018.02.021

Chen, S. R., Hu, Y. M., Chen, H., and Pan, H. L. (2014). Calcineurin inhibitor induces pain hypersensitivity by potentiating pre- and postsynaptic NMDA receptor activity in spinal cords. *J. Physiol.* 592, 215–227. doi: 10.1113/jphysiol.2013.263814

Chen, W., Walwyn, W., Ennes, H. S., Kim, H., Mcroberts, J. A., and Marvizón, J. C. G. (2014). BDNF released during neuropathic pain potentiates NMDA receptors in primary afferent terminals. *Eur. J. Neurosci.* 39, 1439–1454. doi: 10.1111/ejn.12516

Chen, W., Zhang, G., and Marvizón, J. C. G. (2010). NMDA receptors in primary afferents require phosphorylation by Src family kinases to induce substance P release in the rat spinal cord. *Neuroscience* 166, 924–934. doi: 10.1016/j.neuroscience.2010.01.009

Coderre, T. J., and Melzack, R. (1992). The contribution of excitatory amino acids to central sensitization and persistent nociception after formalin-induced tissue injury. *J. Neurosci.* 12, 3665–3670. doi: 10.1523/jneurosci.12-09-03665.1992

Comitato, A., and Bardoni, R. (2021). Presynaptic inhibition of pain and touch in the spinal cord: from receptors to circuits. *Int. J. Mol. Sci.* 22:414. doi: 10.3390/IJMS22010414

Crair, M. C., and Malenka, R. C. (1995). A critical period for long-term potentiation at thalamocortical synapses. *Nature* 375, 325–328. doi: 10.1038/375325a0

Dedek, A., Xu, J., Lorenzo, L. -É, Godin, A. G., Kandegedara, C. M., Glavina, G., et al. (2021). Sexual dimorphism in a neuronal mechanism of spinal hyperexcitability across rodent and human models of pathological pain. *bioRxiv* [Preprint] doi: 10.1101/2021.06.15.447407

Deng, M., Chen, S. R., and Pan, H. L. (2019). Presynaptic NMDA receptors control nociceptive transmission at the spinal cord level in neuropathic pain. *Cell. Mol. Life Sci.* 76, 1889–1899. doi: 10.1007/s00018-019-03047-y

Dore, K., Aow, J., and Malinow, R. (2015). "Agonist binding to the NMDA receptor drives movement of its cytoplasmic domain without ion flow," in *Proceedings of the National Academy of Sciences of the United States of America*, Vol. 112, Washington, DC, 14705–14710. doi: 10.1073/pnas.1520023112

Dore, K., Stein, I. S., Brock, J. A., Castillo, P. E., Zito, K., and Sjöström, P. J. (2017). Unconventional NMDA receptor signaling. *J. Neurosci.* 37, 10800–10807. doi: 10.1523/JNEUROSCI.1825-17.2017

Duguid, I. C., and Smart, T. G. (2008). "Presynaptic NMDA receptors," in *Biology of the NMDA Receptor*, ed. A. M. Van Dongen (Boca Raton, FL: CRC Press/Taylor & Francis), 313–328. doi: 10.1201/9781420044157.ch14

Dunah, A. W., Yasuda, R. P., Wang, Y. H., Luo, J., Dávila-García, M. I., Gbadegesin, M., et al. (1996). Regional and ontogenic expression of the NMDA receptor subunit NR2D protein in rat brain using a subunit-specific antibody. *J. Neurochem.* 67, 2335–2345. doi: 10.1046/j.1471-4159.1996.67062335.x

Ewald, R. C., and Cline, H. T. (2008). "NMDA receptors and brain development," in *Biology of the NMDA Receptor*, ed. A. M. Van Dongen (Boca Raton, FL: CRC Press/Taylor & Francis), 1–15. doi: 10.1201/9781420044157.ch1

Fehrenbacher, J. C., Vasko, M. R., and Duarte, D. B. (2012). Models of inflammation: carrageenan- or unit 5.4 complete freund's adjuvant (CFA)-induced edema and hypersensitivity in the rat. *Curr. Protoc. Pharmacol.* 56, 5.4.1–5.4.9. doi: 10.1002/0471141755.ph0504s56

Garraway, S. M., Xu, Q., and Inturrisi, C. E. (2007). Design and evaluation of small interfering RNAs that target expression of the N-methyl-D-aspartate receptor NR1 subunit gene in the spinal cord dorsal horn. *J. Pharmacol. Exp. Ther.* 322, 982–988. doi: 10.1124/jpet.107.123125

Gray, J. A., Shi, Y., Usui, H., During, M. J., Sakimura, K., and Nicoll, R. A. (2011). Distinct,modes of AMPA receptor suppression at developing synapses by GluN2A and GluN2B: single-cell NMDA receptor subunit deletion in vivo. *Neuron* 71, 1085–1101. doi: 10.1016/j.neuron.2011.08.007

Hildebrand, M. E., Pitcher, G. M., Harding, E. K., Li, H., Beggs, S., and Salter, M. W. (2014). GluN2B and GluN2D NMDARs dominate synaptic responses in the adult spinal cord. *Sci. Rep.* 4:4094. doi: 10.1038/srep04094

Hildebrand, M. E., Xu, J., Dedek, A., Li, Y., Sengar, A. S., Beggs, S., et al. (2016). Potentiation of synaptic GluN2B NMDAR currents by Fyn kinase is gated through BDNF-mediated disinhibition in spinal pain processing. *Cell Rep.* 17, 2753–2765. doi: 10.1016/j.celrep.2016.11.024

Hochman, S., Shreckengost, J., Kimura, H., and Quevedo, J. (2010). Presynaptic inhibition of primary afferents by depolarization: observations supporting nontraditional mechanisms. *Ann. N. Y. Acad. Sci.* 1198, 140–152. doi: 10.1111/J.1749-6632.2010.05436.X

Hsia, A. Y., Malenka, R. C., and Nicoll, R. A. (1998). Development of excitatory circuitry in the hippocampus. *J. Neurophysiol.* 79, 2013–2024. doi: 10.1152/jn.1998.79.4.2013

Huang, Y., Chen, S. R., Chen, H., and Pan, H. L. (2019). Endogenous transient receptor potential ankyrin 1 and vanilloid 1 activity potentiates glutamatergic input to spinal lamina I neurons in inflammatory pain. *J. Neurochem.* 149, 381–398. doi: 10.1111/jnc.14677

Huang, Y., Chen, S. R., Chen, H., Luo, Y., and Pan, H. L. (2020). Calcineurin inhibition causes A2D-1–mediated tonic activation of synaptic NMDA receptors and pain hypersensitivity. *J. Neurosci.* 40, 3707–3719. doi: 10.1523/JNEUROSCI.0282-20.2020

Kato, G., Yasaka, T., Katafuchi, T., Furue, H., Mizuno, M., Iwamoto, Y., et al. (2006). Direct GABAergic and glycinergic inhibition of the substantia gelatinosa from the rostral ventromedial medulla revealed by in vivo patch-clamp analysis in rats. *J. Neurosci.* 26, 1787–1794. doi: 10.1523/JNEUROSCI.4856-05.2006

Kavalali, E. T. (2015). The mechanisms and functions of spontaneous neurotransmitter release. *Nat. Rev. Neurosci.* 16, 5–16. doi: 10.1038/nrn3875

Kehoe, L. A., Bernardinelli, Y., and Muller, D. (2013). GluN3A: an NMDA receptor subunit with exquisite properties and functions. *Neural Plast.* 2013:145387. doi: 10.1155/2013/145387

Krebs, M. O., Desce, J. M., Kemel, M. L., Gauchy, C., Godeheu, G., Cheramy, A., et al. (1991). Glutamatergic control of dopamine release in the rat striatum: evidence for presynaptic N-methyl-D-aspartate receptors on dopaminergic nerve terminals. *J. Neurochem.* 56, 81–85. doi: 10.1111/j.1471-4159.1991.tb02565.x

Kubota, H., Akaike, H., Okamitsu, N., Jang, I. S., Nonaka, K., Kotani, N., et al. (2020). Xenon modulates the GABA and glutamate responses at genuine synaptic levels in rat spinal neurons. *Brain Res. Bull.* 157, 51–60. doi: 10.1016/j.brainresbull.2020.01.016

Kukkar, A., Bali, A., Singh, N., and Jaggi, A. S. (2013). Implications and mechanism of action of gabapentin in neuropathic pain. *Arch. Pharm. Res.* 36, 237–251. doi: 10.1007/s12272-013-0057-y

Kunz, P. A., Roberts, A. C., and Philpot, B. D. (2013). Presynaptic NMDA receptor mechanisms for enhancing spontaneous neurotransmitter release. *J. Neurosci.* 33, 7762–7769. doi: 10.1523/JNEUROSCI.2482-12.2013

Larsen, R. S., Corlew, R. J., Henson, M. A., Roberts, A. C., Mishina, M., Watanabe, M., et al. (2011). NR3A-containing NMDARs promote neurotransmitter release and spike timing-dependent plasticity. *Nat. Neurosci.* 14, 338–344. doi: 10.1038/nn.2750

Li, L., Chen, S. R., Chen, H., Wen, L., Hittelman, W. N., Xie, J. D., et al. (2016). Chloride homeostasis critically regulates synaptic NMDA receptor activity in neuropathic pain. *Cell Rep*. 15, 1376–1383. doi: 10.1016/j.celrep.2016.04.039

Lituma, P. J., Kwon, H. B., Alviña, K., Luján, R., and Castillo, P. E. (2021). Presynaptic nmda receptors facilitate short-term plasticity and bdnf release at hippocampal mossy fiber synapses. *Elife* 10:e66612. doi: 10.7554/ELIFE.66612

Liu, H., Wang, H., Sheng, M., Jan, L. Y., Jan, Y. N., and Basbaum, A. I. (1994). Evidence for presynaptic N-methyl-D-aspartate autoreceptors in the spinal cord dorsal horn. *Proc. Natl. Acad. Sci. U.S.A.* 91, 8383–8387. doi: 10.1073/pnas.91.18.8383

Liu, X. J., Gingrich, J. R., Vargas-Caballero, M., Dong, Y. N., Sengar, A., Beggs, S., et al. (2008). Treatment of inflammatory and neuropathic pain by uncoupling Src from the NMDA receptor complex. *Nat. Med.* 14, 1325–1332. doi: 10.1038/nm.1883

Luo, Z. D., Chaplan, S. R., Higuera, E. S., Sorkin, L. S., Stauderman, K. A., Williams, M. E., et al. (2001). Upregulation of dorsal root ganglion α2δ calcium channel subunit and its correlation with allodynia in spinal nerve-injured rats. *J. Neurosci.* 21, 1868–1875. doi: 10.1523/jneurosci.21-06-01868.2001

Mahmoud, H., Martin, N., and Hildebrand, M. E. (2020). Conserved contributions of NMDA receptor subtypes to synaptic responses in lamina II spinal neurons across early postnatal development. *Mol. Brain* 13:31. doi: 10.1186/s13041-020-00566-9

Mapplebeck, J. C. S., Lorenzo, L. E., Lee, K. Y., Gauthier, C., Muley, M. M., De Koninck, Y., et al. (2019). Chloride dysregulation through downregulation of KCC2 mediates neuropathic pain in both sexes. *Cell Rep.* 28, 590–596.e4. doi: 10.1016/j.celrep.2019.06.059

Marviźon, J. C. G., Martínez, V., Grady, E. F., Bunnett, N. W., and Mayer, E. A. (1997). Neurokinin 1 receptor internalization in spinal cord slices induced by dorsal root stimulation is mediated by NMDA receptors. *J. Neurosci.* 17, 8129–8136. doi: 10.1523/jneurosci.17-21-08129.1997

Mayer, M. L., Westbrook, G. L., and Guthrie, P. B. (1984). Voltage-dependent block by Mg2+ of NMDA responses in spinal cord neurones. *Nature* 309, 261–263. doi: 10.1038/309261a0

McRoberts, J. A., Ennes, H. S., Marvizón, J. C. G., Fanselow, M. S., Mayer, E. A., and Vissel, B. (2011). Selective knockdown of NMDA receptors in primary afferent neurons decreases pain during phase 2 of the formalin test. *Neuroscience* 172, 474–482. doi: 10.1016/j.neuroscience.2010.10.045

Mendell, L. M., and Wall, P. D. (1965). Responses of single dorsal cord cells to peripheral cutaneous unmyelinated fibres [23]. *Nature* 206, 97–99. doi: 10.1038/206097a0

Mogil, J. S., Sternberg, W. F., Kest, B., Marek, P., and Liebeskind, J. C. (1993). Sex differences in the antagonism of swim stress-induced analgesia: effects of gonadectomy and estrogen replacement. *Pain* 53, 17–25. doi: 10.1016/0304-3959(93)90050-Y

Oshima-Takago, T., and Takago, H. (2017). NMDA receptor-dependent presynaptic inhibition at the calyx of Held synapse of rat pups. *Open Biol.* 7:170032. doi: 10.1098/rsob.170032

Paoletti, P., Bellone, C., and Zhou, Q. (2013). NMDA receptor subunit diversity: impact on receptor properties, synaptic plasticity and disease. *Nat. Rev. Neurosci.* 14, 383–400. doi: 10.1038/nrn3504

Peirs, C., and Seal, R. P. (2016). Neural circuits for pain: recent advances and current views. *Science* 354, 578–584. doi: 10.1126/science.aaf8933

Peirs, C., Williams, S. P. G., Zhao, X., Arokiaraj, C. M., Ferreira, D. W., Noh, M. C., et al. (2021). Mechanical allodynia circuitry in the dorsal horn is defined by the nature of the injury. *Neuron* 109, 73–90.e7. doi: 10.1016/j.neuron.2020.10.027

Pittaluga, A. (2021). Presynaptic release-regulating NMDA receptors in isolated nerve terminals: a narrative review. *Br. J. Pharmacol.* 178, 1001–1017. doi: 10.1111/bph.15349

Salter, M. W., and Kalia, L. V. (2004). SRC kinases: a hub for NMDA receptor regulation. *Nat. Rev. Neurosci.* 5, 317–328. doi: 10.1038/nrn1368

Shen, L., Wang, W., Li, S., Qin, J., and Huang, Y. (2018). NMDA receptor antagonists attenuate intrathecal morphine-induced pruritus through ERK phosphorylation. *Mol. Brain* 11:35. doi: 10.1186/s13041-018-0379-2

Sorge, R. E., LaCroix-Fralish, M. L., Tuttle, A. H., Sotocinal, S. G., Austin, J. S., Ritchie, J., et al. (2011). Spinal cord toll-like receptor 4 mediates inflammatory and neuropathic hypersensitivity in male but not female mice. *J. Neurosci.* 31, 15450–15454. doi: 10.1523/JNEUROSCI.3859-11.2011

Sorge, R. E., Mapplebeck, J. C. S., Rosen, S., Beggs, S., Taves, S., Alexander, J. K., et al. (2015). Different immune cells mediate mechanical pain hypersensitivity in male and female mice. *Nat. Neurosci.* 18, 1081–1083. doi: 10.1038/nn.4053

South, S. M., Kohno, T., Kaspar, B. K., Hegarty, D., Vissel, B., Drake, C. T., et al. (2003). A conditional deletion of the NR1 subunit of the NMDA receptor in adult spinal cord dorsal horn reduces NMDA currents and injury-induced pain. *J. Neurosci.* 23, 5031–5040. doi: 10.1523/jneurosci.23-12-05031.2003

Suo, Z. W., Liu, J. P., Xue, M., Yang, Y. H., Yang, X., Xie, J., et al. (2017). Striatal-enriched phosphatase 61 inhibited the nociceptive plasticity in spinal cord dorsal horn of rats. *Neuroscience* 352, 97–105. doi: 10.1016/j.neuroscience.2017.03.048

Temi, S., Rudyk, C., Armstrong, J., Landrigan, J. A., Dedek, C., Salmaso, N., et al. (2021). Differential expression of GluN2 NMDA receptor subunits in the dorsal horn of male and female rats. *Channels* 15, 179–192. doi: 10.1080/19336950.2020.1871205

Todd, A. J. (2010). Neuronal circuitry for pain processing in the dorsal horn. *Nat. Rev. Neurosci.* 11, 823–836. doi: 10.1038/nrn2947

Todd, A. J. (2015). Plasticity of inhibition in the spinal cord. *Handb. Exp. Pharmacol.* 227, 171–190. doi: 10.1007/978-3-662-46450-2_9

Todd, A. J. (2017). Identifying functional populations among the interneurons in laminae I-III of the spinal dorsal horn. *Mol. Pain* 13:1744806917693003. doi: 10.1177/1744806917693003

Tong, C. K., and MacDermott, A. B. (2014). Synaptic GluN2A and GluN2B containing NMDA receptors within the superficial dorsal horn activated following primary afferent stimulation. *J. Neurosci.* 34, 10808–10820. doi: 10.1523/JNEUROSCI.0145-14.2014

Weyerbacher, A. R., Xu, Q., Tamasdan, C., Shin, S. J., and Inturrisi, C. E. (2010). N-methyl-D-aspartate receptor (NMDAR) independent maintenance of inflammatory pain. *Pain* 148, 237–246. doi: 10.1016/j.pain.2009.11.003

Wong, H. H. W., Rannio, S., Jones, V., Thomazeau, A., and Sjöström, P. J. (2021). NMDA receptors in axons: there's no coincidence. *J. Physiol.* 599, 367–387. doi: 10.1113/JP280059

Woolf, C. J. (2011). Central sensitization: implications for the diagnosis and treatment of pain. *Pain* 152, S2–S15. doi: 10.1016/j.pain.2010.09.030

Woolf, C. J., and Thompson, S. W. N. (1991). The induction and maintenance of central sensitization is dependent on N-methyl-D-aspartic acid receptor activation; implications for the treatment of glun2apost-injury pain hypersensitivity states. *Pain* 44, 293–299. doi: 10.1016/0304-3959(91)90100-C

Xie, J. D., Chen, S. R., Chen, H., Zeng, W. A., and Pan, H. L. (2016). Presynaptic N-methyl-D-aspartate (n.d.) receptor activity is increased through protein kinase C in paclitaxel-induced neuropathic pain. *J. Biol. Chem.* 291, 19364–19373. doi: 10.1074/jbc.M116.732347

Yamamoto, T., and Yaksh, T. L. (1992a). Comparison of the antinociceptive effects of pre- and posttreatment with intrathecal morphine and MK801, an NMDA antagonist, on the formalin test in the rat. *Anesthesiology* 77, 757–763. doi: 10.1097/00000542-199210000-00021

Yamamoto, T., and Yaksh, T. L. (1992b). Studies on the spinal interaction of morphine and the NMDA antagonist MK-801 on the hyperesthesia observed in a rat model of sciatic mononeuropathy. *Neurosci. Lett.* 135, 67–70. doi: 10.1016/0304-3940(92)90137-V

Yan, X., Jiang, E., Gao, M., and Weng, H. R. (2013). Endogenous activation of presynaptic NMDA receptors enhances glutamate release from the primary afferents in the spinal dorsal horn in a rat model of neuropathic pain. *J. Physiol.* 591, 2001–2019. doi: 10.1113/jphysiol.2012.250522

Zeng, J., Thomson, L. M., Aicher, S. A., and Terman, G. W. (2006). Primary afferent NMDA receptors increase dorsal horn excitation and mediate opiate tolerance in neonatal rats. *J. Neurosci.* 26, 12033–12042. doi: 10.1523/JNEUROSCI.2530-06.2006

Zhang, G. F., Chen, S. R., Jin, D., Huang, Y., Chen, H., and Pan, H. L. (2021). a2d-1 upregulation in primary sensory neurons promotes NMDA receptor-mediated glutamatergic input in resiniferatoxin-induced neuropathy. *J. Neurosci.* 41, 5963–5978. doi: 10.1523/JNEUROSCI.0303-21.2021

Zhang, Y., and Jordan, J. M. (2010). Epidemiology of osteoarthritis. *Clin. Geriatr. Med.* 26, 355–369. doi: 10.1016/j.cger.2010.03.001

Zhao, Y. L., Chen, S. R., Chen, H., and Pan, H. L. (2012). Chronic opioid potentiates presynaptic but impairs postsynaptic N-methyl-D-aspartic acid receptor activity in spinal cords: implications for opioid hyperalgesia and tolerance. *J. Biol. Chem.* 287, 25073–25085. doi: 10.1074/jbc.M112.378737

Zimmerman, A. L., Kovatsis, E. M., Pozsgai, R. Y., Tasnim, A., Zhang, Q., and Ginty, D. D. (2019). Distinct modes of presynaptic inhibition of cutaneous afferents and their functions in behavior. *Neuron* 102, 420–434.e8. doi: 10.1016/J.NEURON.2019.02.002

Conflict of Interest: The authors declare that the research was conducted in the absence of any commercial or financial relationships that could be construed as a potential conflict of interest.

Publisher's Note: All claims expressed in this article are solely those of the authors and do not necessarily represent those of their affiliated organizations, or those of the publisher, the editors and the reviewers. Any product that may be evaluated in this article, or claim that may be made by its manufacturer, is not guaranteed or endorsed by the publisher.

frontiers | Frontiers in Molecular Neuroscience

ORIGINAL RESEARCH
published: 08 April 2022
doi: 10.3389/fnmol.2022.788620

Mutually Dependent Clustering of SynDIG4/PRRT1 and AMPA Receptor Subunits GluA1 and GluA2 in Heterologous Cells and Primary Neurons

*Kristopher E. Plambeck, Chun-Wei He, Hector H. Navarro and Elva Díaz**

Department of Pharmacology, University of California Davis School of Medicine, Davis, CA, United States

OPEN ACCESS

Edited by:
Dhrubajyoti Chowdhury, Yale University, United States

Reviewed by:
Mohiuddin Ahmad, University of Oklahoma Health Sciences Center, United States
David Soto, University of Barcelona, Spain

***Correspondence:**
Elva Díaz
ediaz@ucdavis.edu

Specialty section:
This article was submitted to Molecular Signalling and Pathways, a section of the journal Frontiers in Molecular Neuroscience

Received: *02 October 2021*
Accepted: *28 February 2022*
Published: *08 April 2022*

Citation:
Plambeck KE, He C-W, Navarro HH and Díaz E (2022) Mutually Dependent Clustering of SynDIG4/PRRT1 and AMPA Receptor Subunits GluA1 and GluA2 in Heterologous Cells and Primary Neurons. Front. Mol. Neurosci. 15:788620. doi: 10.3389/fnmol.2022.788620

Regulation of α-amino-3-hydroxy-5-methyl-4-isoxazolepropionic acid (AMPA)-type glutamate receptors (AMPARs) at synapses is a predominant mechanism for regulating synaptic strength. We identified the transmembrane protein synapse differentiation-induced gene 1 (SynDIG1; SD1) as an AMPAR interacting protein that regulates excitatory synaptic strength and AMPAR number both *in vitro* and *in vivo.* The related protein SynDIG4 (SD4; also known as PRRT1) was identified in several independent proteomic screens in complex with AMPARs, suggesting that it may function as an AMPAR auxiliary factor. Here, we show that the co-expression of SD4 with GluA1 or GluA2 homomeric AMPARs in COS cells leads to a 50 or 33% increase in the mean area of AMPAR puncta, respectively. This effect is accentuated when AMPAR puncta are stratified for co-localization with SD4, resulting in a 100 and 65% increase in GluA1 and GluA2 puncta, respectively. Chimeric proteins expressing only the membrane bound domain of SD4 co-expressed with full-length GluA1 or GluA2 recapitulated the effects of wild-type (WT) SD4. Additionally, the mean puncta area of GluA1 or GluA2 chimeras expressing the membrane and C-terminal domains increased significantly when co-localized with WT SD4. Similarly, the co-expression of GluA1 or GluA2 with SD4 results in a significant increase in the mean area of SD4 puncta co-localized with GluA1 or GluA2, respectively. Last, we observed a significant increase in the co-localization of SD4 with GluA1 after glycine induced long-term potentiation (LTP). The mean size of GluA1 puncta was significantly increased when stratified, indicating that co-localization with SD4 increases synaptic GluA1 cluster size during LTP. These data indicate mutually dependent clustering of SD4 and AMPAR subunits both in COS cells and primary hippocampal neurons, suggesting a mechanism for increased synaptic strength during chemical LTP.

Keywords: AMPA receptor (AMPAR), SynDIG4, PRRT1, SynDIG1, synaptic plasticity

INTRODUCTION

Neurons form precise connections known as synapses that are necessary for cell–cell communication. During excitatory synapse development, pre-synaptic axon terminals responsible for the export of signaling molecules pair with post-synaptic dendritic spines that contain glutamate receptors, scaffolding molecules, and cytoskeletal elements (McAllister, 2007). At excitatory synapses, there are two types of ionotropic glutamate receptors which are recruited to the synaptic site *via* different mechanisms (Lissin et al., 1998): N-methyl-D-aspartate receptors (NMDARs) and α-amino-3-hydroxy-5-methyl-4-isoxazolepropionic acid receptors (AMPARs). NMDARs are first recruited to the dendritic surface during early maturation of excitatory synapses while the later recruitment of AMPARs stabilize the synapse and represent a mature synaptic structure (Scheiffele, 2003). AMPARs are necessary for fast synaptic transmission, and changes in the number of synaptic AMPARs directly reflect changes in synaptic strength (Huganir and Nicoll, 2013). Previous studies have identified a diverse group of AMPAR interacting proteins necessary for the modulation of AMPAR biophysical properties and trafficking to the synapse (Díaz, 2010; Jackson and Nicoll, 2011; Jacobi and von Engelhardt, 2017). For example, the AMPAR auxiliary protein Stargazin, a member of the transmembrane AMPAR regulating protein (TARP) family TARP-γ2, has been observed to decrease the deactivation and desensitization rates of AMPARs, as well as increase forward trafficking of AMPARs to the cell surface (Chen et al., 2000). Stargazin/TARP-γ2 influences AMPARs through interaction with two distinct protein domains (Tomita et al., 2003, 2005), of which the transmembrane (TM) domains TM3 and TM4 and extracellular loop 2 of stargazin/TARP-γ2 have been found to be critically important (Ben-Yaacov et al., 2017). Additional AMPAR auxiliary proteins, such as the Cornichons (CNIHs) (Schwenk et al., 2009) and cysteine-knot AMPAR modulating proteins (CKAMPs) (von Engelhardt et al., 2010) have been shown to affect the functional properties of AMPARs. Therefore, AMPAR localization and channel properties are regulated by a wide array of distinct molecules.

The brain-specific type II transmembrane protein synapse differentiation-induced gene 1 (SynDIG1; SD1) was previously identified as an AMPAR interacting protein which regulates excitatory synapse development (Kalashnikova et al., 2010). Specifically, SD1 clusters with AMPARs in heterologous cells and modulates the number of functional GluA1 and GluA2 containing AMPARs at excitatory synapses. The knockdown of SD1 results in a decrease in the number and strength of excitatory synapses. However, SD1 does not affect the biophysical properties of AMPARs, such as deactivation and desensitization to glutamate (Lovero et al., 2013), indicating SD1 is not a typical auxiliary factor.

Synapse differentiation-induced gene 1 (SynDIG4; SD4), also known as proline-rich transmembrane protein 1 (PRRT1), was identified by three independent proteomic studies (von Engelhardt et al., 2010; Schwenk et al., 2012; Shanks et al., 2012) and demonstrates sequence similarity to SD1 (Kalashnikova et al., 2010). Surprisingly, SD4 is de-enriched at the post-synaptic density (PSD) and co-localizes with the AMPAR subunit GluA1 at extra-synaptic sites in primary neurons (Kirk et al., 2016), implying a role of SD4 outside of the PSD. SD4 has been shown to modify AMPAR gating kinetics in a subunit-dependent manner (Matt et al., 2018). Specifically, SD4 slows the deactivation of GluA1 homomers, as well as GluA1/A2 heteromeric AMPARs. Additionally, SD4 slows the desensitization of GluA1 homomers but not GluA1/A2 heteromers. Interestingly, these effects are potentiated when expressed with TARP-γ8 (Matt et al., 2018), indicating that SD4 may function in AMPAR complexes containing TARP-γ8. In support of this conclusion, a recent cryo-electron microscopy (cryo-EM) study demonstrated that SD4 is associated with native AMPAR complexes that contain both TARP-γ8 and CNIH-2 (Yu et al., 2021).

The primary goal of this study is to further elucidate the role of SD4 in regulating GluA1- and GluA2-containing AMPARs using a structure-function approach. The link between AMPAR subunits and SD4 is necessary to establish a mechanism by which SD4 may affect the localization and trafficking of AMPARs important for synaptic plasticity in the brain. We hypothesize that SD4 is necessary for establishing a reserve pool of AMPARs important for synaptic plasticity through its ability to cluster AMPARs at extra-synaptic sites. The present study identifies the regions sufficient for the clustering of SD4 and the AMPAR subunits GluA1 and GluA2 in heterologous COS cells. Intriguingly, the colocalization of SD4 and AMPAR subunits indicates mutually dependent clustering of AMPAR subunits and SD4, respectively. This observation is recapitulated in primary hippocampal neurons, suggesting a mechanism by which SD4 establishes a reserve pool of extrasynaptic AMPARs that can be employed for SD4-dependent synaptic plasticity.

MATERIALS AND METHODS

Antibodies

The following antibodies were used: mouse IgG1 anti-GluA1 [Neuromab; Cat# 75-327; RRID: AB_2315840; Immunocytochemistry (ICC) 1:200; Immunoblotting (IB) 1:2,000]; mouse IgG2a anti-SynDIG4 (NeuroMab; Cat# 73-409; RRID: AB_2491106; ICC 1:200; IB 1:2,000); mouse IgG2a anti-SynDIG1 (NeuroMab; Cat# 75-251; RRID: AB_10999753; ICC 1:200); rabbit anti- Interferon-induced transmembrane protein 3 (IFITM3) (ProteinTech; ICC 1:200; IB 1:2,000); rat anti-hemagglutinin (HA) (Roche; ICC 1:50; IB 1:1,000); guinea pig anti-vGlut1 (EMD Millipore; ICC 1:500); Alexa 488-conjugated anti-mouse IgG2a (Molecular Probes; ICC 1:200); Alexa 594-conjugated anti-rat (Jackson ImmunoResearch; ICC 1:200); Alexa 555-cross adsorbed anti-mouse IgG1 (Invitrogen; ICC 1:500); Alexa 649-conjugated anti-guinea pig (Jackson ImmunoResearch: ICC 1:500); mouse anti-beta tubulin (MilliporeSigma; Clone: AA2; IB 1:5,000); goat horseradish peroxidase (HRP) conjugated anti-rat (Invitrogen; IB 1:5,000); and goat HRP-conjugated anti-mouse (Invitrogen; IB 1:10,000).

TABLE 1 | Synapse differentiation-induced gene 4 (SD4)/IFITM3 chimeras.

HA-IFITM3/SD4	IFITM3	SD4
1) HA-IF-NTD/SD4-M	a.a. 1–59	a.a. 224–306
2) HA-SD4-NTD/IF-M	a.a. 60–137	a.a. 1–223

TABLE 2 | GluK2/GluA1 chimeras.

HA-K2/A1	GluK2	GluA1
1) M1-3,S2,M4,CT	a.a. 1–561	a.a. 537–907
2) M1-3,M4,CT	a.a. 1–561; a.a. 660–819	a.a. 537–631; a.a. 806–907
3) M1-3, CT	a.a. 1–561; a.a. 660–840	a.a. 537–631; a.a. 827–907
4) M1-3	a.a. 1–561; a.a. 660–908	a.a. 537–631
5) S2,M4,CT	a.a. 1–659	a.a. 632–907
6) M4,CT	a.a. 1–819	a.a. 806–907

Constructs

A full length version of rat SD4 coding sequence was amplified by PCR from pHM6 expression vector and subcloned into pRK5 vector backbone provided by our collaborator Dr. Yael Stern-Bach at the Hebrew University of Jerusalem, Jerusalem, Israel. A full length version of mouse SD1 was expressed using a previously generated pHM6 construct (Kalashnikova et al., 2010). pCMV-HA-mIFITM3 was a gift from Howard Hang & Jacob Yount (Addgene plasmid # 58389; http://n2t.net/addgene:58389; RRID: Addgene_58389). Full length mouse IFITM3 was obtained from AddGene (#58389). SD4/IFITM3 chimeras (**Table 1**) were generated by sequential PCR amplification using megaprimers. Full length wild-type (WT) GluA1 was provided from the Stern-Bach lab and subcloned from the pGEM vector to the pRK5 expression vector. DNA vectors expressing full length GluA2 and GluK2, as well as the GluK2/A1 (**Table 2**, chimera #2–4) and GluK2/A2 le 3, chimera #1 and 2) chimeras, were additionally provided by the Stern-Bach lab. Additional GluK2/A1 (**Table 2**, chimeras #1, 5, and 6) and GluK2/A2 (**Table 3**, chimera #3) constructs were generated by sequential PCR amplification using the megaprimer method. All constructs contain an in-frame HA tag at the N-terminus for detection. **Tables 1–3** identify the amino acid (a.a.) sequences of the indicated protein expressed within each chimeric molecule.

Cell Culture

COS Cells

The primate cell culture line COS-7 (ATCC CRL-1651) was used for all experiments in heterologous cells. COS cells were grown in COS media containing DMEM (Life Technologies) supplemented with 10% Fetal Bovine Serum (Fisher Scientific) and 1% Penicillin/Streptomycin (Life Technologies). Cells were cultured at 37°C with 5% CO_2.

Primary Neurons

Dissociated cultures of primary hippocampal neurons were generated from embryonic day 18 (E18) rat embryos as previously described (Kalashnikova et al., 2010). Cultures used an astrocyte feeder layer derived from rat cortex and grown to 70–90% confluency in 6-well plates in astrocyte plating medium (APM) containing 1X MEM, 10% donor horse serum, 0.6% glucose, and 5 ml pen/strep. Prior to hippocampal dissection, coverslips were treated with 1 M nitric acid and sterilized. Coverslips were then coated with 1 mg/ml poly-L-lysine (PLL) diluted in distilled water and incubated overnight at 37°C. After incubation, coverslips were washed 3 times with distilled water. Dissociated neurons were first cultured on coverslips in Neuronal Plating Media (NPM) containing 1X MEM, 10% donor horse serum, 0.45% glucose, 5 ml sodium pyruvate, and 5 ml pen/strep. After 6 h, neurons on coverslips were transferred to the astrocyte feeder layer that had been changed to Neuronal Maintenance Media (NMM) containing 1X neurobasal, 10 ml Glutamax, 5 ml sodium pyruvate, and 5 ml pen/strep. After 4 days, the anti-mitotic AraC was added at a final concentration of 5 μM. A half volume change of the NMM was performed every 5 days. Neurons were utilized at approximately days *in vitro* (DIV) 12–14 depending on confluency and maturity.

TABLE 3 | GluK2/GluA2 chimeras.

HA-K2/A2	GluK2	GluA2
1) M1-3,S2,M4,CT	a.a. 1–561	a.a. 543–883
2) M1-3,S2,M4	a.a. 1–561; a.a. 841–908	a.a. 543–838
3) M4,CT	a.a. 1–819	a.a. 810–883

Immunoblotting

COS cells were seeded in 6-well plates at a density of 300,000 cells per well in COS media. Transfection was performed with 2 μg of DNA using Lipofectamine 2000 (Invitrogen). Cells were lysed for protein extraction 24 h after transfection using a standard lysis buffer (150 mM NaCl, 50 mM Tris(hydroxymethyl)aminomethane (TRIS) pH 7.4, 5 mM ethylenediaminetetraacetic acid (EDTA), 1% Triton x-100, 1 mM phenylmethylsulfonyl fluoride (PMSF), and protease inhibitor cocktail). Cells were lifted using a cell scraper and then passed through a 22.5-gauge needle before transferring lysates to 1.5 ml microfuge tubes. Lysates were then transferred to a rotator at 4°C for 30 min. After 30 min, lysates were centrifuged at 12,000 rpm for 10 min at 4°C. Supernatant was removed and flash frozen in liquid nitrogen for long term storage. In preparation for immunoblotting, protein samples were thawed on ice. For all blots, 10 μg protein per sample was denatured at 95°C and loaded onto freshly poured 8% sodium dodecyl sulfate–polyacrylamide gel electrophoresis (SDS-PAGE). Gels were run for 90 min at 120 V and transferred to nitrocellulose membrane for 1 h at 100 V. Membranes were blocked in 5% milk diluted in tris-buffered saline with tween-20 (TBST) for 1 h. For testing the expression of AMPAR chimeras, membranes were incubated with both rat anti-HA antibodies and mouse anti-tubulin antibodies at 4°C overnight. For testing the expression of SD4/IFITM3 chimeras, membranes were incubated with anti-SD4, anti-IFITM3, and anti-tubulin antibodies at 4°C overnight. Membranes were washed with TBST and incubated in HRP conjugated goat anti-rat and HRP-conjugated goat anti-mouse secondary antibodies for 1 h at room temperature. Luminata Crescendo reagent was added to membrane for the direct detection of HRP signal (Azure Biosystems).

Immunocytochemistry

COS Cells

COS cells were plated in 6-well plates containing coverslips coated with poly-L-lysine (Sigma-Aldrich). Cells were plated at a density of 300,000 cells per well and cultured for 24 h prior to transfection. All transient transfection experiments contained a total of 2 μg of DNA (1.75 μg receptor and 250 ng of either SD4 or pRK5 empty vector) using Lipofectamine 2000 (Invitrogen) and cells were cultured for an additional 24 h. For live labeling, cells were first incubated at 4°C for 10 min. Cells were washed once with cold PBS and incubated in rat anti-HA antibody diluted in COS media for 20 min at 4°C. After primary staining, cells were washed three times with cold PBS and incubated in donkey Alexa 594-conjugated anti-rat secondary antibody diluted in COS media for 20 min. Cells were washed three times with cold PBS and then with warm COS media. Plates were transferred back to 37°C incubator for 30 min. Cells were washed with PBS and fixed in 4% paraformaldehyde (PFA) for 10 min.

For staining of total SD1 or total SD4, coverslips were incubated in 0.1% Triton-X100 diluted in PBS for 15 min. Cells were blocked with 5% milk in PBS for 30 min and incubated in primary antibody for 1.5 h at room temperature. Coverslips were washed three times with PBS and incubated in donkey Alexa 488-conjugated anti-mouse IgG2a for 1 h. Coverslips were washed three times with PBS and mounted on slides with Fluoromount G (Southern Biotech).

Primary Neurons

For chemical long-term potentiation (LTP), hippocampal neurons at DIV 12–14 were equilibrated in artificial cerebrospinal fluid (aCSF) containing 2 mM magnesium (Mg^{+2}) and 2 mM calcium (Ca^{+2}) at 37°C in incubator for 30 min. Neurons were washed with PBS and replaced with aCSF containing the treatment buffer (2 mM Ca^{+2}; 200 μM glycine; 20 μM bicuculine; 3 μM strychnine), or a vehicle control. Strychnine was diluted in DMSO while glycine and bicuculine were diluted in water, so an equivalent amount of dimethyl sulfoxide (DMSO) or water, respectively, was added as the vehicle control. Neurons were incubated at 37°C for 5 min for chemical-LTP induction. Coverslips were then transferred to a recovery buffer (aCSF w/Mg^{+2}; no drugs) for 20 min at 37°C. For labeling of synaptic GluA1, neurons were washed 3 times with PBS and incubated with anti-GluA1 antibody against the extracellular N-terminus diluted in PBS with 3% bovine serum albumin (BSA) at 37°C for 1 h. Cells were then washed with PBS, fixed with 4% PFA, and then permeabilized with 0.1% Triton X-100 for 15 min. Neurons were blocked with 10% BSA for 30 min. Neurons were then stained for total anti-SD4 and total anti-vGlut1 overnight in 3% BSA at 4°C. After incubation, coverslips were washed 3 times with PBS and incubated in secondary antibodies for each marker for 1 h at room temperature. Neurons were then washed 3 times with PBS and mounted on glass microscope slides for imaging.

Image Analysis

For quantitative analyses, images were taken using either an Olympus FluoView 1000 or Zeiss LSM510 confocal microscope with a 63 × /1.5 NA oil objective with identical settings for laser power, photomultiplier gain, and digital offset. Pinhole (1 AU) and resolution (1,024 × 1,024 pixels) were constant for all images.

Images were analyzed blinded to the experimental condition. Image files were imported into image analysis software (ImageJ) to determine the average size of clusters for each condition. Selected cells were cropped from the original images, saved blinded and subjected to the analysis by an individual not involved in the cell selection and blinding process. The threshold for each independent experiment is determined by averaging the thresholds of at least 25% of images within a dataset. Threshold values were determined by duplicating each image and adjusting the threshold of the duplicated image converted to black and white. Thresholds were determined such that all recognizable puncta were included in the analysis. The average threshold was then applied to all images within a dataset for cluster analysis by inserting values into a pre-written script run through the ImageJ software. The script separates the channels, applies the average threshold values, creates the mask overlay, and analyzes cluster parameters (number and size) defined by the mask. Clusters within the range of 0.1–3.5 μm^2 were measured. After data collection and the unblinding process, the puncta size of all signals was subjected to statistical analysis. For analysis of puncta size based on co-localization with SD4 (stratification analysis), co-localization was defined as overlap of $\geq$ 1 pixel. A mask overlay was then created using ImageJ by overlapping the two channels of sGluA1 and SD4. The colocalized puncta in the image representing the receptor coexpressed with SD4 were then used to select unambiguous single puncta manually in the receptor mask overlay. XY coordinates were used to confirm the selected puncta in the receptor mask overlay that corresponded with the colocalized puncta in the image for the receptor coexpressed with SD4. For figure preparation, signals were adjusted for all panels within a figure by using the equal linear adjustments of levels in Photoshop (Adobe Systems).

Statistical Analysis

Data were collected from at least two independent experiments and a minimum n = 10–15 cells per condition per experiment. All graphs and statistical analyses were generated using GraphPad Prism software. Graphs depict the data average and the standard error of the mean (SEM). Statistical significance was assessed by one-way ANOVA with *post-hoc* Tukey's test or Student's t-test. Significance is defined as $^{*}p < 0.05$; $^{**}p < 0.01$; $^{***}p < 0.001$; and $^{****}p < 0.0001$.

RESULTS

SD4 Clusters GluA1 and GluA2 Containing AMPA Receptors

To characterize the relationship between AMPARs and SD4, we used a clustering assay previously established within our lab (Kalashnikova et al., 2010). The full-length AMPAR subunits GluA1 and GluA2, as well as the kainate receptor subunit (GluK2), were expressed in heterologous COS cells either alone or

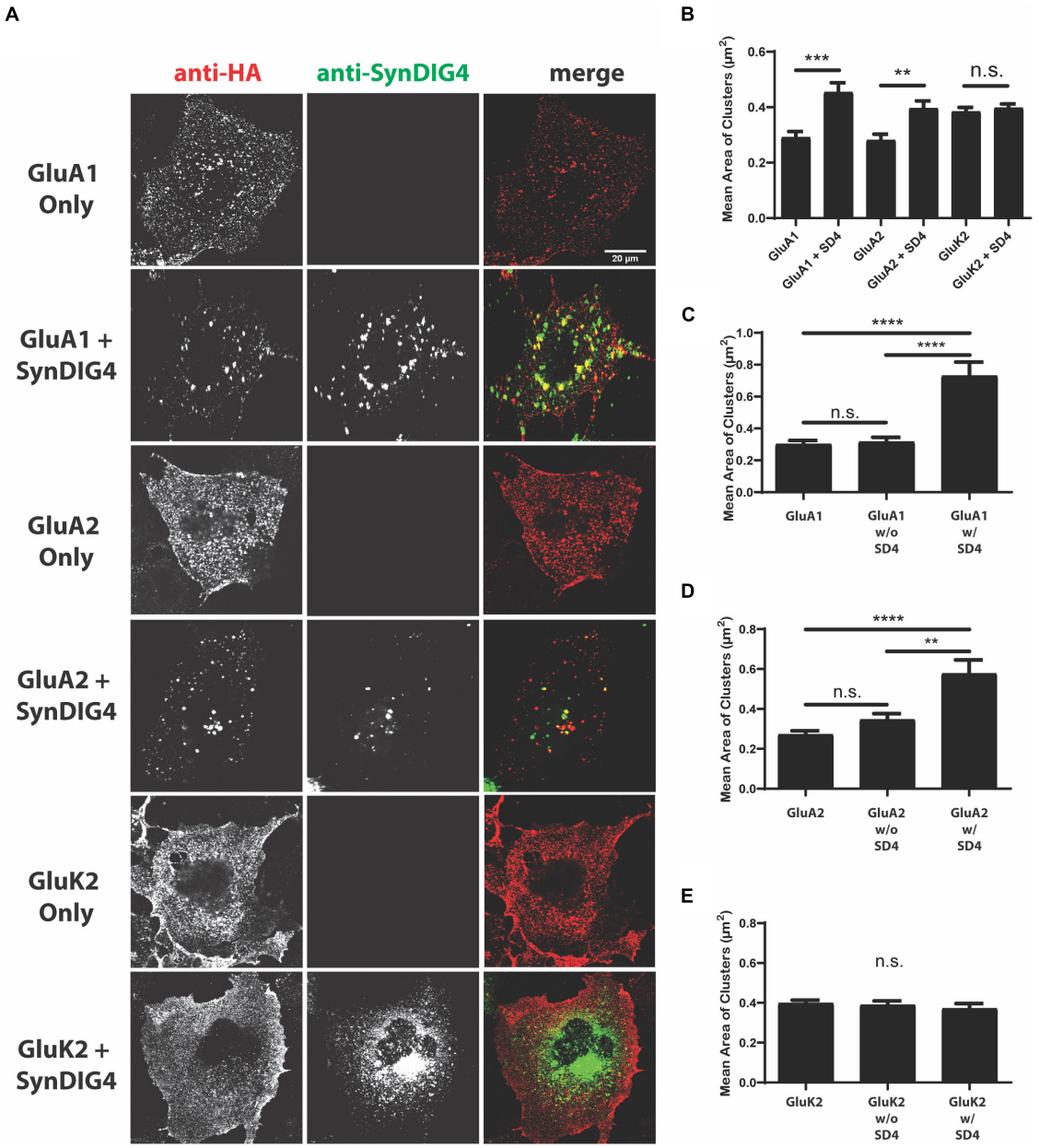

FIGURE 1 | Synapse differentiation-induced gene 4 (SD4) clusters GluA1 and GluA2-containing α-amino-3-hydroxy-5-methyl-4-isoxazolepropionic acid receptors (AMPARs). **(A)** Representative confocal images of COS cells transfected with either receptor alone, or co-transfected with both receptor and SD4. Cells were live labeled with anti-hemagglutinin (HA) antibodies against surface expressing receptors and anti-SD4 antibodies for total SD4. Scale bar = 20 μm. **(B)** Graph depicts the mean cluster size of GluA1 alone (n = 10), GluA1 + SD4 (n = 12), GluA2 alone (n = 16), GluA2 + SD4 (n = 10), GluK2 alone (n = 13), or GluK2 + SD4 (n = 11) puncta. **(C–E)** Graphs depict the stratification of GluA1 **(C)**, GluA2 **(D)**, or GluK2 **(E)** puncta either co-localized or not co-localized with SD4 compared with the average cluster size of receptor alone. Data are represented as mean cluster size ± SEM; n.s. not significant; $^{**}p < 0.01$; $^{***}p < 0.001$; and $^{****}p < 0.0001$; one-way ANOVA with *post-hoc* Tukey's test.

co-expressed with full-length HA-tagged SD4. GluK2 is predicted not to associate with SD4 and served as a negative control. Each receptor subunit contains an N-terminal HA tag for extracellular detection. COS cells were first live-labeled with anti-HA antibodies to examine the distribution of surface expressing GluA1, GluA2, or GluK2. The receptors have extracellular N-termini, while SD4 does not, so only surface GluA1, GluA2, or GluK2 were labeled. After fixation and permeabilization, cells were stained with anti-SD4 antibodies for total SD4. It is important to note that SD4 is a type II transmembrane protein while GluA1 and GluA2 are type I transmembrane proteins; therefore, the HA epitope for the live-labeling of GluA1 or GluA2

is not accessible to HA-SD4 even when the anti-HA antibody is internalized because the HA-tag on SD4 faces the cytoplasm while the anti-HA antibody remains lumenal. Furthermore, the anti-HA antibody used for the surface labeling of HA-GluA1 or HA-GluA2 does not label HA-SD4 when expressed alone (as shown below).

We observed diffuse and even distribution of GluA1, GluA2, and GluK2 when expressed alone. When co-expressed with SD4, a change in the overall distribution of both GluA1 and GluA2 was observed (**Figure 1**). No difference was observed when GluK2 was co-expressed with SD4, indicating the specificity of SD4 for AMPARs (**Figure 1A**). Quantification indicates a significant increase in the mean cluster size of GluA1 and GluA2 puncta when co-expressed with SD4 compared with receptor alone (**Figure 1B**). Although GluK2 puncta are larger at baseline, there is no significant change in puncta size when co-expressed with SD4 (**Figure 1B**).

We noted a distribution of GluA1 or GluA2 cluster sizes in SD4 co-expressing cells. To determine whether cluster size was related to overlap with SD4, which was not captured in the previous analysis, we stratified populations in co-expressing cells into two groups representing glutamate receptor puncta co-localized with SD4 (w/ SD4) or not co-localized with SD4 (w/o SD4). The stratification of GluA1 puncta co-localized with SD4 showed that the mean cluster size is significantly greater when SD4 and GluA1 are co-localized compared to GluA1 expressed alone (**Figure 1C**). In contrast, the size of puncta not co-localized with SD4 were not significantly different compared with GluA1 alone (**Figure 1C**). In addition, the mean size of GluA2 clusters is significantly greater when co-localized with SD4, while non-colocalized clusters are not significantly different compared with GluA2 alone (**Figure 1D**). No significant differences were observed in the size of GluK2 clusters co-localized with SD4 or not co-localized compared with GluK2 alone (**Figure 1E**). These results provide evidence that the co-expression of SD4 is sufficient to re-distribute and cluster GluA1 and GluA2-containing AMPARs in heterologous cells, and the increased cluster size is dependent on co-localization with SD4.

The Proline-Rich N-Terminus of SD4 Is Dispensable for Clustering With GluA1 and GluA2

To identify the region of SD4 sufficient for clustering with GluA1 or GluA2, we generated chimeric proteins by swapping domains between SD4 and the distantly related Dispanin family (Sällman Almén et al., 2012) member IFITM3 with a similar topology (Yount et al., 2010; Ling et al., 2016). One chimera was generated using the intracellular N-terminal region of SD4 and the C-terminal domains of IFITM3, such as the hydrophobic segment that does not span the lipid bilayer, the small intracellular loop, the transmembrane domain, and the short extracellular portion (SD4-NTD/IF-M), and a second chimera was generated using the intracellular N-terminal region of IFITM3 and the corresponding C-terminal domains of SD4 (IF-NTD/SD4-M) (**Figure 2A** and **Table 1**). For brevity, we refer to the C-terminal domains as the "membrane associated region." Constructs were first verified by immunoblot with antibodies that only recognize the N-terminus of their respective proteins (**Figure 2B**). Therefore, signal is only present when the N-terminus is expressed.

Furthermore, GluA1 was expressed in COS cells either alone, or co-expressed with full-length SD4, SD4-NTD/IF-M, or IF-NTD/SD4-M (**Figure 2C**). We observed no difference in the mean cluster size of GluA1 populations either co-localized or not co-localized with SD4-NTD/IF-M compared with GluA1 alone (**Figure 2D**). However, the stratification of GluA1 populations indicated a significant increase in the mean size of GluA1 clusters when co-localized with IF-NTD/SD4-M compared with GluA1 alone (**Figure 2E**). Next, GluA2 was expressed in COS cells either alone, or co-expressed with either IF/SD4 chimeras (**Figure 2F**). The stratification of GluA2 populations co-localized or not co-localized with SD4-NTD/IF-M resulted in no change in the mean size of GluA2 clusters (**Figure 2G**). However, we observed a significant increase in the mean size of GluA2 clusters when co-localized with IF-NTD/SD4-TM compared with GluA2 alone (**Figure 2H**).

These results indicate that the intracellular proline-rich N-terminal portion of SD4 is dispensable for clustering with GluA1 and GluA2. Furthermore, the C-terminal portion of SD4, which consists primarily of membrane associated regions, is sufficient for clustering with GluA1- and GluA2-containing AMPARs, and that clustering of AMPARs is dependent on co-localization with SD4.

The N-Terminus of GluA1 Is Dispensable for Clustering With SD4

To identify the region of GluA1 that is sufficient for clustering with SD4, we generated chimeric GluA1 proteins using the homologous domains of GluK2 (**Table 2**). The expressions of all GluK2/GluA1 chimeras were verified by immunoblot (**Figure 3A**). The chimeras were then transfected and expressed in COS cells either alone or with full-length SD4 (**Figures 3B–F**). The quantification of mean area of clusters shows an increase in puncta size when SD4 is co-expressed with GluA1, but no significant difference when co-expressed with the chimera expressing the M1-3, S2, M4, and CT domains of GluA1 (**Figure 3G**). However, the stratification of GluK2/A1/M1-3/S2/M4/CT chimeric puncta (**Figure 3B**) depicts a significant increase in puncta size when co-localized with SD4 (**Figure 3H**). Therefore, we conclude that the N-terminus of GluA1 is dispensable for clustering with SD4, and cluster size is dependent on co-localization with SD4.

The N-Terminus of GluA2 Is Dispensable for Clustering With SD4

We next generated GluA2 chimeras using the homologous domains of GluK2 (**Table 3**). An expression of GluA2 chimeras was verified by immunoblot (**Figure 4A**). All chimeras were transfected in COS cells either alone or with full-length SD4 (**Figures 4B–D**). We found that only the chimera expressing the M1-3, S2, M4, and CT domains of GluA2 resulted in an altered distribution when co-expressed with SD4 (**Figure 4B**).

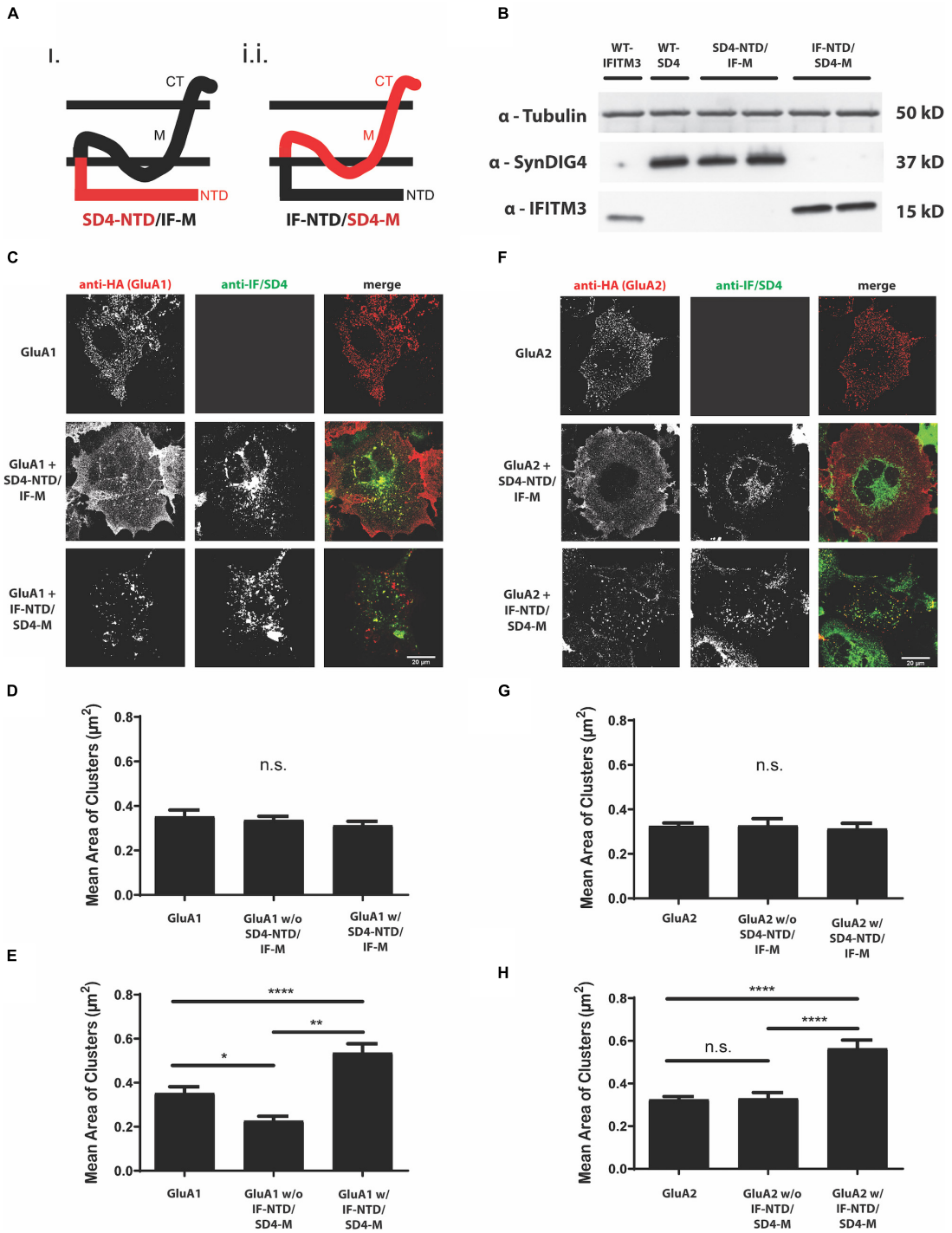

FIGURE 2 | The proline rich N-terminus of SD4 is dispensable for clustering with GluA1 and GluA2. **(A)** Schematic depicting the chimeric protein structures. Chimeras were generated expressing either (i) the N-terminus of SD4 and membrane domain of IFITM3 (SD4-NTD/IF-M) or (ii) the N-terminus of IFITM3 and membrane domain of SD4 (IF-NTD/SD4-M) (as shown in **Table 1** of Methods). **(B)** Immunoblot of COS cell lysates transfected with SD4 and IFITM3 chimeras. β-tubulin was used as the loading control. **(C)** Representative confocal images depict either GluA1 expressed alone or co-expressed with either IF/SD4 chimera. Scale bar = 20 μm. **(D,E)** Graph depicts the mean cluster size of GluA1 puncta from the stratification of GluA1 co-localized or not co-localized with SD4-NTD/IF-M chimeras **(D)** or IF-NTD/SD4-M chimeras **(E)** compared with GluA1 alone. GluA1 alone (n = 10), GluA1 + SD4-NTD/IF-M (n = 12), and GluA1 + IF-NTD/SD4-M (n = 12). **(F)** Representative confocal images of GluA2 alone or co-expressed with IF/SD4 chimeras. Scale bar = 20 μm. **(G,H)** Graph depicts the mean cluster size of GluA2 puncta from the stratification of GluA2 co-localized or not co-localized with SD4-NTD/IF-M chimeras **(G)** or IF-NTD/SD4-M chimeras **(H)** compared with GluA2 alone. GluA2 alone (n = 13), GluA2 + SD4-NTD/IF-M (n = 12), and GluA2 + IF-NTD/SD4-M (n = 16). Data are represented as mean cluster size ± SEM; n.s. not significant; *$p < 0.05$; **$p < 0.01$; ****$p < 0.0001$; one-way ANOVA with *post-hoc* Tukey's test.

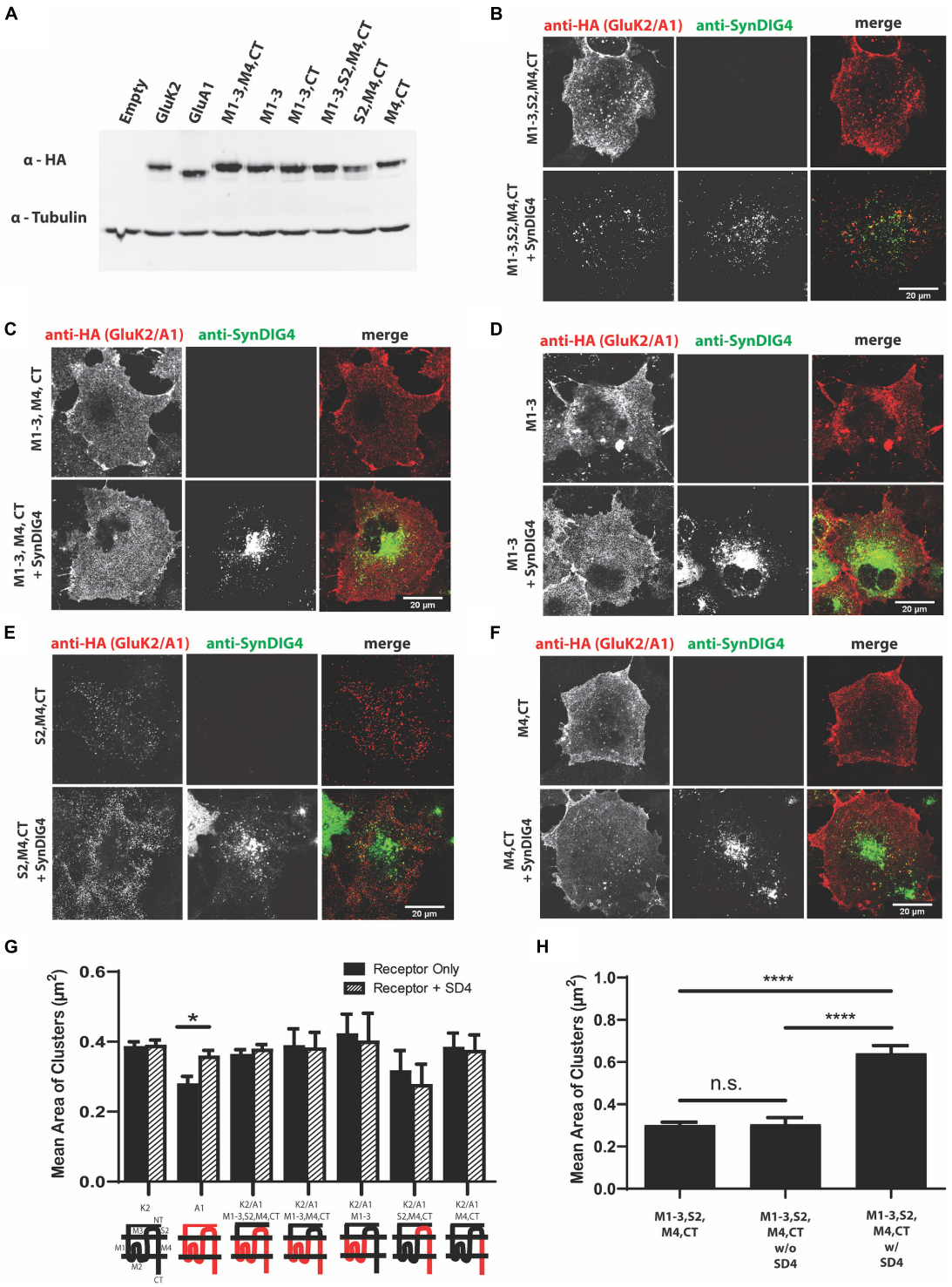

FIGURE 3 | The N-terminus of GluA1 is dispensable for clustering with SD4. **(A)** Immunoblot depicting expression of GluK2/GluA1 chimeras. Homologous domains of GluA1 were inserted into the backbone of GluK2 (as shown in **Table 2** of Methods). β-tubulin was used as the loading control. **(B–F)** Representative confocal images of COS cells transfected with either a GluK2/A1 chimeric receptor alone, or co-transfected with SD4. Scale bar = 20 µm. **(G)** Graph depicts the mean area of clusters when GluK2, GluA1, and each GluK2/A1 chimera is expressed either alone or co-expressed with SD4. **(H)** Graph depicts the mean cluster size of M1-3, S2, M4, CT chimera stratified for either co-localized or not co-localized with SD4. M1-3, S2, M4 alone (n = 11), M1-3, S2, M4 w/o SD4 (n = 13), M1-3, S2, M4 w/ SD4 (n = 13). Data are represented as mean ± SEM; n.s. not significant; *$p < 0.05$; ****$p < 0.0001$; one-way ANOVA with *post-hoc* Tukey's test.

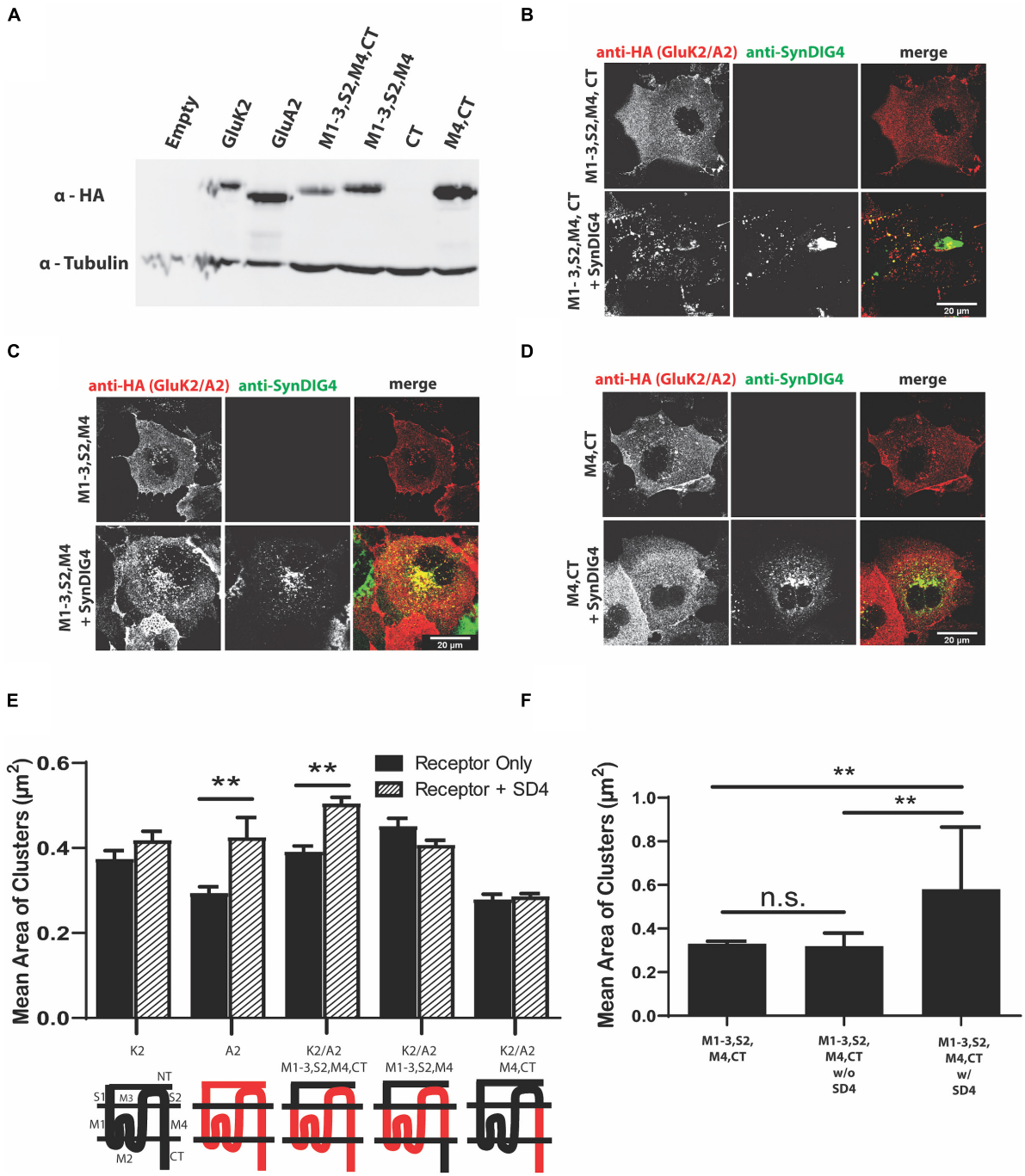

FIGURE 4 | The N-terminus of GluA2 is dispensable for clustering with SD4. **(A)** Immunoblot depicting expression of GluK2/GluA2 chimeras. Homologous domains of GluA2 were inserted into the backbone of GluK2 (as shown in **Table 3** of Methods). β-tubulin was used as the loading control. **(B–D)** Representative confocal images of COS cells transfected with either a GluK2/A2 chimeric receptor alone, or co-transfected with SD4. Scale bar = 20 μm. **(E)** Graph depicts the mean area of clusters when GluK2, GluA2, and each GluK2/A2 chimera is expressed either alone or co-expressed with SD4. **(F)** Graph depicts mean the area of M1-3, S2, M4, CT chimera clusters stratified for either co-localized or non-colocalized with SD4. M1-3, S2, M4, CT alone (n = 14), M1-3, S2, M4, CT w/o SD4 (n = 11), M1-3, S2, M4, CT w/ SD4 (n = 13). Data are represented as mean ± SEM; n.s. not significant; $^{**}p < 0.01$; one-way ANOVA with *post-hoc* Tukey's test.

Additionally, the GluK2/A2/M1-3/S2/M4 chimera, where the GluA2-CT domain was not present, resulted in a loss of the clustering phenotype (**Figure 4C**). Therefore, these experiments show the importance of GluA2 C-terminal domain for clustering with SD4. The quantification of mean area of clusters shows a significant increase in cluster size when SD4 is co-expressed

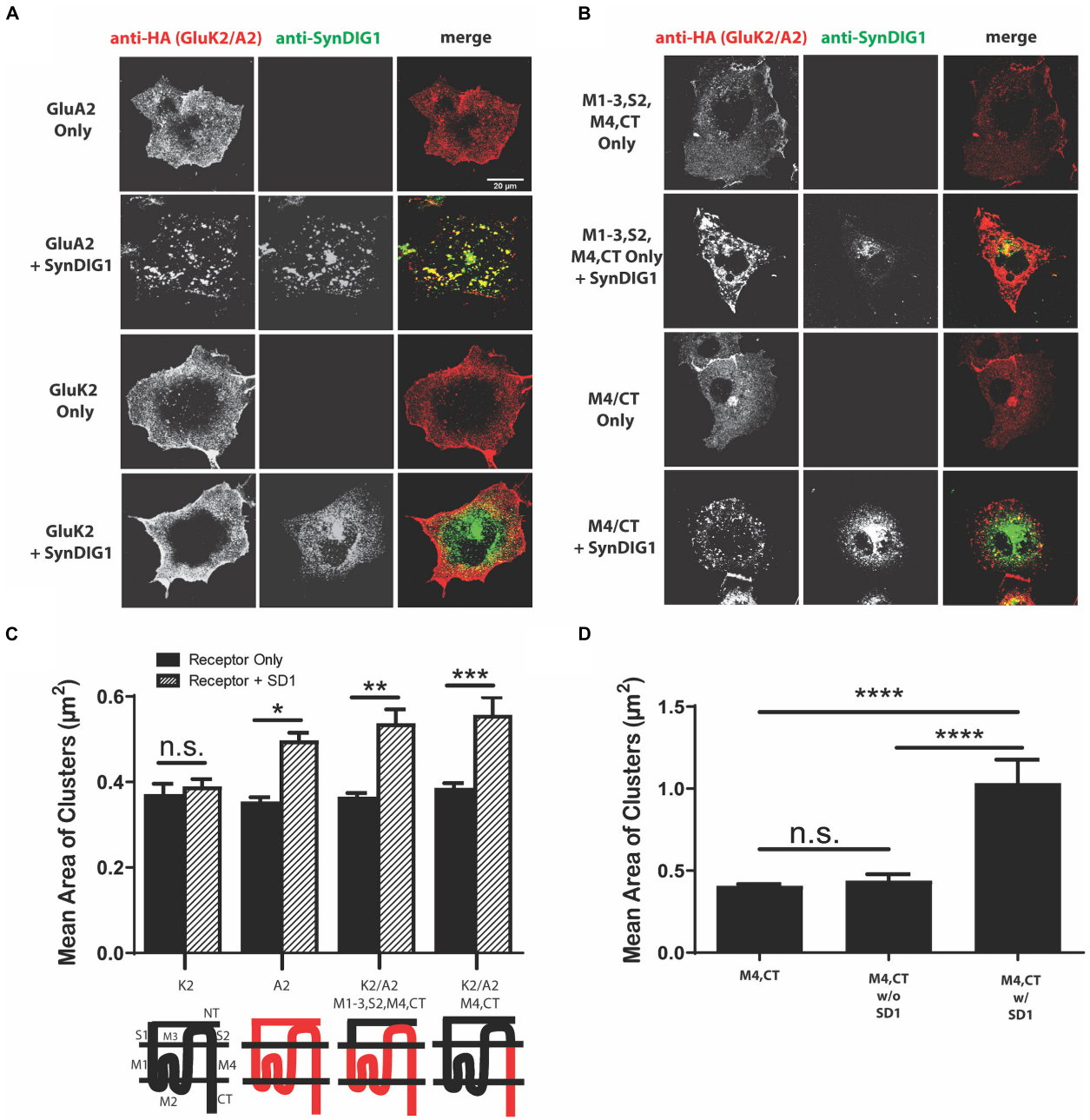

FIGURE 5 | The M4 and C-terminus of GluA2 is sufficient for clustering with synapse differentiation-induced Gene 1 (SD1). **(A)** Representative confocal images of COS cells transfected with GluA2 alone, GluK2 alone, or co-transfected with GluA2 or GluK2 and SD1. Scale bar = 20 µm. **(B)** Representative confocal images of chimeras expressing the M1-3, S2, M4, CT and M4, CT domains of GluA2 either alone or co-expressed with SD1. Scale bar = 20 µm. **(C)** Graph depicts the mean area of clusters when GluK2, GluA2, and each GluK2/A2 chimera is expressed either alone or co-expressed with SD1. **(D)** Graph depicts the mean area of M4, CT chimera clusters stratified for either co-localized or non-colocalized with SD1. M4, CT alone (n = 13), M4, CT w/o SD1 (n = 13), M4, CT w/ SD1 (n = 11). Data are represented as mean ± SEM; n.s. not significant; *$p < 0.05$; **$p < 0.01$; ***$p < 0.001$; ****$p < 0.0001$; one-way ANOVA with *post-hoc* Tukey's test.

with either full-length GluA2 or the GluK2/A2/M1-3/S2/ M4/CT chimera (**Figure 4E**). Furthermore, the stratification of puncta from **Figure 4B** shows a significant increase in puncta area only when co-localized with SD4 (**Figure 4F**). Therefore, we conclude that the N-terminus of GluA2 is dispensable for clustering with SD4, and cluster size is dependent on co-localization with SD4.

The M4 and C-Terminus of GluA2 Is Sufficient for Clustering With SD1

For comparison, we sought to identify a region of AMPAR necessary for clustering with the SD4-related family member SD1. Full-length GluA2 had previously been observed to cluster with SD1 (Kalashnikova et al., 2010); therefore, GluA2 and GluK2 were used as positive and negative controls, respectively. We

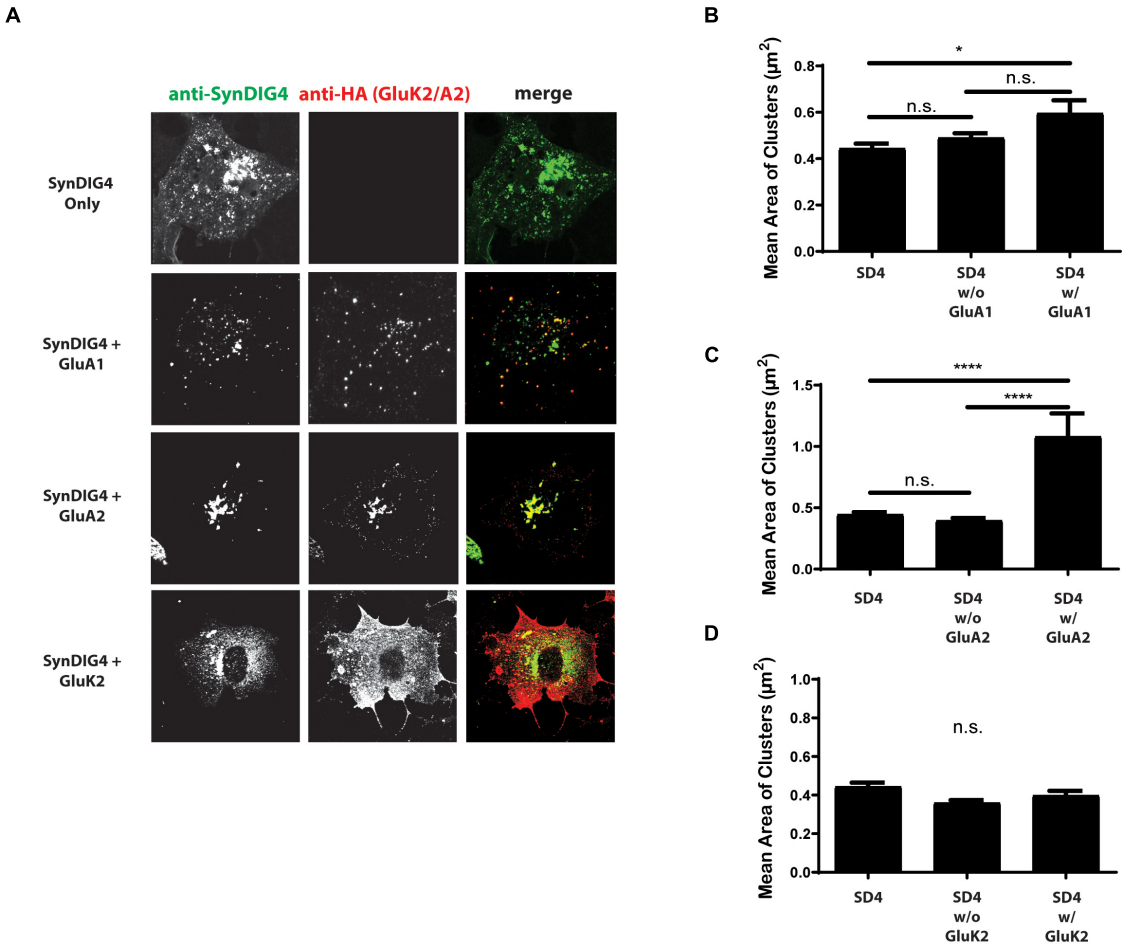

FIGURE 6 | Synapse differentiation-induced gene 4 cluster size increases when colocalized with GluA2. **(A)** Representative confocal images of COS cells expressing SD4 alone, or SD4 co-expressed with either GluA1, GluA2 or GluK2. Scale bar = 20 μm. **(B–D)** Graph depicts the mean area of SD4 clusters stratified for either co-localized or non-colocalized with GluA1 **(B)**, GluA2 **(C)**, or GluK2 **(D)**. **(B)** SD4 alone (n = 12), SD4 w/o A1 (n = 10), SD4 w/ A1 (n = 10). **(C)** SD4 alone (n = 12), SD4 w/o A2 (n = 10), SD4 w/ A2 (n = 10). Data are represented as mean ± SEM; n.s. not significant; *$p < 0.05$; ****$p < 0.0001$; one-way ANOVA with *post-hoc* Tukey's test.

observed altered distribution of GluA2, but not GluK2, when co-expressed with SD1 (**Figure 5A**). Next, we co-expressed two of the key GluA2 chimeras from **Figure 4**. Similar to SD4, we observed clustering when the GluK2/A2/M1-3/S2/M4/CT chimera was co-expressed with SD1. However, in contrast to SD4, we observed clustering when the GluK2/A2/M4/CT chimera was co-expressed with SD1 (**Figure 5B**). Quantification depicts a significant increase in the mean area of clusters when SD1 is co-expressed with GluK2/A2/M1-3/S2/M4/CT and GluK2/A2/M4/CT, but not with GluK2 (**Figure 5C**). Last, the stratification of M4 and CT chimera puncta co-localized with SD1 results in a significant increase in the mean area of clusters (**Figure 5D**). Therefore, the M4 and CT of GluA2 is sufficient for clustering with SD1.

SD4 Cluster Size Increases When Colocalized With GluA1 and GluA2

Next, we were interested in whether the co-expression of AMPARs with SD4 results in a reciprocal increase in the cluster size of SD4. For these experiments, SD4 was expressed in COS cells either alone, or co-expressed with either GluA1, GluA2, or GluK2 (**Figure 6A**). The stratification of SD4 puncta co-localized with GluA1 results in a significant increase in the mean cluster size of SD4 puncta co-localized with GluA1 compared with SD4 alone (**Figure 6B**). Additionally, the mean cluster size of SD4 puncta co-localized with GluA2 is also significantly increased (**Figure 6C**). We observed no difference in the mean cluster size of SD4 puncta whether co-localized or not-colocalized with GluK2 compared with SD4 alone (**Figure 6D**). We conclude that not only does the co-localization of SD4 with AMPARs increase the mean cluster size of the receptor, but colocalization with AMPARs also significantly increase the cluster size of SD4.

SD4 Clustering of GluA1 and GluA2 Is Temperature Dependent

A clustering of GluA2 by SD1 requires a 37°C incubation after the surface labeling at 4°C (Kalashnikova et al., 2010). This observation suggests that a biological process, such as endocytosis is necessary for clustering by SD1. Then, we were

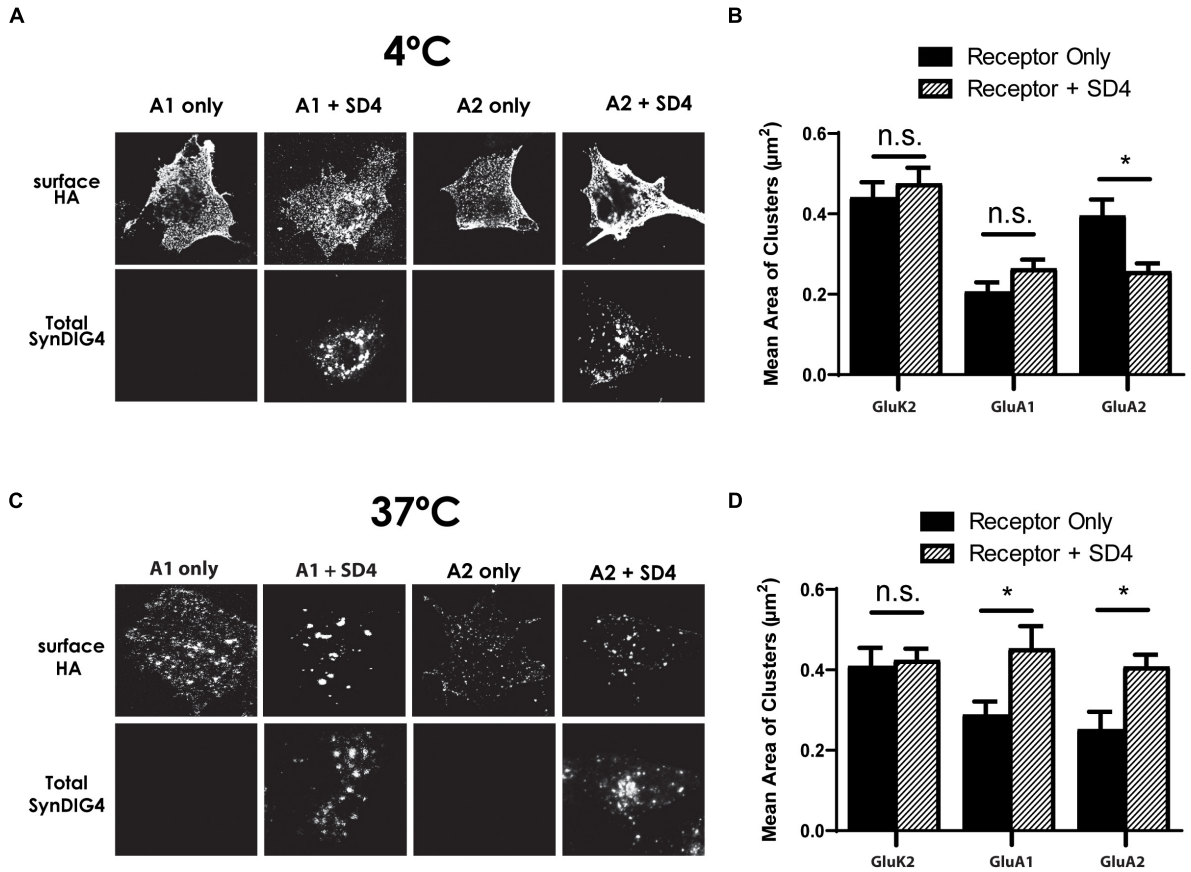

FIGURE 7 | Synapse differentiation-induced gene 4 clustering of GluA1 and GluA2 requires incubation at 37°C. **(A)** Representative confocal images of COS cells expressing either GluK2, GluA1, or GluA2 lone or co-expressed with SD4 after incubation at 4°C. **(B)** Graph depicts the mean area of receptor clusters. GluK2 alone (n = 14), GluK2 + SD4 (n = 12), GluA1 alone (n = 10), GluA1 + SD4 (n = 14), GluA2 alone (n = 12), GluA2 + SD4 (n = 13). **(C)** Representative confocal images of COS cells expressing either GluK2, GluA1, or GluA2 alone or co-expressed with SD4 after incubation at 37°C. GluK2 alone (n = 11), GluK2 + SD4 (n = 16), GluA1 alone (n = 10), GluA1 + SD4 (n = 10), GluA2 alone (n = 10), and GluA2 + SD4 (n = 10). **(D)** Graph depicts mean area of receptor clusters. Data are represented as mean ± SEM; n.s. not significant; *$p < 0.05$; one-way ANOVA with *post-hoc* Tukey's test.

interested to determine whether SD4 clustering of AMPARs is temperature dependent. For these experiments, duplicate plates of COS cells expressing GluK2, GluA1, or GluA1 either alone or co-expressed with SD4 were prepared. For the surface labeling of receptors, all plates were incubated at 4°C. Next, one plate was transferred to a 37°C incubator, while the other plate remained at 4°C. After incubation, coverslips were fixed and imaged. We observed that incubation at 4°C does not result in a change of distribution for any of the receptors, either alone or co-expressed with SD4 (**Figure 7A**). Quantification indicates no significant increase in the mean area of clusters after the 4°C incubation (**Figure 7B**). However, incubation at 37°C resulted in the clustering of receptors as expected (**Figure 7C**). Quantification shows a significant increase in the mean area of clusters when either GluA1 or GluA2 are co-expressed with SD4, but not GluK2 (**Figure 7D**). Therefore, we conclude that the endocytosis of surface labeled AMPARs is most likely to be necessary for clustering with SD4.

Co-localization of SD4 With Synaptic GluA1 Is Increased After Chemical-Long-Term Potentiation

To test the role of SD4-dependent AMPAR clustering in synaptic plasticity, we utilized the primary culture of dissociated rat hippocampal neurons. Neurons were treated with 200 μM glycine or vehicle in aCSF without magnesium at 37°C for 5 min to induce chemical-LTP. Neurons were then transferred to aCSF recovery buffer for 20 min and then stained with anti-GluA1 antibody at 37°C for 1 h. Neurons were then fixed, permeabilized, and stained for total SD4 and vGlut1 (**Figure 8A**; three representative stretches from three individual neurons are shown). The percentage of synaptic GluA1 puncta (defined as overlap with the pre-synaptic marker vGlut1) increased by 2-fold after glycine treatment compared with vehicle (**Figure 8B**), indicating successful chemical-LTP induction. Additionally, the percentage of synaptic GluA1 puncta co-localized with SD4 significantly increased after chemical-LTP (**Figure 8B**),

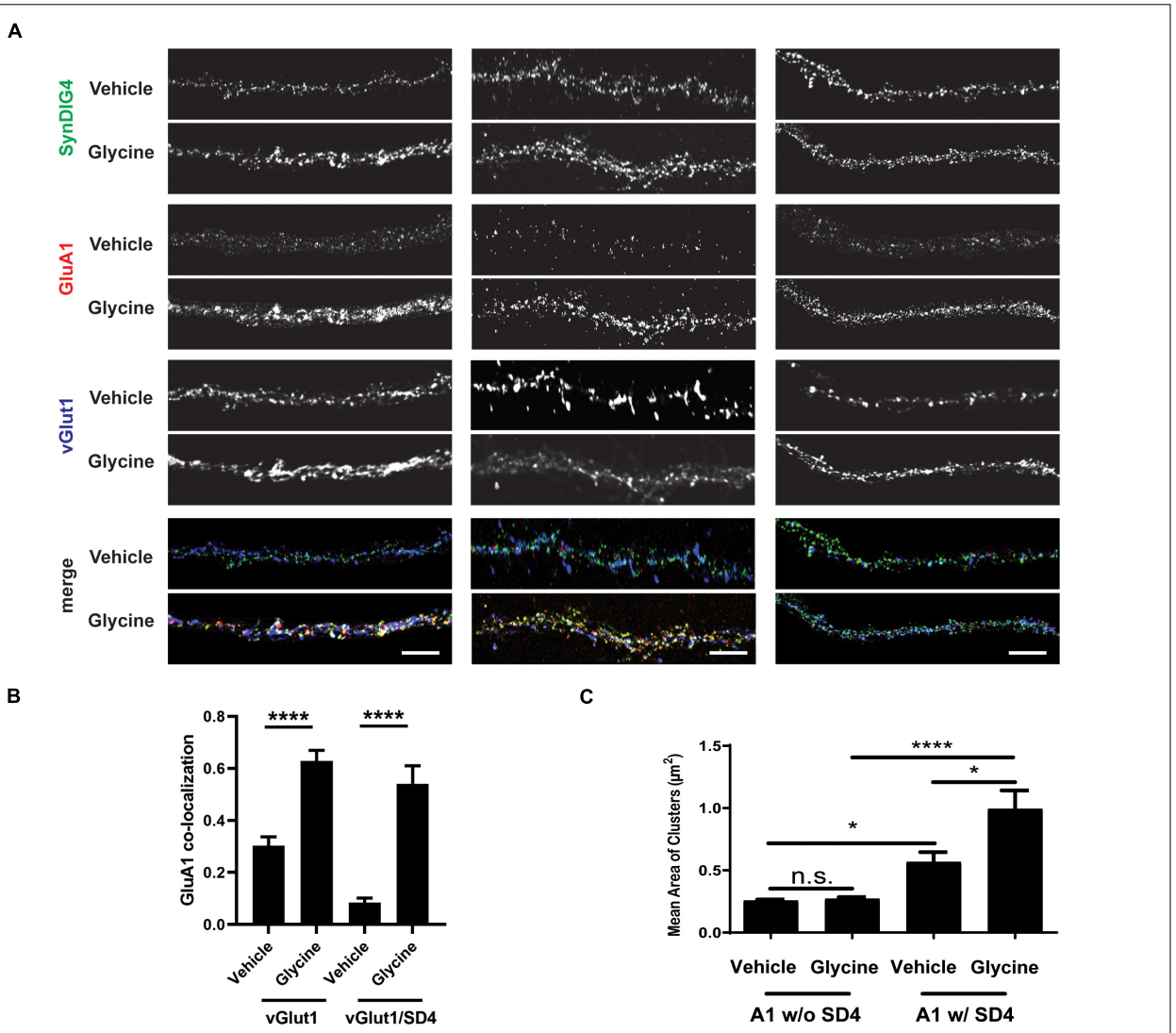

FIGURE 8 | Co-localization of SD4 with synaptic GluA1 is increased after chemical-LTP. **(A)** Representative confocal images of dendritic stretches from primary rat hippocampal neurons at DIV13. Three dendritic stretches are shown for each condition. Neurons were treated with either vehicle or 200 μM glycine in artificial cerebrospinal fluid (aCSF) without magnesium at 37°C for 5 min. Neurons were transferred to aCSF recovery buffer (without drugs) for 20 min and then stained with anti-GluA1 antibody at 37°C for 1 h. Neurons were then fixed, permeabilized, and stained for total SD4 and vGlut1. **(B)** Quantification of co-localization between GluA1, SD4, and vGlut1 upon incubation with vehicle or glycine. **(C)** Quantification of mean area of GluA1 clusters either co-localized or non-colocalized with SD4 after treatment with vehicle or glycine. Data represented as mean ± SEM; n.s., non-significant; $n = 15$ cells per condition; $^{*}p < 0.05$; $^{****}p < 0.0001$; Student's *t*-test **(B)**; one-way ANOVA with *post-hoc* Tukey's test. **(C)** Scale bar = 5 μm.

suggesting that at least a portion of SD4 redistributes to the synapse during glycine induced chemical-LTP. The average number of vGlut1 puncta per stretch was equivalent (vehicle: 27.02 ± 2.39, $n = 42$; glycine: 25.27 ± 1.73, $n = 45$; $p = 0.553$), indicating that the increased percentage of synaptic GluA1 which colocalizes with SD4 is not a result of changes in vGlut1.

Next, we looked at changes in the mean area of GluA1 clusters as a result of chemical-LTP. We stratified these data to determine whether changes in the size of these clusters are dependent on co-localization with SD4. We observed that there was no change in the mean area of GluA1 clusters not colocalized with SD4 after treatment with glycine compared with vehicle (**Figure 8C**). Interestingly, there was a significant increase in the size of GluA1 clusters during vehicle treatment only when GluA1 was co-localized with SD4. Furthermore, we observed a significant increase in the mean area of GluA1 clusters co-localized with SD4 after glycine induced chemical-LTP (**Figure 8C**). As a result of these experiments, we conclude that the co-localization of SD4 with synaptic GluA1 increases after chemical-LTP, and this co-localization results in an increase in the mean area of GluA1 clusters.

DISCUSSION

Previously, we showed that SD4 alters AMPAR biophysical properties in a subunit-specific manner (Matt et al., 2018),

indicating a direct and specific interaction with AMPARs. Indeed, SD4 has been identified in multiple independent proteomic studies as a component of AMPAR complexes (von Engelhardt et al., 2010; Schwenk et al., 2012; Shanks et al., 2012) as well as recent structural studies of native AMPAR complexes from brain (Yu et al., 2021). Although present in synaptosomal membranes, SD4 is de-enriched in the PSD where the majority of SD4 overlaps with GluA1 outside of synapses (Kirk et al., 2016), suggesting that SD4 associates primarily with extra-synaptic AMPARs. Here we present evidence that SD4 and GluA1 or GluA2 AMPARs bi-directionally increase the cluster size of each other in heterologous cells. Distinct regions within SD4, GluA1 and GluA2 are critical for this mutually dependent clustering activity. Intriguingly, the bi-directional clustering requires incubation at 37°C, suggesting that an endocytosis of surface labeled AMPARs is most likely necessary for clustering with SD4. Indeed, a recent study demonstrated overlap of SD4 with early endosomes in hippocampal neurons (Martin et al., 2021), consistent with its role in clustering AMPARs that have been internalized. Importantly, the increased cluster size of GluA1 that overlaps with SD4 is observed in primary hippocampal neurons upon chemical-LTP, suggesting that this clustering activity is a mechanism underlying the strengthening of synapses during synaptic plasticity. Our current model is that the SD4-induced clustering of AMPARs occurs intracellularly after endocytosis to establish a reserve pool of intracellular extrasynaptic AMPARs that can be deployed to the cell surface during LTP. These intracellular clusters of AMPARs co-localized with SD4 presumably remain intracellular in heterologous cells. In addition, others have shown that SD4 KO mice are deficient for LTD (Troyano-Rodriguez et al., 2019); thus, the intracellular clustering of AMPARs could also be employed during LTD as a mechanism to restrict the surface accumulation of AMPARs perhaps upon differential regulation. Additional experiments beyond the scope of this study are needed to investigate the effects of SD4 on AMPAR trafficking in neurons during synaptic plasticity.

Synapse differentiation-induced gene 4 is predicted to contain two membrane-associated domains, with only one that spans the membrane, a large proline-rich intracellular N-terminus, a small intracellular loop, and a small extracellular C-terminus (Kirk et al., 2016), confirmed in a recent study (Martin et al., 2021). Proline residues have often been linked to protein–protein interactions (Kay et al., 2000; Freund et al., 2008). However, our results indicate that only the C-terminal region, such as the membrane bound domains, intracellular loop, and small extracellular tail of SD4 is important for clustering with GluA1 or GluA2. Others reported that SD4 is able to co-immunoprecipitate a small amount (2% of input) of GluA1 or GluA2 when coexpressed in HEK293 cells (Martin et al., 2021). Furthermore, deletion of the intracellular loop, the transmembrane domain, and the small extracellular tail of SD4 eliminated the observed co-immunoprecipitation (Martin et al., 2021), consistent with our results indicating that the proline-rich intracellular N-terminal region is not required for clustering. SD4 does not contain a PDZ binding motif and it is not enriched in the PSD (Kirk et al., 2016). The proline-rich domain may be important for interaction with other auxiliary factors or scaffolds necessary for trafficking and anchoring at synapses. Additional experiments will address this possibility.

To identify the GluA1 AMPAR domain sufficient for clustering with SD4, we used GluK2/GluA1 chimeras which swap homologous protein domains between receptors. All GluK2/GluA1 chimeras lacked the NT domain of GluA1. The total mean area of GluA1 puncta was not significantly larger compared with the chimeras when co-expressed with SD4. However, we did observe some clustering with the GluK2/A1/M1-3/S2/M4/CT chimera when expressed alone, which may have occluded any increase in cluster size in this analysis. In support of this possibility, the mean cluster size of GluK2/A1/M1-3/S2/M4/CT chimeric puncta is significantly increased by the stratification of puncta co-localized with SD4, while no increase is observed by the stratification of other chimeras co-localized with SD4. We observed altered distribution of the receptor only when the entire membrane, S2, and CT domains (GluK2/A1/M1-3/S2/M4/CT) were present and co-localized with SD4 in COS cells. Therefore, we conclude that the NT domain is dispensable, while the entire membrane bound domain of GluA1, in addition to the S2 and CT domains, are necessary for clustering by SD4.

Similar to the GluA1 chimeras, we used GluK2/GluA2 chimeras to identify the region sufficient for clustering with SD4. All GluK2/GluA2 chimeras lacked the NT domains of GluA2. We observed a change in distribution when the entire membrane bound domain, S2 domain, and CT domain of GluA2 (GluK2/A2/M1-3/S2/M4/CT) was expressed with SD4. In these experiments, we saw a significant increase in mean puncta size, with no significant differences with any additional chimeras. Interestingly, we observed that clustering was lost when the CT domain was absent, indicating an importance of the CT for clustering with SD4. Additionally, we did not observe clustering when the M1-3 and S2 domains were absent. We conclude that the entire membrane bound domain of GluA2, in addition to the S2 and CT domains, is necessary for clustering by SD4.

Interestingly, we observed that GluA1 and GluA2 also affected the cluster size of SD4 when co-expressed in COS cells. These results coincide with an increase in cluster size when stratified for co-localization with GluA1 or GluA2. We conclude that the cluster size of both SD4 and AMPAR puncta is significantly increased only when co-localized in COS cells, indicating a bi-directional interaction mechanism.

We were not able to identify a smaller domain of GluA1 or GluA2 sufficient for clustering with SD4. One possibility is that there are multiple regions within the AMPAR necessary for interacting with SD4. Pioneering work by Ben-Yaacov and colleagues using domain swaps demonstrated that AMPAR interaction with stargazin/TARP-γ2 primarily involves the AMPAR membrane domains M1 and M4 of neighboring subunits, with important contributions by the CT (Ben-Yaacov et al., 2017). Structural studies with cryo-EM support these functional results (Twomey et al., 2016;

Zhao et al., 2016; Zhang et al., 2021). Attempts to express three constructs in COS cells were technically problematic; therefore, we could not pursue this approach. Since SD4 has been shown to affect the biophysical properties of GluA1 and GluA2-containing AMPARs (Matt et al., 2018), in future experiments we plan to continue the structure-function approach with electrophysiology to narrow down the critical domain. Moreover, the cryo-EM structures of native AMPARs indicates that SD4 is associated with AMPAR complexes that contain TARP-γ8 and CNIH-2 (Yu et al., 2021). Thus, it will be interesting to determine if SD4-dependent AMPAR clustering is influenced by the presence of TARP-γ8 and/or CNIH-2, or whether SD4 clusters bi-directionally with either of these two auxiliary factors. Furthermore, the co-expression of multiple auxiliary subunits might increase the efficiency of co-immunoprecipitation of AMPAR subunits observed with SD4 alone (Martin et al., 2021). It should be noted that clustering of AMPARs required the co-expression of stargazin/TARP-γ2 and PSD-95; stargazin/TARP-γ2 alone was not sufficient to change the distribution of AMPARs in heterologous cells (Chen et al., 2000). Thus, the mutually dependent clustering activity of SD4 with AMPARs might be unique to this auxiliary factor.

Intriguingly, the mutually dependent clustering requires incubation at 37°C, suggesting that endocytosis of surface labeled AMPARs is most likely necessary for clustering with SD4. In primary hippocampal neurons at steady-state most SD4 overlaps with endosomal markers (Martin et al., 2021) but some protein is available for surface labeling (Kirk et al., 2016; Martin et al., 2021). Thus, it is tempting to speculate that SD4 captures AMPARs at the plasma membrane for clustering *via* transport through an endocytic compartment. Current studies are addressing this possibility. Importantly, the increased cluster size of GluA1 that overlaps with SD4 is observed in primary hippocampal neurons upon chemical-LTP, suggesting that this clustering activity is a mechanism underlying the strengthening of synapses during synaptic plasticity. As the SD4-induced clustering of AMPARs likely occurs after endocytosis in heterologous cells, these intracellular clusters of AMPARs co-localized with SD4 are capable of being deployed to synapses upon chemical-LTP in hippocampal neurons. In addition, SD4 KO mice are deficient for LTD (Troyano-Rodriguez et al., 2019); thus, the intracellular clustering of AMPARs could also be employed during LTD as a mechanism to restrict the surface accumulation of AMPARs. We propose that SD4 establishes an intracellular pool of extrasynaptic AMPARs through the bidirectional clustering of SD4 and AMPARs necessary for regulating synaptic strength.

Our results demonstrate the effects of SD4 on clustering both GluA1 and GluA2 in heterologous cells. In SD4 KO mice, we observed significant reduction in both extrasynaptic GluA2 and extrasynaptic GluA1 puncta density (Matt et al., 2018), consistent with our observations in COS cells. As GluA1/2 heteromers constitute 95% of extrasynaptic AMPAR pool under baseline conditions (Lu et al., 2009), this suggests that SD4 is required to maintain extrasynaptic GluA1/2. Interestingly, certain effects of SD4 were specific for GluA1. For example, puncta size and intensity of both extrasynaptic and synaptic GluA1 (but not GluA2) were slightly reduced in SD4 KO neurons (Matt et al., 2018), indicating an additional role for SD4 in regulating GluA1. GluA1 homomers account for most, if not all, calcium-permeable AMPARs (CP-AMPARs) in hippocampus, which are largely absent at PSDs under basal conditions; however, under certain conditions, CP-AMPARs become transiently detectable at postsynaptic sites including the induction of LTP (Plant et al., 2006) and LTD (Sanderson et al., 2016). Thus, it is tempting to speculate that SD4 might establish reserve pools of GluA1 homomers that are transiently targeted to synapses during synaptic plasticity.

We were able to identify a minimal domain of GluA2 responsible for the interaction with the related protein SD1. SD4 and SD1 share approximately 35% overall amino acid sequence similarity, with higher similarity occurring within the membrane bound domain (Kalashnikova et al., 2010). However, while SD4 and SD1 share similarity only SD4 has been shown to affect the biophysical properties of GluA1 and GluA2-containing AMPARs (Lovero et al., 2013; Matt et al., 2018). The co-expression of GluA2 with SD1 shows the significant clustering of GluA2 when compared to GluA2 expression alone, which fits with previously observed results (Kalashnikova et al., 2010). Conversely, the co-expression of GluK2 with SD1 did not exhibit a clustering phenotype. Using the same GluK2/GluA2 chimeras, we observed the clustering of GluK2/A2/M1-3/S2/M4/CT chimera when co-expressed with SD1. In contrast to SD4, we observed clustering when SD1 was co-expressed with the GluK2/GluA2 chimera expressing only the M4 and CT domain of GluA2. We conclude that the minimal M4/CT domain of GluA2 is sufficient for clustering with SD1, which potentially explains the lack of SD1 effects on biophysical properties.

Most of the excitatory transmission in the brain is mediated by AMPA receptors. Furthermore, many neuropsychiatric and neurological disorders, such as Alzheimer's disease and depression, can be characterized by abnormal AMPA receptor content and trafficking leading to impaired synapse function (Babaei, 2021; Ge and Wang, 2021; Kadriu et al., 2021). Therefore, understanding the complete mechanism behind AMPA receptor function is important for understanding disease. Continuing studies utilizing cultured hippocampal neurons and transgenic mouse models will be important to establish the role of SD4 trafficking to the synapse that may yield a better understanding of underlying mechanism behind neuropsychiatric and neurological disorders.

DATA AVAILABILITY STATEMENT

The raw data supporting the conclusions of this article will be made available by the authors, without undue reservation.

ETHICS STATEMENT

The animal study was reviewed and approved by the UC Davis Institutional Animal Care and Use Committee (IACUC).

AUTHOR CONTRIBUTIONS

KP and ED: methodology and writing. KP, C-WH, and ED: investigation. KP, C-WH, HN, and ED: formal analysis. ED: funding acquisition and supervision. All authors contributed to the article and approved the submitted version.

FUNDING

This project was funded by grants to ED from the Whitehall Foundation (2015-05-106), the National Science Foundation (1322302), and the National Institute of Mental Health (MH119347). HN was a PREP@UCD Scholar funded by the National Institutes of Health (R25GM116690).

ACKNOWLEDGMENTS

We thank members of Diaz, Gray, Hell, and Zito labs, especially CM Meyer and DJ Speca, at UC Davis for comments and suggestions throughout the project as well as Yael Stern-Bach at the Hebrew University of Jerusalem for constructs and advice. pCMV-HA-mIFITM3 was a gift from Howard Hang & Jacob Yount (Addgene plasmid #58389; http://n2t.net/addgene:58389; RRID:Addgene_58389).

REFERENCES

Babaei, P. (2021). NMDA and AMPA receptors dysregulation in Alzheimer's disease. *Eur. J. Pharmacol.* 908:174310. doi: 10.1016/j.ejphar.2021.174310

Ben-Yaacov, A., Gillor, M., Haham, T., Parsai, A., Qneibi, M., and Stern-Bach, Y. (2017). Molecular mechanism of AMPA receptor modulation by TARP/stargazin. *Neuron* 93, 1126.e4–1137.e4. doi: 10.1016/j.neuron.2017.01.032

Chen, L., Chetkovich, D. M., Petralia, R. S., Sweeney, N. T., Kawasaki, Y., Wenthold, R. J., et al. (2000). Stargazin regulates synaptic targeting of AMPA receptors by two distinct mechanisms. *Nature* 408, 936–943. doi: 10.1038/35050030

Díaz, E. (2010). Regulation of AMPA receptors by transmembrane accessory proteins. *Eur. J. Neurosci.* 32, 261–268. doi: 10.1111/j.1460-9568.2010.07357.x

Freund, C., Schmalz, H.-G., Sticht, J., and Kühne, R. (2008). Proline-rich sequence recognition domains (PRD): ligands, function and inhibition. *Handb. Exp. Pharmacol.* 186, 407–429. doi: 10.1007/978-3-540-72843-6_17

Ge, Y., and Wang, Y. T. (2021). GluA1-homomeric AMPA receptor in synaptic plasticity and neurological diseases. *Neuropharmacology* 197:108708. doi: 10.1016/j.neuropharm.2021.108708

Huganir, R. L., and Nicoll, R. A. (2013). AMPARs and synaptic plasticity: the last 25 years. *Neuron* 80, 704–717. doi: 10.1016/j.neuron.2013.10.025

Jackson, A. C., and Nicoll, R. A. (2011). The expanding social network of ionotropic glutamate receptors: TARPs and other transmembrane auxiliary subunits. *Neuron* 70, 178–199. doi: 10.1016/j.neuron.2011.04.007

Jacobi, E., and von Engelhardt, J. (2017). Diversity in AMPA receptor complexes in the brain. *Curr. Opin. Neurobiol.* 45, 32–38. doi: 10.1016/j.conb.2017.03.001

Kalashnikova, E., Lorca, R. A., Kaur, I., Barisone, G. A., Li, B., Ishimaru, T., et al. (2010). SynDIG1: an activity-regulated, AMPA- receptor-interacting transmembrane protein that regulates excitatory synapse development. *Neuron* 65, 80–93. doi: 10.1016/j.neuron.2009.12.021

Kadriu, B., Musazzi, L., Johnston, J. N., Kalynchuk, L. E., Caruncho, H. J., Popoli, M., et al. (2021). Positive AMPA receptor modulation in the treatment of neuropsychiatric disorders: a long and winding road. *Drug Discov. Today* 26, 2816–2838. doi: 10.1016/j.drudis.2021.07.027

Kay, B. K., Williamson, M. P., and Sudol, M. (2000). The importance of being proline: the interaction of proline-rich motifs in signaling proteins with their cognate domains. *FASEB J. Off. Publ. Fed. Am. Soc. Exp. Biol.* 14, 231–241. doi: 10.1096/fasebj.14.2.231

Kirk, L. M., Ti, S. W., Bishop, H. I., Orozco-Llamas, M., Pham, M., Trimmer, J. S., et al. (2016). Distribution of the SynDIG4/proline-rich transmembrane protein 1 in rat brain. *J. Comp. Neurol.* 524, 2266–2280. doi: 10.1002/cne.23945

Ling, S., Zhang, C., Wang, W., Cai, X., Yu, L., Wu, F., et al. (2016). Combined approaches of EPR and NMR illustrate only one transmembrane helix in the human IFITM3. *Sci. Rep.* 6:24029. doi: 10.1038/srep24029

Lissin, D. V., Gomperts, S. N., Carroll, R. C., Christine, C. W., Kalman, D., Kitamura, M., et al. (1998). Activity differentially regulates the surface expression of synaptic AMPA and NMDA glutamate receptors. *Proc. Natl. Acad. Sci. U.S.A.* 95, 7097–7102. doi: 10.1073/pnas.95.12.7097

Lovero, K. L., Blankenship, S. M., Shi, Y., and Nicoll, R. A. (2013). SynDIG1 promotes excitatory synaptogenesis independent of AMPA receptor trafficking and biophysical regulation. *PLoS One* 8:e66171. doi: 10.1371/journal.pone.0066171

Lu, W., Shi, Y., Jackson, A. C., Bjorgan, K., During, M. J., Sprengel, R., et al. (2009). Subunit composition of synaptic AMPA receptors revealed by a single-cell genetic approach. *Neuron* 62, 254–268. doi: 10.1016/j.neuron.2009.02.027

Matt, L., Kirk, L. M., Chenaux, G., Speca, D. J., Puhger, K. R., Pride, M. C., et al. (2018). SynDIG4/Prrt1 is required for excitatory synapse development and plasticity underlying cognitive function. *Cell Rep.* 22, 2246–2253. doi: 10.1016/j.celrep.2018.02.026

Martin, E. E., Wleklinski, E., Hoang, H. T. M., and Ahmad, M. (2021). Interaction and subcellular association of PRRT1/SynDIG4 with AMPA receptors. *Front. Synaptic Neurosci.* 13:705664. doi: 10.3389/fnsyn.2021.705664

McAllister, A. K. (2007). Dynamic aspects of CNS synapse formation. *Annu. Rev. Neurosci.* 30, 425–450. doi: 10.1146/annurev.neuro.29.051605.112830

Plant, K., Pelkey, K. A., Bortolotto, Z. A., Morita, D., Terashima, A., McBain, C. J., et al. (2006). Transient incorporation of native GluR2-lacking AMPA receptors during hippocampal long-term potentiation. *Nat. Neurosci.* 9, 602–604. doi: 10.1038/nn1678

Sällman Almén, M., Bringeland, N., Fredriksson, R., and Schiöth, H. B. (2012). The dispanins: a novel gene family of ancient origin that contains 14 human members. *PLoS One* 7:e31961. doi: 10.1371/journal.pone.0031961

Sanderson, J. L., Gorski, J. A., and Dell'Acqua, M. L. N. M. D. A. (2016). Receptor-dependent LTD requires transient synaptic incorporation of Ca^{2+}-permeable AMPARs mediated by AKAP150-anchored PKA and calcineurin. *Neuron* 89, 1000–1015. doi: 10.1016/j.neuron.2016.01.043

Scheiffele, P. (2003). Cell-cell signaling during synapse formation in the CNS. *Annu. Rev. Neurosci.* 26, 485–508. doi: 10.1146/annurev.neuro.26.043002.094940

Schwenk, J., Harmel, N., Brechet, A., Zolles, G., Berkefeld, H., Müller, C. S., et al. (2012). High-resolution proteomics unravel architecture and molecular diversity of native AMPA receptor complexes. *Neuron* 74, 621–633. doi: 10.1016/j.neuron.2012.03.034

Schwenk, J., Harmel, N., Zolles, G., Bildl, W., Kulik, A., Heimrich, B., et al. (2009). Functional proteomics identify cornichon proteins as auxiliary subunits of AMPA receptors. *Science* 323, 1313–1319. doi: 10.1126/science.1167852

Shanks, N. F., Savas, J. N., Maruo, T., Cais, O., Hirao, A., Oe, S., et al. (2012). Differences in AMPA and kainate receptor interactomes facilitate identification of AMPA receptor auxiliary subunit GSG1L. *Cell Rep.* 1, 590–598. doi: 10.1016/j.celrep.2012.05.004

Tomita, S., Adesnik, H., Sekiguchi, M., Zhang, W., Wada, K., Howe, J. R., et al. (2005). Stargazin modulates AMPA receptor gating and trafficking by distinct domains. *Nature* 435, 1052–1058. doi: 10.1038/nature03624

Tomita, S., Chen, L., Kawasaki, Y., Petralia, R. S., Wenthold, R. J., Nicoll, R. A., et al. (2003). Functional studies and distribution define a family of transmembrane AMPA receptor regulatory proteins. *J. Cell Biol.* 161, 805–816. doi: 10.1083/jcb.200212116

Troyano-Rodriguez, E., Mann, S., Ullah, R., and Ahmad, M. (2019). PRRT1 regulates basal and plasticity-induced AMPA receptor trafficking. *Mol. Cell. Neurosci.* 98, 155–163. doi: 10.1016/j.mcn.2019.06.008

Twomey, E. C., Yelshanskaya, M. V., Grassucci, R. A., Frank, J., and Sobolevsky, A. I. (2016). Elucidation of AMPA receptor-stargazin complexes by cryo-electron microscopy. *Science* 353, 83–86. doi: 10.1126/science.aaf8411

von Engelhardt, J., Mack, V., Sprengel, R., Kavenstock, N., Li, K. W., Stern-Bach, Y., et al. (2010). CKAMP44: a brain-specific protein attenuating short-term synaptic plasticity in the dentate gyrus. *Science* 327, 1518–1522. doi: 10.1126/science.1184178

Yount, J. S., Moltedo, B., Yang, Y.-Y., Charron, G., Moran, T. M., López, C. B., et al. (2010). Palmitoylome profiling reveals s-palmitoylation-dependent antiviral activity of IFITM3. *Nat. Chem. Biol.* 6, 610–614. doi: 10.1038/nchembio.405

Yu, J., Rao, P., Clark, S., Mitra, J., Ha, T., and Gouaux, E. (2021). Hippocampal AMPA receptor assemblies and mechanism of allosteric inhibition. *Nature* 594, 448–453. doi: 10.1038/s41586-021-03540-0

Zhang, D., Watson, J. F., Matthews, P. M., Cais, O., and Greger, I. H. (2021). Gating and modulation of a hetero-octameric AMPA glutamate receptor. *Nature* 594, 454–458. doi: 10.1038/s41586-021-03613-0

Zhao, Y., Chen, S., Yoshioka, C., Baconguis, I., and Gouaux, E. (2016). Architecture of fully occupied GluA2 AMPA receptor-TARP complex elucidated by Cryo-EM. *Nature* 536, 108–111. doi: 10.1038/nature18961

Conflict of Interest: The authors declare that the research was conducted in the absence of any commercial or financial relationships that could be construed as a potential conflict of interest.

Publisher's Note: All claims expressed in this article are solely those of the authors and do not necessarily represent those of their affiliated organizations, or those of the publisher, the editors and the reviewers. Any product that may be evaluated in this article, or claim that may be made by its manufacturer, is not guaranteed or endorsed by the publisher.

frontiers | Frontiers in Molecular Neuroscience

ORIGINAL RESEARCH
published: 03 May 2022
doi: 10.3389/fnmol.2022.880382

Stress Elicits Contrasting Effects on Rac1-Cofilin Signaling in the Hippocampus and Amygdala

*Mihika Bose, Mohammad Sarfaraz Nawaz, Rakhi Pal and Sumantra Chattarji**

National Centre for Biological Sciences, Tata Institute of Fundamental Research, Bangalore, India

There is accumulating evidence for contrasting patterns of stress-induced morphological and physiological plasticity in glutamatergic synapses of the hippocampus and amygdala. The same chronic stress that leads to the formation of dendritic spines in the basolateral amygdala (BLA) of rats, leads to a loss of spines in the hippocampus. However, the molecular underpinnings of these divergent effects of stress on dendritic spines are not well understood. Since the activity of the Rho GTPase Rac1 and the actin-depolymerizing factor cofilin are known to play a pivotal role in spine morphogenesis, we investigated if alterations in this signaling pathway reflect the differential effects of stress on spine plasticity in the hippocampus and amygdala. A day after the end of chronic immobilization stress (2 h/day for 10 days), we found a reduction in the activity of Rac1, as well as its effector p21-activated kinase 1 (PAK1), in the rat hippocampus. These changes, in turn, decreased cofilin phosphorylation alongside a reduction in the levels of profilin isoforms. In striking contrast, the same chronic stress increased Rac1, PAK1 activity, cofilin phosphorylation, and profilin levels in the BLA, which is consistent with enhanced actin polymerization leading to spinogenesis in the BLA. In the hippocampus, on the other hand, the same stress caused the opposite changes, the functional consequences of which would be actin depolymerization leading to the elimination of spines. Together, these findings reveal a role for brain-region specific differences in the dysregulation of Rac1-to-cofilin signaling in the effects of repeated stress on two brain areas that are implicated in the emotional and cognitive symptoms of stress-related psychiatric disorders.

Keywords: chronic stress, synaptic plasticity, dendrite, spine, p-21 activated kinase

OPEN ACCESS

Edited by:
James P. Clement, Jawaharlal Nehru Centre for Advanced Scientific Research, India

Reviewed by:
Sourav Banerjee, National Brain Research Centre (NBRC), India
Laxmi T. Rao, National Institute of Mental Health and Neurosciences (NIMHANS), India

****Correspondence:***
Sumantra Chattarji
shona@ncbs.res.in

Specialty section:
This article was submitted to Molecular Signalling and Pathways, a section of the journal Frontiers in Molecular Neuroscience

Received: *21 February 2022*
Accepted: *07 April 2022*
Published: *03 May 2022*

Citation:
Bose M, Nawaz MS, Pal R and Chattarji S (2022) Stress Elicits Contrasting Effects on Rac1-Cofilin Signaling in the Hippocampus and Amygdala. Front. Mol. Neurosci. 15:880382. doi: 10.3389/fnmol.2022.880382

INTRODUCTION

Stress-related psychiatric disorders are characterized by debilitating symptoms that include impaired cognitive function and heightened emotional problems. These contrasting manifestations at the behavioral level are accompanied by structural and functional aberrations in several brain regions including the hippocampus and amygdala (Bremner et al., 1997; Shin et al., 2005; Lorenzetti et al., 2009; Popoli et al., 2011). Consistent with these clinical findings, decades of research using a wide range of animal models have demonstrated how exposure to stress leads to divergent forms of

morphological and physiological plasticity in neurons and their connections in the hippocampus and amygdala (Luine et al., 1994; Vyas et al., 2002; Mitra et al., 2005; Roozendaal et al., 2009; Chattarji et al., 2015). For instance, pioneering studies in various sub-regions of the rodent hippocampus reported dendritic shrinkage and reduction in spine numbers following chronic restraint stress (Watanabe et al., 1992). Subsequent analyses in the basolateral amygdala (BLA), by contrast, showed that chronic immobilization stress leads to the opposite effect—dendritic growth and spine formation (Vyas et al., 2002; Mitra et al., 2005). These divergent morphological effects are also accompanied by physiological alterations in synaptic plasticity—impaired long-term potentiation (LTP) in the hippocampus (Diamond and Rose, 1994; Kim and Diamond, 2002), but enhanced LTP in the BLA (Suvrathan et al., 2013). Further, consistent with these cellular changes, stress also impairs hippocampus-dependent spatial learning and memory (Luine et al., 1994; Popoli et al., 2011) but facilitates amygdala-dependent fear learning (Conrad et al., 1999; Bauer et al., 2002; Rau et al., 2005; Suvrathan et al., 2013). However, little is known about the molecular underpinning of these contrasting patterns of stress-induced changes at multiple levels of neural organization.

The present study is aimed at addressing this gap in knowledge by focusing on the opposite effects of stress on dendritic spines, the site of glutamatergic excitatory synaptic transmission. Dendritic spines are enriched in actin, a cytoskeletal protein that regulates spine shape and maintains spine stability (Cingolani and Goda, 2008; Hotulainen and Hoogenraad, 2010; Koleske, 2013). The actin-binding proteins cofilin and profilin are involved in actin depolymerization and actin polymerization respectively and play a central role in spine morphogenesis, and the addition and removal of synapses (Pontrello and Ethell, 2009; Hotulainen and Hoogenraad, 2010; Rust, 2015). The phosphorylation and inactivation of cofilin, in turn, are mediated by the Rho family of small guanosine triphosphatases (GTPases), primarily consisting of RhoA and Rac1 (Govek et al., 2005). Moreover, Rac1 is known to be a central regulator of actin cytoskeletal dynamics in dendritic spines thereby exerting control over the structural and functional plasticity of spines (Nakayama et al., 2000; Tashiro et al., 2000; Haditsch et al., 2009; Hedrick et al., 2016). Rac1 mediates phosphorylation of cofilin through its effector p21-activated kinase 1 (PAK1), leading to spine remodeling (Govek et al., 2005; Costa et al., 2020).

Although exposure to repeated stress causes spine removal in the hippocampus and addition in the BLA, whether stress causes any perturbations in Rac1-to-cofilin signaling in these two brain areas remains unexplored. For instance, would repeated exposure to stress affect GTPase activity and would these effects be different in the hippocampus vs. BLA? Further, would the same chronic stress elicit divergent effects on Rac1-cofilin signaling in the two areas? If so, would these stress-induced changes be consistent with the opposite directions of spine density changes reported in the two structures? Here we address these questions using a well-characterized model of chronic immobilization stress in rats (Vyas et al., 2002; Mitra et al., 2005; Rahman et al., 2016).

MATERIALS AND METHODS

Animals

Eight-week-old male Sprague Dawley rats were pair housed in a standard 14 h light and 10 h dark schedule. Rats were housed under controlled humidity and temperature conditions with *ad libitum* access to food and water. All the experimentation procedures were approved by the Institutional Animal Ethics Committee, National Centre for Biological Sciences, Bangalore, India.

Stress Protocol

Rats were subjected to chronic stress as per previously established protocols (Vyas et al., 2002; Mitra et al., 2005; Rahman et al., 2016). Briefly, chronic stress consisted of complete immobilization for 2 h per day for consecutive 10 days in plastic rodent immobilization bags without access to food and water. Prior to stress, rats were handled for three consecutive days and randomly divided into two groups—control and stress at the beginning of the experiment. Rats were sacrificed on the 11th day for further experiments.

Body Weight

To calculate percentage gain in body weights, the net change in body weight of rats between the beginning and end points of the experiments was divided by the starting weight and multiplied by 100.

Coronal Slice Preparation and Tissue Collection

Rats were anesthetized using CO_2 on the 11th day, decapitated and their brains were rapidly dissected out and transferred to an oxygenated, ice-cold cutting solution composed of (in mM): 75 sucrose, 86 NaCl, 25 glucose, 2.5 KCl, 1.2 NaH_2PO_4, 25 $NaHCO_3$, 7 $MgCl_2$, 0.5 $CaCl_2$; equilibrated with 95% $O_2$and 5% CO_2, pH 7.3, 305–310 mOsm. Coronal brain slices of 400 μm thickness containing hippocampus and amygdala were obtained in the cutting solution using Leica VT1200S vibratome (Leica, Germany). Dorsal hippocampus and basolateral amygdala were microdissected from the coronal slices, flash frozen, and stored at −80°C.

Rac1 and RhoA Activation Assay

The G-LISA Rac1 Activation Assay Biochem kit (Cytoskeleton Biochem kit; Denver, USA; catalog no. BK128) and RhoA Activation Assay Biochem kit (Cytoskeleton Biochem kit; Denver, USA; catalog no. BK124) were used to measure the activity of Rac1 and RhoA respectively as per manufacturer's protocol. The kits determine Rac1 or RhoA activity based on the detection of active Rac1 or active RhoA protein bound to GTP. The G-LISA assay uses a 96-well plate coated with either Rac1-GTP binding protein or Rho-GTP binding protein. Active, GTP-bound Rac1 or RhoA in tissue lysate bound to the wells while inactive GDP-bound Rac1 or RhoA were removed during washing steps. The bound active Rac1 or RhoA were detected after incubation with specific Rac1 or RhoA primary antibody respectively followed by HRP-conjugated secondary antibody.

The absorbance was measured at 490 nm using a microplate reader (Tecan Spark, Switzerland).

Synaptoneurosome Preparation

Synaptoneurosomes were prepared from the dorsal hippocampus or basolateral amygdala by differential filtration as described previously with slight modification (Scheetz et al., 2000; Muddashetty et al., 2007). Briefly, microdissected tissue was homogenized at 4°C in 10 volumes of homogenization buffer [composed of (in mM): 118 NaCl, 4.7 KCl, 1.2 $MgSO_4$, 2.5 $CaCl_2$, 1.53 KH_2PO_4, 212.7 glucose, 1 DTT and 20 Tris-HCL, pH 7.4], supplemented with 2× protease inhibitor cocktail (Sigma-Aldrich), 1× phosphatase inhibitor cocktail 2 and 3 (Sigma-Aldrich). The tissue homogenate was passed through three 100 μm nylon mesh filters (Merck Millipore; NY1H02500), followed by one 11 μm nylon net filter (Merck Millipore; NY1102500) and then centrifuged at 1,000× *g* for 15 min. The pellets containing synaptoneurosomeswere resuspended and lysed in RIPA lysis buffer containing 50 mM Tris-HCl (pH 7.4), 1% TritonX, 0.5% Na-deoxycholate, 0.1% SDS, 150 mM NaCl, 1 mM Na_3VO_4, 1 mM EDTA, 1 mM PMSF, 2× protease inhibitor cocktail (Sigma-Aldrich), 1× phosphatase inhibitor cocktail 2 and 3 (Sigma-Aldrich). The protein concentrations were estimated using BCA Protein Assay Kit (Pierce).

Western Blotting

Twenty micrograms of protein from whole tissue lysate or synaptoneurosomes were loaded and separated in a precast gradient gel (NuPAGE 4%–12% Bis-Tris Protein Gels, Thermo Fisher). The resolved proteins were then transferred to a nitrocellulose membrane in a Bio-Rad transfer apparatus. After that, membranes were washed with 1× Tris-buffered saline (TBS). Next, membranes were blocked with 1:1 TBS: Odyssey Blocking Buffer (LI-COR Biosciences, Lincoln, NE, USA) containing 0.1% Tween 20 for 2 h at room temperature followed by overnight incubation at 4°C with primary antibodies (listed below). After subsequent washing with 1× TBST, the membranes were incubated with secondary antibodies (1:10,000 IRDye 800 CW goat anti-rabbit IgG; 1:10,000 IRDye 680 LT goat anti-mouse IgG; LI-COR Biosciences) for 1 h at room temperature. After incubation with respective secondary antibodies, the membranes were washed in 1× TBST. The immunoblots were then dried and digitally scanned using the Fc Odyssey Infrared Imaging System, (LI-COR Biosciences). Densitometric analysis was carried out with the help of Licor Image Studio Lite software.

Primary Antibodies

The following primary antibodies were used in this study: mouse anti-Rac1 (ARC03; 1:500; Cytoskeleton), mouse anti-RhoA (ARH04; 1:500; Cytoskeleton), rabbit anti-PAK1 (2602S; 1:1,000; Cell Signaling Technology), rabbit anti-phospho-PAK1/PAK2 (2606S; Phospho-PAK1 (Ser^{144})/PAK2 (Ser^{141}); 1:1,000; Cell Signaling Technology), rabbit anti-cofilin (5175S; 1:1,000; Cell Signaling Technology), rabbit anti-phospho-cofilin (3313S; Phospho-cofilin (Ser^{3}); 1:1,000; Cell Signaling Technology), rabbit anti-profilin1 (3237S; 1:1,000; Cell Signaling Technology), rabbit anti-GAPDH (2118S; 1:5,000; Cell Signaling Technology), rabbit anti-profilin2 (ab174322; 1:1,000; Abcam).

Statistical Analysis

Statistical analysis of all the data was performed using GraphPad Prism Software (GraphPad software Inc., USA, version 6). Significance was assessed by means of Student's t-test (unpaired, two-tailed) since the sample distributions were normal in the two groups being compared. In the graphs, all the data has been represented as mean ± SEM. For all data analyzed, $p < 0.05$ was considered to be statistically significant.

RESULTS

Contrasting Effects of Stress on Rac1-GTPase Activation in the Hippocampus and Amygdala

First, we verified the efficacy of the chronic immobilization stress (Stress, 2 h/day for 10 days) paradigm (**Figure 1A**) by measuring the relative gain in body weight of rats. Relative to unstressed control rats, stressed rats underwent a significant reduction in the percentage weight gained 1 day after the end of stress (**Figure 1B**; Control: 13.69 ± 0.7%; Stress: −0.32 ± 0.47%; $N = 12$ rats/group; $^{****}p < 0.0001$). Next, we tested if changes in activation patterns of the Rho family of small GTPase may reflect the differential effects of stress on spine plasticity in the hippocampus and amygdala. To this end, we first measured the activity and abundance of Rac1 and RhoA GTPases in the whole tissue lysate obtained from the dorsal hippocampus and basolateral amygdala (BLA) from control and stressed rats. We performed ELISA based GTPase activation assay and immunoblotting was carried out to measure protein abundance. In the hippocampus, we observed a significant reduction of Rac1 GTPase activity in tissue collected from stressed compared to control rats (**Figure 1C**; Control: 1.00 ± 0.05; Stress: 0.86 ± 0.04; data normalized to control animals; $N = 8$ rats/group; $^{*}p < 0.05$), but not in the total abundance of Rac1 protein (**Figures 1D,E**; Control: 1.00 ± 0.05; $N = 12$ rats; Stress: 1.08 ± 0.04; data normalized to control animals; $N = 11$ rats). However, there was no significant difference in the activity (**Figure 1F**; Control: 1.00 ± 0.08; Stress: 1.1 ± 0.09; data normalized to control animals; $N = 8$ rats/group) or abundance of RhoA protein (**Figures 1G,H**; Control: 1.00 ± 0.08; Stress: 0.91 ± 0.12; data normalized to control animals; $N = 12$ rats/group) in the hippocampus of stressed rats relative to controls. In contrast, the same chronic stress led to a significant increase in Rac1 GTPase activity in the BLA of the stressed animals relative to their control counterparts (**Figure 1I**; Control: 1.00 ± 0.06; Stress: 1.55 ± 0.07; data normalized to control animals; $N = 8$ rats/group; $^{****}p < 0.0001$) with no difference in total abundance of Rac1 protein (**Figures 1J,K**; Control: 1.00 ± 0.04; Stress: 1.08 ± 0.05; data normalized to control animals; $N = 12$ rats/group). Also, there was no change in the activity (**Figure 1L**; Control: 1.00 ± 0.10; Stress: 0.92 ± 0.07; data normalized to control animals; $N = 8$ rats/group) or abundance of RhoA protein (**Figures 1M,N**; Control: 1.00 ± 0.04;

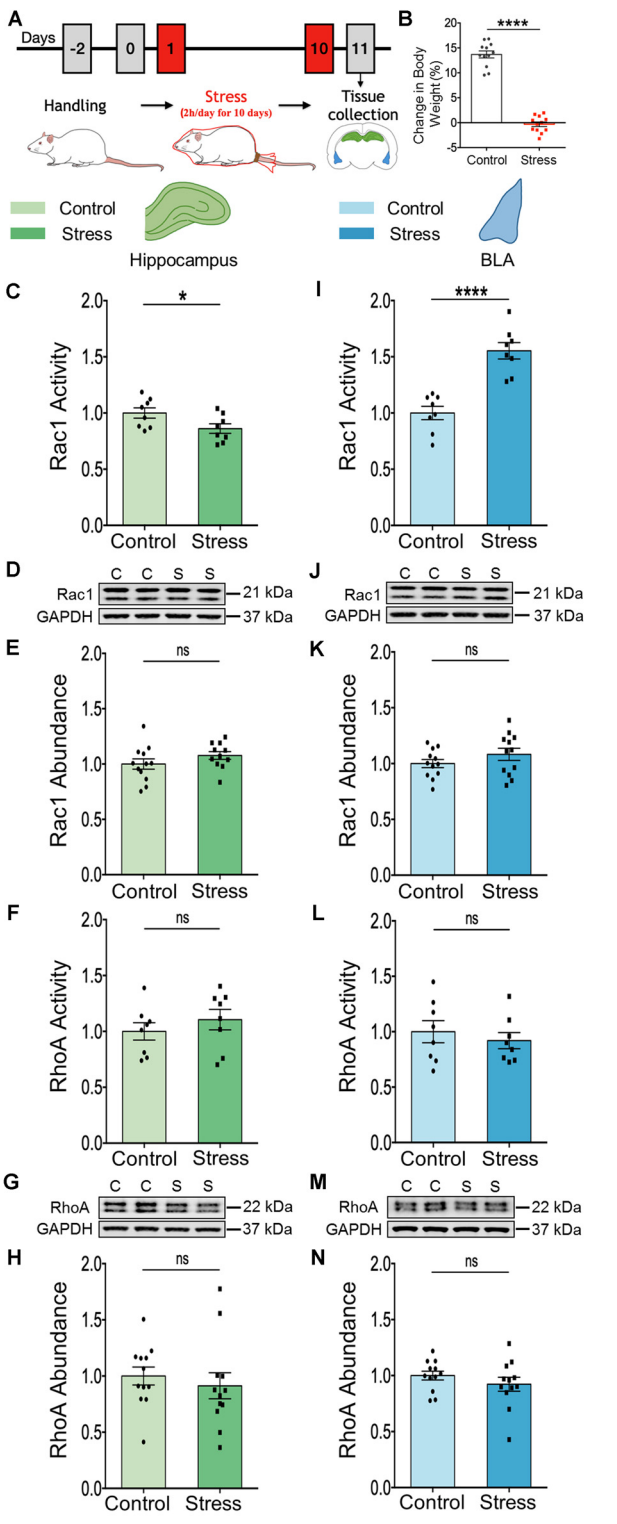

FIGURE 1 | Chronic stress elicits contrasting effects on the activation profile of Rac1-GTPase in the hippocampus and amygdala. **(A)** Schematic representation of experimental protocol. Male rats were subjected to chronic immobilization stress for 2 h/day for 10 days. Animals were then sacrificed for tissue collection. **(B)** Rats subjected to chronic stress show a significant

(*Continued*)

FIGURE 1 | Continued

decrease in percentage gain in body weight compared to control rats. **(C)** Rac1 activity is significantly decreased in the hippocampus of the stressed rats compared to the controls. **(D,E)** No change in the total abundance of Rac1 protein in the hippocampus of the stressed rats has been observed as shown in the representative western blot **(D)** and the summary graph **(E)**. **(F–H)** No change in the activity of RhoA protein **(F)** or the abundance of the RhoA protein **(G,H)** has been observed in the hippocampus of the stressed rats compared to their control counterparts as shown in the representative blot **(G)** or the bar graph **(H)**. **(I)** Rac1 activity is significantly increased in the amygdala of the stressed rats compared to the controls. **(J,K)** No detectable difference in the total abundance of Rac1 protein has been observed in the amygdala of the stressed rats in comparison to control rats, as depicted in the representative blot **(J)** and the bar diagram **(K)**. **(L–N)** No change in the activity of RhoA protein **(L)** or the abundance of RhoA protein **(M,N)** in the amygdala of the stressed rats has been observed compared to control rats as depicted in the representative blot **(M)** and summary graph **(N)**. In the figure, C stands for control, S stands for stress and ns stands for non-significant. Data are represented as means ± SEM; data normalized to control animals except **(B)**; N = 8–12 rats/group; $^{*}p < 0.05$, $^{****}p < 0.0001$.

Stress: 0.92 ± 0.06; data normalized to control animals; N = 12 rats/group) in the BLA of stressed rats compared to controls. Taken together, these data indicate chronic stress modulates Rac1 GTPase activity in opposite directions in the hippocampus and BLA, without affecting RhoA activity.

Contrasting Effects of Stress on PAK1 Activity in the Hippocampus and Amygdala

The PAK1 protein is a critical effector that links Rac1 GTPase activity to cytoskeleton remodeling (Zhao and Manser, 2012; Rane and Minden, 2014). This led us to investigate whether stress can differentially dysregulate PAK1 activity in the hippocampus and amygdala. First, we assessed PAK1 activity by examining its phosphorylation status, as well as abundance of PAK1 in the whole tissue lysate from both brain areas. There was a significant decrease in PAK1 activity in the hippocampus (**Supplementary Figures 1A,B**; Control: 1.00 ± 0.07; Stress: 0.70 ± 0.05; data normalized to control animals; N = 8 rats/group; $^{**}p < 0.01$ and **Supplementary Figure 1E**; Control: 1.00 ± 0.05; Stress: 0.72 ± 0.06; data normalized to control animals; N = 8 rats/group; $^{**}p < 0.01$), without any change in the total abundance of PAK1 protein (**Supplementary Figures 1C,D**; Control: 1.00 ± 0.05; Stress: 0.99 ± 0.06; data normalized to control animals; N = 8 rats/group). In the BLA, however, there was no change in activity of PAK1 (**Supplementary Figures 1F,G**; Control: 1.00 ± 0.11; Stress: 0.94 ± 0.11; data normalized to control animals; N = 8 rats/group and **Supplementary Figure 1J**; Control: 1.00 ± 0.09; N = 8 rats; Stress: 0.99 ± 0.07; data normalized to control animals; N = 7 rats) or its abundance (**Supplementary Figures 1H,I**; Control: 1.00 ± 0.05; Stress: 0.86 ± 0.05; data normalized to control animals; N = 8 rats/group).

Next, to gain a better understanding of stress-induced changes at the synaptic level for which analyses of whole tissue lysates are not optimal, we switched to measurements in synaptoneurosomes. To this end, we isolated synaptoneurosomes from both brain areas to quantify the activity and abundance

of PAK1 protein by immunoblotting. In the hippocampus of stressed animals, we found a significant decrease in PAK1 phosphorylation, at Ser^{144} (**Figures 2A,B**; Control: 1.00 ± 0.07; N = 9 rats; Stress: 0.72 ± 0.05; data normalized to control animals; N = 10 rats; $^{**}p < 0.01$ and **Figure 2E**; Control: 1.00 ± 0.06; N = 9 rats; Stress: 0.77 ± 0.06; data normalized to control animals; N = 10 rats; $^{*}p < 0.05$). This is a primary phosphosite undergoing autophosphorylation upon PAK1 activation and regulates the enzymatic activity of PAK1 (Mayhew et al., 2007). Stress did not change total abundance of hippocampal PAK1 protein (**Figures 2C,D**; Control: 1.00 ± 0.05; N = 9 rats; Stress: 0.96 ± 0.07; data normalized to control animals; N = 10 rats). Notably, a significant increase in PAK1 phosphorylation at Ser^{144} was seen in the BLA of stressed rats (**Figures 2F,G**; Control: 1.00 ± 0.07; N = 11 rats; Stress: 1.46 ± 0.10; data normalized to control animals; N = 12 rats; $^{**}p < 0.01$ and **Figure 2J**; Control: 1.00 ± 0.07; N = 10 rats; Stress: 1.36 ± 0.10; data normalized to control animals; N = 12 rats/group; $^{**}p < 0.01$) without any detectable change in the total abundance of the protein (**Figures 2H,I**; Control: 1.00 ± 0.03; N = 10 rats; Stress: 1.04 ± 0.04; data normalized to control animals; N = 12 rats). However, PAK2 phosphorylation at Ser^{141} was not affected by stress in hippocampal (**Supplementary Figures 2C,D**; Control: 1.00 ± 0.09; N = 9 rats; Stress: 0.89 ± 0.06; data normalized to control animals; N = 10 rats) and BLA (**Supplementary Figures 2G,H**; Control: 1.00 ± 0.07; N = 11 rats; Stress: 1.10 ± 0.08; data normalized to control animals; N = 12 rats) synaptoneurosomes. A similar absence of stress effects was seen in analyses of PAK2 phosphorylation in whole tissue lysates obtained from both areas (**Supplementary Figures 2A,B**; Control: 1.00 ± 0.06; Stress: 0.93 ± 0.08; data normalized to control animals; N = 8 rats/group and **Supplementary Figures 2E,F**; Control: 1.00 ± 0.07; Stress: 0.97 ± 0.05; data normalized to control animals; N = 8 rats/group respectively). Together, these findings also demonstrate divergent effects of chronic stress on PAK1 activity, but not on PAK2, in the hippocampus and amygdala. Further, the decrease in PAK1 activity is consistent with reduced Rac1 activity in the hippocampus, while enhanced activity of both PAK1 and Rac1 was seen in the basolateral amygdala.

Stress Also Leads to Divergent Effects on Cofilin Activity in the Two Brain Areas

The results described thus far point to stress-induced changes in Rac1 and PAK1 (**Figures 1**, **2**). Rac1 is known to exert its effects on spine architecture by modulating the activity of the actin-binding protein cofilin through PAK1. Moreover, cofilin plays a central role in regulating the structure and number of dendritic spines (Yang et al., 1998; Hotulainen et al., 2009; Pontrello and Ethell, 2009). Hence, we next compared the total levels of cofilin protein, as well as the phosphorylation status of cofilin at Ser^{3}, in BLA, and hippocampal synaptoneurosomes. Stress led to a significant reduction in phosphorylation of cofilin at Ser^{3} in the hippocampus (**Figures 3A,B**; Control: 1.00 ± 0.02; N = 8 rats; Stress: 0.58 ± 0.02; data normalized to control

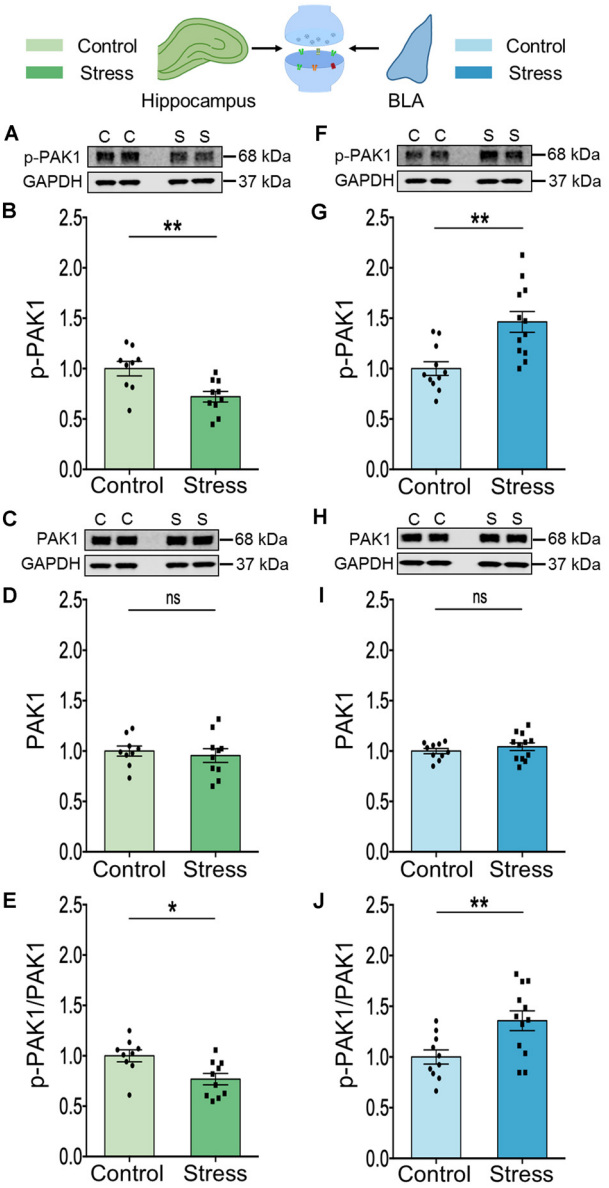

FIGURE 2 | Chronic stress mediates contrasting effect on the activity of the effector molecule PAK1 in the synaptoneurosome fraction isolated from the hippocampus and amygdala. **(A,B)** A significant decrease in the activity of PAK1 protein as represented by a decrease in its phosphorylation status has been observed in the hippocampus of the stressed rats compared to the controls as shown in the representative western blot **(A)** and the summary graph **(B)**. **(C,D)** No change has been observed in the abundance of the PAK1 protein in the hippocampus of stressed rats compared to controls as shown in the representative blot **(C)** and the summary graph **(D)**. **(E)** A significant decrease in the ratio of phospho-PAK1 to total-PAK1 protein has been observed in the hippocampus due to stress confirming a decrease in PAK1 activity. **(F,G)** A significant increase in the activity of PAK1 protein as represented by an increase in its phosphorylation status has been noticed in the amygdala of the stressed rats compared to the controls as shown in the representative western blot **(F)** and the summary data **(G)**. **(H,I)** No detectable difference in the abundance of the PAK1 protein has been viewed in the amygdala of stressed rats compared to controls as shown in the representative blot **(H)** and the summary graph **(I)**. **(J)** A significant increase in

(*Continued*)

FIGURE 2 | Continued
the ratio of phospho-PAK1 to total-PAK1 protein has been observed in the amygdala due to chronic stress confirming an increase in PAK1 activity. In the figure, C stands for control, S stands for stress and ns stands for non-significant. Data are represented as means ± SEM; data normalized to control animals; N = 9–12 rats/group; $^{*}p < 0.05$, $^{**}p < 0.01$. For datasets in **Figures 2**, **3**, the same GAPDH as internal controls has been used for analysis since they are from the same blots. Finally, it may be noted that the blots of p-PAK depicted in panels **(A)** and **(F)** have low signal-to-noise ratio, which gives the impression of a higher background resulting in a smear-like appearance. However, comparisons with Cell Signaling Technology (CST) datasheets for the respective antibodies, as well as previous articles where similar blots for phosphoproteins have been presented (Pyronneau et al., 2017; Brown et al., 2021), suggest that this is caused by a low signal-to-noise ratio.

animals; N = 10 rats; $^{****}p < 0.0001$ and **Figure 3E**; Control: 1.00 ± 0.04; N = 8 rats; Stress: 0.56 ± 0.03; data normalized to control animals; N = 10 rats; $^{****}p < 0.0001$) without any effect on total abundance of the protein (**Figures 3C,D**; Control: 1.00 ± 0.03; N = 9 rats; Stress: 1.06 ± 0.07; data normalized to control animals; N = 10 rats). In the BLA, by contrast, stress caused a significant increase in cofilin phosphorylation at Ser^3 (**Figures 3F,G**; Control: 1.00 ± 0.08; N = 11 rats; Stress: 1.42 ± 0.11; data normalized to control animals; N = 12 rats; $^{**}p < 0.01$ and **Figure 3J**; Control: 1.00 ± 0.08; N = 11 rats; Stress: 1.33 ± 0.11; data normalized to control animals; N = 12 rats; $^{*}p < 0.05$) without any detectable difference in the total abundance of the protein (**Figures 3H,I**; Control: 1.00 ± 0.06; N = 11 rats; Stress: 1.07 ± 0.06; data normalized to control animals; N = 12 rats). Thus, stress-induced decrease in cofilin phosphorylation in the hippocampus, but increase in the BLA, is consistent with enhanced cofilin activity in the hippocampus, but the opposite effect in the BLA. Furthermore, the divergent effects of stress on Rac1-PAK1-cofilin signaling mirrors the loss and formation of spines in the hippocampus and BLA respectively.

Stress Triggers Contrasting Patterns of Expression of Profilin Isoforms in the Two Brain Areas

Similar to cofilin, profilins are actin-binding proteins that also regulate neuronal actin dynamics. Profilins are known to bind G-actin, enhance actin polymerization and play an important role in signal-dependent fine-tuning of spine architecture (Michaelsen et al., 2010). We focused on the two isoforms, profilin 1 and profilin 2 because they are reported to undergo stimulus-dependent accumulation in the spines of excitatory neurons (Ackermann and Matus, 2003; Neuhoff et al., 2005; Lamprecht et al., 2006). In the hippocampus, stress led to a reduction in the levels of both profilin 1 (**Figures 4A,B**; Control: 1.00 ± 0.10; N = 12 rats; Stress: 0.72 ± 0.07; data normalized to control animals; N = 11 rats; $^{*}p < 0.05$) and profilin 2 (**Figures 4C,D**; Control: 1.00 ± 0.06; N = 12 rats; Stress: 0.74 ± 0.06; data normalized to control animals; N = 10 rats; $^{**}p < 0.01$). However, in the BLA stress had the opposite effect on both isoforms (**Figures 4E,F**; Control: 1.00 ± 0.09; Stress: 1.5 ± 0.11; data normalized to control animals; N = 11 rats/group; $^{**}p < 0.01$ and

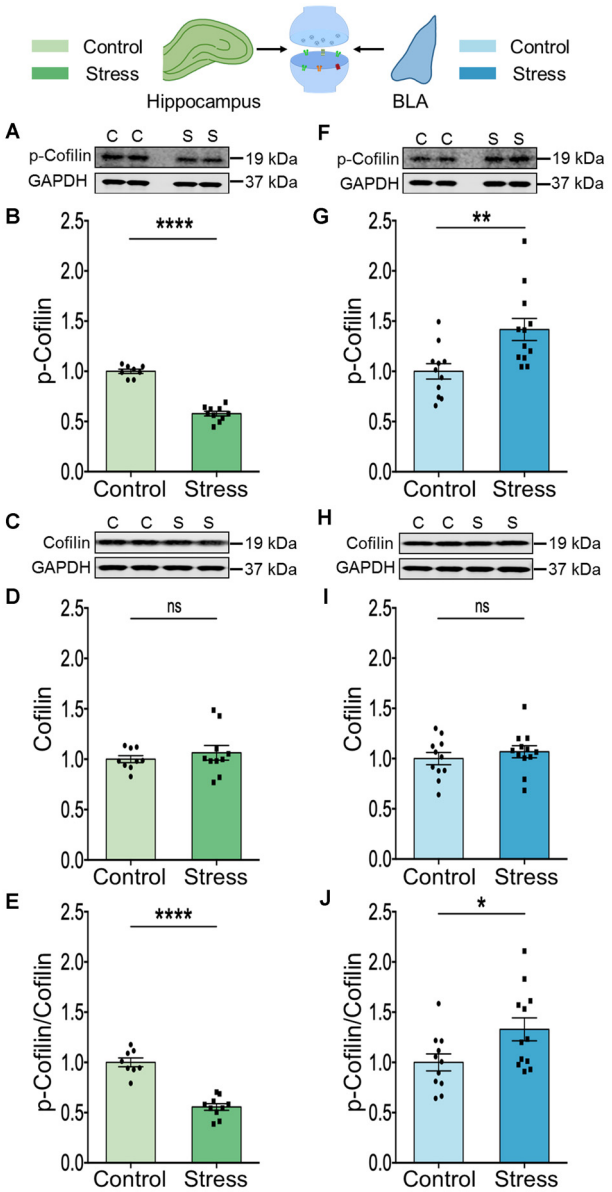

FIGURE 3 | Chronic stress modulates cofilin activity in a differential manner in the hippocampus and amygdala. **(A,B)** A significant decrease in the phosphorylation of the cofilin protein has been observed in the hippocampus of the stressed rats compared to the controls suggesting an increase in the activity of cofilin, as shown in the representative western blot **(A)** and the summary graph **(B)**. **(C,D)** The abundance of the cofilin protein has been observed to undergo no change in the hippocampus of stressed rats compared to controls as shown in the representative blot **(C)** and the summary graph **(D)**. **(E)** A significant decrease in the ratio of phospho-cofilin to total-cofilin has been observed in the hippocampus due to stress confirming an increase in cofilin activity. **(F,G)** A significant increase in the phosphorylation of cofilin protein has been observed in the amygdala of the stressed rats compared to the controls suggesting a decrease in cofilin activity as shown in the representative western blot **(F)** and the summary data **(G)**. **(H,I)** No detectable difference in the abundance of the cofilin protein has been noticed in the amygdala of stressed rats compared to controls as shown in the representative blot **(H)** and the summary graph **(I)**. **(J)** A significant increase in the ratio of phospho-cofilin to total-cofilin has been

(*Continued*)

FIGURE 3 | Continued
observed in the amygdala due to stress confirming a decrease in cofilin activity. In the figure, C stands for control, S stands for stress and ns stands for non-significant. Data are represented as means ± SEM; data normalized to control animals; N = 8–12 rats/group; $^{*}p < 0.05$, $^{**}p < 0.01$, $^{****}p < 0.0001$. For datasets in **Figures 2**, **3**, the same GAPDH as internal controls has been used for analysis since they are from the same blots. Finally, it may be noted that the blots of p-Cofilin depicted in panels 3A and 3F have a low signal to noise ratio, which gives the impression of a higher background resulting in a smear-like appearance. However, comparisons with Cell Signaling Technology (CST) datasheets for the respective antibodies, as well as previous articles where similar blots for phosphoproteins have been presented (Ouyang et al., 2021) suggest that this is caused by a low signal-to-noise ratio.

Figures 4G,H; Control: 1.00 ± 0.04; Stress: 1.24 ± 0.10; data normalized to control animals; N = 11 rats/group; $^{*}p < 0.05$).

DISCUSSION

The analysis presented here is one of the first attempts to characterize the impact of repeated stress on molecular signaling mechanisms underlying spine plasticity in two brain regions that play a pivotal role in regulating the stress response. We found that consistent with the divergent patterns of stress-induced structural plasticity in the hippocampus and amygdala, chronic stress also elicits differential changes in Rac1-PAK1-cofilin signaling and levels of profilin isoforms in these two structures (**Figure 5**). A day after the end of 10 days of chronic stress, we observed contrasting effects in the activation profile of Rac1—a reduction in the hippocampus, but an enhancement in the BLA. However, no detectable difference in RhoA activity was seen in either areas, suggesting that a dysregulation of Rac1 signaling, but not RhoA, is associated with chronic stress-induced structural plasticity. This is interesting in light of an earlier study that reported the involvement of Rac1 activation, but not RhoA, in antidepressant effects (Kato et al., 2018). Stress, in turn, has been implicated in precipitating depressive symptoms (Duman et al., 2019) and animal models of chronic stress have also been used to examine mechanisms of antidepressant action (Govindarajan et al., 2006; Pillai et al., 2012). Consistent with previous studies (Nakayama et al., 2000; Tashiro et al., 2000; Hedrick et al., 2016; Pyronneau et al., 2017), our results demonstrate the importance of Rac1 signaling in the structural plasticity of dendritic spines. RhoA signaling, on the other hand, has been shown to have a complex relationship with spine stability. For instance, RhoA has been implicated in the reduction of spine density (Tashiro et al., 2000; Govek et al., 2005). But, RhoA-ROCK signaling can also phosphorylate and inactivate cofilin, which could promote rather than reduce spine stability (Koleske, 2013). Since Rac1-GTPase mediates its effects by binding and activating PAK1 (Hayashi et al., 2002; Zhao and Manser, 2012; Rane and Minden, 2014), we also analyzed synaptoneurosomes; this revealed lower PAK1 activity in the hippocampus, but the opposite effect in the BLA. A downstream target of Rac1 is the actin-depolymerizing factor cofilin, which upon phosphorylation at its Ser^{3} residue, becomes inactive. As a result, it fails to bind and sever F-actin (Yang et al., 1998).

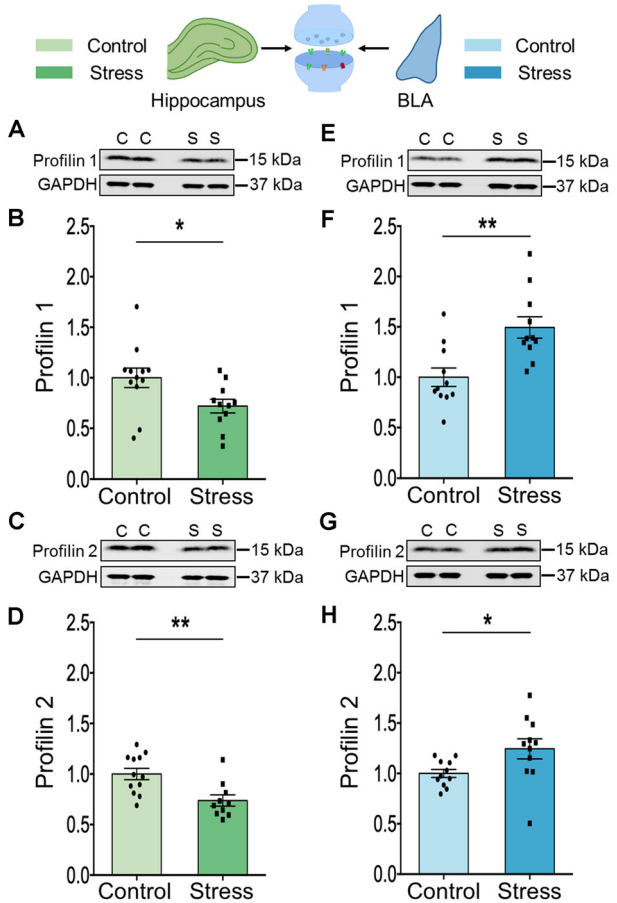

FIGURE 4 | Chronic stress leads to contrasting effect on the expression profile of profilin isoforms in the hippocampus and amygdala. **(A–D)** A significant decrease in the expression of both the profilin isoforms, profilin 1 and profilin 2 has been observed in the synaptoneurosome fraction of the hippocampus of the stressed rats compared to controls as shown in the representative western blots **(A,C)** and the summary graphs **(B,D)** respectively. **(E–H)** A significant increase in the expression of both the profilin isoforms, profilin 1, and profilin 2 has been observed in the synaptoneurosome fraction of the amygdala of the stressed rats compared to its control counterparts as shown in the representative western blots **(E,G)**, and the summary graphs **(F)** and **(H)** respectively. In the figure, C stands for control and S stands for stress. Data are represented as means ± SEM; data normalized to control animals; N = 10–12 rats/group; $^{*}p < 0.05$, $^{**}p < 0.01$. Out of 11 data points in **(F)**, five data points have used the same internal control for analysis as in **Figures 2G**, **3G** since they are from the same blots.

Cofilin-mediated cytoskeletal remodeling plays a significant role in dendritic spine morphogenesis and alterations in spine density (Hotulainen et al., 2009; Mizuno, 2013; Ben Zablah et al., 2020). Following exposure to repeated stress, we found a significant increase in cofilin phosphorylation in the BLA, which is indicative of reduced cofilin activity. In striking contrast, the same stress led to a decrease in cofilin phosphorylation, suggesting its activation, in the hippocampus. High cofilin activity in the hippocampus, in turn, would result in a shift toward actin depolymerization that is consistent with a stress-induced reduction in hippocampal spine density reported in

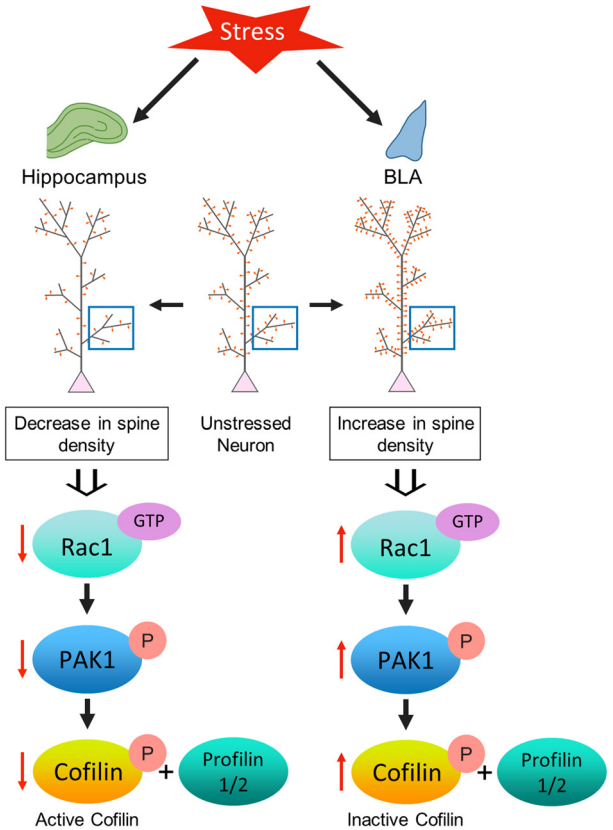

FIGURE 5 | Model depicting the proposed mechanism underlying the contrasting effect of stress-induced structural plasticity in the hippocampus and amygdala. **(Left)** Schematic representation of the effect of stress on the hippocampus. Chronic stress leads to an aberrant decrease in Rac1 activity in the hippocampus which in turn leads to a decrease in PAK1 phosphorylation. A decrease in PAK1 activity ultimately brings about a decrease in cofilin phosphorylation. An increase in cofilin activity along with a simultaneous decrease in the levels of profilin isoforms may correlate with a decrease in spine density in the hippocampus due to stress. **(Right)** Schematic representation of the effect of stress on the amygdala. Chronic stress leads to an aberrant increase in Rac1 activity in the amygdala that effectuates an increase in PAK1 phosphorylation. An increase in PAK1 activity causes an increase in cofilin phosphorylation. A decrease in cofilin activity along with a simultaneous increase in the profilin isoforms may be linked with an increase in spine density in the amygdala due to stress.

earlier studies (Watanabe et al., 1992; Vyas et al., 2002). Conversely, the opposite effect of the same chronic stress on BLA cofilin activity would cause a shift towards elevated actin polymerization, and thereby cause increased spine density. Together, these findings show how the differential dysregulation of Rac1-PAK1-cofilin signaling is consistent with the contrasting effects of stress on spine numbers in the hippocampus vs. the amygdala.

These findings are also consistent with cofilin being the convergence point of Rac1 signaling that ultimately modulates actin cytoskeleton dynamics. Similar to cofilin, the other actin-binding protein profilin also plays an important role in regulating actin dynamics and spine architecture (Michaelsen et al., 2010; Michaelsen-Preusse et al., 2016). Both profilin1 and profilin2 are required for synaptogenesis, while the latter is also important for spine stability and plasticity (Michaelsen et al., 2010). Here, we report that exposure to chronic stress decreases levels of profilin1 and profilin2 expression in the hippocampus, but increases their levels in the BLA. This decrease in cofilin activity, alongside higher profilin levels, would be consistent with enhanced actin polymerization leading to spinogenesis in the BLA. In the hippocampus, on the other hand, the same stress increased cofilin activity but decreased profilin levels, which would lead to actin depolymerization and loss of spines.

Our findings using a rodent model of stress add to a growing body of evidence for the central role played by Rac1-PAK1-cofilin signaling in modulating spine plasticity in both *in vitro* and *in vivo* rodent models. For example, in the developing neuron, Rac1 has been shown to mediate spine formation and activity-induced changes in spine size (Murakoshi et al., 2011; Koleske, 2013), as well as spine stability in adult neurons (Nakayama et al., 2000; Koleske, 2013). Increased or decreased Rac1 signaling has also been associated with elevated and reduced spine density in slice cultures (Tashiro et al., 2000; Tashiro and Yuste, 2004), in primary neuronal cultures (Pennucci et al., 2019), and in mice (Bongmba et al., 2011; Huang et al., 2011; Ohashi, 2015). Reduction in spine density has been seen following knockdown of profilin1 and profilin2 as well (Michaelsen et al., 2010; Michaelsen-Preusse et al., 2016). In light of the pivotal role of Rac1 in learning and memory, this small GTPase and its downstream molecules have also been associated with a range of brain disorders. For instance, in a rodent model of Alzheimer's disease, spine density is reduced due to cofilin activation, which has also been seen in patient brain tissue (Zhao et al., 2006; Shankar et al., 2007). Also, in a mouse model of Fragile X Syndrome, elevated activation of Rac1-PAK1-cofilin signaling has been linked to enhanced dendritic spine density in the somatosensory cortex (Pyronneau et al., 2017). Of relevance to the findings reported here, in a recent study using a rat model of depression, PAK1 gene expression was downregulated in the hippocampus whereas the Rac1 gene was upregulated in the amygdala (Andrus et al., 2012). It should also be noted that our study is based on analyses of synaptoneurosomes, a method that is not amenable to differentiating between excitatory and inhibitory neurons. Further, inhibitory interneurons are aspiny or spine-sparse (Sala, 2002; Goldberg et al., 2003; Sancho and Bloodgood, 2018), and comprise of a relatively smaller proportion of the total population of neurons in the hippocampus and amygdala (Perumal and Sah, 2021). Thus, the divergent effect of stress on Rac1 reported here is more likely to reflect alterations in excitatory neurons.

The divergent patterns of Rac1 activation following chronic stress are consistent with the loss and formation of dendritic spines in the hippocampus and amygdala respectively. But, the significance of the opposite effects of stress on Rac1 activation is not limited to morphological plasticity of spines, and may also have physiological consequences. For instance, the regulation of normal cytoskeletal stability is important for maintaining long-term changes in synaptic efficacy, such as long-term

potentiation (LTP) and depression (LTD) (Koleske, 2013). Consistent with this, the same chronic stress paradigm used here has been shown to facilitate LTP in the lateral amygdala, while various forms of stress are known to impair hippocampal LTP, but enhance LTD, in the hippocampus (Kim and Diamond, 2002; Chattarji et al., 2015). Further, LTP is associated with enhanced F actin content in dendritic spines along with their enlargement (Fukazawa et al., 2003; Okamoto et al., 2004), whereas LTD is associated with spine shrinkage and an increase in G actin content (Okamoto et al., 2004). Interestingly, cofilin inactivation is also associated with spine stabilization and enlargement during LTP (Fukazawa et al., 2003; Ben Zablah et al., 2020). Thus, future studies will be necessary to further explore the physiological consequences of the divergent manifestations of stress-induced alterations in Rac1 signaling for synaptic transmission and plasticity in the hippocampus and amygdala.In conclusion, accumulating evidence has characterized how exposure to repeated stress triggers a range of structural and functional changes across biological scales—from behavior to synapses—that are strikingly different in the hippocampus vs. the amygdala. Our findings on the divergent effects of stress on Rac1-cofilin signaling in these two brain areas add a new dimension to this multi-level framework.

DATA AVAILABILITY STATEMENT

The original contributions presented in the study are included in the article/**Supplementary Material**, further inquiries can be directed to the corresponding author.

ETHICS STATEMENT

The animal study was reviewed and approved by The Institutional Animal Ethics Committee at the National Centre for Biological Sciences.

AUTHOR CONTRIBUTIONS

MB and SC designed the study. MB and MN conducted the experiments and analyzed data. MB, RP, and SC wrote the manuscript along with input from all the authors. All authors contributed to the article and approved the submitted version.

FUNDING

This work was supported by intramural funds from NCBS-TIFR, Department of Atomic Energy, Government of India.

ACKNOWLEDGMENTS

We thank Dr. Dasaradhi Palakodeti and Dr. Aditi Bhattacharya for helpful discussions and advice. We acknowledge the NCBS Animal Care and Resource Center.

SUPPLEMENTARY MATERIAL

The Supplementary Material for this article can be found online at: https://www.frontiersin.org/articles/10.3389/fnmol.2022.880382/full#supplementary-material.

REFERENCES

Ackermann, M., and Matus, A. (2003). Activity-induced targeting of profilin and stabilization of dendritic spine morphology. *Nat. Neurosci.* 6, 1194–1200. doi: 10.1038/nn1135

Andrus, B. M., Blizinsky, K., Vedell, P. T., Dennis, K., Shukla, P. K., Schaffer, D. J., et al. (2012). Gene expression patterns in the hippocampus and amygdala of endogenous depression and chronic stress models. *Mol. Psychiatry* 17, 49–61. doi: 10.1038/mp.2010.119

Bauer, E. P., Schafe, G. E., and LeDoux, J. E. (2002). NMDA receptors and L-type voltage-gated calcium channels contribute to long-term potentiation and different components of fear memory formation in the lateral amygdala. *J. Neurosci.* 22, 5239–5249. doi: 10.1523/JNEUROSCI.22-12-05239.2002

Ben Zablah, Y., Merovitch, N., and Jia, Z. (2020). The role of ADF/cofilin in synaptic physiology and Alzheimer's disease. *Front. Cell Dev. Biol.* 8:594998. doi: 10.3389/fcell.2020.594998

Bongmba, O. Y. N., Martinez, L. A., Elhardt, M. E., Butler, K., and Tejada-Simon, M. V. (2011). Modulation of dendritic spines and synaptic function by Rac1: a possible link to Fragile X syndrome pathology. *Brain Res.* 1399, 79–95. doi: 10.1016/j.brainres.2011.05.020

Bremner, J. D., Randall, P., Vermetten, E., Staib, L., Bronen, R. A., Mazure, C., et al. (1997). Magnetic resonance imaging-based measurement of hippocampal volume in posttraumatic stress disorder related to childhood physical and sexual abuse—a preliminary report. *Biol. Psychiatry* 41, 23–32. doi: 10.1016/s0006-3223(96)00162-x

Brown, T. L., Hashimoto, H., Finseth, L. T., Wood, T. L., and Macklin, W. B. (2021). PAK1 positively regulates oligodendrocyte morphology and myelination. *J. Neurosci.* 41, 1864–1877. doi: 10.1523/JNEUROSCI.0229-20.2021

Chattarji, S., Tomar, A., Suvrathan, A., Ghosh, S., and Rahman, M. M. (2015). Neighborhood matters: divergent patterns of stress-induced plasticity across the brain. *Nat. Neurosci.* 18, 1364–1375. doi: 10.1038/nn.4115

Cingolani, L. A., and Goda, Y. (2008). Actin in action: the interplay between the actin cytoskeleton and synaptic efficacy. *Nat. Rev. Neurosci.* 9, 344–356. doi: 10.1038/nrn2373

Conrad, C. D., LeDoux, J. E., Magariños, A. M., and McEwen, B. S. (1999). Repeated restraint stress facilitates fear conditioning independently of causing hippocampal CA3 dendritic atrophy. *Behav. Neurosci.* 113, 902–913. doi: 10.1037//0735-7044.113.5.902

Costa, J. F., Dines, M., and Lamprecht, R. (2020). The role of Rac GTPase in dendritic spine morphogenesis and memory. *Front. Synaptic Neurosci.* 12:12. doi: 10.3389/fnsyn.2020.00012

Diamond, D. M., and Rose, G. M. (1994). Stress impairs LTP and hippocampal-dependent memory. *Ann. N. Y. Acad. Sci.* 746, 411–414. doi: 10.1111/j.1749-6632.1994.tb39271.x

Duman, R. S., Sanacora, G., and Krystal, J. H. (2019). Altered connectivity in depression: GABA and glutamate neurotransmitter deficits and reversal by novel treatments. *Neuron* 102, 75–90. doi: 10.1016/j.neuron.2019.03.013

Fukazawa, Y., Saitoh, Y., Ozawa, F., Ohta, Y., Mizuno, K., and Inokuchi, K. (2003). Hippocampal LTP is accompanied by enhanced F-actin content within the dendritic spine that is essential for late LTP maintenance *in vivo*. *Neuron* 38, 447–460. doi: 10.1016/s0896-6273(03)00206-x

Goldberg, J. H., Tamas, G., Aronov, D., and Yuste, R. (2003). Calcium microdomains in aspiny dendrites. *Neuron* 40, 807–821. doi: 10.1016/s0896-6273(03)00714-1

Govek, E.-E., Newey, S. E., and Van Aelst, L. (2005). The role of the Rho GTPases in neuronal development. *Genes Dev.* 19, 1–49. doi: 10.1101/gad.1256405

Govindarajan, A., Rao, B. S. S., Nair, D., Trinh, M., Mawjee, N., Tonegawa, S., et al. (2006). Transgenic brain-derived neurotrophic factor expression causes both anxiogenic and antidepressant effects. *Proc. Natl. Acad. Sci. U S A* 103, 13208–13213. doi: 10.1073/pnas.0605180103

Haditsch, U., Leone, D. P., Farinelli, M., Chrostek-Grashoff, A., Brakebusch, C., Mansuy, I. M., et al. (2009). A central role for the small GTPase Rac1 in hippocampal plasticity and spatial learning and memory. *Mol. Cell. Neurosci.* 41, 409–419. doi: 10.1016/j.mcn.2009.04.005

Hayashi, K., Ohshima, T., and Mikoshiba, K. (2002). Pak1 is involved in dendrite initiation as a downstream effector of Rac1 in cortical neurons. *Mol. Cell. Neurosci.* 20, 579–594. doi: 10.1006/mcne.2002.1144

Hedrick, N. G., Harward, S. C., Hall, C. E., Murakoshi, H., McNamara, J. O., and Yasuda, R. (2016). Rho GTPase complementation underlies BDNF-dependent homo- and heterosynaptic plasticity. *Nature* 538, 104–108. doi: 10.1038/nature19784

Hotulainen, P., and Hoogenraad, C. C. (2010). Actin in dendritic spines: connecting dynamics to function. *J. Cell Biol.* 189, 619–629. doi: 10.1083/jcb.201003008

Hotulainen, P., Llano, O., Smirnov, S., Tanhuanpää, K., Faix, J., Rivera, C., et al. (2009). Defining mechanisms of actin polymerization and depolymerization during dendritic spine morphogenesis. *J. Cell Biol.* 185, 323–339. doi: 10.1083/jcb.200809046

Huang, W., Zhou, Z., Asrar, S., Henkelman, M., Xie, W., and Jia, Z. (2011). p21-activated kinases 1 and 3 control brain size through coordinating neuronal complexity and synaptic properties. *Mol. Cell Biol.* 31, 388–403. doi: 10.1128/MCB.00969-10

Kato, T., Fogaça, M. V., Deyama, S., Li, X.-Y., Fukumoto, K., and Duman, R. S. (2018). BDNF release and signaling are required for the antidepressant actions of GLYX-13. *Mol. Psychiatry* 23, 2007–2017. doi: 10.1038/mp.2017.220

Kim, J. J., and Diamond, D. M. (2002). The stressed hippocampus, synaptic plasticity and lost memories. *Nat. Rev. Neurosci.* 3, 453–462. doi: 10.1038/nrn849

Koleske, A. J. (2013). Molecular mechanisms of dendrite stability. *Nat. Rev. Neurosci.* 14, 536–550. doi: 10.1038/nrn3486

Lamprecht, R., Farb, C. R., Rodrigues, S. M., and LeDoux, J. E. (2006). Fear conditioning drives profilin into amygdala dendritic spines. *Nat. Neurosci.* 9, 481–483. doi: 10.1038/nn1672

Lorenzetti, V., Allen, N. B., Fornito, A., and Yücel, M. (2009). Structural brain abnormalities in major depressive disorder: a selective review of recent MRI studies. *J. Affect. Disord.* 117, 1–17. doi: 10.1016/j.jad.2008.11.021

Luine, V., Villegas, M., Martinez, C., and McEwen, B. S. (1994). Repeated stress causes reversible impairments of spatial memory performance. *Brain Res.* 639, 167–170. doi: 10.1016/0006-8993(94)91778-7

Mayhew, M. W., Jeffery, E. D., Sherman, N. E., Nelson, K., Polefrone, J. M., Pratt, S. J., et al. (2007). Identification of phosphorylation sites in βPIX and PAK1. *J. Cell Sci.* 120, 3911–3918. doi: 10.1242/jcs.008177

Michaelsen, K., Murk, K., Zagrebelsky, M., Dreznjak, A., Jockusch, B. M., Rothkegel, M., et al. (2010). Fine-tuning of neuronal architecture requires two profilin isoforms. *Proc. Natl. Acad. Sci. U S A* 107, 15780–15785. doi: 10.1073/pnas.1004406107

Michaelsen-Preusse, K., Zessin, S., Grigoryan, G., Scharkowski, F., Feuge, J., Remus, A., et al. (2016). Neuronal profilins in health and disease: relevance for spine plasticity and Fragile X syndrome. *Proc. Natl. Acad. Sci. U S A* 113, 3365–3370. doi: 10.1073/pnas.1516697113

Mitra, R., Jadhav, S., McEwen, B. S., Vyas, A., and Chattarji, S. (2005). Stress duration modulates the spatiotemporal patterns of spine formation in the basolateral amygdala. *Proc. Natl. Acad. Sci. U S A* 102, 9371–9376. doi: 10.1073/pnas.0504011102

Mizuno, K. (2013). Signaling mechanisms and functional roles of cofilin phosphorylation and dephosphorylation. *Cell Signal.* 25, 457–469. doi: 10.1016/j.cellsig.2012.11.001

Muddashetty, R. S., Kelić, S., Gross, C., Xu, M., and Bassell, G. J. (2007). Dysregulated metabotropic glutamate receptor-dependent translation of AMPA receptor and postsynaptic density-95 mRNAs at synapses in a mouse model of fragile X syndrome. *J. Neurosci.* 27, 5338–5348. doi: 10.1523/JNEUROSCI.0937-07.2007

Murakoshi, H., Wang, H., and Yasuda, R. (2011). Local, persistent activation of Rho GTPases during plasticity of single dendritic spines. *Nature* 472, 100–104. doi: 10.1038/nature09823

Nakayama, A. Y., Harms, M. B., and Luo, L. (2000). Small GTPases Rac and Rho in the maintenance of dendritic spines and branches in hippocampal pyramidal neurons. *J. Neurosci.* 20, 5329–5338. doi: 10.1523/JNEUROSCI.20-14-05329.2000

Neuhoff, H., Sassoè-Pognetto, M., Panzanelli, P., Maas, C., Witke, W., and Kneussel, M. (2005). The actin-binding protein profilin I is localized at synaptic sites in an activity-regulated manner. *Eur. J. Neurosci.* 21, 15–25. doi: 10.1111/j.1460-9568.2004.03814.x

Ohashi, K. (2015). Roles of cofilin in development and its mechanisms of regulation. *Dev. Growth Differ.* 57, 275–290. doi: 10.1111/dgd.12213

Okamoto, K.-I., Nagai, T., Miyawaki, A., and Hayashi, Y. (2004). Rapid and persistent modulation of actin dynamics regulates postsynaptic reorganization underlying bidirectional plasticity. *Nat. Neurosci.* 7, 1104–1112. doi: 10.1038/nn1311

Ouyang, J., Chen, X., Su, S., Li, X., Xu, X., Yu, X., et al. (2021). Neuroligin1 contributes to neuropathic pain by promoting phosphorylation of cofilin in excitatory neurons. *Front. Mol. Neurosci.* 14:640533. doi: 10.3389/fnmol.2021.640533

Pennucci, R., Gucciardi, I., and de Curtis, I. (2019). Rac1 and Rac3 GTPases differently influence the morphological maturation of dendritic spines in hippocampal neurons. *PLoS One* 14:e0220496. doi: 10.1371/journal.pone.0220496

Perumal, M. B., and Sah, P. (2021). Inhibitory circuits in the basolateral amygdala in aversive learning and memory. *Front. Neural Circuits* 15:633235. doi: 10.3389/fncir.2021.633235

Pillai, A. G., Anilkumar, S., and Chattarji, S. (2012). The same antidepressant elicits contrasting patterns of synaptic changes in the amygdala vs hippocampus. *Neuropsychopharmacology* 37, 2702–2711. doi: 10.1038/npp.2012.135

Pontrello, C. G., and Ethell, I. M. (2009). Accelerators, brakes and gears of actin dynamics in dendritic spines. *Open Neurosci. J.* 3, 67–86. doi: 10.2174/1874082000903020067

Popoli, M., Yan, Z., McEwen, B. S., and Sanacora, G. (2011). The stressed synapse: the impact of stress and glucocorticoids on glutamate transmission. *Nat. Rev. Neurosci.* 13, 22–37. doi: 10.1038/nrn3138

Pyronneau, A., He, Q., Hwang, J.-Y., Porch, M., Contractor, A., and Zukin, R. S. (2017). Aberrant Rac1-cofilin signaling mediates defects in dendritic spines, synaptic function and sensory perception in fragile X syndrome. *Sci. Signal.* 10:eaan0852. doi: 10.1126/scisignal.aan0852

Rahman, M. M., Callaghan, C. K., Kerskens, C. M., Chattarji, S., and O'Mara, S. M. (2016). Early hippocampal volume loss as a marker of eventual memory deficits caused by repeated stress. *Sci. Rep.* 6:29127. doi: 10.1038/srep29127

Rane, C. K., and Minden, A. (2014). P21 activated kinases: structure, regulation and functions. *Small GTPases* 5:e28003. doi: 10.4161/sgtp.28003

Rau, V., DeCola, J. P., and Fanselow, M. S. (2005). Stress-induced enhancement of fear learning: an animal model of posttraumatic stress disorder. *Neurosci. Biobehav. Rev.* 29, 1207–1223. doi: 10.1016/j.neubiorev.2005.04.010

Roozendaal, B., McEwen, B. S., and Chattarji, S. (2009). Stress, memory and the amygdala. *Nat. Rev. Neurosci.* 10, 423–433. doi: 10.1038/nrn2651

Rust, M. B. (2015). ADF/cofilin: a crucial regulator of synapse physiology and behavior. *Cell. Mol. Life Sci.* 72, 3521–3529. doi: 10.1007/s00018-015-1941-z

Sala, C. (2002). Molecular regulation of dendritic spine shape and function. *Neurosignals* 11, 213–223. doi: 10.1159/000065433

Sancho, L., and Bloodgood, B. L. (2018). Functional distinctions between spine and dendritic synapses made onto parvalbumin-positive interneurons in mouse cortex. *Cell Rep.* 24, 2075–2087. doi: 10.1016/j.celrep.2018.07.070

Scheetz, A. J., Nairn, A. C., and Constantine-Paton, M. (2000). NMDA receptor-mediated control of protein synthesis at developing synapses. *Nat. Neurosci.* 3, 211–216. doi: 10.1038/72915

Shankar, G. M., Bloodgood, B. L., Townsend, M., Walsh, D. M., Selkoe, D. J., and Sabatini, B. L. (2007). Natural oligomers of the Alzheimer amyloid-beta protein induce reversible synapse loss by modulating an NMDA-type glutamate receptor-dependent signaling pathway. *J. Neurosci.* 27, 2866–2875. doi: 10.1523/JNEUROSCI.4970-06.2007

Shin, L. M., Wright, C. I., Cannistraro, P. A., Wedig, M. M., McMullin, K., Martis, B., et al. (2005). A functional magnetic resonance imaging study of amygdala and medial prefrontal cortex responses to overtly presented fearful faces in posttraumatic stress disorder. *Arch. Gen. Psychiatry* 62, 273–281. doi: 10.1001/archpsyc.62.3.273

Suvrathan, A., Bennur, S., Ghosh, S., Tomar, A., Anilkumar, S., and Chattarji, S. (2013). Stress enhances fear by forming new synapses with greater capacity for long-term potentiation in the amygdala. *Philos. Trans. R. Soc. Lond. B Biol. Sci.* 369:20130151. doi: 10.1098/rstb.2013.0151

Tashiro, A., Minden, A., and Yuste, R. (2000). Regulation of dendritic spine morphology by the rho family of small GTPases: antagonistic roles of Rac and Rho. *Cereb. Cortex* 10, 927–938. doi: 10.1093/cercor/10.10.927

Tashiro, A., and Yuste, R. (2004). Regulation of dendritic spine motility and stability by Rac1 and Rho kinase: evidence for two forms of spine motility. *Mol. Cell. Neurosci.* 26, 429–440. doi: 10.1016/j.mcn.2004.04.001

Vyas, A., Mitra, R., Shankaranarayana Rao, B. S., and Chattarji, S. (2002). Chronic stress induces contrasting patterns of dendritic remodeling in hippocampal and amygdaloid neurons. *J. Neurosci.* 22, 6810–6818. doi: 10.1523/JNEUROSCI.22-15-06810.2002

Watanabe, Y., Gould, E., and McEwen, B. S. (1992). Stress induces atrophy of apical dendrites of hippocampal CA3 pyramidal neurons. *Brain Res.* 588, 341–345. doi: 10.1016/0006-8993(92)91597-8

Yang, N., Higuchi, O., Ohashi, K., Nagata, K., Wada, A., Kangawa, K., et al. (1998). Cofilin phosphorylation by LIM-kinase 1 and its role in Rac-mediated actin reorganization. *Nature* 393, 809–812. doi: 10.1038/31735

Zhao, L., Ma, Q.-L., Calon, F., Harris-White, M. E., Yang, F., Lim, G. P., et al. (2006). Role of p21-activated kinase pathway defects in the cognitive deficits of Alzheimer disease. *Nat. Neurosci.* 9, 234–242. doi: 10.1038/nn1630

Zhao, Z.-S., and Manser, E. (2012). PAK family kinases: physiological roles and regulation. *Cell. Logist.* 2, 59–68. doi: 10.4161/cl.21912

Conflict of Interest: The authors declare that the research was conducted in the absence of any commercial or financial relationships that could be construed as a potential conflict of interest.

Publisher's Note: All claims expressed in this article are solely those of the authors and do not necessarily represent those of their affiliated organizations, or those of the publisher, the editors and the reviewers. Any product that may be evaluated in this article, or claim that may be made by its manufacturer, is not guaranteed or endorsed by the publisher.

frontiers | Frontiers in Molecular Neuroscience

REVIEW
published: 20 June 2022
doi: 10.3389/fnmol.2022.855752

Role of Ca^{2+}/Calmodulin-Dependent Protein Kinase Type II in Mediating Function and Dysfunction at Glutamatergic Synapses

*Archana G. Mohanan[1], Sowmya Gunasekaran[1,2†], Reena Sarah Jacob[1,2†] and R. V. Omkumar[1]**

[1] Neurobiology Division, Rajiv Gandhi Centre for Biotechnology, Thiruvananthapuram, India, [2] Research Scholar, Manipal Academy of Higher Education, Manipal, India

Glutamatergic synapses harbor abundant amounts of the multifunctional Ca^{2+}/calmodulin-dependent protein kinase type II (CaMKII). Both in the postsynaptic density as well as in the cytosolic compartment of postsynaptic terminals, CaMKII plays major roles. In addition to its Ca^{2+}-stimulated kinase activity, it can also bind to a variety of membrane proteins at the synapse and thus exert spatially restricted activity. The abundance of CaMKII in glutamatergic synapse is akin to scaffolding proteins although its prominent function still appears to be that of a kinase. The multimeric structure of CaMKII also confers several functional capabilities on the enzyme. The versatility of the enzyme has prompted hypotheses proposing several roles for the enzyme such as Ca^{2+} signal transduction, memory molecule function and scaffolding. The article will review the multiple roles played by CaMKII in glutamatergic synapses and how they are affected in disease conditions.

Keywords: Ca^{2+}/calmodulin-dependent protein kinase type II (CaMKII), glutamatergic synapse, LTP, LTD, synaptic plasticity, CaMKII genetic models, CaMKII mutations

OPEN ACCESS

Edited by:
Dhrubajyoti Chowdhury, Yale University, United States

Reviewed by:
Johannes W. Hell, University of California, Davis, United States
Shahid Khan, Molecular Biology Consortium, United States

****Correspondence:***
R. V. Omkumar
omkumar@rgcb.res.in

† These authors have contributed equally to this work

Specialty section:
This article was submitted to Molecular Signalling and Pathways, a section of the journal Frontiers in Molecular Neuroscience

Received: *15 January 2022*
Accepted: *21 March 2022*
Published: *20 June 2022*

Citation:
Mohanan AG, Gunasekaran S, Jacob RS and Omkumar RV (2022) Role of Ca^{2+}/Calmodulin-Dependent Protein Kinase Type II in Mediating Function and Dysfunction at Glutamatergic Synapses. Front. Mol. Neurosci. 15:855752. doi: 10.3389/fnmol.2022.855752

INTRODUCTION

Glutamatergic synapses are the main excitatory synapses in the brain particularly in the cerebral cortex and hippocampus. More than 80% of synapses in the cortex are glutamatergic (Micheva et al., 2010). Glutamatergic transmission plays a major role in neuronal functions in the brain. Imbalances in glutamatergic signaling can lead to several neurodegenerative and psychiatric conditions (Moretto et al., 2018).

Calcium (Ca^{2+}) signaling is an essential component in signal transduction at glutamatergic synapses. Calcium signals are tightly regulated since sustained elevation in Ca^{2+} levels can lead to toxicity. In glutamatergic synapses, the spike patterns of Ca^{2+} signals are thought to encode information. Decoding these signals requires the participation of efficient protein machineries that convert them into long-lasting biochemical and cellular changes representing memories. Calcium (Ca^{2+})/calmodulin (CaM)-dependent protein kinase II (CaMKII) at synapses plays a significant role in decoding Ca^{2+} spike patterns and in converting them to corresponding biochemical states. Thus, CaMKII has gained the status of a "memory molecule" by being the initiator of biochemical memory in the brain. However, the multiple isoforms and splice variants of CaMKII that assemble in varying combinations to give rise to several holoenzyme subtypes, makes it so

versatile that it is involved in several other functions both in the brain and in other tissues. The phylogenetic relations of CaMKII with other kinases, its structure, its different isoforms and splice variants, biochemical and physiological functions, especially in long-term potentiation (LTP) and long-term depression (LTD), and its role in various diseases have been reviewed recently (Bayer and Schulman, 2019; Giese, 2021; Sloutsky and Stratton, 2021). Its functions specifically in the glutamatergic postsynaptic compartment have also been previously described (Hell, 2014). This article covers the basics on CaMKII including the recent advances in structure, isoforms, activation mechanisms, role in LTP and LTD, regulation of its translation, role in synapse morphology regulation, role in presynaptic mechanisms and role in various pathological conditions with emphasis on its functioning at glutamatergic synapses. *In vivo* models of CaMKII mutants with the associated behavioral phenotypes and CaMKII mutations reported in neurodevelopmental disorders and learning disabilities in humans have also been included in the present review.

Ca^{2+}/CALMODULIN-DEPENDENT PROTEIN KINASE TYPE II ISOFORMS AND THEIR FUNCTION IN GLUTAMATERGIC SYNAPSES

Even though CaMKII has four distinct isoforms (α, β, γ, and δ) encoded by four different genes with molecular weight ranging from 52 to 83 kDa, α and β are the predominant ones in neurons. CaMKIIα has distinct roles in neuronal plasticity and memory. It is predominant in the hippocampal and in the neocortical areas of the brain. CaMKIIβ is enriched in cerebellum and is involved in neuronal development. While both CaMKIIα and CaMKIIβ are expressed in excitatory pyramidal neurons in the cortex and hippocampus, only CaMKIIβ is found in inhibitory interneurons in these regions (Nicole and Pacary, 2020). CaMKIIδ isoform participates in long-lasting memory storage in the hippocampus (Zalcman et al., 2018, 2019). CaMKIIγ isoform is attributed with the main function of synapse-to-nucleus communication, conveying Ca^{2+} signals to the nucleus and regulating gene expression that is essential for neural plasticity involved in memory (Ma et al., 2014; Cohen et al., 2018).

Ca^{2+}/CALMODULIN-DEPENDENT PROTEIN KINASE TYPE II STRUCTURE IN RELATION TO ITS FUNCTION

CaMKII forms large homo or hetero oligomeric assemblies of either single or multiple isoforms (Hoelz et al., 2003; Bayer and Schulman, 2019). The core sequence for the CaMKII isoforms includes an N-terminal catalytic domain, followed by a CaM binding autoregulatory domain containing Thr^{286}/Thr^{287}, a variable domain that is subject to alternative splicing and a C-terminal self-association domain. A linear representation of a CaMKII subunit is shown in **Figure 1A**.

Under basal state, the enzyme is present in an autoinhibited state with the regulatory segment bound to the substrate-docking groove on each kinase domain. It can be activated by the binding of Ca^{2+}/CaM to the autoregulatory domain which releases the regulatory segment off the kinase domain. Activation of adjacent subunits can result in trans-autophosphorylation at Thr^{286} site (Rich and Schulman, 1998) in the regulatory segment which generates 'autonomous' kinase activity even after the initial Ca^{2+}-stimulus subsides (Miller and Kennedy, 1986) by preventing the regulatory segment binding on the kinase domain. This inter-subunit autophosphorylation mechanism enables Ca^{2+}-spike frequency-detection by CaMKII (De Koninck and Schulman, 1998). The autophosphorylation at Thr^{286} can also increase the affinity of the enzyme for CaM by about 1000-fold, a process termed as CaM trapping. A single autophosphorylated subunit can also rapidly phosphorylate its neighbors. Thus, a brief Ca^{2+} stimulus in the synapse can lead to the persistence of Thr^{286}-autophosphorylated CaMKII that represents molecular memory (**Figure 2**). Autophosphorylation at Thr^{286} is an essential event in the induction of LTP that underlies memory formation.

Once Ca^{2+}/CaM dissociates from the kinase, *cis*-autophosphorylation occurs at the CaM binding domain of CaMKII at the $Thr^{305/306}$ position. Phosphorylation at these sites, termed as "inhibitory" or "burst" autophosphorylation, prevents the binding of Ca^{2+}/CaM and hence kinase cannot be further stimulated. Autophosphorylation at Thr^{305} and Thr^{306} before phosphorylation of Thr^{286} makes the kinase non-responsive to Ca^{2+}/CaM stimulus and such a kinase cannot be activated. On the other hand, if Thr^{286} gets autophosphorylated first, it leads to a holoenzyme in which Thr^{305} and Thr^{306} are protected by Ca^{2+}/CaM and cannot be phosphorylated (Bhattacharyya et al., 2020). It is also reported that CaMKII phosphorylation at $Thr^{305/306}$ is selectively promoted by LTD inducing stimuli and not by LTP inducing stimuli, and phosphorylation at $Thr^{305/306}$ directs CaMKII movement during LTD from excitatory to inhibitory synapses. This phosphorylation can also reduce the activity of phospho-Thr^{286} CaMKII in the absence of Ca^{2+} (Cook et al., 2021).

The first snapshot of the 3D structure of this enzyme was an electron microscopy (EM) image of CaMKII purified from rabbit skeletal muscle (Woodgett et al., 1983) that revealed a symmetrical hexagonal structure, composed of two stacked 6-membered rings. Since then, several hypotheses have been proposed about its structure in relation to its function. The catalytic/autoregulatory domains of each subunit are attached to the hexameric ring by a stalk-like appendage that presumably allows subunits to behave independently of one another for activity and Ca^{2+}/CaM binding, but in concert with one another for the intra-holoenzyme autophosphorylation reaction (**Figure 1B**). Most of the crystallographic studies provided structures at atomic resolution of truncated forms having single or multiple domains (Hoelz et al., 2003; Rosenberg et al., 2006) giving insights on the mechanism of catalytic activity and atomic level details

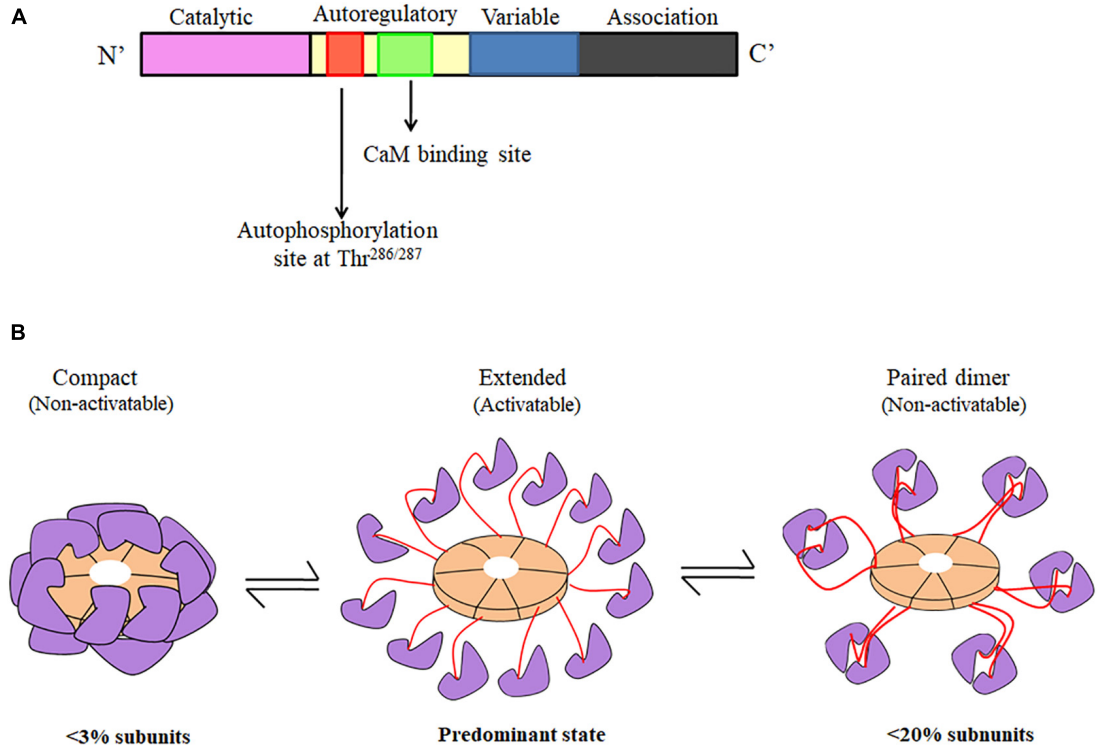

FIGURE 1 | (A) Linear representation of CaMKII structure showing catalytic, autoregulatory, variable and association domains. **(B)** CaMKII holoenzyme structure in three different forms-CaMKII can exist predominantly in the activatable state with an extended conformation along with some non-activatable states, which are represented as both compact form and kinase domain paired form. The different subunits of a single CaMKII holoenzyme can exist in any combination of the three forms. Purple color indicates kinase domain, peach color denotes association domain, and red color indicates regulatory domain (Myers et al., 2017).

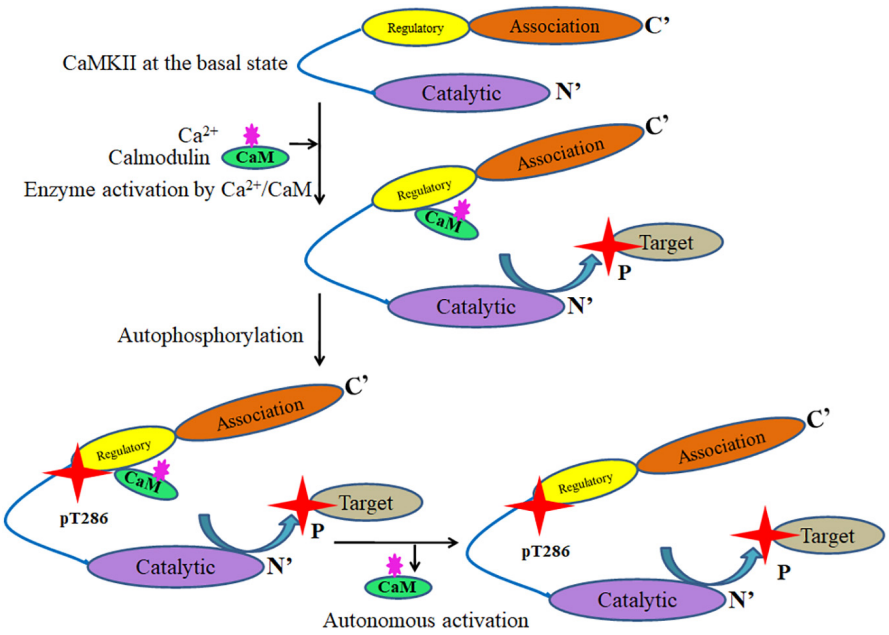

FIGURE 2 | Basic activation mechanism of CaMKII that leads to autonomy resulting from Thr^{286} autophosphorylation. Under basal conditions, the enzyme is present in an autoinhibited state with the regulatory segment bound to the catalytic domain. This can be activated by the binding of Ca^{2+}/CaM to the regulatory domain which releases the regulatory segment from the catalytic domain. The activated enzyme can autophosphorylate at Thr^{286} or any other substrates. The autonomous CaMKII thus generated can be catalytically active even in the absence of Ca^{2+}/CaM.

of the interactions holding the 3D structure and interactions between domains.

The recent studies based on single-particle EM (Myers et al., 2017; Bhattacharyya et al., 2020) in combination with biochemical and live-cell imaging experiments (Buonarati et al., 2021) further substantiated the multimeric structure of CaMKII holoenzyme having a rigid central hub complex formed by the association domains. The kinase domains are linked to the hub by the intrinsically disordered and highly flexible linker regions (residues 301–344) so that they can readily perform inter-subunit autophosphorylation. The holoenzymes range from 15–35 nm in diameter. This model also predicts that CaMKII holoenzymes can exist in three different conformations. Among these three conformations, <3% of the holoenzymes are in the compact conformation, ∼20% appears to form kinase dimers and most of the kinase domains are ordered independently both *in vitro* and inside the cells. CaMKII holoenzymes which appear as either compact or kinase dimers are inactive, whereas the fraction with fully extended kinase domains is in the activatable state (**Figure 1B**; Myers et al., 2017; Bayer and Schulman, 2019).

The formation of extended intra-holoenzyme kinase dimers could enable cooperative activation by CaM in both α and β isoforms (Myers et al., 2017; Bhattacharyya et al., 2020; Buonarati et al., 2021) but there could be distinct steric positioning of kinase domains in the CaMKIIα versus β holoenzyme due to differences in the linker length. This explains the differences in the autophosphorylation states of both the isoforms; CaMKIIα acquires Thr^{286} phosphorylation more readily than $Thr^{305/306}$ phosphorylation whereas inhibitory autophosphorylation at $Thr^{306/307}$ in CaMKIIβ occurs more readily. Inter-holoenzyme kinase dimer formation is thought to involve a high order clustering among CaMKII holoenzymes and is present in minimal quantities under normal physiological conditions for both the isoforms. But it is enhanced in both excitotoxic and ischemic conditions and the high-order CaMKII clustering formed by inter-holoenzyme kinase domain dimerization is reduced for the β isoform for both basal and excitotoxicity-induced clusters, both *in vitro* and in neurons (Buonarati et al., 2021). Much of the studies on holoenzyme structure have been carried out using homomers of either α or β isoforms. However, heteromultimeric CaMKII formed by α and β is known to play key functions in the brain. Structural insights into heteromultimeric forms of CaMKII would help in further advancing the understanding of the physiological functioning of this enzyme. It has been also noted that a small percentage (<4%) of holoenzymes of CaMKIIα were found as 14-mers even with full-length kinase domains (Myers et al., 2017) whereas CaMKIIβ can even exist in 16-mers (Buonarati et al., 2021). The existence of a full-length 14-mer is thought to be an intermediate state in which the exchange of subunits is possible (Myers et al., 2017) and it entails the exchange of activated subunits between two activated, or an activated and a non-activated holoenzyme (Bhattacharyya et al., 2020). This hypothesis was supported by the finding that proteolytic cleavage of the kinase domains from a 12-meric holoenzyme preparation results in the subsequent formation of 14-meric hub domain assemblies (Rosenberg et al., 2006). The function of this kind of subunit exchange is currently unknown, but it is speculated that it can be a part of repair mechanisms of individual subunits and/or synaptic plasticity mechanisms (Bayer and Schulman, 2019).

Ca^{2+}/CALMODULIN-DEPENDENT PROTEIN KINASE TYPE II ACTIVATION IN RESPONSE TO Ca^{2+} INFLUX THROUGH *N*-METHYL-*D*-ASPARTATE RECEPTOR

N-Methyl-D-aspartate receptor (NMDAR) is an ionotropic glutamate receptor with high Ca^{2+} permeability that plays an important role in excitatory neurotransmission in the central nervous system (CNS). Glutamate binding to α-amino-3-hydroxy-5-methyl-4-isoxazole propionic acid receptors (AMPARs) can induce depolarization in the postsynaptic membrane of glutamatergic synapses. The binding of glutamate and glycine and the depolarization-induced removal of Mg^{2+} block causes NMDAR to open and conduct Ca^{2+} and Na^{+} into the cell. This Ca^{2+} influx activates several important signaling pathways involving different protein kinases including CaMKII and phosphatases. Activated CaMKII can bind to various membrane proteins as listed in **Table 1**. The enzyme can interact with each of these proteins either in the Ca^{2+}/CaM activated form or in the autophosphorylated form. It can bind with high affinity at the GluN2B subunit of NMDAR and phosphorylate GluN2B-Ser^{1303} (Omkumar et al., 1996). GluN2B-binding can also happen at the T-site of CaMKII (site where Thr^{286} is bound in the inactive state) making the enzyme permanently active even after the Ca^{2+} stimulus subsides (Bayer et al., 2001). In addition, the kinetic parameters of CaMKII activity and its affinity for ATP are altered in an allosteric manner upon binding to GluN2B (Pradeep et al., 2009; Cheriyan et al., 2011; Madhavan et al., 2020) and this regulation is limited only to the subunit of the enzyme that binds GluN2B (Cheriyan et al., 2012). CaMKII activated in the cytosol can translocate to the postsynaptic membrane where the NMDAR complex is embedded in the postsynaptic density (PSD). CaMKII reversibly translocates to synaptic sites in response to brief stimuli, but its resident time at the synapse increases after longer stimulation (Bayer et al., 2006). It is also reported that the phosphorylation status of GluN2B at Ser^{1303} also regulates GluN2B-CaMKII interaction (Raveendran et al., 2009), whereas the phosphorylation status of Ser^{1303}, in turn, is regulated by the action of kinases and phosphatases (Ramya et al., 2012). In the GluN2B-bound state, the enzyme becomes resistant to the action of phosphatases (Cheriyan et al., 2011) indicating GluN2B-induced structural changes which can be abolished by specific mutations in CaMKII (Mayadevi et al., 2016). This could be a possible reason for the resistance of phospho-Thr^{286}-CaMKIIα to phosphatases in the PSD (Mullasseril et al., 2007). Autonomy of CaMKII due to GluN2B-binding can be terminated only by dissociation of CaMKII from GluN2B. Repeated Ca^{2+} influx through NMDAR promotes the persistent binding of CaMKII to GluN2B which occurs during LTP (Bayer et al., 2006).

TABLE 1 | Protein ligands of CaMKII in the postsynaptic compartment of glutamatergic synapses.

Sl. No.	Protein ligand to which CaMKII binds	Region of binding	Functional implications of this binding	Reference(s)
1	NMDAR subunit GluN2B	839–1120	The binding requires auto phosphorylated CaMKII; tethering at the synaptic membrane; LTP	Lisman et al., 2012
2	NMDAR subunit GluN2B	1289–1310	Activated CaMKII can bind; tethering at the synaptic membrane; LTP	Lisman et al., 2012
3	NMDAR subunit GluN2A	1349–1464	Synaptic targeting	Gardoni et al., 1999
4	NMDAR subunit GluN1	845–863	Synaptic targeting	Leonard et al., 2002
5	Cav1.2	1589–1690	Tethering at the synaptic membrane	Hudmon et al., 2005
6	Densin-180	1247–1495	Membrane localization	Strack et al., 2000b; Robison et al., 2005
7	Tiam 1	1540–1560	Constitutive CaMKII activation; LTP	Saneyoshi et al., 2019
8	Ether-a-go-go (Eag)	731–803	Constitutive CaMKII activation; LTP	Sun et al., 2004

Long Term Potentiation Induction by the Activation of *N*-Methyl-D-Aspartate Receptors-Role of Ca^{2+}/Calmodulin-Dependent Protein Kinase Type II in *N*-Methyl-D-Aspartate Receptor-Dependent Long Term Potentiation

LTP is a process in which brief periods of synaptic activity produces long-lasting increase in the strength of a synapse, as shown by an increase in the size of the excitatory postsynaptic current (EPSC) (Lisman et al., 2012; Bliss and Collingridge, 2019). Several studies have shown that LTP has the essential characteristics of a cellular mechanism that could underlie memory and can serve as an excellent cellular model of memory. Impairment in LTP formation predicts memory impairment in human subjects (Di Lorenzo et al., 2020). LTP occurring at CA3-CA1 synapses (between Schaffer collateral (SC) terminals and CA1 pyramidal neurons) of the hippocampal region is mainly mediated through NMDARs and occurs predominantly by postsynaptic modifications (MacDonald et al., 2006). This model of LTP is a suitable model for associative learning (Baltaci et al., 2019).

LTP has an early phase which is independent of protein synthesis, called early-LTP (E-LTP), and a late phase (L-LTP) which involves the activation of transcription factors and is dependent on protein synthesis, during which structural changes are observed. Single brief tetanus leads to E-LTP that lasts up to 1–3 h and intermittent and repetitive stimulations (or single stronger tetanus) produce L-LTP that lasts at least 24 h (Baltaci et al., 2019). During the induction of LTP, Ca^{2+} influx through NMDARs activates signaling pathways that lead to synaptic modifications (Malenka et al., 1989). NMDAR-dependent LTP requires one or more trains of 100 Hz stimulations (Baltaci et al., 2019).

Over three decades of study suggests that CaMKII is one of the key players in LTP (Zalcman et al., 2018). Inhibition of CaMKII activity blocks the induction as well as maintenance of LTP (Malenka et al., 1989; Malinow et al., 1989; Tao et al., 2021). In response to sufficient influx of Ca^{2+} into the postsynaptic neuron, CaMKII gets activated by the binding of Ca^{2+}/CaM and autophosphorylated at Thr^{286}. Both these forms of CaMKII can translocate to PSD and bind to GluN2B. Autonomously active nature of Thr^{286} phosphorylated CaMKII as well as GluN2B-bound CaMKII is proposed to contribute toward molecular memory. But Thr^{286} autophosphorylation does not have an essential role in NMDAR dependent synaptic potentiation in early postnatal development and in adult dentate gyrus, where neurogenesis occurs (Giese, 2021). Persistent nature of GluN2B-CaMKII interaction could also contribute towards its role in maintaining synaptic strength (Sanhueza et al., 2011). If this interaction is impaired by mutations on the binding sites on CaMKII and/or GluN2B (Yang and Schulman, 1999; Strack et al., 2000a; Mayadevi et al., 2002; Pradeep et al., 2009), then LTP gets impaired (Barria and Malinow, 2005). The binding of GluN2B locks CaMKII in an active conformation and the enzyme can phosphorylate its substrates present in the PSD. The protein substrates of CaMKII in the PSD and the physiological consequences of their phosphorylation status are listed out in **Supplementary Table 1** (McGlade-McCulloh et al., 1993; Inagaki et al., 1997; Gardoni et al., 2003, 2006; Oh et al., 2004; Chen and Roche, 2007; Shin et al., 2012; Zhang et al., 2019; Zybura et al., 2020). One of the main effectors of LTP is AMPAR. CaMKII that is localized in PSD through interaction with GluN2B can phosphorylate Ser^{831} residue of the GluA1 subunit of AMPAR causing potentiation of the single channel conductance of AMPAR (**Figure 3**; Barria et al., 1997a,b). As part of LTP, more AMPARs are recruited to the synapses and this process is called *AMPAfication* (Malenka and Nicoll, 1999). The process of *AMPAfication* makes the transmission even stronger (Zhu and Malinow, 2002). It is also reported that the interaction of CaMKII with GluN2B effects a liquid-liquid phase separation with co-segregation of AMPA receptors and the synaptic adhesion molecule neuroligin into a phase-in-phase assembly indicating the formation of functional nanodomains in the synapse (Hosokawa et al., 2021).

Other than AMPAR, CaMKII has other downstream targets such as transmembrane AMPAR-regulatory proteins (TARPs). TARPs are auxiliary proteins that help in AMPAR functions and trafficking (Jackson and Nicoll, 2011). They have several phosphorylation sites for CaMKII which are implicated in the positioning and trapping of AMPAR in PSD (**Supplementary Table 1**). The C-tail of the TARP family

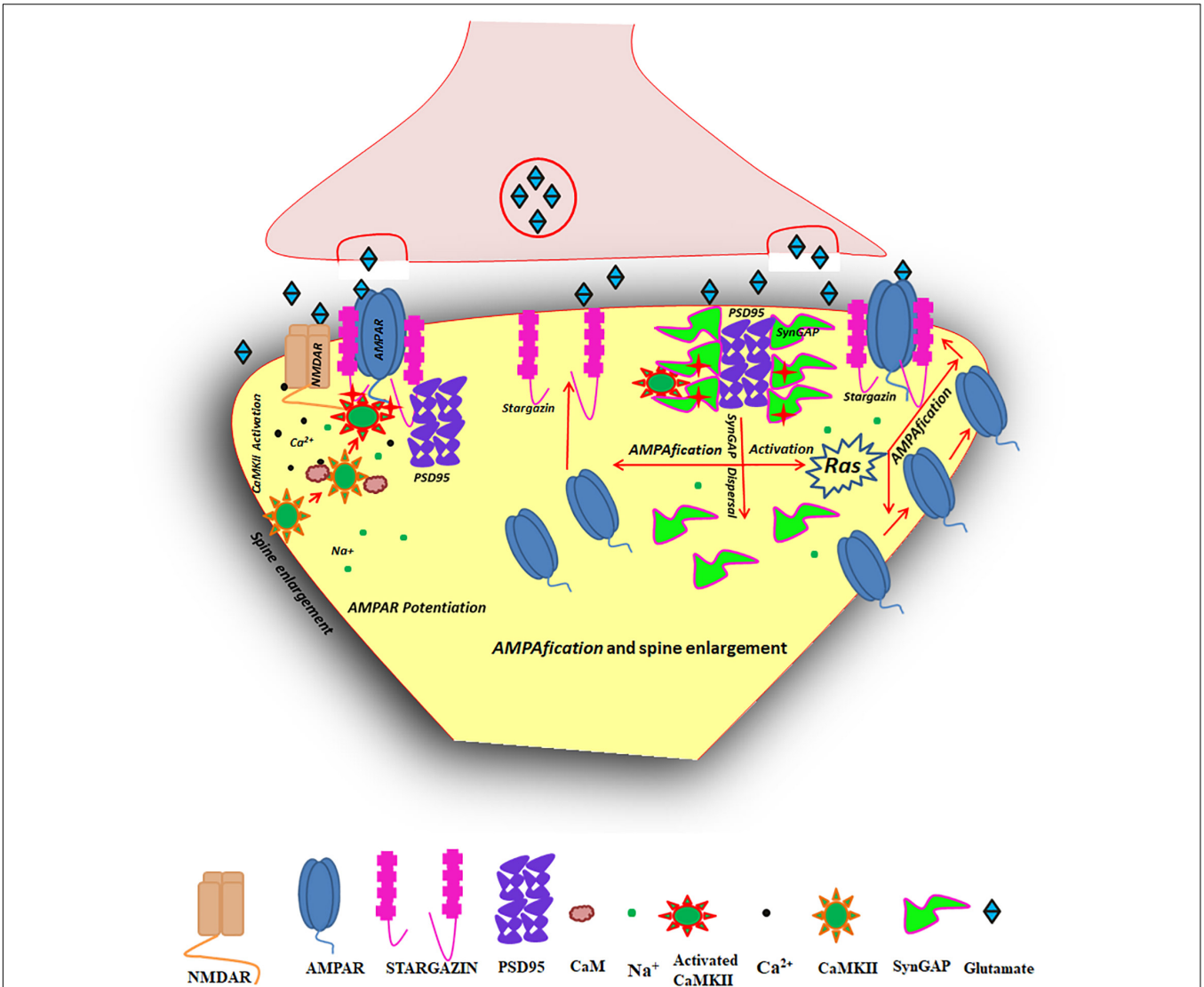

FIGURE 3 | Schematic diagram shows the role of CaMKII in LTP. CaMKII activity at the PSD is essential for the induction and maintenance of LTP, either through (i) enhancement of AMPAR conductance or through (ii) AMPAfication of the postsynaptic site. In either of these functions, activation of CaMKII along with its translocation to its own adapters at the PSD, especially to the GluN2B subunit of NMDAR is essential. The translocated CaMKII can phosphorylate its substrates involved in the induction and maintenance of LTP. (i) AMPAR potentiation-The phosphorylation at Ser^{831} of GluA1 of AMPAR by CaMKII enhances the single channel conductance of AMPAR especially AMPAR formed by GluA1 homomers (Derkach et al., 1999). (ii) AMPAfication (conversion of silent synapses to active synapses)-AMPARs are positioned in the PSD by interaction with many proteins, especially stargazin. Phosphorylation of stargazin by CaMKII results in its dissociation from lipid rafts and binding to PSD95 to make more AMPAR slots on the membrane (slot hypothesis for AMPAfication). In addition to this, CaMKII can phosphorylate SynGAP which results in its elimination from the synapse followed by the activation of Ras/ERK signaling which mediates AMPAfication or AMPAR recruitment to the PSD. These signaling cascades finally lead to spine enlargement.

member, stargazin (TARPγ-2) can be phosphorylated by CaMKII which disrupts the interaction of stargazin with phospholipids in the membrane and eventually allows stargazin to bind with PSD95, a major scaffolding protein in PSD to which many other proteins can bind. In this way, stargazin can trap AMPAR in the PSD (Opazo et al., 2010; Hafner et al., 2015). It is also known that the hippocampally enriched TARPγ-8, but not TARPγ-2/3/4, is a critical CaMKII substrate necessary for LTP induction. The residues of TARPγ-8, Ser^{277} and Ser^{281} are major phosphorylation sites for CaMKII, which sufficiently enhances AMPAR transmission. Mutations of these residues impair LTP, without affecting AMPAR-mediated basal transmission and protein levels of AMPAR in PSD or extrasynaptic regions (Park et al., 2016).

CaMKII can also trap AMPAR in the postsynaptic site through other pathways such as Ras/ERK signaling. In the postsynaptic site, SynGAP (synaptic Ras/Rap GTPase-activating protein) is highly enriched and harbors phosphorylation sites for CaMKII. SynGAP contains C-terminal PDZ binding domain which interacts with PSD95 under basal conditions. During

LTP induction, CaMKII can phosphorylate this protein. This phosphorylation decreases the affinity of SynGAP toward PSD95, which in turn dissociates away from the same. The massive removal of SynGAP makes more PSD95 available for binding of TARPs and thereby AMPAR trapping in the postsynaptic site (**Figure 3**; Gamache et al., 2020).

The synaptic SynGAP dispersion also decreases its RasGAP activity, leading to the activation of Ras/ERK signaling crucial for AMPAR delivery (Walkup et al., 2016). The phosphorylation of SynGAP by CaMKII leads to activation of Ras/ERK signaling and inactivation of Rap. The activation of Ras/ERK signaling drives AMPAR delivery to the postsynaptic site whereas Rap mediates AMPAR removal upon its activation. Thus, SynGAP phosphorylation by CaMKII can enhance AMPAR recruitment during LTP (Zhu et al., 2002; Rumbaugh et al., 2006; Wang C.C. et al., 2013; Araki et al., 2015; Walkup et al., 2015).

LTP is also accompanied by increase in spine volume mediated by activation of CaMKII. Activated CaMKII can influence the activity of Rho GTPase–regulatory proteins [e.g., RhoGEFs (guanine nucleotide exchange factors that activate Rho GTPases) and/or RhoGAPs (GTPase-activating proteins that inhibit Rho GTPases)] to promote actin polymerization in the head and neck region of dendritic spines (Herring and Nicoll, 2016). This results in an increase in size of the spine head and diameter of the neck. Increased actin polymerization also results in the reorganization of PSD proteins in such a way that more AMPARs can be incorporated. SynGAP dispersion from PSD resulting from CaMKII phosphorylation is also related to spine enlargement (Araki et al., 2015).

LTP induction is also associated with the rapid formation of a positive feedback loop, formed by a reciprocally activating kinase-effector complex (RAKEC) in dendritic spines, which consist of CaMKII and Tiam1, a Rac1-specific guanine nucleotide exchange factor (Rac-GEF). Activated CaMKII can persistently interact with Tiam1, in stimulated spines enabling the persistence and confinement of a molecular memory (Saneyoshi et al., 2019). The constitutive activation of CaMKII by occupation of its T-site would help to maintain Tiam1 phosphorylation even after Ca^{2+} concentration subsides. This mechanism can therefore convert transient Ca^{2+} signaling into a persistent activation of Rac1 (protein required for spine formation and enlargement) and its downstream actin regulators. This pathway helps in the maintenance of the enlarged spine and thereby contributes to structural LTP (Kojima et al., 2019).

NMDAR activation in pyramidal neurons causes CaMKII-dependent phosphorylation of the guanine-nucleotide exchange factor (GEF), kalirin-7 at residue Thr^{95}, regulating its GEF activity, leading to activation of Rac1 and rapid enlargement of existing spines. Kalirin-7 also interacts with AMPA receptors and controls their synaptic expression (Xie et al., 2007).

During LTP maintenance, the levels of protein kinase M zeta (PKMζ), a constitutively active protein kinase C (PKC) isoform, are elevated. PKMζ maintains synaptic potentiation by preventing AMPAR endocytosis and promoting stabilization of dendritic spine growth. Inhibition of PKMζ, with zeta-inhibitory peptide (ZIP), can reverse LTP and impair established long-term memories (LTMs). Activated CaMKII can release the translational block on PKMζ mRNA, thereby helping in long-term maintenance of LTP (Patel and Zamani, 2021). It has been shown by direct evidence that CaMKII is essential for memory storage (Rossetti et al., 2017) by using a kinase-dead mutant (K42M) in the hippocampus where the mutant disrupted CaMKII signaling *in vivo*.

Putative Mechanisms of Memory Storage by Ca^{2+}/Calmodulin-Dependent Protein Kinase Type II

While considerable insights have been obtained on the mechanisms by which LTP-inducing tetanic stimuli are converted to enhanced AMPAR activity at the postsynaptic side, the mechanisms by which the potentiated state is maintained has been intensively debated (Giese et al., 1998; Buard et al., 2010; Coultrap et al., 2012; Chang et al., 2017; Giese, 2021; Tao et al., 2021). Even long-lasting structural changes such as spine enlargement are maintained by dynamic molecular mechanisms (Gamache et al., 2020). Among the several molecular systems that were proposed to sustain altered biochemical states, the bistable switch model involving CaMKII (Lisman and Zhabotinsky, 2001) has attracted considerable attention, in which the unphosphorylated and Thr^{286}-phosphorylated states of CaMKII represented the "OFF" and "ON" states respectively. The ability of the CaMKII oligomer to sustain its autophosphorylated state by autonomous activity has initially been proposed to convert information encoded in Ca^{2+}-spikes into stable biochemical traces (Miller and Kennedy, 1986; Hudmon and Schulman, 2002). However, rigorous computational modeling studies showed that successful functioning of the switch requires the participation of protein phosphatase 1 (PP1) and GluN2B (Miller et al., 2005; Michalski, 2013; Urakubo et al., 2014; Lisman and Raghavachari, 2015). The switch was predicted to function in an energy-efficient manner and remain active despite protein turnover (Lisman and Zhabotinsky, 2001). In the unpotentiated synapse, the switch will be in the "OFF" state with CaMKII mostly unphosphorylated. Any phosphorylation supported by resting Ca^{2+} concentration will be successfully annihilated by PP1–mediated dephosphorylation thereby preventing a slow drift to the autophosphorylated "ON" state thus providing stability to the "OFF" state.

LTP-inducing stimulus causes extensive CaMKII autophosphorylation at Thr^{286} due to high Ca^{2+} levels. Autophosphorylated CaMKII that translocates to the PSD will be more than sufficient to saturate the available PP1 activity. Thus, autophosphorylated CaMKII would compete out PP1 activity and thus the high level of autophosphorylation and autonomous activity will be maintained thereby giving stability to the "ON" state. Continued phosphorylation required to negate the effect of PP1 activity while maintaining the "ON" state, leads to consumption of energy in the form of ATP. The model predicted the switch to function in an energy-efficient manner with minimal consumption of ATP and remain active despite protein turnover (Lisman and Zhabotinsky, 2001). Evidence obtained later was in accordance with these predictions on the final functional outcome of the switch, although it involved additional mechanisms than the predicted ones. Accordingly, the revised model (Lisman and Raghavachari, 2015) predicts that energy efficiency is achieved by the reduced dephosphorylation rate of the GluN2B-bound CaMKII (Cheriyan et al., 2011;

Mayadevi et al., 2016). Stability against protein turnover is possible since protein turnover operates by subunit exchange between holoenzymes. Thus, replacement of a phosphorylated subunit with a new, unphosphorylated subunit will be followed by phosphorylation of the newly recruited subunit by adjacent autonomous subunits (Stratton et al., 2014; Lisman and Raghavachari, 2015).

In its "ON" state, the switch can initiate and maintain long-term strengthening of the synapse by the multiple mechanisms described above (see section entitled "LTP Induction by the Activation of NMDARs-Role of CaMKII in NMDAR-Dependent LTP"). But later studies indicated that the autophosphorylation of CaMKIIα was required only for rapid learning especially induced by a single stimulus but was not essential for memory formed by multiple trial learning (Irvine et al., 2005, 2011). This was further supported by the evidence that autophosphorylation at Thr^{286} lowers the stimulation frequency required to induce synaptic plasticity and permits CaMKII to better integrate Ca^{2+} signals at physiologically relevant frequencies that would happen only in LTP induction and not in maintenance (Chang et al., 2017). These findings are not consistent with the bistable switch model in which Thr^{286} autophosphorylation is an essential element. These studies suggest that Thr^{286} autophosphorylation might have a major role in the initial capture of information encoded in the synaptic Ca^{2+} spikes with more efficiency. However, inhibition of CaMKII activity can erase LTP showing the involvement of CaMKII in LTP maintenance, further suggesting that CaMKII acts as a molecular storage device (Tao et al., 2021).

CaMKII activity necessary for LTP maintenance at resting Ca^{2+} concentrations could be arising from the autonomous forms of CaMKII, Thr^{286}-phosphorylated or GluN2B-bound. If Thr^{286} is dispensable (Irvine et al., 2005, 2011; Chang et al., 2017) as mentioned above, the GluN2B-bound form of CaMKII could provide the autonomous activity. However, in the PSD, all the CaMKII subunits in a holoenzyme need not be bound by GluN2B unlike the *in vitro* experiments (Bayer et al., 1999) in which all CaMKII subunits could be bound by GluN2B. Whether the autonomous activity of the GluN2B-bound subunits of CaMKII in the PSD would be sufficient to maintain LTP needs further investigation, since GluN2B-binding does not spread to other subunits of a holoenzyme of CaMKII like Thr^{286} autophosphorylation.

REGULATION OF TRANSLATION OF Ca^{2+}/CALMODULIN-DEPENDENT PROTEIN KINASE TYPE II IN SYNAPTIC PLASTICITY

Gene expression needed for long-lasting synaptic plasticity is tightly regulated. In particular, protein synthesis, regulation of mRNA transport and mRNA stability contribute to the control of gene expression. mRNA translation happens in synaptic locations - dendrites and dendritic spines, which are filled with polyribosomes, translation factors, and mRNAs (Steward and Levy, 1982; Crino and Eberwine, 1996; Job and Eberwine, 2001; Steward and Schuman, 2001).

Regulation of Ca^{2+}/Calmodulin-Dependent Protein Kinase Type II by Cytoplasmic Polyadenylation Element-Binding Protein in Long Term Potentiation

Cytoplasmic polyadenylation element (CPE) present in the 3′ untranslated region (UTR) of mRNAs plays a major role in the regulation of translation in response to cellular signals (Klann and Dever, 2004). CPE sequence present in CaMKIIα mRNA helps in its rapid translation during LTP (Ouyang et al., 1997; Giovannini et al., 2001).

The neuronal CPE-binding protein (CPEB) protein from *Aplysia* has an amino-terminal extension, which can be converted into a prion-like molecule and this mechanism will aid in sustained protein synthesis. Thus, this process would play crucial roles during synaptic plasticity (Si et al., 2003). CPEB blocks translation when it is bound to CPE. Upon phosphorylation, CPEB can dissociate from CPE thereby triggering a series of molecular events leading to initiation of translation. CPEB can be phosphorylated by CaMKII (Wu et al., 1998). CPE-mediated translation following membrane depolarization is also CaMKII-dependent (Lisman et al., 2002). The 3′UTR of CaMKII and other specific mRNAs bind CPEB and polyadenylation specificity factor (CPSF) leading to translational arrest. With NMDAR activation, aurora kinase and CaMKII get activated leading to phosphorylation of CPEB. This is followed by CPEB-CPSF interaction which allows poly(A) polymerase (PAP) recruitment to this complex. PAP initiates the poly(A) tail elongation. This in turn activates poly(A)-binding protein (PABP) which binds to poly(A) tail and initiates interaction with elongation factor eIF4G and thereby activates translation.

Hence, CaMKII activation after LTP activates the CPE-dependent translation which in turn translates CaMKIIα mRNA. This feedforward mechanism is very important for maintaining sustained protein synthesis in LTP and memory (Klann and Dever, 2004).

Regulation of Ca^{2+}/Calmodulin-Dependent Protein Kinase Type II by Elongation Factors in Long Term Potentiation

Translation can be regulated even at the elongation level via phosphorylation of the eukaryotic elongation factor 2 (eEF2), which is a GTP binding protein (Moldave, 1985). eEF2 kinase is regulated by mammalian target of rapamycin (mTOR) activation, which phosphorylates the eEF2 kinase near the CaM binding site, resulting in decreased kinase activity (Browne and Proud, 2004).

In dendrites of cultured cortical neurons (Marin et al., 1997) and tadpole tecta (Scheetz et al., 1997), NMDAR activation leads to phosphorylation of the eEF2 factor thus leading to elongation becoming a rate-limiting step in translation. This is correlated with increased CaMKIIα synthesis but decrease in overall protein

synthesis (Scheetz et al., 2000). Similarly, chemically-induced LTP also leads to increased eEF2 phosphorylation with decreased protein synthesis, but with increase in Arc and Fos protein levels (Chotiner et al., 2003). So, phosphorylation of eEF2 leads to overall decrease in protein synthesis but with exceptions of increased translation like that of CaMKIIα (Scheetz et al., 2000).

REGULATION OF NEUROMODULATOR RELEASE BY Ca^{2+}/CALMODULIN-DEPENDENT PROTEIN KINASE TYPE II

The neurotrophins (NTs) are involved as major players in synaptic development and synaptic plasticity (Poo, 2001). Among the NTs – Neuregulin (NRG), BDNF, NT-3 and NT-4, extensive research has been done on BDNF and its role in synaptic plasticity. Postsynaptic NMDAR gating is regulated by BDNF signaling (Levine et al., 1995, 1998). BDNF is important in LTP, as seen by lack of proper establishment of LTP in BDNF knockout (KO) mouse models (Korte et al., 1995; Patterson et al., 1996). BDNF supports high-frequency transmitter release, which is required for LTP induction (Figurov et al., 1996; Gottschalk et al., 1998; Pozzo-Miller et al., 1999; Abidin et al., 2006).

Moro et al. (2020) reported reduced BDNF secretion in mouse deficient in α and β CaMKII [αβCaMKII double-knockout (DKO)] hippocampal neurons. These neurons had drastically reduced levels of BDNF and fewer BDNF containing dense core vesicles (DCV) targeted to the axon, leading to fewer DCVs per synapse and thus reduced BDNF secretion upon stimulation. CaMKIIβ is crucial for increasing the amount of secreted BDNF by CaMKIV and phospho-cAMP-response element binding protein (CREB) pathway. Interestingly, active CaMKIIβ and not CaMKIIα or inactive CaMKIIβ/CaMKIIα could restore the reduced levels of BDNF expression (Moro et al., 2020). BDNF binds to TrkB and this activates CaMKIIβ further leading to a series of downstream signaling events. Subsequently, Ca^{2+}/CaM enters into the nucleus and CaMKIV gets activated, phosphorylating CREB at Ser^{133} position, along with nuclear-localized neurogranin. Phosphorylated CREB promotes BDNF transcription (Wheeler et al., 2008; Ma et al., 2014; Wang et al., 2017). Thus, BDNF-mediated activation of CaMKIIβ acts as a positive feedback loop to initiate the expression of the neuromodulator (Moro et al., 2020).

Ca^{2+}/CALMODULIN-DEPENDENT PROTEIN KINASE TYPE II IN AXONAL/DENDRITIC GROWTH REGULATION PROMOTING SYNAPTIC STRENGTH

Role of Ca^{2+}/Calmodulin-Dependent Protein Kinase Type II α

Alterations in synaptic strength are brought about majorly through post-translational modifications such as phosphorylation or dephosphorylation of synapse associated proteins (Davis and Squire, 1984; Yan-You Huang et al., 1996). Miller et al. showed that mutating the targeting signal at the 3′UTR of CaMKIIα mRNA caused significant reduction in the level of CaMKIIα in PSDs and impairments in L-LTP and LTM. The 3′UTR mutants in BL6 mice showed poor behavioral performances in fear conditioning, water maze and object recognition indicating cognitive alterations (Miller et al., 2002).

Wu et al. (1998) and Wells et al. (2001) demonstrated that dendritic CaMKIIα is inducible by showing an increase in CaMKIIα in synaptosomes prepared from the visual cortex of dark-reared rat pups that were transferred to light. Tetanic stimulation was found to increase CaMKIIα levels in stratum radiatum of CA1 (Ouyang et al., 1999), which suggests that CaMKIIα present in PSDs, might arise from the activity-dependent translation of dendritic mRNAs. Assembly of CaMKII holoenzymes occur after the translation of the subunits. The β subunit facilitates the association of the holoenzyme with actin cytoskeleton and thereby localization to the synapses (Shen et al., 1998). Since the mRNA of β subunit is located only in the soma (Burgin et al., 1990), some of the CaMKIIα might be transported into dendrites as pre-assembled holoenzyme (Miller et al., 2002).

Miller et al. (2002) also showed that disrupting the dendritic localization of CaMKIIα mRNA disrupted LTM but not short-term memory (STM) formation. Hence, dendritic CaMKIIα might be a requirement for memory consolidation. Local CaMKIIα synthesis might facilitate transmission by regulating AMPAR phosphorylation (Barria et al., 1997b) or by inserting additional AMPARs into the synapse (Hayashi et al., 2000). CaMKIIα has also been reported to be stabilizing the dendritic arbors and thus regulating synapse shape and density (Wu and Cline, 1998; Koh et al., 1999; Rongo and Kaplan, 1999). Filopodia-like extensions and movements in the dendritic arbors play an important role for neurons in order to determine new contact sites, which can then evolve into nascent synapses and mature into functional synaptic connections (Vaughn, 1989; Jontes and Smith, 2000; Wong and Wong, 2000; Ahmari and Smith, 2002). For all these mechanisms, continued supply of CaMKIIα is mandatory and this might be supported via the dendritic translation of CaMKIIα.

Role of Ca^{2+}/Calmodulin-Dependent Protein Kinase Type II β

Motility and plasticity of axonal and dendritic arbors, leading to alterations in synaptic contacts (Fischer et al., 1998; Zou and Cline, 1999; Jontes et al., 2000; Colicos et al., 2001), play significant roles in developing and mature neurons. Shen et al. (1998) showed localization of CaMKIIβ to the actin cytoskeleton, thus demonstrating its role in actin-related morphology modifications. CaMKIIβ overexpression increased the number of synapses whereas inhibiting CaMKIIβ caused significant reduction in motility of filopodia as well as in small dendritic branches with long-term decrease in the degree of dendritic arborization (Fink et al., 2003). In developing hippocampal neurons, CaMKIIβ promotes arborization of the

dendritic tree whereas in mature neurons, it has a strong morphogenic effect, leading to dendritic remodeling rather than overall arborization. CaMKIIβ, and not CaMKIIα is expressed in early development when the neurons build the dendritic arbor (Bayer et al., 1999). Even in the hippocampal region where CaMKIIα expression is exceedingly high, CaMKIIβ dominates during the first postnatal week, thus implying its direct role in morphogenic activity. A small insert in CaMKIIβ is responsible for its F-actin localization and for selective upregulation of dendritic motility. Wang Q. et al. reported that CaMKIIβ that has a longer linker of 93 amino acids (aa) binds more strongly and efficiently to F-actin than does CaMKIIα which has only a 30 aa linker (Wang Q. et al., 2019). They show that peptides derived from the regulatory, linker and association domains of CaMKIIβ can bind F-actin. Based on simulations, they calculated that about 20% of free energy of binding is contributed by the regulatory domain. The remaining energy is derived from the linker and association domains with nearly equal contribution. The linker domain is flexible (Myers et al., 2017) and contributes to the thermodynamics of binding unlike the association domain which has higher rigidity and thus helps in maintaining strict geometry between CaMKIIβ and the bound actin filaments. Thus, the formation of the CaMKII/F-actin complex requires the linker, regulatory and association domains of CaMKIIβ (Wang Q. et al., 2019).

When a short sequence of the variable region of CaMKIIβ was inserted in CaMKIIα, a partial colocalization and partial effect on the dendritic morphology was observed. Thus, neurons high in β isoform would have higher degree of arborization with larger numbers of synapses, an example being the cerebellar neurons having persistently high CaMKIIβ levels than in neurons in the forebrain (Miller and Kennedy, 1985). This is reflected in the highly branched morphology of cerebellar neurons when compared to neurons present in the forebrain.

Another important question is how CaMKIIβ is activated. One report suggested that actin and Ca^{2+}/CaM involve in competitive binding to CaMKIIβ (Shen and Meyer, 1999). Fink et al. (2003) reported the involvement of Ca^{2+}/CaM binding to CaMKII for dendritic mobility. Ca^{2+}/CaM levels present in the unstimulated neurons were sufficient to induce CaMKIIβ-dependent dendritic extension/motility. Hence, Ca^{2+}/CaM stimulus provided by basal neuronal activity in cultures is sufficient for the morphogenic function of CaMKIIβ. Since autophosphorylation at Thr^{287}, which requires Ca^{2+}/CaM binding, was possible at basal conditions (25% of CaMKII phosphorylation) (Molloy and Kennedy, 1991), sufficient Ca^{2+}/CaM should be present during basal neuronal activity leading to partial CaMKIIβ activation. In contrast, CaMKIIα requires stronger stimulation to activate AMPA receptors. Thus, differential expression of the two CaMKII isoforms leads to either strengthening of the synapse if CaMKIIα function dominates or filopodia extension with synapse formation if CaMKIIβ dominates.

The mRNA of CaMKIIα, and not β is present in the dendrites and hence the protein translated in dendrites would have CaMKIIα homomers which would not be actin localized. The mixed population of both the isoforms, translated in the cell body would create α/β hetero-oligomers that might bind to actin and regulate filopodia extension and synapse formation (Mori et al., 2000; Aakalu et al., 2001).

Protein kinase C-mediated phosphorylation of CaMKIIβ is required for maintenance of spine morphology. PKC phosphorylates CaMKIIβ at Ser^{315} during group I metabotropic glutamate receptor (mGluR1) signaling which results in CaMKIIβ/F-actin complex dissociation thereby repressing formation and elongation of spines in mature Purkinje cells (Sugawara et al., 2017).

Puram et al. (2011) found a centrosomal targeting sequence (CTS) within the variable region of CaMKIIβ. The CTS mediates the required CaMKII - pericentriolar material 1 (PCM1, a centrosomal targeting protein) interaction which is required for CaMKII localization to the centrosome. In the centrosome, CaMKIIβ phosphorylates the E3 ubiquitin ligase Cdc20-APC (cell division cycle 20–anaphase promoting complex) at Ser^{51}, thereby inducing Cdc20 dispersion from the centrosome and thus inhibiting centrosomal Cdc20-APC activity. This triggers the switch to retraction mode from growth of the dendrites. This CaMKIIβ function at the centrosome is independent of CaMKIIα.

Ca^{2+}/Calmodulin-Dependent Protein Kinase Type II Phosphorylation States in Spine Size and Regulation

Spine size and synaptic strength were shown to covary in experiments involving photolysis of caged glutamate, which is present in individual spines (Matsuzaki et al., 2004; Zhang et al., 2008). The spines present on dendrites can vary in size (Lisman and Harris, 1993), which might correlate with postsynaptic strength of the synapse at that particular spine (Matsuzaki et al., 2001; Asrican et al., 2007). It is known that by overexpressing autonomous (T286D)-CaMKIIα in CA1 hippocampal cells, there is enhancement in the synaptic strength with Thr^{305}/Thr^{306} sites not being phosphorylated. But there is a decrease in synaptic strength when Thr^{305}/Thr^{306} sites are phosphorylated (Lisman et al., 2012). Interestingly, Pi et al. (2010) showed that CaMKII and its various phosphorylation states can regulate spine size. They found that all autonomous forms of CaMKII can increase spine size. In other words, CaMKII leads to spine enlargement irrespective of Thr^{305}/Thr^{306} phosphorylation. Also, the T286D/T305D/T306D form can increase spine size but at the same time decrease synaptic strength. Thus, the mechanisms through which CaMKII regulates spine structure and synaptic strength have different levels of dependence on the phosphorylation state of the enzyme. A T286D form with an additional mutation, K42R, that inhibits enzymatic activity, could actually enhance spine size, with no effect on synaptic strength, thus showing the importance of the structural (non-enzymatic) role of CaMKIIα in this postsynaptic process. Thus, the overall process might involve two steps in which initial enzymatic activity is required for initiating autophosphorylation at Thr^{286} followed by spine

enlargement that does not require enzymatic activity. This explains why the kinase-dead T286D mutant (K42R/T286D) can support spine enlargement but not the T286A mutant (Pi et al., 2010).

Role of Presynaptic Ca^{2+}/Calmodulin-Dependent Protein Kinase Type II in Axon Terminal Growth

Extensive structural remodeling on the presynaptic and postsynaptic sides of the synapse is important for synaptogenesis. The axon growth cone is very dynamic as it responds to its surrounding signals ultimately growing toward the target region forming the synapse (Nesler et al., 2016). Alterations in axon terminals occur very fast and also at distant sites from the cell body. To enable these changes, the local machinery should be active and working in the growth cone and presynaptic boutons.

Ca^{2+} is an important secondary messenger in axon growth and guidance (Sutherland et al., 2014). Increased intracellular Ca^{2+} levels can activate even enzymes such as protein kinase A (PKA) through S100A1, a Ca^{2+}-binding protein (Melville et al., 2017). Ca^{2+} influx results in activating Ca^{2+}/CaM-dependent enzymes like calcineurin (CaN) and CaMKII (Faas et al., 2011). Activation of CaMKII and PKA promotes attraction of the growth cone toward external cues and dual inhibition of both the enzymes leads to repulsion (Wen et al., 2004). Synapsin is an important target for phosphorylation by CaMKII in the presynaptic nerve terminals. The association of synapsin with synaptic vesicles is reversible and it facilitates vesicle clustering and presynaptic plasticity. This mechanism is regulated by phosphorylation at specific sites by CaMKII and PKA (Stefani et al., 1997; Hosaka et al., 1999). Synapsin gets redistributed to sites of activity-dependent axon terminal growth and thus regulates outgrowth via a PKA-dependent pathway (Vasin et al., 2014).

CaMKII expression is post-transcriptionally regulated at the level of translation by the microRNA (miRNA) containing RNA-induced silencing complex (RISC) (Ashraf et al., 2006). Nesler et al. (2013) observed that growth of new synaptic boutons in response to spaced depolarization requires the function of activity-regulated neuronal miRNAs including miR-8, miR-289 and miR-958 in *Drosophila* larval ventral ganglia. This suggests that mRNAs encoding synaptic proteins might be regulated by these miRNAs. The fly CaMKII 3′UTR has two putative binding sites for activity-regulated miR-289 (Ashraf et al., 2006). It is also reported that miR-148a/b can target CaMKIIα through bioinformatics analysis and luciferase assay (Liu et al., 2010). In animal models of schizophrenia wherein the levels of miR-148b were significantly upregulated, increased levels of CaMKIIα transcript did not lead to a concomitant increase in protein levels (Gunasekaran et al., 2022), implying miR-148b involvement in regulation of CaMKIIα *in vivo*. Knockdown of CaMKII in the presynaptic compartment using transgenic RNAi, disrupted activity-dependent presynaptic growth as it prevented the formation of new ghost boutons in response to spaced stimulus. Abundant levels of phosphorylated CaMKII were found at the presynaptic axon terminal. Spaced stimulation leads to accumulation of a significant amount of total CaMKII protein in the axon terminals. This increase was blocked by treatment with either the translational inhibitor cycloheximide or presynaptic overexpression of miR-289 suggesting a translation-dependent mechanism. Similarly, presynaptic CaMKII has been implicated in controlling both bouton number and morphology during development of the larval neuromuscular junction (NMJ) (Nesler et al., 2016). Presynaptic CaMKII has also been shown to be involved in axon pathfinding in cultured neurons of Xenopus (Wen et al., 2004).

ACTIVATION IN RESPONSE TO VOLTAGE GATED CALCIUM CHANNELS

Voltage gated calcium channels (VGCCs) are present throughout the neuronal membrane and are a major source of Ca^{2+}, especially in dendritic spines after a depolarization of the membrane. Different subtypes of VGCCs are known with distinct functions; mainly involved in Ca^{2+} influx into the cell as well as in regulating gene transcription. Activation of dendritic VGCCs can generate LTP, STP (short-term potentiation) or LTD. Perhaps because of the distinct subcellular localization of VGCCs, LTP induced due to their activation may use mechanisms distinct from NMDAR-dependent LTP (Malenka and Nicoll, 1999). With aging, LTP induction through NMDAR becomes lesser compared to VGCC-dependent LTP, as shown by the limited sensitivity of LTP generated in slices from older rats to NMDAR antagonists and increased sensitivity to antagonists of L-type VGCC (Izumi and Zorumski, 1998). Studies have also shown that repetitive activation of VGCCs is involved in LTD (Pöschel and Manahan-Vaughan, 2007) in a Ca^{2+}-dependent manner. Among the various categories of VGCCs, L-type VGCCs are mainly involved in synaptic plasticity mechanisms.

In the CA1 area of hippocampus, an LTP component has been found that is dependent only on the activation of VGCCs without NMDAR (Grover and Teyler, 1990; Alkadhi, 2021) which was later termed as VDCC LTP. Ca^{2+} entry through VGCCs mediates LTP at thalamic input synapses to the lateral nucleus of amygdala, which may be mechanistically different from the NMDAR-dependent form of plasticity found in the hippocampus but is still dependent on activated CaMKII (Weisskopf et al., 1999). The conditional hippocampus/neocortex Cav1.2 (L-type VGCCs) KO mouse demonstrates an essential role of Cav1.2 in CREB signaling during LTP and spatial learning (Moosmang et al., 2005). In the cortical neurons, activation of T-type VGCCs enhanced LTP and CaMKII autophosphorylation (Moriguchi et al., 2012a). Even in the NMDAR-dependent mechanisms of LTP and LTD (Di Biase et al., 2008), Cav channels are involved (Zhao et al., 2021) by enhancing Ca^{2+} influx into the synaptic site and through CREB mediated events.

Upon aging, the expression of NMDAR diminishes and its subunit composition also changes (Zhao et al., 2009), whereas VGCCs, especially the L-type channels, increase in expression (Thibault and Landfield, 1996; Wang and Mattson, 2014) and can majorly involve in LTP or LTD mechanisms. Activation of

L-type VGCCs, especially Cav1.2 localized in the postsynaptic membrane (Patriarchi et al., 2018) leads to Ca^{2+} influx into the spine, which can activate CaMKII. Even if the expression levels of GluN2B are lower, CaMKII can still tether to the postsynaptic site by binding with the C-terminus of Cav1.2 (Hudmon et al., 2005). This binding, however, does not lead to constitutively active CaMKII and hence, cannot support molecular memory. The enzyme tethered at the membrane can easily get activated with the trains of depolarization stimulus and can facilitate further Ca^{2+} influx through these channels (Ca^{2+}-dependent facilitation).

ROLE OF Ca^{2+}/CALMODULIN-DEPENDENT PROTEIN KINASE TYPE II IN LONG TERM DEPRESSION

LTD is an activity-dependent reduction in the efficacy of neuronal synapses (Malenka and Nicoll, 1999) and is thought to be involved in learning and memory. It brings about a long-lasting decrease in synaptic strength or a reversal of LTP mechanisms. LTD is triggered by synaptic activation of either NMDARs or metabotropic glutamate receptors (mGluRs). A low frequency stimulation (LFS) of NMDARs (700–900 pulses at 1 Hz) can activate LTD mechanisms (**Figure 4**). If the Ca^{2+} influx is low in intensity (if the activation is only for a postsynaptic compartment), it will majorly activate phosphatases and result in LTD (Baltaci et al., 2019). Initially it was thought that protein kinases are required for LTP and phosphatases are involved in LTD. But recent findings suggest that kinases are involved in LTD mechanisms also. It has been noted that the bath application of CaMKII inhibitor KN-62 could block LTD during low-frequency SC collateral stimulation (1 Hz/15 min) (Stanton and Gage, 1996). Experiments with CaMKIIα KO mice also pointed to the role of CaMKII in LTD (Stevens et al., 1994). Even though these initial experiments indicated the role of CaMKII in LTD, the exact mechanism by which CaMKII participates in the process is unknown. In contrast to the previously accepted dogma, it has also been shown by using T286A mutant mouse that Thr^{286} autophosphorylation is a requisite for LTD (Coultrap et al., 2014). The most recent studies on CaMKII autophosphorylation indicates that the autophosphorylation at $Thr^{305/306}$ is selectively induced by LTD stimuli and the mutation of these residues impairs LFS-induced LTD but not HFS-induced LTP (Cook et al., 2021). Both the autophosphorylations are necessary for LTD but the exact role of Thr^{286} with respect to $Thr^{305/306}$ in LTD remains controversial. The death-associated protein kinase 1 (DAPK1) can regulate CaMKII-GluN2B interaction to facilitate LTD. DAPK1 is a CaM kinase family member and is enriched in excitatory synapses. They can bind to GluN2B at a site overlapping the CaMKII binding site. The enzyme gets activated by CaN, a Ca^{2+}-activated protein phosphatase. LTD-stimuli can activate DAPK1 in hippocampal slices in a CaN-dependent manner. Inhibition of DAPK1 or CaN allowed the accumulation of CaMKII at excitatory synapses after LTD-stimuli (Goodell et al., 2017). This indicates that during LTD, DAPKI activated by phosphatases will compete for GluN2B binding and would reduce the binding of activated CaMKII generated by the low frequency stimuli.

CaMKII can phosphorylate Ser^{567} residue of GluA1 subunit of AMPAR, a unique phosphorylation site for CaMKII in the C-terminal loop of GluA1. The C-terminal tail of GluA1 is involved in AMPAR trafficking from extra-synaptic pool to the synapses. Phosphorylation of GluA1 at Ser^{567} by CaMKII inhibits AMPAR trafficking to the synapses (Lu et al., 2010). It has been noted that LTD-inducing stimulation of hippocampal slices produced a robust phosphorylation of Ser^{567} whereas LTP-inducing stimulus could yield only Ser^{831} phosphorylation. The differential phosphorylation of GluA1 by CaMKII under the two synaptic plasticity conditions underlies the role of CaMKII in LTD (Coultrap et al., 2014).

In contrast to spine enlargement in LTP, LTD is associated with spine shrinkage aided by the removal of the AMPA receptor regulatory scaffold protein, A-kinase anchoring protein (AKAP) 79/150. The synaptic removal of AKAP79/150 is brought about by the phosphorylation of the substrate sites within the AKAP79/150 N-terminal polybasic membrane-cytoskeletal targeting domain (residues 1–153) by CaMKII. Phosphorylation by CaMKII inhibits AKAP79/150 association with F-actin, thus facilitating AKAP79/150 removal from spines (**Figure 4**). In addition to the direct phosphorylation of AKAP79/150, CaMKII is also responsible for its depalmitoylation on two Cys residues within the N-terminal targeting domain. Depalmitoylation also promotes synaptic elimination of AKAP79/150. Since the protein harbors PKA and protein phosphatase 2B (PP2B) at the PSD, it can regulate both synaptic insertion and elimination of AMPARs. Under LTP stimulation, PKA can phosphorylate Ser^{845} of GluA1 of AMPAR and thereby more AMPAR trafficking to the synapse occurs, whereas in LTD conditions due to the elimination of AKAP79/150 along with activation of phosphatases, AMPAR dephosphorylation at Ser^{845} and its endocytosis is promoted which eventually leads to spine shrinkage (Woolfrey et al., 2018).

The stimulation pattern-dependent activation of NMDAR that yields either LTP or LTD, causes activation of CaMKII in either case. With the differing stimuli the enzyme targets different substrates and thereby activates specific signaling mechanisms to yield either form of synaptic plasticity.

Ca^{2+}/CALMODULIN-DEPENDENT PROTEIN KINASE TYPE II IN SIGNALING COMPLEXES IN GLUTAMATERGIC SYNAPSES

CaMKII plays an important role in several physiological pathways including synaptic plasticity and hence its localization in the cytosol and PSD are crucial determinants of its function. Immunoelectron microscopy studies show that CaMKIIα is significantly higher in dendritic shafts when compared to dendritic spines. When it gets any proper stimulus, it will abundantly translocate to the spines (Shen and Meyer, 1999;

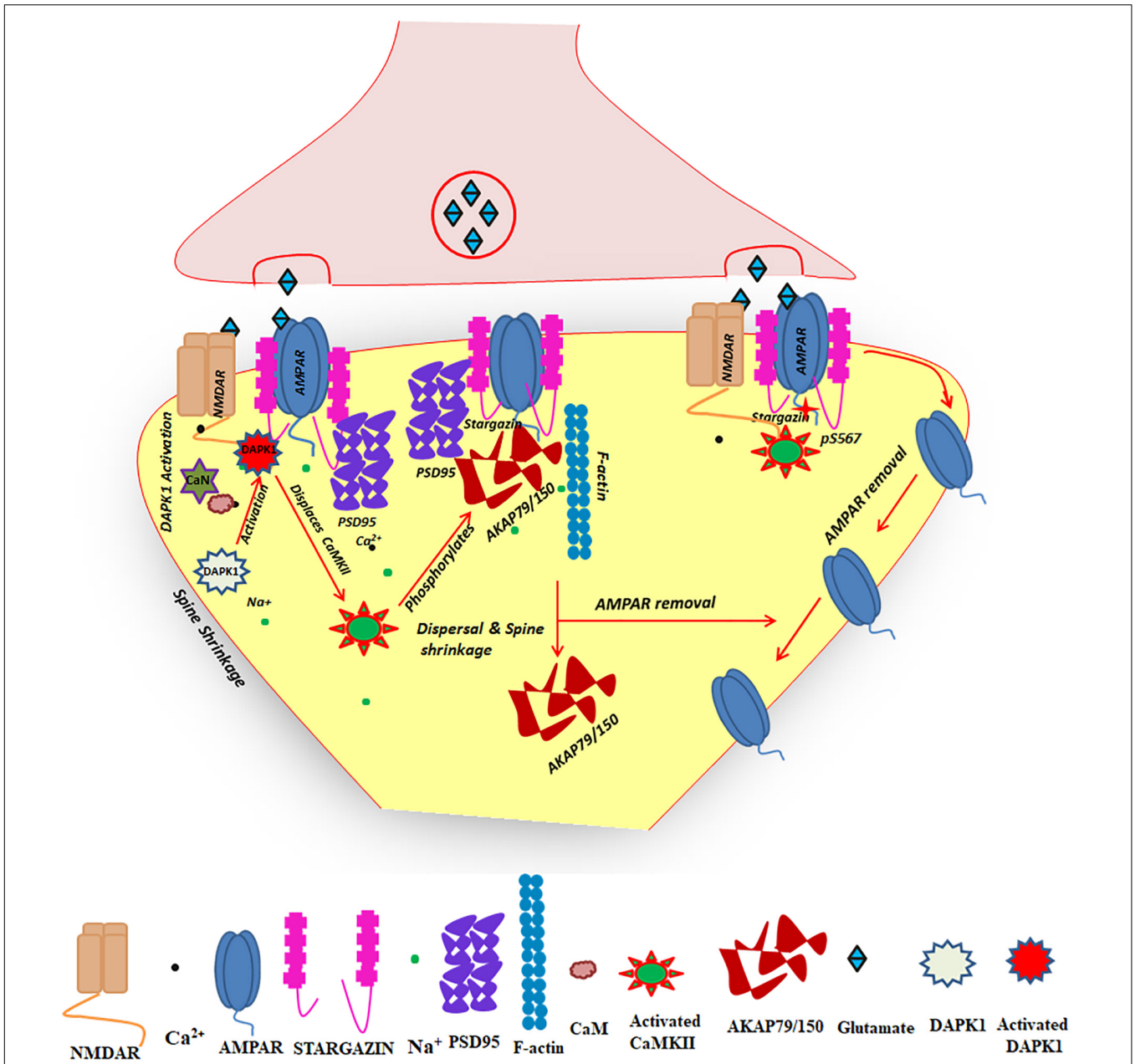

FIGURE 4 | The schematic representation showing the role of CaMKII in LTD. The low tetanic stimulation leading to LTD activates more phosphatases than kinases. Calcineurin thus activated can activate DAPK1 and it can translocate to GluN2B where CaMKII binds. The activation of DAPK1 can even displace activated CaMKII generated under minimal Ca^{2+} stimulus from its binding with GluN2B. The role of CaMKII in LTD involves inhibition of AMPAfication and facilitation of spine shrinkage. Phosphorylation of GluA1 of AMPAR at Ser^{567} obstructs AMPAfication of synapses; CaMKII mediated phosphorylation and depalmitoylation of AKAP79/150 results in its synaptic elimination. Since AKAP79/150 is a major adapter for many proteins required for LTP, its elimination due to dissociation from F-actin can result in AMPAR endocytosis and spine shrinkage.

Shen et al., 2000; Ding et al., 2013). In the basal condition, more CaMKII will be available in the dendritic shaft than in spines. Whenever activation happens the activated CaMKII can translocate to the spines.

Translocated CaMKII can bind with various protein ligands in the PSD as indicated in **Table 1**. One such protein is densin-180, which is a core protein in the PSD that does not span the membrane. Though densin-180 is the only documented interaction partner for the association domain of CaMKII, it will not bind with CaMKII holoenzymes which contain β isoform (Penny and Gold, 2018). The PDZ domain of densin-180 contributes to its binding to α-actinin. A distinct domain of α-actinin interacts with the kinase domains of both α and β subunits of CaMKII. Thus, these three proteins can form a

ternary complex in the PSD stabilized by multiple interactions (Walikonis et al., 2001). This ternary complex within the PSD is an additional mode of localization of CaMKII to PSD apart from its binding to GluN2B.

SAP97, a member of membrane-associated guanylate kinase protein family, has been implicated in the processes of targeting ionotropic glutamate receptors such as NMDARs and AMPARs at postsynaptic sites and is enriched in PSD. SAP97 shares its interaction with AKAP79/150 in addition to the C-terminal region of GluA1. AKAP79/150 in turn harbors PKC, PKA and PP2B. This molecular arrangement inside the PSD works in accordance with the stimuli received. The most important function of this complex is the regulation of AMPARs in synapses including both potentiation and trafficking. CaMKIIα displays a high degree of co-localization with SAP97. CaMKII phosphorylation of Ser^{39} in the N-terminus of SAP97 modulates trafficking of SAP97 (Mauceri et al., 2004) and the associated proteins; in contrast, CaMKII phosphorylation of Ser^{232} in the first PDZ domain of SAP97 may modulate binding of other proteins, such as NMDAR and AMPAR subunits (Nikandrova et al., 2010), especially GluA1 of AMPAR. SAP97 is in close association with AKAP 79/150, but the phosphorylation of SAP97 at Ser^{39} by CaMKII disengages AKAP79/150 from regulating GluA1-AMPARs.

Another complex associated with CaMKII in the PSD is the complex formed by SynGAP, MUPP1 and CaMKII. SynGAP and CaMKII are brought together by direct physical interaction with the PDZ domains of MUPP1, a multi-PDZ domain-containing protein (Krapivinsky et al., 2004). In this complex, SynGAP is phosphorylated by CaMKII which enhances its Ras GTPase activity which in turn promotes AMPAR trafficking as shown in **Figure 3**.

CaMKII has an important role in dendritic spine remodeling upon synaptic stimulation. Electron micrographic studies showed that at physiological molar ratios, single CaMKII holoenzymes cross-linked multiple F-actin filaments at random, whereas at higher CaMKII/F-actin ratios, filaments bundled. From this bundled state CaMKII is released upon Ca^{2+}/CaM activation, triggering network disassembly and expansion leading to spine enlargement. Upon subsequent disappearance of Ca^{2+}, compaction will occur (Khan et al., 2019).

ROLE OF Ca^{2+}/CALMODULIN-DEPENDENT PROTEIN KINASE TYPE II IN CALCIUM OVERLOAD-INDUCED EXCITOTOXICITY

Excitotoxicity is a pathological condition triggered by excessive stimulation of receptors by excitatory neurotransmitters, primarily glutamate, causing Ca^{2+} overload in the cytosol and thereby resulting in neuronal dysfunction and cell death. Increased Ca^{2+} influx and high intracellular Ca^{2+} ($[Ca^{2+}]_i$) rise trigger gene expression (Ortuño-Sahagún et al., 2012) and long-lasting activation of CaMKIIα in hippocampal neurons (Otmakhov et al., 2015). Autophosphorylation of CaMKII at Thr^{253}, Thr^{286} (Vest et al., 2010; Otmakhov et al., 2015; Rostas et al., 2017) and simultaneous S-nitrosylation at Cys^{280}/Cys^{289} by nitric oxide (NO) (Coultrap and Bayer, 2014) generates autonomous activity of the kinase during excitotoxic cell death. Activated CaMKII redistributes to the spines (Otmakhov et al., 2015), promotes its interaction with synaptic GluN2B (Wang N. et al., 2014; Buonarati et al., 2020) and mediates the NMDA-induced caspase-3-dependent cell death pathway (Goebel, 2009). During a glutamate-induced excitotoxic event, CaMKII can also modulate the activity of neuronal nitric oxide synthase (nNOS) (Araki et al., 2020), can cause axonal degeneration via necroptosis (Hou et al., 2009; Arrazola and Court, 2019) and also contribute to the regulated necrosis (RN) pathway (Wang S. et al., 2019).

Contrastingly both overexpression (Vest et al., 2010) and sustained CaMKII inhibition during excitotoxicity can exacerbate cell death of cultured neurons (Ashpole and Hudmon, 2011; Ashpole et al., 2012). Loss of CaMKII activity in astrocytes results in dysregulated Ca^{2+} homeostasis and reduced glutamate uptake (Ashpole et al., 2013) by excitatory amino acid transporter 1 (EAAT1) (Chawla et al., 2017). On the whole, dysregulated CaMKII function upon excitotoxic insult shifts the tight homeostatic balance maintained between kinases and phosphatases in the cell, resulting in dysfunction of excitatory synaptic transmission (Farinelli et al., 2012). The following section reviews the role of CaMKII at glutamatergic synapses in a few diseases in which excitotoxicity is one of the causes.

Alzheimer's Disease

Alzheimer's disease (AD) is a progressive neurodegenerative condition characterized by loss of memory and cognitive function. The presence of amyloid β (Aβ) plaques and neurofibrillary tangles (NFTs) composed of hyperphosphorylated tau protein, is the distinctive feature in AD neuropathology. CaMKII catalyzes the hyperphosphorylation of tau protein at multiple Ser/Thr sites in the AD brain (Yoshimura et al., 2003). Loss of synapses and cognitive decline associated with AD positively correlate to the accumulation of soluble Aβ (Lue et al., 1999; Näslund et al., 2000; Almeida et al., 2005), which leads to reduced CaMKII activation (Zeng et al., 2010; Ly and Song, 2011; Ghosh and Giese, 2015) and inhibition of LTP-induced CaMKII trafficking to excitatory synapses (Cook et al., 2019). A significant reduction in the density and number of synapses (Terry et al., 1991; Scheff and Price, 1993, 1998; Scheff et al., 2006) and altered expression of synaptic proteins (Masliah et al., 2001; Almeida et al., 2005) contributes to synaptic dysfunction and cognitive decline in the AD brain.

In amyloid precursor protein (APP) transgenic mice, Aβ-induced change in CaMKII subcellular distribution aids in the removal of AMPARs from the synaptic membrane (Gu et al., 2009). Opazo et al. (2018) showed that oligomeric forms of Aβ peptide engage in synaptic metaplasticity via aberrant activation of CaMKII, mediated through GluN2B-containing NMDARs, which leads to LTP deficits and destabilization of AMPARs in the early stages of AD.

Epilepsy

Epilepsy is a neurological disorder characterized by recurrent seizures, caused by abnormal brain activity. A strong epileptic stimulus can induce alterations in the composition of PSD proteins (Wyneken et al., 2001) and loss of CA3 cells in a kainic acid (KA)-induced seizure model, wherein hippocampal injury correlates with increased CaMKII activity (Lee et al., 2001). Activation of CaMKIIα is concomitant with a reduction in density of hippocampal dendritic spines and spine PSDs during epileptiform activity (Zha et al., 2009). Also, CaMKII activation via L-type VGCCs and NMDARs are essential for the development and maintenance of an *in vitro* kindling-like state and EPSP-spike potentiation in CA1 pyramidal cells (Semyanov and Godukhin, 2001).

However, a few studies have reported an NMDAR-dependent reduction in CaMKII activity with increased neuronal excitability (Kochan et al., 1999; Churn et al., 2000). Regulation of CaMKII activity during seizures either by the reversible formation of inactivated CaMKII (Yamagata and Obata, 2004; Yamagata et al., 2006) or by modulating different CaMKII isoforms (Murray et al., 2003; Savina et al., 2013), can prevent excessive CaMKII activation due to Ca^{2+} overload (Yamagata et al., 2006). Recently, Vieira et al. (2020) functionally characterized the epilepsy-associated *de novo* variant of GluN2A, S1459G. This mutation disrupts CaMKIIα phosphorylation of GluN2A resulting in defects in NMDAR trafficking and reduced synaptic function (Vieira et al., 2020).

Huntington's Disease

Huntington's disease (HD) is an autosomal, dominantly inherited disorder caused by the expansion of a polyglutamine repeat in the N-terminus of the huntingtin (htt) protein. Progressive and selective degeneration of the striatal medium spiny neurons (MSNs) in HD results in abnormalities of movement, cognition, personality and mood. Being an abundant protein in striatal MSNs (Erondu and Kennedy, 1985), reduced levels of both CaMKII and CaMKII-Thr^{286} phosphorylation have been reported in various mouse models of HD (Deckel et al., 2001, 2002a,b; Brito et al., 2014; Blum et al., 2015; Gratuze et al., 2015). Altered expression levels of CaMKII in the hippocampus can disrupt GluA1-Ser^{831} phosphorylation (Brito et al., 2014) and disturb AMPAR surface diffusion (Zhang et al., 2018). CaMKII inhibition in striatal MSNs causes a reduction in functional glutamatergic synapses and an enhancement in intrinsic excitability (Klug et al., 2012). Although the role of altered CaMKII function in HD is not extensively studied, it is evident that it could contribute to cognitive dysfunction observed in HD (Giralt et al., 2012; Zhang et al., 2018).

Parkinson's Disease (PD)

Parkinson's disease (PD) is a progressive neurodegenerative movement disorder caused by degeneration of dopaminergic neurons in the substantia nigra, that project to the striatum. At the molecular level, dopamine (DA) can modulate or gate the cortical glutamatergic inputs onto striatal MSNs (Freund et al., 1984; Gardoni and Bellone, 2015). Striatal DA depletion causes selective loss of dendritic spines and glutamatergic synapses on striatopallidal MSNs (Day et al., 2006) and differentially affects the expression and phosphorylation of glutamate receptor subunits and CaMKIIα (Brown et al., 2005; Gardoni et al., 2010; Koutsokera et al., 2014).

Dopamine denervation *in vivo* induces an increase in CaMKIIα-Thr^{286} phosphorylation in the striatum (Brown et al., 2005; Koutsokera et al., 2014), concurrent with increased recruitment of activated CaMKIIα to GluN2A-GluN2B subunits (Picconi et al., 2004). On the other hand, reduced levels of CaMKIIα autophosphorylation and GluA1-Ser^{831} phosphorylation in the hippocampus correlates with impaired CA1 LTP in 1-methyl-4-phenyl-1,2,3,6-tetrahydropyridine (MPTP)-treated mice (Moriguchi et al., 2012b). Overall, DA deficiency can induce deficits in synaptic plasticity and motor behavior by altering striatal glutamatergic signaling and CaMKII activity (Picconi et al., 2004; Brown et al., 2005; Deutch, 2006; Paillé et al., 2010; Moriguchi et al., 2012b; Koutsokera et al., 2014).

Cerebral Ischemia

Cerebral ischemia is a condition in which restricted blood supply to the brain causes tissue damage and cell death. Excess glutamate release and high $[Ca^{2+}]_i$ trigger a range of downstream neurotoxic cascades leading to apoptosis or necrosis (Szydlowska and Tymianski, 2010). Ca^{2+} influx ensuing an ischemic insult significantly increases NMDAR-mediated activation of CaMKII (Meng et al., 2003) followed by its phosphorylation at Thr^{253} (Gurd et al., 2008) and Thr^{286} (Shamloo et al., 2000; Matsumoto et al., 2002). CaMKII-Thr^{253} autophosphorylation enhances its association with PSD (Migues et al., 2006) and induces the persistent activation of the enzyme (Rostas et al., 2017). Oxidation of $Met^{281/282}$ (Cys^{281}/Met^{282} in CaMKIIα) in the auto-regulatory domain of the enzyme, by reactive oxygen species (ROS) generated during glutamate excitotoxicity and oxidative stress, can also lead to autonomous activity of the kinase (Anderson, 2015), which in turn augments reperfusion injury in acute ischemic stroke (Gu et al., 2016; Qu et al., 2019; Zhang et al., 2021). Autophosphorylated CaMKII translocates to the synaptic membrane (Matsumoto et al., 2004), binds to synaptic GluN2B (Buonarati et al., 2020) and phosphorylates serine residue(s) of the GluN2B subunit (Meng and Zhang, 2002; Meng et al., 2003) to mediate ischemic cell death. However, a recent study by Tullis et al. (2021), reported that neuronal death in global cerebral ischemia *in vivo* is promoted by the binding of CaMKII to GluN2B and not by CaMKII-mediated GluN2B-Ser^{1303} phosphorylation (Kumar et al., 2019; Buonarati et al., 2020; Tullis et al., 2021). CaMKII activation dependent on NMDARs or L-type VGCCs can also phosphorylate serine residues of GluR6 subunit of kainate receptors via the assembly of GluR6-PSD95-CaMKII signaling module in cerebral ischemia injury (Hao et al., 2005; Xu et al., 2010).

The changes observed in expression levels and activity of CaMKII are dependent on the duration of ischemic insult

(Gurd et al., 2008), which in turn can regulate NMDAR-mediated field excitatory postsynaptic potentials (fEPSPs) (Wang N. et al., 2014). Likewise, 10 min oxygen-glucose deprivation (OGD) treatment *in vitro* can induce NMDAR-mediated postischemic LTP, mediated by CaMKII-NMDAR interaction and NMDAR trafficking to the membrane (Wang N. et al., 2014).

Traumatic Brain Injury

Traumatic brain injury (TBI) is a disruption in the normal function of the brain caused by an external mechanical force. It is associated with the release of excitatory amino acids, particularly glutamate, in the extracellular space (Faden et al., 1989; Chamoun et al., 2010). Overactivation of glutamate receptors (Faden et al., 1989; Liu et al., 2017) and elevated levels of $[Ca^{2+}]_i$ (Deshpande et al., 2008; Sun et al., 2008) transiently activates CaMKIIα (Atkins et al., 2006; Folkerts et al., 2007; Liu et al., 2017) and CaMKIIδ (Zhang et al., 2012). Alterations in NMDAR function, CaMKIIα expression and dendritic spine anatomy in the hippocampus prevent LTP induction after lateral fluid percussion injury (Schwarzbach et al., 2006), thereby causing cognitive impairment often associated with CNS trauma (Atkins et al., 2006; Schwarzbach et al., 2006; Folkerts et al., 2007; Deshpande et al., 2008). Long-term alterations in Ca^{2+} homeostasis mechanisms (Sun et al., 2008) contributes to morbidity and mortality following TBI.

FUNCTIONAL IMPLICATIONS OF Ca^{2+}/CALMODULIN-DEPENDENT PROTEIN KINASE TYPE II MUTATIONS IN SYNAPTIC PLASTICITY

CaMKII plays a versatile role in different regulatory processes involved in synaptic plasticity. This section reviews the different CaMKII mutant animal models generated to study the physiological role of the kinase in synaptic plasticity and its associated behavioral phenotype. Targeted disruption of CaMKIIα/β/γ function *in vivo* dysregulates different types of synaptic plasticity (Silva et al., 1992a; Stevens et al., 1994; Mayford et al., 1995; Giese et al., 1998; Elgersma et al., 2002; Miller et al., 2002; Cho et al., 2007; van Woerden et al., 2009; Yamagata et al., 2009; Yin et al., 2017; Cohen et al., 2018; Kool et al., 2019) and impairs learning (Silva et al., 1992b, 1996; Bach et al., 1995; Giese et al., 1998; Elgersma et al., 2002; Irvine et al., 2005; Yamagata et al., 2009; Borgesius et al., 2011; Achterberg et al., 2014; Cohen et al., 2018), memory (Miller et al., 2002; von Hertzen and Giese, 2005; Cho et al., 2007) and the emotional state (Chen et al., 1994; Yamasaki et al., 2008; Hasegawa et al., 2009; Bachstetter et al., 2014). Although the behavior exhibited varies slightly with the genetic background of the mouse strain used (Gordon et al., 1996; Silva et al., 1996; Hinds et al., 1998; Need and Giese, 2003), the molecular and electrophysiological alterations remain largely unchanged.

Ca^{2+}/Calmodulin-Dependent Protein Kinase Type II α

Ca^{2+}/Calmodulin-Dependent Protein Kinase Type II α Global Knockout Mice

Silva et al. (1992a) reported the production of the first genetically altered mice lacking the α subunit of CaMKII. LTP, STP and LTD were either absent or significantly attenuated in the sensory neocortex and hippocampal slices from young homozygous CaMKIIα$^{-/-}$ KO mice (Silva et al., 1992a; Stevens et al., 1994; Kirkwood et al., 1997; Hinds et al., 1998; Elgersma et al., 2002). Long-term plasticity and reversal of LTP were normal in the CA1 hippocampal region of heterozygous CaMKIIα$^{+/-}$ mice (Silva et al., 1996; Elgersma et al., 2002); however, they exhibited impaired short-lived plasticity (SLP) and paired-pulse facilitation (PPF) and an enhanced post-tetanic potentiation (PTP) response expressed within seconds of stimulation (Silva et al., 1992a, 1996; Chapman et al., 1995; Hojjati et al., 2007).

Plasticity deficits due to either partial or complete loss of CaMKIIα activity manifest as abnormalities in various behavioral paradigms. CaMKIIα null mutant mice have been reported to exhibit pronounced deficits in spatial learning (Silva et al., 1992b; Elgersma et al., 2002; Achterberg et al., 2014), working memory (Yamasaki et al., 2008) and Pavlovian fear conditioning (Chen et al., 1994; Silva et al., 1996; Elgersma et al., 2002; Achterberg et al., 2014). Dysregulated emotional states like increased aggression, decreased anxiety and depression-like behavior and an exaggerated infradian rhythm have also been observed in CaMKIIα$^{+/-}$ mice (Silva et al., 1992b; Chen et al., 1994; Yamasaki et al., 2008).

Dysfunction of the dentate gyrus (DG) due to the immaturity of DG neurons (Yamasaki et al., 2008; Matsuo et al., 2009) and ectopic projection of mossy fibers (Nakahara et al., 2015), causes suppressed induction of activity-dependent genes like *c-fos* and *arc*, resulting in altered behavior exhibited by CaMKIIα KO mice (Yamasaki et al., 2008; Matsuo et al., 2009). Disrupted regulation of *Zif268* gene expression and growth associated protein 43 (GAP43), a synaptogenesis marker, by CaMKIIα$^{+/-}$ mutation can also impair the maturation of cortical circuits necessary for remote memory (Frankland et al., 2004).

Ca^{2+}/Calmodulin-Dependent Protein Kinase Type II α-Thr^{286} Mutant Mice (T286A/T286D)

The Ca^{2+}/CaM-independent, autonomous state of CaMKIIα, induced by autophosphorylation of Thr^{286}, is required for NMDAR-dependent LTP and LTD at CA1 pyramidal cells (Giese et al., 1998), spatial learning (Giese et al., 1998; Need and Giese, 2003), fear learning (Irvine et al., 2005, 2011) and regulation of synapse development *in vivo* (Gustin et al., 2011). During induction of synaptic plasticity, CaMKIIα-Thr^{286} phosphorylation is essential for optimal integration of Ca^{2+} signals; however, it is dispensable for LTP maintenance and memory (Irvine et al., 2005; Chang et al., 2017). High-frequency synaptic stimulation can rescue impaired LTP induction in CA1 neurons from *Camk2a*^{T286A} mice (Chang et al., 2017). Although L-LTP could not be induced at CA1 synapses of T286A mutants (Irvine et al., 2011), mTOR-mediated upregulation of PSD95

expression and a persistent generation of multi-innervated spines (MIS) can contribute to LTM formation in these mutant animals where functional strengthening of synapses is impaired (Radwanska et al., 2011).

The deficit in spatial learning of CaMKIIα-T286A mutant mice is due to decreased spatial selectivity, stability and experience-dependent tuning of CA1 hippocampal place cells (Cho et al., 1998; Cacucci et al., 2007) and an impaired precision of spatial memory (Śliwińska et al., 2020). Pre-adolescent KI mice had disruption in synaptic targeting of CaMKII and enhanced activity of GluN2B-containing-NMDARs at CA3-CA1 synapses along with impaired cognition and anxiety phenotypes (Gustin et al., 2011). The T286A knockin (KI) mutants have normal neurogenesis in their DG (Kee et al., 2007). Therefore, alternate signaling mechanisms involving either PKA or CaMKIIβ are activated in the absence of CaMKIIα autophosphorylation at excitatory synapses in the neonatal rodent hippocampus (Yasuda et al., 2003), hippocampal inhibitory interneurons (Lamsa et al., 2007) and the medial perforant path-granule cell synapses in adult mice (Cooke et al., 2006) to induce LTP.

Constitutive expression of the Ca^{2+}-independent, autonomously active form of CaMKIIα (CaMKIIα-T286D) *in vivo* favors LTD at LTP-inducing θ frequencies (5–10 Hz) and consequently influences spatial learning and fear conditioning (Bach et al., 1995; Mayford et al., 1995, 1996; Wiedenmayer et al., 2000; Bejar et al., 2002; Yasuda and Mayford, 2006). The use of the tetracycline transactivator (tTA) system to limit the expression of CaMKIIα-T286D regionally and temporally, has shed light on the role of CaMKIIα signaling in synaptic plasticity during development, memory encoding and memory storage (Mayford et al., 1996; Glazewski et al., 2001; Bejar et al., 2002; Yasuda and Mayford, 2006). CA1 hippocampal place cells in these mutant animals are less common, less precise and less stable, thereby affecting spatial memory storage (Rotenberg et al., 1996).

Ca^{2+}/Calmodulin-Dependent Protein Kinase Type II α-Thr^{305}/Thr^{306} Mutant Mice

Inhibitory phosphorylation of CaMKIIα at Thr^{305}/Thr^{306} is essential to modulate the association of the kinase with PSD, the threshold for induction of NMDAR-dependent LTP at SC-CA1 synapses, hippocampal-dependent spatial learning and fear conditioning, reversal learning and to induce LTP at inhibitory synapses (iLTP) (Elgersma et al., 2002; Cook et al., 2021). Phosphorylation of CaMKIIα-Thr^{305}/Thr^{306} during an excitatory LTD stimulus blocks the translocation of CaMKIIα to glutamatergic excitatory synapses and directs CaMKIIα to GABAergic inhibitory synapses to induce iLTP. In this way, Thr^{305}/Thr^{306} phosphorylation governs the fundamental LTP vs. LTD decision at excitatory synapses (Cook et al., 2021). Similar to CaMKIIα-T286D mutant, CaMKIIα-T305D favors LTD over LTP at weak tetanic stimulations (Elgersma et al., 2002).

Ca^{2+}/Calmodulin-Dependent Protein Kinase Type II α-K42R Mutant Mice

Similar to the CaMKIIα mutant models reviewed above, the kinase-dead CaMKIIα (CaMKIIα-K42R) KI mouse also exhibited deficits in NMDAR-dependent LTP and hippocampus-dependent learning and memory (Yamagata et al., 2009, 2018). Although the levels of PSD associated CaMKIIα and activity-dependent postsynaptic translocation of CaMKIIα were intact in the mutants, the stimulus-induced increase in spine volume was severely impaired compared to WT mice (Yamagata et al., 2009). Amygdala-dependent fear memory is only partially affected by the loss of kinase activity (Yamagata et al., 2018). Stronger conditioning or multi-trial training could achieve slight or no improvement in the memory deficits of CaMKIIα-K42R mutant mice (Yamagata et al., 2009, 2018).

Conditional Mutant Models

Apart from the models described above, there are a few other transgenic (Tg) mouse models generated to study specific functions of CaMKII in synaptic plasticity. The CaMKIIα-3′UTR mutant has reduced expression of the kinase in the dendrites and its association to PSD (Miller et al., 2002), with no substantial alteration in other protein constituents of the synaptic membrane (Li et al., 2007). Disruption in the local translation of the protein causes a reduction in L-LTP, memory consolidation and LTM storage, with no change in E-LTP and STM formation (Miller et al., 2002).

Using an inducible and forebrain specific CaMKIIα-F89G Tg mouse model, Joe Z. Tsien and group have shown that the levels of CaMKIIα protein can affect the degree and direction of synaptic plasticity (Wang et al., 2003, 2008). A switch between the normal and higher activity state of CaMKIIα during the memory consolidation phase can severely disrupt LTM formation. The synaptic consolidation of LTMs requires the reactivation of CaMKIIα, during the first week after training, to the level present at the time of initial learning (Wang et al., 2003); on the other hand, a shift in CaMKIIα activation status within the immediate post-learning 10 min can alter STM formation (Wang et al., 2008).

In the study reported by Achterberg et al. (2014), conditional *Camk2a* mutant mice models were employed to achieve regional and temporal specific deletion of CaMKIIα. Telencephalon-specific deletion of the *Camk2a* gene ($Camk2a^{flox/Emx-Cre}$) resulted in severe deficits in spatial and contextual learning and hippocampal LTP in adult mice, whereas mice with deletion specific to Purkinje cells in the cerebellum ($Camk2a^{flox/L7-cre}$) learned normally (Achterberg et al., 2014).

At hippocampal synapses, CaMKIIα functions non-enzymatically by limiting the size of docked vesicles (Hojjati et al., 2007) and by regulating neurotransmitter release at glutamatergic synapses (Chapman et al., 1995; Hinds et al., 2003), thereby modulating short-term presynaptic plasticity. A few of the CaMKIIα Tg mice also exhibited seizures (Butler et al., 1995; Mayford et al., 1995; Elgersma et al., 2002; Yamagata et al., 2009). With a potential role for CaMKIIα in controlling the state of emotion, these models can also be exploited in the study of neuropsychiatric diseases (Yamasaki et al., 2008;

Hasegawa et al., 2009; Matsuo et al., 2009; Nakahara et al., 2015; Yamagata et al., 2018).

Ca^{2+}/Calmodulin-Dependent Protein Kinase Type II β

The first Tg mouse model of CaMKIIβ was generated by Cho et al. (2007), by selectively overexpressing CaMKIIβ-F90G in the DG. Elevated CaMKIIβ activity does not affect baseline glutamatergic neurotransmission but causes deficits in LTP (Cho et al., 2007) and in NMDAR-dependent LTD (Yin et al., 2017). The Tg mice displayed normal acquisition, retention and recall of 1-day-old LTM, but showed severe impairments in 10-day-old contextual fear memory (Cho et al., 2007) and behavioral flexibility (Yin et al., 2017). Overexpression of CaMKIIβ decreases the activity of PP1/protein phosphatase 2A (PP2A) and glycogen synthase kinase 3β (GSK3β), which can shift the direction of synaptic plasticity toward potentiation during LTD induction. This disrupts the regulation of synaptic stargazin and interrupts the internalization of AMPAR and dephosphorylation of Ser^{831} and Ser^{845} of GluA1 during NMDAR-LTD (Yin et al., 2017).

Global KO models of CaMKIIβ (*Camk2b*$^{-/-}$) have been generated by deletion of exon sequences of the *Camk2b* gene (van Woerden et al., 2009; Bachstetter et al., 2014; Kool et al., 2016). *Camk2b*$^{-/-}$ mice exhibited cerebellar ataxia and severe deficits in locomotion (Kool et al., 2016), motor coordination (van Woerden et al., 2009), balance and cognition (Bachstetter et al., 2014). Interestingly, they showed reduced anxiety in a gene dose-dependent manner (Bachstetter et al., 2014).

Loss of CaMKIIβ, in *Camk2b*$^{-/-}$ mice, results in bidirectional inversion of postsynaptic plasticity at the parallel fiber (PF)-Purkinje cell (PC) synapse (van Woerden et al., 2009; Pinto et al., 2020). Failure of proper targeting of CaMKIIα to dendritic spines in the absence of CaMKIIβ in the *Camk2b*$^{-/-}$ mice results in impaired hippocampal NMDAR-dependent LTP and fear learning (Borgesius et al., 2011). This disrupted phenotype was absent in the *Camk2b*$^{A303R/A303R}$ KI model in which Ca^{2+}/CaM-dependent kinase activation of CaMKIIβ is disabled but F-actin binding and bundling functions are preserved (Borgesius et al., 2011). During LTP induction, a transient detachment of CaMKIIβ from F-actin, triggered by Ca^{2+} influx through glutamate receptors and the associated autophosphorylation of the F-actin binding region, is necessary for spine enlargement and LTP maintenance (Kim et al., 2015). Persistent binding of CaMKIIβ to F-actin in the amygdala could be causing deficits in LTP (Kim et al., 2015, 2019). To study the regulation of CaMKIIβ-F-actin interaction by autophosphorylation, a KI mouse model was generated by substituting Thr and Ser residues with Ala at exon 13 of *Camk2b* (CaMKIIβ$^{exon13:TS/A}$). This KI mouse exhibited reduced freezing in fear conditioning tests (Kim et al., 2019). The absence of impairment in fear learning in the CaM-binding deficient mutant reported by Borgesius et al. (2011) might be due to phosphorylation of the F-actin binding domain in the non-activable CaMKIIβ-A303R mutant by neighboring α-subunits of the same oligomer (Kim et al., 2019).

Regardless of normal hippocampal plasticity, *Camk2b*$^{A303R/A303R}$ mice exhibited severe deficits in motor behavior. However, the autophosphorylation deficient *Camk2b* mice, *Camk2b*$^{T287A/T287A}$, showed no significant change in locomotion compared to WT littermates, indicating a crucial role for Ca^{2+}/CaM-dependent activity, but not autonomous activity in normal mouse locomotion (Kool et al., 2016). Among the different *Camk2b* conditional mutants generated (Kool et al., 2016), *Camk2b*$^{f/f}$;*L7-cre* mice with specific loss of CaMKIIβ in cerebellar Purkinje cells showed impaired motor learning when tested for five consecutive days, indicating that cerebellar CaMKIIβ is essential for motor function (Kool et al., 2016).

Camk2a-Camk2b Double Mutants

The use of single mutants of *Camk2a* or *Camk2b* to study their function during development and in the mature brain can be inadequate when crucial functions are masked by compensation by the non-deleted form. For this purpose, double mutants of both isoforms (*Camk2a*$^{-/-}$;*Camk2b*$^{-/-}$) were generated (Kool et al., 2019). Germline or adult deletion of both CaMKIIα and CaMKIIβ in mice is lethal. Similarly, the Ca^{2+}-dependent and -independent activities of CaMKIIα and CaMKIIβ are also essential for survival. Acute deletion of both CaMKII isoforms does not overtly affect the biochemical composition of PSD. Adult loss of CaMKIIα and CaMKIIβ also abolished LTP in the hippocampal CA3-CA1 SC pathway. This deficit was absent in mice containing a specific deletion of CaMKII isoforms in the CA3 region of the hippocampus (*Camk2a*$^{f/f}$;*Camk2b*$^{f/f}$;*CA3-Cre*), indicating that presynaptic CaMKIIα and CaMKIIβ are dispensable for LTP at the CA3-CA1 synapses. However, deletion of CaMKII in the CA3 region resulted in significant reduction in LTP at the associational/commissural pathway (CA3-CA3 synapse) (Kool et al., 2019).

Ca^{2+}/Calmodulin-Dependent Protein Kinase Type II γ

Similar to CaMKIIα and CaMKIIβ, global CaMKIIγ KO mice (CaMKIIγ$^{-/-}$) displayed pronounced impairments in hippocampal-dependent memory tasks and avoidance behavior (Cohen et al., 2018). Training-induced increase in the expression of plasticity genes – *BDNF*, *c-Fos* and *Arc* – was prevented in CaMKIIγ$^{-/-}$ mice. While E-LTP was intact, L-LTP was strongly affected at SC-CA1 synapses of CaMKIIγ$^{-/-}$ mice, indicating deficits in LTM, but not STM. KO mice harboring a selective deletion of CaMKIIγ in excitatory neurons (CaMKIIγ-exc-KO), also exhibited impaired spatial learning and a decrease in training-induced nuclear translocation of CaM and *c-Fos* expression, suggesting a role for NMDAR activation upstream to CaMKIIγ-mediated cytonuclear signaling in CaMKIIγ$^{-/-}$ mice (Cohen et al., 2018). *In vivo* deletion of CaMKIIγ in parvalbumin (PV)-expressing inhibitory interneurons (CaMKIIγ PV-KO) eliminates NMDAR-induced synaptic potentiation of excitatory synapses onto inhibitory neurons ($LTP_{E\rightarrow I}$) and impairs experience-dependent neural oscillations, thereby

disrupting memory consolidation and hippocampus-dependent LTM (He et al., 2021).

FUNCTIONAL IMPLICATIONS OF Ca^{2+}/CALMODULIN-DEPENDENT PROTEIN KINASE TYPE II MUTATIONS IN DISEASES

In humans, *de novo* mutations in CaMKII have been identified and reported majorly in cases of neurodevelopmental disorders (NDDs) (Study, 2017; Akita et al., 2018) and intellectual disability (ID) (Küry et al., 2017). The role of CaMKII and glutamatergic signaling in neuropsychiatric diseases has been reviewed by Robison (Robison, 2014; see also Nicole and Pacary, 2020). **Supplementary Table 2** summarizes the different CaMKII variants reported with their functional implications and clinical manifestations if any. The type of mutation (synonymous, missense, splice region, frameshift, deletion), the specific CaMKII isoform (α, β and γ) that is mutated and the protein domain (catalytic, auto-regulatory or association) affected determine the disease phenotype. The zygosity of inheritance (heterozygous/homozygous) can also influence the pathogenicity of the variant (Chia et al., 2018); however, intrafamilial variations in the expression of disease symptoms by subjects carrying the same heterozygous variant, have also been reported (Heiman et al., 2021).

Clinical manifestations of the identified mutations range from global neurodevelopmental delay, seizures, mild to severe ID, hypotonia, delayed development of motor and speech/language skills, abnormal emotional behavior, cerebellar atrophy, facial dysmorphism, visual impairment and gastrointestinal issues. Dysfunction of CaMKIIα can cause seizure-associated activity in the forebrain (Akita et al., 2018) and pronounced motor delay (Küry et al., 2017), while individuals with CaMKIIβ variants exhibit severe ID accompanied with hypotonia (Küry et al., 2017) and cerebellar atrophy (Akita et al., 2018). Facial dysmorphisms along with severe ID and severe hypotonia has been reported in patients carrying a *CAMK2G* variant (Proietti Onori et al., 2018). The vast majority of the variants identified, affect amino acids conserved across species (Küry et al., 2017; Stephenson et al., 2017; Akita et al., 2018; Chia et al., 2018; Proietti Onori et al., 2018), which may explain the degree of severity of pathogenicity.

Stephenson et al. (2017) reported the first characterization of a *de novo* missense mutation in the *CAMK2A* gene, encoding for CaMKIIα, that was found in a patient with autism spectrum disorder (ASD) (Iossifov et al., 2014). Replacement of Glu with Val at 183rd position in the catalytic domain of CaMKIIα (CaMKIIα^{Glu183Val}) disrupts the interaction of CaMKII with ASD-associated proteins, such as Shank3 (SH3 and multiple ankyrin repeat domains 3) (Jiang and Ehlers, 2013), GluN2B (Pan et al., 2015) and the metabotropic glutamate receptor mGlu5 (Chana et al., 2015), which can reduce targeting of CaMKIIα to spines (Stephenson et al., 2017). Neuronal expression of CaMKIIα^{Glu183Val} disrupts AMPAR-mediated synaptic transmission, interferes with CaMKII autophosphorylation and reduces dendritic spine density. Heterozygous (*Camk2a*$^{WT/E183V}$) and homozygous (*Camk2a*$^{E183V/E183V}$) KI mice displayed enhanced repetitive behaviors and deficits in social interactions, which mimic symptoms of ASD (Stephenson et al., 2017). Decreased autoinhibition and increased Thr^{286} autophosphorylation of the CaMKIIα^{Pro212Gln} mutant, identified in an individual with NDD, affects the efficiency of excitatory synaptic transmission by enhancing K^+ currents in dendrites *in vitro* (Akita et al., 2018).

A biallelic, germline, loss-of-function *CAMK2A* missense mutation, *CAMK2A*$^{p.(His477Tyr)}$ in the association domain of CaMKIIα, was reported in two siblings displaying psychomotor retardation, frequent seizures and severe ID (Chia et al., 2018). Compared to the WT enzyme, the mutant form disrupts CaMKIIα self-oligomerization and holoenzyme assembly which in turn affects its subcellular localization in neurons and ability to support synaptic function *in vivo* (Chia et al., 2018). Recently, Brown et al. (2021) characterized six heterozygous variants of *CAMK2A* found in patients with schizophrenia. The p.(Arg396*) mutation in the association domain of CaMKIIα ablates holoenzyme formation, impairs GluN2B binding and consequently fails to accumulate at excitatory synapses in response to a LTP stimulus. While both p.(Arg396*) and p.(Arg8His) variants of *CAMK2A* exhibited impaired autophosphorylation at Thr^{286}, only the p.(Arg8His) mutation in the kinase domain significantly affected the Ca^{2+}/CaM-stimulated kinase activity (Brown et al., 2021). The absence of impaired function or expression for the remaining four mutants studied indicates that the mere occurrence of a mutation in a patient does not imply that the disease is caused by the mutation (Brown et al., 2021).

In addition to NDDs and ID, *CAMK2A* variants/single nucleotide polymorphisms (SNPs)/single nucleotide variants (SNVs) have been reported to be associated with risk for bipolar disorder (BD) in cohorts of European descent (Ament et al., 2015), in sporadic AD patients belonging to the Han Chinese population (Fang et al., 2019) and mild cognitive impairment (MCI) subjects in a Spanish population (Bufill et al., 2015). Deletion of the chromosome at 5q32, covering *CAMK2A*, might be responsible for mild ID observed in two patients diagnosed with mandibulofacial dysostosis (Vincent et al., 2014). Interestingly, *CAMK2A* genetic variants have been reported to be nominally associated with non-verbal communication in ASD cohorts (Chiocchetti et al., 2018) and logical memory performance in the elderly people (Rhein et al., 2020). *CAMK2A* polymorphisms can also influence spatial working memory in Caucasian adolescents (Easton et al., 2013) and cognitive ability in Taiwanese senior high school students (Lee et al., 2021). Recruitment of higher number of subjects from distinct populations is warranted to further validate the association of *CAMK2A* SNPs in genotype-phenotype association studies (Chiocchetti et al., 2018; Rhein et al., 2020).

Apart from mutations in *CAMK2A*, *de novo* mutations in *CAMK2B* have also been reported in 10 unrelated individuals exhibiting mild to severe ID (Küry et al., 2017). There are 19 rare variants of *CAMK2A* and *CAMK2B* that are heterozygous nonsense, missense or splice-site mutations affecting the catalytic

or auto-regulatory domain of CaMKII. The identified variants could affect protein expression and autophosphorylation at Thr^{286}/Thr^{287} when expressed *in vitro*, and cause deficits in neuronal migration *in vivo* (Küry et al., 2017). *De novo* mutations in *CAMK2A* and *CAMK2B* can also result in varying neurodevelopmental phenotypes (Akita et al., 2018). The missense variants disrupted the interaction between the catalytic domain and the regulatory segment, leading to increased Ca^{2+}-independent activity (Akita et al., 2018).

A heterozygous c.85C>T, p.(Arg29*) mutation in *CAMK2B* was found in a patient with mild ID, delayed speech development and seizures (Küry et al., 2017). This mutation was also reported in a 3-year-old European girl with complex focal seizures and global neurodevelopmental delay (Heiman et al., 2021). This maternally inherited pathogenic variant of the *CAMK2B* gene only mildly affected the patient's sibling, with the same variant, while the mother was phenotypically healthy and intellectually normal (Heiman et al., 2021). Similarly, a heterozygous c.416C>T, p.(Pro139Leu) variant of *CAMK2B* found in four Caucasian patients presented with severe ID, global developmental delay, hypotonia and microcephaly (Küry et al., 2017), was also reported in a 22-year-old South Asian woman (Rizzi et al., 2020) as well as in a *MECP-2* (methyl-CpG binding protein 2) negative proband of Japanese origin (Iwama et al., 2019). The recurrence of a few pathogenic variants of *CAMK2A* and *CAMK2B* (Küry et al., 2017) calls for elaborate functional studies of the mutant proteins both *in vitro* and *in vivo* (Onori and van Woerden, 2021).

De novo mutations in *CAMK2G* have also been identified and reported in cases of NDDs and severe ID (De Ligt et al., 2012; Study, 2017; Proietti Onori et al., 2018). Whole-exome sequencing performed on two patients revealed c.875G>C, p.(Arg292Pro) mutation in the auto-regulatory domain of CaMKIIγ, which is a putative CaM trapping region. One research group showed that $CAMK2G^{p.(Arg292Pro)}$ affects protein stability *in vitro* and functions as a pathogenic gain-of-function mutation by rendering it constitutively active and by blocking neuronal migration during development *in vivo* (Proietti Onori et al., 2018). The pathogenicity of the mutant is dependent on its catalytic activity (Proietti Onori et al., 2018). Cohen et al. (2018) reported that the ID observed in these patients might be due to the inability of $CaMKII\gamma^{Arg292Pro}$ to effectively trap CaM and shuttle Ca^{2+}/CaM complex to the nucleus, thereby disrupting a major link connecting activation of NMDARs and Cav1 channels to nuclear transcription of *BDNF*, *c-Fos* and *Arc*. This in turn adversely affects synaptic strengthening and LTM *in vivo*. Similar to *CAMK2A* SNPs reported, a genetic cluster containing *CAMK2G* polymorphisms has been identified to be associated with episodic memory performance (Dominique and Papassotiropoulos, 2006).

Although the *CAMK2* variants reported so far shed light on the probable role of the kinase in mediating disease symptoms, the number of human subjects identified with the mutation is insufficient, compared to the samples tested, to correlate the variant to the disease with good statistical power. Neither is it mandatory for the identified variant(s) to be a causal factor in the diseased phenotype (Brown et al., 2021), nor can an indirect role by the mutant protein be overlooked. More detailed functional characterization of the identified and reported CaMKII mutations than what is already reported, both *in vitro* (Küry et al., 2017; Stephenson et al., 2017; Akita et al., 2018; Chia et al., 2018; Cohen et al., 2018; Proietti Onori et al., 2018; Brown et al., 2021) and *in vivo* (Stephenson et al., 2017; Chia et al., 2018), can further substantiate the critical role of CaMKII mutants in disease conditions. Nonetheless, screening for either sporadic or inherited *CAMK2* variants in disorders majorly affecting cognition, can help in unraveling the theragnostic potential of CaMKII, if any.

Ca^{2+}/CALMODULIN-DEPENDENT PROTEIN KINASE TYPE II AS A DRUGGABLE TARGET FOR TREATING GLUTAMATERGIC DYSFUNCTION

Antagonists against glutamate receptors, majorly NMDARs, have been designed, synthesized and evaluated for their efficacy in preventing excitotoxicity in CNS diseases (Liu et al., 2020; Chandran et al., 2021). Signaling molecules downstream to NMDARs, like CaMKII, can also be targeted to restore Ca^{2+} and glutamate homeostasis at synapses (Vest et al., 2010). Likewise, CaMKII has been exploited as a potential drug target in neuropsychiatric and neurodegenerative diseases (Sałaciak et al., 2021).

Based on the differential regulation of CaMKII function during neurotoxicity, the modulators either enhance (Yamamoto et al., 2009; Zeng et al., 2010; Wang D.M. et al., 2013; Wei et al., 2013; Wang S.Q. et al., 2014) or inhibit CaMKII activity (Wang D. et al., 2013; Jiang et al., 2019). Their *modus operandi* includes binding to Ca^{2+}/CaM binding site of CaMKII (Brooks and Tavalin, 2011; Wong et al., 2019), targeting autonomous CaMKII activity (Coultrap et al., 2011; Wang D.M. et al., 2013; Wang et al., 2016; Deng et al., 2017), interacting with CaMKII hub domain (Leurs et al., 2021), preventing CaMKII translocation to the synaptic membrane (Matsumoto et al., 2008), inhibiting GluN2B-CaMKII binding (Tullis et al., 2021) or by modulating CaMKII-mediated signaling pathways (Liu et al., 2012; Matsumoto et al., 2013; Wei et al., 2013; Zhang et al., 2017; Islam et al., 2019; Wu et al., 2019; Izumi et al., 2020; Chen et al., 2021). The different CaMKII modulators reported from studies involving glutamatergic synapses in neurons are listed below:

1. Synthetic small molecule inhibitors like KN-62 and KN-93 (Tokumitsu et al., 1990; Sumi et al., 1991; Vest et al., 2010; Ashpole and Hudmon, 2011; Brooks and Tavalin, 2011).
2. Synthetic peptide inhibitors like AIP (autocamtide-2-related inhibitory peptide) (Fan et al., 2006; Goebel, 2009; Zha et al., 2009; Ashpole and Hudmon, 2011) and AC3-I (autocamtide-3 derived inhibitory peptide) (Leonard et al., 1999).
3. The natural CaMKII inhibitor protein CaM-KIIN (CN) and its peptide derivatives, CaM-KIINtide (CN27) (Chang et al., 1998; Saha et al., 2006; Mayadevi et al., 2016), CN21 (Vest et al., 2007, 2010;

Ashpole and Hudmon, 2011; Ahmed et al., 2017), CN19 (Coultrap and Bayer, 2011; Chalmers et al., 2020) and CN17β (Gomez-Monterrey et al., 2013).
4. CaMKII antisense oligodeoxynucleotides (Liu et al., 2012).
5. Long non-coding RNA *CAMK2D*-associated transcript 1 (*C2dat1*) (Xu et al., 2016).
6. Analogs of γ-hydroxybutyrate (GHB) (Leurs et al., 2021).
7. Volatile anesthetics like isoflurane (Matsumoto et al., 2008).
8. Compounds isolated from natural sources like nobiletin (Yamamoto et al., 2009), curcumin (Mayadevi et al., 2012), β-asarone (Wei et al., 2013), paeoniflorin (Wang D. et al., 2013; Zhang et al., 2017), naringin (Wang D.M. et al., 2013), *Ganoderma lucidum* polysaccharides (GLP) (Wang S.Q. et al., 2014), baicalin (Wang et al., 2016), theobromine (Islam et al., 2019), tilianin (Jiang et al., 2019) and gastrodin (Chen et al., 2021).
9. The histone deacetylase (HDAC) inhibitor, vorinostat (Matsumoto et al., 2013).
10. SAK3, a T-type calcium channel enhancer (Izumi et al., 2020).

Although a majority of the modulators have been widely employed to combat neuronal glutamatergic dysfunction *in vitro* and *in vivo*, their clinical use will require extensive studies on possible side effects and toxicity to cardiac health too (Nassal et al., 2020).

FUTURE PERSPECTIVES

Majority of the biochemical and structural studies on CaMKII have been performed on homomeric holoenzymes of one of the isoforms. However, under physiological conditions the enzyme can form hetero-multimers with different subunit stoichiometries. The relative abundance of different heteromeric subtypes under different developmental stages and in different regions would be an important determinant in the physiological functioning of CaMKII. Detailed studies on the functional variation among heteromers and their participation in specific cellular functions would be essential in making further progress in understanding the physiological functions of CaMKII. Further refinement of molecular genetic techniques for ectopic expression of isoforms and mutants of CaMKII with better control on heteromer formation would be essential for progress toward this goal.

The binding of CaMKII to GluN2B modulates the kinetic parameters of CaMKII enzyme activity and attenuates dephosphorylation of CaMKII (Pradeep et al., 2009; Cheriyan et al., 2011). These regulatory events strongly support the bistable switch model of molecular memory involving CaMKII and PP1. However, the physiological relevance of these regulatory events and the existence of the bistable switch *in vivo* needs to be demonstrated. Elucidation of the structure of the CaMKII-GluN2B complex could contribute significantly toward understanding the physiological functions of this complex.

CaMKII activation is a prerequisite for both LTP and LTD and recently it has been shown (Woolfrey et al., 2018) that two types of substrates (high autonomy, low autonomy) are preferred under each condition. If so, what are the exact signaling events with respect to the amount of Ca^{2+} entry into the postsynaptic site responsible for each of these events?

The recurrence of a few pathogenic variants of *CAMK2A* and *CAMK2B* (Küry et al., 2017) calls for elaborate functional studies of the mutant proteins both *in vitro* and *in vivo* (Onori and van Woerden, 2021). It also encourages more extensive screening for genetic variants of CaMKII in human populations.

CONCLUSION

CaMKII is an enzyme highly enriched in the brain. It has important roles to play in the functioning of glutamatergic synapses. Significant advances have been made in understanding the structure, function and physiological role of CaMKII. Its contribution to learning and memory has been investigated extensively with the help of most modern techniques. This has unequivocally established the integral part played by this enzyme in learning and memory. However, there is still more to be understood about the exact manner in which CaMKII participates in the underlying cellular mechanisms such as synaptic plasticity. Novel features of the structure and biochemical regulation of CaMKII are still being revealed by biophysical and biochemical experiments. Since the molecular properties of CaMKII holoenzyme are among the foundations on which most of the models of synaptic plasticity, learning and memory are built, progress in structural studies would continue to necessitate revisions in these models. Powerful molecular genetic techniques have permitted the controlled expression of isoforms and mutants of CaMKII in specific cell types in the brain of model organisms leading to important insights into its role in the cellular and systemic mechanisms. However, it has been difficult to dissect out all of its synaptic functions from cellular functions due to technical hurdles. The occurrence of heteromeric subtypes of CaMKII and the redundancy in the function among the isozymes also poses challenges to molecular genetic interrogation of its cellular functions. Progress in the understanding of CaMKII has prompted attempts to pursue it as a therapeutic target for pharmacological and genetic interventions since it is part of impaired Ca^{2+} signaling in many disease conditions. A limited number of genetic variants of CaMKII have been found associated with human neurological disease conditions. The central role of CaMKII in brain functions calls for large scale screening for CaMKII variants in human populations.

AUTHOR CONTRIBUTIONS

AM and RO contributed to conception and design of the manuscript. AM, SG, RJ, and RO co-wrote the manuscript. All authors

contributed to manuscript revision, read and approved the submitted version.

FUNDING

This work was supported by Rajiv Gandhi Center for Biotechnology (RGCB) (Grant No: RGCB-LRF), Department of Science and Technology (DST) (Grant Nos: DST INSPIRE Fellowships, IF150643 and IF150638), Government of India and Science and Engineering Research Board, Government of India (Grant No. CRG/2018/004528).

SUPPLEMENTARY MATERIAL

The Supplementary Material for this article can be found online at: https://www.frontiersin.org/articles/10.3389/fnmol.2022.855752/full#supplementary-material

REFERENCES

Aakalu, G., Smith, W. B., Nguyen, N., Jiang, C., and Schuman, E. M. (2001). Dynamic visualization of local protein synthesis in hippocampal neurons. *Neuron* 30, 489–502. doi: 10.1016/s0896-6273(01)00295-1

Abidin, I., Köhler, T., Weiler, E., Zoidl, G., Eysel, U. T., Lessmann, V., et al. (2006). Reduced presynaptic efficiency of excitatory synaptic transmission impairs LTP in the visual cortex of BDNF-heterozygous mice. *Eur. J. Neurosci.* 24, 3519–3531. doi: 10.1111/j.1460-9568.2006.05242.x

Achterberg, K. G., Buitendijk, G. H., Kool, M. J., Goorden, S. M., Post, L., Slump, D. E., et al. (2014). Temporal and region-specific requirements of αCaMKII in spatial and contextual learning. *J. Neurosci.* 34, 11180–11187. doi: 10.1523/JNEUROSCI.0640-14.2014

Ahmari, S. E., and Smith, S. J. (2002). Knowing a nascent synapse when you see it. *Neuron* 34, 333–336. doi: 10.1016/s0896-6273(02)00685-2

Ahmed, M. E., Dong, Y., Lu, Y., Tucker, D., Wang, R., and Zhang, Q. (2017). Beneficial effects of a CaMKIIα inhibitor TatCN21 peptide in global cerebral ischemia. *J. Mole. Neurosci.* 61, 42–51. doi: 10.1007/s12031-016-0830-8

Akita, T., Aoto, K., Kato, M., Shiina, M., Mutoh, H., Nakashima, M., et al. (2018). De novo variants in CAMK2A and CAMK2B cause neurodevelopmental disorders. *Ann. Clin. Transl. Neurol.* 5, 280–296. doi: 10.1002/acn3.528

Alkadhi, K. A. (2021). NMDA receptor-independent LTP in mammalian nervous system. *Prog. Neurob.* 200:101986. doi: 10.1016/j.pneurobio.2020.101986

Almeida, C. G., Tampellini, D., Takahashi, R. H., Greengard, P., Lin, M. T., Snyder, E. M., et al. (2005). Beta-amyloid accumulation in APP mutant neurons reduces PSD-95 and GluR1 in synapses. *Neurobiol. Dis.* 20, 187–198. doi: 10.1016/j.nbd.2005.02.008

Ament, S. A., Szelinger, S., Glusman, G., Ashworth, J., Hou, L., Akula, N., et al. (2015). Rare variants in neuronal excitability genes influence risk for bipolar disorder. *Proc. Natl. Acad. Sci.* 112, 3576–3581. doi: 10.1073/pnas.1424958112

Anderson, M. E. (2015). Oxidant stress promotes disease by activating CaMKII. *J. Mole. Cell. Cardiol.* 89, 160–167. doi: 10.1016/j.yjmcc.2015.10.014

Araki, S., Osuka, K., Takata, T., Tsuchiya, Y., and Watanabe, Y. (2020). Coordination between Calcium/Calmodulin-Dependent Protein Kinase II and Neuronal Nitric Oxide Synthase in Neurons. *Internat. J. Mole. Sci.* 21:7997. doi: 10.3390/ijms21217997

Araki, Y., Zeng, M., Zhang, M., and Huganir, R. L. (2015). Rapid dispersion of SynGAP from synaptic spines triggers AMPA receptor insertion and spine enlargement during LTP. *Neuron* 85, 173–189. doi: 10.1016/j.neuron.2014.12.023

Arrazola, M. S., and Court, F. A. (2019). Compartmentalized necroptosis activation in excitotoxicity-induced axonal degeneration: a novel mechanism implicated in neurodegenerative disease pathology. *Neur. Regenerat. Res.* 14:1385. doi: 10.4103/1673-5374.253520

Ashpole, N. M., Chawla, A. R., Martin, M. P., Brustovetsky, T., Brustovetsky, N., and Hudmon, A. (2013). Loss of calcium/calmodulin-dependent protein kinase II activity in cortical astrocytes decreases glutamate uptake and induces neurotoxic release of ATP. *J. Biol. Chem.* 288, 14599–14611. doi: 10.1074/jbc.M113.466235

Ashpole, N. M., and Hudmon, A. (2011). Excitotoxic neuroprotection and vulnerability with CaMKII inhibition. *Mole. Cell. Neurosci.* 46, 720–730. doi: 10.1016/j.mcn.2011.02.003

Ashpole, N. M., Song, W., Brustovetsky, T., Engleman, E. A., Brustovetsky, N., Cummins, T. R., et al. (2012). Calcium/calmodulin-dependent protein kinase II (CaMKII) inhibition induces neurotoxicity via dysregulation of glutamate/calcium signaling and hyperexcitability. *J. Biol. Chem.* 287, 8495–8506. doi: 10.1074/jbc.M111.323915

Ashraf, S. I., McLoon, A. L., Sclarsic, S. M., and Kunes, S. (2006). Synaptic protein synthesis associated with memory is regulated by the RISC pathway in Drosophila. *Cell* 124, 191–205. doi: 10.1016/j.cell.2005.12.017

Asrican, B., Lisman, J., and Otmakhov, N. (2007). Synaptic strength of individual spines correlates with bound ca2+–calmodulin-dependent kinase ii. *J. Neurosci.* 27, 14007–14011. doi: 10.1523/JNEUROSCI.3587-07.2007

Atkins, C. M., Chen, S., Alonso, O. F., Dietrich, W. D., and Hu, B. R. (2006). Activation of calcium/calmodulin-dependent protein kinases after traumatic brain injury. *J. Cereb. Blood Flow Metab.* 26, 1507–1518. doi: 10.1038/sj.jcbfm.9600301

Bach, M. E., Hawkins, R. D., Osman, M., Kandel, E. R., and Mayford, M. (1995). Impairment of spatial but not contextual memory in CaMKII mutant mice with a selective loss of hippocampal LTP in the range of the θ frequency. *Cell* 81, 905–915. doi: 10.1016/0092-8674(95)90010-1

Bachstetter, A. D., Webster, S. J., Tu, T., Goulding, D. S., Haiech, J., Watterson, D. M., et al. (2014). Generation and behavior characterization of CaMKIIβ knockout mice. *PLoS One* 9:e105191. doi: 10.1371/journal.pone.0105191

Baltaci, S. B., Mogulkoc, R., and Baltaci, A. K. (2019). Molecular mechanisms of early and late LTP. *Neurochem. Res.* 44, 281–296. doi: 10.1007/s11064-018-2695-4

Barria, A., Derkach, V., and Soderling, T. (1997a). Identification of the Ca2+/calmodulin-dependent protein kinase II regulatory phosphorylation site in the α-amino-3-hydroxyl-5-methyl 4-isoxazole-propionate-type glutamate receptor. *J. Biol. Chem.* 272, 32727–32730. doi: 10.1074/jbc.272.52.32727

Barria, A., Muller, D., Derkach, V., Griffith, L. C., and Soderling, T. R. (1997b). Regulatory phosphorylation of AMPA-type glutamate receptors by CaM-KII during long-term potentiation. *Science* 276, 2042–2045. doi: 10.1126/science.276.5321.2042

Barria, A., and Malinow, R. (2005). NMDA receptor subunit composition controls synaptic plasticity by regulating binding to CaMKII. *Neuron* 48, 289–301. doi: 10.1016/j.neuron.2005.08.034

Bayer, K. U., LeBel, E., McDonald, G. L., O'Leary, H., Schulman, H., and De Koninck, P. (2006). Transition from reversible to persistent binding of CaMKII to postsynaptic sites and NR2B. *J. Neurosci.* 26, 1164–1174. doi: 10.1523/JNEUROSCI.3116-05.2006

Bayer, K. U., Löhler, J., Schulman, H., and Harbers, K. (1999). Developmental expression of the CaM kinase II isoforms: ubiquitous γ-and δ-CaM kinase II are the early isoforms and most abundant in the developing nervous system. *Mole. Brain Res.* 70, 147–154. doi: 10.1016/s0169-328x(99)00131-x

Bayer, K. U., and Schulman, H. (2019). CaM kinase: still inspiring at 40. *Neuron* 103, 380–394. doi: 10.1016/j.neuron.2019.05.033

Bayer, K. U. D. K., De Koninck, P., Leonard, A. S., Hell, J. W., and Schulman, H. (2001). Interaction with the NMDA receptor locks CaMKII in an active conformation. *Nature* 411, 801–805. doi: 10.1038/35081080

Bejar, R., Yasuda, R., Krugers, H., Hood, K., and Mayford, M. (2002). Transgenic calmodulin-dependent protein kinase II activation: dose-dependent effects on synaptic plasticity, learning, and memory. *J. Neurosci.* 22, 5719–5726. doi: 10.1523/JNEUROSCI.22-13-05719.2002

Bhattacharyya, M., Karandur, D., and Kuriyan, J. (2020). Structural insights into the regulation of Ca2+/calmodulin-dependent protein kinase II (CaMKII). *Cold Spring Harb. Perspect. Biol.* 12:a035147. doi: 10.1101/cshperspect.a035147

Bliss, T. V. P., and Collingridge, G. L. (2019). Persistent memories of long-term potentiation and the N-methyl-d-aspartate receptor. *Brain Neurosci. Adv.* 3:2398212819848213. doi: 10.1177/2398212819848213

Blum, D., Herrera, F., Francelle, L., Mendes, T., Basquin, M., Obriot, H., et al. (2015). Mutant huntingtin alters Tau phosphorylation and subcellular distribution. *Hum. Molec. Genet.* 24, 76–85. doi: 10.1093/hmg/ddu421

Borgesius, N. Z., van Woerden, G. M., Buitendijk, G. H., Keijzer, N., Jaarsma, D., Hoogenraad, C. C., et al. (2011). βCaMKII plays a nonenzymatic role in hippocampal synaptic plasticity and learning by targeting αCaMKII to synapses. *J. Neurosci.* 31, 10141–10148. doi: 10.1523/JNEUROSCI.5105-10.2011

Brito, V., Giralt, A., Enriquez-Barreto, L., Puigdellívol, M., Suelves, N., Zamora-Moratalla, A., et al. (2014). Neurotrophin receptor p75 NTR mediates Huntington's disease-associated synaptic and memory dysfunction. *J. Clin. Invest.* 124, 4411–4428. doi: 10.1172/JCI74809

Brooks, I. M., and Tavalin, S. J. (2011). Ca2+/calmodulin-dependent protein kinase II inhibitors disrupt AKAP79-dependent PKC signaling to GluA1 AMPA receptors. *J. Biol. Chem.* 286, 6697–6706. doi: 10.1074/jbc.M110.183558

Brown, A. M., Deutch, A. Y., and Colbran, R. J. (2005). Dopamine depletion alters phosphorylation of striatal proteins in a model of Parkinsonism. *Eur. J. Neurosci.* 22, 247–256. doi: 10.1111/j.1460-9568.2005.04190.x

Brown, C. N., Cook, S. G., Allen, H. F., Crosby, K. C., Singh, T., Coultrap, S. J., et al. (2021). Characterization of six CaMKIIα variants found in patients with schizophrenia. *Iscience* 24:103184. doi: 10.1016/j.isci.2021.103184

Browne, G. J., and Proud, C. G. (2004). A novel mTOR-regulated phosphorylation site in elongation factor 2 kinase modulates the activity of the kinase and its binding to calmodulin. *Molec. Cell. Biol.* 24, 2986–2997. doi: 10.1128/MCB.24.7.2986-2997.2004

Buard, I., Coultrap, S. J., Freund, R. K., Lee, Y. S., Dell'Acqua, M. L., Silva, A. J., et al. (2010). CaMKII "autonomy" is required for initiating but not for maintaining neuronal long-term information storage. *J. Neurosci.* 30, 8214–8220. doi: 10.1523/JNEUROSCI.1469-10.2010

Bufill, E., Roura-Poch, P., Sala-Matavera, I., Antón, S., Lleó, A., Sánchez-Saudinós, B., et al. (2015). Reelin signaling pathway genotypes and Alzheimer disease in a Spanish population. *Alzheimer Dis. Assoc. Dis.* 29, 169–172. doi: 10.1097/WAD.0000000000000002

Buonarati, O. R., Cook, S. G., Goodell, D. J., Chalmers, N. E., Rumian, N. L., Tullis, J. E., et al. (2020). CaMKII versus DAPK1 binding to GluN2B in ischemic neuronal cell death after resuscitation from cardiac arrest. *Cell Rep.* 30, 1–8. doi: 10.1016/j.celrep.2019.11.076

Buonarati, O. R., Miller, A. P., Coultrap, S. J., Bayer, K. U., and Reichow, S. L. (2021). Conserved and divergent features of neuronal CaMKII holoenzyme structure, function, and high-order assembly. *Cell Rep.* 37:110168. doi: 10.1016/j.celrep.2021.110168

Burgin, K. E., Waxham, M. N., Rickling, S., Westgate, S. A., Mobley, W. C., and Kelly, P. T. (1990). In situ hybridization histochemistry of Ca2+/calmodulin-dependent protein kinase in developing rat brain. *J. Neurosci.* 10, 1788–1798. doi: 10.1523/JNEUROSCI.10-06-01788.1990

Butler, L. S., Silva, A. J., Abeliovich, A., Watanabe, Y., Tonegawa, S., and McNamara, J. O. (1995). Limbic epilepsy in transgenic mice carrying a Ca2+/calmodulin-dependent kinase II alpha-subunit mutation. *Proc. Natl. Acad. Sci.* 92, 6852–6855. doi: 10.1073/pnas.92.15.6852

Cacucci, F., Wills, T. J., Lever, C., Giese, K. P., and O'Keefe, J. (2007). Experience-dependent increase in CA1 place cell spatial information, but not spatial reproducibility, is dependent on the autophosphorylation of the α-isoform of the calcium/calmodulin-dependent protein kinase II. *J. Neurosci.* 27, 7854–7859. doi: 10.1523/jneurosci.1704-07.2007

Chalmers, N. E., Yonchek, J., Steklac, K. E., Ramsey, M., Bayer, K. U., Herson, P. S., et al. (2020). Calcium/calmodulin-dependent kinase (CaMKII) inhibition protects against Purkinje cell damage following CA/CPR in mice. *Mole. Neurob.* 57, 150–158. doi: 10.1007/s12035-019-01765-9

Chamoun, R., Suki, D., Gopinath, S. P., Goodman, J. C., and Robertson, C. (2010). Role of extracellular glutamate measured by cerebral microdialysis in severe traumatic brain injury. *J. Neurosurg.* 113, 564–570. doi: 10.3171/2009.12.JNS09689

Chana, G., Laskaris, L., Pantelis, C., Gillett, P., Testa, R., Zantomio, D., et al. (2015). Decreased expression of mGluR5 within the dorsolateral prefrontal cortex in autism and increased microglial number in mGluR5 knockout mice: Pathophysiological and neurobehavioral implications. *Brain Behav. Imm.* 49, 197–205. doi: 10.1016/j.bbi.2015.05.009

Chandran, R., Vijayan, D., Reddy, E. K., Kumar, M., Kesavan, L., Jacob, R., et al. (2021). Neuroprotective derivatives of tacrine that target NMDA receptor and acetylcholinesterase-Design, synthesis and biological evaluation. *Comp. Struct. Biotechnol. J.* 19, 4517–4537. doi: 10.1016/j.csbj.2021.07.041

Chang, B. H., Mukherji, S., and Soderling, T. R. (1998). Characterization of a calmodulin kinase II inhibitor protein in brain. *Proc. Natl. Acad. Sci.* 95, 10890–10895. doi: 10.1073/pnas.95.18.10890

Chang, J. Y., Parra-Bueno, P., Laviv, T., Szatmari, E. M., Lee, S. J. R., and Yasuda, R. (2017). CaMKII autophosphorylation is necessary for optimal integration of Ca2+ signals during LTP induction, but not maintenance. *Neuron* 94, 800–808. doi: 10.1016/j.neuron.2017.04.041

Chapman, P. F., Frenguelli, B. G., Smith, A., Chen, C. M., and Silva, A. J. (1995). The α-Ca2+/calmodulin kinase II: a bidirectional modulator of presynaptic plasticity. *Neuron* 14, 591–597. doi: 10.1016/0896-6273(95)90315-1

Chawla, A. R., Johnson, D. E., Zybura, A. S., Leeds, B. P., Nelson, R. M., and Hudmon, A. (2017). Constitutive regulation of the glutamate/aspartate transporter EAAT 1 by Calcium-Calmodulin-Dependent Protein Kinase II. *J. Neurochem.* 140, 421–434. doi: 10.1111/jnc.13913

Chen, B. S., and Roche, K. W. (2007). Regulation of NMDA receptors by phosphorylation. *Neuropharmacology* 53, 362–368. doi: 10.1016/j.neuropharm.2007.05.018

Chen, C., Rainnie, D. G., Greene, R. W., and Tonegawa, S. (1994). Abnormal fear response and aggressive behavior in mutant mice deficient for alpha-calcium-calmodulin kinase II. *Science* 266, 291–294. doi: 10.1126/science.7939668

Chen, T. T., Zhou, X., Xu, Y. N., Li, Y., Wu, X. Y., Xiang, Q., et al. (2021). Gastrodin ameliorates learning and memory impairment in rats with vascular dementia by promoting autophagy flux via inhibition of the Ca2+/CaMKII signal pathway. *Aging* 13:9542. doi: 10.18632/aging.202667

Cheriyan, J., Kumar, P., Mayadevi, M., Surolia, A., and Omkumar, R. V. (2011). Calcium/calmodulin dependent protein kinase II bound to NMDA receptor 2B subunit exhibits increased ATP affinity and attenuated dephosphorylation. *PLoS One* 6:e16495. doi: 10.1371/journal.pone.0016495

Cheriyan, J., Mohanan, A. G., Kurup, P. K., Mayadevi, M., and Omkumar, R. V. (2012). Effect of multimeric structure of CaMKII in the GluN2B-mediated modulation of kinetic parameters of ATP. *PLoS one* 7:e45064. doi: 10.1371/journal.pone.0045064

Chia, P. H., Zhong, F. L., Niwa, S., Bonnard, C., Utami, K. H., Zeng, R., et al. (2018). A homozygous loss-of-function CAMK2A mutation causes growth delay, frequent seizures and severe intellectual disability. *Elife* 7:e32451. doi: 10.7554/eLife.32451

Chiocchetti, A. G., Yousaf, A., Bour, H. S., Haslinger, D., Waltes, R., Duketis, E., et al. (2018). Common functional variants of the glutamatergic system in Autism spectrum disorder with high and low intellectual abilities. *J. Neural Trans.* 125, 259–271. doi: 10.1007/s00702-017-1813-9

Cho, M. H., Cao, X., Wang, D., and Tsien, J. Z. (2007). Dentate gyrus-specific manipulation of β-Ca2+/calmodulin-dependent kinase II disrupts memory consolidation. *Proc. Natl. Sci.* 104, 16317–16322. doi: 10.1073/pnas.0703344104

Cho, Y. H., Giese, K. P., Tanila, H., Silva, A. J., and Eichenbaum, H. (1998). Abnormal hippocampal spatial representations in αCaMKIIT286A and CREBαΔ− mice. *Science* 279, 867–869. doi: 10.1126/science.279.5352.867

Chotiner, J. K., Khorasani, H., Nairn, A. C., O'dell, T. J., and Watson, J. B. (2003). Adenylyl cyclase-dependent form of chemical long-term potentiation triggers translational regulation at the elongation step. *Neuroscience* 116, 743–752. doi: 10.1016/s0306-4522(02)00797-2

Churn, S. B., Sombati, S., Jakoi, E. R., Sievert, L., and DeLorenzo, R. J. (2000). Inhibition of calcium/calmodulin kinase II alpha subunit expression results in epileptiform activity in cultured hippocampal neurons. *Proc. Natl. Acad. Sci.* 97, 5604–5609. doi: 10.1073/pnas.080071697

Cohen, S. M., Suutari, B., He, X., Wang, Y., Sanchez, S., Tirko, N. N., et al. (2018). Calmodulin shuttling mediates cytonuclear signaling to trigger experience-dependent transcription and memory. *Nat. Comm.* 9, 1–12. doi: 10.1038/s41467-018-04705-8

Colicos, M. A., Collins, B. E., Sailor, M. J., and Goda, Y. (2001). Remodeling of synaptic actin induced by photoconductive stimulation. *Cell* 107, 605–616. doi: 10.1016/s0092-8674(01)00579-7

Cook, S. G., Buonarati, O. R., Coultrap, S. J., and Bayer, K. U. (2021). CaMKII holoenzyme mechanisms that govern the LTP versus LTD decision. *Sci. Adv.* 7:eabe2300. doi: 10.1126/sciadv.abe2300

Cook, S. G., Goodell, D. J., Restrepo, S., Arnold, D. B., and Bayer, K. U. (2019). Simultaneous live imaging of multiple endogenous proteins reveals a mechanism for Alzheimer's-related plasticity impairment. *Cell Rep.* 27, 658–665. doi: 10.1016/j.celrep.2019.03.041

Cooke, S. F., Wu, J., Plattner, F., Errington, M., Rowan, M., Peters, M., et al. (2006). Autophosphorylation of αCaMKII is not a general requirement for NMDA receptor-dependent LTP in the adult mouse. *J. Phys.* 574, 805–818. doi: 10.1113/jphysiol.2006.111559

Coultrap, S. J., Barcomb, K., and Bayer, K. U. (2012). A significant but rather mild contribution of T286 autophosphorylation to Ca2+/CaM-stimulated CaMKII activity. *PLoS One* 7:e37176. doi: 10.1371/journal.pone.0037176

Coultrap, S. J., and Bayer, K. U. (2011). Improving a natural CaMKII inhibitor by random and rational design. *PLoS One* 6:e25245. doi: 10.1371/journal.pone.0025245

Coultrap, S. J., and Bayer, K. U. (2014). Nitric oxide induces Ca2+-independent activity of the Ca2+/calmodulin-dependent protein kinase II (CaMKII). *J. Biol. Chem.* 289, 19458–19465. doi: 10.1074/jbc.M114.558254

Coultrap, S. J., Freund, R. K., O'Leary, H., Sanderson, J. L., Roche, K. W., Dell'Acqua, M. L., et al. (2014). Autonomous CaMKII mediates both LTP and LTD using a mechanism for differential substrate site selection. *Cell Rep.* 6, 431–437. doi: 10.1016/j.celrep.2014.01.005

Coultrap, S. J., Vest, R. S., Ashpole, N. M., Hudmon, A., and Bayer, K. U. (2011). CaMKII in cerebral ischemia. *Acta Pharm. Sin.* 32, 861–872. doi: 10.1038/aps.2011.68

Crino, P. B., and Eberwine, J. (1996). Molecular characterization of the dendritic growth cone: regulated mRNA transport and local protein synthesis. *Neuron* 17, 1173–1187. doi: 10.1016/s0896-6273(00)80248-2

Davis, H. P., and Squire, L. R. (1984). Protein synthesis and memory: a review. *Psychol. Bull.* 96:518. doi: 10.1037/0033-2909.96.3.518

Day, M., Wang, Z., Ding, J., An, X., Ingham, C. A., Shering, A. F., et al. (2006). Selective elimination of glutamatergic synapses on striatopallidal neurons in Parkinson disease models. *Nat. Neurosci.* 9, 251–259. doi: 10.1038/nn1632

De Koninck, P., and Schulman, H. (1998). Sensitivity of CaMKII to the frequency of Ca2+ oscillations. *Science* 279, 227–230.

De Ligt, J., Willemsen, M. H., Van Bon, B. W., Kleefstra, T., Yntema, H. G., Kroes, T., et al. (2012). Diagnostic exome sequencing in persons with severe intellectual disability. *New Engl. J. Med.* 367, 1921–1929. doi: 10.1056/NEJMoa1206524

Deckel, A. W., Gordinier, A., Nuttal, D., Tang, V., Kuwada, C., Freitas, R., et al. (2001). Reduced activity and protein expression of NOS in R6/2 HD transgenic mice: effects of L-NAME on symptom progression. *Brain Res.* 919, 70–81. doi: 10.1016/s0006-8993(01)03000-1

Deckel, A. W., Tang, V., Nuttal, D., Gary, K., and Elder, R. (2002a). Altered neuronal nitric oxide synthase expression contributes to disease progression in Huntington's disease transgenic mice. *Brain Res.* 939, 76–86. doi: 10.1016/s0006-8993(02)02550-7

Deckel, A. W, Elder, R., and Fuhrer, G. (2002b). Biphasic developmental changes in Ca2+/calmodulin-dependent proteins in R6/2 Huntington's disease mice. *Neuroreport* 13, 707–711. doi: 10.1097/00001756-200204160-00034

Deng, G., Orfila, J. E., Dietz, R. M., Moreno-Garcia, M., Rodgers, K. M., Coultrap, S. J., et al. (2017). Autonomous CaMKII activity as a drug target for histological and functional neuroprotection after resuscitation from cardiac arrest. *Cell Rep.* 18, 1109–1117. doi: 10.1016/j.celrep.2017.01.011

Derkach, V., Barria, A., and Soderling, T. R. (1999). Ca2+/calmodulin-kinase II enhances channel conductance of α-amino-3-hydroxy-5-methyl-4-isoxazolepropionate type glutamate receptors. *Proc. Natl. Acad. Sci.* 96, 3269–3274. doi: 10.1073/pnas.96.6.3269

Deshpande, L. S., Sun, D. A., Sombati, S., Baranova, A., Wilson, M. S., Attkisson, E., et al. (2008). Alterations in neuronal calcium levels are associated with cognitive deficits after traumatic brain injury. *Neurosci. Lett.* 441, 115–119. doi: 10.1016/j.neulet.2008.05.113

Deutch, A. Y. (2006). Striatal plasticity in parkinsonism: dystrophic changes in medium spiny neurons and progression in Parkinson's disease. *Parkins. Dis. Relat. Dis.* 2006, 67–70. doi: 10.1007/978-3-211-45295-0_12

Di Biase, V., Obermair, G. J., Szabo, Z., Altier, C., Sanguesa, J., Bourinet, E., et al. (2008). Stable membrane expression of postsynaptic CaV1. 2 calcium channel clusters is independent of interactions with AKAP79/150 and PDZ proteins. *J. Neurosci.* 28, 13845–13855. doi: 10.1523/JNEUROSCI.3213-08.2008

Di Lorenzo, F., Motta, C., Casula, E. P., Bonnì, S., Assogna, M., Caltagirone, C., et al. (2020). LTP-like cortical plasticity predicts conversion to dementia in patients with memory impairment. *Brain Stimul.* 13, 1175–1182. doi: 10.1016/j.brs.2020.05.013

Ding, J. D., Kennedy, M. B., and Weinberg, R. J. (2013). Subcellular organization of camkii in rat hippocampal pyramidal neurons. *J. Comp. Neurol.* 521, 3570–3583. doi: 10.1002/cne.23372

Dominique, J. F., and Papassotiropoulos, A. (2006). Identification of a genetic cluster influencing memory performance and hippocampal activity in humans. *Proc. Natl. Acad. Sci.* 103, 4270–4274. doi: 10.1073/pnas.0510212103

Easton, A. C., Lourdusamy, A., Loth, E., Torro, R., Giese, K. P., Kornhuber, J., et al. (2013). CAMK2A polymorphisms predict working memory performance in humans. *Mole. Psych.* 18, 850–852. doi: 10.1038/mp.2012.114

Elgersma, Y., Fedorov, N. B., Ikonen, S., Choi, E. S., Elgersma, M., Carvalho, O. M., et al. (2002). Inhibitory autophosphorylation of CaMKII controls PSD association, plasticity, and learning. *Neuron* 36, 493–505. doi: 10.1016/s0896-6273(02)01007-3

Erondu, N. E., and Kennedy, M. B. (1985). Regional distribution of type II Ca2+/calmodulin-dependent protein kinase in rat brain. *J. Neurosci.* 5, 3270–3277. doi: 10.1523/JNEUROSCI.05-12-03270.1985

Faas, G. C., Raghavachari, S., Lisman, J. E., and Mody, I. (2011). Calmodulin as a direct detector of Ca 2+ signals. *Nat. Neurosci.* 14, 301–304. doi: 10.1038/nn.2746

Faden, A. I., Demediuk, P., Panter, S. S., and Vink, R. (1989). The role of excitatory amino acids and NMDA receptors in traumatic brain injury. *Science* 244, 798–800. doi: 10.1126/science.2567056

Fan, W., Agarwal, N., and Cooper, N. G. (2006). The role of CaMKII in BDNF-mediated neuroprotection of retinal ganglion cells (RGC-5). *Brain Res.* 1067, 48–57. doi: 10.1016/j.brainres.2005.10.030

Fang, X., Tang, W., Yang, F., Lu, W., Cai, J., Ni, J., et al. (2019). A comprehensive analysis of the CaMK2A gene and susceptibility to Alzheimer's disease in the Han Chinese population. *Front. Aging Neurosci.* 11:84. doi: 10.3389/fnagi.2019.00084

Farinelli, M., Heitz, F. D., Grewe, B. F., Tyagarajan, S. K., Helmchen, F., and Mansuy, I. M. (2012). Selective regulation of NR2B by protein phosphatase-1 for the control of the NMDA receptor in neuroprotection. *PLoS One* 7:e34047. doi: 10.1371/journal.pone.0034047

Figurov, A., Pozzo-Miller, L. D., Olafsson, P., Wang, T., and Lu, B. (1996). Regulation of synaptic responses to high-frequency stimulation and LTP by neurotrophins in the hippocampus. *Nature* 381, 706–709. doi: 10.1038/381706a0

Fink, C. C., Bayer, K. U., Myers, J. W., Ferrell, J. E. Jr., Schulman, H., and Meyer, T. (2003). Selective regulation of neurite extension and synapse formation by the β but not the α isoform of CaMKII. *Neuron* 39, 283–297. doi: 10.1016/s0896-6273(03)00428-8

Fischer, M., Kaech, S., Knutti, D., and Matus, A. (1998). Rapid actin-based plasticity in dendritic spines. *Neuron* 20, 847–854. doi: 10.1016/s0896-6273(00)80467-5

Folkerts, M. M., Parks, E. A., Dedman, J. R., Kaetzel, M. A., Lyeth, B. G., and Berman, R. F. (2007). Phosphorylation of calcium calmodulin-dependent protein kinase II following lateral fluid percussion brain injury in rats. *J. Neurotr.* 24, 638–650. doi: 10.1089/neu.2006.0188

Frankland, P. W., Bontempi, B., Talton, L. E., Kaczmarek, L., and Silva, A. J. (2004). The involvement of the anterior cingulate cortex in remote contextual fear memory. *Science* 304, 881–883. doi: 10.1126/science.1094804

Freund, T. F., Powell, J. F., and Smith, A. (1984). Tyrosine hydroxylase-immunoreactive boutons in synaptic contact with identified striatonigral neurons, with particular reference to dendritic spines. *Neuroscience* 13, 1189–1215. doi: 10.1016/0306-4522(84)90294-x

Gamache, T. R., Araki, Y., and Huganir, R. L. (2020). Twenty years of SynGAP research: from synapses to cognition. *J. Neurosci.* 40, 1596–1605. doi: 10.1523/JNEUROSCI.0420-19.2020

Gardoni, F., and Bellone, C. (2015). Modulation of the glutamatergic transmission by Dopamine: a focus on Parkinson, Huntington and Addiction diseases. *Front. Cell. Neurosci.* 9:25. doi: 10.3389/fncel.2015.00025

Gardoni, F., Ghiglieri, V., Di Luca, M., and Calabresi, P. (2010). Assemblies of glutamate receptor subunits with post-synaptic density proteins and their

alterations in Parkinson's disease. *Prog. Brain Res.* 183, 169–182. doi: 10.1016/S0079-6123(10)83009-2

Gardoni, F., Mauceri, D., Fiorentini, C., Bellone, C., Missale, C., Cattabeni, F., et al. (2003). CaMKII-dependent phosphorylation regulates SAP97/NR2A interaction. *J. Biol. Chem.* 278, 44745–44752. doi: 10.1074/jbc.M303576200

Gardoni, F., Polli, F., Cattabeni, F., and Di Luca, M. (2006). Calcium–calmodulin-dependent protein kinase II phosphorylation modulates PSD-95 binding to NMDA receptors. *Eur. J. Neurosci.* 24, 2694–2704. doi: 10.1111/j.1460-9568.2006.05140.x

Gardoni, F., Schrama, L. H., Van Dalen, J. J. W., Gispen, W. H., Cattabeni, F., and Di Luca, M. (1999). αCaMKII binding to the C-terminal tail of NMDA receptor subunit NR2A and its modulation by autophosphorylation. *FEBS Lett.* 456, 394–398. doi: 10.1016/s0014-5793(99)00985-0

Ghosh, A., and Giese, K. P. (2015). Calcium/calmodulin-dependent kinase II and Alzheimer's disease. *Mole. Brain* 8, 1–7.

Giese, K. P. (2021). The role of CaMKII autophosphorylation for NMDA receptor-dependent synaptic potentiation. *Neuropharmacology* 193:108616. doi: 10.1016/j.neuropharm.2021.108616

Giese, K. P., Fedorov, N. B., Filipkowski, R. K., and Silva, A. J. (1998). Autophosphorylation at Thr286 of the α calcium-calmodulin kinase II in LTP and learning. *Science* 279, 870–873. doi: 10.1126/science.279.5352.870

Giovannini, M. G., Blitzer, R. D., Wong, T., Asoma, K., Tsokas, P., Morrison, J. H., et al. (2001). Mitogen-activated protein kinase regulates early phosphorylation and delayed expression of Ca2+/calmodulin-dependent protein kinase II in long-term potentiation. *J. Neurosci.* 21, 7053–7062. doi: 10.1523/JNEUROSCI.21-18-07053.2001

Giralt, A., Saavedra, A., Alberch, J., and Pérez-Navarro, E. (2012). Cognitive dysfunction in Huntington's disease: humans, mouse models and molecular mechanisms. *J. Hunting. Dis.* 1, 155–173. doi: 10.3233/JHD-120023

Glazewski, S., Bejar, R., Mayford, M., and Fox, K. (2001). The effect of autonomous alpha-CaMKII expression on sensory responses and experience-dependent plasticity in mouse barrel cortex. *Neuropharmacology* 41, 771–778. doi: 10.1016/s0028-3908(01)00097-1

Goebel, D. J. (2009). Selective blockade of CaMKII-α inhibits NMDA-induced caspase-3-dependent cell death but does not arrest PARP-1 activation or loss of plasma membrane selectivity in rat retinal neurons. *Brain Res.* 1256, 190–204. doi: 10.1016/j.brainres.2008.12.051

Gomez-Monterrey, I., Sala, M., Rusciano, M. R., Monaco, S., Maione, A. S., Iaccarino, G., et al. (2013). Characterization of a selective CaMKII peptide inhibitor. *Eur. J. Med. Chem.* 62, 425–434. doi: 10.1016/j.ejmech.2012.12.053

Goodell, D. J., Zaegel, V., Coultrap, S. J., Hell, J. W., and Bayer, K. U. (2017). DAPK1 mediates LTD by making CaMKII/GluN2B binding LTP specific. *Cell Rep.* 19, 2231–2243. doi: 10.1016/j.celrep.2017.05.068

Gordon, J. A., Cioffi, D., Silva, A. J., and Stryker, M. P. (1996). Deficient plasticity in the primary visual cortex of α-calcium/calmodulin-dependent protein kinase II mutant mice. *Neuron* 17, 491–499. doi: 10.1016/s0896-6273(00)80181-6

Gottschalk, W., Pozzo-Miller, L. D., Figurov, A., and Lu, B. (1998). Presynaptic modulation of synaptic transmission and plasticity by brain-derived neurotrophic factor in the developing hippocampus. *J. Neurosci.* 18, 6830–6839. doi: 10.1523/JNEUROSCI.18-17-06830.1998

Gratuze, M., Noël, A., Julien, C., Cisbani, G., Milot-Rousseau, P., Morin, F., et al. (2015). Tau hyperphosphorylation and deregulation of calcineurin in mouse models of Huntington's disease. *Hum. Mole. Genet.* 24, 86–99. doi: 10.1093/hmg/ddu456

Grover, L. M., and Teyler, T. J. (1990). Two components of long-term potentiation induced by different patterns of afferent activation. *Nature* 347, 477–479. doi: 10.1038/347477a0

Gu, S. X., Blokhin, I. O., Wilson, K. M., Dhanesha, N., Doddapattar, P., Grumbach, I. M., et al. (2016). Protein methionine oxidation augments reperfusion injury in acute ischemic stroke. *JCI Insight* 1:7. doi: 10.1172/jci.insight.86460

Gu, Z., Liu, W., and Yan, Z. (2009). β-Amyloid impairs AMPA receptor trafficking and function by reducing Ca2+/calmodulin-dependent protein kinase II synaptic distribution. *J. Biol. Chem.* 284, 10639–10649. doi: 10.1074/jbc.M806508200

Gunasekaran, S., Jacob, R. S., and Omkumar, R. V. (2022). Differential expression of miR-148b, miR-129-2 and miR-296 in animal models of schizophrenia-Relevance to NMDA receptor hypofunction. *Neuropharmacology* 2022:109024. doi: 10.1016/j.neuropharm.2022.109024

Gurd, J. W., Rawof, S., Huo, J. Z., Dykstra, C., Bissoon, N., Teves, L., et al. (2008). Ischemia and status epilepitcus result in enhanced phosphorylation of calcium and calmodulin-stimulated protein kinase II on threonine 253. *Brain Res.* 1218, 158–165. doi: 10.1016/j.brainres.2008.04.040

Gustin, R. M., Shonesy, B. C., Robinson, S. L., Rentz, T. J., Baucum, A. J. II, and Jalan-Sakrikar, N. (2011). Loss of Thr286 phosphorylation disrupts synaptic CaMKIIα targeting, NMDAR activity and behavior in pre-adolescent mice. *Mole. Cell. Neurosci.* 47, 286–292. doi: 10.1016/j.mcn.2011.05.006

Hafner, A. S., Penn, A. C., Grillo-Bosch, D., Retailleau, N., Poujol, C., Philippat, A., et al. (2015). Lengthening of the stargazin cytoplasmic tail increases synaptic transmission by promoting interaction to deeper domains of PSD-95. *Neuron* 86, 475–489. doi: 10.1016/j.neuron.2015.03.013

Hao, Z. B., Pei, D. S., Guan, Q. H., and Zhang, G. Y. (2005). Calcium/calmodulin-dependent protein kinase II (CaMKII), through NMDA receptors and L-Voltage-gated channels, modulates the serine phosphorylation of GluR6 during cerebral ischemia and early reperfusion period in rat hippocampus. *Molecular Brain Res.* 140, 55–62. doi: 10.1016/j.molbrainres.2005.07.005

Hasegawa, S., Furuichi, T., Yoshida, T., Endoh, K., Kato, K., Sado, M., et al. (2009). Transgenic up-regulation of alpha-CaMKII in forebrain leads to increased anxiety-like behaviors and aggression. *Mole. Brain* 2, 1–11. doi: 10.1186/1756-6606-2-6

Hayashi, Y., Shi, S. H., Esteban, J. A., Piccini, A., Poncer, J. C., and Malinow, R. (2000). Driving AMPA receptors into synapses by LTP and CaMKII: requirement for GluR1 and PDZ domain interaction. *Science* 287, 2262–2267. doi: 10.1126/science.287.5461.2262

He, X., Li, J., Zhou, G., Yang, J., McKenzie, S., Li, Y., et al. (2021). Gating of hippocampal rhythms and memory by synaptic plasticity in inhibitory interneurons. *Neuron* 109, 1013–1028. doi: 10.1016/j.neuron.2021.01.014

Heiman, P., Drewes, S., and Ghaloul-Gonzalez, L. (2021). A familial case of CAMK2B mutation with variable expressivity. *SAGE Open Med. Case Rep.* 9:2050313X21990982. doi: 10.1177/2050313X21990982

Hell, J. W. (2014). CaMKII: claiming center stage in postsynaptic function and organization. *Neuron* 81, 249–265. doi: 10.1016/j.neuron.2013.12.024

Herring, B. E., and Nicoll, R. A. (2016). Long-term potentiation: from CaMKII to AMPA receptor trafficking. *Annu. Rev. Phys.* 78, 351–365. doi: 10.1146/annurev-physiol-021014-071753

Hinds, H. L., Goussakov, I., Nakazawa, K., Tonegawa, S., and Bolshakov, V. Y. (2003). Essential function of α-calcium/calmodulin-dependent protein kinase II in neurotransmitter release at a glutamatergic central synapse. *Proc. Natl. Acad. Sci.* 100, 4275–4280. doi: 10.1073/pnas.0530202100

Hinds, H. L., Tonegawa, S., and Malinow, R. (1998). CA1 long-term potentiation is diminished but present in hippocampal slices from α-CaMKII mutant mice. *Learn. Mem.* 5, 344–354. doi: 10.1101/lm.5.4.344

Hoelz, A., Nairn, A. C., and Kuriyan, J. (2003). Crystal structure of a tetradecameric assembly of the association domain of Ca2+/calmodulin-dependent kinase II. *Mole. Cell* 11, 1241–1251. doi: 10.1016/s1097-2765(03)00171-0

Hojjati, M. R., Van Woerden, G. M., Tyler, W. J., Giese, K. P., Silva, A. J., Pozzo-Miller, L., et al. (2007). Kinase activity is not required for αCaMKII-dependent presynaptic plasticity at CA3-CA1 synapses. *Nat. Neurosci.* 10, 1125–1127. doi: 10.1038/nn1946

Hosaka, M., Hammer, R. E., and Südhof, T. C. (1999). A phospho-switch controls the dynamic association of synapsins with synaptic vesicles. *Neuron* 24, 377–387. doi: 10.1016/s0896-6273(00)80851-x

Hosokawa, T., Liu, P. W., Cai, Q., Ferreira, J. S., Levet, F., Butler, C., et al. (2021). CaMKII activation persistently segregates postsynaptic proteins via liquid phase separation. *Nature Neurosci.* 24, 777–785. doi: 10.1038/s41593-021-00843-3

Hou, S. T., Jiang, S. X., Aylsworth, A., Ferguson, G., Slinn, J., Hu, H., et al. (2009). CaMKII phosphorylates collapsin response mediator protein 2 and modulates axonal damage during glutamate excitotoxicity. *J. Neurochem.* 111, 870–881. doi: 10.1111/j.1471-4159.2009.06375.x

Hudmon, A., and Schulman, H. (2002). Neuronal CA2+/calmodulin-dependent protein kinase II: the role of structure and autoregulation in cellular function. *Annu. Rev. Biochem.* 71, 473–510. doi: 10.1146/annurev.biochem.71.110601.135410

Hudmon, A., Schulman, H., Kim, J., Maltez, J. M., Tsien, R. W., and Pitt, G. S. (2005). CaMKII tethers to L-type Ca2+ channels, establishing a local and dedicated integrator of Ca2+ signals for facilitation. *J. Cell Biol.* 171, 537–547. doi: 10.1083/jcb.200505155

Inagaki, N., Goto, H., Ogawara, M., Nishi, Y., Ando, S., and Inagaki, M. (1997). Spatial patterns of Ca^{2+} signals define intracellular distribution of a signaling by Ca^{2+}/calmodulin-dependent protein kinase II. *J. Biol. Chem.* 272, 25195–25199. doi: 10.1074/jbc.272.40.25195

Iossifov, I., O'roak, B. J., Sanders, S. J., Ronemus, M., Krumm, N., Levy, D., et al. (2014). The contribution of de novo coding mutations to autism spectrum disorder. *Nature* 515, 216–221. doi: 10.1038/nature13908

Irvine, E. E., Danhiez, A., Radwanska, K., Nassim, C., Lucchesi, W., Godaux, E., et al. (2011). Properties of contextual memory formed in the absence of αCaMKII autophosphorylation. *Mole. Brain* 4, 1–10. doi: 10.1186/1756-6606-4-8

Irvine, E. E., Vernon, J., and Giese, K. P. (2005). αCaMKII autophosphorylation contributes to rapid learning but is not necessary for memory. *Nat. Neurosci.* 8, 411–412. doi: 10.1038/nn1431

Islam, R., Matsuzaki, K., Sumiyoshi, E., Hossain, M. E., Hashimoto, M., Katakura, M., et al. (2019). Theobromine improves working memory by activating the CaMKII/CREB/BDNF pathway in rats. *Nutrients* 11:888. doi: 10.3390/nu11040888

Iwama, K., Mizuguchi, T., Takeshita, E., Nakagawa, E., Okazaki, T., Nomura, Y., et al. (2019). Genetic landscape of Rett syndrome-like phenotypes revealed by whole exome sequencing. *J. Med. Genet.* 56, 396–407. doi: 10.1136/jmedgenet-2018-105775

Izumi, H., Kawahata, I., Shinoda, Y., Helmstetter, F. J., and Fukunaga, K. (2020). SAK3 administration improves spine abnormalities and cognitive deficits in appNL-GF/NL-GF knock-in mice by increasing proteasome activity through CaMKII/Rpt6 signalling. *Internat. J. Mole. Sci.* 21, 3833. doi: 10.3390/ijms21113833

Izumi, Y., and Zorumski, C. F. (1998). LTP in CA1 of the adult rat hippocampus and voltage-activated calcium channels. *Neurorep.* 9, 3689–3691. doi: 10.1097/00001756-199811160-00022

Jackson, A. C., and Nicoll, R. A. (2011). The expanding social network of ionotropic glutamate receptors: TARPs and other transmembrane auxiliary subunits. *Neuron* 70, 178–199. doi: 10.1016/j.neuron.2011.04.007

Jiang, H., Fang, J., Xing, J., Wang, L., Wang, Q., Wang, Y., et al. (2019). Tilianin mediates neuroprotection against ischemic injury by attenuating CaMKII-dependent mitochondrion-mediated apoptosis and MAPK/NF-κB signalling. *Life Sci.* 216, 233–245. doi: 10.1016/j.lfs.2018.11.035

Jiang, Y. H., and Ehlers, M. D. (2013). Modeling autism by SHANK gene mutations in mice. *Neuron* 78, 8–27. doi: 10.1016/j.neuron.2013.03.016

Job, C., and Eberwine, J. (2001). Localization and translation of mRNA in dentrites and axons. *Nat. Rev. Neurosci.* 2, 889–898. doi: 10.1038/35104069

Jontes, J. D., Buchanan, J., and Smith, S. J. (2000). Growth cone and dendrite dynamics in zebrafish embryos: early events in synaptogenesis imaged in vivo. *Nat. Neurosci.* 3, 231–237. doi: 10.1038/72936

Jontes, J. D., and Smith, S. J. (2000). Filopodia, spines, and the generation of synaptic diversity. *Neuron* 27, 11–14. doi: 10.1016/s0896-6273(00)00003-9

Kee, N., Teixeira, C. M., Wang, A. H., and Frankland, P. W. (2007). Preferential incorporation of adult-generated granule cells into spatial memory networks in the dentate gyrus. *Nat. Neurosci.* 10, 355–362. doi: 10.1038/nn1847

Khan, S., Downing, K. H., and Molloy, J. E. (2019). Architectural dynamics of CaMKII-actin networks. *Biophys. J.* 116, 104–119. doi: 10.1016/j.bpj.2018.11.006

Kim, K., Lakhanpal, G., Lu, H. E., Khan, M., Suzuki, A., Hayashi, M. K., et al. (2015). A temporary gating of actin remodeling during synaptic plasticity consists of the interplay between the kinase and structural functions of CaMKII. *Neuron* 87, 813–826. doi: 10.1016/j.neuron.2015.07.023

Kim, K., Suzuki, A., Kojima, H., Kawamura, M., Miya, K., Abe, M., et al. (2019). Autophosphorylation of F-actin binding domain of CaMKIIβ is required for fear learning. *Neurobiol. Learn. Memory* 157, 86–95. doi: 10.1016/j.nlm.2018.12.003

Kirkwood, A., Silva, A., and Bear, M. F. (1997). Age-dependent decrease of synaptic plasticity in the neocortex of αCaMKII mutant mice. *Proc. Natl. Acad. Sci.* 94, 3380–3383. doi: 10.1073/pnas.94.7.3380

Klann, E., and Dever, T. E. (2004). Biochemical mechanisms for translational regulation in synaptic plasticity. *Nat. Rev. Neurosci.* 5, 931–942. doi: 10.1038/nrn1557

Klug, J. R., Mathur, B. N., Kash, T. L., Wang, H. D., Matthews, R. T., Robison, A. J., et al. (2012). Genetic inhibition of CaMKII in dorsal striatal medium spiny neurons reduces functional excitatory synapses and enhances intrinsic excitability. *PLoS One* 7:e45323. doi: 10.1371/journal.pone.0045323

Kochan, L. D., Churn, S. B., Omojokun, O., Rice, A., and DeLorenzo, R. J. (1999). Status epilepticus results in an N-methyl-D-aspartate receptor-dependent inhibition of Ca2+/calmodulin-dependent kinase II activity in the rat. *Neuroscience* 95, 735–743. doi: 10.1016/s0306-4522(99)00462-5

Koh, Y. H., Popova, E., Thomas, U., Griffith, L. C., and Budnik, V. (1999). Regulation of DLG localization at synapses by CaMKII-dependent phosphorylation. *Cell* 98, 353–363. doi: 10.1016/s0092-8674(00)81964-9

Kojima, H., Rosendale, M., Sugiyama, Y., Hayashi, M., Horiguchi, Y., Yoshihara, T., et al. (2019). The role of CaMKII-Tiam1 complex on learning and memory. *Neurobiol. Learn. Memory* 166:107070. doi: 10.1016/j.nlm.2019.107070

Kool, M. J., Onori, M. P., Borgesius, N. Z., van de Bree, J. E., Elgersma-Hooisma, M., Nio, E., et al. (2019). CAMK2-dependent signaling in neurons is essential for survival. *J. Neurosci.* 39, 5424–5439. doi: 10.1523/JNEUROSCI.1341-18.2019

Kool, M. J., Van De Bree, J. E., Bodde, H. E., Elgersma, Y., and van Woerden, G. M. (2016). The molecular, temporal and region-specific requirements of the beta isoform of Calcium/Calmodulin-dependent protein kinase type 2 (CAMK2B) in mouse locomotion. *Scientif. Rep.* 6, 1–12. doi: 10.1038/srep26989

Korte, M., Carroll, P., Wolf, E., Brem, G., Thoenen, H., and Bonhoeffer, T. (1995). Hippocampal long-term potentiation is impaired in mice lacking brain-derived neurotrophic factor. *Proc. Natl. Acad. Sci.* 92, 8856–8860. doi: 10.1073/pnas.92.19.8856

Koutsokera, M., Kafkalias, P., Giompres, P., Kouvelas, E. D., and Mitsacos, A. (2014). Expression and phosphorylation of glutamate receptor subunits and CaMKII in a mouse model of Parkinsonism. *Brain Res.* 1549, 22–31. doi: 10.1016/j.brainres.2013.12.023

Krapivinsky, G., Medina, I., Krapivinsky, L., Gapon, S., and Clapham, D. E. (2004). SynGAP-MUPP1-CaMKII synaptic complexes regulate p38 MAP kinase activity and NMDA receptor-dependent synaptic AMPA receptor potentiation. *Neuron* 43, 563–574. doi: 10.1016/j.neuron.2004.08.003

Kumar, M., John, M., Madhavan, M., James, J., and Omkumar, R. V. (2019). Alteration in the phosphorylation status of NMDA receptor GluN2B subunit by activation of both NMDA receptor and L-type voltage gated calcium channel. *Neurosci. Lett.* 709:134343. doi: 10.1016/j.neulet.2019.134343

Küry, S., van Woerden, G. M., Besnard, T., Onori, M. P., Latypova, X., Towne, M. C., et al. (2017). De novo mutations in protein kinase genes CAMK2A and CAMK2B cause intellectual disability. *Am. J. Hum. Genet.* 101, 768–788. doi: 10.1016/j.ajhg.2017.10.003

Lamsa, K., Irvine, E. E., Giese, K. P., and Kullmann, D. M. (2007). NMDA receptor-dependent long-term potentiation in mouse hippocampal interneurons shows a unique dependence on Ca2+/calmodulin-dependent kinases. *J. Phys.* 584, 885–894. doi: 10.1113/jphysiol.2007.137380

Lee, L. C., Su, M. T., Huang, H. Y., Cho, Y. C., Yeh, T. K., and Chang, C. Y. (2021). Association of CaMK2A and MeCP2 signaling pathways with cognitive ability in adolescents. *Mole. Brain* 14, 1–14. doi: 10.1186/s13041-021-00858-8

Lee, M. C., Ban, S. S., Woo, Y. J., and Kim, S. U. (2001). Calcium/calmodulin kinase II activity of hippocampus in kainate-induced epilepsy. *J. Korean Med. Sci.* 16, 643–648. doi: 10.3346/jkms.2001.16.5.643

Leonard, A. S., Bayer, K. U., Merrill, M. A., Lim, I. A., Shea, M. A., Schulman, H., et al. (2002). Regulation of calcium/calmodulin-dependent protein Kinase II docking toN-Methyl-d-aspartate receptors by calcium/calmodulin and α-actinin. *J. Biol. Chem.* 277, 48441–48448. doi: 10.1074/jbc.M205164200

Leonard, A. S., Lim, I. A., Hemsworth, D. E., Horne, M. C., and Hell, J. W. (1999). Calcium/calmodulin-dependent protein kinase II is associated with the N-methyl-D-aspartate receptor. *Proc. Natl. Acad. Sci.* 96, 3239–3244. doi: 10.1073/pnas.96.6.3239

Leurs, U., Klein, A. B., McSpadden, E. D., Griem-Krey, N., Solbak, S. M., Houlton, J., et al. (2021). GHB analogs confer neuroprotection through specific interaction with the CaMKIIα hub domain. *Proc. Natl. Acad. Sci.* 118:31. doi: 10.1073/pnas.2108079118

Levine, E. S., Crozier, R. A., Black, I. B., and Plummer, M. R. (1998). Brain-derived neurotrophic factor modulates hippocampal synaptic transmission by increasing N-methyl-D-aspartic acid receptor activity. *Proc. Natl. Acad. Sci.* 95, 10235–10239. doi: 10.1073/pnas.95.17.10235

Levine, E. S,., Dreyfus, C. F., Black, I. B., and Plummer, M. R. (1995). Brain-derived neurotrophic factor rapidly enhances synaptic transmission in hippocampal

neurons via postsynaptic tyrosine kinase receptors. *Proc. Natl. Acad. Sci.* 92, 8074–8077. doi: 10.1073/pnas.92.17.8074

Li, K. W., Miller, S., Klychnikov, O., Loos, M., Stahl-Zeng, J., Spijker, S., et al. (2007). Quantitative proteomics and protein network analysis of hippocampal synapses of CaMKIIα mutant mice. *J. Prot. Res.* 6, 3127–3133. doi: 10.1021/pr070086w

Lisman, J., and Raghavachari, S. (2015). Biochemical principles underlying the stable maintenance of LTP by the CaMKII/NMDAR complex. *Brain Res.* 1621, 51–61. doi: 10.1016/j.brainres.2014.12.010

Lisman, J., Schulman, H., and Cline, H. (2002). The molecular basis of CaMKII function in synaptic and behavioural memory. *Nat. Rev. Neurosci.* 3, 175–190. doi: 10.1038/nrn753

Lisman, J., Yasuda, R., and Raghavachari, S. (2012). Mechanisms of CaMKII action in long-term potentiation. *Nat. Rev. Neurosci.* 13, 169–182. doi: 10.1038/nrn3192

Lisman, J. E., and Harris, K. M. (1993). Quantal analysis and synaptic anatomy—integrating two views of hippocampal plasticity. *Trends Neurosci.* 16, 141–147. doi: 10.1016/0166-2236(93)90122-3

Lisman, J. E., and Zhabotinsky, A. M. (2001). A model of synaptic memory: a CaMKII/PP1 switch that potentiates transmission by organizing an AMPA receptor anchoring assembly. *Neuron* 31, 191–201. doi: 10.1016/s0896-6273(01)00364-6

Liu, W., Jiang, X., Zu, Y., Yang, Y., Liu, Y., Sun, X., et al. (2020). A comprehensive description of GluN2B-selective N-methyl-D-aspartate (n.d.) receptor antagonists. *Eur. Opean J. Med. Chem.* 200:112447. doi: 10.1016/j.ejmech.2020.112447

Liu, X., Qiu, J., Alcon, S., Hashim, J., Meehan, W. P. III, and Mannix, R. (2017). Environmental enrichment mitigates deficits after repetitive mild traumatic brain injury. *J. Neurotr.* 34, 2445–2455. doi: 10.1089/neu.2016.4823

Liu, X., Zhan, Z., Xu, L., Ma, F., Li, D., Guo, Z., et al. (2010). MicroRNA-148/152 impair innate response and antigen presentation of TLR-triggered dendritic cells by targeting CaMKIIα. *J. Immunol.* 185, 7244–7251. doi: 10.4049/jimmunol.1001573

Liu, Z., Xu, J., Shen, X., Lv, C., Xu, T., and Pei, D. (2012). CaMKII antisense oligodeoxynucleotides protect against ischemia-induced neuronal death in the rat hippocampus. *J. Neurol. Sci.* 314, 104–110. doi: 10.1016/j.jns.2011.10.012

Lu, W., Isozaki, K., Roche, K. W., and Nicoll, R. A. (2010). Synaptic targeting of AMPA receptors is regulated by a CaMKII site in the first intracellular loop of GluA1. *Proc. Natl. Acad. Sci.* 107, 22266–22271. doi: 10.1073/pnas.1016289107

Lue, L. F., Kuo, Y. M., Roher, A. E., Brachova, L., Shen, Y., Sue, L., et al. (1999). Soluble amyloid β peptide concentration as a predictor of synaptic change in Alzheimer's disease. *Am. J. Pathol.* 155, 853–862. doi: 10.1016/s0002-9440(10)65184-x

Ly, P. T., and Song, W. (2011). Loss of activated CaMKII at the synapse underlies Alzheimer's disease memory loss. *J. Neurochem.* 119, 673–675. doi: 10.1111/j.1471-4159.2011.07473.x

Ma, H., Groth, R. D., Cohen, S. M., Emery, J. F., Li, B., Hoedt, E., et al. (2014). γCaMKII shuttles Ca2+/CaM to the nucleus to trigger CREB phosphorylation and gene expression. *Cell* 159, 281–294. doi: 10.1016/j.cell.2014.09.019

MacDonald, J. F., Jackson, M. F., and Beazely, M. A. (2006). Hippocampal long-term synaptic plasticity and signal amplification of NMDA receptors. *Crit. Rev. Neurob.* 18, 1–2. doi: 10.1615/critrevneurobiol.v18.i1-2.80

Madhavan, M., Mohanan, A. G., Jacob, R. S., Gunasekaran, S., Nair, R. R., and Omkumar, R. V. (2020). Glu60 of α-Calcium/calmodulin dependent protein kinase II mediates crosstalk between the regulatory T-site and protein substrate binding region of the active site. *Archiv. Biochem. Biophys.* 685:108348. doi: 10.1016/j.abb.2020.108348

Malenka, R. C., Kauer, J. A., Perkel, D. J., Mauk, M. D., Kelly, P. T., Nicoll, R. A., et al. (1989). An essential role for postsynaptic calmodulin and protein kinase activity in long-term potentiation. *Nature* 340, 554–557. doi: 10.1038/340554a0

Malenka, R. C., and Nicoll, R. A. (1999). Long-term potentiation–a decade of progress? *Science* 285, 1870–1874. doi: 10.1126/science.285.5435.1870

Malinow, R., Schulman, H., and Tsien, R. W. (1989). Inhibition of postsynaptic PKC or CaMKII blocks induction but not expression of LTP. *Science* 245, 862–866. doi: 10.1126/science.2549638

Marin, P., Nastiuk, K. L., Daniel, N., Girault, J. A., Czernik, A. J., Glowinski, J., et al. (1997). Glutamate-dependent phosphorylation of elongation factor-2 and inhibition of protein synthesis in neurons. *J. Neurosci.* 17, 3445–3454. doi: 10.1523/JNEUROSCI.17-10-03445.1997

Masliah, E., Mallory, M., Alford, M., DeTeresa, R., Hansen, L. A., and McKeel, D. W. (2001). Altered expression of synaptic proteins occurs early during progression of Alzheimer's disease. *Neurology* 56, 127–129. doi: 10.1212/wnl.56.1.127

Matsumoto, S., Murozono, M., Nagaoka, D., Matsuoka, S., Takeda, A., Narita, H., et al. (2008). Isoflurane Inhibits Protein Kinase Cγ and Calcium/Calmodulin Dependent Protein Kinase II-α Translocation to Synaptic Membranes in Ischemic Mice Brains. *Neurochem. Res.* 33, 2302–2309. doi: 10.1007/s11064-008-9727-4

Matsumoto, S., Shamloo, M., Isshiki, A., and Wieloch, T. (2002). Persistent phosphorylation of synaptic proteins following middle cerebral artery occlusion. *J. Cereb. Blood Flow Metab.* 22, 1107–1113. doi: 10.1097/00004647-200209000-00008

Matsumoto, S., Shamloo, M., Matsumoto, E., Isshiki, A., and Wieloch, T. (2004). Protein kinase C-γ and calcium/calmodulin-dependent protein kinase II-α are persistently translocated to cell membranes of the rat brain during and after middle cerebral artery occlusion. *J. Cereb. Blood Flow Metab.* 24, 54–61. doi: 10.1097/01.WCB.0000095920.70924.F5

Matsumoto, Y., Morinobu, S., Yamamoto, S., Matsumoto, T., Takei, S., Fujita, Y., et al. (2013). Vorinostat ameliorates impaired fear extinction possibly via the hippocampal NMDA-CaMKII pathway in an animal model of posttraumatic stress disorder. *Psychopharmacology* 229, 51–62. doi: 10.1007/s00213-013-3078-9

Matsuo, N., Yamasaki, N., Ohira, K., Takao, K., Toyama, K., Eguchi, M., et al. (2009). Neural activity changes underlying the working memory deficit in alpha-CaMKII heterozygous knockout mice. *Front. Behav. Neurosci.* 3:20. doi: 10.3389/neuro.08.020.2009

Matsuzaki, M., Ellis-Davies, G. C., Nemoto, T., Miyashita, Y., Iino, M., and Kasai, H. (2001). Dendritic spine geometry is critical for AMPA receptor expression in hippocampal CA1 pyramidal neurons. *Nat. Neurosci.* 4, 1086–1092. doi: 10.1038/nn736

Matsuzaki, M., Honkura, N., Ellis-Davies, G. C., and Kasai, H. (2004). Structural basis of long-term potentiation in single dendritic spines. *Nature* 429, 761–766. doi: 10.1038/nature02617

Mauceri, D., Cattabeni, F., Di Luca, M., and Gardoni, F. (2004). Calcium/calmodulin-dependent protein kinase II phosphorylation drives synapse-associated protein 97 into spines. *J. Biol. Chem.* 279, 23813–23821. doi: 10.1074/jbc.M402796200

Mayadevi, M., Lakshmi, K., Suma Priya, S. D., John, S., and Omkumar, R. V. (2016). Protection of α-CaMKII from dephosphorylation by GluN2B subunit of NMDA receptor is abolished by mutation of Glu96 or His282 of α-CaMKII. *PLoS One* 11:e0162011. doi: 10.1371/journal.pone.0162011

Mayadevi, M., Praseeda, M., Kumar, K. S., and Omkumar, R. V. (2002). Sequence determinants on the NR2A and NR2B subunits of NMDA receptor responsible for specificity of phosphorylation by CaMKII. *Biochimica et Biophysica Acta* 1598, 40–45. doi: 10.1016/s0167-4838(02)00315-1

Mayadevi, M., Sherin, D. R., Keerthi, V. S., Rajasekharan, K. N., and Omkumar, R. V. (2012). Curcumin is an inhibitor of calcium/calmodulin dependent protein kinase II. *Bioorg. Med. Chem.* 20, 6040–6047. doi: 10.1016/j.bmc.2012.08.029

Mayford, M., Bach, M. E., Huang, Y. Y., Wang, L., Hawkins, R. D., and Kandel, E. R. (1996). Control of memory formation through regulated expression of a CaMKII transgene. *Science* 274, 1678–1683. doi: 10.1126/science.274.5293.1678

Mayford, M., Wang, J., Kandel, E. R., and O'Dell, T. J. (1995). CaMKII regulates the frequency-response function of hippocampal synapses for the production of both LTD and LTP. *Cell* 81, 891–904. doi: 10.1016/0092-8674(95)90009-8

McGlade-McCulloh, E., Yamamoto, H., Tan, S. E., Brickey, D. A., and Soderling, T. R. (1993). Phosphorylation and regulation of glutamate receptors by calcium/calmodulin-dependent protein kinase II. *Nature* 362, 640–642. doi: 10.1038/362640a0

Melville, Z., Hernández-Ochoa, E. O., Pratt, S. J., Liu, Y., Pierce, A. D., Wilder, P. T., et al. (2017). The activation of protein kinase A by the calcium-binding protein S100A1 is independent of cyclic AMP. *Biochemistry* 56, 2328–2337. doi: 10.1021/acs.biochem.7b00117

Meng, F., Guo, J., Zhang, Q., Song, B., and Zhang, G. (2003). Autophosphorylated calcium/calmodulin-dependent protein kinase IIα (CaMKIIα) reversibly targets to and phosphorylates N-methyl-D-aspartate receptor subunit 2B

(NR2B) in cerebral ischemia and reperfusion in hippocampus of rats. *Brain Res.* 967, 161–169. doi: 10.1016/s0006-8993(02)04267-1

Meng, F., and Zhang, G. (2002). Autophosphorylated calcium/calmodulin-dependent protein kinase II α induced by cerebral ischemia immediately targets and phosphorylates N-methyl-D-aspartate receptor subunit 2B (NR2B) in hippocampus of rats. *Neurosci. Lett.* 333, 59–63. doi: 10.1016/s0304-3940(02)00961-8

Michalski, P. J. (2013). The delicate bistability of CaMKII. *Biophys. J.* 105, 794–806. doi: 10.1016/j.bpj.2013.06.038

Micheva, K. D., Busse, B., Weiler, N. C., O'Rourke, N., and Smith, S. J. (2010). Single-synapse analysis of a diverse synapse population: proteomic imaging methods and markers. *Neuron* 68, 639–653. doi: 10.1016/j.neuron.2010.09.024

Migues, P. V., Lehmann, I. T., Fluechter, L., Cammarota, M., Gurd, J. W., Sim, A. T., et al. (2006). Phosphorylation of CaMKII at Thr253 occurs in vivo and enhances binding to isolated postsynaptic densities. *J. Neurochem.* 98, 289–299. doi: 10.1111/j.1471-4159.2006.03876.x

Miller, P., Zhabotinsky, A. M., Lisman, J. E., and Wang, X. J. (2005). The stability of a stochastic CaMKII switch: dependence on the number of enzyme molecules and protein turnover. *PLoS Biol.* 3:e107. doi: 10.1371/journal.pbio.0030107

Miller, S., Yasuda, M., Coats, J. K., Jones, Y., Martone, M. E., and Mayford, M. (2002). Disruption of dendritic translation of CaMKIIα impairs stabilization of synaptic plasticity and memory consolidation. *Neuron* 36, 507–519. doi: 10.1016/s0896-6273(02)00978-9

Miller, S. G., and Kennedy, M. B. (1985). Distinct forebrain and cerebellar isozymes of type II Ca2+/calmodulin-dependent protein kinase associate differently with the postsynaptic density fraction. *J. Biol. Chem.* 260, 9039–9046. doi: 10.1016/s0021-9258(17)39454-1

Miller, S. G., and Kennedy, M. B. (1986). Regulation of brain Type II Ca2+ calmodulin-dependent protein kinase by autophosphorylation: a Ca2+-triggered molecular switch. *Cell* 44, 861–870. doi: 10.1016/0092-8674(86)90008-5

Moldave, K. (1985). Eukaryotic protein synthesis. *Ann. Rev. Biochem.* 54, 1109–1149.

Molloy, S. S., and Kennedy, M. B. (1991). Autophosphorylation of type II Ca2+/calmodulin-dependent protein kinase in cultures of postnatal rat hippocampal slices. *Proc. Natl. Acad. Sci.* 88, 4756–4760. doi: 10.1073/pnas.88.11.4756

Moosmang, S., Haider, N., Klugbauer, N., Adelsberger, H., Langwieser, N., Müller, J., et al. (2005). Role of hippocampal Cav1. 2 Ca2+ channels in NMDA receptor-independent synaptic plasticity and spatial memory. *J. Neurosci.* 25, 9883–9892. doi: 10.1523/JNEUROSCI.1531-05.2005

Moretto, E., Murru, L., Martano, G., Sassone, J., and Passafaro, M. (2018). Glutamatergic synapses in neurodevelopmental disorders. *Prog. Neuro-Psychopharm. Biol. Psych.* 84, 328–342. doi: 10.1016/j.pnpbp.2017.09.014

Mori, Y., Imaizumi, K., Katayama, T., Yoneda, T., and Tohyama, M. (2000). Two cis-acting elements in the 3′ untranslated region of α-CaMKII regulate its dendritic targeting. *Nat. Neurosci.* 3, 1079–1084. doi: 10.1038/80591

Moriguchi, S., Shioda, N., Yamamoto, Y., Tagashira, H., and Fukunaga, K. (2012a). The T-type voltage-gated calcium channel as a molecular target of the novel cognitive enhancer ST101: enhancement of long-term potentiation and CaMKII autophosphorylation in rat cortical slices. *J. Neurochem.* 121, 44–53. doi: 10.1111/j.1471-4159.2012.07667.x

Moriguchi, S., Yabuki, Y., and Fukunaga, K. (2012b). Reduced calcium/calmodulin-dependent protein kinase II activity in the hippocampus is associated with impaired cognitive function in MPTP-treated mice. *J. Neurochem.* 120, 541–551. doi: 10.1111/j.1471-4159.2011.07608.x

Moro, A., Van Woerden, G. M., Toonen, R. F., and Verhage, M. (2020). CaMKII controls neuromodulation via neuropeptide gene expression and axonal targeting of neuropeptide vesicles. *PLoS biol.* 18:e3000826. doi: 10.1371/journal.pbio.3000826

Mullasseril, P., Dosemeci, A., Lisman, J. E., and Griffith, L. C. (2007). A structural mechanism for maintaining the 'on-state'of the CaMKII memory switch in the post-synaptic density. *J. Neurochem.* 103, 357–364. doi: 10.1111/j.1471-4159.2007.04744.x

Murray, K. D., Isackson, P. J., and Jones, E. G. (2003). N-methyl-D-aspartate receptor-dependent transcriptional regulation of two calcium/calmodulin-dependent protein kinase type II isoforms in rodent cerebral cortex. *Neuroscience* 122, 407–420. doi: 10.1016/j.neuroscience.2003.07.015

Myers, J. B., Zaegel, V., Coultrap, S. J., Miller, A. P., Bayer, K. U., and Reichow, S. L. (2017). The CaMKII holoenzyme structure in activation-competent conformations. *Nat. Comm.* 8, 1–15.

Nakahara, S., Miyake, S., Tajinda, K., and Ito, H. (2015). Mossy fiber mis-pathfinding and semaphorin reduction in the hippocampus of α-CaMKII hKO mice. *Neurosci. Lett.* 598, 47–51. doi: 10.1016/j.neulet.2015.05.012

Näslund, J., Haroutunian, V., Mohs, R., Davis, K. L., Davies, P., Greengard, P., et al. (2000). Correlation between elevated levels of amyloid β-peptide in the brain and cognitive decline. *Jama* 283, 1571–1577. doi: 10.1001/jama.283.12.1571

Nassal, D., Gratz, D., and Hund, T. J. (2020). Challenges and opportunities for therapeutic targeting of calmodulin kinase II in heart. *Front. Pharm.* 11:35. doi: 10.3389/fphar.2020.00035

Need, A. C., and Giese, K. P. (2003). Handling and environmental enrichment do not rescue learning and memory impairments in αCamKIIT286A mutant mice. *Genes Brain Behav.* 2, 132–139. doi: 10.1034/j.1601-183x.2003.00020.x

Nesler, K. R., Sand, R. I., Symmes, B. A., Pradhan, S. J., Boin, N. G., Laun, A. E., et al. (2013). The miRNA pathway controls rapid changes in activity-dependent synaptic structure at the Drosophila melanogaster neuromuscular junction. *PLoS One* 8:e68385. doi: 10.1371/journal.pone.0068385

Nesler, K. R., Starke, E. L., Boin, N. G., Ritz, M., and Barbee, S. A. (2016). Presynaptic CamKII regulates activity-dependent axon terminal growth. *Mole. Cell. Neurosci.* 76, 33–41. doi: 10.1016/j.mcn.2016.08.007

Nicole, O., and Pacary, E. (2020). Camkiiβ in neuronal development and plasticity: an emerging candidate in brain diseases. *Internat. J. Mole. Sci.* 21:7272. doi: 10.3390/ijms21197272

Nikandrova, Y. A., Jiao, Y., Baucum, A. J., Tavalin, S. J., and Colbran, R. J. (2010). Ca2+/calmodulin-dependent protein kinase II binds to and phosphorylates a specific SAP97 splice variant to disrupt association with AKAP79/150 and modulate α-amino-3-hydroxy-5-methyl-4-isoxazolepropionic acid-type glutamate receptor (AMPAR) activity. *J. Biol. Chem.* 285, 923–934. doi: 10.1074/jbc.M109.033985

Oh, J. S., Manzerra, P., and Kennedy, M. B. (2004). Regulation of the neuron-specific Ras GTPase-activating protein, synGAP, by Ca^{2+}/calmodulin-dependent protein kinase II. *J. Biol. Chem.* 279, 17980–17988. doi: 10.1074/jbc.M314109200

Omkumar, R. V., Kiely, M. J., Rosenstein, A. J., Min, K. T., and Kennedy, M. B. (1996). Identification of a phosphorylation site for calcium/calmodulin dependent protein kinase II in the NR2B subunit of the N-methyl-D-aspartate receptor. *J. Biol. Chem.* 271, 31670–31678. doi: 10.1074/jbc.271.49.31670

Onori, M. P., and van Woerden, G. M. (2021). Role of calcium/calmodulin-dependent kinase 2 in neurodevelopmental disorders. *Brain Res. Bull.* 171, 209–220. doi: 10.1016/j.brainresbull.2021.03.014

Opazo, P., da Silva, S. V., Carta, M., Breillat, C., Coultrap, S. J., Grillo-Bosch, D., et al. (2018). CaMKII metaplasticity drives Aβ oligomer-mediated synaptotoxicity. *Cell Rep.* 23, 3137–3145. doi: 10.1016/j.celrep.2018.05.036

Opazo, P., Labrecque, S., Tigaret, C. M., Frouin, A., Wiseman, P. W., De Koninck, P., et al. (2010). CaMKII triggers the diffusional trapping of surface AMPARs through phosphorylation of stargazin. *Neuron* 67, 239–252. doi: 10.1016/j.neuron.2010.06.007

Ortuño-Sahagún, D., Rivera-Cervantes, M. C., Gudiño-Cabrera, G., Junyent, F., Verdaguer, E., Auladell, C., et al. (2012). Microarray analysis of rat hippocampus exposed to excitotoxicity: reversal Na+/Ca2+ exchanger NCX3 is overexpressed in glial cells. *Hippocampus* 22, 128–140. doi: 10.1002/hipo.20869

Otmakhov, N., Gorbacheva, E. V., Regmi, S., Yasuda, R., Hudmon, A., and Lisman, J. (2015). Excitotoxic insult results in a long-lasting activation of CaMKIIα and mitochondrial damage in living hippocampal neurons. *PLoS One* 10:e0120881. doi: 10.1371/journal.pone.0120881

Ouyang, Y., Kantor, D., Harris, K. M., Schuman, E. M., and Kennedy, M. B. (1997). Visualization of the distribution of autophosphorylated calcium/calmodulin-dependent protein kinase II after tetanic stimulation in the CA1 area of the hippocampus. *J. Neurosci.* 17, 5416–5427. doi: 10.1523/JNEUROSCI.17-14-05416.1997

Ouyang, Y., Rosenstein, A., Kreiman, G., Schuman, E. M., and Kennedy, M. B. (1999). Tetanic stimulation leads to increased accumulation of Ca2+/calmodulin-dependent protein kinase II via dendritic protein synthesis in hippocampal neurons. *J. Neurosci.* 19, 7823–7833. doi: 10.1523/JNEUROSCI.19-18-07823.1999

Paillé, V., Picconi, B., Bagetta, V., Ghiglieri, V., Sgobio, C., Di Filippo, M., et al. (2010). Distinct levels of dopamine denervation differentially alter striatal synaptic plasticity and NMDA receptor subunit composition. *J. Neurosci.* 30, 14182–14193. doi: 10.1523/JNEUROSCI.2149-10.2010

Pan, Y., Chen, J., Guo, H., Ou, J., Peng, Y., Liu, Q., et al. (2015). Association of genetic variants of GRIN2B with autism. *Sci. Rep.* 5, 1–5. doi: 10.1038/srep08296

Park, J., Chávez, A. E., Mineur, Y. S., Morimoto-Tomita, M., Lutzu, S., Kim, K. S., et al. (2016). CaMKII phosphorylation of TARPγ-8 is a mediator of LTP and learning and memory. *Neuron* 92, 75–83. doi: 10.1016/j.neuron.2016.09.002

Patel, H., and Zamani, R. (2021). The role of PKMζ in the maintenance of long-term memory: a review. *Rev. Neurosci.* 32, 481–494. doi: 10.1515/revneuro-2020-0105

Patriarchi, T., Buonarati, O. R., and Hell, J. W. (2018). Postsynaptic localization and regulation of AMPA receptors and Cav1. 2 by β2 adrenergic receptor/PKA and Ca2+/CaMKII signaling. *EMBO J.* 37:e99771. doi: 10.15252/embj.201899771

Patterson, S. L., Abel, T., Deuel, T. A., Martin, K. C., Rose, J. C., and Kandel, E. R. (1996). Recombinant BDNF rescues deficits in basal synaptic transmission and hippocampal LTP in BDNF knockout mice. *Neuron* 16, 1137–1145. doi: 10.1016/s0896-6273(00)80140-3

Penny, C. J., and Gold, M. G. (2018). Mechanisms for localising calcineurin and CaMKII in dendritic spines. *Cell. Signal.* 49, 46–58. doi: 10.1016/j.cellsig.2018.05.010

Pi, H. J., Otmakhov, N., El Gaamouch, F., Lemelin, D., De Koninck, P., and Lisman, J. (2010). CaMKII control of spine size and synaptic strength: role of phosphorylation states and nonenzymatic action. *Proc. Natl. Acad. Sci.* 107, 14437–14442. doi: 10.1073/pnas.1009268107

Picconi, B., Gardoni, F., Centonze, D., Mauceri, D., Cenci, M. A., Bernardi, G., et al. (2004). Abnormal Ca2+-calmodulin-dependent protein kinase II function mediates synaptic and motor deficits in experimental parkinsonism. *J. Neurosci.* 24, 5283–5291. doi: 10.1523/JNEUROSCI.1224-04.2004

Pinto, T. M., Schilstra, M. J., Roque, A. C., and Steuber, V. (2020). Binding of Filamentous Actin to CaMKII as Potential Regulation Mechanism of Bidirectional Synaptic Plasticity by β CaMKII in Cerebellar Purkinje Cells. *Sci. Rep.* 10, 1–16. doi: 10.1038/s41598-020-65870-9

Poo, M. M. (2001). Neurotrophins as synaptic modulators. *Nat. Rev. Neurosci.* 2, 24–32. doi: 10.1038/35049004

Pöschel, B., and Manahan-Vaughan, D. (2007). Persistent (> 24 h) long-term depression in the dentate gyrus of freely moving rats is not dependent on activation of NMDA receptors, L-type voltage-gated calcium channels or protein synthesis. *Neuropharmacology* 52, 46–54. doi: 10.1016/j.neuropharm.2006.07.019

Pozzo-Miller, L. D., Gottschalk, W., Zhang, L., McDermott, K., Du, J., Gopalakrishnan, R., et al. (1999). Impairments in high-frequency transmission, synaptic vesicle docking, and synaptic protein distribution in the hippocampus of BDNF knockout mice. *J. Neurosci.* 19, 4972–4983. doi: 10.1523/JNEUROSCI.19-12-04972.1999

Pradeep, K. K., Cheriyan, J., Suma Priya, S. D., Rajeevkumar, R., Mayadevi, M., Praseeda, M., et al. (2009). Regulation of Ca2+/calmodulin-dependent protein kinase II catalysis by N-methyl-D-aspartate receptor subunit 2B. *Biochem. J.* 419, 123–136. doi: 10.1042/BJ20081707

Proietti Onori, M., Koopal, B., Everman, D. B., Worthington, J. D., Jones, J. R., Ploeg, M. A., et al. (2018). The intellectual disability-associated CAMK2G p. Arg292Pro mutation acts as a pathogenic gain-of-function. *Hum. Mutat.* 39, 2008–2024. doi: 10.1002/humu.23647

Puram, S. V., Kim, A. H., Ikeuchi, Y., Wilson-Grady, J. T., Merdes, A., Gygi, S. P., et al. (2011). A CaMKIIβ signaling pathway at the centrosome regulates dendrite patterning in the brain. *Nat. Neurosci.* 14, 973–983. doi: 10.1038/nn.2857

Qu, J., Mei, Q., and Niu, R. (2019). Oxidative CaMKII as a potential target for inflammatory disease. *Mole. Med. Rep.* 20, 863–870. doi: 10.3892/mmr.2019.10309

Radwanska, K., Medvedev, N. I., Pereira, G. S., Engmann, O., Thiede, N., Moraes, M. F., et al. (2011). Mechanism for long-term memory formation when synaptic strengthening is impaired. *Proc. Natl. Acad. Sci.* 108, 18471–18475. doi: 10.1073/pnas.1109680108

Ramya, R. P., Priya, S. S., Mayadevi, M., and Omkumar, R. V. (2012). Regulation of phosphorylation at Ser1303 of GluN2B receptor in the postsynaptic density. *Neurochem. Internat.* 61, 981–985. doi: 10.1016/j.neuint.2012.08.016

Raveendran, R., Devi Suma, Priya, S., Mayadevi, M., Steephan, M., Santhoshkumar, T. R., et al. (2009). Phosphorylation status of the NR2B subunit of NMDA receptor regulates its interaction with calcium/calmodulin-dependent protein kinase II. *J. Neurochem.* 110, 92–105. doi: 10.1111/j.1471-4159.2009.06108.x

Rhein, C., Mühle, C., Lenz, B., Richter-Schmidinger, T., Kogias, G., Boix, F., et al. (2020). Association of a CAMK2A genetic variant with logical memory performance and hippocampal volume in the elderly. *Brain Res. Bull.* 161, 13–20. doi: 10.1016/j.brainresbull.2020.05.001

Rich, R. C., and Schulman, H. (1998). Substrate-directed function of calmodulin in autophosphorylation of Ca2+/calmodulin-dependent protein kinase II. *J. Biol. Chem.* 273, 28424–28429. doi: 10.1074/jbc.273.43.28424

Rizzi, S., Spagnoli, C., Salerno, G. G., Frattini, D., Caraffi, S. G., Trimarchi, G., et al. (2020). Severe intellectual disability, absence of language, epilepsy, microcephaly and progressive cerebellar atrophy related to the recurrent de novo variant p.(P139L) of the CAMK2B gene: a case report and brief review. *Am. J. Med. Genet. Part A* 182, 2675–2679. doi: 10.1002/ajmg.a.61803

Robison, A. J. (2014). Emerging role of CaMKII in neuropsychiatric disease. *Trends Neurosci.* 37, 653–662. doi: 10.1016/j.tins.2014.07.001

Robison, A. J., Bass, M. A., Jiao, Y., MacMillan, L. B., Carmody, L. C., Bartlett, R. K., et al. (2005). Multivalent interactions of calcium/calmodulin-dependent protein kinase II with the postsynaptic density proteins NR2B, densin-180, and α-actinin-2. *J. Biol. Chem.* 280, 35329–35336. doi: 10.1074/jbc.M502191200

Rongo, C., and Kaplan, J. M. (1999). CaMKII regulates the density of central glutamatergic synapses in vivo. *Nature* 402, 195–199. doi: 10.1038/46065

Rosenberg, O. S., Deindl, S., Comolli, L. R., Hoelz, A., Downing, K. H., Nairn, A. C., et al. (2006). Oligomerization states of the association domain and the holoenyzme of Ca2+/CaM kinase II. *FEBS J.* 273, 682–694. doi: 10.1111/j.1742-4658.2005.05088.x

Rossetti, T., Banerjee, S., Kim, C., Leubner, M., Lamar, C., Gupta, P., et al. (2017). Memory erasure experiments indicate a critical role of CaMKII in memory storage. *Neuron* 96, 207–216. doi: 10.1016/j.neuron.2017.09.010

Rostas, J. A., Hoffman, A., Murtha, L. A., Pepperall, D., McLeod, D. D., and Dicksosn, P. W. (2017). Ischaemia-and excitotoxicity-induced CaMKII-Mediated neuronal cell death: the relative roles of CaMKII autophosphorylation at T286 and T253. *Neurochem. Internat.* 104, 6–10. doi: 10.1016/j.neuint.2017.01.002

Rotenberg, A., Mayford, M., Hawkins, R. D., Kandel, E. R., and Muller, R. U. (1996). Mice expressing activated CaMKII lack low frequency LTP and do not form stable place cells in the CA1 region of the hippocampus. *Cell* 87, 1351–1361. doi: 10.1016/s0092-8674(00)81829-2

Rumbaugh, G., Adams, J. P., Kim, J. H., and Huganir, R. L. (2006). SynGAP regulates synaptic strength and mitogen-activated protein kinases in cultured neurons. *Proceedings of the National Academy of Sciences* 103, 4344–4351. doi: 10.1073/pnas.0600084103

Saha, S., Ramanathan, A., and Rangarajan, P. N. (2006). Regulation of Ca2+/calmodulin kinase II inhibitor α (CaMKIINα) in virus-infected mouse brain. *Biochem. Biophys. Res. Comm.* 350, 444–449. doi: 10.1016/j.bbrc.2006.09.066

Sałaciak, K., Koszałka, A., Żmudzka, E., and Pytka, K. (2021). The Calcium/Calmodulin-Dependent Kinases II and IV as Therapeutic Targets in Neurodegenerative and Neuropsychiatric Disorders. *Internat. J. Mole. Sci.* 22:4307. doi: 10.3390/ijms22094307

Saneyoshi, T., Matsuno, H., Suzuki, A., Murakoshi, H., Hedrick, N. G., and Agnello, E. (2019). Reciprocal activation within a kinase-effector complex underlying persistence of structural LTP. *Neuron* 102, 1199–1210. doi: 10.1016/j.neuron.2019.04.012

Sanhueza, M., Fernandez-Villalobos, G., Stein, I. S., Kasumova, G., Zhang, P., Bayer, K. U., et al. (2011). Role of the CaMKII/NMDA receptor complex in the maintenance of synaptic strength. *J. Neurosci.* 31, 9170–9178. doi: 10.1523/JNEUROSCI.1250-11.2011

Savina, T. A., Shchipakina, T. G., and Godukhin, O. V. (2013). Effects of Convulsive Activity on the Subunit Composition of Ca 2+/Calmodulin-Dependent Protein Kinase II in the Hippocampus of Krushinskii–Molodkina Rats. *Neurosci. Behav. Physiol.* 43, 267–274. doi: 10.1007/s11055-013-9727-y

Scheetz, A. J., Nairn, A. C., and Constantine-Paton, M. (1997). N-methyl-D-aspartate receptor activation and visual activity induce elongation factor-2 phosphorylation in amphibian tecta: a role for N-methyl-D-aspartate receptors in controlling protein synthesis. *Proc. Natl. Acad. Sci.* 94, 14770–14775. doi: 10.1073/pnas.94.26.14770

Scheetz, A. J., Nairn, A. C., and Constantine-Paton, M. (2000). NMDA receptor-mediated control of protein synthesis at developing synapses. *Nat. Neurosci.* 3, 211–216. doi: 10.1038/72915

Scheff, S. W., and Price, D. A. (1993). Synapse loss in the temporal lobe in Alzheimer's disease. *Ann. Neurol.* 33, 190–199. doi: 10.1002/ana.410330209

Scheff, S. W., and Price, D. A. (1998). Synaptic density in the inner molecular layer of the hippocampal dentate gyrus in Alzheimer disease. *J. Neuropathol. Exp. Neurol.* 57, 1146–1153. doi: 10.1097/00005072-199812000-00006

Scheff, S. W., Price, D. A., Schmitt, F. A., and Mufson, E. J. (2006). Hippocampal synaptic loss in early Alzheimer's disease and mild cognitive impairment. *Neurobiol. Aging* 27, 1372–1384. doi: 10.1016/j.neurobiolaging.2005.09.012

Schwarzbach, E., Bonislawski, D. P., Xiong, G., and Cohen, A. S. (2006). Mechanisms underlying the inability to induce area CA1 LTP in the mouse after traumatic brain injury. *Hippocampus* 16, 541–550. doi: 10.1002/hipo.20183

Semyanov, A., and Godukhin, O. (2001). Epileptiform activity and EPSP-spike potentiation induced in rat hippocampal CA1 slices by repeated high-K+: involvement of ionotropic glutamate receptors and Ca2+/calmodulin-dependent protein kinase II. *Neuropharmacology* 40, 203–211. doi: 10.1016/s0028-3908(00)00147-7

Shamloo, M., Kamme, F., and Wieloch, T. (2000). Subcellular distribution and autophosphorylation of calcium/calmodulin-dependent protein kinase II-α in rat hippocampus in a model of ischemic tolerance. *Neuroscience* 96, 665–674. doi: 10.1016/s0306-4522(99)00586-2

Shen, K., and Meyer, T. (1999). Dynamic control of CaMKII translocation and localization in hippocampal neurons by NMDA receptor stimulation. *Science* 284, 162–167. doi: 10.1126/science.284.5411.162

Shen, K., Teruel, M. N., Connor, J. H., Shenolikar, S., and Meyer, T. (2000). Molecular memory by reversible translocation of calcium/calmodulin-dependent protein kinase II. *Nat. Neurosci.* 3, 881–886. doi: 10.1038/78783

Shen, K., Teruel, M. N., Subramanian, K., and Meyer, T. (1998). CaMKIIβ functions as an F-actin targeting module that localizes CaMKIIα/β heterooligomers to dendritic spines. *Neuron* 21, 593–606. doi: 10.1016/s0896-6273(00)80569-3

Shin, S. M., Zhang, N., Hansen, J., Gerges, N. Z., Pak, D. T., Sheng, M., et al. (2012). GKAP orchestrates activity-dependent postsynaptic protein remodeling and homeostatic scaling. *Nat. Neurosci.* 15, 1655–1666. doi: 10.1038/nn.3259

Si, K., Lindquist, S., and Kandel, E. R. (2003). A neuronal isoform of the aplysia CPEB has prion-like properties. *Cell* 115, 879–891. doi: 10.1016/s0092-8674(03)01020-1

Silva, A. J., Paylor, R., Wehner, J. M., and Tonegawa, S. (1992b). Impaired spatial learning in alpha-calcium-calmodulin kinase II mutant mice. *Science* 257, 206–211. doi: 10.1126/science.1321493

Silva, A. J., Rosahl, T. W., Chapman, P. F., Marowitz, Z., Friedman, E., Frankland, P. W., et al. (1996). Impaired learning in mice with abnormal short-lived plasticity. *Curr. Biol.* 6, 1509–1518. doi: 10.1016/s0960-9822(96)00756-7

Silva, A. J., Stevens, C. F., Tonegawa, S., and Wang, Y. (1992a). Deficient hippocampal long-term potentiation in alpha-calcium-calmodulin kinase II mutant mice. *Science* 257, 201–206. doi: 10.1126/science.1378648

Śliwińska, M. A., Cały, A., Borczyk, M., Ziółkowska, M., Skonieczna, E., Chilimoniuk, M., et al. (2020). Long-term memory upscales volume of postsynaptic densities in the process that requires autophosphorylation of αCaMKII. *Cereb. Cortex* 30, 2573–2585. doi: 10.1093/cercor/bhz261

Sloutsky, R., and Stratton, M. M. (2021). Functional implications of CaMKII alternative splicing. *Eur. J. Neurosci.* 54, 6780–6794. doi: 10.1111/ejn.14761

Stanton, P. K., and Gage, A. T. (1996). Distinct synaptic loci of Ca2+/calmodulin-dependent protein kinase II necessary for long-term potentiation and depression. *J. Neurophys.* 76, 2097–2101. doi: 10.1152/jn.1996.76.3.2097

Stefani, G., Onofri, F., Valtorta, F., Vaccaro, P., Greengard, P., and Benfenati, F. (1997). Kinetic analysis of the phosphorylation-dependent interactions of synapsin I with rat brain synaptic vesicles. *J. Physiol.* 504, 501–515. doi: 10.1111/j.1469-7793.1997.501bd.x

Stephenson, J. R., Wang, X., Perfitt, T. L., Parrish, W. P., Shonesy, B. C., and Marks, C. R. (2017). A novel human CAMK2A mutation disrupts dendritic morphology and synaptic transmission and causes ASD-related behaviors. *J. Neurosci.* 37, 2216–2233. doi: 10.1523/JNEUROSCI.2068-16.2017

Stevens, C. F., Tonegawa, S., and Wang, Y. (1994). The role of calcium–calmodulin kinase II in three forms of synaptic plasticity. *Curr. Biol.* 4, 687–693. doi: 10.1016/s0960-9822(00)00153-6

Steward, O., and Levy, W. B. (1982). Preferential localization of polyribosomes under the base of dendritic spines in granule cells of the dentate gyrus. *J. Neurosci.* 2, 284–291. doi: 10.1523/JNEUROSCI.02-03-00284.1982

Steward, O., and Schuman, E. M. (2001). Protein synthesis at synaptic sites on dendrites. *Ann. Rev. Neurosci.* 24, 299–325. doi: 10.1146/annurev.neuro.24.1.299

Strack, S., McNeill, R. B., and Colbran, R. J. (2000a). Mechanism and regulation of calcium/calmodulin-dependent protein kinase II targeting to the NR2B subunit of the N-methyl-D-aspartate receptor. *J. Biol. Chem.* 275, 23798–23806. doi: 10.1074/jbc.M001471200

Strack, S., Robison, A. J., Bass, M. A., and Colbran, R. J. (2000b). Association of calcium/calmodulin-dependent kinase II with developmentally regulated splice variants of the postsynaptic density protein densin-180. *J. Biol. Chem.* 275, 25061–25064. doi: 10.1074/jbc.C000319200

Stratton, M., Lee, I. H., Bhattacharyya, M., Christensen, S. M., Chao, L. H., Schulman, H., et al. (2014). Activation-triggered subunit exchange between CaMKII holoenzymes facilitates the spread of kinase activity. *Elife* 3:e01610.

Study, T. D. D. D. (2017). Prevalence and architecture of de novo mutations in developmental disorders. *Nature* 542:433. doi: 10.1038/nature21062

Sugawara, T., Hisatsune, C., Miyamoto, H., Ogawa, N., and Mikoshiba, K. (2017). Regulation of spinogenesis in mature Purkinje cells via mGluR/PKC-mediated phosphorylation of CaMKIIβ. *Proc. Natl. Acad. Sci.* 114, E5256–E5265. doi: 10.1073/pnas.1617270114

Sumi, M., Kiuchi, K., Ishikawa, T., Ishii, A., Hagiwara, M., Nagatsu, T., et al. (1991). The newly synthesized selective Ca2+ calmodulin dependent protein kinase II inhibitor KN-93 reduces dopamine contents in PC12h cells. *Biochem. Biophys. Res. Comm.* 181, 968–975. doi: 10.1016/0006-291x(91)92031-e

Sun, D. A., Deshpande, L. S., Sombati, S., Baranova, A., Wilson, M. S., Hamm, R. J., et al. (2008). Traumatic brain injury causes a long-lasting calcium (Ca2+)-plateau of elevated intracellular Ca levels and altered Ca2+ homeostatic mechanisms in hippocampal neurons surviving brain injury. *Eur. J. Neurosci.* 27, 1659–1672. doi: 10.1111/j.1460-9568.2008.06156.x

Sun, X. X., Hodge, J. J., Zhou, Y., Nguyen, M., and Griffith, L. C. (2004). The eag potassium channel binds and locally activates calcium/calmodulin-dependent protein kinase II. *J. Biol. Chem.* 279, 10206–10214. doi: 10.1074/jbc.M310728200

Sutherland, D. J., Pujic, Z., and Goodhill, G. J. (2014). Calcium signaling in axon guidance. *Trends Neurosci.* 37, 424–432. doi: 10.1016/j.tins.2014.05.008

Szydlowska, K., and Tymianski, M. (2010). Calcium, ischemia and excitotoxicity. *Cell Cal.* 47, 122–129. doi: 10.1016/j.ceca.2010.01.003

Tao, W., Lee, J., Chen, X., Díaz-Alonso, J., Zhou, J., Pleasure, S., et al. (2021). Synaptic memory requires CaMKII. *Elife* 10:e60360. doi: 10.7554/eLife.60360

Terry, R. D., Masliah, E., Salmon, D. P., Butters, N., DeTeresa, R., Hill, R., et al. (1991). Physical basis of cognitive alterations in Alzheimer's disease: synapse loss is the major correlate of cognitive impairment. *Ann. Neurol.* 30, 572–580. doi: 10.1002/ana.410300410

Thibault, O., and Landfield, P. W. (1996). Increase in single L-type calcium channels in hippocampal neurons during aging. *Science* 272, 1017–1020. doi: 10.1126/science.272.5264.1017

Tokumitsu, H., Chijiwa, T., Hagiwara, M., Mizutani, A., Terasawa, M., and Hidaka, H. (1990). KN-62, 1-[N, O-bis (5-isoquinolinesulfonyl)-N-methyl-L-tyrosyl]-4-phenylpiperazi ne, a specific inhibitor of Ca2+/calmodulin-dependent protein kinase II. *J. Biol. Chem.* 265, 4315–4320. doi: 10.1016/s0021-9258(19)39565-1

Tullis, J. E., Buonarati, O. R., Coultrap, S. J., Bourke, A. M., Tiemeier, E. L., Kennedy, M. J., et al. (2021). GluN2B S1303 phosphorylation by CaMKII or DAPK1: no indication for involvement in ischemia or LTP. *Iscience* 24:103214. doi: 10.1016/j.isci.2021.103214

Urakubo, H., Sato, M., Ishii, S., and Kuroda, S. (2014). In vitro reconstitution of a CaMKII memory switch by an NMDA receptor-derived peptide. *Biophys. J.* 106, 1414–1420. doi: 10.1016/j.bpj.2014.01.026

van Woerden, G. M., Hoebeek, F. E., Gao, Z., Nagaraja, R. Y., Hoogenraad, C. C., Kushner, S. A., et al. (2009). βCaMKII controls the direction of plasticity at

parallel fiber–Purkinje cell synapses. *Nat. Neurosci.* 12, 823–825. doi: 10.1038/nn.2329

Vasin, A., Zueva, L., Torrez, C., Volfson, D., Littleton, J. T., and Bykhovskaia, M. (2014). Synapsin regulates activity-dependent outgrowth of synaptic boutons at the Drosophila neuromuscular junction. *J. Neurosci.* 34, 10554–10563. doi: 10.1523/JNEUROSCI.5074-13.2014

Vaughn, J. E. (1989). Fine structure of synaptogenesis in the vertebrate central nervous system. *Synapse* 3, 255–285. doi: 10.1002/syn.890030312

Vest, R. S., Davies, K. D., O'Leary, H., Port, J. D., and Bayer, K. U. (2007). Dual mechanism of a natural CaMKII inhibitor. *Mole. Biol. Cell* 18, 5024–5033. doi: 10.1091/mbc.e07-02-0185

Vest, R. S., O'Leary, H., Coultrap, S. J., Kindy, M. S., and Bayer, K. U. (2010). Effective post-insult neuroprotection by a novel Ca2+/calmodulin-dependent protein kinase II (CaMKII) inhibitor. *J. Biol. Chem.* 285, 20675–20682. doi: 10.1074/jbc.M109.088617

Vieira, M. M., Nguyen, T. A., Wu, K., Badger, J. D. II, Collins, B. M., Anggono, V., et al. (2020). An Epilepsy-Associated GRIN2A rare variant disrupts CaMKIIα phosphorylation of GluN2A and NMDA receptor trafficking. *Cell Rep.* 32:108104. doi: 10.1016/j.celrep.2020.108104

Vincent, M., Collet, C., Verloes, A., Lambert, L., Herlin, C., Blanchet, C., et al. (2014). Large deletions encompassing the TCOF1 and CAMK2A genes are responsible for Treacher Collins syndrome with intellectual disability. *Eur. J. Hum. Genet.* 22, 52–56. doi: 10.1038/ejhg.2013.98

von Hertzen, L. S., and Giese, K. P. (2005). Alpha-isoform of Ca2+/calmodulin-dependent kinase II autophosphorylation is required for memory consolidation-specific transcription. *Neuroreport* 16, 1411–1414. doi: 10.1097/01.wnr.0000175244.51084.bb

Walikonis, R. S., Oguni, A., Khorosheva, E. M., Jeng, C. J., Asuncion, F. J., and Kennedy, M. B. (2001). Densin-180 forms a ternary complex with the α-subunit of Ca2+/calmodulin-dependent protein kinase II and α-actinin. *J. Neurosci.* 21, 423–433. doi: 10.1523/JNEUROSCI.21-02-00423.2001

Walkup, W. G. IV, Mastro, T. L., Schenker, L. T., Vielmetter, J., Hu, R., Iancu, A., et al. (2016). A model for regulation by SynGAP-α1 of binding of synaptic proteins to PDZ-domain'Slots' in the postsynaptic density. *Elife* 5:e16813.

Walkup, W. G., Washburn, L., Sweredoski, M. J., Carlisle, H. J., Graham, R. L., Hess, S., et al. (2015). Phosphorylation of synaptic GTPase-activating protein (synGAP) by Ca2+/calmodulin-dependent protein kinase II (CaMKII) and cyclin-dependent kinase 5 (CDK5) alters the ratio of its GAP activity toward Ras and Rap GTPases. *J. Biol. Chem.* 290, 4908–4927. doi: 10.1074/jbc.M114.614420

Wang, C. C., Held, R. G., and Hall, B. J. (2013). SynGAP regulates protein synthesis and homeostatic synaptic plasticity in developing cortical networks. *PLoS One* 8:e83941. doi: 10.1371/journal.pone.0083941

Wang, D., Tan, Q. R., and Zhang, Z. J. (2013). Neuroprotective effects of paeoniflorin, but not the isomer albiflorin, are associated with the suppression of intracellular calcium and calcium/calmodulin protein kinase II in PC12 cells. *J. Mole. Neurosci.* 51, 581–590. doi: 10.1007/s12031-013-0031-7

Wang, D. M., Yang, Y. J., Zhang, L., Zhang, X., Guan, F. F., and Zhang, L. F. (2013). Naringin enhances CaMKII activity and improves long-term memory in a mouse model of Alzheimer's disease. *Internat. J. Mole. Sci.* 14, 5576–5586. doi: 10.3390/ijms14035576

Wang, H., Feng, R., Wang, L. P., Li, F., Cao, X., and Tsien, J. Z. (2008). CaMKII activation state underlies synaptic labile phase of LTP and short-term memory formation. *Curr. Biol.* 18, 1546–1554. doi: 10.1016/j.cub.2008.08.064

Wang, H., Shimizu, E., Tang, Y. P., Cho, M., Kyin, M., Zuo, W., et al. (2003). Inducible protein knockout reveals temporal requirement of CaMKII reactivation for memory consolidation in the brain. *Proc. Natl. Acad. Sci.* 100, 4287–4292. doi: 10.1073/pnas.0636870100

Wang, N., Chen, L., Cheng, N., Zhang, J., Tian, T., and Lu, W. (2014). Active calcium/calmodulin-dependent protein kinase II (CaMKII) regulates NMDA receptor-mediated postischemic long-term potentiation (i-LTP) by promoting the interaction between CaMKII and NMDA receptors in ischemia. *Neur. Plast.* 2014:827161. doi: 10.1155/2014/827161

Wang, P., Cao, Y., Yu, J., Liu, R., Bai, B., Qi, H., et al. (2016). Baicalin alleviates ischemia-induced memory impairment by inhibiting the phosphorylation of CaMKII in hippocampus. *Brain Res.* 1642, 95–103. doi: 10.1016/j.brainres.2016.03.019

Wang, Q., Chen, M., Schafer, N. P., Bueno, C., Song, S. S., Hudmon, A., et al. (2019). Assemblies of calcium/calmodulin-dependent kinase II with actin and their dynamic regulation by calmodulin in dendritic spines. *Proc. Natl. Acad. Sci.* 116, 18937–18942. doi: 10.1073/pnas.1911452116

Wang, S., Liao, L., Huang, Y., Wang, M., Zhou, H., Chen, D., et al. (2019). Pin1 is regulated by CaMKII activation in glutamate-induced retinal neuronal regulated necrosis. *Front. Cell. Neurosci.* 13:276. doi: 10.3389/fncel.2019.00276

Wang, S. Q., Li, X. J., Qiu, H. B., Jiang, Z. M., Simon, M., Ma, X. R., et al. (2014). Anti-epileptic effect of Ganoderma lucidum polysaccharides by inhibition of intracellular calcium accumulation and stimulation of expression of CaMKII α in epileptic hippocampal neurons. *PLoS One* 9:e102161. doi: 10.1371/journal.pone.0102161

Wang, X., Marks, C. R., Perfitt, T. L., Nakagawa, T., Lee, A., Jacobson, D. A., et al. (2017). A novel mechanism for Ca2+/calmodulin-dependent protein kinase II targeting to L-type Ca2+ channels that initiates long-range signaling to the nucleus. *J. Biol. Chem.* 292, 17324–17336. doi: 10.1074/jbc.M117.788331

Wang, Y., and Mattson, M. P. (2014). L-type Ca2+ currents at CA1 synapses, but not CA3 or dentate granule neuron synapses, are increased in 3xTgAD mice in an age-dependent manner. *Neurobiol. Aging* 35, 88–95. doi: 10.1016/j.neurobiolaging.2013.07.007

Wei, G., Chen, Y. B., Chen, D. F., Lai, X. P., Liu, D. H., Deng, R. D., et al. (2013). β-Asarone inhibits neuronal apoptosis via the CaMKII/CREB/Bcl-2 signalling pathway in an in vitro model and AβPP/PS1 mice. *J. Alzheimer's Dis.* 33, 863–880. doi: 10.3233/jad-2012-120865

Weisskopf, M. G., Bauer, E. P., and LeDoux, J. E. (1999). L-type voltage-gated calcium channels mediate NMDA-independent associative long-term potentiation at thalamic input synapses to the amygdala. *J. Neurosci.* 19, 10512–10519. doi: 10.1523/JNEUROSCI.19-23-10512.1999

Wells, D. G., Dong, X., Quinlan, E. M., Huang, Y. S., Bear, M. F., Richter, J. D., et al. (2001). A role for the cytoplasmic polyadenylation element in NMDA receptor-regulated mRNA translation in neurons. *J. Neurosci.* 21, 9541–9548. doi: 10.1523/JNEUROSCI.21-24-09541.2001

Wen, Z., Guirland, C., Ming, G. L., and Zheng, J. Q. (2004). A CaMKII/calcineurin switch controls the direction of Ca2+-dependent growth cone guidance. *Neuron* 43, 835–846. doi: 10.1016/j.neuron.2004.08.037

Wheeler, D. G., Barrett, C. F., Groth, R. D., Safa, P., and Tsien, R. W. (2008). CaMKII locally encodes L-type channel activity to signal to nuclear CREB in excitation–transcription coupling. *J. Cell Biol.* 183, 849–863. doi: 10.1083/jcb.200805048

Wiedenmayer, C. P., Myers, M. M., Mayford, M., and Barr, G. A. (2000). Olfactory based spatial learning in neonatal mice and its dependence on CaMKII. *Neuroreport* 11, 1051–1055. doi: 10.1097/00001756-200004070-00030

Wong, M. H., Samal, A. B., Lee, M., Vlach, J., Novikov, N., Niedziela-Majka, A., et al. (2019). The KN-93 molecule inhibits calcium/calmodulin-dependent protein kinase II (CaMKII) activity by binding to Ca2+/CaM. *J. Mole. Biol.* 431, 1440–1459. doi: 10.1016/j.jmb.2019.02.001

Wong, W. T., and Wong, R. O. (2000). Rapid dendritic movements during synapse formation and rearrangement. *Curr. Opin. Neurob.* 10, 118–124. doi: 10.1016/s0959-4388(99)00059-8

Woodgett, J. R., Davison, M. T., and Cohen, P. (1983). The calmodulin-dependent glycogen synthase kinase from rabbit skeletal muscle: purification, subunit structure and substrate specificity. *Eur. J. Biochem.* 136, 481–487. doi: 10.1111/j.1432-1033.1983.tb07766.x

Woolfrey, K. M., O'Leary, H., Goodell, D. J., Robertson, H. R., Horne, E. A., Coultrap, S. J., et al. (2018). CaMKII regulates the depalmitoylation and synaptic removal of the scaffold protein AKAP79/150 to mediate structural long-term depression. *J. Biol. Chem.* 293, 1551–1567. doi: 10.1074/jbc.M117.813808

Wu, G. Y., and Cline, H. T. (1998). Stabilization of dendritic arbor structure in vivo by CaMKII. *Science* 279, 222–226. doi: 10.1126/science.279.5348.222

Wu, L., Wells, D., Tay, J., Mendis, D., Abbott, M. A., Barnitt, A., et al. (1998). CPEB-mediated cytoplasmic polyadenylation and the regulation of experience-dependent translation of α-CaMKII mRNA at synapses. *Neuron* 21, 1129–1139. doi: 10.1016/s0896-6273(00)80630-3

Wu, S. P., Li, D., Wang, N., Hou, J. C., and Zhao, L. (2019). YiQi tongluo granule against cerebral ischemia/reperfusion injury in rats by freezing GluN2B and CaMK II through NMDAR/ERK1/2 signalling. *Chem. Pharm. Bull.* 67, 244–252. doi: 10.1248/cpb.c18-00806

Wyneken, U., Smalla, K. H., Marengo, J. J., Soto, D., De La Cerda, A., Tischmeyer, W., et al. (2001). Kainate-induced seizures alter protein composition and

N-methyl-D-aspartate receptor function of rat forebrain postsynaptic densities. *Neuroscience* 102, 65–74. doi: 10.1016/s0306-4522(00)00469-3

Xie, Z., Srivastava, D. P., Photowala, H., Kai, L., Cahill, M. E., Woolfrey, K. M., et al. (2007). Kalirin-7 controls activity-dependent structural and functional plasticity of dendritic spines. *Neuron* 56, 640–656. doi: 10.1016/j.neuron.2007.10.005

Xu, J., Liu, Z. A., Pei, D. S., and Xu, T. J. (2010). Calcium/calmodulin-dependent kinase II facilitated GluR6 subunit serine phosphorylation through GluR6-PSD95-CaMKII signaling module assembly in cerebral ischemia injury. *Brain Res.* 1366, 197–203. doi: 10.1016/j.brainres.2010.09.087

Xu, Q., Deng, F., Xing, Z., Wu, Z., Cen, B., Xu, S., et al. (2016). Long non-coding RNA C2dat1 regulates CaMKII δ expression to promote neuronal survival through the NF-κ B signalling pathway following cerebral ischemia. *Cell Death Dis.* 7, e2173–e2173. doi: 10.1038/cddis.2016.57

Yamagata, Y., Imoto, K., and Obata, K. (2006). A mechanism for the inactivation of Ca2+/calmodulin-dependent protein kinase II during prolonged seizure activity and its consequence after the recovery from seizure activity in rats in vivo. *Neuroscience* 140, 981–992. doi: 10.1016/j.neuroscience.2006.02.054

Yamagata, Y., Kobayashi, S., Umeda, T., Inoue, A., Sakagami, H., and Fukaya, M. (2009). Kinase-dead knock-in mouse reveals an essential role of kinase activity of Ca2+/calmodulin-dependent protein kinase IIα in dendritic spine enlargement, long-term potentiation, and learning. *J. Neurosci.* 29, 7607–7618. doi: 10.1523/JNEUROSCI.0707-09.2009

Yamagata, Y., and Obata, K. (2004). Ca2+/calmodulin-dependent protein kinase II is reversibly autophosphorylated, inactivated and made sedimentable by acute neuronal excitation in rats in vivo. *J. Neurochem.* 91, 745–754. doi: 10.1111/j.1471-4159.2004.02753.x

Yamagata, Y., Yanagawa, Y., and Imoto, K. (2018). Differential involvement of kinase activity of Ca2+/calmodulin-dependent protein kinase IIα in hippocampus-and amygdala-dependent memory revealed by kinase-dead knock-in mouse. *Eneuro* 5, e133–e118. doi: 10.1523/ENEURO.0133-18.2018

Yamamoto, Y., Shioda, N., Han, F., Moriguchi, S., Nakajima, A., Yokosuka, A., et al. (2009). Nobiletin improves brain ischemia-induced learning and memory deficits through stimulation of CaMKII and CREB phosphorylation. *Brain Res.* 1295, 218–229. doi: 10.1016/j.brainres.2009.07.081

Yamasaki, N., Maekawa, M., Kobayashi, K., Kajii, Y., Maeda, J., Soma, M., et al. (2008). Alpha-CaMKII deficiency causes immature dentate gyrus, a novel candidate endophenotype of psychiatric disorders. *Mole. Brain* 1, 1–21. doi: 10.1186/1756-6606-1-6

Yang, E., and Schulman, H. (1999). Structural examination of autoregulation of multifunctional calcium/calmodulin-dependent protein kinase II. *J. Biol. Chem.* 274, 26199–26208. doi: 10.1074/jbc.274.37.26199

Yan-You Huang, P. V., Nguyen, T. A., and Kandel, E. R. (1996). Long-lasting forms of synaptic potentiation in the mammalian hippocampus. *Learn. Memory.* 3, 74–85. doi: 10.1101/lm.3.2-3.74

Yasuda, H., Barth, A. L., Stellwagen, D., and Malenka, R. C. (2003). A developmental switch in the signaling cascades for LTP induction. *Nat. Neurosci.* 6, 15–16. doi: 10.1038/nn985

Yasuda, M., and Mayford, M. R. (2006). CaMKII activation in the entorhinal cortex disrupts previously encoded spatial memory. *Neuron* 50, 309–318. doi: 10.1016/j.neuron.2006.03.035

Yin, P., Xu, H., Wang, Q., Wang, J., Yin, L., Xu, M., et al. (2017). Overexpression of βCaMKII impairs behavioral flexibility and NMDAR-dependent long-term depression in the dentate gyrus. *Neuropharmacology* 116, 270–287. doi: 10.1016/j.neuropharm.2016.12.013

Yoshimura, Y., Ichinose, T., and Yamauchi, T. (2003). Phosphorylation of tau protein to sites found in Alzheimer's disease brain is catalyzed by Ca2+/calmodulin-dependent protein kinase II as demonstrated tandem mass spectrometry. *Neurosci. Lett.* 353, 185–188. doi: 10.1016/j.neulet.2003.09.037

Zalcman, G., Federman, N., Fiszbein, A., de la Fuente, V., Ameneiro, L., Schor, I., et al. (2019). Sustained CaMKII delta gene expression is specifically required for long-lasting memories in mice. *Mole. Neurob.* 56, 1437–1450. doi: 10.1007/s12035-018-1144-3

Zalcman, G., Federman, N., and Romano, A. (2018). CaMKII isoforms in learning and memory: localization and function. *Front. Mole. Neurosci.* 11:445. doi: 10.3389/fnmol.2018.00445

Zeng, Y., Zhao, D., and Xie, C. W. (2010). Neurotrophins enhance CaMKII activity and rescue amyloid-β-induced deficits in hippocampal synaptic plasticity. *J. Alzheimer's Dis.* 21, 823–831. doi: 10.3233/JAD-2010-100264

Zha, X. M., Dailey, M. E., and Green, S. H. (2009). Role of Ca2+/calmodulin-dependent protein kinase II in dendritic spine remodelling during epileptiform activity in vitro. *J. Neurosci. Res.* 87, 1969–1979. doi: 10.1002/jnr.22033

Zhang, H., Zhang, C., Vincent, J., Zala, D., Benstaali, C., Sainlos, M., et al. (2018). Modulation of AMPA receptor surface diffusion restores hippocampal plasticity and memory in Huntington's disease models. *Nat. Comm.* 9, 1–16. doi: 10.1038/s41467-018-06675-3

Zhang, M., Shan, H., Gu, Z., Wang, D., Wang, T., Wang, Z., et al. (2012). Increased expression of calcium/calmodulin-dependent protein kinase type II subunit delta after rat traumatic brain injury. *J. Mole. Neurosci.* 46, 631–643. doi: 10.1007/s12031-011-9651-y

Zhang, X., Connelly, J., Levitan, E. S., Sun, D., and Wang, J. Q. (2021). Calcium/Calmodulin–Dependent Protein Kinase II in Cerebrovascular Diseases. *Transl. Stroke Res.* 12, 513–529. doi: 10.1007/s12975-021-00901-9

Zhang, Y., Qiao, L., Xu, W., Wang, X., Li, H., Xu, W., et al. (2017). Paeoniflorin attenuates cerebral ischemia-induced injury by regulating Ca2+/CaMKII/CREB signalling pathway. *Molecules* 22:359. doi: 10.3390/molecules22030359

Zhang, Y. P., Holbro, N., and Oertner, T. G. (2008). Optical induction of plasticity at single synapses reveals input-specific accumulation of αCaMKII. *Proc. Natl. Acad. Sci.* 105, 12039–12044. doi: 10.1073/pnas.0802940105

Zhang, W., Chuang, Y. A., Na, Y., Ye, Z., Yang, L., Lin, R., et al. (2019). Arc oligomerization is regulated by CaMKII phosphorylation of the GAG domain: an essential mechanism for plasticity and memory formation. *Mol. Cell* 75, 13–25.e5. doi: 10.1016/j.molcel.2019.05.004

Zhao, N., Huang, W., Cătălin, B., Scheller, A., and Kirchhoff, F. (2021). L-Type Ca2+ Channels of NG2 Glia Determine Proliferation and NMDA Receptor-Dependent Plasticity. *Front. Cell Dev. Biol.* 2021:9. doi: 10.3389/fcell.2021.759477

Zhao, X., Rosenke, R., Kronemann, D., Brim, B., Das, S. R., Dunah, A. W., et al. (2009). The effects of aging on N-methyl-D-aspartate receptor subunits in the synaptic membrane and relationships to long-term spatial memory. *Neuroscience* 162, 933–945. doi: 10.1016/j.neuroscience.2009.05.018

Zhu, J. J., and Malinow, R. (2002). Acute versus chronic NMDA receptor blockade and synaptic AMPA receptor delivery. *Nat. Neurosci.* 5, 513–514. doi: 10.1038/nn0602-850

Zhu, J. J., Qin, Y., Zhao, M., Van Aelst, L., and Malinow, R. (2002). Ras and Rap control AMPA receptor trafficking during synaptic plasticity. *Cell* 110, 443–455. doi: 10.1016/s0092-8674(02)00897-8

Zou, D. J., and Cline, H. T. (1999). Postsynaptic calcium/calmodulin-dependent protein kinase II is required to limit elaboration of presynaptic and postsynaptic neuronal arbors. *J. Neurosci.* 19, 8909–8918. doi: 10.1523/JNEUROSCI.19-20-08909.1999

Zybura, A. S., Baucum, A. J., Rush, A. M., Cummins, T. R., and Hudmon, A. (2020). CaMKII enhances voltage-gated sodium channel Nav1. 6 activity and neuronal excitability. *J. Biol. Chem.* 295, 11845–11865. doi: 10.1074/jbc.RA120.014062

Conflict of Interest: The authors declare that the research was conducted in the absence of any commercial or financial relationships that could be construed as a potential conflict of interest.

frontiers | Frontiers in Molecular Neuroscience

ORIGINAL RESEARCH
published: 15 July 2022
doi: 10.3389/fnmol.2022.842772

Glutamatergic Synapse Dysfunction in *Drosophila* Neuromuscular Junctions Can Be Rescued by Proteostasis Modulation

Anushka Chakravorty[1], *Ankit Sharma*[2], *Vasu Sheeba*[2]* *and Ravi Manjithaya*[1,3]*

[1] *Autophagy Laboratory, Molecular Biology and Genetics Unit, Jawaharlal Nehru Centre for Advanced Scientific Research, Bangalore, India,* [2] *Chronobiology and Behavioural Neurogenetics Laboratory, Neuroscience Unit, Jawaharlal Nehru Centre for Advanced Scientific Research, Bangalore, India,* [3] *Neuroscience Unit, Jawaharlal Nehru Centre for Advanced Scientific Research, Bangalore, India*

Glutamate is the major excitatory neurotransmitter in the nervous system, and the *Drosophila* glutamatergic neuromuscular junctions (NMJs) offer a tractable platform to understand excitatory synapse biology both in health and disease. Synaptopathies are neurodegenerative diseases that are associated with synaptic dysfunction and often display compromised proteostasis. One such rare, progressive neurodegenerative condition, Spinocerebellar Ataxia Type 3 (SCA3) or Machado-Joseph Disease (MJD), is characterized by cerebellar ataxia, Parkinsonism, and degeneration of motor neuron synapses. While the polyQ repeat mutant protein ataxin-3 is implicated in MJD, it is unclear how it leads to impaired synaptic function. In this study, we indicated that a *Drosophila* model of MJD recapitulates characteristics of neurodegenerative disorders marked by motor neuron dysfunction. Expression of 78 polyQ repeats of mutant ataxin-3 protein in *Drosophila* motor neurons resulted in behavioral defects, such as impaired locomotion in both larval and adult stages. Furthermore, defects in eclosion and lifespan were observed in adult flies. Detailed characterization of larval glutamatergic neuromuscular junctions (NMJs) revealed defects in morphological features along with compromised NMJ functioning. Autophagy, one of the key proteostasis pathways, is known to be impaired in the case of several synaptopathies. Our study reveals that overexpression of the autophagy-related protein Atg8a rescued behavioral defects. Thus, we present a model for glutamatergic synapse dysfunction that recapitulates synaptic and behavioral deficits and show that it is an amenable system for carrying out genetic and chemical biology screens to identify potential therapeutic targets for synaptopathies.

Keywords: Spinocerebellar Ataxia Type 3, *Drosophila* neuromuscular junctions, glutamatergic synapse, synapse dysfunction, synaptopathy, autophagy

OPEN ACCESS

Edited by:
Dhrubajyoti Chowdhury,
Yale University, United States

Reviewed by:
Vimlesh Kumar,
Indian Institute of Science Education and Research Bhopal, India
Srinivasa Subramaniam,
The Scripps Research Institute, United States

***Correspondence:**
Vasu Sheeba
sheeba@jncasr.ac.in
Ravi Manjithaya
ravim@jncasr.ac.in

Specialty section:
This article was submitted to Molecular Signalling and Pathways, a section of the journal Frontiers in Molecular Neuroscience

Received: *24 December 2021*
Accepted: *25 April 2022*
Published: *15 July 2022*

Citation:
Chakravorty A, Sharma A, Sheeba V and Manjithaya R (2022) Glutamatergic Synapse Dysfunction in Drosophila Neuromuscular Junctions Can Be Rescued by Proteostasis Modulation. Front. Mol. Neurosci. 15:842772. doi: 10.3389/fnmol.2022.842772

INTRODUCTION

Synapses, the terminal ends of neurons, are highly complex structures. Properly functioning synapses are critical to the integrity of neuronal networks in the brain, and any dysfunction of synapses may lead to the manifestation of neurodegenerative disorders (Lepeta et al., 2016; Bae and Kim, 2017). The term "synaptopathy" was introduced to include brain disorders arising as

a result of synaptic dysfunction (Li et al., 2003). Synaptopathy of one of the major excitatory synapses, i.e., the glutamatergic synapse, has been reported in several neurodegenerative and neurodevelopmental disorders, including autism spectrum disorders (ASD), Down syndrome (DS), and intellectual disabilities (ID) (Südhof, 2008; Hussain et al., 2014; Tang et al., 2014; Volk et al., 2015). Although postsynaptic dysfunction, due to defects in α-amino-3-hydroxy-5-methyl-4-isoxazole propionic acid receptors (AMPARs), N-methyl-d-aspartate receptors (NMDARs), and metabotropic glutamate receptors (mGluRs), is well studied, the contribution of impaired presynapses in the manifestation of synaptopathies has not been well-characterized.

Spinocerebellar Ataxia Type 3 (SCA3; also known as Machado-Joseph disease, MJD) is a disease belonging to a group of progressive neurodegenerative disorders that are characterized by gait ataxia, ophthalmoplegia, and amyotrophy (Maciel et al., 1995; Paulson, 2012; McLoughlin et al., 2020). Although muscle weakness and loss of muscles are common signs of this late-onset neurodegenerative disease, the involvement of the peripheral nervous system in the progression of the disease is less understood. The pathogenesis of the disease is attributed to the expanded CAG (coding for Glutamine – Q) repeats in the coding region of the *ATXN3* gene (formerly known as the *MJD1* gene) that encodes a 42 kDa protein, ataxin-3 (or ATXN3). ATXN3 is a deubiquitinating enzyme that preferentially binds to and cleaves long polyubiquitin chains. It harbors multiple ubiquitin-interacting motifs (UIMs) and a catalytic Josephin domain (Nicastro et al., 2010). Non-pathogenic ATXN3 contains polyQs that may range from ∼12 to 43 repeats in length, which could increase beyond 60, in the case of the pathogenic form. PolyQ-expanded ATXN3 has been reported to aggregate in the nuclei of cultured cells and in neurons of various model organisms (Chai et al., 1999; Colomer Gould, 2005; Bichelmeier et al., 2007; Koeppen, 2018). These reports are consistent with patient sample data, which show the formation of inclusions in the brains of patients with MJD (Schmidt et al., 1998; Goti et al., 2004). Although the protein is ubiquitously expressed in several cell types, the mutant form of ATXN3 specifically affects some regions of the brain (Toonen et al., 2018). Extensive research has been done to understand the pathophysiology of MJD in the central nervous system (Alves et al., 2008; Nguyen et al., 2013; Nóbrega et al., 2013; Konno et al., 2014). However, the involvement of polyQ-expanded mutant ATXN3 in the etiology of peripheral nervous system dysfunction is less explored. We investigated the contribution of the polyQ-expanded mutant ATXN3 in the pathogenesis of peripheral nervous system disorders and glutamatergic synapse dysfunction.

We took advantage of the genetic amenability of the fly *Drosophila melanogaster* to generate a model of synaptopathy by targeting the pathogenic form of ATXN3 protein, containing 78 polyQ repeats to the neuromuscular junction. We observed morphological and functional defects in the synapses of motor neurons, which correlate with behavioral deficits observed both in the larval as well as adult stages of flies. As with many other polyQ disorders, we also observed proteostasis impairment in the motor neurons of flies. PolyQ aggregates have been shown to contribute to the pathology of several neurodegenerative disorders by impairment of the autophagy pathway and genetic or pharmacological induction of the pathway might help restore proteostatic imbalance. Here, we show that, with the aid of tissue-specific motor neuron overexpression of one of the core autophagy proteins, Atg8a, there is significant improvement in the behavioral and functional defects of glutamatergic synapses *in vivo*.

MATERIALS AND METHODS

Fly Husbandry

Drosophila melanogaster was reared on standard cornmeal agar supplemented with yeast, at 25°C with 12:12 h light-dark cycle. All crosses were set up at 25°C. The following stocks were obtained from Bloomington *Drosophila* Stock Center (BDSC): *UAS-MJDtrQ27* (8149), *UAS-MJDtrQ78* (8150), *UAS-mCherry-Atg8a* (37750), and *D42-Gal4* (8816).

Larval NMJ Fillet Preparation and Immunohistochemistry

Third instar larvae were dissected in HL3 buffer (70 mM NaCl, 5 mM KCl, 20 mM $MgCl_2$, 5 mM trehalose, 115 mM sucrose, 5 mM HEPES, 10 mM $NaHCO_3$, pH 7.2), internal organs were removed, and muscle fillet was prepared. The dissected fillets were fixed in 4% paraformaldehyde for 20 min and incubated in 0.1% PBT (0.1% Triton X-100 in PBS) for 30 min. Blocking was done in 0.2% PBTB (0.2% BSA in PBT) for 1 h, followed by incubation in 2% PBTN (2% normal goat serum in PBTB) for 30 min. After blocking, samples were kept for overnight primary antibody incubation at 4°C. After several washes and blocking in 2% PBTN, samples were incubated in secondary antibody at room temperature for 2 h. Following washes, the samples were mounted in Vectashield (Vector Laboratories). The following antibodies and their dilutions were used: mouse anti-Brp at 1:200 (Developmental Studies Hybridoma Bank), mouse anti-synaptotagmin at 1:50 (Developmental Studies Hybridoma Bank), mouse anti-HA at 1:200 (Invitrogen), and rabbit anti-GABARAP at 1:200 (Abcam). Secondary antibodies used were goat anti-mouse Atto 633 at 1:1,000 (Sigma-Aldrich), goat anti-mouse Atto 550 at 1:1,000 (Sigma-Aldrich), goat anti-rabbit Atto 633 at 1:1,000 (Sigma-Aldrich), goat anti-rabbit Atto 550 at 1:1,000 (Sigma-Aldrich), FITC-HRP, and Dylight-HRP at 1:200 (Jackson ImmunoResearch Laboratories, Inc.). Images for morphometric analysis were acquired on an LSM 880 confocal microscope using Zen software (Zeiss). Images for synaptotagmin intensity quantification were acquired on a DeltaVision microscope using SoftWorx software (GE Healthcare). For comparison of protein levels between different genotypes, all the samples were processed on the same day under identical conditions. Z-stacks were acquired with 0.25 μm spacing.

Larval Ventral Nerve Cord Preparation and Immunohistochemistry

Brains from third instar larvae were dissected in ice-cold PBS and fixed in 4% paraformaldehyde at room temperature for half an

hour. Following fixation, the samples were washed three times for 10 min with 0.5% PBT (0.5% Triton X-100 in PBS). After washes, the larval brains were blocked using 10% horse serum (prepared in 0.5% PBT). The brains were incubated overnight in primary antibody at 4°C. Following washes (four times, 10 min each using 0.5% PBT), the brains were incubated in secondary antibody at room temperature. Finally, the samples were washed, mounted in a glycerol-containing medium with DAPI, and imaged using a Zeiss LSM 880 confocal microscope and a 63X/1.4 DIC oil immersion objective using Zen software (Zeiss). The following antibodies were used: mouse anti-HA at 1:200 (Invitrogen) and FITC-HRP at 1:200 (Jackson ImmunoResearch Laboratories, Inc.). The secondary antibody used was goat anti-mouse 546 (1:3,000, Invitrogen).

Analysis of Larval NMJ

For quantification of bouton numbers, NMJs of muscle 6/7 of hemisegment A2 were acquired with a 40X objective using a laser-scanning confocal microscope (Zeiss LSM 880). The respective muscle area was acquired with a 20X objective. The number of boutons was normalized to the muscle area. For quantification of the bouton area and branch length, NMJs of muscle 6/7 of hemisegment A4-A6 were used. Quantification of synaptotagmin intensity was done on NMJs of muscle 4 of hemisegment A2. Manual quantification of the number of boutons, bouton area, NMJ branch length, and satellite boutons was done on maximum intensity projection (MIP) of images using ImageJ software (National Institutes of Health, NIH). Quantification of Brp puncta was done using Particle Analysis tool in ImageJ on thresholded images in NMJs of muscle 6/7 of hemisegment A2-A4. Genotype-blind quantification was carried out for all the acquired images.

Behavioral Assays

Larval Locomotion Assay

Third instar larvae of desired genotypes were collected, washed in distilled water, and subjected to a locomotion assay on 1% charcoal agar plates. Four larvae were placed at the center of the plate, and recordings were carried out for 2 min per video at ambient room temperature (25°C). Eight such videos (thus, 32 larvae per genotype) were captured at a frame rate of 30 fps and were uncompressed and processed for further analysis using VirtualDub 1.10.4. Analysis was done using WrmTrck plugin of ImageJ with the following parameters: rolling ball radius – 0.7, minimum object area – 10, maximum object area – 400, maximum velocity – 10, maximum area change – 200, minimum track length – 500, the threshold for turn – 2, size of a bin for speed histogram – 0, frames per second – 30, thresholding method – Otsu. Analysis for coiling behavior, bends and turns, and orientation counts were done using FIMTrack version 2 (Risse et al., 2017). Representative figures were made using iPython (Jupyter Notebook).

Eclosion Assay and Wing Defect Phenotype Assay

Crosses were set up for indicated genotypes and maintained at a 12:12 h light-dark cycle. Eclosion patterns were studied from four replicate vials, containing ∼5 ml of cornmeal agar and housing > 60 pupae per vial. All the vials were monitored till eclosion, and the number of flies eclosing was counted every 6 h for 4 consecutive days. Following eclosion, the number of flies with different wing phenotypes (fully expanded, or degenerated, or half expanded) was counted. Images for wing phenotypes were captured using an SZX16 Olympus stereomicroscope.

Activity Counts

Male flies were collected post-eclosion. Then, two three-day-old flies were loaded onto activity tubes with cornmeal food and monitored using *Drosophila* Activity Monitors (DAM, TriKinetics). Recordings were done under 12:12 h light-dark cycles (light intensity, ∼250lx) at a constant temperature of 25°C. Collected data were binned (20-min bin length) using DAM File Scanner and the activity counts were analyzed using Microsoft Excel.

Adult Lifespan Assay

To perform the lifespan assay, freshly eclosed males and females were collected and aged for 3 days, separated according to sex, and transferred into 4 replicate vials containing cornmeal agar food in groups of 15 flies/vial. Thus, 60 male and female flies of each genotype were assayed. The flies were transferred to fresh media every alternate day, and longevity was estimated by counting the number of flies alive in each vial. The assay was performed for 28 days.

Statistical Analysis

Statistical analysis was done using GraphPad Prism (version 8.4.2) and Statistica 7. Statistics employed for quantification are described in legends of respective figures and in the results section.

RESULTS

Expression of Mutant Q78 in Motor Neurons Causes Locomotory Deficits in Larvae

Previous studies have revealed an intricate association of locomotory deficits with synaptic dysfunction, such as decrease in synaptic connections, changes in the presynaptic and postsynaptic proteomes, and reduced neurotransmitter release (Mhatre et al., 2014; Kashima et al., 2017). To examine the effect of polyglutamine repeats of ATXN3 protein on the peripheral nervous system and glutamatergic synapses at the gross behavioral level, we made use of the GAL4-UAS system (Brand and Perrimon, 1993). Fly motor neurons were targeted using the *D42-Gal4* driver, the expression of which is restricted to motor neurons and interneurons within the larval nervous system and to motor neurons in the adult nervous system (Yeh et al., 1995; Gustafson and Boulianne, 1996). We expressed 78 polyQ repeats flanked upstream by 12 amino acids and downstream by 43 amino acids of ATXN3 protein containing an N-terminal HA tag (MJDtrQ78, henceforth called Q78). Non-pathogenic ATXN3 containing 27 polyQ repeats (MJDtrQ27, henceforth called Q27) served as the control. The Gal4 driver served as the parental driver control. Third instar larvae were

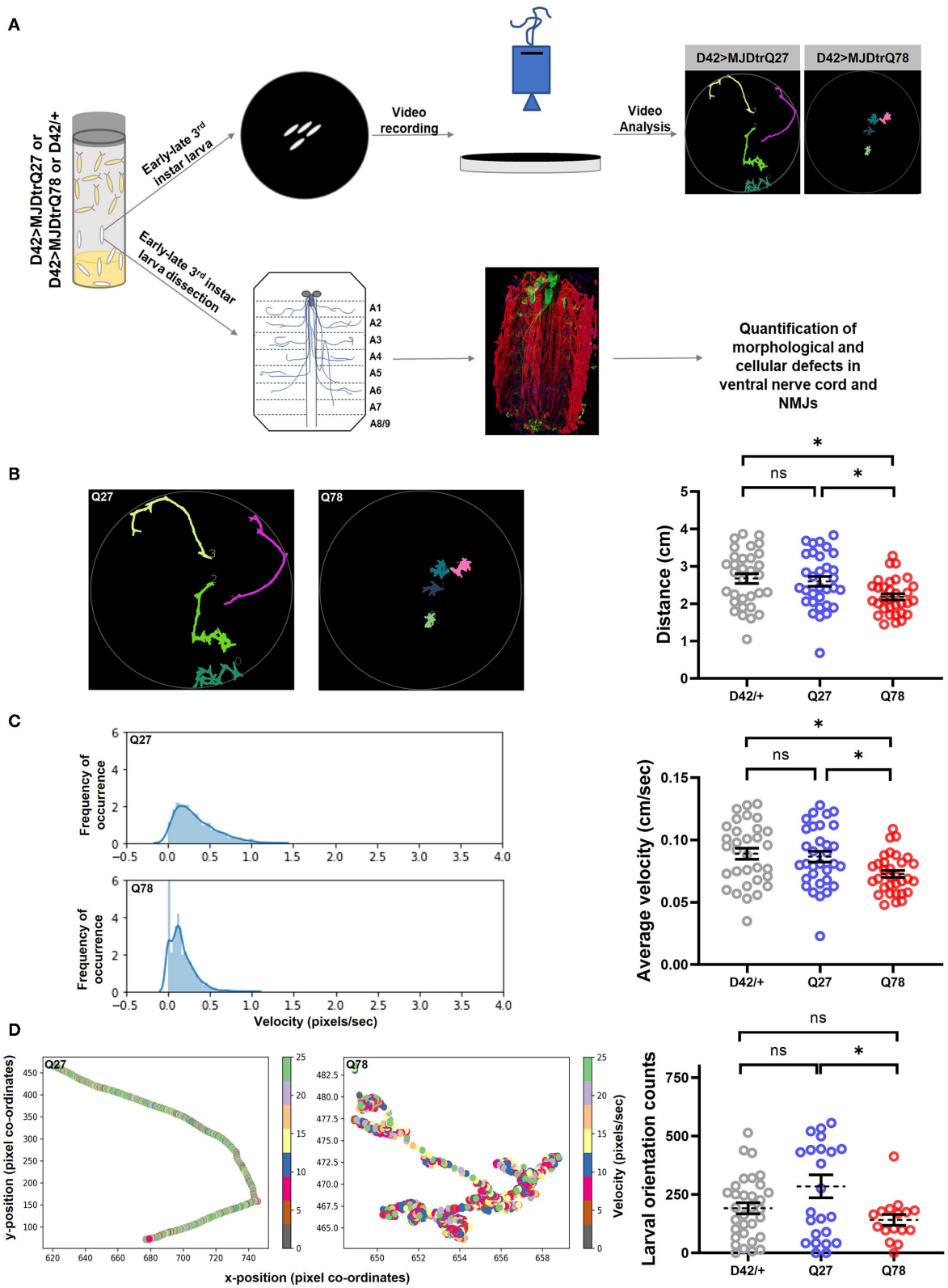

FIGURE 1 | Q78 expression in motor neurons leads to larval locomotion defect. **(A)** A flow chart of approaches to characterize behavioral and cellular defects upon expression of mutant MJDtrQ78. Third instar larvae expressing non-pathogenic Q27 or pathogenic Q78 along with driver control D42/+ were subjected to a larval locomotion assay and simultaneously assessed for phenotypic and functional defects in NMJs. **(B)** Path diagrams for Q27 and Q78 larvae monitored in 1% charcoal

(Continued)

FIGURE 1 | agar plates and quantification of the total distance traversed by the driver-only control larvae (D42/+) vs. non-pathogenic Q27 and pathogenic Q78 larvae. $n = 32$ larvae; one-way ANOVA; *post-hoc* Tukey's multiple comparison test; ns, non-significant; $^*p < 0.05$; error bars represent mean ± SEM. **(C)** Representative images of the velocity distribution of non-pathogenic Q27 and pathogenic Q78 larvae and quantification of the average velocity of larvae. $n = 32$ larvae; one-way ANOVA; *post-hoc* Tukey's multiple comparison test; ns, non-significant; $^*p < 0.05$; error bar represents ± SEM. **(D)** A representative scatter plot showing instantaneous velocity per coordinate for non-pathogenic Q27 and pathogenic Q78 larvae. The number of times the larvae traversed linearly in the arena without reorientation/coiling was plotted as orientation counts. $n = 32$ larvae; one-way ANOVA; *post-hoc* Tukey's multiple comparison test; ns, non-significant; $^*p < 0.05$; error bar represents mean ± SEM.

subjected to a larval locomotion assay with various parameters in 1% charcoal agar plates, including distance traveled in the arena and average velocity, and were quantified as a surrogate readout for proper functioning of motor neurons (**Figure 1A**). We observed defects in larval locomotion on the expression of Q78 in motor neurons.

We first quantified the total path traversed by the larvae and observed a significant reduction in path length traveled by Q78 expressing larvae as compared to both Q27 and D42/+ control larvae [genotype, $F_{(2,93)} = 5.005$, $p = 0.0086$ ANOVA; D42/+ vs. Q27 ($p = 0.8902$), D42/+ vs. Q78 ($p = 0.0114$), Q27 vs. Q78 ($p = 0.0392$) Tukey's multiple comparison] (**Figure 1B**). Furthermore, we assessed the average velocity of locomotion and observed a similar significant reduction in velocity of Q78 expressing larvae as compared to both the controls [genotype, $F_{(2,93)} = 5.004$, $p = 0.0086$, ANOVA; D42/+ vs. Q27 ($p = 0.9037$), D42/+ vs. Q78 ($p = 0.0118$), Q27 vs. Q78 ($p = 0.0374$), Tukey's multiple comparison] (**Figure 1C**). The larval orientation counts were also reduced upon the expression of mutant Q78; however, this parameter was not significantly different from the D42/+ control [genotype, $F_{(2,69)} = 3.773$, $p = 0.0279$, ANOVA; D42/+ vs. Q27 ($p = 0.1137$), D42/+ vs. Q78 ($p = 0.6095$), Q27 vs. Q78 ($p = 0.0304$), Tukey's multiple comparison] (**Figure 1D**). Other features of locomotion, such as the number of linear crawling events (go-phase counts), number of coiling events, and number of reorientation counts (left and right bends), were, however, unchanged as compared to controls (**Supplementary Figures 1A–C**). These results show that the expression of expanded polyQ repeats of ATXN3 in motor-neurons leads to locomotory deficits at the larval stage.

Expression of Mutant Q78 in Motor Neurons Leads to Various Behavioral Defects in Adult Flies

Following defects observed at the larval stages, we explored how the expression of mutant Q78 protein affects adult flies. Previous studies have shown that the expression of Q78 protein in *Drosophila* brain using the pan-neuronal driver *Elav-Gal4* leads to eclosion, wing, locomotor, and lifespan defects (Singh et al., 2014). Since this driver has a very broad expression, it is not possible to pinpoint the spatial and temporal patterns of the defects obtained. We maintained a restricted tissue target to examine the impact of Q78 mutant protein in motor neurons on adult fly behaviors. We studied various behavioral parameters, such as eclosion, wing, locomotion, and lifespan, in these flies (**Figure 2A**). For these experiments, the D42/+ served as the parental control. Upon quantification, we observed that motor-neuron-driven Q78 expression in adult flies led to defects or failure of eclosion, while both the control flies exhibited eclosion of > 90% [$\chi_{(df=2)} = 96.51$, $p = 0.000$, D42 vs. Q78 ($p < 0.00001$), D42 vs. Q27 ($p = 0.7504$), Q27 vs. Q78 ($p < 0.00001$)] (**Figure 2B**). Furthermore, out of all the eclosed flies, the proportion of female flies was higher in comparison to male flies (**Figure 2C**), whereas controls showed the expected 1:1 sex ratio. These results suggest higher male susceptibility toward Q78 pathology. This result is in line with available literature in humans, which report gender bias in the progression of many neurodegenerative conditions (Hanamsagar and Bilbo, 2016; Piscopo et al., 2021). We also observed wing defects in eclosed flies on the expression of Q78 protein. The majority of the flies had completely degenerated wings followed by a small fraction of flies, showing half degenerated wings and very few with fully expanded wings. Such wing defects were absent in control flies, wherein all the wings were fully expanded (**Figure 2D**). Locomotion in adult Q78 flies was also assessed using *Drosophila* Activity Monitors (DAM). Q78-expressing flies had significantly lower activity counts per day as compared to both control flies [genotype, $F_{(2,54)} = 18.76$, $p < 0.0001$, ANOVA; D42/+ vs. Q27 ($p = 0.3945$), D42/+ vs. Q78 ($p = 0.0003$), Q27 vs. Q78 ($p \leq 0.0001$), Tukey's multiple comparison] (**Figure 2E**). Finally, we assessed the survival of male and female Q78-expressing flies. We observed that both male and female flies had a comparatively shorter lifespan as compared to control flies. Moreover, we observed similar sex-based differences, wherein female flies showed a slightly longer lifespan in comparison to male flies (**Figure 2F**). Overall, these results showed that, upon expression of mutant Q78 protein in motor neurons, there are behavioral defects at both larval as well as adult stages of flies.

Expression of Q78 in Motor Neurons Leads to Morphological Changes in *Drosophila* NMJs

Mutant Q78 may aggregate as neuronal nuclear inclusions (NNIs), which contain ubiquitin, heat shock proteins, transcription factors, and polyQ proteins (Fujigasaki et al., 2000; Breuer et al., 2010). It may also aggregate as neuronal cytoplasmic inclusions (NCIs), which are majorly ubiquitin negative (Hayashi et al., 2003; Yamada et al., 2004). The role of either of these inclusions in the progression of MJD pathology in the peripheral nervous system is hitherto unknown. To investigate the distribution of the mutant protein expressed under *D42-Gal4* motor neuron driver *in vivo*, we dissected third instar larvae and immunostained for the truncated form of ATXN3 tagged with HA. In control Q27-expressing larvae, the non-pathogenic ATXN3 was distributed throughout the ventral nerve cord (VNC), axons, and neuromuscular junctions (NMJs,

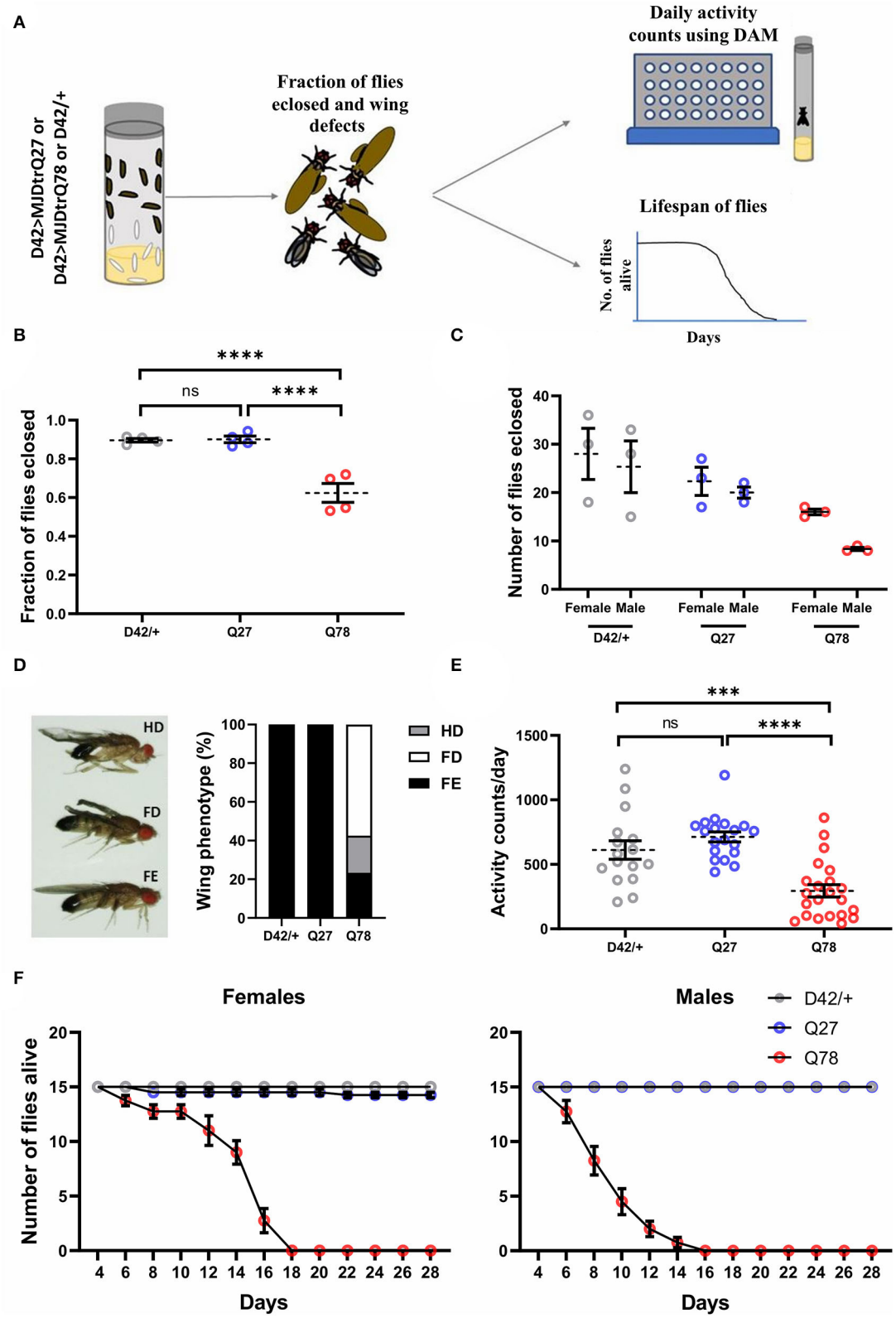

FIGURE 2 | Eclosion, locomotion, and lifespan are affected in adult flies on the expression of Q78 in motor neurons. **(A)** A flow chart depicting phenotypes characterized in adult flies expressing non-pathogenic Q27 or pathogenic Q78 in motor neurons using the *D42-Gal4* driver. A fraction of adult flies that successfully emerged from pupae, wing phenotypes, locomotion, and adult lifespan was assayed. **(B)** Quantification of fraction of flies eclosed. n > 280 pupae from 4 vials; 3x2

(Continued)

FIGURE 2 | contingency test followed by Fisher's Exact test; ****$p < 0.0001$; ns, non-significant; error bars represent mean ± SEM. **(C)** Quantification of the number of male and female flies eclosed. $n \geq 70$ flies. **(D)** Images depicting wing phenotypes of adult flies expressing pathogenic Q78 under *D42-Gal4* and quantification of the percentage of wing phenotypes observed. $n \geq 47$ flies; FD, full degeneration; HD, half degeneration; FE, fully expanded. **(E)** Quantification of activity counts per day. $n \geq 16$ flies per genotype; one-way ANOVA; *post-hoc* Tukey's HSD; ****$p < 0.0001$; ***$p < 0.001$; ns, non-significant; error bars represent mean ± SEM. **(F)** Survivorship plots showing the number of flies alive across 28 days. $n = 60$ flies for both males and females; error bars depict mean ± SEM.

the varicosities or the presynaptic terminals of motor neurons). However, we found that Q78 expression was restricted to the cell bodies in VNC, where it accumulated as aggregates but was rarely present in the NMJs (**Figure 3A**, **Supplementary Figures 2A,B**). This result was in line with the previously observed distribution pattern of Q78 in flies using the *Elav-Gal4* driver (Lee et al., 2004).

We next assessed whether the accumulation of Q78 aggregates in the cell bodies of motor neurons led to changes in the overall morphology of glutamatergic synapses. The motor neurons MN 6/7-Ib and MNSN b/d-Is emanating from the VNC, innervate the musculature present in abdominal hemisegments 6/7 (Budnik, 1996; Menon et al., 2013). A bouton was defined as a swollen presynaptic terminal emanating from the main arbor of NMJ immunostained by FITC-HRP. The accumulation of mutant Q78 in the VNC led to characteristic morphological changes in the NMJs (**Figure 3B**). Structural analysis of the NMJs 6/7 showed that the number of boutons per NMJ was reduced by ∼50% upon expression of mutant Q78 [$t_{(20)} = 3.271$, $p = 0.0038$, *t*-test] (**Figure 3C**). Upon expression of mutant Q78, however, we observed an ∼2-fold increase in the individual bouton area, as compared to Q27 controls [$t_{(366)} = 10.32$, $p < 0.0001$, *t*-test] (**Figure 3D**). The number of branching arbors of NMJs was also decreased in the Q78 expressing motor neurons [$t_{(26)} = 3.552$, $p = 0.0015$, *t*-test] (**Figure 3E**). Moreover, we observed heterogeneity among the affected NMJs, with some exhibiting more severe defects compared to others (**Supplementary Figure 2C**). Altogether, these observations suggest that the expression of mutant Q78 in motor neurons led to structural changes in the glutamatergic NMJs of *Drosophila*.

Motor Neuronal Expression of Q78 Leads to Functional Defects in Glutamatergic Synapses

Since our initial locomotion assays (**Figure 1A**) showed deficits in the larval locomotory behavior, we examined if the presynapses of motor neurons were affected in terms of neurotransmitter release. For this, we quantified two aspects of neurotransmitter release; the clustering of release-ready pools of synaptic vesicles (SVs) at the active zones and for the fusion of SVs.

In addition, the aberrant bouton morphology observed upon expression of Q78 led us to ask whether there were functional defects in the glutamatergic synapses as well, for which we assessed the levels of the *Drosophila* ortholog of ELKS/CAST/ERC protein called Bruchpilot (Brp) (Chou et al., 2020). Active zone sites in presynapses of *Drosophila* NMJs are marked by an increased accumulation of Brp (Van Vactor and Sigrist, 2017). Another SNARE protein involved in the fusion of the glutamate-rich vesicles is Synaptotagmin (Syt) (Paul et al., 2015; Kittel and Heckmann, 2016). We compared the levels of Brp and Syt in *Drosophila* NMJs and visualized Brp positive puncta and Syt intensity using confocal microscopy. When compared to control Q27 larvae, Q78 expression in motor neurons under *D42-Gal4* led to a reduction in the number of Brp positive puncta, indicating a reduction in active zones of NMJs [$t_{(21)} = 3.177$, $p = 0.0045$, *t*-test] (**Figure 4A**). However, no significant reduction in levels of Syt, indicated by changes in Syt intensity, was detectable [$t_{(26)} = 0.9060$, $p = 0.3733$, *t*-test] (**Figure 4B**).

The overgrowth of boutons can lead to the formation of satellite boutons, which are additional boutons that bud off from the parent bouton or from the main arbor of NMJs (Dickman et al., 2006; O'Connor-Giles and Ganetzky, 2008). We quantified the number of satellite boutons as a measure of aberrant growth of the NMJs and observed that Q78 expression in motor neurons led to the appearance of numerous satellite boutons budding off from the main boutons of NMJs ($p < 0.0001$, Mann–Whitney *U*-test) (**Figure 4C**). Such satellite boutons were rarely seen in the NMJs of Q27 controls.

Proteostasis impairment due to polyQ aggregate accumulation can be a leading cause of neuronal dysfunction. One of the important proteostasis pathways is autophagy, and recent studies have shown that it is highly compartmentalized in neurons (Maday and Holzbaur, 2014, 2016). Several lines of research indicate presynaptic autophagy to be important for the normal functioning and development of synapses (Vijayan and Verstreken, 2017; Kuijpers et al., 2021). Apart from physiological substrates generally degraded *via* the general autophagy pathway, pathophysiological substrates, such as amyloid fibrils, hyperphosphorylated tau tangles, and polyQ aggregates, are also known to be degraded *via* the selective autophagy pathway called aggrephagy (Ravikumar et al., 2002; Rubinsztein, 2006; Yamamoto and Simonsen, 2011; Lamark and Johansen, 2012). However, overwhelming levels of aggregate accumulation in neurons can lead to severe impairment in proteostasis pathways, including the ubiquitin-proteasome system and autophagy (Nassif and Hetz, 2012; Hipp et al., 2014; Klaips et al., 2018; Thibaudeau et al., 2018). We, therefore, asked if the accumulation of Q78 aggregates in motor neuron cell bodies could possibly lead to basal-level autophagy impairment and probed for endogenous levels of Atg8a, the ortholog of LC3 in *Drosophila*. We observed that, in comparison to Q27 expressing larvae, Q78 expression in motor neurons led to a significant reduction in the levels of endogenous Atg8a, indicating a possible block in the pathway [$t_{(22)} = 2.422$, $p = 0.0241$, *t*-test] (**Figure 4D**). Taken together, these results suggest

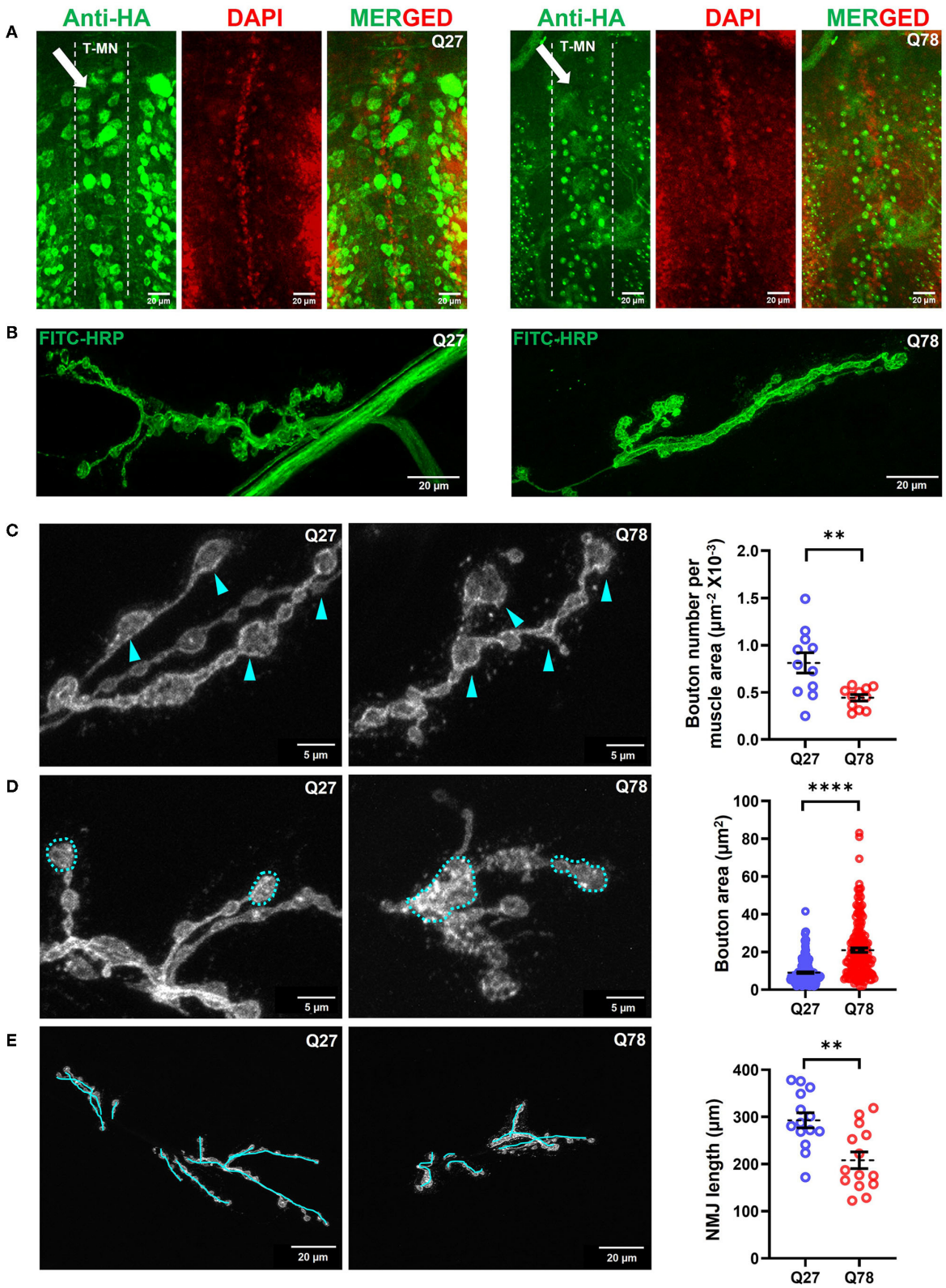

FIGURE 3 | Q78 expression in motor neurons leads to multiparametric changes in the morphology of NMJs. **(A)** An image depicting the cell bodies of motor neurons in the ventral nerve cord (VNCs) of *Drosophila* larvae. An arrow depicts the alignment of the thoracic motor neuron (T-MN) cell bodies. FITC-HRP marks the neuronal membrane. HA antibody was used for staining the pathogenic or non-pathogenic ATXN3 polyQ protein. **(B)** Image depicting the NMJs of the third instar larva

(Continued)

FIGURE 3 | marked by FITC-HRP in Q27 and Q78-expressing larvae. The morphometric changes observed are further quantified. **(C)** The number of boutons per muscle area in Q27 and Q78-expressing larvae and quantification of the same. Arrowheads depict the varicosities or boutons. All quantifications were done on NMJs of muscle 6/7 of abdominal hemisegment A2. $n > 11$; Student's *t*-test; $^{**}p < 0.01$. An error bar represents mean ± SEM. **(D)** The area of boutons in Q27 and Q78-expressing larvae and quantification of the same. Markings indicate the areas considered for quantification. All quantifications were done on NMJs of muscle 6/7 of abdominal segments A4-A6. $n > 160$; Student's *t*-test; $^{****}p < 0.0001$. An error bar represents mean ± SEM. **(E)** Length of NMJ branches and the main arbor in Q27 and Q78-expressing larvae and quantification of the same. Markings represent the lengths considered for quantification. All quantifications were done on NMJs of muscle 6/7 of abdominal segments A4-A6. $n > 12$; Student's *t*-test; $^{**}p < 0.01$. An error bar represents mean ± SEM.

that Q78 expression in motor neurons leads to functional changes in the glutamatergic synapses of *Drosophila* NMJs.

Overexpression of Atg8a in Motor Neurons Leads to Rescue of Defects in Glutamatergic Synapses

Previous studies have shown that restoring the imbalance in proteostasis pathways either by genetic or pharmacological means can reduce the toxicity caused by the accumulation of mutant proteins in the central nervous system (Simonsen et al., 2008; Ordonez et al., 2012; Yi et al., 2013; Charif et al., 2022). We thus wanted to understand if genetic overexpression of Atg8a specifically in motor neurons, can lead to a rescue of the behavioral and synaptic defects in the ATXN3 polyQ model. To assess for rescue in behavioral deficits, we performed the locomotion assay at the larval stage. *D42-Gal4* served as the control, while *D42-Gal4 > UASQ78* and *D42-Gal4 > UASQ78; UASAtg8a* were the experimental genotypes. We observed that Q78 expression under *D42-Gal4* led to a significant reduction in average velocity in comparison to control. This defect was significantly rescued upon overexpression of Atg8a in the background of mutant Q78 under *D42-Gal4* [genotype, $F_{(2,117)} = 20.45$, $p < 0.0001$, ANOVA; D42/+ vs. Q78 ($p < 0.0001$), D42/+ vs. Atg8a; Q78 ($p = 0.0011$), Q78 vs. Atg8a; Q78 ($p = 0.0204$), Tukey's multiple comparison] (**Figure 5A**, right). Similarly, the total distance traveled by the larvae was also rescued on Atg8a overexpression [genotype, $F_{(2,117)} = 20.53$, $p < 0.0001$, ANOVA; D42/+ vs. Q78 ($p < 0.0001$), D42/+ vs. Atg8a; Q78 ($p = 0.0004$), Q78 vs. Atg8a; Q78 ($p = 0.0477$), Tukey's multiple comparison] (**Figure 5A**, left).

Since we observed a rescue in the larval crawling behavior upon overexpression of Atg8a, we wanted to understand if there were significant changes in the morphology and/or function of glutamatergic synapses as well. To answer this question, we imaged the FITC-HRP-labeled NMJs of muscle 6/7 and scored for aberrant bouton phenotype rescue upon overexpression of Atg8a in the background of Q78. We observed that the number of boutons per NMJ was significantly increased upon overexpression of Atg8a as compared to Q78-expressing larvae [genotype, $F_{(2,30)} = 3.730$, $p = 0.0080$, ANOVA; Q27 vs. Q78 ($p = 0.0003$), Q27 vs. Atg8a; Q78 ($p = 0.7325$), Q78 vs. Atg8a; Q78 ($p < 0.0001$), Tukey's multiple comparison) (**Figure 5B**, left). Furthermore, the NMJ arbor length was also increased significantly upon overexpression of Atg8a, comparable to controls [genotype, $F_{(2,42)} = 7.569$, $p = 0.0016$, ANOVA; Q27 vs. Q78 ($p = 0.0072$), Q27 vs. Atg8a; Q78 ($p = 0.6093$), Q78 vs. Atg8a; Q78 ($p = 0.0678$), Tukey's multiple comparison] (**Figure 5B**, right). The bouton area of NMJs in these Atg8a-overexpressed larvae showed a comparable area of boutons similar to controls in comparison to the increased bouton area of Q78-expressing larvae [genotype, $F_{(2,551)} = 77.17$, $p < 0.0001$, ANOVA; Q27 vs. Q78 ($p < 0.0001$), Q27 vs. Atg8a; Q78 ($p = 0.4190$), Q78 vs. Atg8a; Q78 ($p < 0.0001$), Tukey's multiple comparison) (**Figure 5B**, center). We next assessed the levels of Ref(2)P (fly ortholog of p62), a ubiquitin-binding scaffold protein involved in the capture and degradation of cargo, and a substrate of the autophagy pathway. We observed that, in larvae co-expressing Q78 and Atg8a, the intensity of p62 puncta was reduced compared to those expressing Q78 alone [$t_{(14)} = 3.289$, $p = 0.0054$, *t*-test] (**Supplementary Figure 3**), suggesting autophagy-dependent degradation of p62.

Altogether, these results suggest that overexpression of Atg8a in Q78 mutants significantly rescued the phenotypes observed both at the behavioral level and at the cellular level. Thus, we show that genetic overexpression of the core autophagy protein Atg8a has the potential to rescue behavioral and cellular defects arising out of glutamatergic synapse dysfunction in a *Drosophila* model of MJD.

DISCUSSION

Synapses are important communication centers of neuronal networks through which information in the form of electrical or chemical cues is transferred. Synaptic dysfunction is known to be an early sign of many neurodegenerative disorders, such as Alzheimer's, Parkinson's, Huntington's, and prion disease (Graveland et al., 1985; Kitamoto et al., 1992; Scheff and Price, 2003; Coleman et al., 2004; DiProspero et al., 2004; Compta and Revesz, 2021). Such dysfunction may be a result of various insults, including the accumulation of misfolded and aggregated proteins, thereby hampering the normal functioning of synapses (Scott et al., 2010; Zhou et al., 2017; Ghiglieri et al., 2018). Polyglutamine-(polyQ) expansion diseases are a group of neurodegenerative conditions, encompassing nine heritable genetic disorders. The pathogenicity of these diseases is attributed to unstable CAG trinucleotide repeats within protein-coding regions, resulting in the formation of polyQ repeat-containing proteins (Riley and Orr, 2006).

Various studies have shown the involvement of polyQ repeats in ATXN3 in the pathogenesis and disease progression of the central nervous system. However, peripheral nervous system dysfunction is relatively unexplored (Colomer Gould et al., 2007; Schmidt et al., 2019; Wiatr et al., 2021). Human neurodegenerative diseases have been modeled in relatively simpler invertebrates, such as *D. melanogaster* and

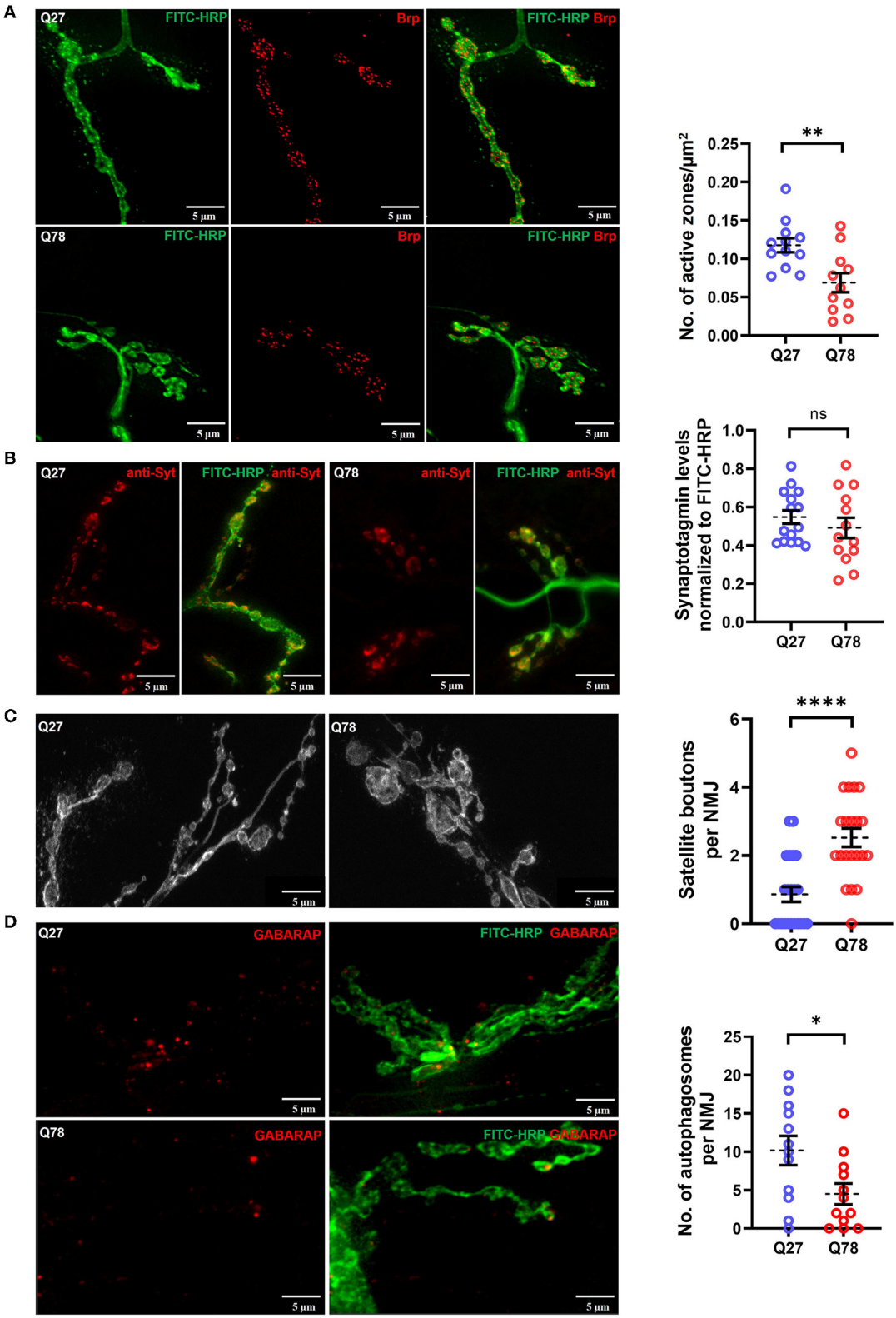

FIGURE 4 | Q78 expression in larval NMJs leads to functional changes in glutamatergic synapses. **(A)** A representative image of active zones marked by anti-Brp in the NMJs of the third-instar larva marked by FITC-HRP in Q27 and Q78-expressing larvae. Quantification of the number of active zones normalized to the area of NMJ. All quantifications were done on NMJs of muscle 6/7 of abdominal segments A4-A6. $n \geq 12$; Student's *t*-test; $^{**}p < 0.01$. An error bar represents mean ±

(Continued)

FIGURE 4 | SEM. **(B)** Representative images of synaptotagmin (Syt) intensity in the third instar larval NMJ marked by FITC-HRP in Q27 and Q78-expressing larvae and quantification of Syt signal intensity in the boutons. All quantifications were done on NMJs of muscle 6/7 of abdominal segments A4-A6. $n \geq 15$; Student's *t*-test; ns, non-significant. An error bar represents mean ± SEM. **(C)** Representative images depicting satellite boutons budding from the main boutons in NMJs with Q78 expression along with quantification of the number of satellite boutons per NMJ. All quantifications were done on NMJs of muscle 6/7 of abdominal segments A4-A6. $n > 25$; Student's *t*-test; $^{****}p < 0.0001$. An error bar represents mean ± SEM. **(D)** The figure depicts the number of autophagosomes marked by anti-GABARAP in NMJs stained by FITC-HRP in Q27- and Q78-expressing larvae. All quantifications were done on NMJs of muscle 6/7 of abdominal segments A4-A6. $n > 12$; Student's *t*-test; $^{*}p < 0.05$. An error bar represents mean ± SEM.

Caenorhabditis elegans, as these systems serve as excellent *in vivo* models to understand mechanisms of disease pathology, owing to homology to the human genome, and the vast number of tools available to genetically manipulate these organisms (Lu and Vogel, 2009; Caldwell et al., 2020). Using *Drosophila* as the model organism, Warrick et al. showed that targeted expression of the mutant Ataxin-3 in different cell types led to neurodegeneration. Particularly, neuronal cells were most susceptible to degeneration (Warrick et al., 1998). While their study explored the effects of expressing MJDtr-Q78 under different *GAL4* drivers (*gmr-GAL4, elav-GAL4, 24B-Gal4, and dpp-GAL4*), in our study, we focused on the dysfunction of synapses associated with neurodegenerative diseases. We used this model as a tool to understand synaptopathy associated with Spinocerebellar Ataxia Type-3, with a particular focus to assess if modulating proteostatic machinery in the synapses can lead to a rescue of the defects. While expressing MJDtr-Q78 (strong) under *elav-GAL4* is lethal, our study has utilized targeted expression of MJDtr-Q78 (strong) in the motor neurons. These flies do not show lethality in the early stages, allowing us to utilize larval NMJs as model glutamatergic synapses to understand the dysfunction associated with SCA3, thus enabling a narrow dissection of behavioral and physiological defects and their causation.

Behavioral and Physiological Functions Are Affected Due to Expression of Pathogenic Q78 in Glutamatergic Motor Circuits

In our study, we were able to characterize the defects at the behavioral level in the larval and adult stages. With the well-established locomotion assay, we could characterize various aspects of locomotory defects in the larval stage as well as other behavioral defects associated with mutant Q78 expression in motor neurons in the adult stage. Our results are in line with previous studies, which have shown similar behavioral defects in other neurodegenerative models of *Drosophila* larvae and adults, owing to aggregate protein expression and, hence, cellular malfunctioning (Mershin et al., 2004; Mhatre et al., 2014; Wu et al., 2017; Delfino et al., 2020).

Synapse Morphology and Health Are Compromised by the Presence of Pathogenic ATXN3 in Motor Neuron Soma

The rhythmic movements of the larvae have been attributed to concerted actions of motor neurons, sensory neurons, and interneurons (Kohsaka et al., 2012). Indeed, electrophysiological recordings from the larval NMJs during wave contractions of the larval body have shown concurrent rhythmic patterns (Fox et al., 2006; Imlach et al., 2012; Ruiz et al., 2013). Thus, any dysfunction in this circuitry can lead to locomotion impairment. We explored the possibility of glutamatergic synapses becoming dysfunctional upon expression of Q78. We found that mutant Q78 accumulated as aggregates in the ventral nerve cord (VNC) unlike in controls. This finding suggests the possibility of the truncated form of MJDtrQ78 containing 78 polyQ repeats being retained in the nucleus, as reported by several groups (Lee et al., 2004; Bichelmeier et al., 2007; Macedo-Ribeiro et al., 2009). Accumulation of mutant Q78 led to morphological changes in the NMJs. A possible reason could be relative transcriptional changes in proteins or modification in the levels of proteins/phosphoproteins required for synapse maintenance and/or functioning, as has been reported by various groups for ATXN3 models (Ramani et al., 2017; Wiatr et al., 2021). Moreover, the heterogeneity in terms of defects in the NMJs might be attributed to differences in expression of the driver *D42-Gal4*, which would require further investigation.

It is known that morphological changes in the NMJs are often correlated with functional defects as well, which might lead to behavioral deficits (Sleigh et al., 2014; Cappello and Francolini, 2017). We further assessed for functional defects in the boutons of NMJs. Synaptic vesicles loaded with neurotransmitters are brought close to the presynaptic membrane of the *Drosophila* NMJ by the concerted actions of presynaptic proteins, such as Bruchpilot (Brp) and another vesicular SNARE, Synaptotagmin (Syt), thus leading to the docking and fusion of these vesicles and concomitant release of glutamate (Quiñones-Frías and Littleton, 2021; Sauvola and Littleton, 2021). Brp and Syt are also essential at the *Drosophila* neuromuscular junctions for the clustering of calcium channels (Kittel et al., 2006; Wagh et al., 2006). *Brp* null mutants (brp^{69}) have been shown to be defective in the fusion of glutamate-containing neurotransmitter vesicles in *Drosophila* NMJs (Paul et al., 2015). Thus, any changes in the levels of Brp and Syt may alter the functioning of glutamatergic synapses. Our results showed that Q78 expression in larval motor neurons led to a reduction in Brp-containing active zones but no change in Syt levels. The abundance of Brp positively correlates with neurotransmitter release (Matz et al., 2010; Weyhersmüller et al., 2011; Ehmann et al., 2014). However, in our study, it might be possible that the mutant Q78 NMJs are defective in releasing glutamate, thus correlating with behavioral deficits.

Satellite boutons are often characteristic of endocytic mutants, such as *endo* as well as mutants of the BMP signaling pathway and actin regulation. These supernumerary boutons are usually functional boutons (unlike other overgrowth phenotypes, such as "ghost" boutons) since they contain Brp and Synapsin, which

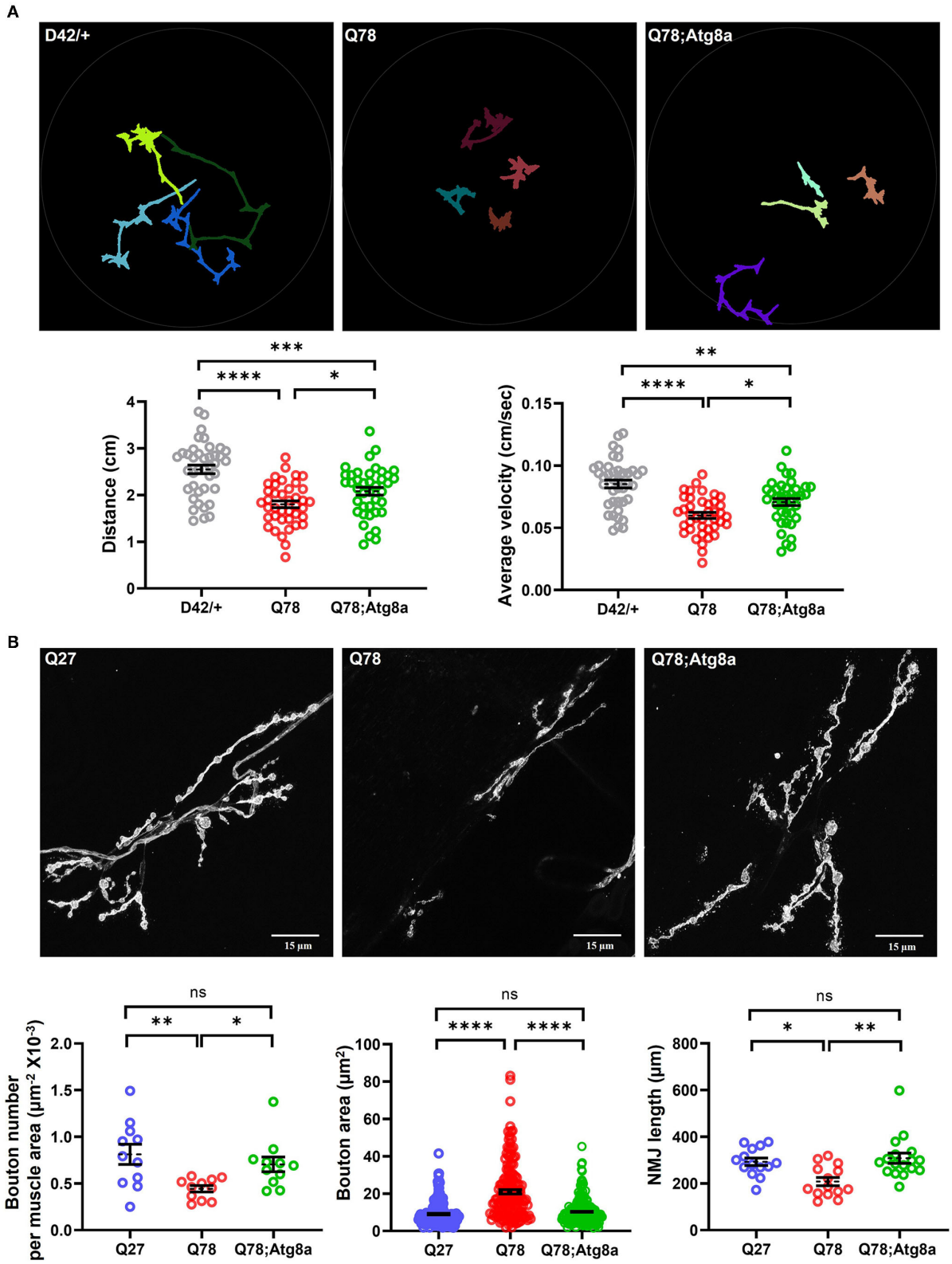

FIGURE 5 | The behavioral and morphological defects in larval glutamatergic synapses are rescued upon Atg8a overexpression. **(A)** Path diagrams for indicated larvae monitored in 1% charcoal agar plates and quantification of total distance traversed and average velocity of the driver-only control larvae (D42/+) vs. pathogenic Q78 and rescue Q78; Atg8a larvae. $n = 40$ larvae; one-way ANOVA; *post-hoc* Tukey's multiple comparison test; $^{*}p < 0.05$; $^{**}p < 0.01$; $^{***}p < 0.001$; $^{****}p < 0.0001$;

(Continued)

FIGURE 5 | ns, non-significant. Error bars represent mean ± SEM. **(B)** Representative images of NMJs of indicated larvae from muscle 6/7 of abdominal hemisegment A2. Quantification of the number of boutons per muscle area ($n > 11$ NMJs), bouton area ($n > 160$ boutons), and NMJ arbor length ($n > 12$ NMJs). Quantifications for the number of boutons per area of muscle were done on hemisegment A2. Quantifications for the bouton area and NMJ arbor length were done on NMJs of muscle 6/7 of abdominal segments A4-A6. One-way ANOVA; *post-hoc* Tukey's multiple comparison test; $^{*}p < 0.05$, $^{**}p < 0.01$, $^{***}p < 0.001$, $^{****}p < 0.0001$. ns, non-significant. Error bars represent mean ± SEM.

are in apposition to postsynaptic GluR and Dlg (Dickman et al., 2006). Our observation of the appearance of numerous satellite boutons in Q78 mutants might indicate defects in the endocytic pathway as well. The appearance of satellite boutons could also be a compensatory mechanism against functional defects in the NMJs. Future studies would be required to understand the underlying cause. Our results thus show changes in the physiology and health of glutamatergic synapses in mutant Q78 *Drosophila* NMJs. Such changes in NMJs have been previously reported in several neurodegenerative disorders across various models (Menalled et al., 2003; Dupuis and Loeffler, 2009; Steinert et al., 2012; Pratt et al., 2015; Rodríguez Cruz et al., 2020; Alhindi et al., 2021).

Harnessing Proteostatic Pathways Can Mitigate the Toxicity of Malformed ATXN3

In synapses, fast protein turnover is a prerequisite for the proper functioning of synaptic vesicle cycles, which might exceed 100 Hz in some cases (de Kock and Sakmann, 2008). Such a turnover might not be possible in cases of long motor neurons where the main site of protein synthesis (soma) is often separated from the distal ends (synapses) by over a meter in length. Thus, local proteostatic mechanisms, such as autophagy and the ubiquitin-proteasome system, are often required to mediate the fast turnover and maintenance of these synapses (Ding and Shen, 2008; Gorenberg and Chandra, 2017; Vijayan and Verstreken, 2017; Andres-Alonso et al., 2021). Any impairment in these pathways, for example, due to aggregate accumulation as reported in the case of many neurodegenerative disorders, can lead to synaptopathies (Bridi and Hirth, 2018). Studies pertaining to the impaired autophagy pathway in MJD have shed light upon the role of ATXN3 as a regulator of this pathway. Ashkenazi and colleagues have shown that the polyQ domain of wild-type ATXN3 is important for regulating autophagy by interacting with beclin1, preventing its degradation *via* UPS. However, other polyQ proteins or mutant ATXN3 itself, harboring long polyQ repeats, competes for this interaction of wild-type ATXN3 with beclin1, thus leading to impairment in autophagy by mediating the degradation of beclin1 (Ashkenazi et al., 2017). We also detected impairment in the autophagy pathway as indicated by a reduction in autophagosome numbers in fly NMJs. Future studies will reveal more details of the mechanism of impairment upon Q78 expression in the NMJs. Several previous studies have suggested that restoring the proteostasis imbalance *via* genetic or pharmacological means can have therapeutic value (Corti et al., 2020; Joshi et al., 2020; Bastien et al., 2021). Overexpression of Atg8a has been shown to promote longevity and reduce age-induced oxidative stress in adult flies (Simonsen et al., 2008). Therefore, we examined whether overexpression of Atg8a in *Drosophila* motor neurons could suppress synaptic dysfunction caused by the presence of mutant ATXN3. Indeed, our results indicate that tissue-specific overexpression of one of the core autophagy proteins, Atg8a, in the motor neurons of *Drosophila* facilitated a rescue in morphological and functional defects in the glutamatergic synapses of ATXN3 models, which is further recapitulated in the improvement of behavioral defects at the larval stage. The NMJ morphology is rescued in terms of bouton number. However, we do see a satellite bouton phenotype similar to Q78, which might explain the partial rescue in the locomotory behavior of the larvae. Co-expression of Atg8a with Q78 also resulted in lower levels of Ref(2)P in the NMJs, implicating the involvement of the autophagy pathway.

Our study sheds light on the pathogenesis of glutamatergic synapses *in vivo* in MJD. The defects observed in the glutamatergic synapses at the cellular and behavioral levels are consistent with other aggregate-induced neurodegenerative models (Jacobsen et al., 2006; Kohsaka et al., 2012; Hall et al., 2015; Maulik et al., 2017; Rattray et al., 2017; Caldwell et al., 2020). The genetic amenability of this model allows for quick forward genetic and modifier screens to identify potential mediators of synaptopathies. Furthermore, the observed rescue of defects demonstrates the usefulness of this model in screening for pharmacological and genetic candidates with therapeutic potential for the treatment of synaptopathies.

DATA AVAILABILITY STATEMENT

The raw data supporting the conclusions of this article will be made available by the authors, without undue reservation.

AUTHOR CONTRIBUTIONS

AC contributed to the conceptualization of the original study, performed the larval behavioral experiments, larval NMJ dissections, larval NMJ image acquisition, analysis, and manuscript writing. AS performed adult fly experiments, larval brain dissection, image acquisition of larval brain, statistical analysis, and data curation. VS and RM conceptualized and supervised the study. All authors contributed to the article and approved the submitted version.

FUNDING

This work was supported by the Department of Biotechnology (DBT) grant in Life Sciences Research, Education and Training at JNCASR (BT/INF/22/SP27679/2018), the Intramural funds from

JNCASR to RM and VS, and the JNCASR doctoral fellowships to AC and AS.

ACKNOWLEDGMENTS

We are thankful to the members of the Chronobiology and Behavioral Neurogenetics Laboratory (JNCASR), the Autophagy Laboratory (JNCASR), and Aparna Hebbar for their input and critical review of the manuscript. We are thankful to Rutvij Kulkarni for his help with the cartoons and statistical analyses.

SUPPLEMENTARY MATERIAL

The Supplementary Material for this article can be found online at: https://www.frontiersin.org/articles/10.3389/fnmol.2022.842772/full#supplementary-material

REFERENCES

Alhindi, A., Boehm, I., and Chaytow, H. (2021). Small junction, big problems: neuromuscular junction pathology in mouse models of amyotrophic lateral sclerosis (ALS). *J. Anat*. doi: 10.1111/joa.13463. [Epub ahead of print].

Alves, S., Régulier, E., Nascimento-Ferreira, I., Hassig, R., Dufour, N., Koeppen, A., et al. (2008). Striatal and nigral pathology in a lentiviral rat model of Machado-Joseph disease. *Hum. Mol. Genet.* 17, 2071–2083. doi: 10.1093/hmg/ddn106

Andres-Alonso, M., Kreutz, M. R., and Karpova, A. (2021). Autophagy and the endolysosomal system in presynaptic function. *Cell. Mol. Life Sci.* 78, 2621–2639. doi: 10.1007/s00018-020-03722-5

Ashkenazi, A., Bento, C. F., Ricketts, T., Vicinanza, M., Siddiqi, F., Pavel, M., et al. (2017). Polyglutamine tracts regulate beclin 1-dependent autophagy. *Nature* 545, 108–111. doi: 10.1038/nature22078

Bae, J. R., and Kim, S. H. (2017). Synapses in neurodegenerative diseases. *BMB Rep.* 50, 237–246. doi: 10.5483/BMBRep.2017.50.5.038

Bastien, J., Menon, S., Messa, M., and Nyfeler, B. (2021). Molecular targets and approaches to restore autophagy and lysosomal capacity in neurodegenerative disorders. *Mol. Aspects Med.* 82, 101018. doi: 10.1016/j.mam.2021.101018

Bichelmeier, U., Schmidt, T., Hübener, J., Boy, J., Rüttiger, L., Häbig, K., et al. (2007). Nuclear localization of ataxin-3 is required for the manifestation of symptoms in SCA3: *in vivo* evidence. *J. Neurosci.* 27, 7418–7428. doi: 10.1523/JNEUROSCI.4540-06.2007

Brand, A. H., and Perrimon, N. (1993). Targeted gene expression as a means of altering cell fates and generating dominant phenotypes. *Development* 118, 401–415. doi: 10.1242/dev.118.2.401

Breuer, P., Haacke, A., Evert, B. O., and Wüllner, U. (2010). Nuclear aggregation of polyglutamine-expanded ataxin-3: fragments escape the cytoplasmic quality control. *J. Biol. Chem.* 285, 6532–6537. doi: 10.1074/jbc.M109.036335

Bridi, J. C., and Hirth, F. (2018). Mechanisms of α-Synuclein induced synaptopathy in Parkinson's Disease. *Front. Neurosci.* 12, 80. doi: 10.3389/fnins.2018.00080

Budnik, V. (1996). Synapse maturation and structural plasticity at *Drosophila* neuromuscular junctions. *Curr. Opin. Neurobiol.* 6, 858–867. doi: 10.1016/S0959-4388(96)80038-9

Caldwell, K. A., Willicott, C. W., and Caldwell, G. A. (2020). Modeling neurodegeneration in *Caenorhabditis elegans*. *Dis. Model. Mech.* 13, dmm046110. doi: 10.1242/dmm.046110

Cappello, V., and Francolini, M. (2017). Neuromuscular junction dismantling in Amyotrophic Lateral Sclerosis. *Int. J. Mol. Sci.* 18, 2092. doi: 10.3390/ijms18102092

Chai, Y., Koppenhafer, S. L., Shoesmith, S. J., Perez, M. K., and Paulson, H. L. (1999). Evidence for proteasome involvement in polyglutamine disease: localization to nuclear inclusions in SCA3/MJD and suppression of polyglutamine aggregation *in vitro*. *Hum. Mol. Genet.* 8, 673–682. doi: 10.1093/hmg/8.4.673

Charif, S. E., Vassallu, M. F., Salvañal, L., and Igaz, L. M. (2022). Protein synthesis modulation as a therapeutic approach for amyotrophic lateral sclerosis and frontotemporal dementia. *Neural Regen. Res.* 17, 1423–1430. doi: 10.4103/1673-5374.330593

Chou, V. T., Johnson, S. A., and Van Vactor, D. (2020). Synapse development and maturation at the *Drosophila* neuromuscular junction. *Neural Dev.* 15, 11. doi: 10.1186/s13064-020-00147-5

Coleman, P., Federoff, H., and Kurlan, R. (2004). A focus on the synapse for neuroprotection in Alzheimer disease and other dementias. *Neurology* 63, 1155–1162. doi: 10.1212/01.WNL.0000140626.48118.0A

Colomer Gould, V. F. (2005). Mouse models of Machado-Joseph disease and other polyglutamine spinocerebellar ataxias. *NeuroRx* 2, 480–483. doi: 10.1602/neurorx.2.3.480

Colomer Gould, V. F., Goti, D., Pearce, D., Gonzalez, G. A., Gao, H., Bermudez de Leon, M., et al. (2007). A mutant ataxin-3 fragment results from processing at a site N-terminal to amino acid 190 in brain of Machado-Joseph disease-like transgenic mice. *Neurobiol. Dis.* 27, 362–369. doi: 10.1016/j.nbd.2007.06.005

Compta, Y., and Revesz, T. (2021). Neuropathological and biomarker findings in Parkinson's disease and Alzheimer's disease: from protein aggregates to synaptic dysfunction. *J. Parkinsons. Dis.* 11, 107–121. doi: 10.3233/JPD-202323

Corti, O., Blomgren, K., Poletti, A., and Beart, P. M. (2020). Autophagy in neurodegeneration: new insights underpinning therapy for neurological diseases. *J. Neurochem.* 154, 354–371. doi: 10.1111/jnc.15002

de Kock, C. P., and Sakmann, B. (2008). High frequency action potential bursts (>or= 100 Hz) in L2/3 and L5B thick tufted neurons in anaesthetized and awake rat primary somatosensory cortex. *J. Physiol.* 586, 3353–3364. doi: 10.1113/jphysiol.2008.155580

Delfino, L., Mason, R. P., Kyriacou, C. P., Giorgini, F., and Rosato, E. (2020). Rab8 promotes mutant HTT aggregation, reduces neurodegeneration, and ameliorates behavioural alterations in a *Drosophila*model of Huntington's disease. *J. Huntingtons. Dis.* 9, 253–263. doi: 10.3233/JHD-200411

Dickman, D. K., Lu, Z., Meinertzhagen, I. A., and Schwarz, T. L. (2006). Altered synaptic development and active zone spacing in endocytosis mutants. *Curr. Biol.* 16, 591–598. doi: 10.1016/j.cub.2006.02.058

Ding, M., and Shen, K. (2008). The role of the ubiquitin proteasome system in synapse remodeling and neurodegenerative diseases. *Bioessays* 30, 1075–1083. doi: 10.1002/bies.20843

DiProspero, N. A., Chen, E. Y., Charles, V., Plomann, M., Kordower, J. H., and Tagle, D. A. (2004). Early changes in Huntington's disease patient brains involve alterations in cytoskeletal and synaptic elements. *J. Neurocytol.* 33, 517–533. doi: 10.1007/s11068-004-0514-8

Dupuis, L., and Loeffler, J. P. (2009). Neuromuscular junction destruction during amyotrophic lateral sclerosis: insights from transgenic models. *Curr. Opin. Pharmacol.* 9, 341–346. doi: 10.1016/j.coph.2009.03.007

Ehmann, N., van de Linde, S., Alon, A., Ljaschenko, D., Keung, X. Z., Holm, T., et al. (2014). Quantitative super-resolution imaging of Bruchpilot distinguishes active zone states. *Nat. Commun.* 5, 4650. doi: 10.1038/ncomms5650

Fox, L. E., Soll, D. R., and Wu, C. F. (2006). Coordination and modulation of locomotion pattern generators in *Drosophila* larvae: effects of altered biogenic amine levels by the tyramine beta hydroxlyase mutation. *J. Neurosci.* 26, 1486–1498. doi: 10.1523/JNEUROSCI.4749-05.2006

Fujigasaki, H., Uchihara, T., Koyano, S., Iwabuchi, K., Yagishita, S., Makifuchi, T., et al. (2000). Ataxin-3 is translocated into the nucleus for the formation of intranuclear inclusions in normal and Machado-Joseph disease brains. *Exp. Neurol.* 165, 248–256. doi: 10.1006/exnr.2000.7479

Ghiglieri, V., Calabrese, V., and Calabresi, P. (2018). Alpha-Synuclein: from early synaptic dysfunction to neurodegeneration. *Front. Neurol.* 9, 295. doi: 10.3389/fneur.2018.00295

Gorenberg, E. L., and Chandra, S. S. (2017). The role of co-chaperones in synaptic proteostasis and neurodegenerative disease. *Front. Neurosci.* 11, 248. doi: 10.3389/fnins.2017.00248

Goti, D., Katzen, S. M., Mez, J., Kurtis, N., Kiluk, J., Ben-Haïem, L., et al. (2004). A mutant ataxin-3 putative-cleavage fragment in brains of Machado-Joseph disease patients and transgenic mice is cytotoxic above a critical concentration. *J. Neurosci.* 24, 10266–10279. doi: 10.1523/JNEUROSCI.2734-04.2004

Graveland, G. A., Williams, R. S., and DiFiglia, M. (1985). Evidence for degenerative and regenerative changes in neostriatal spiny neurons in Huntington's disease. *Science* 227, 770–773. doi: 10.1126/science.3155875

Gustafson, K., and Boulianne, G. L. (1996). Distinct expression patterns detected within individual tissues by the GAL4 enhancer trap technique. *Genome* 39, 174–182. doi: 10.1139/g96-023

Hall, K., Yang, S., Sauchanka, O., Spillantini, M. G., and Anichtchik, O. (2015). Behavioural deficits in transgenic mice expressing human truncated (1-120 amino acid) alpha-synuclein. *Exp. Neurol.* 264, 8–13. doi: 10.1016/j.expneurol.2014.11.003

Hanamsagar, R., and Bilbo, S. D. (2016). Sex differences in neurodevelopmental and neurodegenerative disorders: focus on microglial function and neuroinflammation during development. *J. Steroid Biochem. Mol. Biol.* 160, 127–133. doi: 10.1016/j.jsbmb.2015.09.039

Hayashi, M., Kobayashi, K., and Furuta, H. (2003). Immunohistochemical study of neuronal intranuclear and cytoplasmic inclusions in Machado-Joseph disease. *Psychiatry Clin. Neurosci.* 57, 205–213. doi: 10.1046/j.1440-1819.2003.01102.x

Hipp, M. S., Park, S. H., and Hartl, F. U. (2014). Proteostasis impairment in protein-misfolding and -aggregation diseases. *Trends Cell Biol.* 24, 506–514. doi: 10.1016/j.tcb.2014.05.003

Hussain, N. K., Diering, G. H., Sole, J., Anggono, V., and Huganir, R. L. (2014). Sorting Nexin 27 regulates basal and activity-dependent trafficking of AMPARs. *Proc. Natl. Acad. Sci. U.S.A.* 111, 11840–11845. doi: 10.1073/pnas.1412415111

Imlach, W. L., Beck, E. S., Choi, B. J., Lotti, F., Pellizzoni, L., and McCabe, B. D. (2012). SMN is required for sensory-motor circuit function in *Drosophila*. *Cell* 151, 427–439. doi: 10.1016/j.cell.2012.09.011

Jacobsen, J. S., Wu, C. C., Redwine, J. M., Comery, T. A., Arias, R., Bowlby, M., et al. (2006). Early-onset behavioral and synaptic deficits in a mouse model of Alzheimer's disease. *Proc. Natl. Acad. Sci. U.S.A.* 103, 5161–5166. doi: 10.1073/pnas.0600948103

Joshi, V., Upadhyay, A., Prajapati, V. K., and Mishra, A. (2020). How autophagy can restore proteostasis defects in multiple diseases? *Med. Res. Rev.* 40, 1385–1439. doi: 10.1002/med.21662

Kashima, R., Redmond, P. L., Ghatpande, P., Roy, S., Kornberg, T. B., Hanke, T., et al. (2017). Hyperactive locomotion in a *Drosophila* model is a functional readout for the synaptic abnormalities underlying fragile X syndrome. *Sci. Signal.* 10, eaai8133. doi: 10.1126/scisignal.aai8133

Kitamoto, T., Shin, R. W., Doh-ura, K., Tomokane, N., Miyazono, M., Muramoto, T., et al. (1992). Abnormal isoform of prion proteins accumulates in the synaptic structures of the central nervous system in patients with Creutzfeldt-Jakob disease. *Am. J. Pathol.* 140, 1285–1294.

Kittel, R. J., and Heckmann, M. (2016). Synaptic vesicle proteins and active zone plasticity. *Front. Synaptic Neurosci.* 8, 8. doi: 10.3389/fnsyn.2016.00008

Kittel, R. J., Wichmann, C., Rasse, T. M., Fouquet, W., Schmidt, M., Schmid, A., et al. (2006). Bruchpilot promotes active zone assembly, Ca2+ channel clustering, and vesicle release. *Science* 312, 1051–1054. doi: 10.1126/science.1126308

Klaips, C. L., Jayaraj, G. G., and Hartl, F. U. (2018). Pathways of cellular proteostasis in aging and disease. *J. Cell Biol.* 217, 51–63. doi: 10.1083/jcb.201709072

Koeppen, A. H. (2018). The neuropathology of Spinocerebellar Ataxia Type 3/Machado-Joseph disease. *Adv. Exp. Med. Biol.* 1049, 233–241. doi: 10.1007/978-3-319-71779-1_11

Kohsaka, H., Okusawa, S., Itakura, Y., Fushiki, A., and Nose, A. (2012). Development of larval motor circuits in *Drosophila*. *Dev. Growth Differ.* 54, 408–419. doi: 10.1111/j.1440-169X.2012.01347.x

Konno, A., Shuvaev, A. N., Miyake, N., Miyake, K., Iizuka, A., Matsuura, S., et al. (2014). Mutant ataxin-3 with an abnormally expanded polyglutamine chain disrupts dendritic development and metabotropic glutamate receptor signaling in mouse cerebellar Purkinje cells. *Cerebellum* 13, 29–41. doi: 10.1007/s12311-013-0516-5

Kuijpers, M., Kochlamazashvili, G., Stumpf, A., Puchkov, D., Swaminathan, A., Lucht, M. T., et al. (2021). Neuronal autophagy regulates presynaptic neurotransmission by controlling the axonal endoplasmic reticulum. *Neuron* 109, 299-313.e299. doi: 10.1016/j.neuron.2020.10.005

Lamark, T., and Johansen, T. (2012). Aggrephagy: selective disposal of protein aggregates by macroautophagy. *Int. J. Cell Biol.* 2012, 736905. doi: 10.1155/2012/736905

Lee, W. C., Yoshihara, M., and Littleton, J. T. (2004). Cytoplasmic aggregates trap polyglutamine-containing proteins and block axonal transport in a *Drosophila* model of Huntington's disease. *Proc. Natl. Acad. Sci. U.S.A.* 101, 3224–3229. doi: 10.1073/pnas.0400243101

Lepeta, K., Lourenco, M. V., Schweitzer, B. C., Martino Adami, P. V., Banerjee, P., Catuara-Solarz, S., et al. (2016). Synaptopathies: synaptic dysfunction in neurological disorders - a review from students to students. *J. Neurochem.* 138, 785–805. doi: 10.1111/jnc.13713

Li, J. Y., Plomann, M., and Brundin, P. (2003). Huntington's disease: a synaptopathy? *Trends Mol. Med.* 9, 414–420. doi: 10.1016/j.molmed.2003.08.006

Lu, B., and Vogel, H. (2009). *Drosophila* models of neurodegenerative diseases. *Annu. Rev. Pathol.* 4, 315–342. doi: 10.1146/annurev.pathol.3.121806.151529

Macedo-Ribeiro, S., Cortes, L., Maciel, P., and Carvalho, A. L. (2009). Nucleocytoplasmic shuttling activity of ataxin-3. *PLoS ONE* 4, e5834. doi: 10.1371/journal.pone.0005834

Maciel, P., Gaspar, C., DeStefano, A. L., Silveira, I., Coutinho, P., Radvany, J., et al. (1995). Correlation between CAG repeat length and clinical features in Machado-Joseph disease. *Am. J. Hum. Genet.* 57, 54–61.

Maday, S., and Holzbaur, E. L. (2014). Autophagosome biogenesis in primary neurons follows an ordered and spatially regulated pathway. *Dev. Cell* 30, 71–85. doi: 10.1016/j.devcel.2014.06.001

Maday, S., and Holzbaur, E. L. (2016). Compartment-specific regulation of autophagy in primary neurons. *J. Neurosci.* 36, 5933–5945. doi: 10.1523/JNEUROSCI.4401-15.2016

Matz, J., Gilyan, A., Kolar, A., McCarvill, T., and Krueger, S. R. (2010). Rapid structural alterations of the active zone lead to sustained changes in neurotransmitter release. *Proc. Natl. Acad. Sci. U.S.A.* 107, 8836–8841. doi: 10.1073/pnas.0906087107

Maulik, M., Mitra, S., Bult-Ito, A., Taylor, B. E., and Vayndorf, E. M. (2017). Behavioral phenotyping and pathological indicators of Parkinson's Disease in *C. elegansmodels. Front. Genet.* 8, 77. doi: 10.3389/fgene.2017.00077

McLoughlin, H. S., Moore, L. R., and Paulson, H. L. (2020). Pathogenesis of SCA3 and implications for other polyglutamine diseases. *Neurobiol. Dis.* 134, 104635. doi: 10.1016/j.nbd.2019.104635

Menalled, L. B., Sison, J. D., Dragatsis, I., Zeitlin, S., and Chesselet, M. F. (2003). Time course of early motor and neuropathological anomalies in a knock-in mouse model of Huntington's disease with 140 CAG repeats. *J. Comp. Neurol.* 465, 11–26. doi: 10.1002/cne.10776

Menon, K. P., Carrillo, R. A., and Zinn, K. (2013). Development and plasticity of the *Drosophila* larval neuromuscular junction. *Wiley Interdiscip. Rev. Dev. Biol.* 2, 647–670. doi: 10.1002/wdev.108

Mershin, A., Pavlopoulos, E., Fitch, O., Braden, B. C., Nanopoulos, D. V., and Skoulakis, E. M. (2004). Learning and memory deficits upon TAU accumulation in *Drosophila* mushroom body neurons. *Learn. Mem.* 11, 277–287. doi: 10.1101/lm.70804

Mhatre, S. D., Satyasi, V., Killen, M., Paddock, B. E., Moir, R. D., Saunders, A. J., et al. (2014). Synaptic abnormalities in a *Drosophila* model of Alzheimer's disease. *Dis. Model. Mech.* 7, 373–385. doi: 10.1242/dmm.012104

Nassif, M., and Hetz, C. (2012). Autophagy impairment: a crossroad between neurodegeneration and tauopathies. *BMC Biol.* 10, 78. doi: 10.1186/1741-7007-10-78

Nguyen, H. P., Hübener, J., Weber, J. J., Grueninger, S., Riess, O., and Weiss, A. (2013). Cerebellar soluble mutant ataxin-3 level decreases during disease progression in Spinocerebellar Ataxia Type 3 mice. *PLoS ONE* 8, e62043. doi: 10.1371/journal.pone.0062043

Nicastro, G., Todi, S. V., Karaca, E., Bonvin, A. M., Paulson, H. L., and Pastore, A. (2010). Understanding the role of the Josephin domain in the PolyUb binding and cleavage properties of ataxin-3. *PLoS ONE* 5, e12430. doi: 10.1371/journal.pone.0012430

Nóbrega, C., Nascimento-Ferreira, I., Onofre, I., Albuquerque, D., Conceição, M., Déglon, N., et al. (2013). Overexpression of mutant ataxin-3 in mouse cerebellum induces ataxia and cerebellar neuropathology. *Cerebellum* 12, 441–455. doi: 10.1007/s12311-012-0432-0

O'Connor-Giles, K. M., and Ganetzky, B. (2008). Satellite signaling at synapses. *Fly* 2, 259–261. doi: 10.4161/fly.7133

Ordonez, M. P., Roberts, E. A., Kidwell, C. U., Yuan, S. H., Plaisted, W. C., and Goldstein, L. S. (2012). Disruption and therapeutic rescue of autophagy in a human neuronal model of Niemann Pick type C1. *Hum. Mol. Genet.* 21, 2651–2662. doi: 10.1093/hmg/dds090

Paul, M. M., Pauli, M., Ehmann, N., Hallermann, S., Sauer, M., Kittel, R. J., et al. (2015). Bruchpilot and Synaptotagmin collaborate to drive rapid glutamate release and active zone differentiation. *Front. Cell. Neurosci.* 9, 29. doi: 10.3389/fncel.2015.00029

Paulson, H. (2012). Machado-Joseph disease/spinocerebellar ataxia type 3. *Handb. Clin. Neurol.* 103, 437–449. doi: 10.1016/B978-0-444-51892-7.00027-9

Piscopo, P., Bellenghi, M., Manzini, V., Crestini, A., Pontecorvi, G., Corbo, M., et al. (2021). A sex perspective in neurodegenerative diseases: microRNAs as possible peripheral biomarkers. *Int. J. Mol. Sci.* 22, 4423. doi: 10.3390/ijms22094423

Pratt, S. J. P., Valencia, A. P., Le, G. K., Shah, S. B., and Lovering, R. M. (2015). Pre- and postsynaptic changes in the neuromuscular junction in dystrophic mice. *Front. Physiol.* 6, 252. doi: 10.3389/fphys.2015.00252

Quiñones-Frías, M. C., and Littleton, J. T. (2021). Function of *Drosophila* synaptotagmins in membrane trafficking at synapses. *Cell. Mol. Life Sci.* 78, 4335–4364. doi: 10.1007/s00018-021-03788-9

Ramani, B., Panwar, B., Moore, L. R., Wang, B., Huang, R., Guan, Y., et al. (2017). Comparison of spinocerebellar ataxia type 3 mouse models identifies early gain-of-function, cell-autonomous transcriptional changes in oligodendrocytes. *Hum. Mol. Genet.* 26, 3362–3374. doi: 10.1093/hmg/ddx224

Rattray, I., Smith, E. J., Crum, W. R., Walker, T. A., Gale, R., Bates, G. P., et al. (2017). Correlations of behavioral deficits with brain pathology assessed through longitudinal MRI and histopathology in the HdhQ150/Q150 mouse model of Huntington's Disease. *PLoS ONE* 12, e0168556. doi: 10.1371/journal.pone.0168556

Ravikumar, B., Duden, R., and Rubinsztein, D. C. (2002). Aggregate-prone proteins with polyglutamine and polyalanine expansions are degraded by autophagy. *Hum. Mol. Genet.* 11, 1107–1117. doi: 10.1093/hmg/11.9.1107

Riley, B. E., and Orr, H. T. (2006). Polyglutamine neurodegenerative diseases and regulation of transcription: assembling the puzzle. *Genes Dev.* 20, 2183–2192. doi: 10.1101/gad.1436506

Risse, B., Berh, D., Otto, N., Klämbt, C., and Jiang, X. (2017). FIMTrack: An open source tracking and locomotion analysis software for small animals. *PLoS Comput. Biol.* 13, e1005530. doi: 10.1371/journal.pcbi.1005530

Rodríguez Cruz, P. M., Cossins, J., Beeson, D., and Vincent, A. (2020). The neuromuscular junction in health and disease: molecular mechanisms governing synaptic formation and homeostasis. *Front. Mol. Neurosci.* 13, 610964. doi: 10.3389/fnmol.2020.610964

Rubinsztein, D. C. (2006). The roles of intracellular protein-degradation pathways in neurodegeneration. *Nature* 443, 780–786. doi: 10.1038/nature05291

Ruiz, S., Ferreiro, M. J., Menhert, K. I., Casanova, G., Olivera, A., and Cantera, R. (2013). Rhythmic changes in synapse numbers in *Drosophila melanogaster* motor terminals. *PLoS ONE* 8, e67161. doi: 10.1371/journal.pone.0067161

Sauvola, C. W., and Littleton, J. T. (2021). SNARE regulatory proteins in synaptic vesicle fusion and recycling. *Front. Mol. Neurosci.* 14, 733138. doi: 10.3389/fnmol.2021.733138

Scheff, S. W., and Price, D. A. (2003). Synaptic pathology in Alzheimer's disease: a review of ultrastructural studies. *Neurobiol. Aging* 24, 1029–1046. doi: 10.1016/j.neurobiolaging.2003.08.002

Schmidt, J., Mayer, A. K., Bakula, D., Freude, J., Weber, J. J., Weiss, A., et al. (2019). Vulnerability of frontal brain neurons for the toxicity of expanded ataxin-3. *Hum. Mol. Genet.* 28, 1463–1473. doi: 10.1093/hmg/ddy437

Schmidt, T., Landwehrmeyer, G. B., Schmitt, I., Trottier, Y., Auburger, G., Laccone, F., et al. (1998). An isoform of ataxin-3 accumulates in the nucleus of neuronal cells in affected brain regions of SCA3 patients. *Brain Pathol.* 8, 669–679. doi: 10.1111/j.1750-3639.1998.tb00193.x

Scott, D. A., Tabarean, I., Tang, Y., Cartier, A., Masliah, E., and Roy, S. (2010). A pathologic cascade leading to synaptic dysfunction in alpha-synuclein-induced neurodegeneration. *J. Neurosci.* 30, 8083–8095. doi: 10.1523/JNEUROSCI.1091-10.2010

Simonsen, A., Cumming, R. C., Brech, A., Isakson, P., Schubert, D. R., and Finley, K. D. (2008). Promoting basal levels of autophagy in the nervous system enhances longevity and oxidant resistance in adult *Drosophila*. *Autophagy* 4, 176–184. doi: 10.4161/auto.5269

Singh, M. D., Raj, K., and Sarkar, S. (2014). *Drosophila* Myc, a novel modifier suppresses the poly(Q) toxicity by modulating the level of CREB binding protein and histone acetylation. *Neurobiol. Dis.* 63, 48–61. doi: 10.1016/j.nbd.2013.11.015

Sleigh, J. N., Grice, S. J., Burgess, R. W., Talbot, K., and Cader, M. Z. (2014). Neuromuscular junction maturation defects precede impaired lower motor neuron connectivity in Charcot-Marie-Tooth type 2D mice. *Hum. Mol. Genet.* 23, 2639–2650. doi: 10.1093/hmg/ddt659

Steinert, J. R., Campesan, S., Richards, P., Kyriacou, C. P., Forsythe, I. D., and Giorgini, F. (2012). Rab11 rescues synaptic dysfunction and behavioural deficits in a *Drosophila* model of Huntington's disease. *Hum. Mol. Genet.* 21, 2912–2922. doi: 10.1093/hmg/dds117

Südhof, T. C. (2008). Neuroligins and neurexins link synaptic function to cognitive disease. *Nature* 455, 903–911. doi: 10.1038/nature07456

Tang, G., Gudsnuk, K., Kuo, S. H., Cotrina, M. L., Rosoklija, G., Sosunov, A., et al. (2014). Loss of mTOR-dependent macroautophagy causes autistic-like synaptic pruning deficits. *Neuron* 83, 1131–1143. doi: 10.1016/j.neuron.2014.07.040

Thibaudeau, T. A., Anderson, R. T., and Smith, D. M. (2018). A common mechanism of proteasome impairment by neurodegenerative disease-associated oligomers. *Nat. Commun.* 9, 1097. doi: 10.1038/s41467-018-03509-0

Toonen, L. J. A., Overzier, M., Evers, M. M., Leon, L. G., van der Zeeuw, S. A. J., Mei, H., et al. (2018). Transcriptional profiling and biomarker identification reveal tissue specific effects of expanded ataxin-3 in a spinocerebellar ataxia type 3 mouse model. *Mol. Neurodegener.* 13, 31. doi: 10.1186/s13024-018-0261-9

Van Vactor, D., and Sigrist, S. J. (2017). Presynaptic morphogenesis, active zone organization and structural plasticity in *Drosophila*. *Curr. Opin. Neurobiol.* 43, 119–129. doi: 10.1016/j.conb.2017.03.003

Vijayan, V., and Verstreken, P. (2017). Autophagy in the presynaptic compartment in health and disease. *J. Cell Biol.* 216, 1895–1906. doi: 10.1083/jcb.201611113

Volk, L., Chiu, S.-L., Sharma, K., and Huganir, R. L. (2015). Glutamate synapses in human cognitive disorders. *Annu. Rev. Neurosci.* 38, 127–149. doi: 10.1146/annurev-neuro-071714-033821

Wagh, D. A., Rasse, T. M., Asan, E., Hofbauer, A., Schwenkert, I., Dürrbeck, H., et al. (2006). Bruchpilot, a protein with homology to ELKS/CAST, is required for structural integrity and function of synaptic active zones in *Drosophila*. *Neuron* 49, 833–844. doi: 10.1016/j.neuron.2006.02.008

Warrick, J. M., Paulson, H. L., Gray-Board, G. L., Bui, Q. T., Fischbeck, K. H., Pittman, R. N., et al. (1998). Expanded polyglutamine protein forms nuclear inclusions and causes neural degeneration in *Drosophila*. *Cell* 93, 939–949. doi: 10.1016/s0092-8674(00)81200-3

Weyhersmüller, A., Hallermann, S., Wagner, N., and Eilers, J. (2011). Rapid active zone remodeling during synaptic plasticity. *J. Neurosci.* 31, 6041–6052. doi: 10.1523/JNEUROSCI.6698-10.2011

Wiatr, K., Marczak, Ł., Pérot, J. B., Brouillet, E., Flament, J., and Figiel, M. (2021). Broad influence of mutant Ataxin-3 on the proteome of the adult brain, young neurons, and axons reveals central molecular processes and biomarkers in SCA3/MJD using knock-in mouse model. *Front. Mol. Neurosci.* 14, 658339. doi: 10.3389/fnmol.2021.658339

Wu, C. H., Giampetruzzi, A., Tran, H., Fallini, C., Gao, F. B., and Landers, J. E. (2017). A *Drosophila* model of ALS reveals a partial loss of function of causative human PFN1 mutants. *Hum. Mol. Genet.* 26, 2146–2155. doi: 10.1093/hmg/ddx112

Yamada, M., Tan, C. F., Inenaga, C., Tsuji, S., and Takahashi, H. (2004). Sharing of polyglutamine localization by the neuronal nucleus and cytoplasm in CAG-repeat diseases. *Neuropathol. Appl. Neurobiol.* 30, 665–675. doi: 10.1111/j.1365-2990.2004.00583.x

Yamamoto, A., and Simonsen, A. (2011). The elimination of accumulated and aggregated proteins: a role for aggrephagy in neurodegeneration. *Neurobiol. Dis.* 43, 17–28. doi: 10.1016/j.nbd.2010.08.015

Yeh, E., Gustafson, K., and Boulianne, G. L. (1995). Green fluorescent protein as a vital marker and reporter of gene expression in *Drosophila*. *Proc. Natl. Acad. Sci. U.S.A.* 92, 7036–7040. doi: 10.1073/pnas.92.15.7036

Yi, J., Zhang, L., Tang, B., Han, W., Zhou, Y., Chen, Z., et al. (2013). Sodium valproate alleviates neurodegeneration in SCA3/MJD via suppressing apoptosis and rescuing the hypoacetylation levels of histone H3 and H4. *PLoS ONE* 8, e54792. doi: 10.1371/journal.pone.0054792

Zhou, L., McInnes, J., Wierda, K., Holt, M., Herrmann, A. G., Jackson, R. J., et al. (2017). Tau association with synaptic vesicles causes presynaptic dysfunction. *Nat. Commun.* 8, 15295. doi: 10.1038/ncomms15295

Conflict of Interest: The authors declare that the research was conducted in the absence of any commercial or financial relationships that could be construed as a potential conflict of interest.

Publisher's Note: All claims expressed in this article are solely those of the authors and do not necessarily represent those of their affiliated organizations, or those of the publisher, the editors and the reviewers. Any product that may be evaluated in this article, or claim that may be made by its manufacturer, is not guaranteed or endorsed by the publisher.

frontiers | Frontiers in Molecular Neuroscience

TYPE Original Research
PUBLISHED 21 September 2022
DOI 10.3389/fnmol.2022.943980

OPEN ACCESS

EDITED BY
James P. Clement,
Jawaharlal Nehru Centre for Advanced Scientific Research, India

REVIEWED BY
Vasudharani Devanathan,
Indian Institute of Science Education and Research, Tirupati, India
Aurnab Ghose,
Indian Institute of Science Education and Research, Pune, India

*CORRESPONDENCE
Sourav Banerjee
souravnbrc@gmail.com;
sourav@nbrc.ac.in

SPECIALTY SECTION
This article was submitted to Molecular Signaling and Pathways, a section of the journal Frontiers in Molecular Neuroscience

RECEIVED 14 May 2022
ACCEPTED 29 August 2022
PUBLISHED 21 September 2022

CITATION
Sharma G and Banerjee S (2022) Activity-regulated E3 ubiquitin ligase TRIM47 modulates excitatory synapse development.
Front. Mol. Neurosci. 15:943980.
doi: 10.3389/fnmol.2022.943980

Activity-regulated E3 ubiquitin ligase TRIM47 modulates excitatory synapse development

Gourav Sharma and Sourav Banerjee*

National Brain Research Centre, Gurgaon, India

The Ubiquitin Proteasome System (UPS) has been shown to regulate neuronal development and synapse formation. Activity-dependent regulation of E3 ligase, a component of the UPS that targets specific proteins for proteasome-mediated degradation, is emerging as a pivotal player for the establishment of functional synapses. Here, we identified TRIM47 as a developmentally regulated E3 ligase that is expressed in rat hippocampus during the temporal window of synapse formation. We have demonstrated that the expression of TRIM47 is regulated by the glutamate-induced synaptic activity of hippocampal neurons in culture. In addition, the activity-dependent enhancement of TRIM47 expression is recapitulated following the object location test, a hippocampus-dependent spatial memory paradigm. We observed that this enhancement of TRIM47 expression requires NMDA receptor activation. The knockdown of TRIM47 leads to an enhancement of spine density without affecting dendritic complexity. Furthermore, we observed an increase in excitatory synapse development upon loss of TRIM47 function. Comprehensively, our study identified an activity-regulated E3 ligase that drives excitatory synapse formation in hippocampal neurons.

KEYWORDS

synapse, spine, E3 Ub ligase, neuronal activation, TRIM47

Introduction

Information transfer from one neuron to another requires a highly specialized structure known as a synapse (Südhof, 2021). Synapses are formed in the developing as well as in the adult brain while performing cognitive functions (Cohen-Cory, 2002; Zito and Svoboda, 2002; Cornelia Koeberle et al., 2017; Nguyen et al., 2020). Although the initial phase of synapse formation occurs without neuronal activity, the maturation of these nascent synapses requires neuronal activity (Fertuck and Salpeter, 1976; Salpeter and Harris, 1983; Rao and Craig, 1997; Hall and Ghosh, 2008; Lin et al., 2008). Synapse formation is initiated as early as postnatal day 1 (P1) (Fiala et al., 1998). The density of synapses gradually increases from P7 to P15 and reaches a peak at P21 after which newly established synapses undergo maturation till P60 (Harris and Stevens, 1989; Harris and Jensen, 1992; Lohmann and Kessels, 2014; Zhu et al., 2018; Cizeron et al., 2020). Synapse

development in dissociated neuronal culture follows a similar temporal pattern as detected in postnatal rodents (Fletcher et al., 1994; Papa et al., 1995; Boyer et al., 1998).

The development of functional synapses relies on a myriad of factors that operate gene expression both at the transcriptional and post-transcriptional level. The transcriptional regulation of synapse formation has been extensively studied. These studies identified the involvement of immediate early genes, such as NPAS4, in inhibitory synapse development (Lin et al., 2008). A screen for calcium-regulated transcription factors identified MEF2A/D as a regulator of excitatory synapse formation (Flavell et al., 2006; Polleux et al., 2007). A genome-wide RNA interference (RNAi) screen has identified transcriptionally regulated cell adhesion proteins, such as Cadherin 11 and 13, as regulators of functional synapse development (Paradis et al., 2007). More recently, post-transcriptional control of synapse formation has gained significant attention. Among various post-transcriptional regulators, protein ubiquitination and subsequent degradation by the Ubiquitin Proteasome System (UPS) has emerged as a key regulator. The UPS involves an enzymatic cascade to ubiquitinate a subset of proteins by E3 ubiquitin ligase and degrade the ubiquitinated proteins by the proteasome (Mabb and Ehlers, 2010). An initial unbiased genetic screen identified *Highwire*, an E3 ubiquitin ligase in *Drosophila* and its homolog *rpm-1* in *Caenorhabditis elegans,* to be involved in the regulation of synapse development (Wan et al., 2000; Nakata et al., 2005). The Ube3A, an E3 ubiquitin ligase mutated in Angelman Syndrome, has been shown to ubiquitinate Arc and trigger its degradation by proteasome upon induction of neuronal activity (Greer et al., 2010). The Arc degradation regulates the insertion of AMPA-type glutamatergic receptor subunit on the post-synaptic membrane that governs the development of excitatory synapses (Greer et al., 2010). Emerging studies have pointed out the non-degradative functions of E3 ubiquitin ligases. Neuralized1 (Neurl1) ubiquitinates cytoplasmic polyadenylation element binding protein 3 (CPEB3) and promotes its enzymatic activity for polyadenylation and translational regulation by transcripts containing binding sites for CPEB3 (Pavlopoulos et al., 2011). The E3 Ubiquitin ligase activity of Neurl1 is enhanced upon exposure to a spatial memory paradigm leading to the growth of new dendritic spines and synthesis of AMPA-type glutamatergic receptor subunits GluA1 and GluA2 (Pavlopoulos et al., 2011). Activity-dependent self-polyubiquitination of E3 ubiquitin ligase Rnf2 stabilizes its function and prevents its degradation *via* Ube3A-mediated polyubiquitination (Kumari et al., 2017). The self-polyubiquitination of Rnf2 regulates functional synapse development by modulating the insertion of AMPA-type glutamatergic receptors on the post-synaptic membrane (Kumari et al., 2017). Our screen for activity-regulated E3 ubiquitin ligase identified several E3 ubiquitin ligases, such as TRIM9, TRIM47, and PDZRN3 that could potentially regulate synapse formation (Kumari et al., 2017). Previous studies have implicated TRIM47, a RING domain containing E3 ubiquitin ligase, in the regulation of glioma cell proliferation and migration (Chen et al., 2020) and tumor progression in pancreatic cancer (Li et al., 2021). However, the function of TRIM47 remains elusive in the nervous system. These observations prompted us to evaluate the importance of TRIM47 in functional synapse development in hippocampal neurons.

In this study, we have identified TRIM47 as a synapse-associated E3 ubiquitin ligase and expressed during the temporal window of synapse formation. Our study demonstrated that TRIM47 is localized in neuronal dendrites and synapses of developing hippocampal neurons. We observed that glutamate-induced neuronal activity and exposure to a spatial learning paradigm enhance the NMDA-dependent expression of TRIM47. The knockdown of TRIM47 enhances spine density without affecting dendritic development. The loss of TRIM47 increases excitatory synapse formation. Our data establish TRIM47 as a negative regulator of the dendritic spine and synapse development.

Materials and methods

Primary hippocampal neuronal culture

Rat (Sprague-Dawley) primary hippocampal neuronal cultures were prepared and maintained as described previously (Kaech and Banker, 2006). Briefly, hippocampi were dissected out from embryonic day 18 (E18) pups, treated with trypsin (0.25%), and dissociated by trituration to a make single cell suspension. Cells were plated onto poly-L-lysine (1 mg/ml) coated glass coverslip (200–300 cells/mm^2). About 190–200 cells/mm^2 were used for imaging experiments and 300 cells/mm^2 were used for all biochemical experiments. Neurons were maintained in the Neurobasal medium (Gibco, #21103-049) containing B27 supplements (Gibco, #17504-001) (NB27) at 5% CO_2 and 37°C. Animals were generated at the animal house of the National Brain Research Centre and experiments were performed as per the guidelines approved by the Institutional Animal Ethics (IAEC) committee of the National Brain Research Centre.

Lentivirus production and transduction

Lentivirus preparation and transduction into hippocampal neuronal cultures were performed as described previously (Banerjee et al., 2009). shRNA against TRIM47 was cloned into *Mlu*I and *Cla*I sites of the pLVTHM vector

(Addgene plasmid #12247) and verified by sequencing. pLVTHM vectors containing TRIM47 shRNA (shRNA #1: ACTTGGTGAAGCTGAGTTCCC) or (shRNA #2: AGAAAGCTGACTGAATCCGCC) and non-targeting control (Universal Control: ATCTCGCTTGGGCGAGAGTAAG) were used for lentivirus preparation. *Escherichia coli* Stbl3 strain was used to propagate shRNA containing pLVTHM plasmid and DH5α was used to propagate psPAX2 (Addgene plasmid #12260) packaging plasmid and the pMD2.G (Addgene plasmid #12259) envelope plasmid. Purified plasmids were prepared by the Endotoxin-free Maxiprep kit (Qiagen). Lentiviruses were produced by co-transfecting 20 μg transfer vector (mCherry cassette under EF1α promoter and shRNA cassette against TRIM47 or non-targeting control under H1 promoter in pLVTHM plasmid), 15 μg psPAX2, and 6 μg pMD2.G into HEK293T cells. The cells were grown in low glucose DMEM media (Gibco) with 10% Fetal Bovine Serum (FBS) (Gibco) and maintained at 5% CO_2 and 37°C. HEK293T (2×10^6) cells were transfected by the calcium phosphate method. Following transfection, the media containing the transfection mixture was replaced with the fresh media after 8 h. Culture supernatant containing lentivirus particles were collected 72 h post-transfection and viruses were concentrated by ultracentrifugation. Viral titers were determined by infecting HEK293K cells followed by counting cells using a fluorescence-based cell counter. Titers were typically $1–3 \times 10^7$ TU/ml.

RNAi was performed by infecting primary rat hippocampal neuronal cultures at *Days-In Vitro* (DIV) 3 with lentivirus expressing shRNAs against TRIM47 and non-targeting control. Virus infection was tracked by visualizing mCherry expression in infected neurons. The efficiency of knockdown was verified by preparing lysates from TRIM47 and non-targeting shRNA virus-infected neurons at DIV 21 in Laemmli buffer and resolving equal volumes on sodium dodecyl-sulfate polyacrylamide gel electrophoresis (SDS-PAGE). We have used two shRNAs against TRIM47 (Construct 1 and 2) for its effective knockdown and also a non-targeting shRNA to eliminate the possibility of an off-target effect. Viral infections were performed at a multiplicity of infection (MOI) of 2 for 6 h following which lentivirus-containing media was replaced with fresh neurobasal media supplemented with B27 (NB27). Neurons were incubated up to DIV 21 prior to immunocytochemistry and imaging experiments.

Stimulation of hippocampal neurons

Hippocampal neurons (DIV 7) were stimulated by glutamate (20 μM) for 45 min as described previously (Banerjee et al., 2009) with minor modifications. Neurons were incubated in low-KCl-HBS (290 mOSm) [110 mM NaCl, 5.4 mM KCl, 1.8 mM $CaCl_2$, 0.8 mM $MgCl_2$, 10 mM D-glucose, and 10 mM HEPES-KOH (pH 7.4)] for 60 min prior to stimulation. To block NMDA receptor function, neurons were pretreated with its antagonist, AP5 (50 μM) for 50 min. To block Ca^{2+} activity, neurons were pretreated with EGTA (5 μM) for 50 min. Furthermore, neurons were stimulated with NMDA (20 μM), in low-KCl-HBS for 45 min. AP5 and EGTA remained in the incubation buffer for the entire duration of the experiment. After stimulation, neurons were harvested for protein lysate preparation using 1X Laemmli buffer.

Western blot analysis

Samples from the stimulated or un-stimulated neurons or lentivirus infected neurons from 2 to 3 coverslips for each experimental condition were lysed using 1X Laemmli buffer and pooled together for western blot analysis. Equal volumes of lysates were resolved on 10% SDS polyacrylamide gel, transferred onto nitrocellulose membrane (Millipore), blocked with 5% skim milk (Merck), and probed with antibodies specific for TRIM47 (1:500; Bethyl Laboratories, #A301-194A), c-Fos (1:500; Calbiochem, #OP17), Tuj1 (1:10,000; Sigma, #T8578), and GAPDH (1:25000; Sigma, #G9545). For each lane, immunoblotting was performed with Tuj1 or GAPDH as the internal control to normalize protein levels.

To evaluate the developmental expression pattern of TRIM47, hippocampal tissue lysates from post-natal day pups (P0, P4, P7, P14, P21, P60, and P120) were analyzed by SDS-PAGE against TRIM47 antibody and Tuj1 expression was used for normalization.

For the spatial object recognition test-related protein expression analysis, the Long-Evans rats were euthanized and the dorsal hippocampus was isolated within 30 min after the test session for each animal to prepare a lysate using lysis buffer and 0.1% SDS. Protein estimation was done using Bradford's protein estimation method Bradford (1976). An equal amount of protein was resolved on 10% SDS polyacrylamide gels and probed for TRIM47, c-Fos, and Tuj1.

Blots were detected by the chemiluminescence kit (Pierce) on X-ray films or the UVITEC gel documentation system. Band intensities were quantified using ImageJ (NIH). Statistical significance was measured by an unpaired two-tailed *t*-test or ANOVA.

Synaptoneurosome preparation

Synaptoneurosomes were prepared as described previously (Steward et al., 1991). Briefly, hippocampi from P14 and P60 rat brains were homogenized in the homogenization buffer (0.32 M Sucrose, 2 mM HEPES pH 7.4, 0.1 mM EDTA, and 0.25 mM DTT) containing a protease inhibitor cocktail (Roche) using a Dounce tissue homogenizer (Kontes). Nuclei

and cell debris were removed by centrifugation at 2,000 g for 2 min. The supernatant fraction containing the crude synaptoneurosome fraction was pelleted after centrifugation at 14,000 g for 10 min. The pellet (P2) was then resuspended in homogenization buffer (0.32M sucrose, 0.1 mM EDTA, 0.25 mM DTT, 200 mM HEPES-KOH, pH 7.4) and layered onto a 5–13% discontinuous Ficoll (Sigma) gradient that was equilibrated at 4°C for 60 min. The gradient was centrifuged at 20,000 g for 45 min at 4°C. A synaptoneurosome fraction located at the interface of 5–13% gradient was obtained. Ficoll was removed from the synaptoneurosome fraction by centrifugation at 20,000 g for 20 min at 4°C and resuspending the pellet in homogenization buffer. The synaptoneurosome pellet was resuspended in the synaptoneurosome buffer (10 mM Tris pH 7.5, 2.2 mM $CaCl_2$, 0.5 mM Na_2HPO_4, 0.4 mM KH_2PO_4, 4 mM $NaHCO_3$, and 80 mM NaCl) and lysed using 0.1% SDS. The protein concentration of total hippocampal lysate (mentioned here as crude, containing both nuclear and cytoplasmic fraction) and synaptoneurosome fraction was measured by the BCA protein estimation kit (Pierce). The quality of synaptoneurosome fraction was assessed using an equal amount of crude as well as synaptoneurosome lysate by western blot analysis using antibodies specific for the synaptic compartment (PSD95, 1:1,000; clone K28/43; Neuromab, #75-028 and Synapsin I, 1:5,000; Millipore, #AB1543), glia (GFAP, 1:1,000; abcam, #ab7260), and nucleus (Histone H1, 1:1,000; Millipore, #ab05-457).

Calcium-phosphate transfection of neurons for spine analysis

Hippocampal neuronal cultures were transfected with a plasmid expressing enhanced green fluorescent protein (EGFP) under the chicken β-actin promoter (CAG-GFP) at DIV 2 as described previously (Jiang and Chen, 2006; Sun et al., 2013). Briefly, hippocampal neurons were transfected with 1 μg of CAG-GFP mixed with 25 μl of 2X-Hepes Buffer Saline (2x-HBS, pH 7.04) and 2.48 μl of 2.5M $CaCl_2$ in ultrapure Milli-Q, bringing the volume up-to 50 μl per coverslip. Each mixing step was done with constant agitation, and the mixture was left undisturbed for about 15 min. About 50 μl of transfection mix was added to each well containing cultured neurons on glass coverslips and was mixed thoroughly. The cells were then incubated in 5% CO_2 at 37°C for 1-h and 30 min. Each coverslip was then washed with Neurobasal media kept at 5% CO_2 and 37°C at-least 3 times to wash off all the precipitates from the coverslip. The cells were then incubated in glial preconditioned NB27 at 5% CO_2 and 37°C. Coverslips that showed green fluorescent protein (GFP) the next day (DIV 3) were then selected and transduced with lentivirus expressing shRNAs against TRIM47 and non-targeting control for 6 h and complete media was replaced. Half volume of glial conditioned NB27 media was replaced every third day for maintenance of the culture up to DIV 21.

Immunocytochemistry for synapse formation assay

Hippocampal neurons (DIV 3) infected with lentivirus co-expressing mCherry along with non-targeting control shRNA, or shRNAs targeting TRIM47 were immunostained on (DIV 21) as described previously (Banerjee et al., 2009) with minor modifications. Neurons were washed three times in Minimum Essential Medium (MEM) with HEPES modification (MEM-H) (Sigma, #M2645-10L) and fixed with 4% paraformaldehyde (PFA) in 1X-PBS containing 4% sucrose at 37°C for 15 min. Following fixation, neurons were washed in MEM-H three times, permeabilized with 0.1% Triton-X-100 in 1X-PBS (PBST) for 90 s and washed one time in MEM-H. Neurons were incubated in blocking solution (1% bovine serum albumin [BSA] and 10% horse serum in MEM-H) at RT for 1 h. These neurons were incubated with antibodies specific for PSD95 (1:300; clone K28/43; Neuromab, #75-028.) and Synapsin I (1:1,000, Millipore, #AB1543) overnight at 4°C. Following primary antibody incubation, neurons were washed three times in MEM-H and incubated with respective secondary antibodies (mouse or rabbit) conjugated with Ms-Alexa–488 (Invitrogen Molecular probes, #A21202, for PSD95) or Rb-Alexa–633 (Invitrogen Molecular probes, #A21071, for Synapsin I) dyes at RT for 35 min. Neurons were washed three times in MEM-H, treated with methanol at –20°C for 5 min, air dried, and mounted on glass slides using Vectashield mounting medium containing DAPI (Vector Laboratory, #H1200).

Immunocytochemistry for TRIM47 localization in hippocampal neurons

Hippocampal neurons (DIV 7 and DIV 21) were immunostained as described previously (Banerjee et al., 2009) with minor modifications. Neurons were washed three times in MEM with HEPES modification (MEM-H) (Sigma, #M2645-10L) and fixed with 4% PFA in 1X-PBS containing 4% sucrose at 37°C for 15 min. Following fixation, neurons were washed in MEM-H three times, permeabilized with 0.1% Triton-X-100 in 1X-PBS (PBST) for 90 s, and washed one time in MEM-H. Neurons were incubated in a blocking solution (1% BSA and 10% horse serum in MEM-H) at RT for 2 h. These neurons were incubated with antibodies specific for PSD95 (1:300; abcam, #ab12093) and TRIM47 (1:300, Bethyl lab, #A301-194A) overnight at 4°C. Following primary antibody incubation, neurons were washed three times in MEM-H and incubated with respective secondary antibodies (mouse or rabbit) conjugated with Rb-Alexa–488 (Invitrogen Molecular

probes, #A11034, for TRIM47) or Goat-Alexa–594 (Invitrogen Molecular probes, #A11058, for PSD95) dyes at RT for 35 min. Neurons were washed two times in MEM-H, followed by 1 h blocking in the blocking solution and then incubated with Tuj1 antibody (1:10,000; Sigma, #T8578). Neurons were washed with MEM-H two times and then incubated with secondary antibody Ms-Alexa-647 (Invitrogen Molecular probes, #A21236, for Tuj1) followed by three MEM-H washes for 5 min each. Neurons were air dried and mounted on glass slides using Vectashield mounting medium containing DAPI (Vector Laboratory, #H1200).

Immunohistochemistry

Long-Evans rats aged P14 and P60 were sedated using a lethal dose of Ketamine (300 mg/kg) and a Xylazine (30 mg/kg) cocktail. Rats were perfused intracardially with phosphate buffer saline (PBS—137 mM NaCl, 2.7 mM KCl, 8 mM Na_2HPO_4, and 2 mM KH_2PO_4) and 4% PFA in PBS. Brains were isolated and kept in 4% PFA in PBS for 2 days post perfusion. Brains were transferred to 30% sucrose solution in PBS till they settle down at the bottom and are ready for sectioning. About 50 μm sections were prepared using cryotome and mounted on gelatin-coated slides. Sections were washed with PBS three times for 5 min each and then permeabilized using 0.1% TritonX-100 in PBS (0.1% PBST) for 60 min. Sections were again washed with 0.1% PBST three times for 5 min each. Blocking was done using 2% BSA + 5% Horse Serum in 0.1% PBST at RT for 2 h. Primary antibody incubation for MAP2 (5 μg/ml, abcam, #ab28032) and TRIM47 (1:250, bethyl lab, #A301-194A) in blocking solution was done for 20 h at 4°C. Following primary antibody incubation, sections were washed three times in 0.1% PBST and incubated with respective secondary antibodies (mouse or rabbit) conjugated with Rb-Alexa–488 (Invitrogen Molecular probes, #A11034, for TRIM47) or Ms-Alexa–647 (Invitrogen Molecular probes, #A21236, for MAP2) dyes at RT for 4 h. Neurons were washed three times in 0.1% PBST and mounted using Vectashield (#H1200) mounting medium containing DAPI.

Confocal microscopy and image analysis

Using a Nikon Ti-2 point scan confocal microscope with a Plan Apo λ 60X Oil NA, oil immersion objective at 1,024 × 1,024 pixel resolution and at ×0.7 optical zoom, 16-bit images of pyramidal neurons were acquired. High-magnification images were obtained using a Plan Apo 100× OIL DIC N2 oil immersion objective at ×2 optical zoom at 1,024 × 1,024 pixel resolution. We obtained 6–8 optical sections with 0.75 μm step size (×60), and a maximum intensity projection was created for image analysis. Furthermore, 8–16 optical sections with a 0.5 μm step size (×100) were deconvolved with Nikon elements AR software for spine analysis and synapse formation assay.

Alexa 488 (PSD95), mCherry (Lentivirus RNAi), and Alexa 633(Synapsin I) were visualized by excitation of the 488-nm argon ion laser, 561 nm Helium–Neon laser (HeNe1), and 640-nm Helium–Neon (HeNe2) laser, respectively. We have used emission filters BP 505–530 for GFP, LP 560 for Alexa 546, and the Meta setting for Alexa 633. All images were acquired with identical settings for laser power, detector gain, amplifier offset, and pinhole diameter for each experiment and between experiments. Image analysis was performed as described previously (Paradis et al., 2007) with minor modifications.

For analyzing PSD95 and Synapsin I colocalization puncta density values, maximum intensity projections were created from the optical sections obtained from the images of all three channels (488, 546, and 633). mCherry images of multiple frames of all the neurons were used to trace the dendrites using NeuronStudio software (CNIC, Mt Sinai School of Medicine). Synapse density was quantified as the overlap of images of all three channels (488, 546, and 633) using a custom program in Matlab software (Mathworks). For TRIM47 colocalization with PSD95 on Tuj1 labeled neurons, the channels were 488, 594, and 647, respectively, and localization was quantified as the overlap of signals in all three channels.

The threshold for each channel (488/633 or 488/594) in each image was calculated as the mean pixel intensity for the entire image plus two standard deviations (SDs) above the mean. The threshold for GFP (488) was set at the mean pixel intensity plus one standard deviation for each image. A binary mask that included all pixels above threshold was created for each channel. Then, using the mask for each channel and trace files from NeuronStudio, regions of triple co-localizations lesser than 10 μm in size were considered as synaptic puncta. To calculate synapse density (per μm dendrite), the number of objects was divided by the length of the dendrite as measured using NeuronStudio traces. The synapse density for each condition within an experiment was calculated by averaging the synapse density from all of the images corresponding to a particular experimental condition. Statistical significance was assessed using a Student *t*-test and one-way ANOVA as indicated. All analyses were performed blind to the experimental condition.

For spine morphology analysis, neurons that showed expression of both mCherry (RNAi) and GFP (CAG-GFP transfection) were included. Neurons were processed using Neurolucida 360 (MBF Bioscience) to generate a three dimensional (3D) dendritic skeleton automatically using the Rayburst Crawl tracing algorithm. Following successful tracing of the dendritic branch, the spines were detected and classified automatically using the detect spine program feature. Structures that were not spines and spines that were ambiguous in shape were manually removed or reclassified.

The statistical significance in spine morphology and density changes were assessed using a Student *t*-test and one-way ANOVA as indicated. All analyses were performed blind to the experimental condition.

Sholl analysis

Sholl analysis was performed on neurons transduced with CAG-GFP and infected with lentivirus to evaluate the neuronal morphology post RNAi. SynD (Schmitz et al., 2011) was used for the analysis. The cell soma was determined and the intersections were counted in concentric circles with increasing radii of 10 μm from the center of the cell soma. A number of intersections were plotted against their distances from the center of the cell soma. The statistical significance between non-targeting control RNAi and TRIM47 RNAi was measured using the Kolmogorov–Smirnov (K–S) test.

Spatial object recognition

The object recognition test performed is an adaptation of the traditional object recognition test for location memory in rats previously described (Cavoy and Delacour, 1993; Sutcliffe et al., 2007; Wimmer et al., 2012). The spatial object recognition test consists of 7 days of animal handling phase followed by 5 test sessions. In the first session, the animal is presented to the empty test arena (white floor and gray wall box with 80 cm × 80 cm × 50 cm dimensions along with spatial cues on its walls) for 10 min to be familiarized with the test environment, which differs from the home cage. Following the habituation session, the animal is returned to the home cage for a minimal time of not more than 5 min, which is necessary to clean the arena with 70% alcohol and to place the objects into the arena. In the next 3 phases that are spaced 5 min apart, the animal is allowed to explore two objects which remain at the same position in the box for 10 min in all three sessions. After the 4th session, the animal is returned to the home cage for 24 h following which the 5th session (test session) is carried out. In the test session, objects are either placed at the same location as in the last training session (object not displaced) or one of the two objects is moved to a different location (object displaced) with respect to the other object and the spatial cues on the wall of the arena, and the animal is allowed to explore the two objects freely for 10 min. The videos of the exploration sessions were recorded using an overhead mounted camera (Logitech HD webcam C270). The time spent exploring each object (interaction time) was recorded using MATLAB-based autotyping software (Patel et al., 2014) and manually by an observer blind to the experimental details and the identity of control and test animals. Exploration is defined as approaching the object with the nose closer than 2 cm. The recognition memory readout is the percentage of time spent with each object during test sessions (Denninger et al., 2018). Long-Evans rats of age 6–8 weeks were tested for object location memory (spatial object recognition test). Animals were generated at the animal house of the National Brain Research Centre and experiments were performed as per the guidelines approved by the IAEC of the National Brain Research Centre.

Statistical methods

Statistical analyses were performed for all experiments. Data are represented as the percentage mean ± standard error of mean (SEM). The "*n*" number mentioned in each experiment refers to the number of independent experiments performed or for imaging experiments "*n*" is the number of neurons analyzed. Western blots were analyzed using an unpaired 2-tailed Student's *t*-test assuming unequal variances or one-way ANOVA or as indicated. Synaptic puncta density analyses for co-localization of GFP/PSD95/Synapsin I puncta, spine density, and morphology analysis was performed using one-way ANOVA with Dunnett's T3 multiple comparison test. We used the K–S test to determine the statistical differences in the distribution data from our Sholl analysis. The statistical significance was judged to be $p < 0.05$, and *p*-values are indicated in the respective figure legends. A statistical analysis was performed using GraphPad Prism 9.

Results

Activity-regulated TRIM47 expression during synapse development

To visualize the expression pattern of TRIM47 during the synapse formation, we measured the protein expression level at various stages of developing and adult hippocampus, starting from P0 (postnatal day 0) to P120. Our western blot analysis showed a detectable level of TRIM47 from P4 and its expression reaches to the maximum level at P21 (**Figures 1A,B**). We observed a significant increase in the level of TRIM47 at both P14 (8.30814 ± 1.671-fold increase, $p < 0.0048$) and P21 (9.60853 ± 2.887-fold increase, $p < 0.0125$) as compared with its level at P0 (**Figures 1A,B**). This observation indicates that the expression of TRIM47 coincides with the temporal window of synapse formation (Harris and Stevens, 1989; Harris and Jensen, 1992; Fletcher et al., 1994; Papa et al., 1995; Boyer et al., 1998; Fiala et al., 1998; Li and Sheng, 2003).

Synapse development has been shown to be regulated by neuronal activity (Nelson et al., 1990; Shatz and Katz, 1996; Zito and Svoboda, 2002; Yu et al., 2004; Andreae and Burrone, 2014). Synaptic activation triggers the translocation of proteasome machineries to dendritic spines and promotes

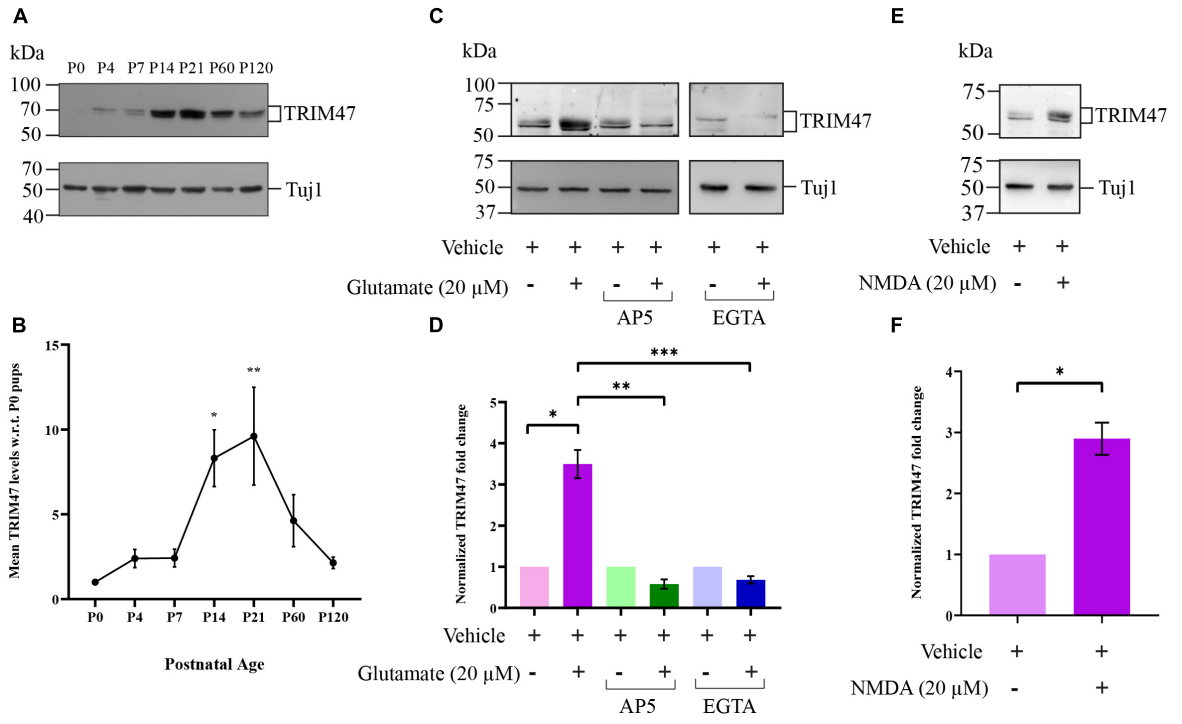

FIGURE 1
Developmental and activity-dependent expression of TRIM47. **(A)** A photomicrograph showing the postnatal developmental expression pattern of TRIM47 protein in rat hippocampus. **(B)** Quantification of western blot results is shown. $n = 5$, $^{**}p < 0.0048$, and $^{*}p < 0.0215$. One-way ANOVA with Tukey's test is conducted. **(C)** A photomicrograph showing western blot analysis of activity-induced TRIM47 protein expression following glutamate (20 μM) stimulation in the presence or absence of NMDA antagonist AP5 (50 μM) and chelating agent EGTA (5 μM). **(D)** Quantitation of TRIM47 expression is shown. $n = 8$; $^{*}p < 0.0002$, $^{**}p < 0.003$, and $^{***}p < 0.01$; and an unpaired t-test with Welch's correction. **(E)** A photomicrograph showing the TRIM47 level following NMDA (20 μM) stimulation. **(F)** Quantitation of TRIM47 expression after NMDA stimulation; $n = 12$; and $^{****}p < 0.0001$. An unpaired t-test with Welch's correction is shown. The data represent the mean ± SEM.

protein ubiquitination *via* NMDA receptor activation (Bingol and Schuman, 2006). Prompted by these observations, we have analyzed the impact of neuronal activity on TRIM47 expression. Hippocampal neurons (DIV 7) were treated with glutamate (20 μM) for 45 min and the TRIM47 protein level was analyzed by western blot. We observed that the glutamate stimulation enhances the TRIM47 protein level (3.496 ± 0.3417-fold increase as compared with vehicle treated neurons, $p < 0.0002$, $n = 8$) (**Figures 1C,D**). To evaluate the contribution of NMDA receptor in the activity-regulated enhancement of TRIM47, hippocampal neurons (DIV 7) were treated with AP5 (50 μM), NMDA antagonist, in the presence or absence of glutamate. We observed that blockade of NMDA activity prevented activity-induced enhancement of TRIM47 (**Figures 1C,D**). However, AP5 alone did not affect the TRIM47 level (**Figures 1C,D**). Furthermore, we have tested whether NMDA receptor activation alone is sufficient for an enhanced expression of TRIM47. Our western blot analysis from NMDA-treated hippocampal neurons (DIV 7) demonstrated that the NMDA receptor activation alone is sufficient for increase in TRIM47 protein level (2.89 ± 0.91-fold increase as compared with vehicle treated neurons, $p < 0.0001$, $n = 12$) (**Figures 1E,F**).

The NMDA-induced Ca^{++} activity triggers protein ubiquitination (Bingol and Schuman, 2006; Djakovic et al., 2009; Xu et al., 2018). To evaluate the role of Ca^{++} influx in activity-dependent enhancement of TRIM47, neurons were stimulated with glutamate in the presence or absence of the chelating agent EGTA. Our western blot analysis demonstrated that chelation of Ca^{++} by the application of EGTA (5 μM) prevented glutamate-induced enhancement of TRIM47 (**Figures 1C,D**). However, EGTA alone did not influence the TRIM47 level (**Figures 1C,D**), indicating that NMDA-induced Ca^{++} activity influences enhancement of TRIM47.

Since TRIM47 expression is enhanced in hippocampal neuronal culture following the application of glutamate, we have tested whether neuronal activity could regulate TRIM47 expression *in vivo*. We have analyzed its abundance in the dorsal hippocampus during spatial memory formation. We have used object location task, a spatial memory paradigm that induces synaptic activity in the physiological environment (Oliveira et al., 2010; Barbosa et al., 2013; Cohen et al., 2013; Cinalli et al., 2020). Consistent with previous observations (Ennaceur et al., 1997; Ennaceur, 2010; Oliveira et al., 2010), we observed that rat showed preferential exploration of displaced

object after the training in arena with two identical objects. The dorsal hippocampus from these rats were isolated and the TRIM47 level was analyzed by western blot. Our data showed an enhancement of TRIM47 (2.76 ± 0.52-fold increase, $p < 0.0434$, $n = 4$) in the dorsal hippocampus of the rats that preferentially explored the displaced object (Figures 2C–E).

Localization of TRIM47 at the synapse

Since TRIM47 showed an activity-dependent enhancement during the temporal window of synapse formation, we anticipate that the E3 ubiquitin ligase could possibly be localized at the synapto-dendritic compartment to drive synapse formation with spatial resolution. We have purified synaptoneurosome, a biochemical fraction enriched with synaptic compartment, from P14 and P60 rat hippocampi using ficoll density-gradient fractionation (Steward et al., 1991; Figure 3A. The purity of the synaptoneurosomal fractions were evaluated by immunoblotting of synaptic proteins, such as PSD-95 and Synapsin I, which showed enrichment in the synaptoneurosomal fraction as compared with the crude fraction. The glial protein GFAP and nuclear protein histone H1 being absent from the synaptoneurosomal fractions further confirmed their purity (Figures 3B,D). We detected that endogenous TRIM47 was enriched (3.05 ± 0.5992-fold increase, $p < 0.0417$, $n = 4$) and at P60 (2.35 ± 0.4172-fold increase, $p < 0.0476$, $n = 4$) in the synaptic fraction compared with the total cellular (crude) fraction (Figures 3C,E). We immunostained P14 and P60 rat brain sections using TRIM47 and the dendritic marker microtubule-associated protein 2 (MAP2). TRIM47 was found in a variety of brain areas, including the hippocampus (Supplementary Figure 1). Our data detected TRIM47 puncta in dendrites of hippocampal

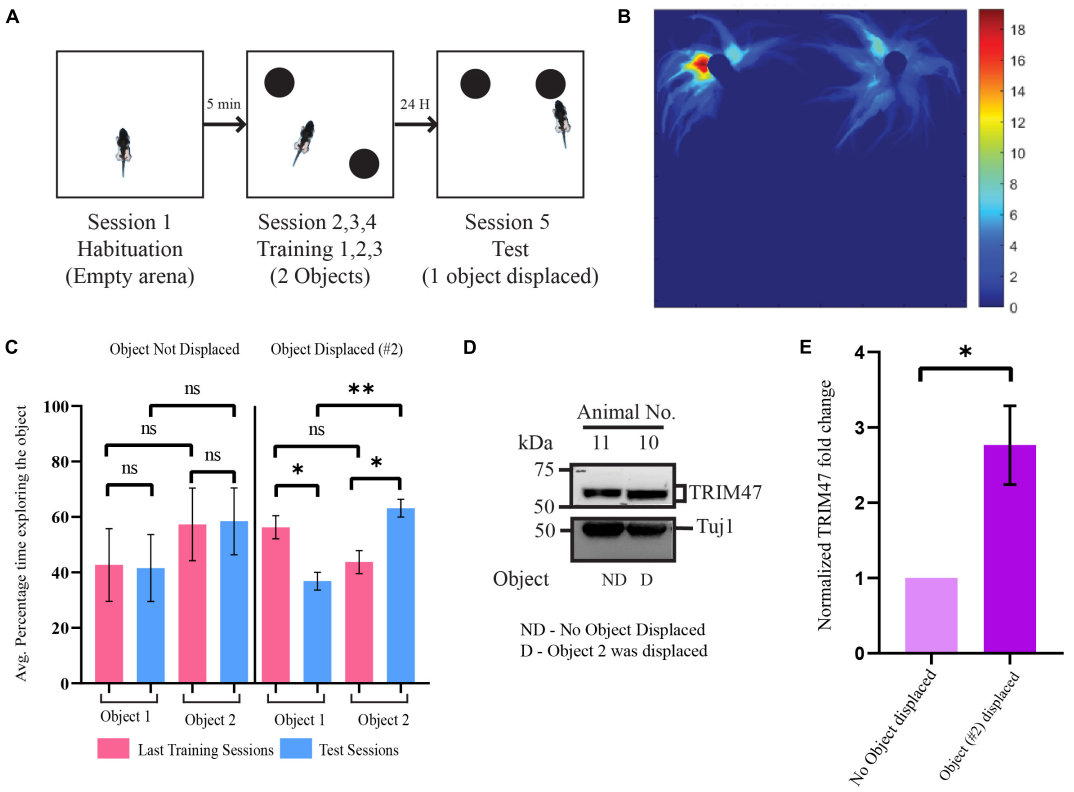

FIGURE 2
Enhancement of TRIM47 expression during spatial memory formation. **(A)** Schematic of the Spatial Object Recognition (SOR) memory test. **(B)** A representative heatmap showing the time spent by rat in the arena during the test session. **(C)** Quantitation of the average percentage time spent by rats exploring each object during the last training sessions and test sessions. Rats which were tested for object location memory where object location was same during the training and the test sessions (object not displaced or ND) and object location altered (object displaced or D) during test sessions. *$p < 0.0114$, **$p < 0.0012$; $n = 4$. Data are shown as the mean ± SEM, one-way ANOVA, and Fisher's least significant difference (LSD). **(D)** Enhancement of TRIM47 in the hippocampus was detected from animals showing preferential exploration of the displaced object. A photomicrograph showing TRIM47 and Tuj1 proteins expression levels in tissue isolated from dorsal hippocampi of rats subjected to a spatial object recognition memory test. ND—rats subjected to SOR where the object location was same during the test and training sessions; D—rats subjected to SOR where the location of one of the objects was changed during the test session relative to the training sessions. **(E)** Quantitation of western blot analysis post SOR. *$p < 0.0434$; $n = 4$. An unpaired t-test with Welch's correction is conducted. Data represent the mean ± SEM.

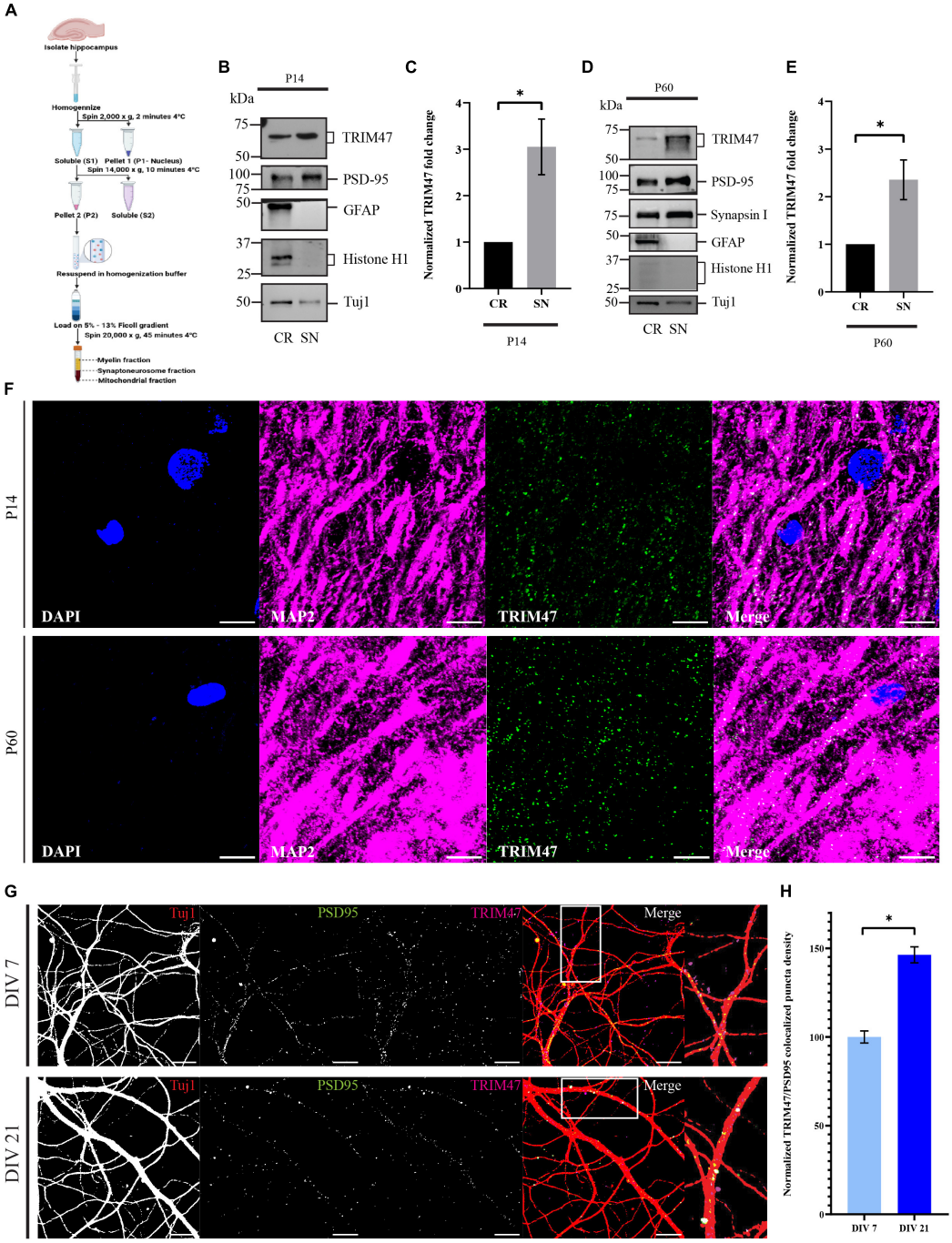

FIGURE 3
Localization of TRIM47 at the hippocampal synapse. **(A)** The schematic representation of synaptoneurosome preparation. Synaptoneurosome is prepared from rat hippocampus (P14 and P60) by ficoll density gradient (5–13%) centrifugation. **(B,D)** Synaptoneurosome purity is characterized by western blot analysis using antibodies specific for proteins enriched at the synapse (PSD95 and Synapsin I), astrocyte (GFAP), and nucleus (Histone H1). Tuj1 is used for normalization. Crude (CR) represents both nuclear and cytoplasmic proteins and synaptoneurosome (SN) represents synaptic proteins. Western blot showing synaptic localization of TRIM47. **(C,E)** Quantitation of TRIM47 protein levels showing synaptic enrichment. Data represent the mean ± SEM; $n = 4$; $^*p < 0.05$; and an unpaired t-test with Welch's correction. Icons in schematic representation **(A)** created in biorender.com. **(F)** Rat brain sections at P14 and P60 are immunostained for TRIM47, dendrites marked by MAP2, and sections are mounted in a medium containing DAPI. Scale—10 μm. **(G)** Neurons at DIV7 and DIV21 are immunostained for TRIM47 (magenta) as well as postsynaptic density protein PSD95 (green). Localization of TRIM47 at the synapses is visualized by apposing TRIM47 and PSD95 puncta onto hippocampal neurons labeled for Tuj1 (red). TRIM47/PSD95 co-localized puncta per micrometer of dendrite is measured to detect the puncta density. Scale: 10 μm. **(H)** Quantitation of synapse localized TRIM47 puncta density is measured from neurons at DIV7 and DIV21. $n = 12–13$; $^*p < 0.0001$; and an unpaired t-test with Welch's correction. Data represents the mean ± SEM.

neurons from rat brain at P14 and P60 (Figure 3F). Furthermore, synaptic localization in dissociated hippocampal neuron (DIV 7 and DIV 21) were detected by the colocalization of TRIM47 puncta with PSD95 labeled synaptic puncta (Figure 3G). We observed that the TRIM47 showed an increased colocalization with PSD95 at DIV 21 (46.3 ± 4.52% increase, $p < 0.0001$, $n = 12–13$) as compared with neurons at DIV 7 (Figure 3H).

Role of TRIM47 in dendritic development

Enhanced expressions of TRIM47 starting from P4 to P21 coincides with the temporal window of dendritic development (Pokorný and Yamamoto, 1981; Kroon et al., 2019). We have analyzed the importance of TRIM47 in dendritic development following the effective knockdown of TRIM47 by two distinct shRNAs. Hippocampal neurons were transduced (DIV 3) with lentivirus expressing shRNAs against TRIM47. The efficacy of knockdown in hippocampal neurons (DIV 21) was analyzed by western blot. We observed that both shRNA against TRIM47 led to significant reduction of the protein (shRNA #1—66.4 ± 5.28% decrease, $p < 0.0063$, $n = 3$; and shRNA #2—78.43 ± 4.59% decrease, $p < 0.0034$, $n = 3$) (Figures 4A,B). To evaluate the importance of TRIM47 in dendritic development, hippocampal neurons (DIV 2) were transfected with the chicken β-actin promoter driven EGFP (CAG-GFP) to visualize neuronal processes, and these neurons (DIV 3) were transduced with lentivirus expressing two distinct shRNAs against TRIM47 along with mCherry. Sholl analysis was performed using confocal images from neurons (DIV 21) expressing non-targeting control shRNA or shRNAs against TRIM47. We observed that knockdown of TRIM47 by two distinct shRNAs has no effect on dendritic development (Figures 4C,D).

TRIM47 affects dendritic spine density and spine morphology

Factors influencing dendritic spine structure have been shown to influence development and functions of synapse (Sala et al., 2001; Pavlopoulos et al., 2011; Gao et al., 2017; Sell et al., 2021). We have tested the impact of TRIM47 knockdown on dendritic spine development. Hippocampal neurons (DIV 3) were transduced with lentivirus expressing shRNAs against TRIM47 along with mCherry. Prior to transduction, CAG-GFP was transfected in hippocampal neurons (DIV 2) to visualize the dendritic spine. These EGFP-labeled dendritic spines were imaged from hippocampal neurons (DIV 21) to evaluate their structural change following the loss of TRIM47 function. We observed that knockdown of TRIM47 led to a significant increase (16.34 ± 3.2%, $p < 0.0009$ for shRNA#1; and 14.11 ± 2.85%, $p < 0.0029$ for shRNA#2) of total dendritic spine density (Figures 5A,B). We have measured spine type and observed that the loss of TRIM47 enhances mushroom spine (15.09 ± 2.05%, $p < 0.0001$ for shRNA#1; and 16.18 ± 1.36%, $p < 0.0001$ for shRNA#2) without influencing thin (shRNA #1—1.03 ± 1.92%, $p < 0.8$; and shRNA #2—1.09 ± 1.8%, $p < 0.75$) and stubby spines (shRNA #1—2.18 ± 2.57%, $p < 0.59$; and shRNA #2—0.7 ± 3.16%, $p < 0.95$) (Figures 5A–E). Our observations indicate that TRIM47 is a negative regulator of dendritic spine structure.

TRIM47 regulates glutamatergic synapse density

Synapses are formed on dendritic spines (Amaral and Pozzo-Miller, 2009; Zito et al., 2009). Prompted by our observation that TRIM47 negatively regulates dendritic spine development, we have analyzed synapse formation in excitatory neurons of the hippocampus following loss of TRIM47 function. Hippocampal neurons (DIV 3) were transduced with lentivirus expressing two distinct shRNAs along with mCherry. These neurons (DIV 21) were immunostained with the postsynaptic protein PSD95 and presynaptic protein Synapsin I. Synapse density was measured from confocal images by analyzing the number of colocalized PSD95 and Synapsin I puncta onto mCherry expressing dendrite. We observed that the knockdown of TRIM47 significantly enhanced (0.56 ± 0.037 synapse per μm, $p < 0.0001$ for shRNA #1 and 0.46 ± 0.042 synapse per μm, $p < 0.0001$ for shRNA #2 as compared with 0.24 ± 0.032 synapse per μm for control shRNA) (Figures 6A,B) synapse density. These observations indicate that TRIM47 functions as a negative regulator of excitatory synapse development in hippocampal neurons.

Discussion

Our study identified an E3 ubiquitin ligase that is expressed during the temporal window of synapse formation in the hippocampus. TRIM47 is localized in developing synapses (Figure 3) and its expression is regulated by neuronal activity in the developing as well as in the adult hippocampus (Figures 1, 2). The loss of TRIM47 function by two shRNAs enhances dendritic spine density as well as the number of mushroom spines without affecting dendritic complexity (Figures 4, 5). Furthermore, TRIM47 knockdown leads to an increase in glutamatergic synapse density (Figure 6). Similar phenotypic observations by distinct shRNA-mediated knockdown of TRIM47 eliminates the possibility of off-target effect of shRNA and support our observation that TRIM47 is a negative regulator of dendritic spine development and excitatory synapse formation. The localization of TRIM47

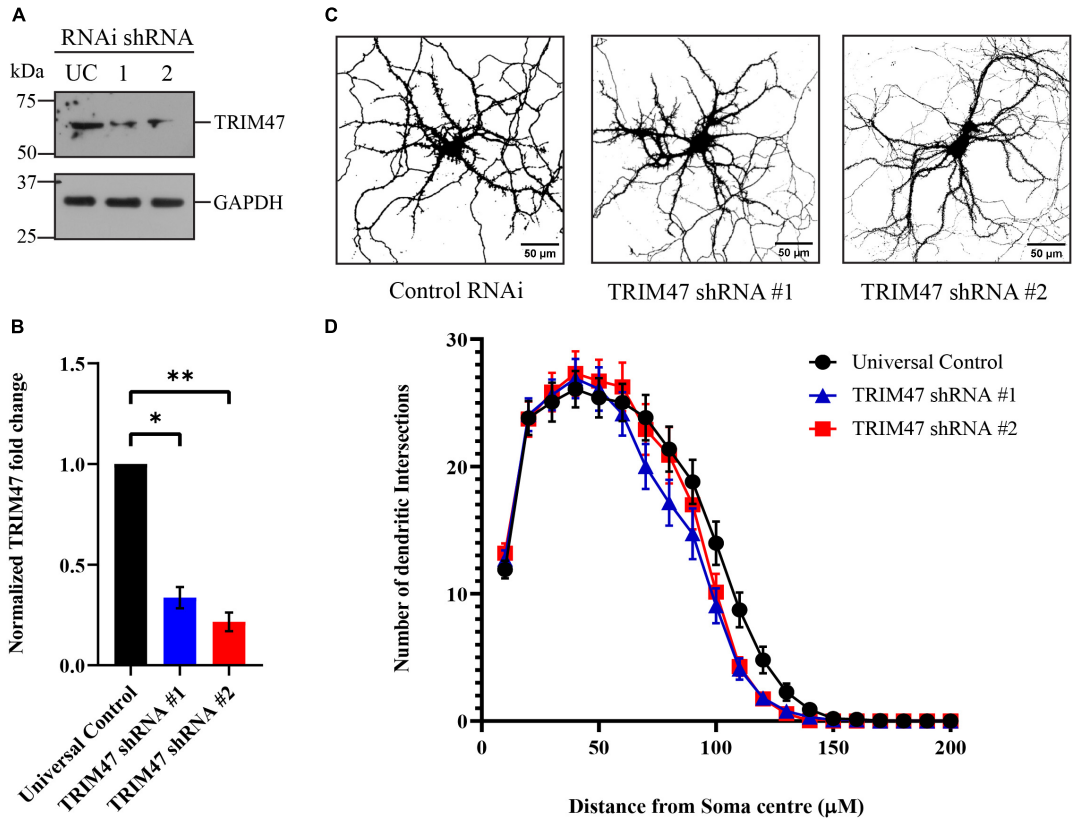

FIGURE 4
Effect of TRIM47 knockdown in dendritic development. **(A)** Photomicrograph showing effective knockdown of TRIM47 protein level in hippocampal neurons (DIV 21) by two distinct shRNAs. **(B)** Quantitation of TRIM47 normalized protein level following knockdown. $n = 3$; $^{*}p < 0.006$ and $^{**}p < 0.003$; and an unpaired t-test with Welch's correction. **(C)** Representative photomicrographs showing dendritic complexity (DIV 21) from hippocampal neurons transduced with lentivirus expressing two distinct shRNAs against TRIM47 (DIV 3). Dendritic development is analyzed by Sholl analysis. Scale as indicated. **(D)** Quantitation of Sholl analysis showing dendritic intersections at concentric circles drawn at 10 µm radius interval from the center of the soma. $n = 30–32$. One-way ANOVA with Dunnett's T3 multiple comparisons test was used to measure the statistical significance. $P < 0.92$ (control RNAi *vs.* TRIM47 knockdown by shRNA#1) and $p < 0.98$ (control RNAi *vs.* TRIM47 knockdown by shRNA#2); and the Kolmogorov–Smirnov test. Data represents mean ± SEM.

in developing synapse during the temporal window of synaptogenesis suggests that the TRIM47 could provide the spatial control of synapse formation.

Consistent with previous observation showing activity-dependent ubiquitination of synaptic proteins (Bingol and Schuman, 2006), our study suggests that the TRIM47 could function as a key regulator of activity-dependent *de novo* polyubiquitination of synaptic proteins. TRIM47 enrichment at the synapse and enhancement of its expression in hippocampal neurons by glutamate application or exposure to spatial memory paradigm indicate that TRIM47 function could spatially control spine architecture in developing as well as adult brain during learning. We observed that the NMDA receptor activation is sufficient for an increase in TRIM47 expression, and the calcium chelator EGTA blocks this enhancement. This observation suggests calcium-dependent TRIM47 expression upon NMDA receptor activation. These observations, along with previous studies, prompted us to anticipate that NMDA-mediated enhancement of TRIM47 could regulate the synaptic proteome for functional activity of the synapse (Ferreira et al., 2021).

The dendritic spine is an actin rich structure. Several factors influencing actin polymerization or depolymerization have been shown to be regulated by ubiquitin-dependent degradation by the proteasome (Schreiber et al., 2015; Lohraseb et al., 2022). We anticipate that proteasome-mediated degradation of factors influencing actin depolymerization following activity-dependent enhancement of TRIM47 could modulate the structure of the dendritic spine. The alteration of dendritic spine structure is directly correlated with the development of functional synapses and regulating synaptic potentiation during learning (Sell et al., 2021). Consistent with this logical proposition, we observed that TRIM47 also acts as a negative regulator of excitatory synapse development. It could be possible that TRIM47 promotes ubiquitination of proteins, negatively influencing synaptogenesis *via* canonical or non-canonical functions of ubiquitination.

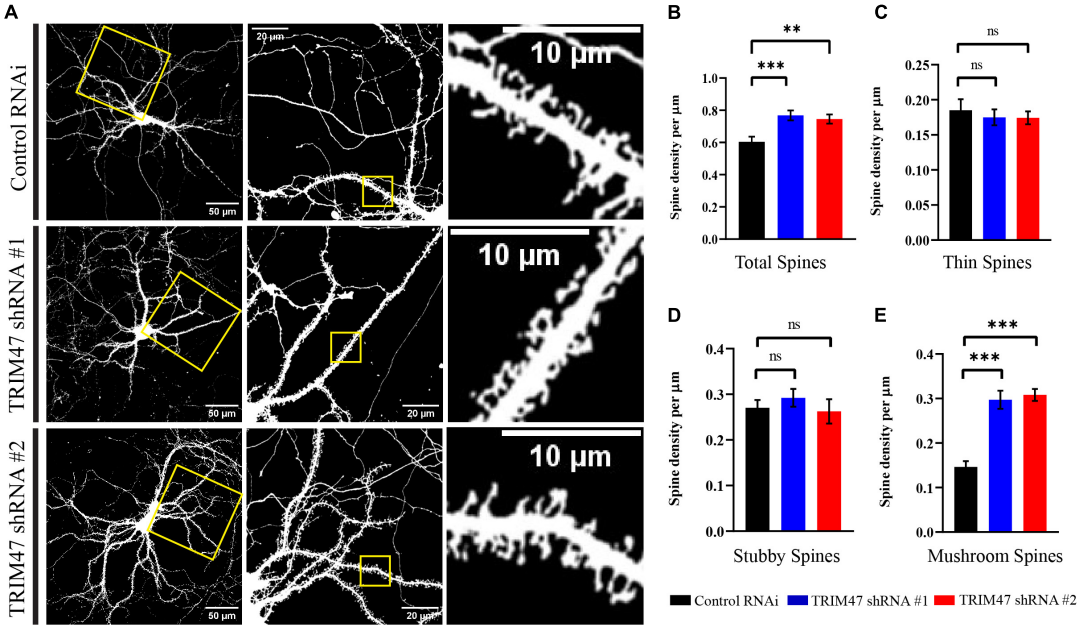

FIGURE 5
Dendritic spine morphology following TRIM47 knockdown. **(A)** Representative photomicrograph showing dendritic spine morphology from hippocampal neurons (DIV 21) that are transduced with two shRNAs against TRIM47 (DIV 3) and transfected with chicken βactin promoter driven GFP to visualize dendritic spine. Scale as indicated. **(B)** Quantitation of the total dendritic spine density following TRIM47 knockdown. Spine density per micrometer of dendritic length is measured from confocal images using Neurolucida 360. $^{***}p < 0.0009$ for shRNA#1, $^{**}p < 0.0029$ for shRNA#2. **(C–E)** Quantitation of thin spine **(C)**, stubby spines **(D)**, and mushroom spines **(E)** following TRIM47 knockdown. $^{***}p < 0.0001$ for **(E)**, ns = not significant for **(C,D)**. n = 16–25. One-way ANOVA with Dunnett's T3 multiple comparisons test. Data are shown as the mean ± SEM.

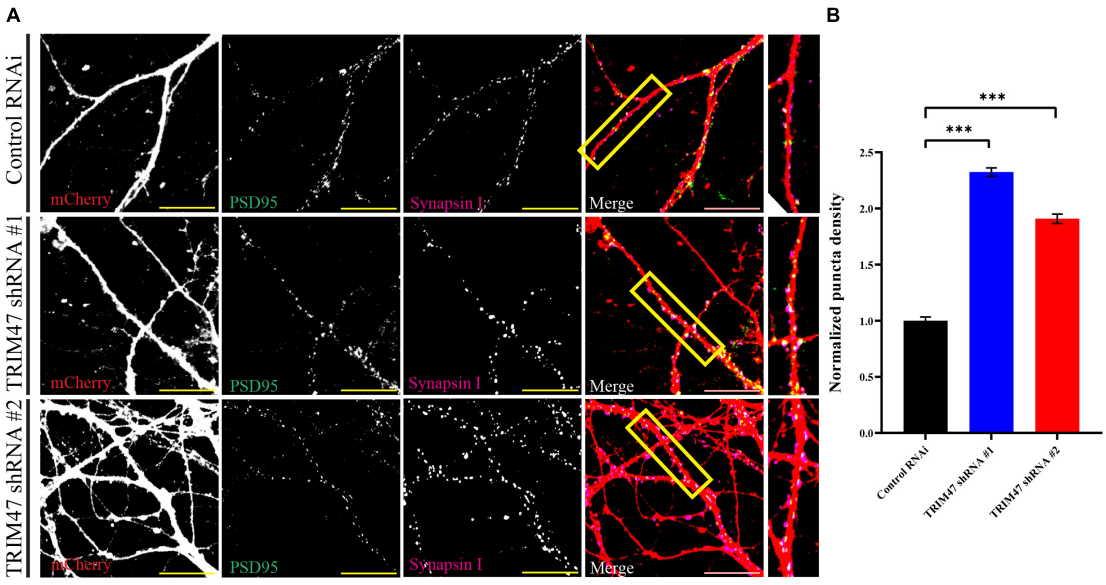

FIGURE 6
Excitatory synapse formation following TRIM47 knockdown. **(A)** Synapse density is measured from hippocampal neurons after effective knockdown of TRIM47. Neurons (DIV 3) are transduced with two distinct shRNAs against TRIM47 and these neurons (DIV 21) are immunostained using presynaptic protein Synapsin I (magenta) as well as postsynaptic protein PSD95 (green). Synapses are visualized by apposing Synapsin I and PSD95 puncta onto hippocampal neurons expressing mCherry (red). PSD95/Synapsin I colocalized puncta per micrometer of dendrite is measured to detect synapse density. Scale 20 µm. **(B)** Quantitation of synapse density is measured from neurons expressing control shRNA (Control RNAi) and two distinct shRNAs (shRNA # 1 and shRNA# 2) against TRIM47. n = 15–21. $^{***}p < 0.001$; one-way ANOVA with Dunnett's T3 multiple comparisons test. Data represent the mean ± SEM.

Analyzing the impact of TRIM47 knockdown on synaptic maturation would require functional characterization of synapses by electrophysiological recording of synaptic activity and distribution of glutamatergic receptor in the synaptic compartment. To gain a mechanistic insight into the activity-regulated functions of TRIM47 in dendritic spine development and synapse formation, targets of TRIM47 needs to be identified. Detailed characterization of these targets will elucidate mechanistic aspects of TRIM47-mediated spine development and synaptogenesis.

Data availability statement

The original contributions presented in this study are included in the article/**Supplementary material**, further inquiries can be directed to the corresponding author.

Ethics statement

This animal study was reviewed and approved by the Institutional Animal Ethics Committee of National Brain Research Centre.

Author contributions

SB conceived the idea. GS performed all experiment and analysis. SB and GS wrote the manuscript. Both authors contributed to the article and approved the submitted version.

Funding

This research was supported by a core grant to the National Brain Research Centre and a Ramalingaswami Fellowship from the Department of Biotechnology, Government of India.

Acknowledgments

We thank the members of the Synapse Biology Laboratory for the insightful discussions.

Conflict of interest

The authors declare that the research was conducted in the absence of any commercial or financial relationships that could be construed as a potential conflict of interest.

Publisher's note

Supplementary material

The Supplementary Material for this article can be found online at: https://www.frontiersin.org/articles/10.3389/fnmol.2022.943980/full#supplementary-material

SUPPLEMENTARY FIGURE 1
Localization of TRIM47 in rat brain. **(A)** P14 and **(B)** P60 Rat brain sections of 50 μm thickness are immunostained for TRIM47 and MAP2. Confocal images of whole brain section at ×10 (left panel), ×20 showing hippocampus (middle panel), and ×100 (right panel) shows TRIM47 localization in hippocampal neurons. Part of the image magnified is marked in yellow box.

References

Amaral, M. D., and Pozzo-Miller, L. (2009). The dynamics of excitatory synapse formation on dendritic spines. *Cellscience* 5, 19–25.

Andreae, L. C., and Burrone, J. (2014). The role of neuronal activity and transmitter release on synapse formation. *Curr. Opin. Neurobiol.* 27, 47–52. doi: 10.1016/j.conb.2014.02.008

Banerjee, S., Neveu, P., and Kosik, K. S. (2009). A coordinated local translational control point at the synapse involving relief from silencing and MOV10 degradation. *Neuron* 64, 871–884. doi: 10.1016/j.neuron.2009.11.023

Barbosa, F. F., Santos, J. R., Meurer, Y. S. R., Macêdo, P. T., Ferreira, L. M. S., Pontes, I. M. O., et al. (2013). Differential cortical c-Fos and Zif-268 expression after object and spatial memory processing in a standard or episodic-like object recognition task. *Front. Behav. Neurosci.* 7:112. doi: 10.3389/fnbeh.2013.00112

Bingol, B., and Schuman, E. M. (2006). Activity-dependent dynamics and sequestration of proteasomes in dendritic spines. *Nature* 441, 1144–1148. doi: 10.1038/nature04769

Boyer, C., Schikorski, T., and Stevens, C. F. (1998). Comparison of hippocampal dendritic spines in culture and in brain. *J. Neurosci.* 18, 5294–5300. doi: 10.1523/jneurosci.18-14-

Bradford, M. (1976). A rapid and sensitive method for the quantitation of microgram quantities of protein utilizing the principle of protein-dye binding. *Anal. Biochem.* 72, 248–254. doi: 10.1016/0003-2697(76)90527-3

Cavoy, A., and Delacour, J. (1993). Spatial but not object recognition is impaired by aging in rats. *Physiol. Behav.* 53, 527–530. doi: 10.1016/0031-9384(93)90148-9

Chen, L., Li, M., Li, Q., Xu, M., and Zhong, W. (2020). Knockdown of TRIM47 inhibits glioma cell proliferation, migration and invasion through the inactivation

of Wnt/β-catenin pathway. *Mol. Cell. Probes* 53:101623. doi: 10.1016/j.mcp.2020.101623

Cinalli, D. A., Cohen, S. J., Guthrie, K., and Stackman, R. W. (2020). Object recognition memory: distinct yet complementary roles of the mouse CA1 and Perirhinal cortex. *Front. Mol. Neurosci.* 13:527543. doi: 10.3389/fnmol.2020.527543

Cizeron, M., Qiu, Z., Koniaris, B., Gokhale, R., Komiyama, N. H., Fransén, E., et al. (2020). A brainwide atlas of synapses across the mouse life span. *Science* 369:aba3163. doi: 10.1126/science.aba3163

Cohen, S. J., Munchow, A. H., Rios, L. M., Zhang, G., Ásgeirsdóttir, H. N., and Stackman, R. W. (2013). The rodent hippocampus is essential for nonspatial object memory. *Curr. Biol.* 23, 1685–1690. doi: 10.1016/j.cub.2013.07.002

Cohen-Cory, S. (2002). The developing synapse: Construction and modulation of synaptic structures and circuits. *Science* 298, 770–776. doi: 10.1126/science.1075510

Cornelia Koeberle, S., Tanaka, S., Kuriu, T., Iwasaki, H., Koeberle, A., Schulz, A., et al. (2017). Developmental stage-dependent regulation of spine formation by calcium-calmodulin-dependent protein kinase IIα and Rap1. *Sci. Rep.* 7:13409. doi: 10.1038/s41598-017-13728-y

Denninger, J. K., Smith, B. M., and Kirby, E. D. (2018). Novel object recognition and object location behavioral testing in mice on a budget. *J. Vis. Exp.* 2018, 1–10. doi: 10.3791/58593

Djakovic, S. N., Schwarz, L. A., and Patrick, G. N. (2009). Regulation of the proteasome by neuronal activity and Calcium-Calmodulin dependent protein kinase II - Gentry N. *J. Biol. Chem.* 284, 26655–22665.

Ennaceur, A. (2010). One-trial object recognition in rats and mice: Methodological and theoretical issues. *Behav. Brain Res.* 215, 244–254. doi: 10.1016/j.bbr.2009.12.036

Ennaceur, A., Neave, N., and Aggleton, J. P. (1997). Spontaneous object recognition and object location memory in rats: The effects of lesions in the cingulate cortices, the medial prefrontal cortex, the cingulum bundle and the fornix. *Exp. Brain Res.* 113, 509–519. doi: 10.1007/PL00005603

Ferreira, J. S., Kellermayer, B., Carvalho, A. L., and Groc, L. (2021). Interplay between NMDA receptor dynamics and the synaptic proteasome. *Eur. J. Neurosci.* 54, 6000–6011. doi: 10.1111/ejn.15427

Fertuck, H. C., and Salpeter, M. M. (1976). Quantitation of junctional and extrajunctional acetylcholine receptors by electron microscope autoradiography after 125I-α-bungarotoxin binding at mouse neuromuscular junctions. *J. Cell Biol.* 69, 144–158. doi: 10.1083/jcb.69.1.144

Fiala, J. C., Feinberg, M., Popov, V., and Harris, K. M. (1998). Synaptogenesis Via Dendritic Filopodia in Developing Hippocampal Area CA1. *J. Neurosci.* 18, 8900–8911. doi: 10.1523/JNEUROSCI.18-21-08900.1998

Flavell, S. W., Cowan, C. W., Kim, T.-K., Greer, P. L., Lin, Y., Paradis, S., et al. (2006). Activity-dependent regulation of MEF2 transcription factors suppresses excitatory synapse number. *Science* 311, 1008–1012. doi: 10.1126/science.1122511

Fletcher, T. L., De Camilli, P., and Banker, G. (1994). Synaptogenesis in hippocampal cultures: Evidence indicating that axons and dendrites become competent to form synapses at different stages of neuronal development. *J. Neurosci.* 14, 6695–6706. doi: 10.1523/jneurosci.14-11-06695.1994

Gao, J., Marosi, M., Choi, J., Achiro, J. M., Kim, S., Li, S., et al. (2017). The E3 ubiquitin ligase IDOL regulates synaptic ApoER2 levels and is important for plasticity and learning. *eLife* 6:e29178. doi: 10.7554/eLife.29178

Greer, P. L., Hanayama, R., Bloodgood, B. L., Mardinly, A. R., Lipton, D. M., Flavell, S. W., et al. (2010). The Angelman Syndrome Protein Ube3A regulates synapse development by Ubiquitinating arc. *Cell* 140, 704–716. doi: 10.1016/j.cell.2010.01.026

Hall, B. J., and Ghosh, A. (2008). Regulation of AMPA receptor recruitment at developing synapses. *Trends Neurosci.* 31, 82–89. doi: 10.1016/j.tins.2007.11.010

Harris, K. M., and Stevens, J. K. (1989). Dendritic spines of CA1 pyramidal cells in the rat hippocampus: Serial electron microscopy with reference to their biophysical characteristics. *J. Neurosci.* 9, 2982–2997. doi: 10.1523/jneurosci.09-08-02982.1989

Harris, M., and Jensen, E. (1992). Three-dimensional structure of dendritic spines and synapses in rat hippocampus (CA1) at postnatal day 15 and adult ages. *J. Neurosci.* 12, 2665–2705. doi: 10.1523/JNEUROSCI.12-07-02685.1992

Jiang, M., and Chen, G. (2006). High Ca2+-phosphate transfection efficiency in low-density neuronal cultures. *Nat. Protoc.* 1, 695–700. doi: 10.1038/nprot.2006.86

Kaech, S., and Banker, G. (2006). Culturing hippocampal neurons. *Nat. Protoc.* 1, 2406–2415. doi: 10.1038/nprot.2006.356

Kroon, T., van Hugte, E., van Linge, L., Mansvelder, H. D., and Meredith, R. M. (2019). Early postnatal development of pyramidal neurons across layers of the mouse medial prefrontal cortex. *Sci. Rep.* 9:5037. doi: 10.1038/s41598-019-41661-9

Kumari, P., Srinivasan, B., and Banerjee, S. (2017). Modulation of hippocampal synapse maturation by activity-regulated E3 ligase via non-canonical pathway. *Neuroscience* 364, 226–241. doi: 10.1016/j.neuroscience.2017.08.057

Li, L., Yu, Y., Zhang, Z., Guo, Y., Yin, T., Wu, H., et al. (2021). TRIM47 accelerates aerobic glycolysis and tumor progression through regulating ubiquitination of FBP1 in pancreatic cancer. *Pharmacol. Res.* 166:105429. doi: 10.1016/j.phrs.2021.105429

Li, Z., and Sheng, M. (2003). Some assembly required: The development of neuronal synapses. *Nat. Rev. Mol. Cell Biol.* 4, 833–841. doi: 10.1038/nrm1242

Lin, Y., Bloodgood, B. L., Hauser, J. L., Lapan, A. D., Koon, A. C., Kim, T. K., et al. (2008). Activity-dependent regulation of inhibitory synapse development by Npas4. *Nature* 455, 1198–1204. doi: 10.1038/nature07319

Lohmann, C., and Kessels, H. W. (2014). The developmental stages of synaptic plasticity. *J. Physiol.* 592, 13–31. doi: 10.1113/jphysiol.2012.235119

Lohraseb, I., McCarthy, P., Secker, G., Marchant, C., Wu, J., Ali, N., et al. (2022). Global ubiquitinome profiling identifies NEDD4 as a regulator of Profilin 1 and actin remodelling in neural crest cells. *Nat. Commun.* 13:2018. doi: 10.1038/s41467-022-29660-3

Mabb, A. M., and Ehlers, M. D. (2010). Ubiquitination in postsynaptic function and plasticity. *Annu. Rev. Cell Dev. Biol.* 26, 179–210. doi: 10.1146/annurev-cellbio-100109-104129

Nakata, K., Abrams, B., Grill, B., Goncharov, A., Huang, X., Chisholm, A. D., et al. (2005). Regulation of a DLK-1 and p38 MAP kinase pathway by the ubiquitin ligase RPM-1 is required for presynaptic development. *Cell* 120, 407–420. doi: 10.1016/j.cell.2004.12.017

Nelson, P. G., Fields, R. D., Yu, C., and Neale, E. A. (1990). Mechanisms involved in activity-dependent synapse formation in mammalian central nervous system cell cultures. *J. Neurobiol.* 21, 138–156. doi: 10.1002/neu.480210110

Nguyen, A. Q., Koeppen, J., Woodruff, S., Mina, K., Figueroa, Z., and Ethell, I. M. (2020). Astrocytic Ephrin-B1 Controls Synapse Formation in the Hippocampus During Learning and Memory. *Front. Synaptic Neurosci.* 12:10. doi: 10.3389/fnsyn.2020.00010

Oliveira, A. M. M., Hawk, J. D., Abel, T., and Havekes, R. (2010). Post-training reversible inactivation of the hippocampus enhances novel object recognition memory. *Learn. Mem.* 17, 155–160. doi: 10.1101/lm.1625310

Papa, M., Bundman, M. C., Greenberger, V., and Segal, M. (1995). Morphological analysis of dendritic spine development in primary cultures of hippocampal neurons. *J. Neurosci.* 15, 1–11. doi: 10.1523/jneurosci.15-01-00001.1995

Paradis, S., Harrar, D. B., Lin, Y., Koon, A. C., Hauser, J. L., Griffith, E. C., et al. (2007). An RNAi-Based Approach Identifies Molecules Required for Glutamatergic and GABAergic Synapse Development. *Neuron* 53, 217–232. doi: 10.1016/j.neuron.2006.12.012

Patel, T. P., Gullotti, D. M., Hernandez, P., O'Brien, W. T., Capehart, B. P., Morrison, B., et al. (2014). An open-source toolbox for automated phenotyping of mice in behavioral tasks. *Front. Behav. Neurosci.* 8:349. doi: 10.3389/fnbeh.2014.00349

Pavlopoulos, E., Trifilieff, P., Chevaleyre, V., Fioriti, L., Zairis, S., Pagano, A., et al. (2011). Neuralized1 activates CPEB3: A function for nonproteolytic ubiquitin in synaptic plasticity and memory storage. *Cell* 147, 1369–1383. doi: 10.1016/j.cell.2011.09.056

Pokorný, J., and Yamamoto, T. (1981). Postnatal ontogenesis of hippocampal CA1 area in rats. I. Development of dendritic arborisation in pyramidal neurons. *Brain Res. Bull.* 7, 113–120. doi: 10.1016/0361-9230(81)90075-7

Polleux, F., Ince-Dunn, G., and Ghosh, A. (2007). Transcriptional regulation of vertebrate axon guidance and synapse formation. *Nat. Rev. Neurosci.* 8, 331–340. doi: 10.1038/nrn2118

Rao, A., and Craig, A. M. (1997). Activity regulates the synaptic localization of the NMDA receptor in hippocampal neurons. *Neuron* 19, 801–812. doi: 10.1016/S0896-6273(00)80962-9

Sala, C., Piech, V., Wilson, N. R., Passafaro, M., Liu, G., and Sheng, M. (2001). Regulation of Dendritic Spine Morphology and Synaptic Function by Shank and Homer. *Neuron* 31, 115–130. doi: 10.24033/bsmf.2510

Salpeter, M. M., and Harris, R. (1983). Distribution and turnover rate of acetylcholine receptors throughout the junction folds at a vertebrate neuromuscular junction. *J. Cell Biol.* 96, 1781–1785. doi: 10.1083/jcb.96.6.1781

Schmitz, S. K., Hjorth, J. J. J., Joemai, R. M. S., Wijntjes, R., Eijgenraam, S., de Bruijn, P., et al. (2011). Automated analysis of neuronal morphology, synapse number and synaptic recruitment. *J. Neurosci. Methods* 195, 185–193. doi: 10.1016/j.jneumeth.2010.12.011

Schreiber, J., Végh, M. J., Dawitz, J., Kroon, T., Loos, M., Labonté, D., et al. (2015). Ubiquitin ligase TRIM3 controls hippocampal plasticity and learning by regulating synaptic γ-actin levels. *J. Cell Biol.* 211, 569–586. doi: 10.1083/jcb.201506048

Sell, G. L., Xin, W., Cook, E. K., Zbinden, M. A., Schaffer, T. B., O'Meally, R. N., et al. (2021). Deleting a UBE3A substrate rescues impaired hippocampal physiology and learning in Angelman syndrome mice. *Sci. Rep.* 11:19414. doi: 10.1038/s41598-021-97898-w

Shatz, C. J., and Katz, L. C. (1996). Synaptic activity and the construction of cortical circuits. *ScienJce* 274, 1133–1138.

Steward, O., Pollack, A., and Rao, A. (1991). Evidence that protein constituents of postsynaptic membrane specializations are locally synthesized: Time course of appearance of recently synthesized proteins in synaptic junctions. *J. Neurosci. Res.* 30, 649–660. doi: 10.1002/jnr.490300408

Südhof, T. C. (2021). The cell biology of synapse formation. *J. Cell Biol.* 220:e202103052. doi: 10.1083/jcb.202103052

Sun, M., Bernard, L. P., Dibona, V. L., Wu, Q., and Zhang, H. (2013). Calcium phosphate transfection of primary hippocampal neurons. *J. Vis. Exp.* 81:e50808. doi: 10.3791/50808

Sutcliffe, J. S., Marshall, K. M., and Neill, J. C. (2007). Influence of gender on working and spatial memory in the novel object recognition task in the rat. *Behav. Brain Res.* 177, 117–125. doi: 10.1016/j.bbr.2006.10.029

Wan, H. I., DiAntonio, A., Fetter, R. D., Bergstrom, K., Strauss, R., and Goodman, C. S. (2000). Highwire regulates synaptic growth in Drosophila. *Neuron* 26, 313–329. doi: 10.1016/S0896-6273(00)81166-6

Wimmer, M. E., Hernandez, P. J., Blackwell, J., and Abel, T. (2012). Aging impairs hippocampus-dependent long-term memory for object location in mice. *Neurobiol. Aging* 33, 2220–2224. doi: 10.1016/j.neurobiolaging.2011.07.007

Xu, J., Kurup, P., Nairn, A. C., and Lombroso, P. J. (2018). Synaptic NMDA receptor activation induces Ubiquitination and degradation of STEP61. *Mol. Neurobiol.* 55, 3096–3111. doi: 10.1007/s12035-017-0555-x

Yu, C. R., Power, J., Barnea, G., O'Donnell, S., Brown, H. E. V., Osborne, J., et al. (2004). Spontaneous neural activity is required for the establishment and maintenance of the olfactory sensory map. *Neuron* 42, 553–566. doi: 10.1016/S0896-6273(04)00224-7

Zhu, F., Cizeron, M., Qiu, Z., Benavides-Piccione, R., Kopanitsa, M. V., Skene, N. G., et al. (2018). Architecture of the mouse brain synaptome. *Neuron* 99, 781.e–799.e. doi: 10.1016/j.neuron.2018.07.007

Zito, K., Scheuss, V., Knott, G., Hill, T., and Svoboda, K. (2009). Rapid functional maturation of nascent dendritic spines. *Neuron* 61, 247–258. doi: 10.1016/j.neuron.2008.10.054

Zito, K., and Svoboda, K. (2002). Activity-dependent synaptogenesis in the adult mammalian cortex. *Neuron* 35, 1015–1017. doi: 10.1016/S0896-6273(02)00903-0

Frontiers in Molecular Neuroscience

Leading research into the brain's molecular structure, design and function

Part of the most cited neuroscience series, this journal explores and identifies key molecules underlying the structure, design and function of the brain across all levels.

Discover the latest Research Topics

See more →

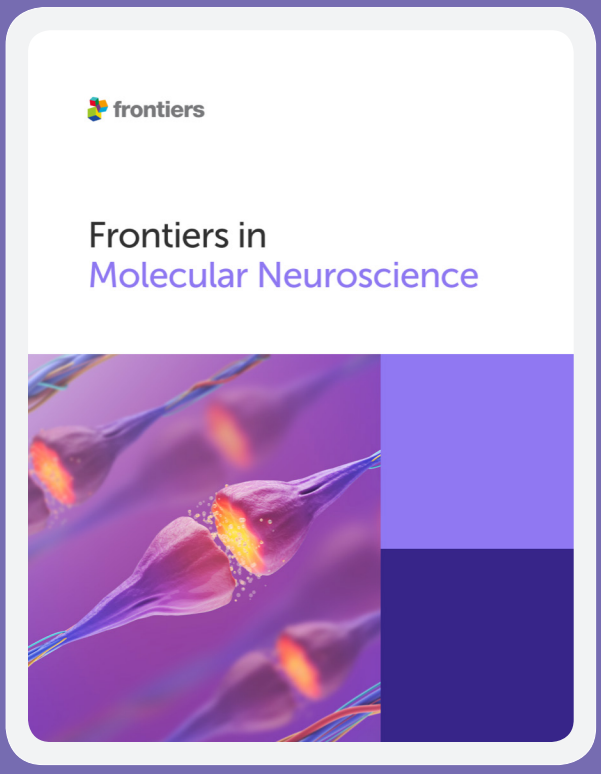

Frontiers

Avenue du Tribunal-Fédéral 34
1005 Lausanne, Switzerland
frontiersin.org

Contact us

+41 (0)21 510 17 00
frontiersin.org/about/contact